UNIVERZITA KARLOVA V PRAZE
LÉKAŘSKÁ FAKULTA V PLZNI
ŠIKLŮV ÚSTAV PATOLOGIE

MORFOLOGIE, IMUNOHISTOCHEMIE A MOLEKULÁRNÍ GENETIKA V DIAGNOSTICE RENÁLNÍCH NEOPLÁZIÍ

MORPHOLOGY, IMMUNOHISTOCHEMISTRY AND MOLECULAR GENETICS IN DIAGNOSTICS OF THE RENAL NEOPLASMS

HABILITAČNÍ PRÁCE

MUDr. KRISTÝNA PIVOVARČÍKOVÁ, Ph.D.

PLZEŇ 2021

Prohlášení

Prohlašuji, že jsem habilitační práci zpracovala samostatně a že jsem řádně uvedla a citovala všechny použité prameny a literaturu. Souhlasím s trvalým uložením elektronické verze mé práce v databázi UK LF Plzeň.

V Plzni, 20. března 2021

MUDr. Kristýna Pivovarčíková, Ph.D

OBSAH

SEZNAM POUŽITÝCH ZKRATEK

2SC	Imunohistochemická protilátka detekující „S-(2-succino) cysteine“
aCGH	Array Comparative Genomic Hybridization
ACN	Adult cystic nephroma (adultní cystický nefrom)
AE1/3	Směs imunohistochemických protilátek detekující cytokeratiny
AMACR	Imunohistochemická protilátka detekující enzym α-methylacyl-CoA racemasu
ATRX	a-thalassaemia/mental retardation syndrome X-linked
BSARCC	Biphasic squamoid alveolar renal cell carcinoma (bifazický skvamo-alveolární renální karcinom)
CAIX	Imunohistochemická protilátka detekující anhydrázu kyseliny uhličité *CA9*
CAM5.2	Imunohistochemická protilátka detekující cytokeratin *KRT8*
CD10	Imunohistochemická protilátka detekující metaloendopeptidázu MME
CD117	Imunohistochemická protilátka detekující extracelulární část transmembránového tyrozin-kinázového receptoru c-Kit
CCRCC	Clear cell renal cell carcinoma (světlobuněčný renální karcinom)
CK7	Imunohistochemická protilátka detekující protein cytokeratinu *KRT7*
CK20	Imunohistochemická protilátka detekující protein cytokeratinu *KRT20*
CNV	Copy number variation (variace počtu kopií)
DAXX	Death-domain associated protein X
EVT	Eosinophilic vacuolated tumor (eosinofilní tumor s vakuolami)
FFPE	formalin-fixed, paraffin-embedded
FH	Fumarat hydratase (fumarát hydratáza)
FHRCC	Fumarat hydratase deficient renal cell carcinoma (fumarát hydratáza deficientní renální karcinom)
FISH	Fluorescence in situ hybridization
GUPS	The Genitourinary Pathology Society (Genitourinární Patologická Společnost)
HE	Barvení hematoxylin-eosin
HIF-2	Hypoxia-inducible factor 2
HLRCC	Hereditary leiomyomatosis and renal cell carcinoma-associated renal cell carcinoma (karcinom ledviny asociovaný se syndromem familiární leiomyomatózy a karcinomem ledvin)
HMB45	Imunohistochemická protilátka detekující antigen PMEL
HOT	High-grade oncocytic tumor (high-grade onkocytický tumor)
HPF	High power field (pole velkého zvětšení)
INI-1	Imunohistochemická protilátka detekující „chromatin remodeling protein“ INI-1/ SMARCB1
INSM1	Imunohistochemická protilátka detekující insulinoma-associated protein 1
LOH	Loss of heterozygosity (ztráta heterozygozity)
MELAN A	Imunohistochemická protilátka detekující produkt genu *MELANA*
MEST	Mixed epithelial and stromal tumor (smíšený epiteliální a stromální tumor ledviny)
MESTF	Mixed epithelial and stromal tumor family (rodina smíšených epiteliálních a stromálních tumorů ledviny)
MITF RCC	MiT rodina translokačního renálního karcinomu
MTS RCC	Mucinous tubular and spindle cell renal cell carcinoma (mucinózní tubularní a vřetenobuněčný renální karcinom)

NGS	Next-Generation Sequencing (sekvenování nové generace)
NET	Neuroendocrine tumor (neuroendokrinní tumor)
OPRCC	Oncocytic papillary renal cell carcinoma (onkocytický papilární renální karcinom)
PAX8	Imunohistochemická protilátka detekující protein PAX8
PCN	Pediatric cystic nephroma (pediatrický cystický nefrom)
PCR	Polymerase chain reaction (polymerázová řetězová reakce)
PD-1	Programed cell death 1
PD-L1	Programmed death-ligand 1
PLC	Paneth-like cells (Panethových buňkám podobné buňky)
PRCC	Papillary renal cell carcinoma (papilární renální karcinom)
PRCCM	"Mucin"-secreting papillary penal cell carcinoma ("Mucin"-secernující papilání renální karcinom)
RCC	Renal cell carcinoma (renální karcinom)
SDHB	Imunohistochemická protilátka detekující „Succinate Dehydrogenase Iron-sulfur Subunit B"
SPRCC	Solid papillary renal cell carcinoma (solidní varianta papilárního renálního karcinomu)
TFE3	transkripční faktor TFE3
TFEB	transkripční faktor TFEB
TILs	tumor infiltrující lymfocyty
UC	uroteliální karcinom
VHL	von Hippel-Lindau
WHO	World Health Organization (Světová Zdravotnická Organizace)

ÚVOD

Habilitační práce „Morfologie, imunohistochemie a molekulární genetika v diagnostice renálních neoplázií“ představuje soubor komentovaných dříve publikovaných prací – habilitační práce tak prezentuje celkem 27 vybraných publikací, na kterých se autorka podílela, ať už jako členka autorského kolektivu, či jako první autor. Jedná se zejména o originální práce, které byly publikovány v odborných zahraničních časopisech s impact faktorem, zahrnuty jsou však i práce souhrnné i originální uveřejněné v recenzovaných českých a slovenských časopisech.

Práce je tematicky zaměřena na diagnostiku renálních neoplázií, tedy na jedno z odvětví subspecializace autorky a je rozčleněna do částí podle komentovaných neoplastických jednotek. Práce se v žádném případě nesnaží do široka obsáhnout, detailně popsat a okomentovat aktuální poznatky na poli renálních neoplázií. Předkládaná práce pouze komentuje současnou literaturou diskutované dílčí problémy některých renálních tumorů, na jejichž popisu a prezentaci se autorka svou publikační aktivitou spolupodílela.

Práce je na začátku uvedena krátkým úvodem do problematiky, následuje recentně publikovaná souhrnná publikace autorky z recenzovaného časopisu, která aktuální problematiku morfologie, imunohistochemie a genetiky v rámci renálních neoplázií kompletně shrnuje. Za ní je práce rozčleněna do oddílů dle komentovaných neoplastických entit, kde po krátkém shrnujícím úvodu jsou vždy zařazeny vlastní originální práce, věnující se dílčím problémům v rámci vymezeného tématu. Ty vždy opět s krátkým českým úvodem a připojenými kopiemi reprintů.

SOUBOR KOMENTOVANÝCH PUBLIKACÍ

1 MORFOLOGIE, IMUNOHISTOCHEMIE A GENETIKA RENÁLNÍCH NEOPLÁZIÍ

V posledních 40 letech doznala klasifikace renálních neoplázií výrazných změn – z původně dvou nádorových jednotek nyní rozlišujeme několik desítek renálních neoplázií a spektrum těchto lézí se i na dále velmi dynamicky rozrůstá. Kromě objevu zcela nových nádorových jednotek se v současné době stále častěji setkáváme i s výrazně se měnícím pohledem na dříve definované jednotky. Celkem významně začíná do klasifikace renálních neoplázií v posledním desetiletí promlouvat molekulární genetika, i tak však morfologické znaky zůstávají při diagnostice klíčovými charakteristikami. I přes inovativní přístup s implementací imunohistochemických barvení a molekulárně-genetických metod si však skupina renálních neoplázií kromě morfologického primu ponechává i své půvabné historické specifikum – tradiční „popisné“ názvy entit. Názvy renálních tumorózních entit tak sice můžou na jednu stranu působit krkolomně, z pohledu patologa však jasně vypovídají o prvcích důležitých pro jejich zařazení a určení diagnózy (např. pro Xp11 translokační renální karcinom je diagnostická translokace *TFE3* genu se spektrem genů partnerských, eosinofilní solidně cystický renální karcinom je tumor sestávající z eosinofilních buněk uspořádaných v cystických a solidních okrscích atd.).

V rámci renálních neoplázií se sice nejčastěji setkáváme s tradičními jednotkami, odborná literatura a rutinní diagnostika však jasně ukazuje, že méně časté typy renálních neoplázií nejsou až takovou raritou, jak se předpokládalo. Implementace imunohistochemie a molekulárně genetických metod doplňujících klíčové morfologické rysy ukazuje, že některé dříve diagnostikované tumory ve skutečnosti nejsou entitami, za které byly původně považovány. Řada tumorů dříve spadajících do kategorie neklasifikovatelných renálních karcinomů/tumorů („unclassifiable renal carcinomas/tumors“) představuje množství zcela nových jednotek, které by neměli být opomíjeny. Molekulární genetika a imunohistochemie se pak postupně stala rutinní a neodmyslitelnou součástí diagnostiky renálních neoplázií.

V současné době stojíme na prahu před vydáním nové WHO klasifikace, která, jak lze předpokládat, bude alespoň částečným odrazem recentně publikovaných doporučení Genitourinární Patologické Společnosti (The Genitourinary Pathology Society/GUPS) [44, 45]. Tato doporučení se dopodrobna věnovala dvěma okruhům – jednak novým poznatkům v rámci tradičních a dlouho uznávaných renálních neoplázií [44], jednak objektivní charakteristice některých zcela nově popsaných jednotek (na podkladě revizí dostupné literatury), které se v literatuře začínají objevovat recentně před a po vydání WHO klasifikace z roku 2016 [45]. GUPS doporučení tak rozeznávají zcela nové jednotky, jejichž existence je podložena mnohotnými nezávislými studiemi a lze předpokládat, že tyto jednotky by mohli být oficiálně uznány jako samostatné entity nově připravovanou WHO. Dále v doporučeních najdeme tzv. „emerging entity“ a „provisional entity“, kdy obě tyto skupiny disponují v současné době omezeným počtem publikovaných případů a k další validaci těchto nádorových jednotek jsou nutné nové studie [45]. Kromě nových jednotek, GUPS doporučení věnovala velkou pozornost i novým poznatkům v rámci „starých“ a „tradičních“ renálních neoplastických jednotek [44]. Velké změny se v posledních letech uskutečňují především na poli papilárního renálního karcinomu (PRCC), který se jako skupina stává velice heterogenní [36].

Na rozdíl od mohutného pokroku na poli morfologie, imunohistochemie a molekulární genetiky u renálních neoplázií bohužel prozatím nedochází k výraznějšímu posunu v léčbě pacientů. Diagnostika tak výrazně předběhla terapeutické možnosti a v tuto chvíli stále platí, že různé renální karcinomy jsou léčeny prakticky totožně. Mohlo by se tak zdát, že posun na

poli diagnostickém se nesetkává s tíženým klinickým efektem a tedy vlastně ani není žádoucí a jedná se o zbytečné snahy a nadbytečnou „vědu“. Velký rozkvět na poli renálních neoplázií však podle nás má své opodstatnění. Znalost morfologického spektra, imunohistochemických vlastností a molekulárně-genetických charakteristik je pro správnou finální diagnostiku renálního tumoru nepostradatelná a jen dobrá edukace patologů a literární dostupnost všech těchto důležitých informací může zajistit správnou diagnózu. Do budoucna, s rozvojem personalizované medicíny a cílené léčby, ovšem předpokládáme, že stanovení správné a kompletní diagnózy bude mít výrazný dopad na další léčbu pacienta a prognózu jeho onemocnění.

1.1 Morfologie, imunohistochemie a genetika napříč spektrem různých renálních neoplázií – souhrn

Využití imunohistochemie při diagnostice renálních neoplázií.
Pivovarčíková K, Michalová K, Hes O.
Cesk Patol 2020; 56(3): 130–139

Problematika je do široka shrnuta následující publikací.

1.1.1 Využití imunohistochemie při diagnostice renálních neoplázií

Jedná se o souhrnnou práci publikovanou v recenzovaném časopise „Česko-slovenská patologie“. Článek podává aktuální přehled o využití imunohistochemie a genetických znaků při rutinní diagnostice renálních neoplázií a problematiku tohoto odvětví do široka shrnuje.

Využití imunohistochemie při diagnostice renálních neoplázií

Kristýna Pivovarčíková, Květoslava Michalová, Ondřej Hes

Šiklův ústav patologie LF UK a FN Plzeň

SOUHRN

Tento přehledový článek stručně shrnuje možnosti využití imunohistochemie při vyšetřování především renálních karcinomů a základní molekulárně genetické znaky vybraných neoplázií. Článek však v žádném případě nelze brát jako univerzální návod pro diagnostiku renálních tumorů. Renální karcinomy dokážou mít velmi variabilní morfologický vzhled a to i v rámci jedné léze (nádorová heterogenita) a často velmi nepředvídatelný a neuniformní imunohistochemický profil. Některé renální neoplázie jsou diagnostikovány striktně na podkladě molekulárně-genetických vlastností, bez ohledu na morfologický vzhled.

Klíčová slova: Angiomyolipom – imunohistochemie – chromofóbní renální karcinom – světlobuněčný renální karcinom – renální onkocytom

Immunohistochemistry and renal neoplasias

SUMMARY

We present here a review article dealing with immunohistochemistry and basic molecular-genetic findings/markers in selected renal tumors. The article is not an universal instruction for renal tumor diagnostics. Renal cell carcinomas can have very variable morphological features (even within one neoplastic lesion – i.e. tumoral heterogeneity) and unpredictable and variable immunohistochemical profile. Some renal neoplasias are diagnosed on the base of molecular-genetic signs only (regardless morphologic appearance).

Keywords: Angiomyolipoma – immunohistochemistry – chromophobe renal cell carcinoma – clear cell renal cell carcinoma – renal oncocytoma

Cesk Patol 2020; 56(3): 130–139

Klasifikace renálních neoplázií doznala v posledních 40 letech významných změn a stále se velmi dynamicky mění. Prakticky neustále jsou publikovány práce popisující nové renální nádorové jednotky, zároveň se však začíná významně měnit i pohled a přístup k některým dlouhodobě uznávaným renálním neoplaziím. V současné době platná WHO klasifikace (z roku 2016) odráží významné pokroky na poli morfologie, imunohistochemie, cytogenetiky a molekulární patologie a obsahuje několik desítek nádorových jednotek a čtyři tzv. provizorní jednotky (1).

Není účelem tohoto článku do detailu popsat všechny renální tumory - morfologické spektrum různých jednotek může být opravdu široké. Bez nadsázky lze říct, že typický imunohistochemický profil jednotlivých renálních karcinomů (RCC) neexistuje a stoprocentně se nelze spolehnout ani na molekulárně genetické vyšetření. Pozornost zde tak bude věnována pouze určitým diferenciálně diagnostickým okruhům RCC, které budou stručně komentovány. V žádném případě však nelze brát toto sdělení jako univerzální návod pro diagnostiku renálních neoplázií.

Na prvním místě by v tomto přehledovém článku mělo být zdůrazněno, že u drtivé většiny případů ke správné diagnóze renální neoplázie vystačí obyčejné barvení hematoxylinem-eosinem a dostatečný sampling léze. Histologický nález zůstává nejdůležitějším diagnostickým kritériem, které pokud nedovolí určit diagnózu s definitivní platností, alespoň rozhoduje o dalším diagnostickém postupu. Nutné je však mít též na paměti, že některé renální tumory jsou dnes klasifikovány čistě na podkladě molekulárně genetických znaků (bez ohledu na přítomnost či absenci typických morfologických znaků). Molekulárně genetická analýza tak v urogenitální patologii začíná být součástí rutinní diagnostické praxe a je společně s imunohistochemií hojně využívána. Molekulárně genetickou analýzu a imunohistochemická barvení však nelze v běžné praxi užívat jako univerzální diagnostický nástroj a s tímto vědomím by k nim mělo být přistupováno. Tyto metody tak v žádném případě neřeší diagnostické dilema ve 100 % případů. Diagnostika části renálních neoplázií tedy rozhodně patří do rukou zkušeného urogenitálního patologa a laboratoře disponující výše jmenovanými diagnostickými modalitami.

✉ ***Adresa pro korespondenci:***
MUDr. Kristýna Pivovarčíková, Ph.D.
Šiklův ústav patologie LF UK a FN Plzeň
Alej Svobody 80, 30460 Plzeň
tel.: +420377404633
e-mail: pivovarcikovak@fnplzen.cz

MARKERY RENÁLNÍHO ORIGA

Patology je obecně používáno různé spektrum imunohistochemických markerů, ale asi mezi ty pro renální origo úplně nejčastější patří PAX2, PAX8, RCC, CD10 a vimentin. Při indikaci těchto a jiných barvení je třeba vždy myslet na jejich nízkou specificitu pouze pro renální origo. Též bývá pravidlem, že neobvyklé varianty a „podivné" RCC obvykle mívají stejně tak neobvyklý a podivný imunohistochemický profil, a že imunohistochemický profil metastázy RCC může být zcela odlišný od tumoru primárního.

PAX2 kromě renálního origa (senzitivita 56 % u primárních RCC a 79 % u metastáz RCC (2)) může vykazovat též pozitivitu např. u tumorů i nenádorových lézí Müllerianského origa (3), karcinomu příštítného tělíska či světlobuněčného karcinomu ovaria (4). PAX8 je podle doporučení ISUP považován za patrně nejlepší marker renálního origa (5), se sensitivitou až 95 % u primárních RCC (6), ale ani toto barvení se nevyznačuje specificitou. Nukleární pozitivita PAX8 je též často využívána k potvrzení origa ovariálního karcinomu či karcinomu štítné žlázy (7).

S PAX8 pozitivitou též nutno počítat u B-lymfocytů a B-buněčných lymfomů (zkřížená pozitivita s PAX5) a velkého množství dalších (viz tab. 1) (8). Imunohistochemický marker RCC (**R**enal **C**ell **C**arcinoma marker) vykazuje membránovou a cytoplasmatickou pozitivitu a v publikacích je uváděna sensitivita přes 79 % u primárních RCC a 56 % u metastáz RCC (9). I přes velmi sugestivní název však nutno počítat s pozitivitou tohoto markeru nejen u RCC (pozitivita popsána u karcinomů prsu, embryonálního karcinomu a jiných lézí (9)). CD10 je další oblíbený marker renálního origa, reaguje membránově a kromě RCC vykazuje pozitivitu i u velkého množství různých jiných malignit i nenádorových lézí (ve velmi zkráceném výčtu – různé typy lymfomů, leukémií, uroteliální karcinom, hepatocelulární karcinom, adenokarcinom prostaty atd.). Stejně tak velkou nespecifitou je znám i vimentin.

Tabulka 1. Exprese PAX8 různými tkáněmi a nádor – převzato Cox et kol. (8).

PAX8 běžná a očekávaná exprese
Štítná žláza (nádory i nenádorá tkáň)
Renální tubuly a renální epiteliální neoplázie
Nefroblastom
Příštítná tělíska a jejich neoplázie
Nádory genitálního traktu u ženy (ovárium, endometrium, endocervix)
Nadvarle (nenádorový epitel i z něj vycházející neoplázie)
Meduloblastom
Neuroendokrinní nádory pankreatu
Thymický epitel a neoplázie
Karcinom z Merkelových buněk
Nefrogenní adenom
Yolk sac tumor
B-lymfocyty a část B-lymfomů
PAX8 méně častá exprese
Seminom
Uroteliální karcinom (častěji horních cest močových, ale i nenádorový urotel horního močového traktu)

RENÁLNÍ KARCINOMY SPOJENÉ S PAPILÁRNÍ MORFOLOGIÍ

Renální karcinomy rostoucí pod obrazem papilární léze mají sice překryvné charakteristiky morfologické (tj. papilární růst), avšak odlišné vlastnosti imunohistochemické, molekulárně genetický profil a různé klinické chování. Mezi tyto léze lze ve zkráceném výčtu zařadit papilární renální karcinom (PRCC), renální karcinom asociovaný se syndromem familiární leiomyomatózy a karcinomem ledviny (HLRCC)/fumaráthydratáza deficientní renální karcinom (FHRCC), světlobuněčný papilární renální karcinom (CCPRCC), Xp11.2 translokační renální karcinom (Xp11 TRCC) a metanefrický adenom (MA).

U PRCC je dnes již oproti původnímu smýšlení a dělení (tradičně typ 1 a 2 (10)) evidentní, že PRCC představuje velmi heterogenní skupinu, s neustále expandujícím morfologickým spektrem. PRCC typicky exprimuje cytokeratiny (AE1/AE3, CAM5.2, HMWK), membránový epitelový antigen (EMA), α-methylacyl-CoA-racemasu (AMACR), vimentin a CD10 (1). Variabilní je reaktivita pro CK7, kdy pozitivita CK7 je častější u PRCC typ 1, u PRCC typ 2 se pozitivita pohybuje okolo 50 % případů (11). Za typické molekulárně genetické znaky PRCC jsou tradičně považovány trisomie/polysomie chromosomů 7 a 17 a ztráta gonosomu Y u mužských pacientů (1). Avšak v současné době je zřejmé, že toto všeobecně uznávané dogma je nepravdivé a zůstává v platnosti snad pouze u PRCC typu 1 (12-19).

Renální karcinom asociovaný se syndromem familiární leiomyomatózy a karcinomem ledviny (HLRCC)/fumaráthydratáza deficientní renální karcinom (FHRCC) je nádor s širokým morfologickým spektrem zahrnujícím tumory predominantně s papilární architektonikou, typicky smíšené s jiným růstovým typem (cystický, tubulární, tubulolopapilární, solidní) (20,21), či nádory tubulocystické (22,23). Velká část tumorů v literatuře publikovaných jako HLRCC/FHRCC byla původně klasifikována jako renální karcinomy blíže nespecifikované (RCC NOS dle WHO) (24). V minulosti byl u těchto nádorů popisován jako typický morfologický znak přítomnost eosinofilních makrojadérek s perinukleolárním projasněním. Dnes je jasné, že tento znak není při diagnostice nikterak nápomocný, neboť nemusí být přítomen (25), či je naopak často přítomen i u jiných RCC (21, 26). Pro nádory je tak typická a definující pouze inaktivační mutace genu pro *FH* (1,27). Tato mutace vede ke kompletní ztrátě či redukci aktivity enzymu fumarát hydratasy, která je za normálních okolností zodpovědná za konverzi fumarátu na malát během Krebsova cyklu (28-30). Z toho resultující zvýšené množství fumarátu vede k modifikaci buněčných enzymatických a látkových pochodů, kde jedním z důsledků je i zvýšená produkce S-(2-sukcino)-cysteinu (2SC). Akumulace 2SC vede k pozitivním výsledkům imunohistochemických barvení na 2SC (31,32), naopak ztráta enzymatické aktivity FH způsobuje negativitu imunohistochemického barvení na FH (imunohistochemický profil 2SC+/FH-) (24,31). Imunohistochemická protilátka proti 2SC je komerčně nedostupná, vzhledem k raritě těchto lézí a tedy ne příliš častému užití protilátky je obtížná i interpretace výsledku vyšetření, její využití v rutinní praxi je tedy limitováno. Protilátka proti FH je sice běžně dostupná, avšak četné práce jasně dokazují její významnou nespolehlivost a to ve smyslu jak falešně negativních tak falešně pozitivních výsledků (21,26). Definitivní diagnóza musí být potvrzena molekulárně genetickým vyšetřením s průkazem mutace/ztráty heterozygozity genu *FH* a to i u případů s nespecifickým imunoprofilem a sugestivní morfologií a klinickým průběhem (mladý pacient s agresivním tumorem).

Světlobuněčný papilární renální karcinom (CCPRCC) se skládá z blandně vyhlížejících cylindrických buněk s objemnou „clear" cytoplasmou a jádrem s low-grade morfologií, lehce nadzdviženým od bazální membrány. Tumor roste pod obrazem papilární, tubulární (Obr. 1) či tubulopapilární léze. Imunohistochemicky tyto nádory vykazují difúzní pozitivitu v CK7, HMWK a vimentinu. Karboanhydráza IX (CA-IX) je pozitivní v typické v tzv. cuplike (bazolaterální) distribuci. Naopak negativní jsou nádorové buňky v racemáze (AMACR) a TFE3. Variabilní reaktivitu lze prokázat v CD10 (1,33,34). CCPRCC byl dlouhou dobu považován za tumor bez molekulárně genetických aberací typických ať už pro CCRCC, či pro PRCC (33). U ojedinělých v literatuře popsaných případů však byly detekovány abnormality genu *VHL* (34,35). Podle našeho názoru by však léze s nejednoznačnou morfologií, ne příliš typickým imunohistochemickým profilem a se současně prokázanou abnormalitou *VHL* genu neměly být klasifikovány jako CCPRCC (36).

Xp11.2 translokační renální karcinom (Xp11 TRCC) je renální neoplázií, kde přítomnost translokace transkripčního faktoru TFE3 (se širokým spektrem genů partnerských za vzniku různých fúzních genů) je charakteristikou tuto nádorovou jednotku definující (37-40). Pro nádory je typická velká variabilita morfologického vzhledu, klasicky je však popisována papilární architektonika, buňky s jasnou a eozinofilní objemnou cytoplasmou, psammomatózní tělíska, hyalinní globule, krevní lakuny. Imunohistochemický profil není konstantní, nádory

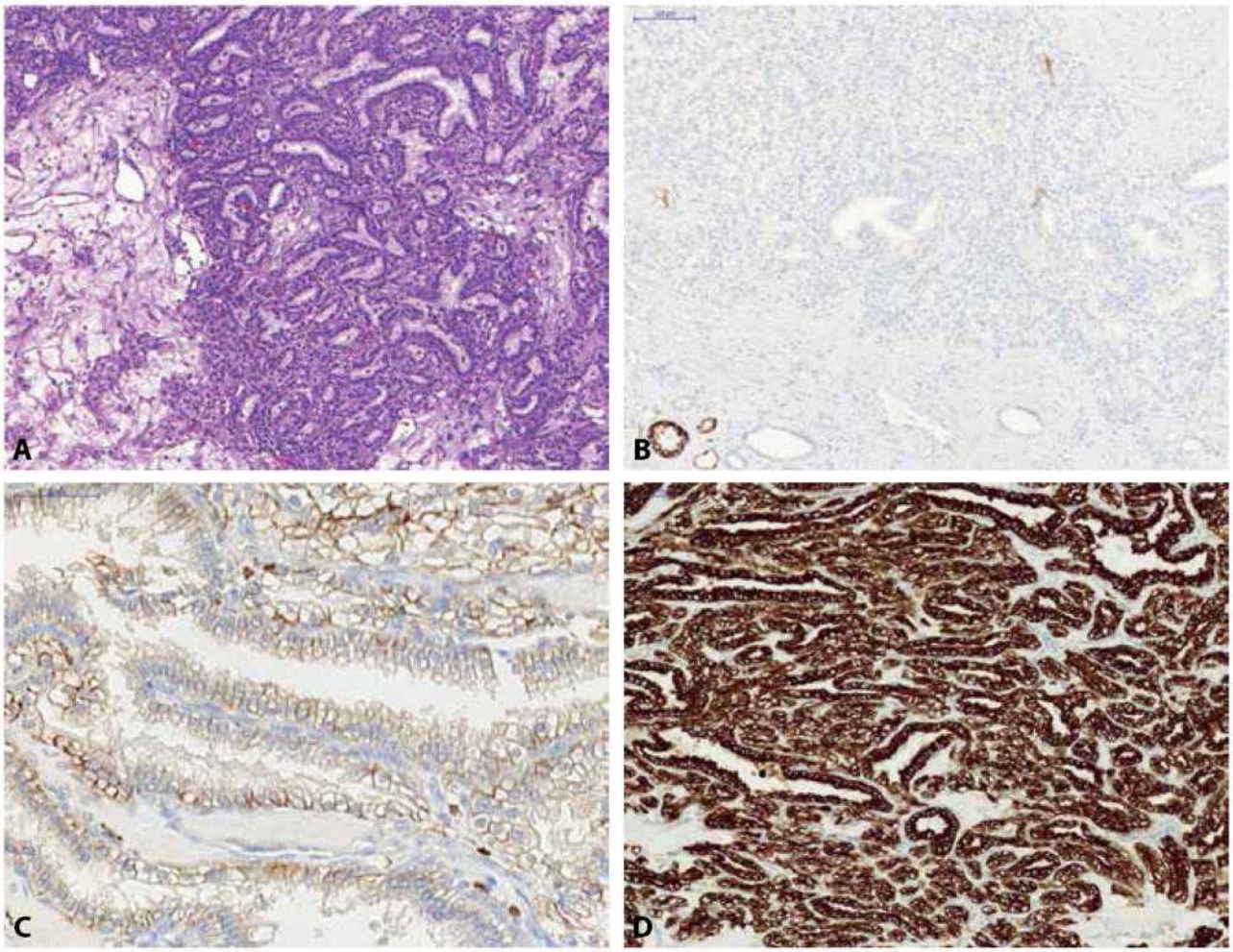

Obr. 1. Světlobuněčný papilární renální karcinom, převážně s tubulárním způsobem růstu (**A**). Nádor je negativní v průkazu α-methylacyl-CoA--racemasy/AMACR (**B**), v imunohistochemickém průkazu karboanhydrázy IX vykazuje charakteristickou bazolaterální/"cup-like" pozitivitu (**C**). Difúzně je nádor pozitivní v CK7.

obyčejně neexprimují cytokeratinové markery, jsou pozitivní v PAX8, někdy jsou reaktivní v průkazu melanomových markerů (Melan A, HMB45), část nádorů je cathepsin K pozitivní. Imunohistochemický průkaz proteinu TFE3 (jaderná reaktivita) je problematický, nevykazuje konstantní pozitivitu (ovlivněn fixací materiálu, vykazuje falešně pozitivní i negativní výsledky) a je tedy nutno k jeho interpretaci přistupovat obezřetně a finální diagnózu konfirmovat molekulárně genetickým vyšetřením zlomu *TFE3* pomocí vyšetření FISH (41).

Metanefrický adenom (MA) se typicky skládá s těsně nahloučených malých uniformních acinů, zhruba polovina případů však může obsahovat papilární okrsky (1) a nádor tak morfologicky může významně připomínat PRCC typ 1 se solidním způsobem růstu (5). MA je však oproti PRCC difúzně pozitivní v barvení WT1 a většinou CD57. Cytokeratin CK7 může být u MA fokálně pozitivní, avšak negativní je nádor v barvení racemázou a EMA (1). Nedávno byla též prokázána užitečnost imunohistochemického barvení s BRAF V600E (88% senzitivita a 100% specificita v barvení MA (42)). Pro MA též není typická polysomie chromozomů 7 a 17 a ztráta chromozomu Y (5,43).

RENÁLNÍ KARCINOMY SE SVĚTLOBUNĚČNOU MORFOLOGIÍ

Na prvním místě je zde potřeba zmínit nejčastější renální tumor vůbec – světlobuněčný renální karcinom (CCRCC). Do této skupiny spadá i nádor, který má s CCRCC překryvný genetický profil – multilokulární cystická renální neoplázie nízkého maligního potenciálu a lze zde zařadit i provizorní jednotku současné WHO – renální karcinom s leiomyomatózním stromatem (RCCLS). Další jednotky v této diferenciálně diagnostické skupině se překrývají s neopláziemi uvedenými výše – mezi ně patří jak CCPRCC, Xp11 TRCC tak i PRCC, který též může vykazovat výrazné světlobuněčné změny.

Světlobuněčný renální karcinom (CCRCC) má typicky acinární či alveolární uspořádání, buňky se světlou cytoplazmou a na pozadí relativně pravidelnou jemnou síť kapilár. Morfologie těchto RCC však může být i velmi různorodá, mohou obsahovat low-grade vřetenité buňky, "syncitiální" obrovské buňky, produkci mucínu, high-grade okrsky s emperipoézou, buňky podobné buňkám Panethovým, mohou být tvořeny buňkami s eosinofilní cytoplazmou (granulární varianta CCRCC) či vzácně mohou vykazovat i papilární způsob růstu. Hlavním klíčem pro správnou diagnózu je u CCRCC dostatečný sampling léze, neboť typické morfologické znaky mohou být v tumorózní mase vyjádřeny pouze fokálně. CCRCC je typicky pozitivní v barvení vimentinem a CA-IX. CK 7 je často vnímán jako marker, který je u CCRCC negativní, není tomu ovšem tak. Recentní práce ukazuje, že CK7 může být pozitivní až u 66 % low-grade CCRCC (Obr. 2) (u CCRCC s high-grade morfologií a cysticky změněných CCRCC je pozitivita CK7 udávána s nižší frekvencí – u 6 %, resp. 25 % takových lézí) (44). Mokelulárně genetické znaky typické pro CCRCC jsou abnormality *VHL* genu (mutace, hypermethylace, LOH3p).

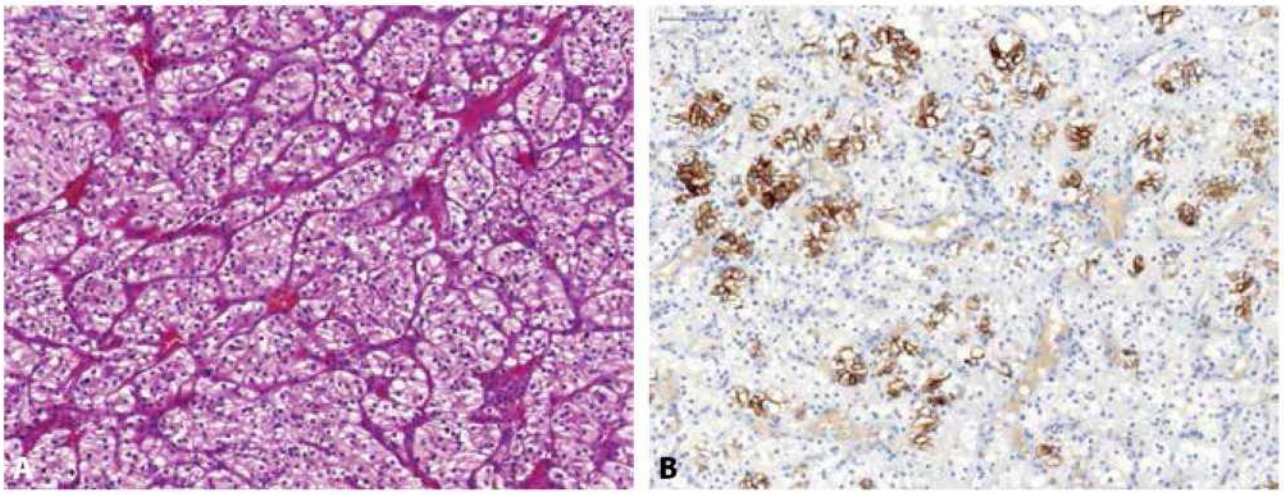

Obr. 2. Low-grade světlobuněčný renální karcinom (**A**), fokálně vykazující pozitivitu barvení s cytokeratinem CK7 (**B**).

Multilokulární cystická renální neoplázie nízkého maligního potenciálu (MCRNLMP) je novou jednotkou WHO 2016, kompletně sestávající z cystických prostor lemovaných low-grade buňkami se světlou cytoplazmou, bez přítomnosti solidních okrsků. Tyto léze vykazují pozitivitu CK7 (44) až v 92 % případů (45). Nádor je též pozitivní v CD10 (63 %), racemáze - AMACR (21 %), vimentinu (58 %), CA-IX (100 %) (45). Genetický profil je stejně jako ten imunohistochemický překryvný s CCRCC, diagnóza (a odlišení od CCRCC) je tak plně závislá pouze na morfologickém nálezu – absenci solidních nádorových okrsků a vyžaduje tak důkladný sampling léze.

Relativně blízko k dříve zmíněné skupině CCPRCC stojí tzv. renální karcinom s objemným leiomyomatózním stromatem (RCCLS), v současné WHO uváděný jako „provizorní" jednotka. Nádory mají epitelovou komponentou prakticky totožnou se světlobuněčným renálním karcinomem a typicky obsahují objemné hladkosvalové stroma. Renální karcinomy s objemným leiomyomatózním stromatem jsou poměrně heterogenní skupinou nádorů, kde většinu tumorů představuje klasický CCRCC, který pouze produkuje objemné stroma. Malá část tumorů této skupiny je tvořena nádory, které reagují pozitivně s CK7 a nemají abnormality ve *VHL* genu. Ještě menší část představují morfologicky identické nádory, které vykazují mutaci v *TCEB1* genu. Pouze malá část těchto lézí nemá prokázány abnormality ani v *VHL*, ani v *TCEB1* genu (46). Shrnout lze vše následujícím způsobem: máme-li nádor se světlobuněčnými elementy a objemným hladkosvalovým stromatem, je vhodné barvit CK7. Je-li léze negativní, popř. slabě či fokálně pozitivní, statisticky pravděpodobněji jde o CCRCC. Jde-li o lézi difuzně CK7 pozitivní, spíše bychom měli myslet na *TCEB1* mutovaný RCC či skutečný RCC s objemným leiomyomatózním stromatem (47). Je nutno říci, že jde o okrajovou část renální patologie.

PRCC se světlobuněčnými změnami je subtyp PRCC s typickou papilární architektonikou, kde papilární struktury jsou lemovány buňkami se světlou cytoplasmou. Některé ze studií věnujících se těmto tumorům připisují světlobuněčný vzhled degenerativním změnám v tumoru, krvácení a/nebo nekróze (48,49). Většina prací popisujících tuto jednotku však po provedení molekulárně genetických vyšetření shledala většinu popsaných tumorů i přes často excesivně vyjádřenou papilární architektoniku za CCRCC (49-52). Jen ojedinělé případy RCC s papilární architektonikou a buňkami se světlou cytoplazmou tak patrně budou opravdovými PRCC. Studie přesně definující diagnostické modality a shrnující biologické chování nejsou v současné době v literatuře k dispozici.

RENÁLNÍ KARCINOMY S ONKOCYTÁRNÍ MORFOLOGIÍ

Do této skupiny lze zařadit onkocytický papilární renální karcinom, renální onkocytom (RO), chromofobní renální karcinom (ChRCC), „granulární" variantu světlobuněčného renálního karcinomu (CCRCC), eozinofilní solidní a cystický renální karcinom (ESC RCC), sukcinátdehydrogenáza deficientní renální karcinom (SDHB-RCC), t(6;11) translokační renální karcinom (t(6;11)TRCC), tzv. hybridní onkocytom-chromofóbní tumory (HOCT), ale morfologickým spektrem do této skupiny může spadat i HLRCC/FHRCC. Recentně jsou pak v literatuře popisovány i neoplázie jako low-grade onkocytický tumor (LOT) (53), či high-grade onkocytický tumor (HOT) (54,55), které si též rozhodně zaslouží být zmíněny. Ač se to může zdát nepravděpodobné, v této skupině bude zmíněn i epiteloidní angiomyolipom (eAML), který svou morfologií může někdy připomínat RCC.

Onkocytický PRCC (OPRCC) je dobře známá morfologická varianta PRCC, u nějž jsou papily lemovány buňkami s hojnou granulární a výrazně eozinofilní cytoplasmou a obyčejně nízkým nukleárním gradem. Imunohistochemický profil těchto lézí vykazuje typicky pozitivitu vimentinu, AMACR a v barvení protilátkou proti mitochondriálnímu antigenu (MIA). CK7 je v pozitivitě variabilní. Zisk chromosomů 7 a 17 je dle dostupných studií nejčastěji detekovanou molekulárně genetickou změnou (56-61), i když významná část OPRCC (dle některých studií až 43,5 % OPRCC (62)) vykazuje disomický status chromosomů 7 a 17. Mezi další chromozomální aberace patří zisk chromosomů 3 a 11, ztráty chromosomů 1, 4, 11, 14 a gonosomu X a Y (56-61). U části tumorů pak byla explicitně detekována delece chromosomu 14, změny v genu *CCND1*, delece 1p (locus 1p36) a ztráta chromosomu Y (62, 63), přičemž tyto změny jsou typicky popisovány i u renálního onkocytomu (RO). Je tedy zřejmé, že OPRCC a RO mají z části překryvný chromozomálně aberační genotyp a molekulárně genetická analýza má v diferenciální diagnostice těchto lézí jen velmi omezený význam.

Renální onkocytom (RO) může mít variabilní morfologický vzhled, nejčastěji je však popisován jako nádor složený z tzv. onkocytů (eozinofilní okrouhlé buňky s denzně granulární cytoplazmou), které jsou uspořádány v solidní hnízda, typické jsou okrsky, kde onkocytické buňky rostou v řídké hypocelulární pojivové tkáni (Obr. 3) (1). RO je difúzně silně pozitivní v barvení MIA (64), toto však není pravidlem (např. malobuněčná varianta RO může reagovat velmi chabě (65) či být negativní (66)). Stejně tak i pozitivita S-100A1 je udávána ve velkém procentu případů RO a je tak některými autory doporučována k odlišení od ChRCC

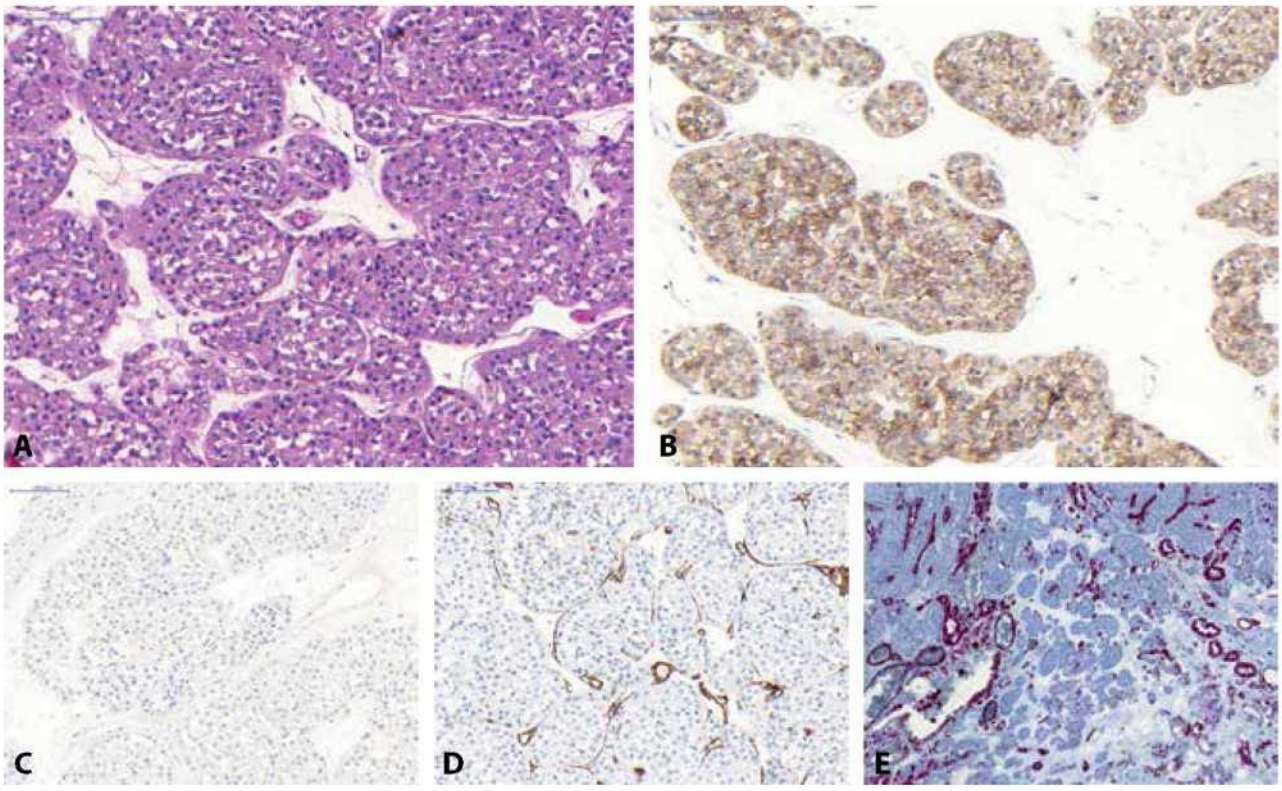

Obr. 3. Renální onkocytom sestávající z „onkocytů" uspořádaných v solidní hnízda, rostoucí na hypocelulárním stromatu (**A**). Nádor je typicky membránově pozitivní v CD117 (**B**), naopak negativní v CK7 (**C**) a vimentinu (**D**). Tumor však může fokálně reagovat pozitivně v CK7 i ve vimentinu (reagují roztroušené individuální buňky či skupiny buněk a to silnou pozitivitou – zde fokální pozitivita vimentinu (**E**)).

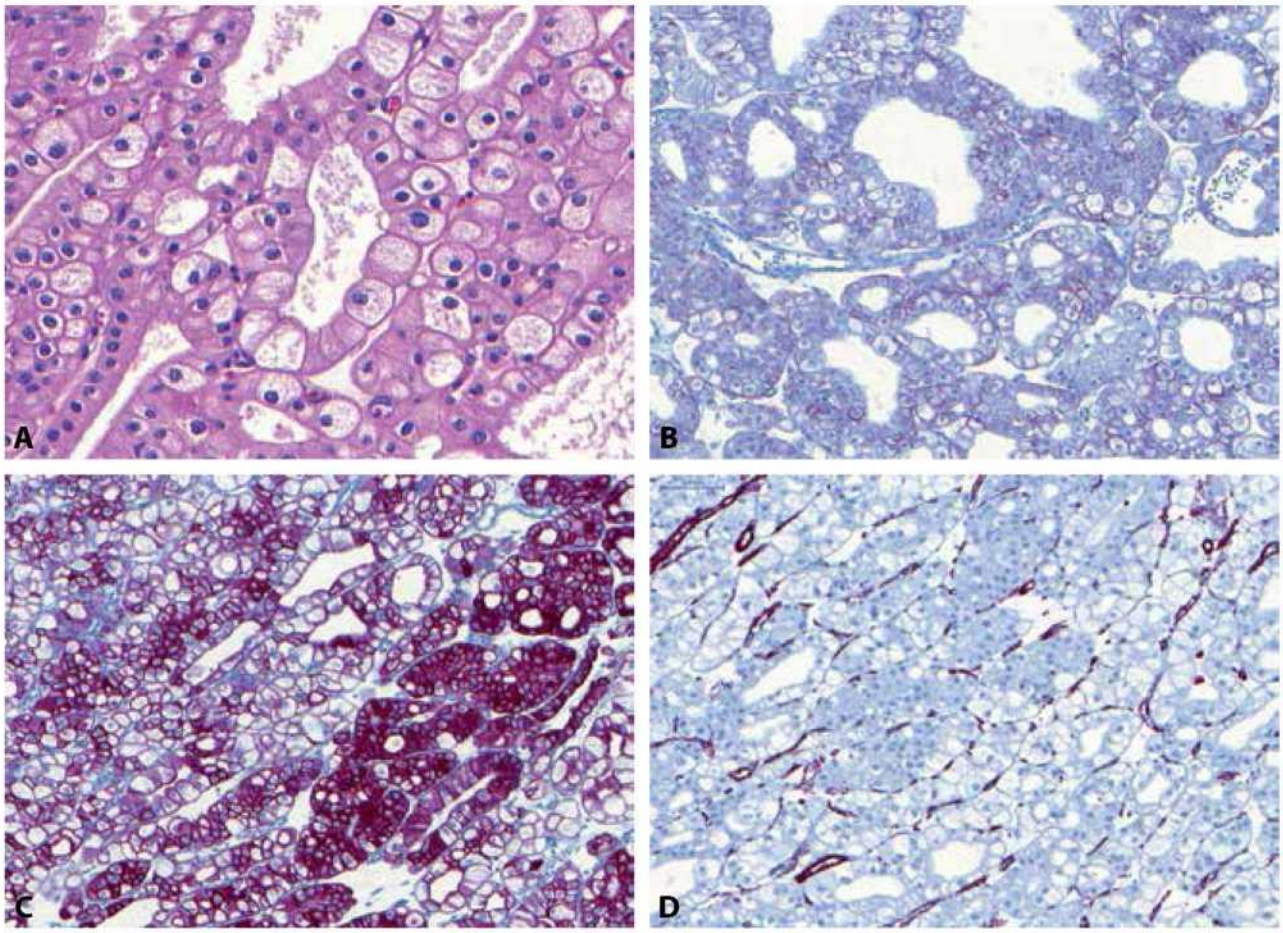

Obr. 4. Chromofóbní renální karcinom s typickými raisinoidními jádry a perinukleárním projasněním (**A**). Nádor je pozitivní v průkazu CD117 (**B**) a CK7 (**C**) a negativní v barvení vimentinem (**D**).

(ChRCC je obvykle S-100A1 negativní) (67), avšak malobuněčná varianta RO bývá popisována též jako S-100A1 negativní (66). Cytokeratin CK7 a vimentin jsou v RO obvykle negativní, ale není ani výjimkou, že tumor může fokálně reagovat pozitivně (68) (s CK7 obvykle reagují roztroušené individuální buňky či skupiny buněk a to silnou pozitivitou (69), též centrální jizevnaté okrsky RO mohou vykazovat reaktivitu jak v CK7, tak i ve vimentinu (70,71)). CD117 je u RO membránově pozitivní (5). Molekulárně genetický profil rozděluje RO do různých cytogenetických kategorií – RO může mít normální karyotyp, některé RO mají aneuploidický chromozomální status se ztrátou chromozomu 1 (celý chromozom, nebo jen jeho část), kombinovaný se ztrátou chromosomu Y či X a/nebo chromosomu 14 a 21 a u některých RO lze detekovat translokaci lokusu 11q13 s alterací *CCND1* a overexpresí cyclinu D1 (72-74).

U chromofóbního renálního karcinomu (ChRCC) jsou klasicky rozeznávány dvě hlavní morfologické varianty (klasická a eozinofilní), morfologické spektrum této neoplázie je ale mnohem širší (v literatuře jsou dokumentovány případy adenomatoidního mikrocystického pigmentovaného ChRCC, tzv. onkocytické varianty ChRCC, ChRCC s neuroendokrinní diferenciací či multicystický ChRCC (75-83)). ChRCC tak může být predominantně tvořený velkými slabě eosinofilními buňkami, které jsou typické pro klasickou variantu ChRCC, naopak menší oxyfilní buňky s granulární cytoplazmou bývají u eosinofilní varianty ChRCC (1). Jádra jsou obvykle velká s nerovnými okraji (tzv. raisinoidní jádra), perinukleárním projasněním (halo efekt) a časté jsou i binukleární buňky (Obr. 4). ChRCC je pozitivní v CD117, EMA, CK8, CK18 a obvykle v parvalbuminu. Cytokeratin CK7 je difúzně pozitivní, nikoliv však ve 100 % případů a na toto pak nelze spoléhat především u eosinofilní varianty ChRCC, kde CK7 bývá často pozitivní jen fokálně, nebo může být i zcela kompletně negativní (5, 84). Difúzní reaktivita CK7 však podle většiny autorů favorizuje diagnózu ChRCC (84). Vimentin je obecně negativní, vzácně však může vykazovat ojedinělou reaktivitu (stejně jako u RO) (68). Obecně lze říci, že ChRCC morfologie je podmíněna řadou fixačních artefaktů (raisinoidní jádra, perinukleární haló) a je tedy nutno počítat s promítnutím tohoto faktu i do výsledků imunohistochemických vyšetření. Chromozomálně aberační status u ChRCC vykazuje mnohočetné ztráty postihující chromozomy 1, 2, 6, 10, 13, 17, 21 či Y (85-87), ale byly dokumentovány i případy se ziskem chromosomů 4, 7, 15, 19, 20 (87), přičemž tyto „gainy" bývají častěji detekovány u ChRCC se sarkomatoidní dediferenciací (změny s větší frekvencí detekovány právě v sarkomatoidní nádorové komponentě) (87,88). Popsány byly i případy ChRCC s disomickým profilem (87).

Eozinofilní solidní a cystický renální karcinom (ESC RCC) je recentně popsaná nádorová jednotka (89), která prozatím není zahrnuta ve WHO 2016, avšak je jednoznačně přijata komunitou urogenitálních patologů. Většina případů byla popsána u žen (90), jen ojedinělé případy byly dokumentovány u mužů (25,47). Případy ESC RCC se mohou vyskytovat u pacientů s tuberózní sklerózou, většina případů však vzniká sporadicky. Typicky je tato neoplázie spojována s indolentním klinickým průběhem, v literatuře jsou ale popsány i případy s metastatickým potenciálem (25,91). Jak je již z názvu této jednotky patrné, jedná se o neoplázii s okrsky solidního a cystického uspořádání (různě velké makro- a mikrocystické okrsky). Buňky mají objemnou eozinofilní cytoplazmu a hrubá až tečkovitá cytoplasmatická granula (granula jsou hrubá do té míry, že mohou připomínat až obraz při leishmaniové infekci – Obr. 5). Jádra jsou často iregulární s prominentními jadérky. Buňky jsou pozitivní v imunohistochemickém průkazu PAX8, AE1/3, CK8/18 a vimentinu. U ESC RCC je přítomna pro renální tumory relativně neobvyklá, avšak pro tento podtyp tumoru zcela charakteristická pozitivita cytokeratinu CK20 ve většině případů, zatímco CK7 je obvykle negativní či pozitivní jen fokálně (47,89,90). CD117 je negativní. Karyotyp těchto lézí vykazuje variabilní genomické alterace (90), četné studie prokázaly somatickou bialelickou ztráta *TSC1/TSC2* genu u většiny ESC RCC (92-95).

Sukcynátdehydrogenáza deficientní renální karcinom (SDHRCC) je definován jako SDH deficientní neoplázie se ztrátou imunohistochemického barvení protilátkou proti SDHB (1) (protilátka SHDB detekuje ztrátu všech SDH podtypů). Mikroskopicky nádor většinou sestává z low-grade neoplastických buněk s eosinofilní jemně zrnitou cytoplazmou a cytoplazmatickými vakuolami (47,96) a kromě definující negativity SDHB imunohistochemicky je obvykle negativní v barvení CA-IX, CD117, většinou negativní CK7, CK20, AE1/3, CK8/18. Difúzně pozitivní je SDHRCC v PAX8, CD10 a EMA (96,97).

t(6;11)/TFEB translokační renální karcinom (t(6;11) TRCC) je v typické morfologii nádor diagnostikovatelný jednoduše i pouze z hematoxylinu a eosinu (bifazicky vypadající tumor s hnízdy větších epiteloidních buněk kombinovaných s klastry menších buněk obklopujících globulární eosinofilní materiál – tzv. pseudorosety (1)). Bohužel, existuje řada morfologických variant, kdy nejsou vyjádřené pseudorozety, epitelová komponenta je spíše světlobuněčná či lehce eosinofilní. Imunohistochemicky většina nádorů exprimuje HMB45, Melan A a kathepsin K. V případě atypické morfologie či imunofenotypu je nutné diagnózu podpořit molekulární genetikou (průkaz zlomu genu *TFEB*). U potvrzených případů pak dále nutno provést vyšetření amplifikace *TFEB* genu, neboť TFEB TRCC s touto amplifikací vykazují agresivní chování (98-100).

Hybridní onkocytom-chromofóbní tumory (HOCT) jsou ve WHO zmiňovány v kapitole chromofóbních renálních karcinomů jako onkocytom připomínající eosinofilní ChRCC (1). Jedná se o typ tumoru s překryvnými morfologickými charakteristikami RO a ChRCC – překryvným/smíšeným morfologickým vzhledem a imunoprofilem. Molekulárně geneticky a klinickým chováním se HOCT zdají být rozdílné od RO a od ChRCC (101). Hybridní onkocytom-chromofóbní tumor se může vzácně vyskytovat sporadicky (jako solitární neoplázie), častěji však vzniká jako multifokální tumor v souvislosti s renální onkocytózou či u pacientů s Birt-Hogg-Dubé syndromem. Tumory často připomínají RO ovšem s perinukleárním cytoplazmatickým projasněním, bez raisinoidních jader. U těchto tumorů byla prokázána pozitivita barvení v CK7, AE1/3, EMA, MIA a fokální pozitivita vimentinu; CD117 bylo slabě či alespoň fokálně exprimováno ve většině případů. Naopak negativní byly nádory v barvení CK20 (102). Molekukárně genetické znaky této jednotky byly prozatím popsány jen v ojedinělých studiích s částečně konfliktními výsledky (101-103).

Již takto nesnadná situace na poli diferenciální diagnostiky onkocytických tumorů je ještě dále komplikována recentně velmi diskutovanými jednotkami – low-grade onkocytický tumor (LOT) a high-grade onkocytický tumor (HOT). Low-grade onkocytický tumor (dříve nejspíše též popsán jako „ChRCC, onkocytární varianta" (77)) je charakterizován jako CD117-/CK7+ tumor s indolentním chováním. Nádor je tvořen uniformní populací buněk s low-grade vzhledem, bez jaderných iregularit, fokálně s perinukleárním projasněním a relativně ostře oddělenými hypocelulární okrsky s řídce rozloženými nádorovými buňkami vytvářející trámce, řídkou síť či s individuálně roztroušenými buňkami (47) (tyto okrsky jsou morfologicky odlišné od okrsků typicky přítomných u RO) (53). Kromě typického imunoprofilu CD117-/CK7+ jsou nádory pozitivní v barvení AE1/3, PAX8, BerEP4 a MOC31 a negativní v CA-IX, CK20, vimentinu, HMB45 a MELAN A (53). U této jednotky nebyl prokázán konsistentní chromozomální aberační status (bez pevně prokázaných

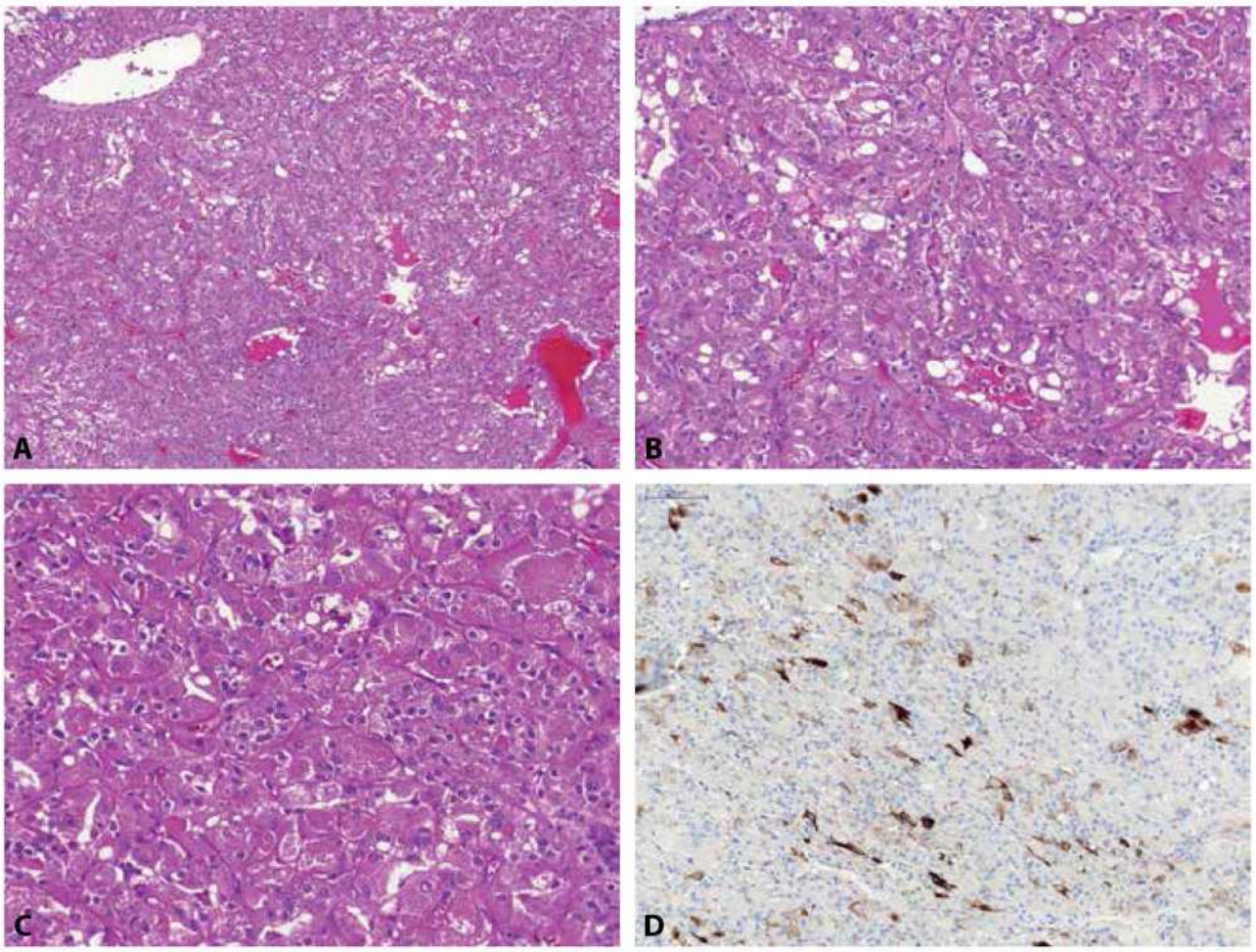

Obr. 5. Eozinofilní solidní a cystický renální karcinom je nádor rostoucí solidně a cysticky (zde solidní okrsek – **A**), buňky mají objemnou eosinofilní cytoplazmu a hrubá až tečkovitá cytoplasmatická granula (**B, C**). Pro nádor je charakteristická fokální pozitivita v CK20 (**D**).

chromozomální ztrát a zisků) (53). High-grade onkocytický tumor sestává z buněk s objemnou eosinofilní či jasnou cytoplazmou s intracytoplazmatickými vakuolami. Jádra vykazují high-grade morfologii - jsou kulatá, s prominentními jadérky (WHO/ISUP grade 3) a většinou s hladkou konturou, bez raisinoidních změn (54). Nádor je ve většině pozitivní v průkazu AE1/3, CK18, PAX8, MIA, CD10, kathepsin K a negativní v TFE3, HMB45, MELAN A a vimentinu. Variabilní je reakce s CD117 a CK7 (většina HOT je CD117 pozitivní a CK7 negativní/jen fokálně pozitivní) (54). I přes high-grade morfologii nebylo u HOT dokumentováno agresivní chování. U tumoru nebyly prokázány kompletní chromozomální zisky ani ztráty, ojedinělé případy prokázaly ztrátu části chromozomů (data však velmi limitovaná malým počtem případů) (54). Recentní práce popisující tento tumor prokázala časté mutace v *TSC1/TSC2* a *mTOR* (104).

Epiteloidní angiomyolipom (eAML) může být predominantně tvořen buňkami s hojnou eosinofilní cytoplazmou a výraznými cytologickými atypiemi. Nádor je na rozdíl od většiny RCC negativní v expresi PAX8 a pozitivní v průkazu HMB45, MELAN A (ale pozor, cytoplazmatická reaktivita může být jen fokální a slabá), či kathepsinu K (8).

UROTEL VERSUS RENÁLNÍ ORIGO?

Uroteliální karcinom (UC) postihující horní močový trakt dokáže velmi věrně napodobit primární renální karcinom a naopak. V ideálních případech je autory doporučován panel protilátek PAX8, GATA3 a p63 (u RCC PAX8+/GATA3-/p63-, naopak u UC PAX8-/GATA3+/p63+). Jedná se však o ideální případ, který v praxi samozřejmě úplně dobře nefunguje. Při indikaci a hodnocení imunohistohemických barvení je třeba myslet na to, že PAX8 vykazuje pozitivitu u 15 – 30 % UC horních močových cest (pozitivita může být silná a difúzní), včetně nenádorového urotelu (7, 105). Některé typy RCC jsou též GATA3 pozitivní a to ve velkém procentu případů (ChRCC 51 % (106), RO 17 % (106), CCPRCC 76 % případů (107)). Spíše než na imunohistochemický profil tak doporučujeme klást důraz na morfologii léze a především dostatečné zpracování materiálu/množství bloků, se zaměřením na oblast renální pánvičky (ve snaze najít uroteliální lézi – ať už uroteliální *CIS* či papilární uroteliální neoplázii). My, na základě našich zkušeností, v praxi využíváme kombinaci CK7, vimentin, GATA3. Pokud je vyšetřovaná léze CK7, GATA 3 pozitivní a vimentin negativní, spíše se kloníme k uroteliálnímu origu. Léze vimentin pozitivní a GATA3 negativní budou pak nejspíše origa renálního.

ZÁVĚR

Morfologie v diagnostice renálních lézí zůstává základním a hlavním diagnostickým kritériem. Klíčem pro správnou diagnózu je především nezapomínat na základní pravidlo při zpracování vzorku - dostatečně rozsáhlé zpracování materiálu (sampling), neboť některé typické morfologické znaky mohou být vyjádřeny pouze fokálně a lze je tedy zastihnout právě pouze při dostatečném až excesivním zablokování materiálu. V ideálních případech je molekulární genetika společně s imunohistochemií nemalou

a velmi cennou pomocnou modalitou, tyto však patří spíše do rukou zkušeného uropatologa než do rutinní praxe.

Ačkoliv výše popsaná expanze morfologického a molekulárně genetického spektra renálních neoplázií zůstává prozatím bez přímého klinického dopadu (neboť léčebný algoritmus se u různých renálních nádorů t.č. zásadně neliší) v budoucnu a s rozvojem cílené léčby, by toto mělo nabýt na významu a mít klinické opodstatnění. Z pohledu patologa je pak znalost morfologického spektra a variabilit neodmyslitelnou součástí každodenní praxe a snad i zárukou správné diagnózy.

PODĚKOVÁNÍ

Podpořeno programem rozvoje vědních oborů Karlovy univerzity (Projekt Q39) a MZ ČR RVO (Fakultní nemocnice Plzeň – FNPl, 00669806).

PROHLÁŠENÍ

Autor práce prohlašuje, že v souvislosti s tématem, vznikem a publikací tohoto článku není ve střetu zájmů a vznik ani publikace článku nebyly podpořeny žádnou farmaceutickou firmou. Toto prohlášení se týká i všech spoluautorů.

LITERATURA

1. **Moch H, Humphrey PA, Ulbright TM, Reuter VE.** WHO classification of tumours of the urinary system and male genital organs. Lyon: IARC; 2016.
2. **Wasco MJ, Pu RT.** Comparison of PAX-2, RCC antigen, and antiphosphorylated H2AX antibody (gamma-H2AX) in diagnosing metastatic renal cell carcinoma by fine-needle aspiration. *Diagn Cytopathol* 2008; 36(8): 568-573.
3. **Ozcan A, Liles N, Coffey D, Shen SS, Truong LD.** PAX2 and PAX8 expression in primary and metastatic mullerian epithelial tumors: a comprehensive comparison. *Am J Surg Pathol* 2011; 35(12): 1837-1847.
4. **Gokden N, Gokden M, Phan DC, McKenney JK.** The utility of PAX-2 in distinguishing metastatic clear cell renal cell carcinoma from its morphologic mimics: an immunohistochemical study with comparison to renal cell carcinoma marker. *Am J Surg Pathol* 2008; 32(10): 1462-1467.
5. **Reuter VE, Argani P, Zhou M, Delahunt B, Members of the IIiDUPG.** Best practices recommendations in the application of immunohistochemistry in the kidney tumors: report from the International Society of Urologic Pathology consensus conference. *Am J Surg Pathol* 2014; 38(8): e35-49.
6. **Sangoi AR, Karamchandani J, Kim J, Pai RK, McKenney JK.** The use of immunohistochemistry in the diagnosis of metastatic clear cell renal cell carcinoma: a review of PAX-8, PAX-2, hKIM-1, RCCma, and CD10. *Adv Anat Pathol* 2010; 17(6): 377-393.
7. **Laury AR, Perets R, Piao H, et al.** A comprehensive analysis of PAX8 expression in human epithelial tumors. *Am J Surg Pathol* 2011; 35(6): 816-826.
8. **Cox RM, Magi-Galluzzi C, McKenney JK.** Immunohistochemical Pitfalls in Genitourinary Pathology: 2018 Update. Advances in anatomic pathology. 2018;25(6):387-99.
9. **McGregor DK, Khurana KK, Cao C, et al.** Diagnosing primary and metastatic renal cell carcinoma: the use of the monoclonal antibody 'Renal Cell Carcinoma Marker'. *Am J Surg Pathol* 2001; 25(12): 1485-1492.
10. **Delahunt B, Eble JN.** Papillary renal cell carcinoma: a clinicopathologic and immunohistochemical study of 105 tumors. *Mod Pathol* 1997; 10(6): 537-544.
11. **Langner C, Wegscheider BJ, Ratschek M, Schips L, Zigeuner R.** Keratin immunohistochemistry in renal cell carcinoma subtypes and renal oncocytomas: a systematic analysis of 233 tumors. *Virchows Arch* 2004; 444(2): 127-134.
12. **Jiang F, Richter J, Schraml P, et al.** Chromosomal imbalances in papillary renal cell carcinoma: genetic differences between histological subtypes. *Am J Pathol* 1998; 153(5): 1467-1473.
13. **Kovac M, Navas C, Horswell S, et al.** Recurrent chromosomal gains and heterogeneous driver mutations characterise papillary renal cancer evolution. *Nat Commun* 2015; 6: 6336.
14. **Yu W, Zhang W, Jiang Y, et al.** Clinicopathological, genetic, ultrastructural characterizations and prognostic factors of papillary renal cell carcinoma: new diagnostic and prognostic information. *Acta Histochem* 2013; 115(5): 452-459.
15. **Marsaud A, Dadone B, Ambrosetti D, et al.** Dismantling papillary renal cell carcinoma classification: The heterogeneity of genetic profiles suggests several independent diseases. *Genes Chromosomes Cancer* 2015; 54(6): 369-382.
16. **Gunawan B, von Heydebreck A, Fritsch T, et al.** Cytogenetic and morphologic typing of 58 papillary renal cell carcinomas: evidence for a cytogenetic evolution of type 2 from type 1 tumors. *Cancer Res* 2003; 63(19): 6200-6205.
17. **Antonelli A, Tardanico R, Balzarini P, et al.** Cytogenetic features, clinical significance and prognostic impact of type 1 and type 2 papillary renal cell carcinoma. *Cancer Genet Cytogenet* 2010; 199(2): 128-133.
18. **Saleeb RM, Brimo F, Farag M, et al**. Toward Biological Subtyping of Papillary Renal Cell Carcinoma With Clinical Implications Through Histologic, Immunohistochemical, and Molecular Analysis. *Am J Surg Pathol* 2017; 41(12): 1618-1629.
19. **Pitra T, Pivovarcikova K, Alaghehbandan R, Hes O.** Chromosomal numerical aberration pattern in papillary renal cell carcinoma: Review article. *Ann Diagn Pathol* 2019; 40: 189-199.
20. **Merino MJ, Torres-Cabala C, Pinto P, Linehan WM.** The morphologic spectrum of kidney tumors in hereditary leiomyomatosis and renal cell carcinoma (HLRCC) syndrome. *Am J Surg Pathol* 2007; 31(10): 1578-1585.
21. **Muller M, Guillaud-Bataille M, Salleron J, et al.** Pattern multiplicity and fumarate hydratase (FH)/S-(2-succino)-cysteine (2SC) staining but not eosinophilic nucleoli with perinucleolar halos differentiate hereditary leiomyomatosis and renal cell carcinoma-associated renal cell carcinomas from kidney tumors without FH gene alteration. *Mod Pathol* 2018; 31(6): 974-983.
22. **Smith SC, Trpkov K, Chen YB, et al.** Tubulocystic Carcinoma of the Kidney With Poorly Differentiated Foci: A Frequent Morphologic Pattern of Fumarate Hydratase-deficient Renal Cell Carcinoma. *Am J Surg Pathol* 2016; 40(11): 1457-1472.
23. **Ulamec M, Skenderi F, Zhou M, et al.** Molecular Genetic Alterations in Renal Cell Carcinomas With Tubulocystic Pattern: Tubulocystic Renal Cell Carcinoma, Tubulocystic Renal Cell Carcinoma With Heterogenous Component and Familial Leiomyomatosis-associated Renal Cell Carcinoma. Clinicopathologic and Molecular Genetic Analysis of 15 Cases. *Appl Immunohistochem Mol Morphol* 2016; 24(7): 521-530.
24. **Trpkov K, Hes O, Agaimy A, et al.** Fumarate Hydratase-deficient Renal Cell Carcinoma Is Strongly Correlated With Fumarate Hydratase Mutation and Hereditary Leiomyomatosis and Renal Cell Carcinoma Syndrome. *Am J Surg Pathol* 2016; 40(7): 865-875.
25. **Li Y, Reuter VE, Matoso A, Netto GJ, Epstein JI, Argani P.** Re-evaluation of 33 'unclassified' eosinophilic renal cell carcinomas in young patients. *Histopathology* 2018; 72(4): 588-600.
26. **Pivovarčíková K, Martínek P, Trpkov K, et al.** Fumarate hydratase deficient renal cell carcinoma and fumarate hydratase deficient-like renal cell carcinoma: Morphologic comparative study of 23 genetically tested cases. *Cesk Patol* 2019; 55(4): 244–249.
27. **Launonen V, Vierimaa O, Kiuru M, et al.** Inherited susceptibility to uterine leiomyomas and renal cell cancer. *Proc Natl Acad Sci U S A* 2001; 98(6): 3387-3392.
28. Tomlinson IP, Alam NA, Rowan AJ, et al. Germline mutations in FH predispose to dominantly inherited uterine fibroids, skin leiomyomata and papillary renal cell cancer. *Nat Genet* 2002; 30(4): 406-410.
29. **Toro JR, Nickerson ML, Wei MH, et al.** Mutations in the fumarate hydratase gene cause hereditary leiomyomatosis and renal cell cancer in families in North America. *Am J Hum Genet* 2003; 73(1): 95-106.
30. **Wei MH, Toure O, Glenn GM, et al.** Novel mutations in FH and expansion of the spectrum of phenotypes expressed in families with hereditary leiomyomatosis and renal cell cancer. *J Med Genet* 2006; 43(1): 18-27.
31. **Bardella C, El-Bahrawy M, Frizzell N, et al.** Aberrant succination of proteins in fumarate hydratase-deficient mice and HLRCC patients is a robust biomarker of mutation status. *J Pathol* 2011; 225(1): 4-11.

32. **Chen YB, Brannon AR, Toubaji A, et al.** Hereditary leiomyomatosis and renal cell carcinoma syndrome-associated renal cancer: recognition of the syndrome by pathologic features and the utility of detecting aberrant succination by immunohistochemistry. *Am J Surg Pathol* 2014; 38(5): 627-637.
33. **Kuroda N, Ohe C, Kawakami F, et al.** Clear cell papillary renal cell carcinoma: a review. *Int J Clin Exp Pathol* 2014; 7(11): 7312-7318.
34. **Aron M, Chang E, Herrera L, et al.** Clear cell-papillary renal cell carcinoma of the kidney not associated with end-stage renal disease: clinicopathologic correlation with expanded immunophenotypic and molecular characterization of a large cohort with emphasis on relationship with renal angiomyoadenomatous tumor. *Am J Surg Pathol* 2015; 39(7): 873-888.
35. **Deml KF, Schildhaus HU, Comperat E, et al.** Clear cell papillary renal cell carcinoma and renal angiomyoadenomatous tumor: two variants of a morphologic, immunohistochemical, and genetic distinct entity of renal cell carcinoma. *Am J Surg Pathol* 2015; 39(7): 889-901.
36. **Hes O, Comperat EM, Rioux-Leclercq N.** Clear cell papillary renal cell carcinoma, renal angiomyoadenomatous tumor, and renal cell carcinoma with leiomyomatous stroma relationship of 3 types of renal tumors: a review. *Ann Diagn Pathol* 2016; 21: 59-64.
37. **Argani P, Zhong M, Reuter VE, et al.** TFE3-Fusion Variant Analysis Defines Specific Clinicopathologic Associations Among Xp11 Translocation Cancers. *Am J Surg Pathol* 2016; 40(6): 723-737.
38. **Argani P, Zhang L, Reuter VE, Tickoo SK, Antonescu CR.** RBM10-TFE3 Renal Cell Carcinoma: A Potential Diagnostic Pitfall Due to Cryptic Intrachromosomal Xp11.2 Inversion Resulting in False-negative TFE3 FISH. *Am J Surg Pathol* 2017; 41(5): 655-662.
39. **Xia QY, Wang XT, Zhan XM, et al.** Xp11 Translocation Renal Cell Carcinomas (RCCs) With RBM10-TFE3 Gene Fusion Demonstrating Melanotic Features and Overlapping Morphology With t(6;11) RCC: Interest and Diagnostic Pitfall in Detecting a Paracentric Inversion of TFE3. *Am J Surg Pathol* 2017; 41(5): 663-676.
40. **Wang XT, Xia QY, Ni H, et al.** SFPQ/PSF-TFE3 renal cell carcinoma: a clinicopathologic study emphasizing extended morphology and reviewing the differences between SFPQ-TFE3 RCC and the corresponding mesenchymal neoplasm despite an identical gene fusion. *Hum Pathol* 2017; 63: 190-200.
41. **Hayes M, Peckova K, Martinek P, et al.** Molecular-genetic analysis is essential for accurate classification of renal carcinoma resembling Xp11.2 translocation carcinoma. *Virchows Arch* 2015; 466(3): 313-322.
42. **Udager AM, Pan J, Magers MJ, et al.** Molecular and immunohistochemical characterization reveals novel BRAF mutations in metanephric adenoma. *Am J Surg Pathol* 2015; 39(4): 549-557.
43. **Brunelli M, Eble JN, Zhang S, Martignoni G, Cheng L.** Metanephric adenoma lacks the gains of chromosomes 7 and 17 and loss of Y that are typical of papillary renal cell carcinoma and papillary adenoma. *Mod Pathol* 2003; 16(10): 1060-1063.
44. **Gonzalez ML, Alaghehbandan R, Pivovarcikova K, et al.** Reactivity of CK7 across the spectrum of renal cell carcinomas with clear cells. *Histopathology* 2019; 74(4): 608-617.
45. **Williamson SR, Halat S, Eble JN, et al.** Multilocular cystic renal cell carcinoma: similarities and differences in immunoprofile compared with clear cell renal cell carcinoma. *Am J Surg Pathol* 2012; 36(10): 1425-1433.
46. **Parilla M, Alikhan M, Al-Kawaaz M, et al.** Genetic Underpinnings of Renal Cell Carcinoma With Leiomyomatous Stroma. *Am J Surg Pathol* 2019; 43(8): 1135-1144.
47. **Trpkov K, Hes O.** New and emerging renal entities: a perspective post-WHO 2016 classification. *Histopathology* 2019; 74(1): 31-59.
48. **Ross H, Martignoni G, Argani P.** Renal cell carcinoma with clear cell and papillary features. *Arch Pathol Lab Med* 2012; 136(4): 391-399.
49. **Fuzesi L, Gunawan B, Bergmann F, Tack S, Braun S, Jakse G.** Papillary renal cell carcinoma with clear cell cytomorphology and chromosomal loss of 3p. *Histopathology* 1999; 35(2): 157-161.
50. **Salama ME, Worsham MJ, DePeralta-Venturina M.** Malignant papillary renal tumors with extensive clear cell change: a molecular analysis by microsatellite analysis and fluorescence in situ hybridization. *Arch Pathol Lab Med* 2003; 127(9): 1176-181.
51. **Jia L, Jayakumaran G, Al-Ahmadie H, et al.** USCAP 2018 Abstracts: Clear cell renal cell carcinoma with prominent papillary architecture: a rare morphologic variant supported by molecular evidence. *Mod Pathol* 2018; 31: 323.
52. **Alaghehbandan R, Ulamec M, Martinek P, et al.** Papillary pattern in clear cell renal cell carcinoma: Clinicopathologic, morphologic, immunohistochemical and molecular genetic analysis of 23 cases. Ann Diagn Pathol 2019; 38: 80-86.
53. **Trpkov K, Williamson SR, Gao Y, et al.** Low-grade Oncocytic Tumor of Kidney (CD117 Negative, Cytokeratin 7 Positive): A Distinct Entity? *Histopathology* 2019; 75(2): 174-184.
54. **He H, Trpkov K, Martinek P, et al.** "High-grade oncocytic renal tumor": morphologic, immunohistochemical, and molecular genetic study of 14 cases. *Virchows Arch* 2018; 473(6): 725-738.
55. **Trpkov K, Bonert M, Gao Y, et al.** High-grade Oncocytic Tumor (HOT) of Kidney in a Patient with Tuberous Sclerosis Complex. *Histopathology* 2019; 75(3): 440-442.
56. **Xia QY, Rao Q, Shen Q, et al.** Oncocytic papillary renal cell carcinoma: a clinicopathological study emphasizing distinct morphology, extended immunohistochemical profile and cytogenetic features. *Int J Clin Exp Pathol* 2013; 6(7): 1392-1399.
57. **Hes O, Brunelli M, Michal M, et al.** Oncocytic papillary renal cell carcinoma: a clinicopathologic, immunohistochemical, ultrastructural, and interphase cytogenetic study of 12 cases. *Ann Diagn Pathol* 2006; 10(3): 133-139.
58. **Park BH, Ro JY, Park WS, et al.** Oncocytic papillary renal cell carcinoma with inverted nuclear pattern: distinct subtype with an indolent clinical course. Pathol Int 2009; 59(3): 137-146.
59. **Lefevre M, Couturier J, Sibony M, et al.** Adult papillary renal tumor with oncocytic cells: clinicopathologic, immunohistochemical, and cytogenetic features of 10 cases. *Am J Surg Pathol* 2005; 29(12): 1576-1581.
60. **Han G, Yu W, Chu J, et al.** Oncocytic papillary renal cell carcinoma: A clinicopathological and genetic analysis and indolent clinical course in 14 cases. *Pathol Res Pract* 2017; 213(1): 1-6.
61. **Kunju LP, Wojno K, Wolf JS, Jr., Cheng L, Shah RB.** Papillary renal cell carcinoma with oncocytic cells and nonoverlapping low grade nuclei: expanding the morphologic spectrum with emphasis on clinicopathologic, immunohistochemical and molecular features. *Hum Pathol* 2008; 39(1): 96-101.
62. **Michalova K, Steiner P, Montiel DP, et al.** Chromosomal Aberration Pattern in Oncocytic Papillary Renal Cell Carcinoma: Analysis of 28 Cases. United States & Canadian Academy of Pathology 106th Annual Meeting; San Antonio: *Mod Pathol* 2017; p. 243 A.
63. **Michalova K, Steiner P, Alaghehbandan R, et al.** Papillary renal cell carcinoma with cytologic and molecular genetic features overlapping with renal oncocytoma: Analysis of 10 cases. *Ann Diagn Pathol* 2018; 35: 1-6.
64. **Tickoo SK, Amin MB, Linden MD, Lee MW, Zarbo RJ.** Antimitochondrial antibody (113-1) in the differential diagnosis of granular renal cell tumors. *Am J Surg Pathol* 1997; 21(8): 922-930.
65. **Hes O, Michal M, Boudova L, Mukensnabl P, Kinkor Z, Miculka P.** Small cell variant of renal oncocytoma--a rare and misleading type of benign renal tumor. *Int J Surg Pathol* 2001; 9(3): 215-222.
66. **Zhang W, Yu W, Wang Q, Jiang Y, Li Y.** The clinicopathological, ultrastructural, genetic features and diagnosis of small cell variant renal oncocytoma. Acta Histochem 2015; 117(6): 505-511.
67. **Rocca PC, Brunelli M, Gobbo S, et al.** Diagnostic utility of S100A1 expression in renal cell neoplasms: an immunohistochemical and quantitative RT-PCR study. *Mod Pathol* 2007; 20(7): 722-728.
68. **Skinnider BF, Folpe AL, Hennigar RA, et al.** Distribution of cytokeratins and vimentin in adult renal neoplasms and normal renal tissue: potential utility of a cytokeratin antibody panel in the differential diagnosis of renal tumors. *Am J Surg Pathol* 2005; 29(6): 747-754.
69. **Mathers ME, Pollock AM, Marsh C, O'Donnell M.** Cytokeratin 7: a useful adjunct in the diagnosis of chromophobe renal cell carcinoma. *Histopathology* 2002; 40(6): 563-567.
70. **Hes O, Michal M, Kuroda N, et al.** Vimentin reactivity in renal oncocytoma: immunohistochemical study of 234 cases. *Arch Pathol Lab Med* 2007; 131(12): 1782-1788.
71. **Wobker SE, Williamson SR.** Modern Pathologic Diagnosis of Renal Oncocytoma. *J Kidney Cancer VHL* 2017; 4(4): 1-12.
72. **Fuzesi L, Frank D, Nguyen C, Ringert RH, Bartels H, Gunawan B.** Losses of 1p and chromosome 14 in renal oncocytomas. *Cancer Genet Cytogenet* 2005; 160(2): 120-125.
73. **Joshi S, Tolkunov D, Aviv H, et al.** The Genomic Landscape of Renal Oncocytoma Identifies a Metabolic Barrier to Tumorigenesis. *Cell Rep* 2015; 13(9): 1895-1908.
74. **Anderson CB, Lipsky M, Nandula SV, et al.** Cytogenetic analysis of 130 renal oncocyto-

mas identify three distinct and mutually exclusive diagnostic classes of chromosome aberrations. *Genes Chromosomes Cancer* 2019; doi: 10.1002/gcc.22766. [Epub ahead of print]

75. **Michal M, Hes O, Svec A, Ludvikova M.** Pigmented microcystic chromophobe cell carcinoma: a unique variant of renal cell carcinoma. *Ann Diagn Pathol* 1998; 2(3): 149-153.
76. **Dundr P, Pesl M, Povysil C, et al.** Pigmented microcystic chromophobe renal cell carcinoma. *Pathol Res Pract* 2007; 203(8): 593-597.
77. **Kuroda N, Tanaka A, Yamaguchi T, et al.** Chromophobe renal cell carcinoma, oncocytic variant: a proposal of a new variant giving a critical diagnostic pitfall in diagnosing renal oncocytic tumors. *Med Mol Morphol* 2013; 46(1): 49-55.
78. **Hes O, Vanecek T, Perez-Montiel DM, et al.** Chromophobe renal cell carcinoma with microcystic and adenomatous arrangement and pigmentation--a diagnostic pitfall. Morphological, immunohistochemical, ultrastructural and molecular genetic report of 20 cases. *Virchows Arch* 2005; 446(4): 383-393.
79. **Kuroda N, Iiyama T, Moriki T, Shuin T, Enzan H.** Chromophobe renal cell carcinoma with focal papillary configuration, nuclear basaloid arrangement and stromal osseous metaplasia containing fatty bone marrow element. *Histopathology* 2005; 46(6): 712-713.
80. **Parada DD, Pena KB.** Chromophobe renal cell carcinoma with neuroendocrine differentiation. *APMIS* 2008; 116(9): 859-865.
81. **Kuroda N, Tamura M, Hes O, Michal M, Gatalica Z.** Chromophobe renal cell carcinoma with neuroendocrine differentiation and sarcomatoid change. *Pathol Int* 2011; 61(9): 552-554.
82. **Foix MP, Dunatov A, Martinek P, et al.** Morphological, immunohistochemical, and chromosomal analysis of multicystic chromophobe renal cell carcinoma, an architecturally unusual challenging variant. *Virchows Arch* 2016; 469(6): 669-678.
83. **Gutierrez FJQ, Panizo A, Tienza A, et al.** Cytogenetic and immunohistochemical study of 42 pigmented microcystic chromophobe renal cell carcinoma (PMChRCC). *Virchows Arch* 2018; 473(2): 209-217.
84. **Williamson SR, Gadde R, Trpkov K, et al.** Diagnostic criteria for oncocytic renal neoplasms: a survey of urologic pathologists. *Hum Pathol* 2017; 63: 149-156.
85. **Brunelli M, Eble JN, Zhang S, Martignoni G, Delahunt B, Cheng L.** Eosinophilic and classic chromophobe renal cell carcinomas have similar frequent losses of multiple chromosomes from among chromosomes 1, 2, 6, 10, and 17, and this pattern of genetic abnormality is not present in renal oncocytoma. *Mod Pathol* 2005; 18(2): 161-169.
86. **Kovacs A, Kovacs G.** Low chromosome number in chromophobe renal cell carcinomas. Genes Chromosomes Cancer. 1992; 4(3): 267-268.
87. **Sperga M, Martinek P, Vanecek T, et al.** Chromophobe renal cell carcinoma--chromosomal aberration variability and its relation to Paner grading system: an array CGH and FISH analysis of 37 cases. Virchows Arch 2013; 463(4): 563-573.
88. **Brunelli M, Gobbo S, Cossu-Rocca P, et al.** Chromosomal gains in the sarcomatoid transformation of chromophobe renal cell carcinoma. Mod Pathol 2007; 20(3): 303-309.
89. **Trpkov K, Hes O, Bonert M, et al.** Eosinophilic, Solid, and Cystic Renal Cell Carcinoma: Clinicopathologic Study of 16 Unique, Sporadic Neoplasms Occurring in Women. *Am J Surg Pathol* 2016; 40(1): 60-71.
90. **Trpkov K, Abou-Ouf H, Hes O, et al.** Eosinophilic Solid and Cystic Renal Cell Carcinoma (ESC RCC): Further Morphologic and Molecular Characterization of ESC RCC as a Distinct Entity. *Am J Surg Pathol* 2017; 41(10): 1299-1308.
91. **McKenney JK, Przybycin CG, Trpkov K, Magi-Galluzzi C.** Eosinophilic solid and cystic renal cell carcinomas have metastatic potential. *Histopathology* 2018; 72(6): 1066-1067.
92. **Argani P.** A Molecular Marker for Eosinophilic Solid and Cystic Renal Cell Carcinoma. *Eur Urol* 2018; 74(4): 487-488.
93. **Mehra R, Vats P, Cao X, et al.** Somatic Bi-allelic Loss of TSC Genes in Eosinophilic Solid and Cystic Renal Cell Carcinoma. *Eur Urol* 2018; 74(4): 483-486.
94. **Palsgrove DN, Li Y, Pratilas CA, et al.** Eosinophilic Solid and Cystic (ESC) Renal Cell Carcinomas Harbor TSC Mutations: Molecular Analysis Supports an Expanding Clinicopathologic Spectrum. *Am J Surg Pathol* 2018; 42(9): 1166-1181.
95. **Parilla M, Kadri S, Patil SA, et al.** Are Sporadic Eosinophilic Solid and Cystic Renal Cell Carcinomas Characterized by Somatic Tuberous Sclerosis Gene Mutations? *Am J Surg Pathol* 2018; 42(7): 911-917.
96. **Gill AJ, Hes O, Papathomas T, et al.** Succinate dehydrogenase (SDH)-deficient renal carcinoma: a morphologically distinct entity: a clinicopathologic series of 36 tumors from 27 patients. *Am J Surg Pathol* 2014; 38(12): 1588-1602.
97. **Williamson SR, Eble JN, Amin MB, et al.** Succinate dehydrogenase-deficient renal cell carcinoma: detailed characterization of 11 tumors defining a unique subtype of renal cell carcinoma. *Mod Pathol* 2015; 28(1): 80-94.
98. **Peckova K, Vanecek T, Martinek P, et al.** Aggressive and nonaggressive translocation t(6;11) renal cell carcinoma: comparative study of 6 cases and review of the literature. *Ann Diagn Pathol* 2014; 18(6): 351-357.
99. **Gupta S, Johnson SH, Vasmatzis G, et al.** TFEB-VEGFA (6p21.1) co-amplified renal cell carcinoma: a distinct entity with potential implications for clinical management. *Mod Pathol* 2017; 30(7): 998-1012.
100. **Williamson SR, Grignon DJ, Cheng L, et al.** Renal Cell Carcinoma With Chromosome 6p Amplification Including the TFEB Gene: A Novel Mechanism of Tumor Pathogenesis? *Am J Surg Pathol* 2017; 41(3): 287-298.
101. **Ruiz-Cordero R, Rao P, Li L, et al.** Hybrid oncocytic/chromophobe renal tumors are molecularly distinct from oncocytoma and chromophobe renal cell carcinoma. *Mod Pathol* 2019; doi: 10.1038/s41379-019-0304-y. [Epub ahead of print].
102. **Petersson F, Gatalica Z, Grossmann P, et al.** Sporadic hybrid oncocytic/chromophobe tumor of the kidney: a clinicopathologic, histomorphologic, immunohistochemical, ultrastructural, and molecular cytogenetic study of 14 cases. *Virchows Arch* 2010; 456(4): 355-365.
103. **Pote N, Vieillefond A, Couturier J, et al.** Hybrid oncocytic/chromophobe renal cell tumours do not display genomic features of chromophobe renal cell carcinomas. *Virchows Arch* 2013; 462(6): 633-638.
104. **Chen YB, Mirsadraei L, Jayakumaran G, et al.** Somatic Mutations of TSC2 or MTOR Characterize a Morphologically Distinct Subset of Sporadic Renal Cell Carcinoma With Eosinophilic and Vacuolated Cytoplasm. *Am J Surg Pathol* 2019; 43(1): 121-131.
105. **Tong GX, Yu WM, Beaubier NT, et al.** Expression of PAX8 in normal and neoplastic renal tissues: an immunohistochemical study. *Mod Pathol* 2009; 22(9): 1218-1227.
106. **Miettinen M, McCue PA, Sarlomo-Rikala M, et al.** GATA3: a multispecific but potentially useful marker in surgical pathology: a systematic analysis of 2500 epithelial and nonepithelial tumors. *Am J Surg Pathol* 2014; 38(1): 13-22.
107. **Mantilla JG, Antic T, Tretiakova M.** GATA3 as a valuable marker to distinguish clear cell papillary renal cell carcinomas from morphologic mimics. *Hum Pathol* 2017; 66: 152-158.

1.2 Papilární renální karcinom, nový pohled na tradiční jednotku a její varianty

(komentář 7 publikací)

Chromosomal numerical aberration pattern in papillary renal cell carcinoma: Review article
Pitra T, Pivovarcikova K, Alaghehbandan R, Hes O.
Ann Diagn Pathol. 2019 Jun;40:189-199.

Renal cell carcinomas with tubulopapillary architecture and oncocytic cells: Molecular analysis of 39 difficult tumors to classify
Pivovarcikova K, Grossmann P, Hajkova V, Alaghehbandan R, Pitra T, Perez Montiel D, Sperga M, Rogala J, Slisarenko M, Bartos Vesela A, Svajdler P, Michalova K, Rotterova P, Hora M, Michal M, Hes O.
Ann Diagn Pathol. 2021 Mar 31;52:151734. doi: 10.1016/j.anndiagpath.2021.151734.

Papillary renal cell carcinoma with cytologic and molecular genetic features overlapping with renal oncocytoma: Analysis of 10 cases
Michalova K, Steiner P, Alaghehbandan R, Trpkov K, Martinek P, Grossmann P, Montiel DP, Sperga M, Straka L, Prochazkova K, Cempirkova D, Horava V, Bulimbasic S, Pivovarcikova K, Daum O, Ondic O, Rotterova P, Michal M, Hora M, Hes O.
Ann Diagn Pathol. 2018 Aug;35:1-6.

Warthin-like papillary renal cell carcinoma: Clinicopathologic, morphologic, immunohistochemical and molecular genetic analysis of 11 cases
Skenderi F, Ulamec M, Vanecek T, Martinek P, Alaghehbandan R, Foix MP, Babankova I, Montiel DP, Alvarado-Cabrero I, Svajdler M, Dubinský P, Cempirkova D, Pavlovsky M, Vranic S, Daum O, Ondic O, Pivovarcikova K, Michalova K, Hora M, Rotterova P, Stehlikova A, Dusek M, Michal M, Hes O.
Ann Diagn Pathol. 2017 Apr;27:48-56.

Biphasic Squamoid Alveolar Renal Cell Carcinoma: A Distinctive Subtype of Papillary Renal Cell Carcinoma?
Hes O, Condom Mundo E, Peckova K, Lopez JI, Martinek P, Vanecek T, Falconieri G, Agaimy A, Davidson W, Petersson F, Bulimbasic S, Damjanov I, Jimeno M, Ulamec M, Podhola M, Sperga M, Pane Foix M, Shelekhova K, Kalusova K, Hora M, Rotterova P, Daum O, Pivovarcikova K, Michal M.
Am J Surg Pathol. 2016 May;40(5):664-75

Cystic and necrotic papillary renal cell carcinoma: prognosis, morphology, immunohistochemical, and molecular-genetic profile of 10 cases
Peckova K, Martinek P, Pivovarcikova K, Vanecek T, Alaghehbandan R, Prochazkova K, Montiel DP, Hora M, Skenderi F, Ulamec M, Rotterova P, Daum O, Ferda J, Davidson W, Ondic O, Dubova M, Michal M, Hes O.
Ann Diagn Pathol. 2017 Feb;26:23-30.

Papillary renal cell carcinoma with prominent spindle cell stroma - tumor mimicking mixed epithelial and stromal tumor of the kidney: Clinicopathologic, morphologic, immunohistochemical and molecular genetic analysis of 6 cases

Rogala J, Kojima F, Alaghehbandan R, Agaimy A, Martinek P, Ondic O, Ulamec M, Sperga M, Michalova K, Pivovarcikova K, Pitra T, Hora M, Ferak I, Marečková J, Michal M, Hes O.

Ann Diagn Pathol. 2020 Feb;44:151441. doi: 10.1016/j.anndiagpath.2019.151441.

Papilární renální karcinom (PRCC) je celkově druhou nejčastější renální neoplázií. Tradiční pojetí této varianty renálního karcinomu se v uplynulých deseti letech otřásá v základech, padají zažitá dogmata. Oproti původnímu smýšlení se jedná o výrazně heterogenní jednotku s velmi širokým a stále expandujícím morfologickým spektrem, variabilním cytogenetickým pozadím a typicky udávanými imunohistochemickými znaky, které však taktéž nejsou absolutní.

Postupně se ukazuje, že původní strohé dělení na PRCC typ 1 a typ 2 [8] je nedostatečné a nově se v literatuře setkáváme s popisy různých morfologických variant PRCC [29], řada publikací pochází z dílny Šiklova ústavu patologie. Různé varianty PRCC jsou okomentovány zevrubně v následujícím přehledu a následně jsou některé z nich představeny podrobně v přiložených původních pracích.

Onkocytický PRCC (OPRCC) byl poprvé popsán v roce 2005 autory Lefevre a kol. na souboru celkem 10 případů [22]. Již pár měsíců po tomto popisu navázal kolektiv autorů Šiklova ústavu patologie vedený prof. Hesem souborem obdobných 12 případů [15] a následovaly další kohorty případů [13, 21, 51]. To dostalo tento podtyp PRCC rychle do všeobecného podvědomí. V roce 2016 pak byl OPRCC poprvé oficiálně uznám jako podtyp PRCC i WHO klasifikací. WHO 2016 definuje OPRCC jako papilárně uspořádaný tumor sestávající z onkocytických buněk, které lemují papily v jedné řadě, bez překryvu jader, bez pseudostratifikací [24]. V různých pracích provedené molekulárně-genetické studie prokázaly pouze nekonzistentní výsledky, OPRCC nemá jasně daná genotypická specifika. Současná definice OPRCC daná WHO klasifikací [24] je však lehce konfliktní, neboť morfologická kritéria pro OPRCC udávaná aktuální WHO klasifikací (2016) jsou částečně v rozporu s diagnózou OPRCC u prvotních případů, které tuto entitu v literatuře popisují. Zároveň, recentně v literatuře představená varianta PRCC, tzv. PRCC s reverzní polaritou [2], je s OPRCC (tak, jak je definovanám WHO 2016) překryvnou jednotkou. Současná situace okolo OPRCC tak naléhavě volá po dalších studiích, oficiálním konsenzu, nové definici a specifikaci diagnostických kritérií. I na základě naší studie však nedoporučujeme v současné době užívat pojem „OPRCC“ jako název jednotky. Pojem OPRCC je patrně pouze popisným termínem pro popis tumorů s papilárním/tubulopapilárním uspořádáním setávajících s onkocytických buněk [30].

Další varianty PRCC jsou sice literaturou dobře zdokumentovány, jedná se však většinou o varianty popsané na kohortách o menším počtu případů, o klinických dopadech těchto variant máme prozatím pouze vágní představy, stejně tak o dopadech rozlišování těchto variant. Znalost morfologického spektra PRCC však lze považovat za kruciální pro správnou diagnózu PRCC, proto je jeho znalost a opora v literatuře nepodstupitelná.

“Mucin“ secernující PRCC/PRCC s mucinózní sekrecí (PRCCM) je varianta PRCC spjatá zejména s autory Val Bernal a kol. [46], ačkoliv první popisy „mucinózní“ produkce u PRCC se datují ještě před tento autorský kolektiv [11, 12]. Už název jasně napovídá, že u tohoto podtypu PRCC byla popsána produkce „mucínu“, resp. mucínu podobného materiálu

v oblasti intracelulární a/nebo intracelulární. Warthinovu tumoru podobný PRCC je tumor mající morfologicky blízko k OPRCC (sestává z papilárních struktur lemovaných buňkami onkocytického vzhledu, často však se zastiženou preudostratifikací), od nějž se odlišuje přítomností prominujícího denzního lymfocytárního infiltrátu. Nádor tak nápadně připomíná Warthinův tumor slinné žlázy, s nímž však nemá žádnou souvislost [38]. Solidní PRCC (SPRCC) se vyznačuje přítomností těšně nahloučených papilárních a tubulárních struktur, což podmiňuje jeho „pseudo"-solidní histologický vzhled. Papilární renální karcinom s vřetenobuněčným stromatem je recentně popsaná varianta PRCC s papilárním, mikropapilárním a/nebo tubulopapilárním způsobem růstu a prominujícím vřetenitým stromatem, připomínajícím stroma u smíšeného epiteliálního a stromálního tumoru ledviny (MEST) či sarkomatoidního karcinomu [33].

Častěji než s dříve jmenovanými raritními subtypy PRCC se však můžeme setkat s tzv. bifázickým skvamoidně alveolární PRCC (BSARCC), v současných doporučených postupech GUPS též označován zjednodušeným názvem „bifazický PRCC" [44]. Varianta popsaná v roce 2012 Peterssonem a kol. [28], se první větší deskriptivní studie dočkala v roce 2016 [16]. Tato varianta PRCC se velmi rychle dostala do podvědomí patologů, neboť se postupně začalo ukazovat, že varianta není až tak vzácná. Deskripnivní název jednotky opět jasně napovídá, jak tumor morfologicky vypadá. Tumor se skládá z dvojí populace morfologicky odlišných buněk - velkých skvamoidních buněk s objemnou eosinofilní cytoplasmou a prominentními velkými vezikulárními jadérky a populací low-grade uniformních buněk s malým množstvím cytoplasmy a kulatými jádry. Typickým znakem je přítomnost emperipoézy (vázané na velké skvamoidní buňky). Alterace *MET* genu byla zastižena asi u 60% BSARCC [9].

Recentně pak byla v literatuře též představena již dříve zmiňovaná jednotka „PRCC s reverzní polaritou" (v literatuře též pod názvem „onkocytický low-grade PRCC"). Tumory jsou popisovány jako papilárně/tubulopapilárně uspořádané a papily s tenkými fibrovaskulárními septy jsou kryty kuboidálními až cylindrickými buňkami s granulární eosinofilní cytoplazmou a apikálně lokalizovanými jádry. Tumory jsou pozitivní v imunohistochemickém průkazu EMA, GATA3, negativní v CD117 a vimentinu a variabilně reagují v racemáze (AMACR). U popsaných případů byly prokázány variabilně polysomie chromozomů 7 a 17 [1] a ve vysokém procentu případů byla prokázána mutace genu *KRAS*, která naopak nebyla prokázána v kontrolní kohortě přípaů PRCC typ 1 a 2 [2, 19]. Morfologicky však podle názoru některých autorů tyto nově popsané tumory kompletně odpovídají aktuální definici OPRCC (tak, jak je specifikována současnou WHO) [24].

1.2.1 Chromosomal numerical aberration pattern in papillary renal cell carcinoma: Review article

U papilárního renálního karcinomu jsou tradičně a „historicky“ rozlišovány dva subtypy - typ 1 a typ 2. Recentní studie však posouvají poznání této nádorové jednotky a začíná být zřejmé, že klasická klasifikace není dostačující a spektrum PRCC je výrazně širší, než bylo původně předpokládáno. V literatuře bylo postupně popsáno několik odlišných podtypů PRCC (většinou malé série případů), které nezapadají do dříve zmiňovaných tradičních subtypů.

V rámci popisu spektra různých molekulárně genetických vlastností PRCC je chromozomální numerický aberační status jeden z nejvíce studovaných a v literatuře popisovaných znaků. Dostupné publikované studie analyzující cytogenetické změny v různých typech PRCC jasně ukázaly, že molekulárně genetický profil je výrazně heterogenní napříč celým spektrem PRCC. Ze všech zdokumentovaných variant/subtypů, PRCC typ 1 se zdá být geneticky nejvíce uniformní skupinou, jiné typy vykazovaly různý stupeň heterogenity.

Ač dlouhá léta byla polysomie chromozomů 7 a 17 a ztráta gonozomu Y u mužských pacientů považována za cytogenetický znak typický pro PRCC, v současné době začíná být evidentní, že tumor-specifický chromozomální numerický aberační status u PRCC patrně neexistuje. Tento přehledový článek založený na review dostupné literatury shrnuje dosavadní znalosti o chromozomálním numerickém aberačním statusu u PRCC.

Annals of Diagnostic Pathology 40 (2019) 189–199

Contents lists available at ScienceDirect

Annals of Diagnostic Pathology

journal homepage: www.elsevier.com/locate/anndiagpath

Review Articles

Chromosomal numerical aberration pattern in papillary renal cell carcinoma: Review article☆

Tomas Pitra[a], Kristyna Pivovarcikova[b], Reza Alaghehbandan[c], Ondrej Hes[b,*]

[a] Department of Urology, Charles University, Medical Faculty, Charles University Hospital Plzen, Czech Republic
[b] Department of Pathology, Charles University, Medical Faculty, Charles University Hospital Plzen, Czech Republic
[c] Department of Pathology, Faculty of Medicine, University of British Columbia, Royal Columbian Hospital, Vancouver, BC, Canada

ARTICLE INFO

Keywords:
Kidney
Papillary renal cell carcinoma
Chromosomal numerical aberration pattern
Review

ABSTRACT

Traditionally, papillary renal cell carcinomas (PRCCs) have been divided in two subgroups – type 1 and type 2. Based on recent molecular and genetic developments in the understanding of RCCs, it seems that this traditional classification may not be adequate and that the spectrum of PRCCs is much wider than initially proposed. Small series of distinct types of PRCC which do not fit into the above mentioned categories have been described in the literature. Published studies investigating molecular genetic changes in various types of PRCCs have shown that the molecular genetic features are remarkably heterogeneous across the whole spectrum of PRCCs. Of all PRCC subtypes/variants, PRCC type 1 seems to be a genetically uniform group, while other types showed different degrees of heterogeneity. Among different molecular-genetic features, chromosomal numerical aberration status is one of the most frequently studied features so far. It is becoming more evident that tumor type-specific chromosomal numerical aberration status in PRCCs may not exist. In this review, we present the most current knowledge concerning chromosomal numerical aberration status in PRCCs.

1. Introduction

Papillary renal cell carcinoma (PRCC) is the second most common type of renal cell carcinoma (RCC) [1]. Historically, PRCCs have been divided in two subgroups (based on morphological and immunohistochemical features) – type 1 and type 2 [2,3]. However, we now know that PRCCs were composed of a heterogeneous group of RCCs including translocation RCCs, hereditary leiomyomatosis associated RCCs, and other mixed and unclassified PRCCs. Based on recent molecular and genetic developments in the understanding of RCCs, it is evident that the traditional PRCC type 1/type 2 classification may not be adequate and that the spectrum of PRCCs is much wider than initially proposed. In fact, on daily surgical pathology practice, it is not uncommon to encounter tumors with overlapping (mixed) histology or even distinct subtypes of PRCC which do not fit into the above-mentioned categories.

In 1997 Kovacs et al. published "The Heidelberg classification of renal cell tumors", which was the first classification integrating molecular genetic features as one of the diagnostic tools applicable to renal cell tumors [4]. In recent years, there have been many studies examining and describing molecular genetic changes in PRCCs. All these studies have shown that the molecular genetic changes are remarkably heterogeneous across the whole spectrum of PRCCs and that molecular-genetic analysis cannot be used as a universal diagnostic tool in this regard.

In this review, we presented the most current knowledge concerning chromosomal numerical aberration pattern (CNAP) as one of the aspects of molecular-genetic backgrounds in PRCCs.

2. PRCC type 1

Traditionally, PRCCs type 1 are composed of neoplastic cells with scant cytoplasm and low-grade nuclei (according to Fuhrman grading system/ISUP) arranged in a single layer (Fig. 1) [3].

Molecular genetic changes in PRCCs type 1 are most uniform among all subtypes of PRCCs. Gains and losses of chromosomes in PRCCs type 1, described in different studies, are summarized in Tables 1 and 2.

Historically, the gains of chromosomes 7 and 17, which are believed to be the most common and characteristic CNAP among the entire spectrum of PRCCs, are most typically seen in PRCC type 1. Other frequently encountered chromosomal gains in PRCCs type 1 are the gains of chromosomes 3, 12, 16, and 20. There are also some studies

☆ The study was supported by the Charles University Research Fund (project number Q39) and by Institutional Research Fund FN 00669806.
* Corresponding author at: Department of Pathology, Charles University, Medical Faculty, Charles University Hospital Plzen, Alej Svobody 80, 304 60 Pilsen, Czech Republic.
E-mail address: hes@medima.cz (O. Hes).

https://doi.org/10.1016/j.anndiagpath.2017.11.004

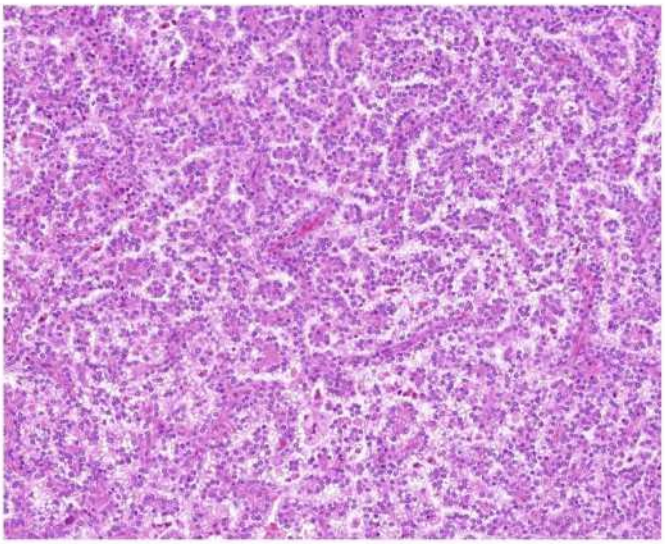

Fig. 1. Papillary renal cell carcinomas type 1 are composed of neoplastic cells with scant cytoplasm and low-grade nuclei arranged in papillary or tubulopapillary pattern.

which have demonstrated the gains of chromosomes 2, 4, 5, 6, 8, 13, and 18 only in a small proportion of cases. (Table 1).

The loss of chromosome Y in male patients is another typical chromosomal aberration pattern observed in PRCC type 1. There are also individual cases showing losses of various chromosomes including 1, 2, 4, 5, 7, 8, 9, 10, 11, 14, 15, 16, 18, 19, 20, 21, and 22 [5-10] (Table 2).

3. PRCC type 2

By definition, PRCC type 2 histologically presents with neoplastic cells with abundant eosinophilic cytoplasm, high-grade nuclear features (according to Fuhrman grading system/ISUP) and nuclear pseudostratification (Fig. 2) [3].

CNAP in PRCC type 2 has not proven to be as constant as seen in PRCC type 1. It is worth noting that although the gains of chromosomes 7 and 17 are most commonly referred within the literature for PRCC type 2, these changes in fact are only found in a smaller percentage of cases. A large number of different chromosomal aberrations have been described in PRCC type 2, but there is a large variability in their occurrence and frequencies in different studies. Nonetheless, the relatively more frequent chromosomal aberrations in PRCCs type 2 are the gains of chromosomes 12, 16 and 20. Of note, other chromosomal gains described with enormous variability in a small percentage of the cases include gains of chromosomes 1, 2, 3, 4, 5, 6, 8, 9, 13, 18, 19 and 22 [5-10] (Table 3).

The loss of chromosome Y in male patients has been reported in PRCC type 2 in different studies. There are also sporadic cases showing losses of different chromosomes and their parts including 1, 2, 3, 4,5, 6, 7, 8, 9, 10, 12, 13, 14, 15, 17, 18, 19, 20, 21, 22, and X [5-10] (Table 4).

4. Oncocytic PRCC

Oncocytic PRCCs (OPRCC) are tumors with papillary architecture, with papillae being covered by single layer of neoplastic cells showing abundant and granular deeply eosinophilic cytoplasm (oncocytic cells) (Fig. 3). Although papillary growth pattern is a constant feature, solid areas may also be seen infrequently. Ultrastructurally, the cytoplasm is packed with numerous mitochondria [11]. These tumors usually show a relatively indolent clinical behavior [11,12], although some tumors can behave aggressively [13,14].

CNAP is not uniform in this poorly understood subtype of PRCC. The gains of chromosomes 7 and 17 are the most common chromosomal aberrations reported by different studies. There are also some studies describing even the gains of chromosomes 3 and 11. Loss of chromosome Y in male patient is occasionally seen in OPRCC. Other described numerical aberrations are the losses of chromosomes 1, 4, 14 as wells as

Table 1
PRCC type 1 - gains of chromosomes.

	1+	2+			3+		4+	5+	6+	7+				8+	9+	12+			13+	16+			17+			18+	19+	20+		21+		22+
	1q+	2+	2p+	2q+	3+	3q+	4+	5+	6+	7+	7p+	7q+	7+,17+	8+	9+	12+	12p+	12q+	13+	16+	16p+	16q+	17+	17p+	17q+	18+	19q+	20+	20q+	21+	21q+	
Jiang et al. [5] CGH											9/9 100%	6/9 66.7%						2/9 22.2%				5/9 55.6%		9/9 100%	9/9 100%				5/9 55.6%			
Kovac et al. [6] Sequence analysis		1/6 16.7%			1/6 16.7%					4/6 66.7%			3/6 50%			3/6 50%				2/6 33.3%			4/6 66.7%									
Yu et al. [7] FISH										20/30 66.7%													26/30 86.7%									
Marsaud et al. [8] aCGH + Karyotyping + FISH		1/15 6.7%			4/15 26.7%			2/15 13.3%	1/15 6.7%	15/15 100%			15/15 100%	1/15 6.7%		6/15 40%			2/15 13.3%	8/15 53.3%			15/15 100%					6/15 40%			1/15 6.7%	2/15 13.3%
Gunaw et al. [9] Cytogenetic analysis		4/34 11.8%			7/34 20.6%			4/34 11.8%	1/34 2.9%	30/34 88.2%			28/34 82.4%	4/34 11.8%		12/34 35.3%			4/34 11.8%	22/34 64.7%			32/34 94.1%			1/34 2.9%		15/34 44.1%				
Antonelli et al. [10] Karyotyping		1/13 7.7%			4/13 30.8%		1/13 7.7%			9/13 69.2%			9/13 69.2%			5/13 38.5 %			1/13 7.7%	4/13 30.8%			11/13 84.6%					4/13 30.8%				

Table 2
PRCC type 1 - chromosomal losses.

	1-		2-	3-		4-		5-	6-		7-	8-	9-			10-	11-		13	14-	15-	16-		17-	18-		19-	20-	21-		22-		X-			Y-
	1p-		2-	3-	3q-	4-	4q-	5-	6p-	6q-	7-	8-	9-	9p-	9q-	10-	11-	11q-	13q-	14-	15-	16-	16p-	17-	18-	18q-	19-	20-	21-	21q-	22-	22q-	X-	Xp-	Xq-	Y-
Jiang et al. [5] CGH	3/9	33.3%					5/9	55.6%		4/9	44.4%				4/9	44.4%			6/9	66.7%														2/9	22.2%	3/9	33.3%	
Kovac et al. [6] Sequence analysis	1/6	16.7%																							1/6	16.7%		1/6	16.7%			2/6	33.3%				
Yu et al. [7] FISH												0/30					2/30	6.7%							6/30	20%										18/20M	90%
Marsaud et al. [8] aCGH + Karyotyping + FISH	1/15	6.7%				1/15	6.7%						1/15	6.7%	1/15	6.7%					1/15	6.7%	1/15	6.7%						1/15	6.7%	1/15	6.7%				9/9M	100%
Gunawan et al. [9] Cytogenetic analysis			1/34	2,9%				3/34	8,8%		1/34	2,9%	3/34	8,8%		1/34	2,9%				3/34	8,8%		1/34	2,9%	3/34	8,8%		1/34	2,9%	2/34	5,9%	4/34	11,8%	1/34	2,9%		24/28M	85,7%
Antonelli et al. [10] Karyotyping													1/13	7.7%						1/13	7.7%			1/13	7.7%				1/13	7.7%			1/13	7.7%		7/9M	77.8%

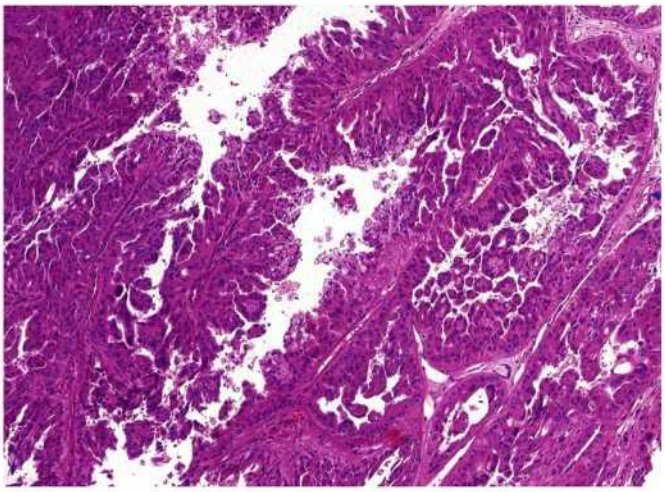

Fig. 2. Papillary renal cell carcinoma type 2 is characterized by papillary growth pattern and neoplastic cells with pseudostratification, eosinophilic cytoplasm with high-grade nuclei.

loss of gonosome X [11-13,15-17]. (Table 5).

The largest study to date investigating CNAP in OPRCC showed interesting results. A substantial proportion of OPRCCs in this study showed disomic status of chromosomes 7 and 17, some with deletion of chromosome 14, deletion of 1p (locus 1p36) and some cases had loss of chromosomes Y. Interestingly, all such patterns are also well-known to be characteristic for renal oncocytoma (RO). The authors reported that approximately one third of cases showed the gains of chromosomes 7 and/or 17. There were a small proportion of tumors demonstrating loss of chromosome Y in male patients, which is one of the chromosomal patterns traditionally believed to be characteristic for PRCC. Some cases (7/24) showed none or variable and nonspecific chromosomal abnormalities (i.e., loss of chromosome 17, gonosome X) [14] (Table 5).

5. Other variants/subtypes of PRCCs

In addition to the most common and well-described variants of PRCCs, a number of small series of other different types of PRCCs have been also described, which interestingly showed variable numerical aberration patterns.

"Mucin"-secreting PRCC has been described in different studies. These tumors have papillary architecture with some cases demonstrating tubulopapillary or solid growth patterns, and producing variable amount of mucin-like material intra- or/and extracellularly (Fig. 4) [18-20]. A recent molecular-genetic study by our group demonstrated the gains of chromosomes 7 (2/4 cases), 17 (3/4 cases), 16 (1/2 cases) and loss of chromosome Y in all male cases (Table 6) [20].

Cystic and necrotic PRCC is an unusual variant of PRCC type 1. These tumors usually present as huge renal cystic lesions filled with large amount of necrotic (liquefactive necrosis) and hemorrhagic contents. The cystic spaces are lined by a very limited amount of viable neoplastic tumor cells, creating potential diagnostic challenges. These tumors are well encapsulated by fibroleiomyomatous stroma, which is

Table 3
PRCC type 2 - Gains of chromosomes.

		Jiang et al. [5] CGH	Kovac et al. [6] Sequence analysis	Yu et al. [7] FISH	Marsaud et al. [8] aCGH + Karyotyping + FISH	Gunawan et al. [9] Cytogenetic analysis	Antonelli et al. [10] Karyotyping
Y+	Y+				1/16 6.3%		
X+	Xq+				1/16 6.3%		
	X+				2/16 12.5%		
22+	22+					1/13 7.7%	
21+	21q+		1/20 5%		21+ 1/16 6.3%		
20+	20q+	4/16 25%			2/16 12.5%		
	20p+				1/16 6.3%		
	20+		2/20 10%		4/16 25%	8/13 61.5%	4/13 30.8%
19+	19q+		1/20 5%		1/16 6.3%		
	19p+				1/16 6.3%		
	19+					2/13 15.4%	
18+	18p+		1/20 5%				
	18+					1/13 7.7%	1/13 7.7%
17+	17q+	11/16 68.8%	3/20 15%		3/16 18.8%		
	17p+	6/16 37.5%					
	17+		10/20 50%	15/26 57.7%	8/16 50%	7/13 53.9%	7/13 53.8%
16+	16q+	3/16 18.8%	1/20 5%		1/16 6.3%		
	16p+		1/20 5%		1/16 6,3%		
	16+		11/20 55%		4/16 25%	10/13 76.9%	7/13 53.8%
15+	15+				1/16 6.3%		
13+	13q+		1/20 50%		1/16 6.3%		
	13+				1/16 6.3%	3/13 23.1%	2/13 15.4%
12+	12q+	5/16 31.2%			1/16 6.3%		
	12p+		1/20 5%				
	12+		5/20 25%		9/16 56.3%	5/13 38.5%	4/13 30.8%
11+							1/13 7.7%
10+	10p+				1/16 6.3%		
	10+				1/16 6.3%	1/13 7.7%	1/13 7.7%
9+	9+		1/20 5%				
8+	8q+				1/16 6.3%		
	8+		2/20 10%		6/16 37.5%	2/13 15.4%	
7+	7+,17+		8/20 40%		5/16 31.3%	5/13 38.5%	6/13 46.2%
	7q+	5/16 31.2%					
	7p+	5/16 31.2%					
	7+		9/20 45%	16/26 61.5%	8/16 50%	9/13 69.2%	8/13 61.5%
6+	6p+		1/20 5%		1/16 6.3%		
	6+						1/13 7.7%
5+	5q+				3/16 18.8%		
	5+		1/20 5%		3/16 18.8%	1/13 7.7%	1/13 7.7%
4+	4+				1/16 6.3%	1/13 7.7%	
3+	3q+		1/20 5%		3/16 18.8%		
	3+		1/20 5%		1/16 6.3%	5/13 38.5%	
2+	2q+		2/20 10%				
	2p+						
	2+		1/20 5%		2/16 12.5%	3/13 23.1%	
1+	1q+		2/20 10%		1/16 6.3%		
	1p+				1/16 6.3%		

Table 4
PRCC type 2 - chromosomal losses.

		Jiang et al. [5] CGH	Kovac et al. [6] Sequence analysis	Yu et al. [7] FISH	Marsaud et al. [8] aCGH + Karyotyping + FISH	Gunawan et al. [9] Cytogenetic analysis	Antonelli et al. [10] Karyotyping
Y-	Y-			8/12M 66.7%	7/11M 63.6%	9/10M 90%	7/10M 70%
X-	Xq-	6/16 37.5%					
	Xp-	5/16 31.2%			1/16 6.3%		
	X-		4/20 20%		3/16 18.8%		2/13 15.4%
22-	22q-		1/20 5%				
	22-		2/20 10%		2/16 12.5%	4/13 30.8%	1/13 7.7%
21-	21q-		1/20 5%				
	21-				5/16 31.3%	2/13 15.4%	1/13 7.7%
20-	20q-				1/16 6,3%		
	20p-		1/20 5%				
	20-					1/13 7.7%	2/13 15.4%
19-	19-				1/16 6.3%	1/13 7.7%	
18-	18q-		1/20 5%		2/16 12.5%		
	18-		2/20 10%	13/26 50%	2/16 12.5%	6/13 46.2%	1/13 7.7%
17-	17p-		1/20 5%				
	17-					3/13 23,1%	1/13 7.7%
16-	16q-				3/16 18.8%		
	16p-				1/16 6.3%		
	16-					1/13 7.7%	
15-	15-				3/16 18.8%	3/13 23,1%	2/13 15.4%
14-	14q-		1/20 5%				
	14-		1/20 5%		8/16 50%	3/13 23,1%	3/13 23.1%
13-	13q-	3/16 18.8%					
	13-				1/16 6.3%	2/13 15.4%	1/13 7.7%
11-	11q-				2/16 12.5%		
	11-		1/20 5%	9/26 34.6%	3/16 18.8%	3/13 23,1%	1/13 7.7%
12-	12-					2/13 15.4%	
10-	10-				1/16 6.3%	2/13 15.4%	3/13 23.1%
9-	9q-	6/16 37.5%					
	9p-		1/20 5%		2/16 12.5%		
	9-		3/20 15%		2/16 12.5%	3/13 23,1%	2/13 15.4%
8-	8p-				1/16 6.3%		
	8-			6/26 23.1%	2/16 12.5%	3/13 23,1%	1/13 7.7%
7-	7q-		1/20 5%		1/16 6.3%		
	7-					1/13 7.7%	
6-	6q-	6/16 37.5%			1/16 6.3%		
	6p-		1/20 5%				
	6-				2/16 12.5%	1/13 7.7%	
5-	5-					2/13 15,4%	3/13 23.1%
4-	4q-	5/16 31.2%	1/20 5%				
	4-				1/16 6.3%	2/13 15.4%	1/13 7.7%
3-	3q-		1/20 5%				
	3p-		4/20 20%		5/16 31.3%		
	3-					1/13 7.7%	1/13 7.7%
2-	2q-		2/20 10%				
	2p-		2/20 10%				
	2-					3/13 23,1%	1/13 7.7%
1-	1q-				2/16 12.5%		
	1p-	4/16 25%	1/20 5%		2/16 12.5%		
	1-				3/16 18.8%	2/13 15.4%	2/13 15.4%

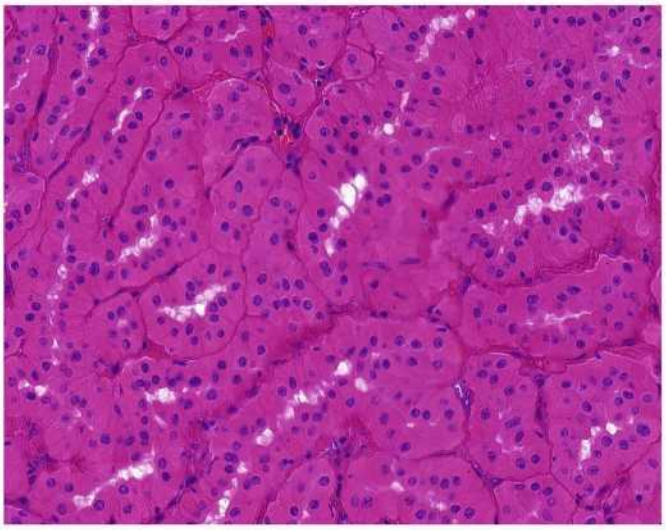

Fig. 3. So-called oncocytic papillary renal cell carcinoma is a poorly understood variant, composed of eosinophilic cells resembling in many aspects those in renal oncocytoma.

histologically indistinguishable from inflammatory pseudotumor. All such tumors were morphologically consistent with the diagnosis of PRCC type 1 and had non-aggressive behavior despite the presence of liquefactive necrosis. A molecular-genetic analysis of 10 cases by Peckova et al. showed non-homogenous changes including 5/8 analyzable cases with polysomy of chromosomes 7 and 17, and 5/7 analyzable male cases with loss of chromosome Y. No molecular-genetic abnormalities were detected in the remaining two cases (Table 7) [21].

Solid PRCC was originally described by Renshaw et al. in 1997 [22]. This type of PRCC is typically composed of tightly packed small compressed tubules (Fig. 5) and short abortive papillae with or without sparse true papillae. The neoplastic cells are monomorphic with scant cytoplasm and small nuclei [23]. Molecular genetic studies showed the gains of chromosomes 7 and 17 and loss of gonosome Y in male patients in high percentage of cases (Table 8) [22,24,25].

Warthin-like PRCC is another subtype of PRCC, which has considerable morphological resemblance to oncocytic PRCC. Warthin-like PRCC has predominant papillary architecture, with oncocytic neoplastic cells admixed with dense lymphoid stroma and tumor infiltrating lymphocytes (Fig. 6). Molecular genetic analysis performed on these tumors showed a wide heterogeneous spectrum of chromosomal changes (not even constant in this subgroup). In some cases no chromosomal changes were detected, while other cases showed the gains of chromosomes 1, 2, 5, 7, 8, 12, 17 and 21, with some cases demonstrated loses of chromosomes 1, 3, 14, 15, 18, 22 and Y [26] (Table 9).

PRCCs with clear cells are tumors with papillary architecture and clear cell morphology (Fig. 7). Some studies have suggested that the clear cell features may be associated with degenerative changes, hemorrhage and/or necrosis [27,28]. There are a number of studies which described such tumors and strictly followed results of molecular genetic analysis in further classifying these neoplasms. Fuzesi et al. reported loss of terminal 3p segment and loss of chromosome 14 in all such cases and further showed other chromosomal changes detected in individual cases. In another study, Salama et al. showed LOH 3p in 6/6 cases, and loss of chromosomes 7 and 17 in 4/6 and 6/6 cases, respectively. It should be noted that tumors examined in these two studies were rather evaluated from clear cell renal cell carcinoma (CCRCC) molecular genetic perspectives than PRCC. Further, the authors did not perform immunohistochemical studies in these cases [29,30]. On the other hand, Gobbo et al. performed immunohistochemical and cytogenetical analysis of 14 cases of RCC with papillary architecture and variable proportion of neoplastic cells with clear cytoplasm. According to their combined immunohistochemical and cytogenetical analysis, 9/14 cases were classified as PRCC, because of AMACR positivity, CK7 reactivity (in most cases), polysomy of chromosomes 7 or 17 and loss of chromosome Y in male cases [27]. Haudebourg et al. studied three RCC cases with the above-mentioned morphology and found polysomy of chromosomes 7 and 17 in 2/3 case (these were classified as PRCCs) and detected polysomy of 7 and 17, loss of gonosome Y concurrently with loss of heterozygosity (LOH) for chromosome 3 in 1/3 cases (this case was classified as hybrid tumor composed of PRCC and CCRCC). All tumors were positive for AMACR and CD10 (3/3), and 2/3 were immunoreactive for CK7 [31] (Table 10).

Biphasic squamoid alveolar RCC (BSARCC) was recently described as a distinct morphologic variant of PRCC. These tumors are composed of a distinctly dual cell populations including low-grade uniform small neoplastic cells with scant cytoplasm and round (or slightly elongated) nuclei and larger squamoid cells containing voluminous pink cytoplasm and large nuclei with prominent nucleoli (Fig. 8). Emperipolesis associated with squamoid cells is constant finding in all described cases [32,33]. Hes et al. showed the gains of chromosomes 7 and 17 in all analyzable cases (11/21) and loss of chromosome Y in 4/5 male cases. Table 11 presents other chromosomal abnormalities described in some cases included in this study [32]. On the other hand, Petersson et al. showed in their one suitable case for molecular-genetic analysis absolutely distinct results [34]. However, this case was later reclassified as unclassified RCC [32]. BSARCCs can be multifocal and also associated with other subtypes of RCC [33,35]. Further, these tumors can occur in a familial context of hereditary PRCC associated with *MET* mutation [36]. This rare morphologic variant of PRCC has also been described in kidney allografts [37].

6. Discussion

The classification of renal neoplasms has dramatically changed in recent years. Although histology and immunohistochemical assays still serve as the main diagnostic drivers, in the era of precision medicine, molecular genetic analysis plays an integral role in diagnostically challenging cases as well as enhancing the classification of renal tumors based on molecular biomarkers.

The traditional general opinion concerning chromosomal numerical aberration status in PRCC includes a combination of gains of chromosomes 7 and 17 with loss of chromosome Y in male patients. One of the challenges in verifying such claim comes with the fact that it would be nearly impossible to distinguish various histologic subtypes of PRCCs used in earlier studies along with employing small number of cases.

From historical perspective, some of "PRCCs" are now recognized as completely different tumors and distinct entities. For instance, translocation PRCC (Xp11.2) was recognized as a separate neoplastic entity in the WHO 2004 classification [38]. RCC associated with hereditary leiomyomatosis (HLRCC) was considered as a hereditary counterpart of PRCC type 2 in the WHO 2004 and was subsequently recognized as a separate entity in the Vancouver ISUP classification. Clear cell papillary RCC (CCPRCC) is another example of such, which was introduced as a new entity by the Vancouver ISUP classification [39]. Both of these neoplasms (HLRCC and CCPRCC) were later adopted by the WHO 2016

Table 5
Oncocytic PRCC – chromosomal gains and losses.

		2+	3+		5+	7+	11+	16+	17+		7+,17+ in common	1-		4-	14-	15-	17-	Y-	X-
		2+	3+	3p+	5+	7+	11q+	16+	17+	17q+	7+,17+	1-	1p-	4q-	14-	15-	17-	Y-	X-
Xia et al. [15]	FISH					3/5 60%			2/5 40%		1/5							1/4 M 25%	
Hes et al. [11]	FISH					7/12 58.3%			8/12 66.7%		5/12 41.7%							3/10M 30%	
Park et al. [13]	Array CGH			3/4 75%			2/4 50%			2/4 50%				1/4 25%					
Lefevre et al. [12]	Karyotyping + CGH	1/5 20%	1/5 20%		1/5 20%			1/5 20%				2/5 40%			3/5 60%	2/5 40%		3/5 M 60%	
Han et al. [16]	FISH					7/14 50%			6/14 42.9%									2/8M 25%	
Kunju et al. [17]	FISH					6/6 100%			6/6 100%		6/6 100%							2/4M 50%	
Michalova et al. [14]	FISH					5/22 22.7%			6/22 27.3%		4/22 18.2%		6/21 28.6%		3/22 13.6%		5/22 22.7%	8/13M 61.3%	2/23 8.7%

classification [1].

The most recent WHO 2016 classification of renal tumors still recognizes the traditional subtyping of PRCC into type 1 and type 2. Oncocytic PRCC is currently mentioned as a provisional entity in the recent WHO 2016, which can be possibly recognized as PRCC type 3. The current WHO classification also recognizes the fact that there are renal tumors with mixed histology which may not fit into any of these categories [1].

During the last 15 years, many subtypes and variants of PRCC have been described, which do not fit in any of the officially recognized WHO tumor categories (i.e., type 1, type 2, possibly oncocytic). There are a number of studies describing small series of morphologically distinct PRCCs such as Warthin-like PRCC [26], solid PRCC [22-25], mucinous PRCC [18-20], biphasic squamoid alveolar RCC [32-36], and PRCC with clear cells [27,29,30,40].

It is evident that PRCCs are composed of a diverse and heterogeneous group of tumors with distinct subgroups of papillary or tubulopapillary architecture. These tumors can show different histological and even immunohistochemical profiles. From histologic point of view, these tumors can present in a wide range of morphological features such as small basophilic cells with scant cytoplasm, cells with abundant eosinophilic cytoplasm (oncocytic), larger basophilic cells with squamoid feature and emperipolesis or even cells with clear cytoplasm. In addition to typical papillary and tubulopapillary architecture, PRCC can present with predominant solid feature, as well as biphasic architecture with solid islands surrounded by alveolar-like structures. PRCCs can produce large necrotic and cystic changes or demonstrate mucin-like production. It is apparent that all such variations in PRCCs can create potential diagnostic challenges.

Imumnohistochemicaly, PRCCs express several different antibodies. Traditionally, vimentin, AMACR and CK7 were considered characteristic. PRCCs are almost constantly positive for vimentin and AMACR, however they show variable reactivity for CK7 [1]. Positivity of CK7 is more common in type 1 PRCC, while it is more variable in PRCC type 2 (some studies reported CK7 positivity in about 50% of PRCCs type 2) [41].

The above-mentioned subtypes/variants of PRCCs are shown to have diverse chromosomal numerical aberration patterns. PRCC type 1 has the most uniform molecular genetic changes across the whole spectrum of PRCCs. Polysomy of chromosomes 7 and 17 are very

Table 6
"Mucin" secreting PRCC – chromosomal gains and losses.

		7+	17+	7+,17+ in common	16+	Y-
Pivovarcikova et al. [20]	ACGH	1/1 100%	1/1 100%	1/1 100%	1/1 100%	1/1 100%
	FISH	2/4 50%	3/4 75%	1/4 25%	1/2 50%	4/4 100%

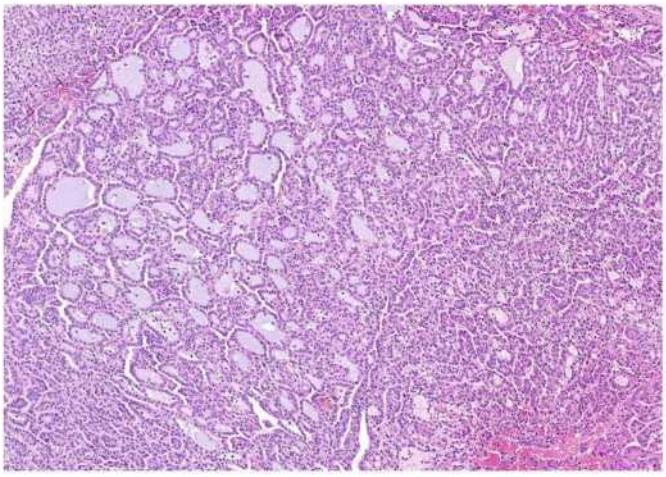

Fig. 4. Papillary renal cell carcinoma with mucicarmin positive deposition is a papillary lesion with areas containing bluish mucinous material.

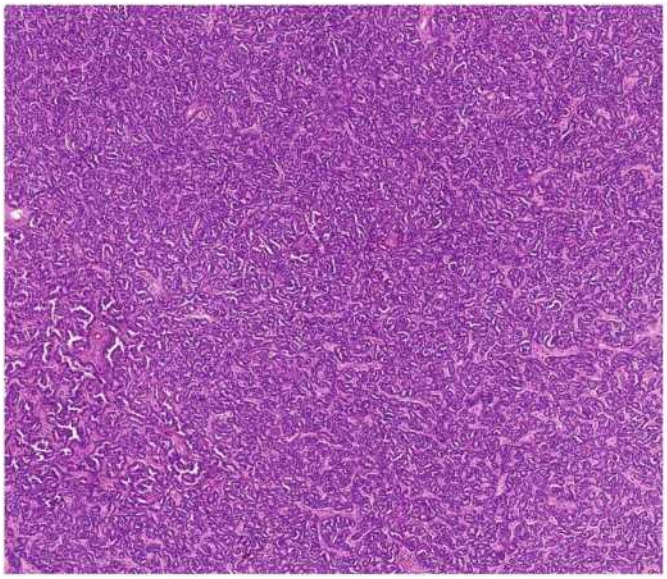

Fig. 5. So-called solid variant of papillary renal cell carcinoma is a compact tumor composed of small tubules, more or less compressed.

common features described in 66.7–100% of cases in different studies [5-10,42]. Loss of gonosome Y can be seen in 77.8–100% of male cases [7-10].

Numerical aberration status in PRCC type 2 is much more variable in contrast to PRCC type 1. In fact, the recent Cancer Genomic Atlas Research Network findings on PRCCs showed that PRCC type 1 and type 2 are clinically and biologically distinct tumors, with type 2 being consisted of at least three subtypes based on molecular features [42]. Nonetheless, the gains of chromosomes 7 and 17 are the most common molecular findings in PRCC type 2. These molecular changes are found in 31.2–69.2% (gain of chromosome 7) and 50–68.8% (polysomy of chromosome 17) in different studies. Other relatively frequent chromosomal changes in these tumors are polysomy of chromosomes 12, 16 and 20 [5-10]. Loss of gonosome Y is also described in 63.6–90% male cases of PRCC type 2 [7-9]. Further, there are a wide spectrum of CNAPs reported in PRCC type 2 (in smaller frequencies) including gains of chromosomes 1, 2, 3, 4, 5, 6, 8, 9, 13, 18, 19 and 22, as well as losses of chromosomes 1, 2, 3, 4,5, 6, 7, 8, 9, 10, 12, 13, 14, 15, 17, 18, 19, 20, 21, 22, and X [5-10].

A peculiar yet particularly interesting finding in chromosomal numerical aberration status has been recently reported in OPRCC. In a large scale study by Michalova et al. 43.5% of OPRCCs showed CNAP very similar to renal oncocytoma (RO). In this study, only 6/22 case (27.3%) showed polysomy of chromosomes 7 and 17. Given considerable CNAP overlap between OPRCC and RO, the reliability of CNAP analysis as a potential diagnostic utility tool in the differential diagnosis workup would be of major concern [14].

Molecular genetic studies performed in solid PRCC showed gains of chromosomes 7 and 17 and loss of chromosome Y in male patients in high percentage of cases (gain of chromosome 7 in 66.7–100% of cases, gain of chromosome 17 in 93.8–100% of cases, and loss of gonosome Y in 100% of cases) (Table 8) [22,24,25].

"Mucin" secreting PRCC is also composed of molecular-genetically heterogeneous tumors. A study by Pivovarcikova et al. demonstrated the gain of chromosomes 7 in 50% of cases, chromosome 17 in 75% of cases, chromosome 16 in 50% of cases, and the loss of chromosome Y in all male cases (100%). However, it should be noted that the sample size in the study was rather small, with only limited number of cases being suitable for genetic analysis [20].

BSARCCs showed numerical chromosomal abnormalities traditionally believed to be characteristic of PRCC. The largest series of BSARCCs, published by Hes et al. showed gains of chromosomes 7 and 17 in all

Table 7
Cystic and necrotic PRCC – chromosomal gains and losses.

		2+	3+	7+	9+	12+	13+	16+	17+	20+	21+	22+	7+,17+ in common	21-	Y-
Peckova et al. [21]	aCGH	1/7 14.3%	1/7 14.3%	3/7 42.9%	1/7 14.3%	3/7 42.9%	1/7 14.9%	2/7 28.6%	4/7 57.1%	2/7 28.6%	1/7 14.3%	1/7 14.3%	3/7 42.9%	1/7 14.3%	2/6M 33.3%
	FISH			5/8 62.5%					6/8 75%				5/8 52.5%		5/7M 71.4%

Table 8
Solid PRCC – chromosomal gains and losses.

		3+	5+	7+	12+	16+	17+	20+	X+	7+17+ in common	Y-	14-	18-	21-
Renshaw et al. [22]	FISH			2/3 66.7%			3/3 100%			2/3 66.7%				
	Cytogenetic study	1/1 100%	1/1 100%		1/1 100%	1/1 100%	1/1 100%	1/1 100%	1/1 100%			1/1 100%	1/1 100%	1/1 100%
Zhang et al. [25]	FISH			2/2 100%			2/2 100%			2/2 100%	2/2 100%			
Mantoan Padilha et al. [24]	FISH			14/16 87.5%			15/16 93.8%			13/16 81%	NP			

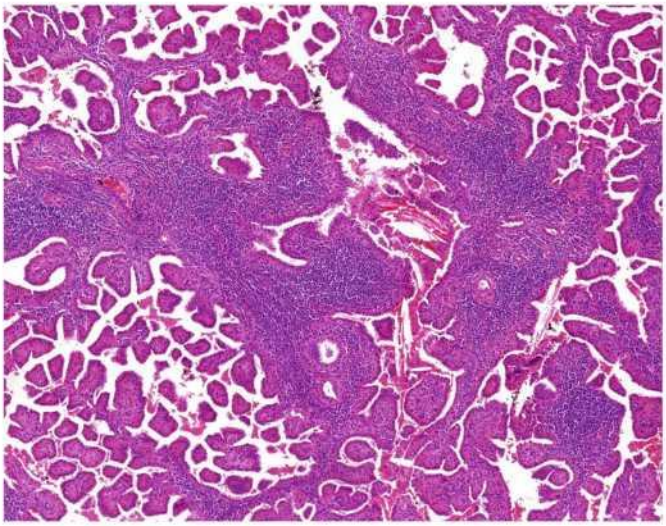

Fig. 6. Warthin-like variant of papillary renal cell carcinoma is a recently described lesion composed of papillary structures with dense lymphoid stroma and oncocytic cells on the surface of papillae.

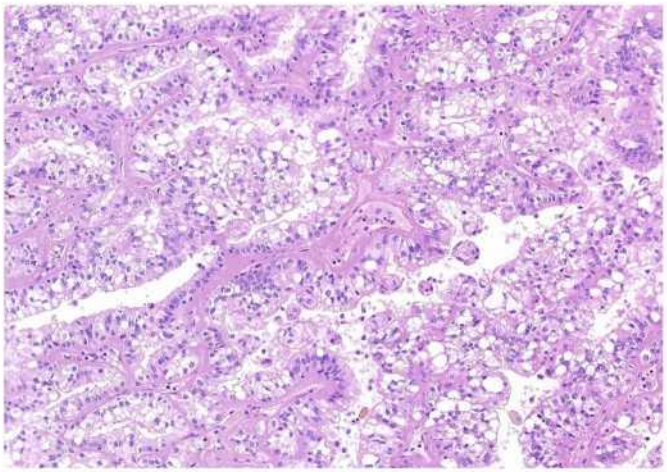

Fig. 7. Papillary renal cell carcinoma with clear cells is a tumor different from clear cell papillary renal cell carcinoma. Tumor is composed of clear cells admixed with cells with granular eosinophilic cytoplasm.

analyzable cases (100%) and the loss of chromosome Y in 80% of male patients. Other chromosomal abnormalities described in this study are presented in Table 11. The high percentage of polysomy of chromosomes 7 and 17 can be explained by the fact that some of these tumors histologically exhibited features compatible with PRCC type 1 [32].

All published studies on PRCC with clear cell changes strictly used results of molecular genetic analysis in classification of these tumors; CNAP was used as an ultimate criterion for the classification of such tumors in these studies [27,29-31]. Fuzesi and Salama presented RCCs with papillary architecture and clear cells, which were classified as clear cell renal cell carcinoma based on cytogenetic finding of loss of terminal 3p chromosomal segment [29,30]. Gobbo et al. assessed 14 RCCs with papillary architecture and clear cells, of which 9 were classified as PRCC based on cytogenetic changes including gains of chromosomes 7 (88.9%) and/or 17 (88.9%) and loss of chromosome Y in all male cases (100%). 3/14 cases in this study were classified as CCRCC (cases with detected 3p deletion), and 2/14 cases remained as unclassified (one case had polysomy of chromosomes 7 and 17 and 3p deletion, one case showed no changes in these three monitored parameters) [27]. Haudebourg's group had similar approach in their three cases included in the study. Two cases with detected polysomy 7 and 17 were labeled as PRCC. One case with polysomy of chromosomes 7 and 17 and concurrently LOH of chromosome 3 was designated as "unclassified RCC" [31].

Warthin-like PRCC has a wide spectrum of chromosomal changes and it is evident that this subgroup is rather heterogeneous. Only one described case of Warthin-like PRCC showed polysomy of chromosomes 7 and 17, which is believed to be characteristic for PRCC. Some published cases had no chromosomal changes, while other cases showed non-characteristic gains and losses of different chromosomes [26].

Table 9
Warthin-like PRCC – chromosomal gains and losses.

		1+	2+	5+	7+	8+	12+	17+	21+	1-	3-	14-	15-	18-	22-	Y-	X-
Skenderi et al. [26]	Low pass whole genome sequencing	1/9 11.1%	1/9 11.1%	2/9 22.2%	1/9 11.1%	1/9 11.1%	1/9 11.1%	1/9 11.1%	1/9 11.1%	3/9 33.3%	2/9 22.2%	2/9 22.2%	1/9 11.1%	1/9 11.1%	1/7 14.3%	2/7M 28.6%	1/7 14.3%

Table 10
PRCC with clear cell changes – chromosomal gains and losses.

		3p-	2+	3+	4+	5+	7+	9+	11+	12+	13+	16+	17+	18+	20+	21+	22+	7+17+ in common	7-	9-	13-	14-	17-	21-	22-	Y-
Gobbo et al. [27]	FISH	0/9 0%					8/9 88.9%						8/9 88.9%					7/9 77.8%								4/4 100%
Fuzesi et al. [29]	Karyotyping	3/3 100%					1/3 33.3%			1/3 33.3%					1/3 33.3%					1/3 33.3%	1/3 33.3%	3/3 100%		1/3 33.3%	1/3 33.3%	
Salama et al. [30]	FISH + microsatellite Analysis	6/7 85.7%					0/6						0/6						4/6 67%				6/6 100%			
Haudebourg et al. [31]	FISH	0	1/3 33.3%	1/3 33.3%			3/3 100%	1/3 33.3%					3/3 100%	1/3 33.3%				3/3 100%								1/1 100%
	SNP array	1/2 50%	2/2 100%	1/2 50%	1/2 50%	1/2 50%	2/2 100%	1/2 50%	1/2 50%	1/2 50%	1/2 50%	1/2 50%	2/2 100%	1/2 50%	1/2 50%	1/2 50%	1/2 50%	2/2 100%								1/1 100%

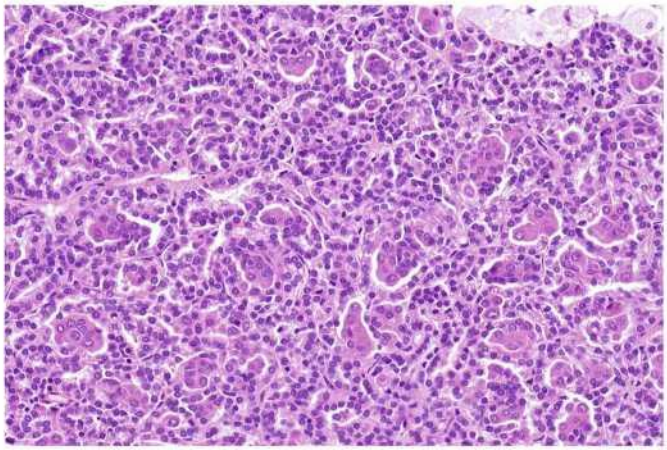

Fig. 8. Biphasic squamoid alveolar (papillary) renal cell carcinoma is a recently described variant, which is composed of dual cell population: small low-grade cells with scanty cytoplasm and large high grade eosinophilic cells almost identical to squamous cells.

Molecular-genetic analysis of cystic and necrotic PRCC showed polysomy of chromosome 7 (62.5% cases) and polysomy of chromosome 17 (75% cases). Loss of chromosome Y was detected in 71.4% of male patients. There were other chromosomal abnormalities reported in these tumors, while no chromosomal numerical aberrations were found in some cases [21]. These findings are somewhat surprising given all cystic and necrotic PRCCs were histologically consistent with PRCC type 1 in viable and preserved areas, where higher percentage of polysomy chromosomes 7 and 17 would have been expected.

Overall, this review highlights the fact that PRCC is composed of a highly heterogeneous group of tumors with broad morphological spectrum and immunohistochemical profile. This fact has also recently been supported by Salleeb et al. [43]. The authors showed high variability and heterogeneity among PRCCs as a group of tumors and proposed 2 new subtypes [43]. From all above mentioned facts, it is evident that chromosomal numerical aberration status is much more complex than traditionally thought. Of all PRCC subtypes/variants, PRCC type 1 seems to be a genetically uniform group, while other types showed different degrees of heterogeneity. We believe that it may not be possible to distinguish various PRCC subtypes merely based on CNAP. In other words, CNAP should be considered only as one of diagnostic tools (like immunohistochemistry) in clinical decision making process. Finally, it is becoming more evident that tumor type-specific chromosomal numerical aberration status in PRCCs may not exist.

Disclosure of conflict of interest

All authors declare no conflict of interest.

Table 11
Biphasic squamoid alveolar RCC – chromosomal gains and losses.

		1+	5+	7+	11+	12+	13+	16+	17+	20+	7+,17+ in common	2-	5-	6-	9-	12-	15-	16-	17-	18-	21-	22-	Xp-	Y-
Hes et al. [32]	Array CGH			5/5 100%		1/5 20%		1/5 20%	5/5 100%	3/5 60%	5/5 100%										1/5 20%		1/5 20%	
	FISH			11/11 100%					11/11 100%		11/11 100%													4/5M 80%

References

[1] Moch H, Humphrey PA, Ulbright TM, Reuter VE. WHO classification of tumours of the urinary system and male genital organs. Lyon: IARC; 2016.
[2] Delahunt B, Eble JN. Papillary renal cell carcinoma: a clinicopathologic and immunohistochemical study of 105 tumors. Mod Pathol 1997;10:537–44.
[3] Delahunt B, Eble JN, McCredie MR, et al. Morphologic typing of papillary renal cell carcinoma: comparison of growth kinetics and patient survival in 66 cases. Hum Pathol 2001;32:590–5.
[4] Kovacs G, Akhtar M, Beckwith BJ, et al. The Heidelberg classification of renal cell tumours. J Pathol 1997;183:131–3.
[5] Jiang F, Richter J, Schraml P, et al. Chromosomal imbalances in papillary renal cell carcinoma: genetic differences between histological subtypes. Am J Pathol 1998;153:1467–73.
[6] Kovac M, Navas C, Horswell S, et al. Recurrent chromosomal gains and heterogeneous driver mutations characterise papillary renal cancer evolution. Nat Commun 2015;6:6336.
[7] Yu W, Zhang W, Jiang Y, et al. Clinicopathological, genetic, ultrastructural characterizations and prognostic factors of papillary renal cell carcinoma: new diagnostic and prognostic information. Acta Histochem 2013;115:452–9.
[8] Marsaud A, Dadone B, Ambrosetti D, et al. Dismantling papillary renal cell carcinoma classification: the heterogeneity of genetic profiles suggests several independent diseases. Genes Chromosomes Cancer 2015;54:369–82.
[9] Gunawan B, von Heydebreck A, Fritsch T, et al. Cytogenetic and morphologic typing of 58 papillary renal cell carcinomas: evidence for a cytogenetic evolution of type 2 from type 1 tumors. Cancer Res 2003;63:6200–5.
[10] Antonelli A, Tardanico R, Balzarini P, et al. Cytogenetic features, clinical significance and prognostic impact of type 1 and type 2 papillary renal cell carcinoma. Cancer Genet Cytogenet 2010;199:128–33.
[11] Hes O, Brunelli M, Michal M, et al. Oncocytic papillary renal cell carcinoma: a clinicopathologic, immunohistochemical, ultrastructural, and interphase cytogenetic study of 12 cases. Ann Diagn Pathol 2006;10:133–9.
[12] Lefevre M, Couturier J, Sibony M, et al. Adult papillary renal tumor with oncocytic cells: clinicopathologic, immunohistochemical, and cytogenetic features of 10 cases. Am J Surg Pathol 2005;29:1576–81.
[13] Park BH, Ro JY, Park WS, et al. Oncocytic papillary renal cell carcinoma with inverted nuclear pattern: distinct subtype with an indolent clinical course. Pathol Int 2009;59:137–46.
[14] Michalova K, Steiner P, Montiel DP, et al. Chromosomal aberration pattern in oncocytic papillary renal cell carcinoma: analysis of 28 cases. United States & Canadian Academy of Pathology 106th Annual Meeting. San Antonio: Mod Pathol; 2017. p. 243A.
[15] Xia QY, Rao Q, Shen Q, et al. Oncocytic papillary renal cell carcinoma: a clinicopathological study emphasizing distinct morphology, extended immunohistochemical profile and cytogenetic features. Int J Clin Exp Pathol 2013;6:1392–9.
[16] Han G, Yu W, Chu J, et al. Oncocytic papillary renal cell carcinoma: a clinicopathological and genetic analysis and indolent clinical course in 14 cases. Pathol Res Pract 2017;213:1–6.
[17] Kunju LP, Wojno K, Wolf Jr. JS, et al. Papillary renal cell carcinoma with oncocytic cells and nonoverlapping low grade nuclei: expanding the morphologic spectrum with emphasis on clinicopathologic, immunohistochemical and molecular features. Hum Pathol 2008;39:96–101.
[18] Val-Bernal JF, Mayorga M, Garcia-Arranz P, Gomez-Roman JJ. Mucin secretion in papillary (chromophil) renal cell carcinoma. Am J Surg Pathol 1998;22:1037–40.
[19] Val-Bernal JF, Gomez-Roman JJ, Vallina T, et al. Papillary (chromophil) renal cell carcinoma with mucinous secretion. Pathol Res Pract 1999;195:11–7.
[20] Pivovarcikova K, Peckova K, Martinek P, et al. "Mucin"-secreting papillary renal cell carcinoma: clinicopathological, immunohistochemical, and molecular genetic analysis of seven cases. Virchows Arch 2016;469:71–80.
[21] Peckova K, Martinek P, Pivovarcikova K, et al. Cystic and necrotic papillary renal cell carcinoma: prognosis, morphology, immunohistochemical, and molecular-genetic profile of 10 cases. Ann Diagn Pathol 2017;26:23–30.
[22] Renshaw AA, Zhang H, Corless CL, et al. Solid variants of papillary (chromophil) renal cell carcinoma: clinicopathologic and genetic features. Am J Surg Pathol 1997;21:1203–9.
[23] Ulamec M, Skenderi F, Trpkov K, et al. Solid papillary renal cell carcinoma: clinicopathologic, morphologic, and immunohistochemical analysis of 10 cases and review of the literature. Ann Diagn Pathol 2016;23:51–7.
[24] Mantoan Padilha M, Billis A, Allende D, et al. Metanephric adenoma and solid variant of papillary renal cell carcinoma: common and distinctive features. Histopathology 2013;62:941–53.
[25] Zhang Y, Yong X, Wu Q, et al. Mucinous tubular and spindle cell carcinoma and solid variant papillary renal cell carcinoma: a clinicopathologic comparative analysis of four cases with similar molecular genetics datum. Diagn Pathol 2014;9:194.
[26] Skenderi F, Ulamec M, Vanecek T, et al. Warthin-like papillary renal cell carcinoma: clinicopathologic, morphologic, immunohistochemical and molecular genetic analysis of 11 cases. Ann Diagn Pathol 2017;27:48–56.
[27] Gobbo S, Eble JN, Grignon DJ, et al. Clear cell papillary renal cell carcinoma: a distinct histopathologic and molecular genetic entity. Am J Surg Pathol 2008;32:1239–45.
[28] Ross H, Martignoni G, Argani P. Renal cell carcinoma with clear cell and papillary features. Arch Pathol Lab Med 2012;136:391–9.
[29] Fuzesi L, Gunawan B, Bergmann F, et al. Papillary renal cell carcinoma with clear cell cytomorphology and chromosomal loss of 3p. Histopathology 1999;35:157–61.
[30] Salama ME, Worsham MJ, DePeralta-Venturina M. Malignant papillary renal tumors with extensive clear cell change: a molecular analysis by microsatellite analysis and fluorescence in situ hybridization. Arch Pathol Lab Med 2003;127:1176–81.
[31] Haudebourg J, Hoch B, Fabas T, et al. Strength of molecular cytogenetic analyses for adjusting the diagnosis of renal cell carcinomas with both clear cells and papillary features: a study of three cases. Virchows Arch 2010;457:397–404.
[32] Hes O, Condom Mundo E, Peckova K, et al. Biphasic squamoid alveolar renal cell carcinoma: a distinctive subtype of papillary renal cell carcinoma? Am J Surg Pathol 2016;40:664–75.
[33] Trpkov K, Athanazio D, Magi-Galluzzi C, et al. Biphasic papillary renal cell carcinoma is a rare and distinct morphologic variant – clinicopathologic study of 24 novel cases. United States & Canadian Academy of Pathology 106th Annual Meeting. San Antonio: Mod Pathol; 2017. p. 264A.
[34] Petersson F, Bulimbasic S, Hes O, et al. Biphasic alveolosquamoid renal carcinoma: a histomorphological, immunohistochemical, molecular genetic, and ultrastructural study of a distinctive morphologic variant of renal cell carcinoma. Ann Diagn Pathol 2012;16:459–69.
[35] Lopez JI. Case report: multifocal biphasic squamoid alveolar renal cell carcinoma. 5. F1000Res; 2016. p. 607.
[36] Chartier S, Mejean A, Richard S, et al. Biphasic squamoid alveolar renal cell carcinoma: 2 cases in a family supporting a continuous spectrum with papillary type I renal cell carcinoma. Am J Surg Pathol 2017;41(7):1011–2.
[37] Troxell ML, Higgins JP. Renal cell carcinoma in kidney allografts: histologic types, including biphasic papillary carcinoma. Hum Pathol 2016;57:28–36.
[38] SG Eble JN, Epstein JI, Sesterhenn IA. World Health Organization classification of tumours pathology and genetics tumours of the urinary system and male genital organs. Lyon: IARC Press; 2004.
[39] Srigley JR, Delahunt B, Eble JN, et al. The International Society of Urological Pathology (ISUP) Vancouver classification of renal neoplasia. Am J Surg Pathol 2013;37:1469–89.
[40] Klatte T, Said JW, Seligson DB, et al. Pathological, immunohistochemical and cytogenetic features of papillary renal cell carcinoma with clear cell features. J Urol 2011;185:30–5.
[41] Langner C, Wegscheider BJ, Ratschek M, et al. Keratin immunohistochemistry in renal cell carcinoma subtypes and renal oncocytomas: a systematic analysis of 233 tumors. Virchows Arch 2004;444:127–34.
[42] Linehan WM, Spellman PT, Ricketts CJ, et al. Comprehensive molecular characterization of papillary renal-cell carcinoma. N Engl J Med 2016;374:135–45.
[43] Saleeb RM, Brimo F, Farag M, et al. Toward biological subtyping of papillary renal cell carcinoma with clinical implications through histologic, immunohistochemical, and molecular analysis. Am J Surg Pathol 2017 Oct 3. http://dx.doi.org/10.1097/PAS.0000000000000962. [Epub ahead of print]. PMID:28984673.

1.2.2 Renal cell carcinomas with tubulopapillary architecture and oncocytic cells: Molecular analysis of 39 difficult tumors to classify

Onkocytický papilární renální karcinom je ne příliš přesně definovaná varianta PRCC. Od prvního popisu OPRCC byla publikována řada studií na toto téma, často s mírně konfliktními výsledky, přesná definice této entity stále chybí.

Celkem bylo touto prací analyzováno 39 PRCC sestávajících z onkocytických buněk, některé ze zařazených tumorů splňovaly kritéria WHO klasifikace 2016 pro označení OPRCC. Případy byly pro účely studie rozděleny do tří kategorií (na základě sledovaných cytogenetických znaků). První skupina zahrnovala celkem 23 případů, u nichž byl prokázán cytogenetický profil typicky přisuzovaný renálnímu onkocytomu (RO). Druhá skupina obsahovala 7 případů s prokázanou polyzomií chromozomů 7 a 17. Do třetí skupiny bylo zahrnuto 9 tumorů s variabilním cytogenetickým pozadím, nezařaditelných do předchozích dvou kategorií. Sledovaná epidemiologická data, morfologické a imunohistochemické charakteristiky byly výrazně variabilní jak v rámci jednotlivých vymezených skupin, tak mezi různými skupinami. Žádný z histomorfologických znaků nebyl specifický pro konkrétní skupinu. Kombinace morfologie, imunohistochemického profilu léze a molekulárně-genetického vyšetření nedovolila odhadnout biologické chování tumorů.

Vzhledem k variabilnímu cytogenetickému pozadí námi analyzovaných „OPRCC“ doporučujeme při hodnocení biopsií těchto tumorů striktní adherenci k morfologii a imunuhistochemickému profilu a to zejména v limitovanému vzorku (např. v punkční biopsii). Výsledky cytogenetických vyšetření v rámci diagnostického algoritmu mohou být potenciálně zavádějící a „OPRCC“ může být chybně diagnostikován jako RO. Onkocytický papilární renální karcinom je velmi variabilní skupina tumorů a užívání termínu „OPRCC“ jakožto názvu neoplastické renální entity je otazné. V současné době tak vyvstává otázka zda, spíše než označení neoplastické entity, by termín „OPRCC“ neměl být používán pouze jako popisný termín.

Annals of Diagnostic Pathology 52 (2021) 151734

Contents lists available at ScienceDirect

Annals of Diagnostic Pathology

journal homepage: www.elsevier.com/locate/anndiagpath

Original Contributions

Renal cell carcinomas with tubulopapillary architecture and oncocytic cells: Molecular analysis of 39 difficult tumors to classify☆

Kristyna Pivovarcikova[a], Petr Grossmann[a], Veronika Hajkova[a], Reza Alaghehbandan[b], Tomas Pitra[c], Delia Perez Montiel[d], Maris Sperga[e], Joanna Rogala[a], Maryna Slisarenko[a], Adriena Bartos Vesela[c], Peter Svajdler[a], Kvetoslava Michalova[a], Pavla Rotterova[a], Milan Hora[c], Michal Michal[a], Ondrej Hes[a,*]

[a] Department of Pathology, Charles University in Prague, Faculty of Medicine in Plzeň, Pilsen, Czech Republic
[b] Department of Pathology, Faculty of Medicine, University of British Columbia, Royal Columbian Hospital, Vancouver, BC, Canada
[c] Department of Urology, Charles University in Prague, Faculty of Medicine in Plzeň, Pilsen, Czech Republic
[d] Department of Pathology, Institute Nacional de Cancerologia, Mexico City, Mexico
[e] Department of Pathology, Stradin's University, Riga, Latvia

ARTICLE INFO

Keywords:
Kidney
Oncocytic renal cell carcinoma
Papillary
Unclassified
Copy number variation pattern
Oncocytoma
Overlapping

ABSTRACT

So-called oncocytic papillary renal cell carcinoma (OPRCC) is a poorly defined variant of papillary renal cell carcinoma. Since its first description, several studies were published with conflicting results, and thus precise definition is lacking.

A cohort of 39 PRCCs composed of oncocytic cells were analyzed. Cases were divided into 3 groups based on copy number variation (CNV) pattern. The first group consisted of 23 cases with CNV equal to renal oncocytoma. The second group consisted of 7 cases with polysomy of chromosomes 7 and 17 and the last group of 9 cases included those with variable CNV.

Epidemiologic, morphologic and immunohistochemical features varied among the groups. There were not any particular histomorphologic features correlating with any of the genetic subgroups. Further, a combination of morphologic, immunohistochemical, and molecular-genetic features did not allow to precisely predict biologic behavior.

Owing to variable CNV pattern in OPRCC, strict adherence to morphology and immunohistochemical profile is recommended, particularly in limited samples (i.e., core biopsy). Applying CNV pattern as a part of a diagnostic algorithm can be potentially misleading.

OPRCC is a highly variable group of tumors, which might be misdiagnosed as renal oncocytoma. Using the term OPRCC as a distinct diagnostic entity is, thanks to its high heterogeneity, questionable.

1. Introduction

Renal cell carcinomas (RCC) composed of oncocytic cells represents a heterogeneous group of renal neoplasms, which can pose diagnostic challenge in routine practice. Despite the existence of well-established renal tumor entities such as renal oncocytoma (RO) and chromophobe RCC, there are several morphologic variants of "oncocytic" tumors, for which rendering exact diagnosis may be very challenging. Among others, group of papillary RCC with oncocytic cells represents example of such challenging tumors. Papillary renal cell carcinoma (PRCC) has traditionally been divided into two morphologic subgroups – PRCC type 1 and PRCC type 2 [1]. However, in the "histo-molecular" classification era, this does not hold true and remains unsatisfactory as many PRCC cannot be classified as per existing criteria [2].

The WHO classification defines oncocytic PRCC (OPRCC) as a PRCC with voluminous, finely granular, evenly distributed eosinophilic

☆ The study was supported by the Charles University Research Fund (project number Q39), by Institutional Research Fund FN 00669806, and by Biobank Research on Telemedical Approaches for Human Biobanks in a European Region, Bavarian-Czech University Agency (BTHA), and by SVV-2020 No. 260 539 provided by the Ministry of Education, Youth, and Sports of the Czech Republic.

* Corresponding author at: Department of Pathology, Medical Faculty, Charles University Hospital Plzen, Alej Svobody 80, 304 60 Pilsen, Czech Republic.
E-mail address: hes@biopticka.cz (O. Hes).

https://doi.org/10.1016/j.anndiagpath.2021.151734

Available online 31 March 2021

cytoplasm and oncocytoma-like nuclei (usually with low nuclear grade), which are single-layered and linearly aligned [3]. Apparently, "OPRCC" fulfilling these WHO criteria fits well in a subgroup of PRCC recently described as "PRCC with reverse polarity" [4]. However from the reverse perspective, PRCCs composed of oncocytic cells are a part of much broader spectrum, where PRCC with reverse polarity is one of the existing variants/subtypes. The whole group of PRCCs composed of oncocytic cells is so far poorly understood and histologic diagnostic criteria have not yet been determined.

In this study, we analyzed morphological, immunohistochemical, and molecular genetic features of renal tumors showing combined papillary/tubullopapillary/papillary, compressed to solid architecture and oncocytic cells (some of them overlapping with OPRCC as defined by WHO classification/PRCC with reverse polarity) in order to better understand the relationship between morphology and genetic background of these heterogeneous group of RCCs.

2. Material and methods

2.1. Case identification

A total of 287 cases of RCC with oncocytic/eosinophilic cells and tubulopapillary/papillary architecture were retrieved from the Pilsen Tumor Registry. A search algorithm including the keywords "oncocytic, papillary, tubular, tubulopapillary, unusual, renal cell carcinoma" was used to identify appropriate renal tumors. All cases were reviewed by 2 pathologists (K.P., O.H.). Basic inclusion criteria were papillary/tubulopapillary/papillary compressed architecture and oncocytic cells. All cases with poorly fixed quality tissue or fixation artifacts were excluded from the study. Further, we excluded high grade clear cell RCCs, unusual chromophobe RCCs, tubulocystic RCCs, as well as cases with limited available material (i.e., core biopsy). Upon completion of initial review of 246 cases, 53 tumors were selected to be tested for DNA quality, of which seven cases with low DNA quality were further excluded. In total, 46 tumors with papillary, tubulopapillary, and/or papillary-solid (compressed papillae) architecture were analyzed and a representative block from each case was stained with antimitochondrial antigen antibody (MIA) to confirm the oncocytic nature of neoplastic cells (for details see below). Only tumors with diffuse and strong cytoplasmic positivity were accepted, leading to the exclusion of seven more cases from the study.

Finally, 39 tumors were enrolled in the study, with 1–20 tissue blocks (median 4) available for each case. One to two representative blocks were selected for immunohistochemical and molecular–genetic studies. It should be noted that 10 cases were previously published in the study of Michalova et al. (cases 1–10) [5].

2.2. Light microscopy

Tissues for light microscopy were fixed in 4% formaldehyde and embedded in paraffin using routine procedure. Sections 2 μm thick were cut from tissue blocks and stained with hematoxylin and eosin (H&E).

2.3. Immunohistochemistry

The immunohistochemical analysis was performed using a Ventana BenchMark ULTRA (Ventana Medical System, Inc., Tucson, Arizona). The following primary antibodies were used: cytokeratin 7 (OV-TL12/30, monoclonal; Dako, Glostrup, Denmark; 1:200), cytokeratin 20 (M7019, monoclonal; Dako; 1:100), racemase/AMACR (P504S, monoclonal; Zeta, Sierra Madre, CA; 1:50), vimentin (V9, monoclonal; Cell Marque, Rocklin, CA; RTU), carbonic anhydrase IX (EP161, monoclonal; Cell Marque; RTU), antimelanosome (HMB45, monoclonal; Dako; 1:200), TFE3 (MRQ-37, monoclonal; Cell Marque; RTU), Melan A (A103, monoclonal; Cell Marque; RTU), mitochondrial antigen antibody/MIA (113-1, Biogenex, San Ramon, CA; 1:100), GATA3 (monoclonal, Biocare Medical, Concord, CA, 1:100), cyclin D1 (SP4-R; monoclonal, Cell Marque, RTU). Appropriate positive controls were used.

2.4. Fluorescent in-situ hybridization (FISH)

Four μm thick FFPE sections were placed onto positively charged slides. The unstained slides were routinely deparaffinized and incubated in the 1× Target Retrieval Solution Citrate pH 6 (Dako, Glostrup, Denmark) at 95 °C for 40 min and subsequently cooled for 20 min at room temperature in the same solution. Slides were washed in deionized water for 5 min and digested in protease solution with Pepsin (0.5 mg/ml, Sigma Aldrich, St. Louis, MO, USA) in 0.01 M HCl at 37 °C for 35 to 60 min, according the sample conditions. Slides were then placed into deionized water for 5 min, dehydrated in a series of ethanol solution (70%, 85%, and 96% for 2 min each) and air-dried. Vysis probes (Vysis/Abbott Molecular, IL, USA) were mixed with water and CEP or LSI/WCP Hybridization buffer (Vysis/Abbott Molecular) in a 1:2:7 ratio respectively. ZytoLight probe (ZytoVision GmbH, Bremerhaven, Germany) was factory premixed. Overview of all used probes is summarized in Supplemental Table 1.

An appropriate amount of probe was applied on specimen, covered with a glass coverslip and sealed with rubber cement. Slides were incubated in the ThermoBrite instrument (StatSpin/Iris Sample Processing, Westwood, MA, USA) with co-denaturation at 85 °C for 8 min and hybridization at 37 °C for 16 h. Rubber cemented coverslip was then removed and the slide was placed in post-hybridization wash solution (2xSSC + 0.3% NP-40) at 72 °C for 2 min. The slides were air-dried in the dark, counterstained with 4′, 6′-diamidino-2-phenylindole DAPI (Vysis/Abbott Molecular), coverslipped and immediately examined.

The sections were examined with an Olympus BX51 fluorescence microscope (Olympus Corporation, Tokyo, Japan) using a 100× objective and filter sets Triple Band Pass (DAPI/SpectrumGreen/SpectrumOrange), Dual Band Pass (SpectrumGreen/SpectrumOrange) and Single Band Pass (SpectrumGreen, SpectrumOrange, SpectrumGold, SpectrumRed and SpectrumAqua). For each probe, one hundred randomly selected nonoverlapping tumor cell nuclei were examined for presence of fluorescent signals.

Scoring of loss 1p was performed by counting the ratio of the number of 1p36 to 1q25. Cut-off value was used 0.7 according to the classification of Mohapatra et al. [6]. Loss and gain for studied centromeres and loci *CCND1* and *IGH* were defined as the presence of one specific signal per nucleus in >45% and three and more signals in >10% (mean value in normal non-neoplastic control tissues +3 standard deviations), respectively [7]. Regarding break-apart probes, yellow signals were considered negative, separate orange and green signals were considered as positive. Cut off value was set to more than 10% of breakpoint signals (mean value in normal non-neoplastic control tissues +3 standard deviations).

2.5. NGS method

DNA from FFPE samples was extracted using QIAsymphony DSP DNA mini kit (Qiagen, Hilden, Germany). Purified DNAs were quantified using the Qubit Broad Range DNA Assays (Thermo Fisher Scientific, Waltham, Massachusetts, USA).

Hotspot mutations in *KRAS* gene were analyzed using the Accel-Amplicon Plus EGFR PAthway Panel (Swift Biosciences, USA). The libraries were prepared following the Accel-Amplicon protocol for Illumina sequencing. Final libraries were multiplexed, spiked with 20% PhiX control and sequenced on a NextSeq 550 (Illumina, San Diego, CA) to achieve at least 150,000 reads per sample. The analysis of the sequencing results (fastq files) was performed using the Varsome Clinical software (Saphetor SA, CH). Parameters for variant reporting were set to a minimum coverage per amplicon 300 and allelic frequency over 5%.

2.6. Evaluation of the cases, study groups

The tumors were divided into three distinct molecular subgroups according to their chromosomal copy number variation (CNV) pattern as follows: 1) PRCC with oncocytic cells and CNV identical to RO (enumeration of chromosome 1 - loss of whole chromosome 1 or its deletion, typically 1p36; and/or loss of chromosome 14; and/or loss of gonosomes; and/or 11q13 rearrangement - gene *CCND1*, or normal karyotype – see in Supplemental Table 2), 2) PRCC with oncocytic cells and gains of chromosomes 7 and 17, and 3) PRCC with oncocytic cells and variable CNV not matching the two previously mentioned subgroups. All neoplasms were analyzed by morphology and immunohistochemistry, and clinical data were compared.

2.7. Statistical analysis

The values of continuous parameters were calculated as means ± standard deviation (SD). Pearson's χ^2 test was used for categorical variables and Student's *t*-test for comparing the means. All tests were two-tailed, and $p < 0.05$ was considered statistically significant. All descriptive and inferential statistical analyses were carried out using the Statistical Package for the Social Sciences (SPSS), version 19.0 (Chicago, IL, USA).

3. Results

All 39 cases of PRCC composed of oncocytic cells were divided into three distinct subgroups according to their chromosomal CNV of selected chromosomes:

3.1. GROUP 1: PRCC with oncocytic cells and renal oncocytoma-like CNV

Basic clinicopathologic data are listed in Table 1. This study subgroup included 23 cases. Patients were 15 males and 8 females, with age range 52 to 81 years (median 68 years, mean 67.9 years). Tumor size (available in 22/23 cases) ranged from 0.8 to 9 cm in greatest dimension (median 3.8 cm, mean 4.4 cm). Pathologic stage included pT1 in 13 cases (pT1a in 11 cases, pT1b in 2 cases), pT2 in 1, and pT3a in 2 cases. No information on pathologic stage was available in 7 cases. Follow-up data were available for 14 patients (range 0.5 to 8 years, mean 4.5 years, median 7.5 years). One patient developed recurrence and metastatic disease (case 15a, for further recurrence details see case 15b in subgroup "PRCC with oncocytic cells and gains of chromosomes 7 and 17"), thirteen patients are alive with no evidence of disease.

Morphologic features are summarized in Table 2. Papillary component was documented, at least focally, in all 23 tumors (Fig. 1A+B). Papillary architecture was the predominant growth pattern in 18/23 cases, with 6/18 cases exhibiting secondary compressed papillary structures, and 5/18 with other minor components (tubulopapillary in 3 cases, tubular in 1 case, and cystic and tubular in 1 case). In the remaining 5/23 cases, the papillary areas were only focally present, of which 3/5 cases showed predominant tubulopapillary areas (in two cases with more tubulopapillary compressed architecture), and 2/5 cases combined papillary areas with tubular structures (even tubular compressed mimicking "solid" areas) (Fig. 2). Two cases (case 3 and case 16) with papillary architecture, uniform eosinophilic cells and round nuclei met criteria for diagnosis of PRCC with reverse polarity (see below) (Fig. 3A+B). 10/23 cases showed WHO/ISUP nuclear grade 2, while the remaining 13/23 cases were nuclear grade 3. Pseudostratification was noted in 8/23 cases (in 5 cases only focally). Macrophages were present in 11 cases. Further, we found necrosis in 2 cases, hemorrhage in 6 cases, so-called bloody lakes in 2 cases, calcifications in 5 cases, and hemosiderin pigmentation in 3 cases (Fig. 4).

Results of immunohistochemical analysis are summarized in Table 3. All cases showed positivity for anti-mitochondrial antigen antibody (MIA) and vimentin (in 2 cases only focally), while all tumors were negative for CD117, Melan A, and HMB45. Twelve cases were positive for CK7 (focally in 5/12 and single cells in 1/12). Racemase (AMACR) showed positive result in 20/21 cases and cyclin D1 in 21/22 cases (focal in 2/22 and single cells in 6/21 cases). Carbonic anhydrase IX was positive in 7/21 cases (focally in all seven cases), GATA3 in 2/21 cases, and CK20 in 1/22 cases. GATA3 positivity corresponded with cases fulfilling morphologic criteria for PRCC with reverse polarity (case 3 and

Table 1
GROUP 1: PRCC with oncocytic cells and renal oncocytoma-like CNV - clinical data.

CASE	SEX	AGE	SIDE	SIZE – in the greatest dimension (cm)	STAGE	FU	
CASE 1*	M	69	L	10	pT3a	6y	ANED
CASE 2*	F	61	L	7	NA	6y	ANED
CASE 3*	F	56	NA	2	pT1a	LFU	LFU
CASE 4*	F	75	L	3.5	pT1a	6y	ANED
CASE 5*	F	68	NA	4	pT1a	1.5y	ANED
CASE 6*	F	58	R	5	NA	13y	ANED
CASE 7*	M	79	R	9	pT2	3y	ANED
CASE 8*	M	73	R	3	pT1a	2y	ANED
CASE 9*	M	76	R	NA	NA	LFU	LFU
CASE 10*	M	63	NA	5.5	pT1b	LFU	LFU
CASE 11	M	76	R	7.9	pT3a	10y	ANED
CASE 12	F	66	R	4	pT1a	2.6y	ANED
CASE 13	M	67	R	2	pT1a	1.5	ANED
CASE 14	F	67	R	3	pT1a	0.5y	ANED
CASE 15a	M	60	R	5	pT1b	8	AWD (see case 15b in subgroup "PRCC with oncocytic cells and gains of chromosomes 7 and 17")
CASE 16	F	71	L	2.1	pT1a	1.4y	ANED
CASE 17	M	73	L	6.5	NA	LFU	LFU
CASE 18	M	66	R	3.5	NA	LFU	LFU
CASE 19	M	68	R	1.5	pT1a	LFU	LFU
CASE 20	M	52	L	4	NA	LFU	LFU
CASE 21	M	65	R	1.8	pT1a	1.6 y	ANED
CASE 22	M	81	NA	5.5	NA	LFU	LFU
CASE 23	M	72	R	0.8	pT1a	LFU	LFU

M male, *F* female, *L* left, *R* right, *NA* not available, *ANED* alive with no evidence of disease, *AWD* alive with the disease, *LFU* lost for follow up, * cases previously included in study by Michalova et al. [5].

Table 2
GROUP 1: PRCC with oncocytic cells and renal oncocytoma-like CNV – morphologic study.

CASE	Pattern of growth		Cytoplasm	Grade ISUP/WHO	Pseudostratification	Calcification (C), necrosis (N), hemosiderin (HEM), hemorrhage (HEMOR)	Macrophages
	Papillary structures	Other growth pattern					
CASE 1[a]	Compressed papillary	Compressed tubular	Granular and eosinophilic, cuboidal cells	2	No	N+	Not present
CASE 2[a]	Only		Granular, abundant, eosinophilic	2, nuclei elevated from BM	No	HEM +, C +	+++
CASE 3[a]	Only		Granular, eosinophilic, cuboidal cells	2	No	Not present	Not present
CASE 4[a]	Only		Granular, abundant, eosinophilic	2	Present focally	Not present	++
CASE 5[a]	Focally	Tubulopapillary	Granular, abundant, eosinophilic	3, nuclei elevated from BM	No	HEMOR +	Not present
CASE 6[a]	Only		Granular, abundant, eosinophilic	3	Present focally	Not present	Not present
CASE 7[a]	Focally, compressed	Tubular, "solid"	Granular, abundant, eosinophilic	2, granular chromatin	no	HEMOR +	++
CASE 8[a]	Predominantly	Tubulopapillary	Granular, abundant, eosinophilic	3	Present focally	Not present	Not present
CASE 9[a]	Only		Granular, abundant, eosinophilic	3	Present	Not present	Not present
CASE 10[a]	Papillary and papillary compressed		Granular, abundant, eosinophilic	2, granular chromatin	No	Not present	Not present
CASE 11	Predominantly	Tubulopapillary	Granular, abundant eosinophilic	2, optically empty, grooves, nuclei luminally located	present focally	C + (discrete), HEMOR + (discrete)	Not present
CASE 12	Papillary compressed to "solid"		Granular, eosinophilic cytoplasm	3, granular chromatin, nuclei centrally located	No	Occasional siderophages	+
CASE 13	Papillary compressed		Granular, abundant eosinophilic	3, elevated from BM	No	C +, HEMOR +	+
CASE 14	Predominantly	Tubular	Granular, abundant eosinophilic	3, granular chromatin	No	Bloody lakes	++
CASE 15a	Focally papillary compressed	Cystic, tubular	Granular, abundant eosinophilic, giant multinucleated cells	3	present focally	C +, bloody lakes, N +, HEMOR +	+ (collections of foamy macrophages)
CASE 16	Only		Granular, abundant eosinophilic, intracytoplasmatic vacuoles	2	No	Not present	Not present
CASE 17	Papillary compressed		Granular, abundant eosinophilic	2, granular chromatin, luminal localization of nuclei	No	Not present	+ (collections of foamy macrophages)
CASE 18	Papillary compressed		Granular, abundant eosinophilic	3	Present	Bloody lakes	+
CASE 19	Only		Granular, abundant eosinophilic	2, granular chromatin, nuclei centrally located	Present	C + cholesterol clefts, bloody lakes	+ (collections of foamy macrophages)
CASE 20	Focally	Tubulopapillary compressed	Granular, abundant eosinophilic	3, granular chromatin, nuclei centrally located	No	Not present	++
CASE 21	Only		Granular, abundant eosinophilic	3	No	Not present	Not present
CASE 22	Focally	Tubulopapillary compressed	Granular, abundant eosinophilic	3	No	HEMOR+	Not present
CASE 23	Predominantly	Tubulopapillary compressed	Granular, abundant eosinophilic	3	Present focally	HEM+	Not present

[a] Cases previously included in study by Michalova et al. [5], *BM* basal membrane, + present.

16). TFE3 staining was positive in two cases (clear nuclear staining in more than 50% of neoplastic cells), while FISH for detection of break in *TFE3* gene was negative in both cases.

Cytogenetic study showed spectrum of changes typically described in RO. Eight cases (8/23) had normal karyotype in tracked characters. Loss of gonosomes was identified in 5/23 cases, including 4/5 cases with loss of Y and 1/5 case with loss of X. Deletion 1p36 (2/23 cases) and combined deletion of 1p36 with loss Y (2/23 cases) were detected. Rearrangement of gene *CCND1* localized on 11q13 was noted in 2/23 cases. The remaining of 6/23 cases each showed combined different cytogenetic changes compatible with RO as follows, one case with deletion 1p36 concurrently with loss 14 and Y, one case with deletion 1p36 concurrently with loss 14, one case with loss 14 concurrently with loss Y, and one case with loss 14. Cases fulfilling the morphologic criteria of PRCC with reverse polarity had rearrangement of gene *CCND1* in one case (case 3) and normal karyotype in the second case (case 16). Mutation of *KRAS* gene was documented in both cases. Overview of all detected changes are presented in Table 4.

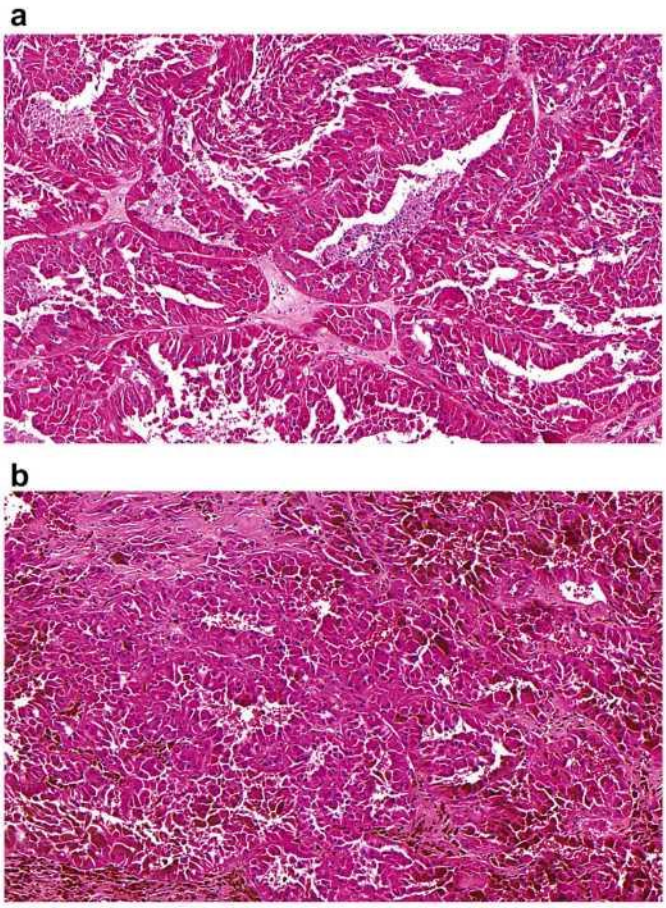

Fig. 1. A: Papillary renal cell carcinoma composed of oncocytic cells. Mild to moderate pseudostratification is present, however, nuclei are round and small with low nucleo-cytoplasmatic ratio.
B: In some tumors from "PRCC with oncocytic cells and renal oncocytoma-like CNV" group, voluminous deposits of hemosiderin were present.

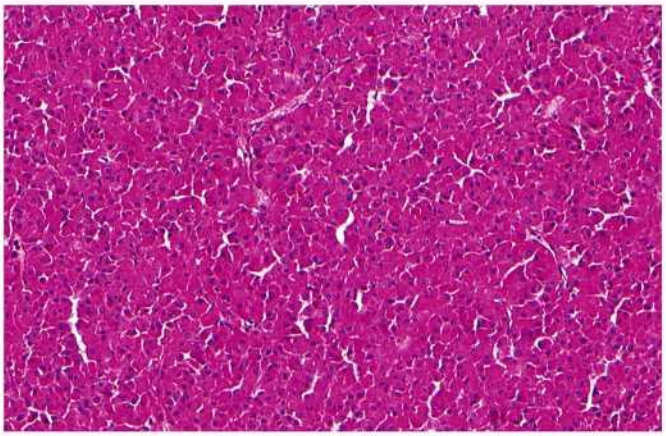

Fig. 2. In some tumors, compressed tubulopapillary structures imparted pseudosolid appearance.

3.2. GROUP 2: PRCC with oncocytic cells and gains of chromosomes 7 and 17

Clinicopathologic data are showed in Table 5. This subgroup contained seven tumors, with 6 males and 1 female. One case (15b) represented a recurrence from a patient initially included in a previous group as case 15a. Clinicopathologic data regarding case 15b are described above. The age of six remaining patients ranged from 40 to 69 years (mean 59.9 years, median 61 years). Tumor size ranged from 1.2 to 5 cm in greatest dimension (median 3 cm, mean 3.3 cm). Pathologic staging was available in 5 cases (pT1a in 3 and pT1b in 2 cases). Follow-up was available in 5/6 patients, ranging 0.5 to 9 years (mean 6.7 years, median 6 years). No records concerning aggressive behavior were found in 4 patients, while one patient died of the disease 6 years post-surgery.

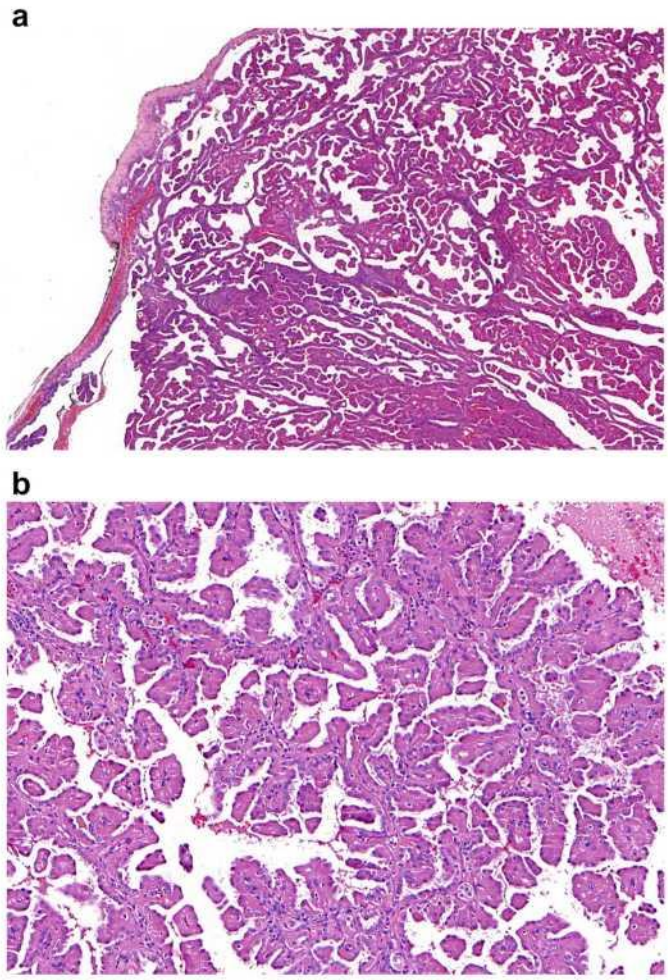

Fig. 3. A: Two cases from "PRCC with oncocytic cells and renal oncocytoma-like CNV group" fulfilled diagnostic criteria for "PRCC with reverse polarity".
B: Neoplastic cells were arranged in single row on papillary cores.

Morphologic data are summarized in Table 6. Morphologically, three cases had only or predominantly papillary architecture (in 1 case with focal tubulopapillary areas, and in 1 case with compressed papillae). In two cases, there were papillary areas admixed with tubular and cystic areas (in 1 case), and with more solid and tubular compressed areas (in 1 case) (Fig. 4A+B). Two cases were composed of compressed tubulopapillary/tubular structures. Nuclear grade was 2 in 3/7 cases, and grade 3 in 4/7 tumors (WHO/ISUP). Pseudostratification was focally present in 1 case, in the remaining 6/7 cases was not documented. Three tumors contained macrophages. Psammoma bodies were found in one case. Hemosiderin deposition was found in one case and large hemorrhage in another case.

The immunohistochemical results are summarized in Table 7. All cases were positive for MIA, racemase (AMACR), and vimentin (in 4/7 cases focally). CD117, Melan A, HMB45, TFE3 were negative. CK7 positivity was found in 4/7 cases (in one case focally), while two cases showed reactivity for CK20. Carbonic anhydrase IX was focally positive in 2/7 tumors and GATA3 in one tumor (case 29, this case did not meet the morphologic criteria of PRCC with reverse polarity). Cyclin D1 was

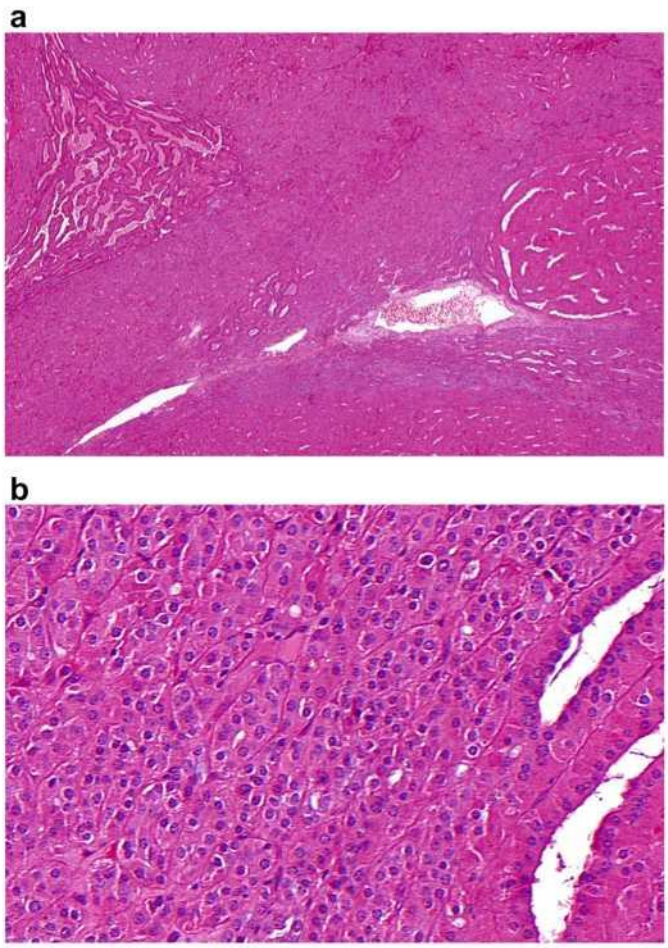

Fig. 4. A: Some cases from group 2 (PRCC with oncocytic cells and gains of chromosomes 7 and 17) showed papillary areas only focally, admixed with more solid and tubular compressed areas.
B: Oncocytic neoplastic cells formed solid component reaching grade 3 (ISUP/WHO).

positive in 7/7 cases (in 3 cases focally).

Cytogenetic study detected gain of chromosomes 7 and 17 in all these cases (Table 8). Loss of chromosome Y was noted in 4/6 male patients and loss of chromosome X in 1/1 female. In four cases, there were additional cytogenetic changes characteristic for RO (1× rearrangement of *CCND1*, 1× deletion 1p36 together with loss 14, 1× loss 14, 1× deletion 1p36). In 2 cases, in addition to the polysomies 7 and 17 and loss Y, we noted gain in locus 11q13.

3.3. GROUP 3: PRCC with oncocytic cells and with variable CNV

Basic clinicopathologic data are summarized in Table 9. In this subgroup, nine cases were collected based on the results of cytogenetic study - PRCCs with oncocytic cells and variable CNV not matching the former subgroups. This group included 7 males and 2 females, with age ranged between 55 and 81 years (median 71 years, mean 71.7 years). Size of tumors ranged between 1.3 and 7 cm in the largest dimension (mean 3.9 cm; median 3 cm). Pathologic stage was pT1 in 3 cases (pT1a in 2 cases, pT1b in 1 case), and pT3a in 3 cases. Information about stage was not available in 3 cases. Follow-up data were available for 6 patients (range 4 to 14.5 years, mean 7.5, median 6.2 years). One patient had metastatic disease (lymph nodes metastasis), and one patient died of the disease 4 years post-surgery. Four patients showed no aggressive behavior.

Morphologic features are shown in Table 10. All 9 cases had predominantly/solely papillary architecture (in 1 case there were focal tubular and cystic areas, and in 1 case focally tubulopapillary areas). In 2/9 cases papillary structures were predominantly compressed. Four tumors had nuclear grade 2, and four tumors had nuclear grade 3 (WHO/ISUP). Nuclear pseudostratification was present in 3 cases (in 2/3 cases focally). Two tumors contained macrophages (Fig. 5), and hemosiderin deposition was found in four cases. One tumor contained psammoma bodies and necrosis was documented in 1 case.

Immunohistochemical findings are summarized in Table 11. All cases were positive for MIA, vimentin (focal positivity in 3 cases), and Cyclin D1 (6 cases with focal positivity, positive single cells in 1 case). CK20, CD117, TFE3, Melan A, HMB45, and GATA3 were negative in all cases. Six cases were positive for CK7 (2/6 cases focally, single cells reactivity in 1/6). Carbonic anhydrase IX showed focal positivity in 3/8 cases.

Cytogenetic study in this subgroup showed variable results (Table 12). Cases frequently showed cytogenetic changes partially overlapping with both PRCC and RO. However, in contrast with the former two subgroups, the full cytogenetic overlap with either of PRCC or RO was not recorded in any of these cases. Namely, 2/9 cases had polysomy of chromosome 17 and loss of chromosome Y; 2/9 cases showed loss of chromosome 17; 1/9 case showed loss of chromosome 7 and loss of chromosome 17. In 1/9 case loss of chromosome 17, together with loss of chromosome Y and deletion 1p36 was found. In 1/9 case loss of chromosome 17 together with loss of chromosome Y was found. In 1/9 case gain of chromosome 7 together with loss of chromosome 17 was documented. Finally, in 1/9 case gain of chromosome 7 together with loss of chromosome Y was encountered.

3.4. Inferential analysis findings

This analysis was carried out to examine statistical significant differences between the above-mentioned three cohorts. No significant statistical differences were found between mean age of patients in group one (PRCC with oncocytic cells and RO-like CNV) and the other two groups. Similar findings were also observed for following variables: sex, tumor size, pathologic staging, and clinical follow-up data. Data on age, sex, and pathologic staging were statistically different between the second group (PRCC with oncocytic cells and gains of chromosomes 7 and 17) and the third group (PRCC with oncocytic cells and with variable CNV).

4. Discussion

The so-called "OPRRC" was first time described in 2005 by Lefevre et al. [8]. The authors published 10 tumors with combined extensive papillary architecture and oncocytic neoplastic cells (packed by mitochondrias, which imparts a finely granular appearance of the cytoplasm) in a single layer. The presence of mitochondrias was further verified by electron-microscopy and supported by specific immunolabeling with anti-mitochondria antigen antibody (MIA). The tumors showed immunohistochemical profile similar to PRCC (AMACR and vimentin positivity). However, the cytogenetic features were similar to RO. None of the cases showed trisomy of chromosome 7 and/or 17. The authors used a descriptive term "adult papillary tumor with oncocytic cells". A few months later, a study of other 12 cases was subsequently published [9]. Similarly to the initial study, the tumors were mostly composed of papillary structures lined by single (occasionally pseudostratified) layers of cells with granular eosinophilic cytoplasm, electron-microscopically filled by numerous mitochondria, and with an immunoprofile "typical" of PRCC. However, few cases showed pseudostratification. Interestingly, in 11/12 cases solid areas with morphological features overlapping with typical RO were documented. Nine cases presented with higher nuclear grade. Cytogenetic study of these tumors detected changes usually described in PRCC (polysomy of chromososome 7 and/or 17) in majority of cases. The authors for the first time used the term

Table 3
GROUP 1: PRCC with oncocytic cells and renal oncocytoma-like CNV – immunohistochemistry.

CASE	MIA	CK7	CK20	CD117	TFE3	Melan A	HMB45	AMACR	VIM	Cyclin D1	GATA3	CANH
CASE 1*	+++	Foc. ++	–	–	–	–	–	+++	Foc. +++	SC +	–	Foc. +++
CASE 2*	+++	–	–	–	–	–	–	+++	+++	SC +++	–	Foc. +++
CASE 3*	+++	+++	–	–	–	–	–	+	Foc. +	+++	+++	–
CASE 4*	+++	+++	–	–	–	–	–	+++	++	+++	–	Foc. +++
CASE 5*	+++	–	–	–	–	–	–	Foc. +++	+++	SC +	–	Foc. +++
CASE 6*	+++	–	–	–	–	–	–	+	+++	++	–	–
CASE 7*	+++	Foc. ++	–	–	–	–	–	+++	+++	+ SC	–	–
CASE 8*	+++	Foc. +++	–	–	–	–	–	NA	+++	Foc. +++	–	–
CASE 9*	++	–	–	–	–	–	–	+++	+++	+ SC	NA	NA
CASE 10*	+++	–	–	–	–	–	–	+++	+++	Foc. +++	–	Foc. +++
CASE 11	+++	++	–	–	–	–	–	+++	+++	++	–	–
CASE 12	+++	–	–	–	–	–	–	+++	+++	++	–	–
CASE 13	++	–	–	–	–	–	–	+++	+++	++	–	–
CASE 14	+++	–	–	–	–	–	–	+++	+++	++	–	–
CASE 15[a]	+++	++ SC	+++	–	–	–	–	+++	+++	–	–	Foc. +++
CASE 16	+++	+++	–	–	–	–	–	–	+++	++	+++	–
CASE 17	+++	–	–	–	–	–	–	+++	+++	+	–	–
CASE 18	+++	+++	–	–	–	–	–	+++	+++	+++	–	–
CASE 19	+++	–	–	–	–	–	–	+++	+++	++	–	–
CASE 20	+++	Foc. +	–	–	–	–	–	++	+++	+ SC	–	–
CASE 21	+++	+++	–	–	–	–	–	+++	+++	++	–	Foc. +++
CASE 22	+++	Foc. +	–	–	++ [a]	–	–	+++	+++	–	–	–
CASE 23	+++	–	–	–	+++ [a]	–	–	+++	+++	++	–	–

– negative, + weak positivity, ++ moderate positivity, +++ strong positivity, *Foc.* focally (up to 50%), *SC* single cells.
[a] FISH (break *TFE3*) negative.
* Cases previously included in study by Michalova et al. [5].

Table 4
GROUP 1: PRCC with oncocytic cells and renal oncocytoma-like CNV - cytogenetic study.

CASE	Del 1p36	Enumeration 1	BA BCL1 (CCND1)	Enumeration BCL1 (CCND1)	Enumeration 7	Enumeration 14	Enumeration 17	X/Y	SWIFT KRAS
CASE 1[a]	Negative	Negative	Negative	Negative	Negative	Negative	Negative	Loss Y	NP
CASE 2[a]	Present	Negative	Negative	Negative	Negative	Loss	Negative	Negative	NP
CASE 3[a]	Negative	Negative	Present	NA	Negative	Negative	Negative	Negative	Mutation KRAS c.35G>A, p.(Gly12Asp), AF:30%
CASE 4[a]	Negative	Negative	Negative	NA	Negative	Negative	Negative	Negative	NP
CASE 5[a]	Negative	Negative	Negative	Negative	Negative	Negative	Negative	Negative	NP
CASE 6[a]	Present	Negative	Negative	Negative	Negative	Negative	Negative	Negative	NP
CASE 7[a]	Negative	Negative	Negative	Negative	Negative	Negative	Negative	Loss Y	NP
CASE8[a]	Negative	Negative	Negative	Negative	Negative	Negative	Negative	Negative	NP
CASE 9[a]	Present	Negative	Negative	Negative	Negative	Negative	Negative	Negative	NP
CASE 10[a]	Present	Negative	Negative	NA	Negative	loss	Negative	Loss Y	NP
CASE 11	Negative	Negative	Present	Negative	Negative	Negative	Negative	NA	NP
CASE 12	Negative	Negative	Negative	Negative	Negative	Negative	Negative	Loss X	NP
CASE 13	Present	Negative	Negative	Negative	Negative	Negative	Negative	Loss Y	NP
CASE 14	Negative	Negative	Negative	Negative	Negative	Negative	Negative	Negative	NP
CASE 15a	NA	NA	Negative	Negative	Negative	Negative	Negative	Negative	NP
CASE 16	Negative	Negative	Negative	Negative	Negative	Negative	Negative	Negative	Mutation KRAS c.181C>A, p.(Gln61Lys), AF:19%
CASE 17	Negative	Negative	Negative	Negative	Negative	Negative	Negative	Loss Y	NP
CASE 18	Negative	Negative	Negative	Negative	Negative	loss	Negative	Negative	NP
CASE 19	Negative	Negative	Negative	Negative	Negative	Negative	Negative	Negative	NP
CASE 20	Negative	Negative	Negative	Negative	Negative	Negative	Negative	Negative	Negative
CASE 21	Negative	Negative	Negative	Negative	Negative	Negative	Negative	Loss Y	Negative
CASE 22	Present	Negative	Negative	Negative	Negative	Negative	Negative	Loss Y	Negative
CASE 23	Negative	Negative	Negative	Negative	Negative	loss	Negative	Loss Y	NA

NA not available, *NP* not performed.
[a] Cases previously included in study by Michalova et al. [5].

oncocytic PRCC, and since then, a number of different studies have been published, mostly with conflicting results [10-12].

The so-called "OPRCC" is not yet fully characterized. The basic morphologic criteria (papillary and/or tubulopapillary architecture and cells with abundant granular/oncocytic cytoplasm) are non-specific and a number of different renal tumors meets these characteristics. Particularly, the term "oncocytic" is frequently erroneously applied to all cells with voluminous eosinophilic cytoplasm, without confirming their true "oncocytic" nature by immunohistochemical or electron microscopic examination. Another problematic point is the definition of OPRCC by WHO 2016. When applying the 2016 WHO criteria, majority of the tumors from the initial studies [8,9] would not fulfill the proposed morphologic characteristics for the diagnosis of OPRCC [3]. However, the majority of these initial cases would mostly be compatible with another recently described PRCC subtype – "PRCC with reverse polarity" [4].

Table 5
GROUP 2: PRCC with oncocytic cells and gains of chromosomes 7 and 17 - clinical data.

CASE	SEX	AGE	SIDE	SIZE – in the greatest dimension (cm)	STAGE	FU	
CASE 24	M	69	R	5	pT1b	6y	DOD
CASE 25	M	63	NA	3	pT1a	9y	DNED
CASE 26	M	59	L	3	pT1a	10y	ANED
CASE 27	F	59	R	1.2	pT1a	8y	ANED
CASE 28	M	40	NA	NA	NA	LFU	LFU
CASE 29	M	67	R	4.5	pT1b	0.5y	ANED
CASE 15b	M	64	R	2.4	pT1a	8y	AWD

M male, *F* female, *L* left, *R* right, *NA* not available, *DNED* death with no evidence of disease, *ANED* alive with no evidence of disease, *AWD* alive with the disease, *DOD* death of the disease, *LFU* lost for follow up.

In this study, we presented a cohort of tumors fulfilling the basic criteria for the diagnosis of so-called "OPRCC" as it has been used in previously published studies (papillary and/or tubulopapillary architecture and cells with abundant oncocytic cytoplasm packed with mitochondria) [8-12]. Following strict criteria accepted by the WHO 2016, substantial part of our cohort cannot be classified as OPRCC. According to WHO 2016, the combination of morphology and immunoprofile of the tumors discussed herein would classify them either as OPRCC or PRCC, NOS. Therefore, we decided to split our cases into 3 distinct categories using CNV and other molecular features as a divider line: RO-like group, 7 and 17 polysomy group, and mixture of patterns.

Our cytogenetic findings showed interesting results and occasional overlapping diagnostic features. Only seven cases (17.9%) showed polysomy of chromosome 7 and 17, which is consistent with traditional cytogenetic changes of PRCC, particularly the so-called type 1 [13]. Interestingly, four cases with chromosome 7 and 17 polysomy concurrently had some RO-like cytogenetic features as well. Molecular genetic changes consistent with the diagnosis of RO were documented in 28/39 cases (71.8%). Five cases showed variable cytogenetic profile, with changes partly consistent with RO or with those of PRCC. Four cases in this study showed changes, which not typically belong to either RO or PRCC (loss of chromosomes 7 and/or 17).

Patients were mostly older, only 7/39 were in age under 60 years (only one patient was 40 years). There was a strong male predominance (27:11). Four patients with documented aggressive behavior showed variable cytogenetic profile, thus we were not able to identify any CNV characteristic features associated with aggressive behavior.

Analysis of architectural growth patterns showed overlapping features across all 3 groups. However, the number of cases in each group is relatively small and does not allow to predict any particular subgroup-specific architecture. In all 3 groups, tumors were mainly arranged in papillary and tubulopapillary patterns, while rarely with "pseudosolid" (compressed) areas. Across the study groups 1–3, nuclear pseudostratification was detected in 8/23, 1/7 and 3/9 cases, respectively (in majority of cases only focally). Further, we evaluated the presence of

Table 6
GROUP 2: PRCC with oncocytic cells and gains of chromosomes 7 and 17 - morphologic study.

CASE	Pattern of growth		Cytoplasm	Grade ISUP/ WHO	Pseudostratification	Calcification (C), necrosis (N), hemosiderin (HEM), hemorrhage (HEMOR)	Macrophages
	Presence of papillary structures						
CASE 24	Predominantly	Tubulopapillary (focally compressed)	Granular, abundant, eosinophilic, areas of cells with clear cytoplasm	3, nuclei elevated from BM	No	HEM +	++
CASE 25	Papillary and papillary compressed		Granular, abundant, eosinophilic, cuboidal to cylindrical cells	3	No	HEM +, C + (psammoma)	++
CASE 26	Only		Granular, eosinophilic, cylindrical cells	3	Present focally	Not present	+
CASE 27	Not present	Compressed tubulopapillary, alveolar	Granular, abundant, eosinophilic	2, granular chromatin	No	Not present	Not present
CASE 28	Not present	Compressed tubular	Granular, abundant	2, granular chromatin	No	Not present	Not present
CASE 29	Focally	Predominantly solid, tubullary compressed	Granular, eosinophilic, cuboidal cells	2, granular chromatin	No	Not present	Not present
CASE 15b	Papillae sporadically	Tubular, cystic	Granular, abundant, eosinophilic, intracytoplasmic vacuoles ("empty")	3	No	HEMOR +	Not present

BM basal membrane, + present.

Table 7
GROUP 2: PRCC with oncocytic cells and gains of chromosomes 7 and 17 – immunohistochemistry.

CASE	MIA	CK7	CK20	CD117	TFE3	Melan A	HMB45	AMACR	VIM	Cyclin D1	GATA3	CANH
CASE 24	+++	–	+++	–	–	–	–	+++	Foc. ++	Foc. ++	–	–
CASE 25	++	+++	–	–	–	–	–	+++	++	Foc. +++	–	Foc. +++
CASE 26	++	+++	–	–	–	–	–	+++	+++	Foc. ++	–	Foc. +++
CASE 27	+++	–	–	–	–	–	–	++	+++	+++	–	–
CASE 28	++	Foc. +++	–	–	–	–	–	+	Foc. +++	++	–	–
CASE 29	+++	+++	–	–	–	–	–	+++	Foc. ++	+++	+++	–
CASE 15b	++	–	+++	–	–	–	–	+++	Foc. ++	++	–	–

– negative, + weak positivity, ++ moderate positivity, +++ strong positivity, *Foc.* focally (up to 50%), *SC* single cells.

Table 8
GROUP 2: PRCC with oncocytic cells and gains of chromosomes 7 and 17 - cytogenetic study.

CASE	Del 1p36	Enumeration 1	BA BCL1 (CCND1)	Enumeration BCL1 (CCND1)	Enumeration 7	Enumeration 14	Enumeration 17	X/Y	SWIFT KRAS
CASE 24	Negative	Negative	Present	NA	Gain	Negative	Gain	Negative	NP
CASE 25	Negative	Negative	NA	NA	Gain	Negative	Gain	Negative	NP
CASE 26	Negative	Negative	Negative	Gain	Gain	Negative	Gain	Loss Y	NP
CASE 27	Present	Negative	Negative	Negative	Gain	Loss	Gain	Loss X	NP
CASE 28	NA	NA	Negative	Gain	Gain	NA	Gain	Loss Y	NP
CASE 29	Negative	Loss	Negative	Negative	Gain	Loss	Gain	Loss Y	NP
CASE 15b	Present	Negative	Negative	Negative	Gain	Negative	Gain	Loss Y	NP

NA not available, *NP* not performed.

Table 9
GROUP 3: PRCC with oncocytic cells and with variable CNV – clinical data.

CASE	SEX	AGE	SIDE	SIZE – in the greatest dimension (cm)	STAGE	FU
CASE 30	M	73	R	3	pT1a	4.3y ANED
CASE 31	M	71	R	3	NA	LFU
CASE 32	M	55	NA	7	pT3a	4y DOD
CASE 33	M	70	R	4	pT3a	10y AWD (Lymph nodes metastasis)
CASE 34	F	81	R	2	NA	LFU
CASE 35	M	69	L	6.5	pT1b	14.5y DNED
CASE 36	F	70	L	6	pT3a	8y ANED
CASE 37	M	75	R	2	pT1a	4.3y ANED
CASE 38	M	81	R	1.3	NA	LFU

M male, *F* female, *L* left, *R* right, *NA* not available, *DNED* death with no evidence of disease, *ANED* alive with no evidence of disease, *AWD* alive with the disease, *DOD* death of the disease, *LFU* lost for follow up.

foam cells, calcifications, hemorrhagia, hemosiderin and necrosis, which yielded no differences between the study groups. There were no significant differences in immunohistochemical profile among the study groups, with all cases positive for MIA, AMACR and vimentin. Immunoreactivity for CK7, CK20, AMACR, cyclin D1, GATA3, and carbonic anhydrase IX was variable across the three groups. All tumors were negative for CD117, HMB45, and Melan A. No correlation between immunoprofile and CNV status was found.

An interesting finding in this study were 2 cases fulfilling the diagnostic criteria (both morphologically and immunohistochemically) for so-called PRCC with reverse polarity. Both cases were listed in the group of PRCC with oncocytic cells and RO-like CNV. Moreover, we showed *KRAS* mutation in both tumors, believed to be another characteristic feature of PRCC with reverse polarity.

Case 15 provided another interesting and study design complicating results. The primary tumor (case 15a) showed molecular genetic pattern similar to RO, while its recurrence (case 15b) presented with polysomy of chromosomes 7 and 17. Primary lesion exhibited mostly tubular architectural pattern with cystic changes, the recurrent tumor was predominantly tubular. However in recurrent lesion, intracytoplasmic vacuoles were focally present. Both primary and recurrent tumor expressed CK20. Such findings demonstrated that renal cell carcinomas with papillary/tubulopapillary patterns and oncocytic cells are heterogeneous and that CNV analysis can potentially be confusing and need to be interpreted with caution.

The differential diagnosis of "oncocytic" renal tumors is rather challenging and includes RO, OPRCC, chromophobe renal cell carcinoma, and less frequently encountered neoplasms such as so-called hybrid oncocytic-chromophobe tumor/low grade oncocytic neoplasia of uncertain malignant potential (according to the WHO 2016 classified as chromophobe RCC), so-called low-grade oncocytic tumor (LOT), and so-called eosinophilic vacuolated tumor [3,14].

Because of oncocytic features of the neoplastic cells and the presence of more "solid" areas in our tumors, RO is a morphological leading differential diagnosis. It should be noted that sometimes, focal papillary foci can even be seen in RO [15]. Alveolar growth pattern, occasionally with island-like structures in a rich fibrotic or edematous background is characteristic for RO. Membranous positivity of CD117 is also typical for RO [16]. AMACR positivity was described in RO [17], and central scar-like areas in RO can show focal positivity for vimentin at the periphery or in small clusters scattered throughout the tumor [18]. The cytogenetic alterations in RO encompass enumeration of chromosome 1 (loss of whole chromosome 1or its deletion – typically 1p36), and/or loss of chromosome 14, and/or loss of gonosomes (X/Y), and/or 11q13 rearrangement (gene *CCND1*) or normal karyotype. Recent study of 130 RO identified three classes of mutually exclusive cytogenetic categories in RO: Rearrangement 11q13 – *CCND1* gene, loss of chromosome 1 and/or losses of Y in males and X in females and divergent types of chromosome abnormalities. The authors raised hypothesis that cytogenetic categories may have different roles in initiation and/or progression of the disease [19]. Cytogenetic study in our cases also showed features overlapping with RO (similar to Lefevre's study [8]). Based on our findings, it seems that extensive sampling of the tumor, aiming to identify papillae with foam cells, is more effective than utilizing expensive genetic testing [9].

Papillary architecture can rarely be seen in chromophobe RCC, but characteristic cytologic features such as so-called raisinoid nuclei and perinuclear clearing, as well as combination of large leaf-like cells and smaller eosinophilic cells can help to establish correct diagnosis [20]. So-called low-grade oncocytic tumor (LOT), and so-called eosinophilic vacuolated tumor are solid tumors, without papillation or well-formed papillae. Both tumors can be easily ruled out using basic morphologic features [14,21].

As previously mentioned, both the primary tumor and the recurrence of one of the cases (case 15) was diffusely reactive for CK20 (with variable intensity). Similar pattern was also documented in another primary tumor in our study. The former case was grouped as "PRCC with oncocytic cells and RO-like CNV" group, while the recurrence and the latter case were listed in group of "PRCC with oncocytic cells and gains of chromosomes 7 and 17". It is important to note that CK20 positivity can be seen in up to 85% of eosinophilic solid and cystic RCC (ESC) RCCs. In our study, CK20 positive cases did show neither solid and cystic architectures, nor voluminous eosinophilic cytoplasm with cytoplasmic stippling, which is typical in ESC RCCs. CNV pattern for ESC is also different, with no polysomy of chromosomes 7 and 17 being reported [22].

Our findings clearly showed that tumors grouped under umbrella term "OPRCC" forms a heterogeneous group of renal tumors. Although they all share papillary/tubulopapillary architecture with oncocytic

Table 10
GROUP 3: PRCC with oncocytic cells and with variable CNV - morphologic study.

CASE	Pattern of growth		Cytoplasm	Grade ISUP/WHO	Pseudostratification	Calcification (C), necrosis (N), hemosiderin (HEM), hemorrhage (HEMOR)	Macrophages
	Presence of papillary structures	Presence of other structures					
CASE 30	Predominantly	Tubular, cystic	Granular, abundant, eosinophilic	3, granular chromatin	No	HEM +	+
CASE 31	Only		granular, abundant, eosinophilic, cylindrical cells	3	Present	Not present	Not present
CASE 32	Papillary compressed, focally to "solid"		Granular, eosinophilic, cuboidal to cylindrical cells	2, granular chromatin	Present focally	Not present	Not present
CASE 33	Only		Granular, eosinophilic, cuboidal cells	2, granular chromatin	No	HEM + (occasionally fine pigmentation in the stalks)	Not present
CASE 34	Only, focally compressed		Abundant, granular, eosinophilic, cuboidal to cylindrical cells	2, nuclei centrally located	No	Not present	Not present
CASE 35	Only		Granular, abundant, eosinophilic, apically slightly granular and eosinophilic "globules", cylindrical cells	3, granular chromatin, luminal localization of nuclei	Present focally	C + (psammomatous), HEM + (prominent granular disperse)	Not present
CASE 36	Predominantly	Tubulopapillary	Granular, eosinophilic, focally clear cell changes, cuboidal cells	3, optically empty, nuclei centrally located	No	HEM + (prominent granular disperse), N +, HEMOR +	Not present
CASE 37	Only		Granular, eosinophilic, cuboidal cells	2, granular chromatin, nuclei centrally located	No	N +, HEM + (fine), bloody lakes	+ (collections of foamy macrophages)
CASE 38	Only		Granular, abundant, eosinophilic	2, nuclei centrally located	No	Not present	+ (collections of foamy macrophages)

BM basal membrane, + present.

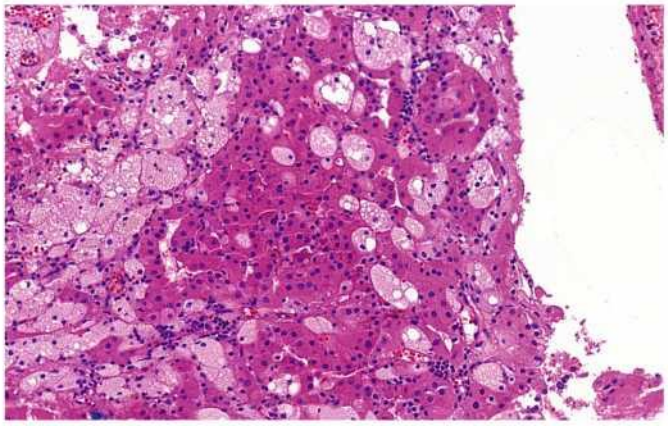

Fig. 5. Some tumors contained voluminous foam cell deposits (e.g. case from group 3: PRCC with oncocytic cells and with variable CNV).

cells, immunohistochemical and molecular genetic profiles are variable. Cytogenetic changes may be similar to RO at one end of the spectrum or identical to typical PRCC "type 1" at the other end. Unfortunately, as broad is the genetic profile, as variable biologic behavior and prognosis would be. In this study, 4/26 cases (15.4%) showed aggressive clinical course. Two cases with stage pT1b (first case was part of PRCC with oncocytic cells and CNV equal to renal oncocytoma and second case was part of PRCC with oncocytic cells and gains of chromosomes 7 and 17) developed aggressive clinical course. The two other cases with stage pT3a also developed metastatic aggressive disease; both were in group 3 "PRCC with oncocytic cells and variable CNV". Abnormalities in *CCND1* gene did not have impact on biologic behavior either.

Our findings suggest that using molecular testing in diagnosing PRCC with oncocytic cells can be potentially misleading, as the majority of such cases show cytogenetic features consistent with the diagnosis of RO. We would also not recommend using cytogenetic analysis in limited material (i.e., core biopsy) to establish the diagnosis as this can be misleading. However, in tumors composed of oncocytic cells but with debatable architecture (i.e., papillary, tubulopapillary and compressed/solid), all available diagnostic modalities should be appropriately utilized. Nonetheless, we recommend generous sampling of surgical

Table 11
GROUP 3: PRCC with oncocytic cells and with variable CNV – immunohistochemistry.

CASE	MIA	CK7	CK20	CD117	TFE3	Melan A	HMB45	AMACR	VIM	Cyclin D1	GATA3	CANH
CASE 30	+++	+++	–	–	–	–	–	+++	+++	SC +	NA	NA
CASE 31	+++	Foc. ++	–	–	–	–	–	+++	++	Foc. +	–	–
CASE 32	+++	–	–	–	–	–	–	+++	++	Foc. +	–	–
CASE 33	+++	–	–	–	–	–	–	NA	Foc. +	Foc. ++	–	–
CASE 34	++	–	–	–	–	–	–	+++	+++	Foc. ++	–	–
CASE 35	+++	+++	–	–	–	–	–	+++	Foc. +++	Foc. ++	–	Foc. +++
CASE 36	+++	+ SC	–	–	–	–	–	+++	+++	Foc. +++	–	–
CASE 37	+++	+++	–	–	–	–	–	+++	Foc. ++	+++	–	Foc. +++
CASE 38	+++	Foc. ++	–	–	–	–	–	+++	+++	+	–	Foc. ++

– negative, + weak positivity, ++ moderate positivity, +++ strong positivity, *Foc.* focally (up to 50%), *SC* single cells.

Table 12
GROUP 3: PRCC with oncocytic cells and with variable CNV – cytogenetic study.

CASE	Del 1p36	Enumeration 1	BA BCL1 (CCND1)	Enumeration BCL1 (CCND1)	Enumeration 7	Enumeration 14	Enumeration 17	X/Y	SWIFT KRAS
CASE 30	Negative	Negative	Negative	Negative	Loss	Negative	Loss	Negative	NP
CASE 31	Negative	Negative	Negative	Negative	Negative	Negative	Gain	Loss Y	NP
CASE 32	Present	Negative	Negative	Negative	Negative	Negative	Loss	Loss Y	NP
CASE 33	Negative	Negative	Negative	Negative	Negative	Negative	Loss	Negative	NP
CASE 34	Negative	Negative	Negative	Negative	Negative	Negative	Loss	Loss Y	Negative
CASE 35	Negative	Negative	Negative	Negative	Negative	Negative	Loss	Negative	NP
CASE 36	Negative	Negative	Negative	Negative	Gain	Negative	Loss	Negative	NP
CASE 37	Negative	Negative	Negative	Negative	Negative	Negative	Gain	Loss Y	NP
CASE 38	Negative	Negative	Negative	Negative	Gain	Negative	Negative	Loss Y	Negative

NA not available, *NP* not performed.

specimen since it seems to be the most reliable method in rendering an accurate diagnosis. For clinical practice and patient management, it is reasonable to potentially "overcall" RO as PRCC than the opposite.

5. Conclusions

Nearly 16 years after the initial description of so-called "OPRCC" and many published and unpublished discussions, "OPRCC" still remains a controversial group of renal carcinomas. With the exception of so-called PRCC with reverse polarity, which seems to be a relatively uniform, compact and well-defined tumor, the vast majority of RCC with papillary/tubulopapillary architecture and oncocytic cells are highly variable in aspects of biologic behavior, morphology, and molecular-genetic features. However, within genitourinary tumors classification this is not an exception. For example, testicular Sertoli cell tumors, NOS share even broader morphologic, immunohistochemical and genetic heterogeneity [3]. Based on our results and existing published data, we would not recommend using the term "OPRCC" as a distinct diagnostic category.

Supplementary data to this article can be found online at https://doi.org/10.1016/j.anndiagpath.2021.151734.

Declaration of competing interest

All authors declare no conflict of interest.

References

[1] Delahunt B, Eble JN. Papillary renal cell carcinoma: a clinicopathologic and immunohistochemical study of 105 tumors. Mod Pathol 1997;10(6):537–44.

[2] Trpkov K, Hes O, Williamson SR, Adeniran AJ, Agaimy A, Alaghehbandan R, et al. New developments in existing WHO entities and evolving molecular concepts: the Genitourinary Pathology Society (GUPS) update on renal neoplasia. Mod Pathol 2021. https://doi.org/10.1038/s41379-021-00779-w [Epub ahead of print].

[3] Moch H, Humphrey PA, Ulbright TM, Reuter VE. WHO classification of tumours of the urinary system and male genital organs. Lyon: IARC; 2016.

[4] Al-Obaidy KI, Eble JN, Cheng L, Williamson SR, Sakr WA, Gupta N, et al. Papillary renal neoplasm with reverse polarity: a morphologic, immunohistochemical, and molecular study. Am J Surg Pathol 2019;43(8):1099–111. https://doi.org/10.1097/PAS.0000000000001288.

[5] Michalova K, Steiner P, Alaghehbandan R, Trpkov K, Martinek P, Grossmann P, et al. Papillary renal cell carcinoma with cytologic and molecular genetic features overlapping with renal oncocytoma: analysis of 10 cases. Ann Diagn Pathol 2018;35:1–6. doi:https://doi.org/10.1016/j.anndiagpath.2018.01.010.

[6] Mohapatra G, Betensky RA, Miller ER, Carey B, Gaumont LD, Engler DA, et al. Glioma test array for use with formalin-fixed, paraffin-embedded tissue: array comparative genomic hybridization correlates with loss of heterozygosity and fluorescence in situ hybridization. The Mol Diagn 2006;8(2):268–76. doi:https://doi.org/10.2353/jmoldx.2006.050109.

[7] Petersson F, Gatalica Z, Grossmann P, Perez Montiel MD, Alvarado Cabrero I, Bulimbasic S, et al. Sporadic hybrid oncocytic/chromophobe tumor of the kidney: a clinicopathologic, histomorphologic, immunohistochemical, ultrastructural, and molecular cytogenetic study of 14 cases. Virchows Arch 2010;456(4):355–65. https://doi.org/10.1007/s00428-010-0898-4.

[8] Lefevre M, Couturier J, Sibony M, Bazille C, Boyer K, Callard P, et al. Adult papillary renal tumor with oncocytic cells: clinicopathologic, immunohistochemical, and cytogenetic features of 10 cases. Am J Surg Pathol 2005;29(12):1576–81. https://doi.org/10.1097/01.pas.0000184821.09871.ec.

[9] Hes O, Brunelli M, Michal M, Cossu Rocca P, Hora M, Chilosi M, et al. Oncocytic papillary renal cell carcinoma: a clinicopathologic, immunohistochemical, ultrastructural, and interphase cytogenetic study of 12 cases. Ann Diagn Pathol 2006;10(3):133–9. doi:https://doi.org/10.1016/j.anndiagpath.2005.12.002.

[10] Kunju LP, Wojno K, Wolf Jr JS, Cheng L, Shah RB. Papillary renal cell carcinoma with oncocytic cells and nonoverlapping low grade nuclei: expanding the morphologic spectrum with emphasis on clinicopathologic, immunohistochemical and molecular features. Hum Pathol 2008;39(1):96–101. https://doi.org/10.1016/j.humpath.2007.05.016.

[11] Xia QY, Rao Q, Shen Q, Shi SS, Li L, Liu B, et al. Oncocytic papillary renal cell carcinoma: a clinicopathological study emphasizing distinct morphology, extended immunohistochemical profile and cytogenetic features. Int J Clin Exp Pathol 2013;6(7):1392–9.

[12] Han G, Yu W, Chu J, Liu Y, Jiang Y, Li Y, et al. Oncocytic papillary renal cell carcinoma: a clinicopathological and genetic analysis and indolent clinical course in 14 cases. Pathol Res Pract 2017;213(1):1–6. https://doi.org/10.1016/j.prp.2016.04.009.

[13] Pitra T, Pivovarcikova K, Alaghehbandan R, Hes O. Chromosomal numerical aberration pattern in papillary renal cell carcinoma: review article. Ann Diagn Pathol 2019;40:189–99. doi:https://doi.org/10.1016/j.anndiagpath.2017.11.004.

[14] Trpkov K, Williamson SR, Gill AJ, Adeniran AJ, Agaimy A, Alaghehbandan R, et al. Novel, emerging and provisional renal entities: the Genitourinary Pathology Society (GUPS) update on renal neoplasia. Mod Pathol 2021. https://doi.org/10.1038/s41379-021-00737-6.

[15] Amin MB, Crotty TB, Tickoo SK, Farrow GM. Renal oncocytoma: a reappraisal of morphologic features with clinicopathologic findings in 80 cases. Am J Surg Pathol 1997;21(1):1–12. https://doi.org/10.1097/00000478-199701000-00001.

[16] Reuter VE, Argani P, Zhou M, Delahunt B, Members of the IIiDUPG. Best practices recommendations in the application of immunohistochemistry in the kidney tumors: report from the International Society of Urologic Pathology consensus conference. Am J Surg Pathol 2014;38(8):e35–49. doi:https://doi.org/10.1097/PAS.0000000000000258.

[17] Tretiakova MS, Sahoo S, Takahashi M, Turkyilmaz M, Vogelzang NJ, Lin F, et al. Expression of alpha-methylacyl-CoA racemase in papillary renal cell carcinoma. Am J Surg Pathol 2004;28(1):69–76. https://doi.org/10.1097/00000478-200401000-00007.

[18] Hes O, Michal M, Kuroda N, Martignoni G, Brunelli M, Lu Y, et al. Vimentin reactivity in renal oncocytoma: immunohistochemical study of 234 cases. Arch Pathol Lab Med 2007;131(12):1782–8. https://doi.org/10.1043/1543-2165(2007)131[1782:VRIROI]2.0.CO;2.

[19] Anderson CB, Lipsky M, Nandula SV, Freeman CE, Matthews T, Walsh CE, et al. Cytogenetic analysis of 130 renal oncocytomas identify three distinct and mutually exclusive diagnostic classes of chromosome aberrations. Genes Chromosomes Cancer 2019. doi:https://doi.org/10.1002/gcc.22766.

[20] Michalova K, Tretiakova M, Pivovarcikova K, Alaghehbandan R, Perez Montiel D, Ulamec M, et al. Expanding the morphologic spectrum of chromophobe renal cell

carcinoma: a study of 8 cases with papillary architecture. Ann Diagn Pathol 2020; 44:151448. doi:https://doi.org/10.1016/j.anndiagpath.2019.151448.
[21] Trpkov K, Hes O. New and emerging renal entities: a perspective post-WHO 2016 classification. Histopathology. 2019;74(1):31–59. doi:https://doi.org/10.1111/his.13727.
[22] Trpkov K, Hes O, Bonert M, Lopez JI, Bonsib SM, Nesi G, et al. Eosinophilic, solid, and cystic renal cell carcinoma: clinicopathologic study of 16 unique, sporadic neoplasms occurring in women. Am J Surg Pathol 2016;40(1):60–71. https://doi.org/10.1097/PAS.0000000000000508.

1.2.3 Papillary renal cell carcinoma with cytologic and molecular genetic features overlapping with renal oncocytoma: Analysis of 10 cases

Tato studie se zaměřila na 10 renálních tumorů kombinujících v sobě morfologický vzhled PRCC, onkocytického PRCC (OPRCC) a renálního onkocytomu (RO) a molekulárně genetické pozadí RO. V rámci prezentované studie tak byly z plzeňského registru nádorů vybrány případy, které vykazovaly unimorfní histologický vzhled s predominantně papilárním, tubulopapilárním či pseudosolidním (komprimované papily) způsobem růstu a sestávali z onkocytických buněk. Od OPRCC (tak jak je definován současnou WHO 2016) se případy odlišovaly pseudostratifikací jader a vyšším nukleárním gradem. Vzhledem k přítomnosti solidnějších okrsků, tumory někdy vzdáleně připomínaly RO. Nádory byly vyšetřeny širokým imunohistochemickým panelem a cytogeneticky. Pro účely této studie pak bylo dále vybráno pouze 10 případů PRCC, u nichž byly geneticky prokázány cytogenetické znaky typicky popisované u RO (tj. ztráta 1p36, ztráta chromozomu Y, rearanže genu *CCND1* a numerické změny chromozomu 14).

Pacienty bylo pět žen a pět mužů, ve věkovém rozmezí 56 - 79 let (průměr 66,8 let). Velikost tumorů se pohybovala v rozmezí 2 - 10 cm (průměr 5,1 cm). Údaje o dalším průběhu onemocnění byly dostupné u 8/10 pacientů (průměrně v délce trvání 5,2 let). Jeden pacient zemřel na následky onemocnění, 7/8 pacientů jsou ve zdravotnických databázích vedeni jako živí a zdraví. Imunohistochenická analýza prokázala reaktivitu všech případů pro racemázu (AMACR), vimentin, PAX8, OSCAR, CAM5.2 a MIA. Exprese SDHB byla zachována ve všech případech. Mírně variabilnější byla pozitivita v CD10 (9/10 případů), CK7 (7/10 případů), Catepsinu K (4/10 případů) a AE1/3 (2/10 případů). Žádný případ nevykazoval pozitivitu v barvení CD117, HMB45 a CK20.

I přes detekované chromozomální numerické abnormality, mluvící ve prospěch RO, jsme všechny případy vzhledem jejich predominantně papilárnímu/tubulopapilárnímu uspořádání a imunofenotypu (pozitivita AMACR, vimentinu a negativita CD117) klasifikovali jako součást spektra PRCC. Tato studie tak dále expanduje spektrum PRCC a přidává kohortu PRCC, která představuje diagnostickou výzvu a může být potenciálně agresivní.

Annals of Diagnostic Pathology 35 (2018) 1–6

Contents lists available at ScienceDirect

Annals of Diagnostic Pathology

journal homepage: www.elsevier.com/locate/anndiagpath

Papillary renal cell carcinoma with cytologic and molecular genetic features overlapping with renal oncocytoma: Analysis of 10 cases

Kvetoslava Michalova[a], Petr Steiner[a], Reza Alaghehbandan[b], Kiril Trpkov[c], Petr Martinek[a], Petr Grossmann[a], Delia Perez Montiel[d], Maris Sperga[e], Lubomir Straka[f], Kristyna Prochazkova[g], Dana Cempirkova[h], Vladimir Horava[i], Stela Bulimbasic[j], Kristyna Pivovarcikova[a], Ondrej Daum[a], Ondrej Ondic[a], Pavla Rotterova[k], Michal Michal[a], Milan Hora[g], Ondrej Hes[a,*]

[a] Department of Pathology, Charles University, Medical Faculty and Charles University Hospital Plzen, Czech Republic
[b] Department of Pathology, Faculty of Medicine, University of British Columbia, Royal Columbian Hospital, Vancouver, BC, Canada
[c] Department of Pathology and Laboratory Medicine, University of Calgary, Calgary Laboratory Services, Calgary, Canada
[d] Department of Pathology, Institute Nacional de Cancerologia, Mexico City, Mexico
[e] Department of Pathology, Rigas Stradins University, Riga, Latvia
[f] Department of Pathology, Alpha Medical, Presov, Slovakia
[g] Department of Urology, Charles University, Medical Faculty and Charles University Hospital Plzen, Czech Republic
[h] Department of Pathology, Regional Hospital Jindrichuv Hradec, Czech Republic
[i] Department of Pathology, Regional Hospital Fridek Mistek, Czech Republic
[j] Department of Pathology, Clinical Hospital Center Zagreb, Zagreb, Croatia
[k] Biopticka laborator, Plzen, Czech Republic

ARTICLE INFO

Keywords:
Kidney
Papillary renal cell carcinoma
Oncocytic
Oncocytoma
High grade
FISH
Chromosomal aberration pattern

ABSTRACT

Background: We present a series of papillary renal cell carcinomas (PRCC) reminiscent of so-called "oncocytic variant of papillary renal cell carcinoma" (OPRCC), included in the 2016 WHO classification as a potential type 3 PRCC. OPRCC is a poorly understood entity, cytologically characterized by oncocytic cells with non-overlapping low grade nuclei. OPRCC is not genotypically distinct and the studies concerning this variant have shown an inconsistent genetic profile. The tumors presented herein demonstrated predominantly papillary/tubulopapillary architecture and differed from OPRCC by pseudostratification and grade 2–3 nuclei (Fuhrman/ISUP). Because there is a morphologic overlap between renal oncocytoma (RO) and PRCC in the cases included in this study, the most frequently affected chromosomes in RO and PRCC were analyzed.

Materials and methods: 147 PRCC composed of oncocytic cells were retrieved from our registry in order to select a group of morphologically uniform tumors. 10 cases with predominantly papillary, tubulopapillary or solid architectural patterns were identified. For immunohistochemical analysis, the following antibodies were used: vimentin, antimitochondrial antigene (MIA), AMACR, PAX8, CK7, CK20, AE1-3, CAM5.2, OSCAR, Cathepsin K, HMB45, SDHB, CD10, and CD117. Enumeration changes of locus 1p36, chromosomes 7, 14, 17, X, Y and rearrangement of *CCND1* were examined by FISH. For further study, only tumors showing karyotype similar to that of RO were selected. The tumors exhibiting either trisomy of chromosomes 7, 17 or gain of Y, thus abnormalities characteristic for PRCC, were excluded.

Results: There were 5 males and 5 females, with patient age ranging from 56 to 79 years (mean 66.8 years). The tumor size ranged from 2 to 10 cm (mean 5.1 cm). Follow-up was available for 8/10 patients (mean 5.2 years); one patient died of the disease, while 7 of 8 are alive and well. Immunohistochemically, all cases were reactive for AMACR, vimentin, PAX8, OSCAR, CAM5.2, and MIA. SDHB was retained in all cases. 9/10 cases were positive for CD10, 7/10 cases reacted with CK7, 4/10 with Cathepsin K, and 2/10 with AE1-3. None of the cases were positive for CD117, HMB45 and CK20. All 10 cases were analyzable by FISH and showed chromosomal abnormalities similar to that usually seen in RO (i.e. loss of 1p36 gene loci, loss of chromosome Y, rearrangement of *CCND1* and numerical changes of chromosome 14).

Conclusions: We analyzed a series of renal tumors combining the features of PRCC/OPRCC and RO, that included pseudostratification and mostly high grade oncocytic cells lining papillary/tubulopapillary structures, karyotype characterized by loss of 1p36, loss of chromosome Y, rearrangement of *CCND1* gene and numerical changes of chromosome 14. Despite the chromosomal numerical abnormalities typical of RO, we classified these tumors as

* Corresponding aurthor at: Department of Pathology, Charles University, Medical Faculty and Charles University Hospital Plzen, Alej Svobody 80, 304 60 Plzen, Czech Republic.
E-mail address: hes@medima.cz (O. Hes).

https://doi.org/10.1016/j.anndiagpath.2018.01.010

part of the spectrum of PRCC because of their predominant papillary/tubulopapillary architecture, immunoprofile that included reactivity for AMACR, vimentin and lack of reactivity for CD117, all of which is incompatible with the diagnosis of RO. This study expands the morphological spectrum of PRCC by adding a cohort of diagnostically challenging cases, which may be potentially aggressive.

1. Introduction

Oncocytic papillary renal cell carcinoma (OPRCC) was first described in a series of 10 cases in 2005 [13], followed by a series of 12 cases published a couple months later [7]. Since then, several studies on OPRCC have been published [12,15,16,18,19,26]. These tumors characteristically show solid to papillary architecture with low grade non-stratified neoplastic cells strikingly resembling renal oncocytoma (RO). There are several aspects of these tumors which are still poorly understood. The cytogenetic results on OPRCC remain controversial in the studies published to date, as some cases show trisomy of chromosome 7 and 17, while others do not [7,12,15,18,19].

We analyzed a cohort of 10 cases selected from a group of morphologically straightforward papillary RCCs composed of oncocytic cells, which we descriptively called "papillary renal cell carcinoma with features of renal oncocytoma" (PRCCRO). PRCCRO differed from "classic" OPRCC mostly by the presence of pseudostratification and high grade nuclei in some cases. With respect to the overlapping features between PRCCRO and OPRCC, we used the same cytogenetic approach when analyzing PRCCRO as in OPRCC. Because of the lack of a comprehensive chromosomal analysis of OPRCC, we decided to evaluate the most frequently affected chromosomes in RO and papillary renal cell carcinoma (PRCC). The goal of this study was to potentially elucidate a morphologic subset of PRCC demonstrating immunohistochemical features of PRCC, but cytogenetic features of RO.

2. Materials and methods

The Pilsen tumor registry was searched using the following keywords "papillary-renal-carcinoma-oncocytic". Of 1563 PRCCs, 147 OPRCCs met the search criteria, during the period 1993–2017. All 147 cases were reviewed by two pathologists (K.M. and O.H.) and subsequently 56 morphologically uniform cases of PRCCs with oncocytic cytoplasm were selected. DNA quality was tested in all OPRCCs and ultimately, 23 cases with good quality of DNA were selected. In order to present as consistent series as possible, we excluded the cases showing either trisomy of chromosomes 7 and 17, chromosomal abnormalities characteristically encountered in PRCC. Within this group, we selected for further analysis 10 cases of PRCC with oncocytic cells which exhibited copy number variation status similar to RO. The clinical information was extracted from the registry records and follow-up data were obtained by contacting the attending clinicians. The tissues for light microscopy was fixed in 4% formaldehyde and embedded in paraffin, using a routine procedure. 5 μm thick sections were cut from the tissue blocks and were stained with hematoxylin and eosin (H&E). One to 18 blocks were available for evaluation per case.

2.1. Immunohistochemistry

The immunohistochemical (IHC) analysis was performed using a Ventana BenchMark ULTRA (Ventana Medical System, Inc., Tucson, Arizona). The following primary antibodies were used: racemase/AMACR (13H4, monoclonal, DAKO, Glostrup, Denmark, 1:200), cytokeratin (CK) 7 (OV-TL12/30, monoclonal, DakoCytomation, Carpinteria CA, USA, 1:200), CK20 (Ks20.8, monoclonal, DAKO, Glostrup, Denmark, 1:100), AE1-3 (AE1/AE3 & PCK26, monoclonal, Ventana Medical Systems, RTU), OSCAR (OSCAR, monoclonal, Covance, Herts, UK, 1:500), (CAM5.2, monoclonal, Ventana, RTU), vimentin (V9, monoclonal, Ventana Medical Systems, RTU), PAX 8 (MRQ-50, monoclonal, CellMarque, Rocklin, CA, RTU), anti-mitochondrial antibody (113-1, monoclonal, Biogenex, San Ramon, CA, 1:500), HMB45 (HMB45, monoclonal, DAKO, Glostrup, Denmark, 1:400), CD117 (polyclonal, DAKO, Glostrup, Denmark, 1:800), CD10 (56C6, Novocastra, Burlingame, CA, 1:20), SDHB (polyclonal, Sigma Aldrich, St. Luis, MS, 1:200), Cathepsin K (3F9, monoclonal, Abcam, Cambridge, UK, 1:100). Antibodies were visualized using the enzymes alkaline phosphatase or peroxidase as detecting systems (both purchased from Ventana Medical System). Appropriate positive controls were used.

2.2. Molecular genetic analysis

2.2.1. Fluorescence in situ hybridization

The enumeration changes of locus 1p36, chromosomes 7, 14, 17, X, Y and rearrangement of *CCND1* (BCL1ba) were examined by Fluorescence In Situ Hybridisation (FISH). In brief, 4-μm-thick formalin fixed paraffin embedded section, were placed on a positively charged slide. Tissues were deparaffinized in xylene two times for 5 min and were washed twice in 96% ethanol and once in deionized water for 5 min. The slides were then heated in the 1 × Target Retrieval Solution (pH 6) (DAKO, Glostrup, Denmark) for 40 min at 95 °C and were cooled for 20 min at room temperature in the same solution. The slides were washed in deionized water for 5 min and digested in protease solution with pepsin (0.5 mg/mL) (Sigma Aldrich) in 0.01 M HCl at 37 °C for 15 min. The slides were then placed into deionized water for 5 min, dehydrated in a series of ethanol solution (70%, 85% and 96% for 2 min each) and air dried. An appropriate amount of FISH probe was diluted according to manufacturer's instructions, and applied onto each

Table 1
Clinicopathologic data.

Case No	Age	Sex	Size (cm)	Follow-up	Pattern	WHO/ISUP nucleolar grade	Stage
1	69	M	10	AW 6 yr; dg of AML	Papillary, compressed papillae	2	NA
2	61	F	7	AW 6 yr	Tubulopapillary	2	NA
3	56	F	2	DOD 4 yr after surgery	Papillary	2	NA
4	65	F	3.5	AW 6 yr	Papillary	2	pT1a
5	68	F	4	AW 1.5 yr	Tubulopapillary	2	pT1a
6	58	F	5	AW 13 yr	Papillary	3	pT1b
7	79	M	9	AW 3 yr	Compressed papillae	2	pT2
8	73	M	3	AW 2 yr	Tubulopapillary	3	pT1a
9	76	M	NA	NA	Papillary	2	NA
10	63	M	3.5	NA	Papillary	3	pT1b

AW alive and well; DOD death of disease; NA not available; yr years, year, dg diagnosis, AML acute myeloid leukemia.

specimen, covered with a glass cover slip and sealed with rubber cement. The slides were incubated in the ThermoBrite™ instrument (StatSpin/Iris Sample Processing, Westwood, MA, USA) with co-denaturation parameters at 85 °C for 8 min and hybridization parameters 37 °C for 16 h. The cover slips were then removed, and the slides were placed in a post-hybridization wash solution (2xSSC/0.3%NP-40) at 72 °C for 2 min. The slides were air-dried in the dark, counterstained with 4′ 6-diamidino-2-phenylindole (DAPI) (VYSIS/Abbott), cover slipped and examined immediately (Probes, used for this study, are showed in Table 3).

Hybridized slides were examined with an Olympus BX51 fluorescence microscope, using a ×100 objective, triple band pass (DAPI/Spectrum Green/Spectrum Orange) filter sets, dual band pass (FITC/Texas Red) and single band pass (Spectrum Green or Spectrum Orange) filters. One hundred randomly selected non-overlapping tumor cell nuclei were examined for the presence of fluorescent signals. Cut-off for loss represented 45% of nuclei with signal losses. For gain and break apart probes, cut-offs were set at 10% of nuclei with more than two signals or with split signals.

3. Results

The clinicopathologic characteristics of the patients are summarized in Table 1. There were 5 males and 5 females with patient age ranging from 56 to 79 years (mean 66.8 years, median 66.5 years). Follow-up was available for 8 of 10 patients (range 1.5–6 year, mean 5.2 years, median 5 years). One patient died of disease 4 years after the surgery, and 7 of 8 were alive. One patient was diagnosed with acute myeloid leukemia 4 years after the surgery, the remaining patients were well and without progression of the disease.

3.1. Gross and microscopic findings

The results are summarized in Table 1. All tumors were solitary, with tumor size ranging from 2 to 10 cm (mean 5.1 cm, median 4.1 cm). Most of the tumors were well demarcated and located in the cortex, containing only occasional hemorrhagic foci. All tumors were confined to the kidney, representing stage pT1 (TNM 2009).

Microscopically, the observed growth patterns included papillary (Fig. 1A), tubulary (Fig. 1B), tubulopapillary (Fig. 1C), solid-papillary, and solid (imparted by compressed papillae) (Fig. 1D) (see Table 1). The tumor cells were arranged in a single, non-overlapping layer (Fig. 2A) or in multiple layers (Fig. 2B) of epithelial cells. The cytoplasm of the neoplastic cells was typically abundant, demonstrating deeply eosinophilic cytoplasm and distinct cell borders (Fig. 2C). The nuclei were located peripherally, and were mostly round to slightly oval, to occasionally irregular in shape, with frequently prominent nucleoli (Fig. 2D) (ISUP nucleolar grading ranged from 2 to 3, see Table 1). At least occasional pseudostratification was documented in all cases. Foci of foamy macrophages were scattered throughout the tumors in variable amounts (Fig. 2E). Occasional psammoma bodies were identified in some tumors (Fig. 2F). Subtle hemorrhagic changes were occasionally present.

3.2. Immunohistochemistry

Immunohistochemical profiles are presented in Table 2. All cases showed diffuse positivity for vimentin (Fig. 3A), AMACR (Fig. 3B), PAX8, cytokeratines OSCAR (positivity was focal in 2 cases) and CAM5.2 (positivity was focal in 6 cases), and MIA. 9/10 cases were positive for CD10, 7/10 cases reacted with CK7 (the positivity was focal in 2 cases), 4/10 cases were positive with Cathepsin K (the positivity was focal in 3 cases) and 2/10 were strongly and diffusely positive with AE1-3. There was single cell positivity with CK20 in Case #2. The remaining cases were completely negative. None of the cases reacted with CD117 and HMB45. SDHB was retained in all cases.

3.3. Fluorescence in situ hybridization

All of the cases were analyzable and the results are shown in Table 3. Briefly, 1p36 locus deletion was detected in 4/10 cases, loss of chromosome Y in 3/10, loss of chromosome 14 in 2/10, while a rearrangement of *CCND1* gene was found in 1/10 cases. None of the tumors showed either trisomy of chromosomes 7 and 17 or gain of chromosome Y.

4. Discussion

PRCC is a malignant tumor derived from the renal tubular epithelium. These tumors were historically sub-classified into type 1 and type 2, based on the absence or presence of cytoplasmic eosinophilia and nuclear pseudostratification [6]. Recently, several distinct variants of PRCC morphologically different from type 1 and type 2 have been described in the literature, reflecting the increasing recognition of the morphologic heterogeneity that exists within the spectrum of PRCC [1,2,8,10,20,25].

Oncocytic cell is defined as an epithelial cell stuffed with mitochondria, which impart a finely granular appearance of the cytoplasm [11]. Oncocytic variants of various tumors are well known in other organs such as in the thyroid (Hurtle cell adenoma/carcinoma), adrenal glands and liver [3,5,17].

The oncocytic variant of PRCC was first described in 2005 by

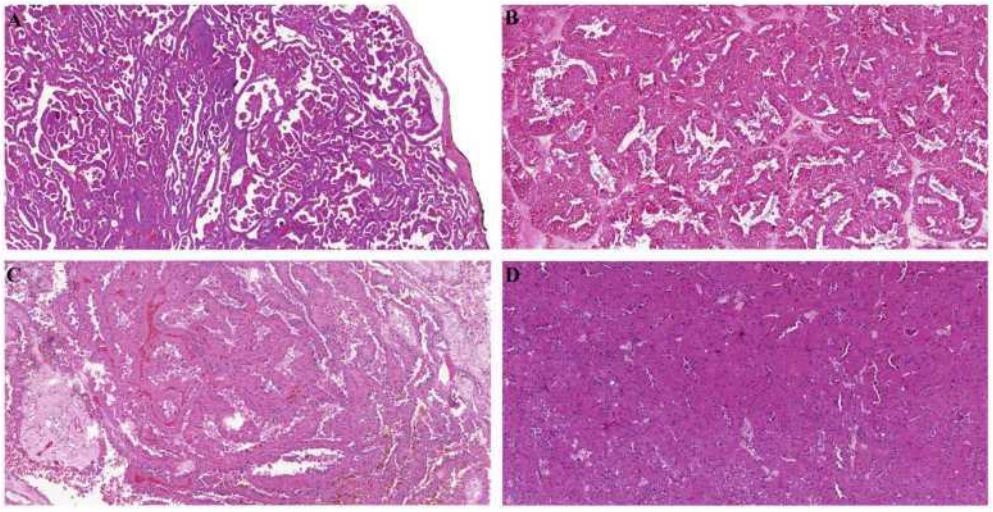

Fig. 1. The growth pattern of the tumors ranged from papillary (A) to tubular (B), with tubulopapillary pattern as an intermediate arrangement (C). Some tumors presented with solid architectural growth pattern resulting from compressed papillae (D).

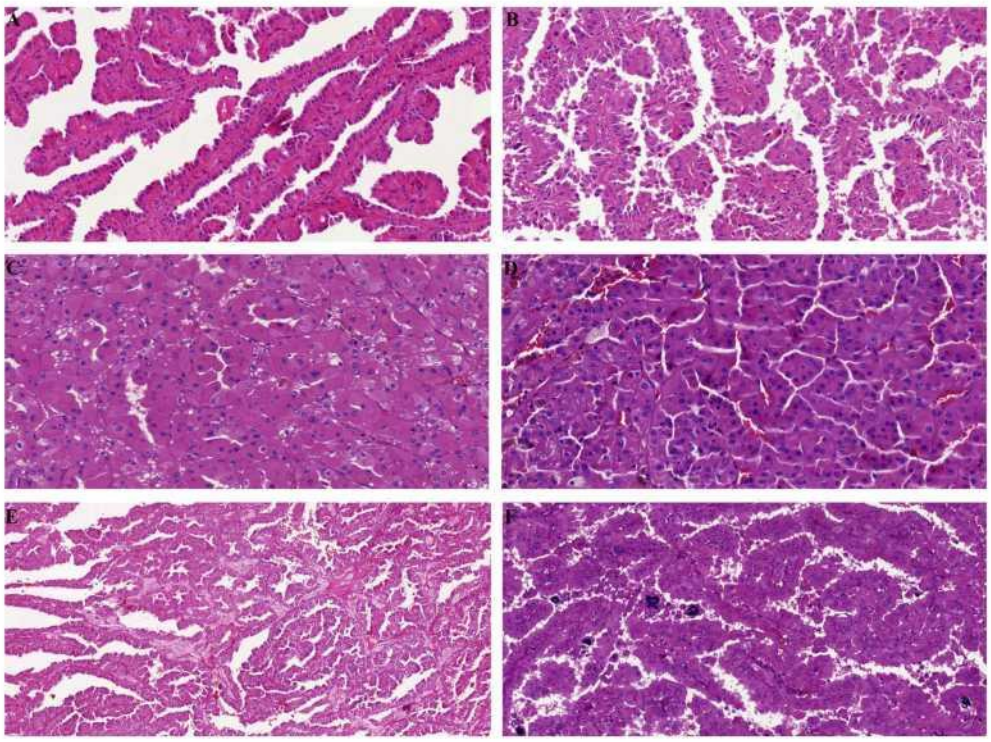

Fig. 2. Tumor cells were mostly arranged in a single layer without pseudostratification (A), endowed by an abundant deeply eosinophilic cytoplasm and distinct cell borders (B). At least occasional pseudostratification was documented in all studied cases (C). Foci of foamy macrophages were dispersed throughout the tumors in variable amounts (D). High grade oncocytic cells (E) and occasional psammoma bodies were identified in some tumors (F).

Table 2
Results of immunohistochemical examination.

Case	HMB45	CD117	Cathepsin K	CK20	AE1-3	CK 7	OSC	CAM5.2	CD10	AMACR	Vim	SDHB	PAX 8	MIA
1	-	-	Foc + +	-	-	+	Foc + + +	+	+ + +	+ + +	+ + +	+ + +	+ +	+ + +
2	-	-	-	-	-	Foc +	+ +	Foc + +	+ + +	+ + +	+ + +	+ + +	+ +	+ + +
3	-	-	Foc +	-	+ + +	+	+ + +	+ +	Foc +	+ +	+ +	+ + +	+ +	+ +
4	-	-	-	-	+ + +	+	+ + +	+ +	Foc + + +	+ + +	+	+ + +	+ +	+ + +
5	-	-	-	-	-	-	Foc + +	Foc +	Foc + + +	+ + +	+ + +	+ + +	+ + +	+ + +
6	-	-	-	-	-	-	+ + +	+ +	+ + +	+	+ + +	+ + +	+ +	+ + +
7	-	-	-	-	-	+	+ + +	Foc +	+ +	+ +	+ + +	+ + +	+ +	+ +
8	-	-	Foc + + +	-	-	+	+ +, Foc + + +	Foc +	+ + +	+ +	+ + +	+ + +	+ +	+ +
9	-	-	-	-	-	−	+ +	Foc + +	-	+ +	+ +	+ + +	+ + +	+ +
10	-	-	+	-	-	Foc +	+ + +	Foc + +	+ + +	+ +	+ + +	+ + +	+	+ +

Foc = focally; + = weak positivity, + + = moderate positivity, + + + = strong positivity, - = negative,* single cell positivity, AE1-3 = AE1-AE3, OSC = cytokeratin OSCAR, vim = vimentin, SDHB = succinate dehydrogenase B, MIA = antimitochondrial antigene.

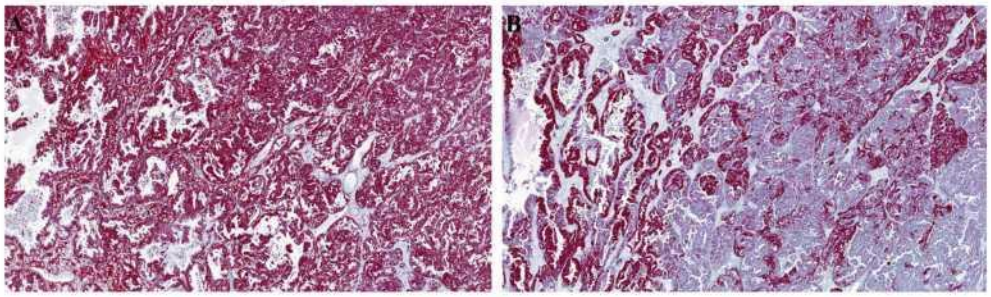

Fig. 3. Immunoreactivity for vimentin was detected in all cases (A). AMACR was also expressed in all cases (B).

Lefevre et al. They presented 10 cases demonstrating papillary morphology with the papillae being covered by distinctly oncocytic cells [13]. In this series, the tumors were diffusely positive for antimitochondrial antigen (MIA), vimentin, and AMACR, but none of the cases was positive for CK7. Although the authors described only single cell layer of oncocytic cells lining the papillae, their illustrations most likely showed multilayered epithelial cells on the papillae in Fig. 2B and C. Another series of 12 oncocytic PRCC with mostly papillary arrangement was published within months in 2006. Some cases in this study, however, showed variable amount of solid component [7]. The cytologic features were identical to those in Lefevre's study, but there was variable positivity for CK7 (4/12 cases were CK7 positive versus 0/10 in the Lefevre et al. study). The oncocytic variant of PRCC has been proposed as "type 3" PRCC [7,13] and it was suggested to represent a possible new variant of PRCC in the 2016 WHO classification [9]. These tumors indeed share histopathological features of PRCC and RO. They are characterized by papillary architecture with the papillae typically lined by single layer of tumor cells with voluminous eosinophilic

Table 3
Molecular-genetic analyses.

Case	1p36	CCND1 (BCL1 ba)	CEP 7	CEP 14	CEP 17	X/Y
1	Neg.	Neg.	Neg.	Neg.	Neg.	Loss Y
2	Pos.	Neg.	Neg.	Loss	Neg.	Neg.
3	Neg.	Pos.	Neg.	Neg.	Neg.	Neg.
4	Neg.	Neg.	Neg.	Neg.	Neg.	Neg.
5	Neg.	Neg.	Neg.	Neg.	Neg.	Neg.
6	Pos.	Neg.	Neg.	Neg.	Neg.	Neg.
7	Neg.	Neg.	Neg.	Neg.	Neg.	Loss Y
8	Neg.	Neg.	Neg.	Neg.	Neg.	Neg.
9	Pos.	Neg.	Neg.	Neg.	Neg.	Neg.
10	Pos.	Neg.	Neg.	Loss	Neg.	Loss Y

Neg = negative.
Pos = positive.
CEP = centromeric probe.

(oncocytic) cytoplasm and nuclei demonstrating a low nucleolar grade (ISUP grade 1). In less typical cases, the architecture can range from solid to cystic [22]. Immunohistochemically, OPRCCs are generally similar to PRCC.

We have encountered many renal tumors in our consultation practice sent with a diagnosis of "possible aggressive oncocytoma" by the submitting pathologist, which we considered both morphologically and immunohistochemically very close to the OPRCC. Therefore, this study was aimed to include these cases of "potentially aggressive oncocytic tumors", histologically characterized by papillary/tubulopapillary architecture with minor solid component. The solid component, due to compressed papillae, was the predominant architectural pattern only in one case (#7). The neoplastic cells demonstrated WHO/ISUP grade 2 nuclei in 7 of 10 cases; 3 of 10 were WHO/ISUP grade 3. The cytoplasm had oncocytic appearance characterized by deep eosinophilic, coarsely granular cytoplasm. The oncocytic appearance of the cytoplasm was similar to the true OPRCC and demonstrated diffuse and strong cytoplasmic immunoreactivity for MIA. The overall immunoprofile, consisting of positivity for AMACR, vimentin, MIA, PAX8, CK7 and negativity for CD117, was in accordance with PRCC/OPRCC. The main differences from the "classic" OPRCC were the presence of high grade nuclei and at least focal pseudostratification, seen in all of the cases. The biologic behavior of PRCCRO was mostly favourable, as majority of the patients (7 of 8 with available follow up) were alive and without metastatic spread during the follow-up. One case (#3), however, behaved in an aggressive manner and the patient succumbed to the disease 4 years post-surgery. Histologically, this case did not differ from the other cases in any aspects. It was a small 2 cm tumor demonstrating ISUP grade 2. This case was also the only one, showing rearrangement of *CCND1* gene.

The increasing number of reported cases and the development of new diagnostic techniques have demonstrated that PRCC, as a group, is more morphologically and genetically diverse than previously thought. PRCC type 1 is considered a distinct entity, typically showing gains of chromosomes 7 and 17 and loss of Y. In contrast, PRCC type 2 is known to show more variable histologic patterns [9]. Linehan et al. published a large complex genetic analysis of 161 primary PRCCs, confirming that genetically, PRCC type 1 is relatively consistent, as opposed to PRCC type 2, which, according to their study, consists of at least 3 subtypes [14]. It is worth noting that the authors did not analyze the chromosomal numerical aberration patterns in detail because their study was mainly focused on changes affecting various genes. In a recent study by Saleeb et al., the authors proposed another type of PRCC designated as PRCC3, demonstrating unique immunohistochemical and chromosomal numerical aberration pattern, while morphologically showing a variable appearance [21].The authors slightly refined the OPRCC category (called PRCC/oncocytic low-grade) in their study. However, the OPRCC cases included in their study were different from the cases we describe here as PRCCRO.

The published data on the chromosomal aberrations of OPRCC remain inconsistent, as some tumors were cytogenetically similar to PRCC type 1, demonstrating polysomy of chromosomes 7, 17 and loss of Y, whereas others were not [7,12,15,18,19]. Considering OPRCC is a possible new variant of PRCC, the available published studies mostly focused on the analysis of the chromosomes 7, 17 and Y.

RO is known for its variable genetic profile which can be characterized by 4 basic patterns: normal karyotype, loss of chromosome 1 and Y, chromosomal translocations involving the CCND1 locus at 11q13, and deletion of chromosome 14 [9].

Because of a lack of comprehensive chromosomal analysis of OPRCC, the current study was carried out to examine the chromosomal numerical abnormalities (CNA) by focusing on chromosomes frequently aberrant in both PRCC and RO. CNA of PRCCRO were highly unusual, as all of our cases (10 of 10) showed several CNA features traditionally associated with RO, including loss of 1p36 gene loci, loss of chromosome Y, rearrangement of *CCND1* gene and numerical changes of chromosome 14. Therefore, it is evident that some cases within the spectrum of PRCC can demonstrate CNAs which are inconsistent with our general postulates about PRCC.

Distinction of PRCCRO from RO is of utmost clinical significance, as RO typically shows an indolent clinical course with only very rare aggressive cases documented to date [4,24], while PRCCRO can generally behave in an aggressive fashion. RO is composed of large neoplastic cells with abundant, eosinophilic, finely granular cytoplasm and round to oval nuclei, forming compact nests and solid areas, particularly at the periphery [9]. Although delicate and focal papillary-like formation can rarely be seen, extensive papillary growth is incompatible with the diagnosis of oncocytoma. Solid areas observed in PRCCRO which were at least focally presented in all of our cases may closely mimic RO. Because the papillary formations were a constant finding in PRCCRO, a meticulous and thorough sampling can ultimately aid in establishing the accurate diagnosis. Nevertheless, sufficient tissue material may not always be available (such as in consultation cases or in core biopsies) which can lead to extremely difficult morphologic distinction between PRCCRO and RO. In such cases, a panel of immunostains including AMACR, vimentin, CK7 and CD117 may be helpful, as RO would be typically positive for CD117 and negative for AMACR, CK7 and vimentin. The reverse immunohistochemical pattern would be true for PRCCRO, with the caveat that these markers may show immunoreactivity in either scattered cells or small groups of cells [9]. Our findings also showed that the chromosomal aberration patterns of RO and PRCCRO are markedly overlapping and thus limiting the utility of a cytogenetic analysis in such a differential diagnosis. In our opinion, in the differential diagnostic work-up of RO and PRCCRO, the morphologic features and the corresponding IHC profile are more robust and superior tools to the cytogenetic evaluation of PRCCRO.

Of note, fumarate hydratase-deficient renal cell carcinoma (FH-deficient RCC), both syndromic (hereditary leiomyomatosis and renal cell carcinoma-associated RCC) and sporadic, can also have some morphologic overlapping features with PRCCRO. FH-deficient RCC often presents with papillary/tubulopapillary architecture and large cells containing abundant eosinophilic cytoplasm. A consistent finding of FH-deficient RCC is the presence of large nuclei with very prominent deep red nucleoli surrounded by a clear halo, reminiscent of the cytomegalovirus inclusions [23]. Although PRCCROs occasionally present with prominent nucleoli, they lack such staining qualities and perinucleolar clearing. The advanced pathologic stage at the time of the diagnosis is another common feature of the FH-deficient RCC (in contrast to PRCCRO). The loss of fumarate hydratase (FH) and overexpression of modified S-(2-succino)-cysteine (2SC) can be visualized by IHC and can serve as an additional differential diagnostic feature. The detection of the *FH* gene mutation on chromosome 1q42.3-q43 can confirm the diagnosis of FH-deficient RCC with certainty.

In conclusion, we provide the first comprehensive morphologic,

IHC, and molecular genetic study of PRCCRO, further confirming the diverse nature of PRCC. Despite the CNAs typical of renal oncocytoma in all studied cases, we classified these tumors under the category of PRCC, because of their predominant papillary/tubulopapillary architecture and the immunoprofile compatible with PRCC (positivity for AMACR, vimentin, MIA, PAX8, CK7 and negativity for CD117). From a practical point of view, we recommend to base the diagnosis of PRCC with oncocytic cells primarily on the morphologic features, including presence of focal pseudostratification and intermediate to high grade nuclei, which should be supported by the appropriate IHC profile. We recommend setting the cytogenetic features aside in such cases to avoid the potential misdiagnosis of a malignant PRCC as a benign renal oncocytoma.

Compliance with ethical standards

Study design has been approved by local ethical committee (Charles University, Medical School Plzen) LEK FN Plzeň.

Funding

The study was supported by Charles University Fund SVV 2017-260391.

Conflict of interest

All authors declare no conflict of interest.

References

[1] Argani P, Netto GJ, Parwani AV. Papillary renal cell carcinoma with low-grade spindle cell foci: a mimic of mucinous tubular and spindle cell carcinoma. Am J Surg Pathol 2008;32:1353–9. http://dx.doi.org/10.1097/PAS.0b013e31816a1c34.

[2] Arroyo MR, Green DM, Perlman EJ, Beckwith JB, Argani P. The spectrum of metanephric adenofibroma and related lesions: clinicopathologic study of 25 cases from the National Wilms Tumor Study Group Pathology Center. Am J Surg Pathol 2001;25:433–44.

[3] Baithun SI, Pollock DJ. Oncocytic hepatocellular tumour. Histopathology 1983;7:107–12.

[4] Cacciamani G, Cima L, Ficial M, Novella G, Siracusano S, Tedeschi U, et al. Liver metastases from renal oncocytoma with vascular extension. Appl Immunohistochem Mol Morphol 2017. http://dx.doi.org/10.1097/PAI.0000000000000490.

[5] Caplan RH, Abellera RM, Kisken WA. Hurthle cell tumors of the thyroid gland. A clinicopathologic review and long-term follow-up. JAMA 1984;251:3114–7.

[6] Delahunt B, Eble JN. Papillary renal cell carcinoma: a clinicopathologic and immunohistochemical study of 105 tumors. Mod Pathol 1997;10:537–44.

[7] Hes O, Brunelli M, Michal M, Cossu Rocca P, Hora M, Chilosi M, et al. Oncocytic papillary renal cell carcinoma: a clinicopathologic, immunohistochemical, ultrastructural, and interphase cytogenetic study of 12 cases. Ann Diagn Pathol 2006;10:133–9. http://dx.doi.org/10.1016/j.anndiagpath.2005.12.002.

[8] Hes O, Condom Mundo E, Peckova K, Lopez JI, Martinek P, Vanecek T, et al. Biphasic squamoid alveolar renal cell carcinoma: a distinctive subtype of papillary renal cell carcinoma? Am J Surg Pathol 2016;40:664–75. http://dx.doi.org/10.1097/pas.0000000000000639.

[9] Moch H, Humphrey PA, Ulbright TM, Reuter VE. WHO Classification of Tumours of the Urinary System and Male Genital Organs. Lyon: IARC; 2016.

[10] Klatte T, Said JW, Seligson DB, Rao PN, de Martino M, Shuch B, et al. Pathological, immunohistochemical and cytogenetic features of papillary renal cell carcinoma with clear cell features. J Urol 2011;185:30–5. http://dx.doi.org/10.1016/j.juro.2010.09.013.

[11] Kumar VAA, Fausto N, Aster JC. Robbins and Cotran Pathologic Basis of Disease, Professional Edition E-Book. Edition 8 Elsevier Health Sciences; 2009.

[12] Kunju LP, Wojno K, Wolf Jr. JS, Cheng L, Shah RB. Papillary renal cell carcinoma with oncocytic cells and nonoverlapping low grade nuclei: expanding the morphologic spectrum with emphasis on clinicopathologic, immunohistochemical and molecular features. Hum Pathol 2008;39:96–101. http://dx.doi.org/10.1016/j.humpath.2007.05.016.

[13] Lefevre M, Couturier J, Sibony M, Bazille C, Boyer K, Callard P, et al. Adult papillary renal tumor with oncocytic cells: clinicopathologic, immunohistochemical, and cytogenetic features of 10 cases. Am J Surg Pathol 2005;29:1576–81.

[14] Linehan WM, Spellman PT, Ricketts CJ, Creighton CJ, Fei SS, Davis C, et al. Comprehensive molecular characterization of papillary renal-cell carcinoma. N Engl J Med 2016;374:135–45. http://dx.doi.org/10.1056/NEJMoa1505917.

[15] Mai KT, Kohler DM, Robertson SJ, Belanger EC, Marginean EC. Oncocytic papillary renal cell carcinoma with solid architecture: mimic of renal oncocytoma. Pathol Int 2008;58:164–8. http://dx.doi.org/10.1111/j.1440-1827.2007.02205.x.

[16] Masuzawa N, Kishimoto M, Nishimura A, Shichiri Y, Yanagisawa A. Oncocytic renal cell carcinoma having papillotubular growth: rare morphological variant of papillary renal cell carcinoma. Pathol Int 2008;58:300–5. http://dx.doi.org/10.1111/j.1440-1827.2008.02227.x.

[17] Mearini L, Del Sordo R, Costantini E, Nunzi E, Porena M. Adrenal oncocytic neoplasm: a systematic review. Urol Int 2013;91:125–33. http://dx.doi.org/10.1159/000345141.

[18] Okada A, Sasaki S, Fujiyoshi Y, Niimi K, Kurokawa S, Umemoto Y, et al. A case of oncocytic papillary renal cell carcinoma. Int J Urol 2009;16:765–7. http://dx.doi.org/10.1111/j.1442-2042.2009.02336.x.

[19] Park BH, Ro JY, Park WS, Jee KJ, Kim K, Gong G, et al. Oncocytic papillary renal cell carcinoma with inverted nuclear pattern: distinct subtype with an indolent clinical course. Pathol Int 2009;59:137–46. http://dx.doi.org/10.1111/j.1440-1827.2009.02341.x.

[20] Pivovarcikova K, Peckova K, Martinek P, Montiel DP, Kalusova K, Pitra T, et al. "Mucin"-secreting papillary renal cell carcinoma: clinicopathological, immunohistochemical, and molecular genetic analysis of seven cases. Virchows Arch 2016;469:71–80. http://dx.doi.org/10.1007/s00428-016-1936-7.

[21] Saleeb RM, Brimo F, Farag M, Rompre-Brodeur A, Rotondo F, Beharry V, et al. Toward biological subtyping of papillary renal cell carcinoma with clinical implications through histologic, Immunohistochemical, and molecular analysis. Am J Surg Pathol 2017;41:1618–29. http://dx.doi.org/10.1097/PAS.0000000000000962.

[22] Srigley JR, Delahunt B. Uncommon and recently described renal carcinomas. Mod Pathol 2009;22(Suppl. 2):S2–23. http://dx.doi.org/10.1038/modpathol.2009.70.

[23] Trpkov K, Hes O, Agaimy A, Bonert M, Martinek P, Magi-Galluzzi C, et al. Fumarate hydratase-deficient renal cell carcinoma is strongly correlated with fumarate hydratase mutation and hereditary leiomyomatosis and renal cell carcinoma syndrome. Am J Surg Pathol 2016;40:865–75. http://dx.doi.org/10.1097/PAS.0000000000000617.

[24] Trpkov K, Yilmaz A, Uzer D, Dishongh KM, Quick CM, Bismar TA, et al. Renal oncocytoma revisited: a clinicopathological study of 109 cases with emphasis on problematic diagnostic features. Histopathology 2010;57:893–906. http://dx.doi.org/10.1111/j.1365-2559.2010.03726.x.

[25] Ulamec M, Skenderi F, Trpkov K, Kruslin B, Vranic S, Bulimbasic S, et al. Solid papillary renal cell carcinoma: clinicopathologic, morphologic, and immunohistochemical analysis of 10 cases and review of the literature. Ann Diagn Pathol 2016;23:51–7. http://dx.doi.org/10.1016/j.anndiagpath.2016.04.008.

[26] Xia QY, Rao Q, Shen Q, Shi SS, Li L, Liu B, et al. Oncocytic papillary renal cell carcinoma: a clinicopathological study emphasizing distinct morphology, extended immunohistochemical profile and cytogenetic features. Int J Clin Exp Pathol 2013;6:1392–9.

1.2.4 Solid papillary renal cell carcinoma: clinicopathologic, morphologic, and immunohistochemical analysis of 10 cases and review of the literature

Solidní PRCC, ačkoliv literaturou není příliš často komentován, je dobře známou variantou PRCC. Varianta se vyznačuje přítomností nahusto nakupených papilárních a tubulárních struktur, což dává tumoru typický mikroskopický „solidní“ vzhled. Tato práce shrnuje dosavadní literární poznatky o solidní variantě PRCC a popisuje dalších 10 nových případů pocházejících z plzeňského registru nádorů.

Případy doposud popsané v literatuře (celkem 53 případů) vykazovaly ve většině imunohistochemický profil typický pro PRCC (pozitivita CK7, EMA, AMACR) a cytogenetické znaky často připisované PRCC (polysomie chromozomů 7/17 a ztráta gonosomu Y). Pacienti byli častěji muži, věk pacientů se pohyboval v rozmezí 17 - 82 let a dostupná data o dalším vývoji onemocnění ukazují, že solidní varianta PRCC vykazuje spíše příznivý klinický průběh onemocnění. Prezentovaná práce pak obohacuje sérii doposud publikovaných solidní PRCC o dalších 10 nových případů, všechny tumory se vyskytly u mužů ve věkovém rozmezí 34 - 70 let a všechny neoplázie byly zastiženy ve stádiu pT1 (dle TNM2009/2017). Velikost tumorů se pohybovala v rozmezí 1,4 – 5,5 cm v největším rozměru (průměr 3,32 cm), tumory byly dobře ohraničené, bělavé až žluté s granulovanou plochou na řezu. Detailní morfologická analýza u tumorů, kromě typických a prominentních komprimovaných abortivních papil a tubulů, zaznamenala i okrsky s „pravým“ solidním vzhledem. Pouze raritně byly přítomny i dobře formované „klasické“ papilární struktury. Všech 10 tumorů bylo difúzně pozitivních v CK7 a negativní ve WT-1. U 9/10 pacientů byl další průběh onemocnění bez rekurencí a progrese, v jednom případě u pacienta došlo k rekurenci onemocnění.

Solidní varianta PRCC je vzácným tumorem s incidencí méně než 1% všech renálních neoplázií. Tumory typicky sestávají s těsně nahloučených abortivních papil a tubulů, což neopláziím propůjčuje typický „solidní“ histologický vzhled. Imunohistochemicky a cytogeneticky pak tumory vykazují profil totožný s „konvenčním“ PRCC. Diferenciálně diagnosticky je důležité tuto variantu PRCC odlišit především od metanefrického adenomu, epiteloidního nefroblastomu a výjimečně i od mucinózního, tubulárního a vřetenobuněčného RCC a onkocytické varianty PRCC.

Annals of Diagnostic Pathology 23 (2016) 51–57

Contents lists available at ScienceDirect

Annals of Diagnostic Pathology

Solid papillary renal cell carcinoma: clinicopathologic, morphologic, and immunohistochemical analysis of 10 cases and review of the literature

Monika Ulamec [a,b], Faruk Skenderi [c], Kiril Trpkov [d], Bozo Kruslin [a,b], Semir Vranic [c], Stela Bulimbasic [b,e], Sandra Trivunic [f], Delia Perez Montiel [g], Kvetoslava Peckova [h], Kristyna Pivovarcikova [h], Ondrej Ondic [h], Ondrej Daum [h], Pavla Rotterova [h], Martin Dusek [h], Milan Hora [i], Michal Michal [h], Ondrej Hes [h,*]

[a] Ljudevit Jurak Pathology Department, Clinical Hospital Center Sestre milosrdnice, Zagreb, Croatia
[b] Pathology Department, Medical University, Medical Faculty Zagreb, Croatia
[c] Department of Pathology, Clinical Centre of the University of Sarajevo, Sarajevo, Bosnia and Herzegovina
[d] Department of Pathology, Calgary Laboratory Services and University of Calgary, Calgary, AB, Canada
[e] Department of Pathology, Clinical Hospital Center Zagreb, Zagreb, Croatia
[f] Department of Pathology, Medical Faculty, University of Novi Sad, Serbia
[g] Department of Pathology, Institute Nacional de Cancerologia, Mexico City, Mexico
[h] Department of Pathology, Charles University, Medical Faculty and Charles University Hospital Plzen, Czech Republic
[i] Department of Urolology, Charles University, Medical Faculty and Charles University Hospital Plzen, Czech Republic

ARTICLE INFO

Keywords:
Kidney
Solid
Papillary renal cell carcinoma
Review
Differential diagnosis

ABSTRACT

Solid papillary renal cell carcinoma is rarely reported in the literature, and its tumor characteristics are not entirely compatible with the concept of 2 histological subtypes of papillary renal cell carcinoma (PRCC). Tumor is composed mostly of small compressed tubules and short abortive papillae giving solid appearance of monomorphic epithelial cells with scanty cytoplasm and small nuclei, sometimes mimicking spindle cells, without or with sparse true papillae. It shows immunohistochemical (+CK7, +EMA, +AMACR) and genetic hallmarks (polysomy/trisomy 7/17, loss of Y) of conventional PRCC. About 53 cases have been described in the literature, with male predominance and age ranging from 17 to 82 years. By available follow-up data, solid PRCC has a favorable clinical course. We describe 10 cases compatible with the diagnosis of solid PRCC. All patients were males age range was from 34 to 70 years, and all but one were pT1 according to TNM 2009. On follow-up, 9 patients were without evidence of disease, and 1 had recurrent tumor. Size of the tumor ranged from 1.4 to 5.5 cm (mean, 3.32 cm). Tumors were well-circumscribed whitish to yellow masses with granular surface. Although solid architecture was a prominent morphologic feature, detailed analysis revealed that the tumors were composed of compressed short abortive papillae and compressed tubules admixed with true solid areas. Well-formed papillae were exceptionally present. All 10 cases were strongly and diffusely positive for CK7 and negative for WT-1. In conclusion, solid PRCC is a rare tumor with an incidence of less than 1% of all renal tumors. In majority of the cases, tumors were composed of tightly compressed tubular structures and short abortive papillae that render a solid morphologic appearance. Immunohistochemical and molecular features do not differ from conventional PRCC. Metanephric adenoma; epithelioid nephroblastoma; and, rarely, mucinous tubular and spindle cell carcinoma and oncocytic variant of PRCC should be considered in the differential diagnosis.

1. Introduction

Papillary renal cell carcinoma (PRCC) was first formally recognized as a specific entity in the Heidelberg classification, and then it was accepted in the 2004 World Health Organization (WHO) classification [1–2]. It was described as a malignant renal tumor with characteristic papillary or tubulopapillary architecture and with specific immunohistochemical and cytogenetic profile. PRCC is the second most common renal cell carcinoma (RCC) subtype occurring in up to 18.5% of all RCCs [3–5]. The description of PRCC dates back to 1974 in the study of Mancilla-Jimenez et al [6]. The authors reported in detail the ultrasonographic, macroscopic, and microscopic features of PRCC and recognized 2 consistent histologic patterns, namely, the papillae lined either by a single row of cells with scant cytoplasm or cells with pseudostratifed nuclei and abundant eosinophilic cytoplasm. Besides these 2 patterns,

Disclosure of conflict of interest: All authors declare no conflict of interest

The study was supported by the Charles University Research Fund (project number P36) and by project CZ.1.05/2.1.00/03.0076 from the European Regional Development Fund.

* Corresponding author at: Department of Pathology, Charles University, Medical Faculty and Charles University Hospital Plzen, Alej Svobody 80, 304 60 Pilsen, Czech Republic.
E-mail address: hes@medima.cz (O. Hes).

http://dx.doi.org/10.1016/j.anndiagpath.2016.04.008
1092-9134/

Table 1
Clinicopathological features and follow-up of solid PRCC

Case	Age (y)	Sex	Size (cm)	Follow-up
1	49	M	5.5	NED-8 y
2	70	M	1.5	DOC-3 y[a]
3	37	M	3.5	NED
4	66	M	2.5	NA
5	60	M	4.5	NED
6	54	M	2.8	NED-5 y
7	63	M	4	NED
8	34	M	2.5	NED-13 y
9	52	M	1.4	NED-9.5 y
10	48	M	5	AWD-8 y[b]

NED, no evidence of desease; DOC, dead for other reasons; NA, not available; AWD, alive with desease.
[a] Bilateral nephrectomy for PRCCs; dead for metastatic prostate cancer 3 years later; MSCT during follow-up diagnostics showed nephrectomy area without tumor.
[b] Only T3N0Mx tumor, recidivant tumor after 8 years, placed in the prior nephrectomy area.

they also reported papillary tumors with clear cells and other morphological features. PRCCs were later characterized in more details in several studies [7–9]. In 2004, the WHO classification adopted 2 types of PRCC: type 1, with papillae lined by a single cell layer of cuboidal cells with scant cytoplasm, and type 2, in which papillae are lined by large eosinophilic cells with pseudostratified nuclei [2]. Although less frequently encountered, several additional patterns were subsequently reported in the literature, including oncocytic [10–11], PRCC with clear cells [12], and solid PRCC. Solid variant of PRCC is composed of monomorphic epithelial cells with scant cytoplasm and small nuclei, arranged in tightly packed, ill-defined tubules or papillae and solid sheets [3,13–18]. It closely resembles metanephric adenoma (MA) and may share similar morphologic features with epitheloid nephroblastoma or mucinous tubular and spindle cell carcinoma (MTSC).

In this study, we describe a series of 10 cases collected from multiple institutions, and we discuss the diagnostic pitfalls and the differential diagnosis of the solid form of PRCC.

2. Material and methods

Ten cases compatible with the diagnosis of solid PRCC were retrieved out of 1311 papillary RCCs (including institutional, consultation, and archive cases) in the Pilsen Tumor Registry. Pathologic examination of all available hematoxylin and eosin–stained sections from each case (range, 1-18 slides) was performed by at least 3 pathologists (MU, FS, and OH). Cases were reevaluated, and solid, tubular, and papillary components were accessed as percentage of the tumor. Tissue for light microscopy was fixed in 4% formaldehyde and embedded in paraffin using routine procedures. Three-micrometer thin sections were cut and stained with hematoxylin and eosin to evaluate the architecture of the tumors. Basal membranes were highlighted by periodic acid Schiff (PAS) stain.

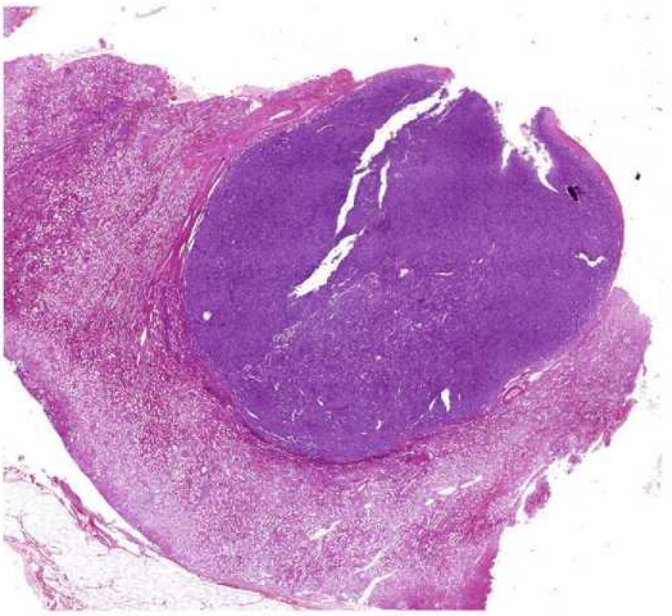

Fig. 1. Using scanning magnification, most of the tumors appeared completely solid.

The immunohistochemical study was performed using a Ventana Benchmark XT automated stainer (Ventana Medical System, Inc, Tucson, AZ).

The following primary antibodies were used in the immunohistochemical study: racemase/AMACR (13H4, monoclonal, DAKO, Glostrup, Denmark, 1:200), cytokeratin 7 (OV-TL12/30, monoclonal, DakoCytomation, Carpenteria CA, 1:200), epithelial membrane antigen (EMA) (E29, monoclonal, DakoCytomation, 1:1000), CD10 (monoclonal, Sp67, Ventana, RTU), CD34 (QBEnd-10, monoclonal, Dako, 1:100), CD57(NK 1, Leica Biosystems, Newcastle upon Tyne, UK, 1:200), WT1 (GF-H2, monoclonal, DakoCytomation, 1:150), Ki-67 (MIB1, monoclonal, Dako, 1:1000). Appropriate positive and negative controls were used. Immunostains were scored as 1+ (focal in small clusters of individual cells), 2+ (up to 50% positive cells), and 3+ (diffuse strong positivity in more than 50% of cells).

3. Results

The clinicopathologic data are summarized in Table 1. The age of the patients ranged from 34 to 70 years (mean age, 53.30); all patients were male. Size of the tumor in the largest diameter ranged from 1.4 to 5.5 cm (mean, 3.32 cm). Most of the cases were pT1 stage (TNM 09); 1 tumor was pT3. Most of the patients (8/10) were alive and well without signs of metastatic disease or relapse within follow-up period of 3-13 years. One patient was faced with recurrent tumor 8 years after resection. One patient had bilateral nephrectomy due to multiple small PRCCs and died of metastatic prostate cancer 3 years later.

Table 2
Gross and microscopic features of solid PRCC

Patient	Gross description	True solid (%)	Compressed tubuli (%)	Compressed abortive papillae; occasional glomeruloid formations (%)	True papillae (%)	Capsule	ISUP grade
1	Yellow well-circumscribed nodule	10	40	50	0	+	1
2	Yellow well-circumscribed nodule, bilateral papillary RCCs	20	70	10	0	+	1
3	Gray well-circumscribed nodule	5	80	10	5	+	2
4	Yellow well-circumscribed nodule	80	10	5	5	+	1
5	Gray well-circumscribed nodule	20	30	50	0	−	1
6	Yellow well-circumscribed nodule	5	10	80	5	+	1
7	Yellow well-circumscribed nodule	20	70	10	0	+	1
8	Yellow well-circumscribed nodule	10	50	40	0	−/+	1
9	Yellow well-circumscribed nodule	30	10	60	0	+	1
10	Yellow well-circumscribed nodule, necrotic −50%	60	20	20	0	+	2

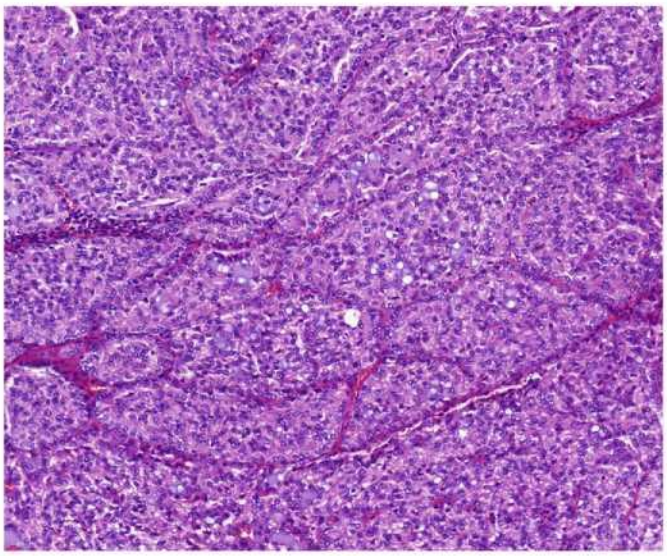

Fig. 2. Only 2 cases from our series were mostly arranged in solid-alveolar pattern.

Morphologic features are summarized in Table 2. Macroscopically, tumors were well-circumscribed yellow to white homogeneous nodules, sometimes with fine-granulated surface. One tumor showed necrotic area in up to 50% of the tumor.

Nine tumors were encapsulated. Using scanning magnification, most of the tumors appeared completely solid (Fig. 1), but on closer examination, true solid areas comprised 5% to 80% of the tumor. On high power and using PAS staining, only 2 tumors were mostly solid (60% and 80% of the tumors, respectively, comprised solid areas) (Fig. 2). Four tumors were composed mostly of compressed tubules (between 50% and 80% of the 2 tumors) (Fig. 3A and B), whereas the remaining 4 were composed mostly of compressed abortive papillae with occasional glomeruloid formations (between 50% and 80% of these contained compressed abortive papillae) (Fig. 4). True papillae with fibrovascular cores were found in 3 cases in up to 5% of the tumor. Tumor cells had scant cytoplasm and small, round to elongated nuclei with occasional nuclear grooves (International Society of Urological Pathology [ISUP] nucleolar grade was 1 or 2) (Fig. 5). In all but 1 case, the cells with scant but eosinophilic cytoplasm were also focally found. Small foci of tubules with cells showing sparse but clear cytoplasm were found in 2 cases.

The immunohistochemistry results are summarized in Table 3. All 10 cases were strongly and diffusely positive for CK7 (Fig. 6) and negative for WT-1. AMACR was diffusely positive in 9 cases (Fig. 7). EMA was positive diffusely in 8 cases and focally in 2. Vimentin was diffusely positive in 6 cases, and 4 were positive focally (less than 50% of cells). CD10 was focally positive in 4 cases. CD57 showed weak and focal positivity in 1 case. Proliferation activity was less than 2% in all tumors using Ki-67 labeling.

4. Discussion and review of the literature

4.1. Clinical and pathological characteristics

So-called solid PRCC, as a part of the morphologic PRCC spectrum, has been described for the first time by Renshaw et al [13]. The incidence was less than 1% of all renal tumors [3], and this estimation corresponds with the proportion of solid PRCCs in this series. In our study, the incidence was actually 0.76% of all PRCCs in the Pilsen Tumor Registry.

In toto, about 53 cases have been described in the literature with tumors showing distinctive solid PRCC features. The data from the English literature are summarized in Table 4. There is a male predominance, with a male to female ratio of 3.5:1. Age at time of diagnosis was from 17 to 82 years. The follow-up data are however limited, and it seems that solid PRCC has favorable clinical course. Most cases were classified as pT1 tumors, with nuclear grade up to 2, according to Fuhrman grading system [3,13–19]. In our study, the age range was from 34 to 70 years (mean age, 53.3), and all patients were male. The largest tumor size ranged from 1.4 to 5.5 cm (mean, 3.3 cm), which is similar to the previously published data. Nine of our cases were pT1 stage (TNM 09). One case was pT3 and demonstrated infiltration through the renal capsule with invasion into the perirenal fat. This patient had recurrent tumor after 8 years. Seven of the 10 cases were without evidence of disease during the follow-up from 3 to 13 years. One patient had multiple small PRCCs and died of metastatic prostate cancer 3 years later.

In the previous studies, the tumors were well-circumscribed, solid, homogeneous, and nodular masses, grayish white in color and located in the renal cortex. Hemorrhage and necrosis in the central areas were also described, as well as presence of multifocal tumors [13,16–17]. In this study, the tumors represented well-circumscribed solid nodules, mostly yellow in color and often showing finely granular cut surface. In 1 case, multifocal, bilateral PRCCs were found, together with the solid PRCC. Abundant necrosis was found in only 1 case.

Solid PRCC is typically composed of cells with scant cytoplasm and small, round to elongated nuclei, cytologically resembling type 1 PRCC. The cells are organized in solid sheets or tubular structures that are tightly packed, sometimes mimicking spindle cells, with no true papillae and lacking fibrovascular stalks. Some tumors may exhibit completely

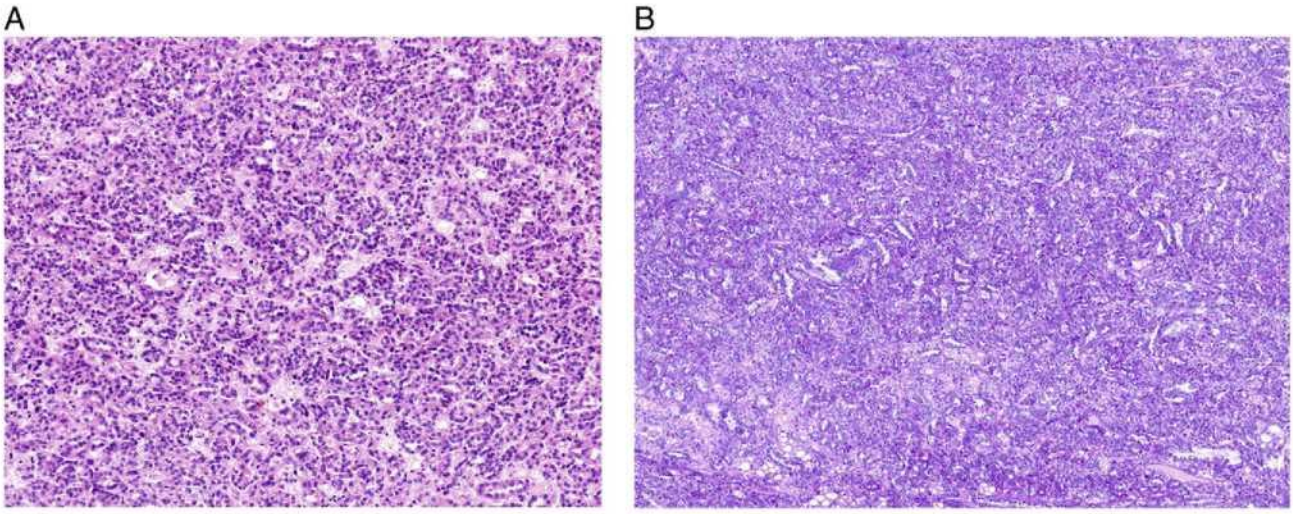

Fig. 3. (A) Four tumors were composed of small tubules. (B) Predominantly tubular architecture highlighted by PAS staining.

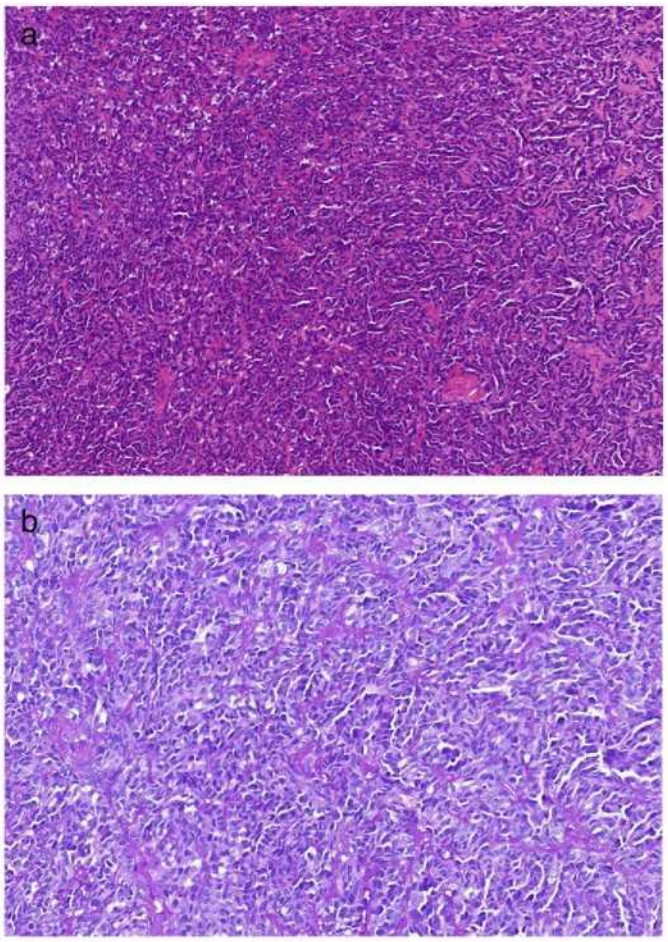

Fig. 4. (A-B) Four tumors in our series were composed of short compressed abortive papillae (hematoxylin and eosin = A, PAS = B).

solid morphology and distinct micronodules, with the cells showing eosinophilic cytoplasm. Abortive papillae are also frequently found.

In the current study, true solid areas comprised 5%-80% of the individual tumors; on high power and PAS stain, only 2 tumors had more than 50% solid pattern, without any visible tubules or papillae. Areas of compressed, tightly packed tubular structures and abortive papillae comprised the rest of the tumors, usually mimicking solid areas and rarely showing focal spindle cell appearance. Four tumors were mostly composed of compressed and abortive papillae, and 4 were composed

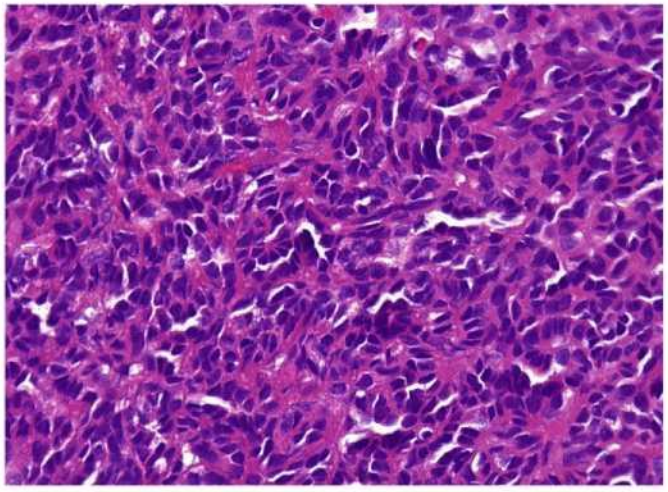

Fig. 5. Tumor cells had scant cytoplasm and small, round to elongated nuclei.

Table 3
Immunohistochemical staining results in solid PRCC

Patient	CK7	AMACR	EMA	WT-1	CD57	CD10	Vim	Ki-67
1	+++	+++	+++	−	+	−	+	≤1%
2	+++	+++	+++	−	−	+	+++	≤1%
3	+++	+++	+	−	−	−	++	≤1%
4	+++	+++	+++	−	−	++	++	≤1%
5	+++	+++	++	−	−	−	+++	≤1%
6	+++	+++	+++	−	−	−	+++	≤1%
7	+++	−	+++	−	−	−	+++	≤1%
8	+++	+++	+++	−	−	−	+++	≤1%
9	+++	+++	+++	−	−	+	+++	≤1%
10	+++	+++	+++	−	−	++	+	≤2%

+: focal positivity, in small clusters or single cells; ++: up to 50% of positive cells; +++: diffuse, strong positivity, more than 50% of positive cells. Vim, vimentin.

mostly of compressed tubules. True papillae with fibrovascular cores were found in 3 cases and formed up to 5% of the tumor volume.

The amount of cytoplasm in the neoplastic cells may be variable. In most of the cases, the cells had scant cytoplasm and appeared basophilic, but cells having more abundant cytoplasm and low-grade nuclear features were also noted. The spindle cell–like component was usually low grade with slightly elongated nuclei, moderate pleomorphism, finely dispersed chromatin, and distinct nucleoli. These cells were different from true sarcomatoid morphology and resembled the cells of mucinous tubular and spindle cell RCC. Mitoses were rarely found [3,13–19]. Cantley et al [16] described a case of a young male patient with renal tumor showing sarcomatoid RCC, with an epithelial component identical to the solid PRCC. In some cases, foamy macrophages and psammoma bodies were found in the stroma of the tumor [17]. Occasionally, isolated foam cells and psammoma bodies were also present in our cases, but mitotic figures were not found. Most of the neoplastic cells had scant cytoplasm and small, round to elongated nuclei, with ISUP nucleolar grade 1 and 2. In all cases, there were low-grade nuclei, except in 1 case in which cells showed scant eosinophilic cytoplasm.

Although small solid areas in conventional PRCC are compatible with the diagnosis of PRCC, specific criteria for the diagnosis of solid PRCC are not provided in the recent renal tumor classifications [5]. In published studies, however, variable percentages of solid architecture, compressed papillae, or tubules were used to define this entity. Some authors proposed that solid PRCC should not contain true papillae, whereas others suggested that true papillae could comprise up to 20% [3,16–17].

4.2. Immunohistochemical profile and genetics

PRCC usually stains positive for cytokeratin AE1/AE3, CAM5.2, high–molecular weight cytokeratins, CK7, EMA, vimentin, CD10, AMACR, and RCC [2,4–5,7–9]. Of note, CK7 positivity can be variable, and it is not a

Fig. 6. All 10 cases were strongly and diffusely positive for CK7.

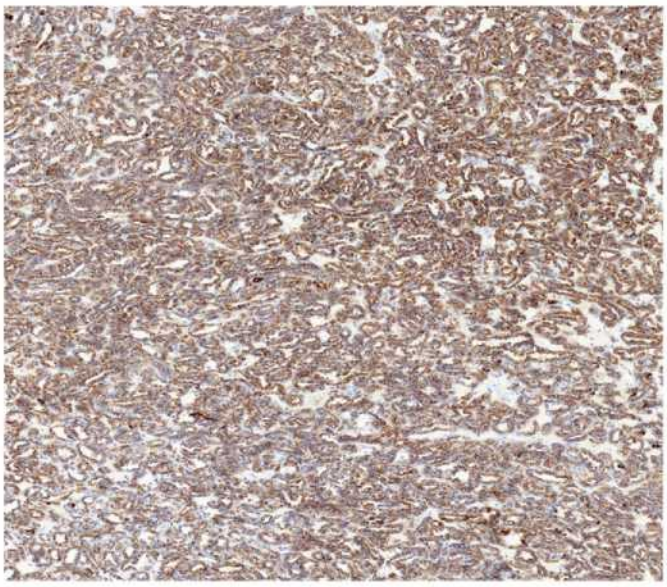

Fig. 7. Racemase (AMACR) was diffusely positive in 9 cases.

constant feature of PRCC; however, CK7 is frequently expressed in PRCC type 1. Solid PRCC shows immunoprofile similar to "conventional type" of PRCC, with strong, diffuse positivity for EMA, CK7, and AMACR and usually focal positivity for CD10 [3,13–19]. According to some studies, vimentin may be also focally positive.

In our experience, all10 evaluated cases were strongly and diffusely positive for CK7 and negative for WT-1. CK7 may in fact highlight the collapsed tubular architecture. AMACR was diffusely positive in 9 and EMA in 7 cases. CD10 was focally positive in 4 cases. CD57 showed weak and individual cell positivity in 9 cases. Proliferation activity, evaluated by Ki-67, was between 1% and 2% in all tumors.

4.3. Molecular genetic profile

Trisomy and tetrasomy of chromosome 7 and trisomy of 17, as well as loss of Y, are nearly pathognomic for PRCC. According to the published data, this also applies to solid PRCC [3,13–19]. According to WHO 2016, however, a wide variety of other chromosomal aberrations can be seen in PRCC, including trisomy 8, 12, 16, and 20 and loss of 1p, 4q, 6q, 7, 9p, 13q, Xp, and Xq, as well as amplification of 8q and overexpression of MYC. Thirteen percent of sporadic PRCCs demonstrate *MET* mutations. Loss of heterozygosity of *VHL* and *FHIT* can also be found. Type 1 PRCC shows gains of 7p and 17p, whereas LOH of 1p, 3p, 5q, 6, 8, 9p, 10, 11, 15, 18, and 22 was found in PRCC type 2. Allelic imbalance of 9q13 has been shown to be of prognostic significance in PRCC [5]. Renshaw et al [13] described cytogenetic changes in 1 case of solid PRCC, which demonstrated a karyotype of 45XXX, +X, +3, +5, +12, −14, +16, +17, −18, +20, and −21.

4.4. Pitfalls and differential diagnosis

Several entities should be considered in the differential diagnosis of solid PRCC, such as MA, epithelioid nephroblastoma, MTSC, and solid oncocytic PRCC (Table 5).

Metanephric adenoma of the kidney is a benign tumor usually found in younger patients, predominantly in women. It accounts for 0.2%-0.7% of adult renal epithelial neoplasms. It is sharply demarcated without a distinct pseudocapsule and consists of bland, small blue cells forming small, tightly packed tubular structures and acini but infrequently may also show more solid growth. Some tubules are typically elongated and branching. Both PRCC and MA may contain glomeruloid bodies with abortive papillae, tightly packed tubules, or solid tumor cell sheets. Psammoma bodies can be present in both MA and solid PRCC [20–22].

MA typically shows CK7−, AMACR−, WT1+, and CD57+ immunoprofile and does not exhibit the chromosomal changes typical of PRCC [20–25]. In fact, MA with polysomy 7 and 17 or loss of Y described in the literature most likely represents solid PRCC [20]. According to more recent data, BRAF V600E mutations were identified in nearly 90% of MAs, but similar BRAF exon 15 mutations are extremely rare in other renal tumors, including PRCCs. Immunohistochemistry for detection of BRAF V600E mutations was also validated, and it can be used as an additional tool in the differential diagnostic process [26]. According to the study of Yakirevich et al [27], majority of MAs are positive for kidney-specific catherin, whereas PRCCs and nephroblastomas are negative.

Table 4
Literature data

	Renshaw et al	Ngan et al	Argani et al	Zhang et al	Mantoan Padilha et al	Kinney et al	Cantley et al
No. cases	6[a]	1	5	2	23	15	1
Age	35-82	36	17-68	50-51	30-80	69-83	31
Sex (M/F)	4/2	1/0	1/0	2/0	15/8	11/?	1/0
Size (cm)	1-12	–	2.1-5.2	2-8	0.9-10	1.9-2	4.5
Nuclear grade 1/2/3/4	2/2/2/0	–	0/5/0/0	0/1/1/0	–	–	–
pTNM	2 T1, 4 T2	–	4T1a, 1T1b	1T1a, 1 T2	11T1a, 9T1b, 3 T2	–	T1b
Follow-up (mo)	2-108	–	Up to 8	8, 14	–	–	24
Follow-up	1 AWD (6 mo) 4 NED	–	5 NED	2 NED	–	–	NED
No. cases	6[a]	1	5	2	23	15	1
Papillae/solid encount	4-S	S	2-S[b]	2-T	10 S	–	T[c]
	2-T		3-T[b]		13 T		
CK7	6+	1+	5+	2+	23+	14+	1+
AMACAR	–	–	–	2+	23+	15+	–
EMA	6+	1+	–	2+	21+	–	1+
Vimentin	–	1−	–	2+	23−	–	1+
CD10	–	–	5+ (focal)	1 (focal)	–	–	–
WT-1	–	–	–	–	23−	15−	1−
CD57	–	–	–	–	16+ (focal)	14−; 1+	1−
Trisomy 7	2	–	5	2	14	8	1
Trisomy 17	3	–	3	2	15	8	–
Y loss	–	–	–	2	–	11	–

S, predominantly solid with small micronodules and abortive papillae; T, mostly tubular pattern and compressed tubules; –, no data; AWD, alive with disease; NED, no evidence of disease; M, male; F, female.
[a] Three were multifocal.
[b] Tumors with spindle cell foci.
[c] Foci with high-grade nuclei, with spindle cells.

Table 5
Differential diagnosis of solid PRCC

Characteristics	S PRCC	MA	EN	MTSC	OPRCC
Age (y)	17-83, average 54	Children, young adults, 5-83, average 49	Mostly children up to 6; in adult 21-67, average 32	32-79, average 56	40-82, average 67
Sex (M/F ratio)	M (3.5/1)	F (1/9)	Equal	F (1/1.5)	M (5/1)
Fibrous pseudocapsule	+	−	+	+	+
Multifocality	+	−	+	−	+
Cytology					
Cells with eosinophilic cytoplasm	+[a]	−	−	+[a]	+ (abundant)
Cells with scant cytoplasm	+	+	+	+	−
Nuclei	Low gr	Low gr	Low-high gr	Low gr	Low-high gr
True solid areas	+	+	+	+	+
Spindle cells with low-grade features	+	−	−	+	−
Compressed tubuli	+	+	+	+	+
Compressed abortive papillae (glomeruloid)	+	+	+	−	−
Real papillae with fibrovasc. CORE	+ (sparse)	+ (sparse)	−	−	+
Visible tubuli on LPF	+ (sparse)	+	+	+	+
Mucinous stroma	−	−	−	+	−
AE1/3	+	−	−	+	+
CK7	+	−	−	+	+
EMA	+	−	−	+	+
AMACAR	+	−	−	−	−
WT-1	−	+	+	−	−
CD57	−	+	+	−	−
Trisomy 7	Y	N	N	N	Y
Trisomy 17	Y	N	N	N	Y
Loss of Y	Y	N	N	N	Y

Y, yes; N, no; LPF, low-power field; SPRCC, solid PRCC; EN, epithelioid nephroblastoma; OPRCC, oncocytic PRCC; gr, grade; MA, metanephric adenoma; MTSC, mucinous tubulary and spindle cell carcinoma.

[a] Not so abundant cytoplasm as in oncocytic PRCC.

In a recently published study, 21 MAs and 23 solid PRCCs shared similar morphologic features. Eleven solid PRCCs lacked papillae completely but showed typical immunoprofile and genetic aberrations of PRCCs [3]. Some of these cases with solid and glomeruloid structures were composed of larger eosinophilic cells and resembled a renal tumor described by Petersson et al [28], provisionally named *biphasic alveolosquamoid renal carcinoma*. This entity was further analyzed in a larger cohort and was recently recognized as a subtype of PRCC. Therefore, a solid-alveolar morphology of this newly described PRCC variant should also be considered in the differential diagnosis of solid PRCC. However, it appears that there is little difference in the clinical management and the prognosis of this entity [29]. It is also worth mentioning that the diagnostic criteria for malignant MA described in the literature were never generally accepted, and likely all malignant MAs represent examples of extremely well-differentiated epithelioid nephroblastomas [20].

Nephroblastoma is very rare in adult patients, but adult nephroblastomas generally do not differ from their pediatric counterpart. Pure epithelioid nephroblastoma is exceptionally rarely seen in adult patients. However, this tumor type should also be considered in the differential diagnosis of solid PRCC. The morphology typically shows tubulopapillar and solid patterns; the cells are small and uniform with scant cytoplasm, and there are absent or very rare mitotic figures [18–19,30–32]. Kinney et al [18] analyzed 37 tumors originally diagnosed as MA, 13 solid PRCCs, and 20 epithelial-predominant nephroblastomas using immunohistochemistry and fluorescence in situ hybridization for trisomy of chromosomes 7 and 17 and loss of Y. All epithelial-predominant nephroblastomas were diffusely positive for WT-1, and only 1 was focally positive for CK7. All tumors showed disomy of chromosomes 7, 17, and Y present [18].

Another renal tumor which frequently shows solid architecture is MTSC. It is characterized by elongated and compressed tubules or cordlike formations of uniform, cuboidal cells with eosinophilic, focally vacuolated cytoplasm and distinct cell spindling, and usually demonstrates low-grade nuclei. The stroma is typically myxoid and contains variable amount of extracellular mucin. Focal clusters of foamy macrophages may also be seen. In cases with limited myxoid stroma (so-called mucin-poor variant) and limited presence of well-formed papillae, it may be difficult to distinguish MTSC from solid PRCC [33–34]. In rare examples of MTSC, the cells form solid and compact areas with minimal amount of interstitial mucin. Such cases can truly mimic solid PRCC, but in well-sampled tumors, more typical areas of MTSC are usually found. Both solid PRCC and MTSC can have tubular structures, papillary architecture, spindle cell appearance, psammoma bodies, foamy macrophages, and interstitial mucin and demonstrate positive staining for vimentin, CK7, CK19, EMA, AMACR, CD10, and RCC [15,17].

There are several studies that consider the issue of MTSC in the differential diagnosis of solid PRCC, raising the possibility that MTSC represents a subtype of PRCC [33–37]. Peckova et al [38] analyzed 54 MTSCs using array comparative genomic hybridization and divided the MTSCs into 3 categories: low grade, high grade, and MTSC overlapping with PRCC. They showed multiple chromosomal losses and no gains in low- and high-grade MTSC groups, supporting the concept that MTSC represents a distinct type of RCC. However, the group showing overlapping features with PRCC demonstrated more heterogeneous status, with frequent gains of chromosomes 7 and/or 17, suggesting that this MTSC subgroup should be considered in the spectrum of PRCC [38].

An oncocytic variant of PRCC different from PRCC type 1 and 2 was also reported, composed of papillae lined by single or rarely pseudostratified layers of cells with granular, deeply eosinophilic cytoplasm and round regular nuclei. In the new 2016 WHO classification of renal tumors, the oncocytic PRCC is considered as a possible new variant of PRCC [5]. This type of PRCC can also show solid pattern in up to 90% of the tumor. The immunoprofile and the genotype are compatible with PRCC [10–11,39–41]. Despite the solid architecture, oncocytic PRCC can be differentiated from solid PRCC mostly by histology. The oncocytic cells of oncocytic PRCC are eosinophilic and contain voluminous cytoplasm and differ from the smaller epithelial cells of solid PRCC which contain scanty cytoplasm.

5. Conclusion

In conclusion, solid PRCC is a rare tumor with an incidence less than 1% of all renal tumors. In the majority of cases, it is composed of solid areas and compressed tubular structures or short abortive papillae that result in a solid appearance. The immunohistochemical and molecular genetic features do not differ from conventional PRCC. Metanephric

adenoma, epithelioid nephroblastoma, and less often MTSC and an oncocytic variant of PRCC should all be considered in the differential diagnosis of solid PRCC.

References

[1] Kovacs G, Akhtar M, Beckwith BJ, Bugert P, Cooper CS, Delahunt B, et al. The Heidelberg classification of renal cell tumours. J Pathol 1997;183(2):131–3.

[2] Eble JN, Sauter G, Epstein JI, Sesterhenn IA, editors. Tumours of the urinary system andmale genital organs. World Health Organization classification of tumours. Press LI; 2004. p. 27–9.

[3] Mantoan Padilha M, Billis A, Allende D, Zhou M, Magi-Galluzzi C. Metanephric adenoma and solid variant of papillary renal cell carcinoma: common and distinctive features. Histopathology 2013;62(6):941–53.

[4] Klatte T, Said JW, Seligson DB, Rao PN, de Martino M, Shuch B, et al. Pathological, immunohistochemical and cytogenetic features of papillary renal cell carcinoma with clear cell features. J Urol 2011;185(1):30–5.

[5] Moch H, Humphrey PA, Ulbright TM, Reuter VE, editors. WHO classification of tumours of the urinary system and male genital organs. 4th ed. Lyon: IARC; 2016.

[6] Mancilla-Jimenez R, Stanley RJ, Blath RA. Papillary renal cell carcinoma: a clinical, radiologic, and pathologic study of 34 cases. Cancer 1976;38(6):2469–80.

[7] Delahunt B, Eble JN. Papillary renal cell carcinoma: a clinicopathologic and immunohistochemical study of 105 tumors. Mod Pathol 1997;10(6):537–44.

[8] Amin MB, Corless CL, Renshaw AA, Tickoo SK, Kubus JK, Schultz DS. Papillary (chromophil) renal cell carcinoma (PRCC): evaluation of conventional pathologic prognostic parameters in 62 cases. Am J Surg Pathol 1997;21:621–35.

[9] Delahunt B, Eble JN, McCredie MR, Bethwaite PB, Stewart JH, Bilous AM. Morphologic typing of papillary renal cell carcinoma: comparison of growth kinetics and patient survival in 66 cases. Hum Pathol 2001;32(6):590–5.

[10] Lefevre M, Couturier J, Sibony M, Bazille C, Boyer K, Callard P, et al. Adult papillary renal tumor with oncocytic cells: clinicopathologic, immunohistochemical, and cytogenetic features of 10 cases. Am J Surg Pathol 2005;29(12):1576–81.

[11] Hes O, Brunelli M, Michal M, Cossu Rocca P, Hora M, Chilosi M, et al. Oncocytic papillary renal cell carcinoma: a clinicopathologic, immunohistochemical, ultrastructural, and interphase cytogenetic study of 12 cases. Ann Diagn Pathol 2006;10(3):133–9.

[12] Gobbo S, Eble JN, Maclennan GT, Grignon DJ, Shah RB, Zhang S, et al. Renal cell carcinomas with papillary architecture and clear cell components: the utility of immunohistochemical and cytogenetical analyses in differential diagnosis. Am J Surg Pathol 2008;32(12):1780–6.

[13] Renshaw AA, Zhang H, Corless CL, Fletcher JA, Pins MR. Solid variants of papillary (chromophil) renal cell carcinoma: clinicopathologic and genetic features. Am J Surg Pathol 1997;21(10):1203–9.

[14] Ngan KW, Ng KF, Chuang CK. Solid variant of papillary renal cell carcinoma. Chang Gung Med J 2001;24(9):582–6.

[15] Argani P, Netto GJ, Parwani AV. Papillary renal cell carcinoma with low-grade spindle cell foci: a mimic of mucinous tubular and spindle cell carcinoma. Am J Surg Pathol 2008;32(9):1353–9.

[16] Cantley R, Gattuso P, Cimbaluk D. Solid variant of papillary renal cell carcinoma with spindle cell and tubular components. Arch Pathol Lab Med 2010;134(8):1210–4.

[17] Zhang Y, Yong X, Wu Q, Wang X, Zhang Q, Wu S, et al. Mucinous tubular and spindle cell carcinoma and solid variant papillary renal cell carcinoma: a clinicopathologic comparative analysis of four cases with similar molecular genetics datum. Diagn Pathol 2014;9:194.

[18] Kinney SN, Eble JN, Hes O, Williamson SR, Grignon DJ, Wang M, et al. Metanephric adenoma: the utility of immunohistochemical and cytogenetic analyses in differential diagnosis, including solid variant papillary renal cell carcinoma and epithelial-predominant nephroblastoma. Mod Pathol 2015 Sep;28(9):1236–48.

[19] Chen L, Deng FM, Melamed J, Zhou M. Differential diagnosis of renal tumors with tubulopapillary architecture in children and young adults: a case report and review of literature. Am J Clin Exp Urol 2014;2(3):266–72.

[20] Arroyo MR, Green DM, Perlman EJ, Beckwith JB, Argani P. The spectrum of metanephric adenofibroma and related lesions: clinicopathologic study of 25 cases from the National Wilms Tumor Study Group Pathology Center. Am J Surg Pathol 2001;25(4):433–44.

[21] Gatalica Z, Grujic S, Kovatich A, Petersen RO. Metanephric adenoma: histology, immunophenotype, cytogenetics, ultrastructure. Mod Pathol 1996;9(3):329–33.

[22] Jones EC, Pins M, Dickersin GR, Young RH. Metanephric adenoma of the kidney. A clinicopathological, immunohistochemical, flow cytometric, cytogenetic, and electron microscopic study of seven cases. Am J Surg Pathol 1995;19(6):615–26.

[23] Brown JA, Anderl KL, Borell TJ, Qian J, Bostwick DG, Jenkins RB. Simultaneous chromosome 7 and 17 gain and sex chromosome loss provide evidence that renal metanephric adenoma is related to papillary renal cell carcinoma. J Urol 1997;158(2):370–4.

[24] Brunelli M, Eble JN, Zhang S, Martignoni G, Cheng L. Metanephric adenoma lacks the gains of chromosomes 7 and 17 and loss of Y that are typical of papillary renal cell carcinoma and papillary adenoma. Mod Pathol 2003;16(10):1060–3.

[25] Obulareddy SJ, Xin J, Truskinovsky AM, Anderson JK, Franklin MJ, Dudek AZ. Metanephric adenoma of the kidney: an unusual diagnostic challenge. Rare Tumors 2010;2(2), e38.

[26] Udager AM, Pan J, Magers MJ, Palapattu GS, Morgan TM, Montgomery JS, et al. Molecular and immunohistochemical characterization reveals novel BRAF mutations in metanephric adenoma. Am J Surg Pathol 2015;39(4):549–57.

[27] Yakirevich E, Magi-Galluzzi C, Grada Z, Lu S, Resnick MB, Mangray S. Cadherin 17 is a sensitive and specific marker for metanephric adenoma. Am J Surg Pathol 2015;39(4):479–86.

[28] Petersson F, Bulimbasic S, Hes O, Slavik P, Martinek P, Michal M, et al. Biphasic alveolosquamoid renal carcinoma: a histomorphological, immunohistochemical, molecular genetic, and ultrastructural study of a distinctive morphologic variant of renal cell carcinoma. Ann Diagn Pathol 2012;16(6):459–69.

[29] Hes O, Condom Mundo E, Peckova K, Lopez JI, Martinek P, Vanecek T, et al. Biphasic Squamoid alveolar renal cell carcinoma: a distinctive subtype of papillary renal cell carcinoma? Am J Surg Pathol 2016;40(5):664–75.

[30] Huser J, Grignon DJ, Ro JY, Ayala AG, Shannon RL, Papadopoulos NJ. Adult Wilms' tumor: a clinicopathologic study of 11 cases. Mod Pathol 1990;3(3):321–6.

[31] Muir TE, Cheville JC, Lager DJ. Metanephric adenoma, nephrogenic rests, and Wilms' tumor: a histologic and immunophenotypic comparison. Am J Surg Pathol 2001;25(10):1290–6.

[32] Reinhard H, Aliani S, Ruebe C, Stockle M, Leuschner I, Graf N. Wilms' tumor in adults: results of the Society of Pediatric Oncology (SIOP) 93-01/Society for Pediatric Oncology and Hematology (GPOH) study. J Clin Oncol 2004;22(22):4500–6.

[33] Fine SW, Argani P, DeMarzo AM, Delahunt B, Sebo TJ, Reuter VE, et al. Expanding the histologic spectrum of mucinous tubular and spindle cell carcinoma of the kidney. Am J Surg Pathol 2006;30(12):1554–60.

[34] Paner GP, Srigley JR, Radhakrishnan A, Cohen C, Skinnider BF, Tickoo SK, et al. Immunohistochemical analysis of mucinous tubular and spindle cell carcinoma and papillary renal cell carcinoma of the kidney: significant immunophenotypic overlap warrants diagnostic caution. Am J Surg Pathol 2006;30(1):13–9.

[35] Alexiev BA, Burke AP, Drachenberg CB, Richards SM, Zou YS. Mucinous tubular and spindle cell carcinoma of the kidney with prominent papillary component, a non-classic morphologic variant. A histologic, immunohistochemical, electron microscopic and fluorescence in situ hybridization study. Pathol Res Pract 2014;210(7):454–8.

[36] Cossu-Rocca P, Eble JN, Delahunt B, Zhang S, Martignoni G, Brunelli M, et al. Renal mucinous tubular and spindle carcinoma lacks the gains of chromosomes 7 and 17 and losses of chromosome Y that are prevalent in papillary renal cell carcinoma. Mod Pathol 2006;19(4):488–93.

[37] Shen SS, Ro JY, Tamboli P, Truong LD, Zhai Q, Jung SJ, et al. Mucinous tubular and spindle cell carcinoma of kidney is probably a variant of papillary renal cell carcinoma with spindle cell features. Ann Diagn Pathol 2007;11(1):13–21.

[38] Peckova K, Martinek P, Sperga M, Montiel DP, Daum O, Rotterova P, et al. Mucinous spindle and tubular renal cell carcinoma: analysis of chromosomal aberration pattern of low-grade, high-grade, and overlapping morphologic variant with papillary renal cell carcinoma. Ann Diagn Pathol 2015;19(4):226–31.

[39] Allory Y, Ouazana D, Boucher E, Thiounn N, Vieillefond A. Papillary renal cell carcinoma. Prognostic value of morphological subtypes in a clinicopathologic study of 43 cases. Virchows Arch 2003;442(4):336–42.

[40] Kunju LP, Wojno K, Wolf Jr JS, Cheng L, Shah RB. Papillary renal cell carcinoma with oncocytic cells and nonoverlapping low grade nuclei: expanding the morphologic spectrum with emphasis on clinicopathologic, immunohistochemical and molecular features. Hum Pathol 2008 Jan;39(1):96–101.

[41] Mai KT, Kohler DM, Robertson SJ, Belanger EC, Marginean EC. Oncocytic papillary renal cell carcinoma with solid architecture: mimic of renal oncocytoma. Pathol Int 2008;58(3):164–8.

1.2.5 Warthin-like papillary renal cell carcinoma: Clinicopathologic, morphologic, immunohistochemical and molecular genetic analysis of 11 cases

Pro tuto práci bylo vybráno 11 případů OPRCC s prominujícím nádorovým lymfocytárním infiltrátem, morfologicky připomínajících Warthinův tumor (tzv. Warthinovu tumoru podobný PRCC/ Warthin-like PRCC).

Tumory pocházely predominantně od mužů (8/11, 73%), věkový průměr pacientů byl 59 let (14-76 let) a průměrná velikost nádoru dosahovala 7cm v největším rozměr (1-22cm). Další průběh onemocnění byl znám u 9 pacientů (v délce trvání v rozmezí 1-132 měsíců, medián 47,6 měsíců), tři pacienti zemřeli na následky onemocnění. Všechny případy obsahovaly denzní zánětlivý infiltrát, u 8/11 případů byla zastižena pseudostratifikace jader. Papilární architektonika byla predominující (tvořící více než 60% tumorózní masy). Tubulární a solidní komponenta byla zastižena v pěti, resp. třech případech. Nádory byly uniformně pozitivní v AMACR, PAX8, MIA, vimentinu a cytokeratinu OSCAR a naopak vesměs negativní v imunuhistochemickém barvení karboanhydrázy 9, CD117, CK20 a TTF-1. Analýza chromozomálních numerických variací prokázala významnou variabilitu u pěti případů, ve spektru od ztrát jediného chromozomu až po komplexní rearanžment genomu. Pouze u jednoho případu byla prokázána polysomie chromosomů 7 a 17 (kromě jiných aberací). Ve čtyřech případech nebyla prokázána žádná numerická imbalance.

Warthin-like PRCC je tumor morfologicky velmi blízký OPRCC, od něhož se liší přítomností denzního lymfoidního stromatu. Numerický chromozomální aberační status těchto tumorů je variabilní. Warthin-like PRCC je potenciálně agresivní, u 3/9 pacientů nádor vedl ke smrti pacientů.

Annals of Diagnostic Pathology 27 (2017) 48–56

Contents lists available at ScienceDirect

Annals of Diagnostic Pathology

Warthin-like papillary renal cell carcinoma: Clinicopathologic, morphologic, immunohistochemical and molecular genetic analysis of 11 cases☆

Faruk Skenderi [a], Monika Ulamec [b], Tomas Vanecek [c], Petr Martinek [c], Reza Alaghehbandan [d], Maria Pane Foix [e], Iva Babankova [f], Delia Perez Montiel [g], Isabel Alvarado-Cabrero [h], Marian Svajdler [c], Pavol Dubinský [i], Dana Cempirkova [j], Michal Pavlovsky [k], Semir Vranic [a], Ondrej Daum [c], Ondrej Ondic [c], Kristyna Pivovarcikova [c], Kvetoslava Michalova [c], Milan Hora [l], Pavla Rotterova [m], Adela Stehlikova [c], Martin Dusek [c], Michal Michal [c], Ondrej Hes [c,*]

[a] Department of Pathology, University of Sarajevo Clinical Center, Sarajevo, Bosnia and Herzegovina
[b] "Ljudevit Jurak" Pathology Department, Clinical Hospital Center "Sestre milosrdnice", Zagreb, Croatia
[c] Department of Pathology, Charles University, Medical Faculty and Charles University Hospital Plzen, Czech Republic
[d] Department of Pathology, University of British Columbia, Royal Columbian Hospital, Vancouver, BC, Canada
[e] Department of Pathology, Bellvitge University Hospital, Barcelona, Spain
[f] Department of Pathology, Masaryk's Oncologic Institute, University Hospital Brno, Czech Republic
[g] Department of Pathology, Instituto Nacional de Cancerologia, Mexico City, Mexico
[h] Department of Pathology, Centro Medico, Mexico City, Mexico
[i] Department of Radiation Oncology, Oncology Institute, Kosice, Slovakia
[j] Department Pathology, Regional Hospital Jindrichuv Hradec, Czech Republic
[k] Department Pathology, Regional Hospital Most, Czech Republic
[l] Department of Urology, Charles University, Medical Faculty and Charles University Hospital Plzen, Czech Republic
[m] Biopticka Laboratory, Pilsen, Czech Republic

ARTICLE INFO

Keywords:
Kidney
Oncocytic papillary renal cell carcinoma
Warthin's tumor
Warthin-like
Lymphoid stroma
Immunohistochemistry
Chromosomal aberration pattern

ABSTRACT

Oncocytic papillary renal cell carcinoma (PRCC) is a distinct subtype of PRCC, listed as a possible new variant of PRCC in the 2016 WHO classification. It is composed of papillae aligned by large single-layered eosinophilic cells showing linearly arranged oncocytoma-like nuclei.

We analyzed clinicopathologic, morphologic, immunohistochemical and molecular-genetic characteristics of 11 oncocytic PRCCs with prominent tumor lymphocytic infiltrate, morphologically resembling Warthin's tumor.

The patients were predominantly males (8/11, 73%), with an average age of 59 years (range 14–76), and a mean tumor size of 7 cm (range 1–22 cm). Tumors had the features of oncocytic PRCCs with focal pseudostratification in 8/11 cases and showed dense stromal inflammatory infiltration in all cases. Papillary growth pattern was predominant, comprising more than 60% of tumor volume. Tubular and solid components were present in 5 and 3 cases, respectively. Uniform immunohistochemical positivity was found for AMACR, PAX-8, MIA, vimentin, and OSCAR. Tumors were mostly negative for carboanhydrase 9, CD117, CK20, and TTF-1. Immunohistochemical stains for DNA mismatch repair proteins MLH1 and PMS2 were retained in all cases, while MSH2 and MSH6 were negative in 1 case. Tumor infiltrating lymphocytes (TILs) consisted of both B and T cells. Chromosomal copy number variation analysis showed great variability in 5 cases, ranging from a loss of one single chromosome to complex genome rearrangements. Only one case showed gains of chromosomes 7 and 17, among other aberrations. In 4 cases no numerical imbalance was found. Follow up data was available for 9 patients (median 47.6 months, range 1–132). In 6 patients no lethal progression was noted, while 3 died of disease.

In conclusion, Warthin-like PRCC is morphologically very close to oncocytic PRCC, from which it differs by the presence of dense lymphoid stroma. Chromosomal numerical aberration pattern of these tumors is variable;

☆ The study was supported by the Charles University Research Fund (project number P36) and by the grant of Ministry of Health of the Czech Republic - Conceptual Development of Research Organization (Faculty Hospital in Pilsen – FN Pl, 00669806).

* Corresponding author at: Department of Pathology, Charles University, Medical Faculty and Charles University Hospital Plzen, Alej Svobody 80, 304 60 Pilsen, Czech Republic.
E-mail address: hes@medima.cz (O. Hes).

http://dx.doi.org/10.1016/j.anndiagpath.2017.01.005
1092-9134/

only one case showed gains of chromosomes 7 and 17. Warthin-like PRCC is a potentially aggressive tumor since a lethal outcome was recorded in 3/9 cases.

1. Introduction

Renal cell carcinoma (RCC) is a highly heterogeneous group of tumors, consisting of at least 14 subtypes recognized in the latest WHO classification, and several additional tentatively distinct variants [1-3]. The subgroup of papillary renal cell carcinoma (PRCC) is further divided into type 1 and 2. Recently, a number of studies have described a small series of morphologically distinctive PRCCs, such as oncocytic, solid, biphasic squamoid alveolar, "mucin"-secreting, or clear cell types, not belonging to any of the two main types [4-9]. These tumors may be associated with foci of type 2-resembling areas and are thus often designated as such, which may contribute to the molecular-genetic heterogeneity of PRCC type 2 tumors [10]. Some of these tumors are even designated as unclassified [11]. Even though the tumor stage remains the best determinant for the survival of patients after nephron sparing surgery within the PRCC group [12], the histological variants of PRCC are important to recognize. This is due to the fact that the papillary morphology is also seen in other RCC subtypes, and thus the treatment and outcome may significantly differ in patients with variant tumors as compared with those who have two classical forms of PRCC.

Oncocytic PRCC [4,13,14] is mentioned in the 2016 WHO classification as a tumor that has a papillary architecture, and is composed of large cells with finely granular eosinophilic cytoplasm, mostly single-layered, and linearly aligned oncocytoma-like nuclei [3]. Such morphology, with addition of a prominent lymphocytic infiltrate in stroma, may commonly be seen in the papillary cystadenoma lymphomatosum (Warthin's tumor) of the salivary glands. To the best of our knowledge, carcinomas resembling benign Warthin's tumor have been described in salivary glands [15] and thyroid [16], but not in the kidney. Tumor infiltrating lymphocytes (TILs) may have prognostic value and that with the advent of novel immune mediated therapies [17], tumors with TILs could be considered for potential immunotherapy in the future. Of note, lymphoid infiltrates are frequently found in tumors of other organs associated with Lynch syndrome. However, a potential link between this hereditary syndrome and lymphoid infiltrates in some renal tumors has not been explored.

The aim of this study was to analyze the clinicopathologic, morphologic, immunohistochemical and molecular-genetic characteristics of 11 oncocytic PRCCs with prominent lymphoid stroma (Warthin-like papillary renal cell carcinoma - WPRCC), morphologically reminiscent of Warthin's tumor.

2. Materials and methods

2.1. Case selection and routine microscopy

There were 1147 in-house and consultation cases of PRCC in Plzen Tumor Registry. We searched the database for keywords "oncocytic, papillary, kidney, lymphoid stroma", and reviewed 147 tumors. We subsequently selected 11 cases with predominant oncocytic cytology and abundant intratumoral lymphocytic infiltrate. All the cases were reviewed by three pathologists (FS, MU, OH). There were 1–10 tissue blocks available for each case, and 1–2 representative blocks were selected for immunohistochemical and molecular–genetic studies. Clinical, gross and follow-up data were collected by review of the institutional medical records and by contacting the consulting pathologists.

Tissue for light microscopy was fixed in 4% formaldehyde, embedded in paraffin using routine procedures. 5 μm thin sections were cut and stained with hematoxylin and eosin. Special stain technique for evaluation of mucin was performed using mucicarmine, periodic acid - Schiff (PAS) and alcian blue at pH 2.5. We evaluated percentages of papillary, tubular, cystic, and solid architectural patterns, abundance of TIL with reference to index case, nuclear grade according to the guidelines of ISUP (International Society of Urologic Pathology), nuclear pseudostratification, single versus multiple cell layers forming papillae, presence of foamy macrophages, and microscopic necrosis.

2.2. Immunohistochemistry

Immunohistochemical study was performed using primary antibodies recognizing following antigens: racemase/AMACR (13H4, monoclonal, Dako, Glostrup, Denmark, 1:200), carbonic anhydrase IX (rhCA9, monoclonal, RD systems, Abingdon, GB, 1:100), vimentin (D9, monoclonal, NeoMarkers, Westinghouse, CA, 1:1000), OSCAR (OSCAR, monoclonal, Covance-SpinChem, San Diego, CA, 1:500), PAX-8 (polyclonal, Cell Marque, Rocklin, CA, 1:25), cytokeratin 7 (OV-TL12/30, monoclonal, Dako, 1:200), cytokeratin 20 (M7019, monoclonal, Dako, 1:100), cytokeratins (AE1-AE3, monoclonal, BioGenex, San Ramon, CA, 1:1000), CD117 (CD117, polyclonal; Dako, Glostrup, Denmark; RTU), EMA (E29, monoclonal; DakoCytomation, Carpinteria, CA; 1:1000), CD10 (56C6, monoclonal; Novocastra, Newcastle upon Tyne, UK; 1:50), TTF-1 (SPT24, monoclonal; Novocastra, 1:400), *anti*-mitochondrial antigen (MIA, monoclonal; BioGenex; 1:100), CD3 (monoclonal, LN10, Novocastra, 1:50), CD5 (monoclonal, 4C7, Novocastra, 1:50), CD20 (monoclonal, L26, DakoCytomation, RTU), MSH2 (monoclonal, G219-1129, Cell Marque, RTU), MSH6 (monoclonal, 44, Ventana, Manheim, Germany, RTU), PMS2 (monoclonal, EPR 3947, Cell Marque, RTU), MLH1 (monoclonal, G168-728, Cell Marque, RTU). The primary antibodies were visualized using the supersensitive streptavidin-biotin-peroxidase complex (BioGenex). Appropriate positive controls were employed for all assays. Immunohistochemical staining was recorded negative if no staining, or less than 5% of staining was observed; as weak (+) for staining of up to 25% of tumor cells; moderate (++) for staining 25–50% of tumor cells; and strong (+++) for staining in more than 50% of tumor cells.

2.3. DNA extraction

DNA was extracted using the QIAsymphony DSP DNA Mini Kit on automated extraction system QIAsymphony SP (QIAGEN, Hilden, Germany) according to the manufacturer's supplementary protocol for FFPE samples. Concentration and purity of isolated DNA were measured using the NanoDrop ND-1000 (NanoDrop Technologies, Inc., Wilmington, DE, USA). DNA integrity was examined by multiplex PCR amplification of five fragments of lengths ranging from 100 to 600 base pairs (bp) [18].

2.4. Low pass whole genome analysis

All samples were tested for copy number variations (CNV) in all chromosomes using low pass whole genome sequencing on Ion Torrent PGM platform using kits and software from Life Technologies (Thermo Fisher Scientific, Waltham, MA USA). The extracted DNA (100 ng) was enzymatically fragmented using a shear enzyme mix contained in Ion Xpress Plus Fragment Library Kit. Samples with DNA integrity control result of 600 bp were sheared 10 min, and samples with lower integrity were sheared 5 min. Sequencing adapters were ligated and the sequencing library was size-selected for 200 bp. Final libraries were

Table 1
Clinicopathological data on Warthin-like papillary renal cell carcinoma.

Case No.	Age	Sex	Size (cm)	TNM stage	Follow-up (months)
Case 1	48	M	1.0[a]	–	DUD 1 months, autopsy, no generalization
Case 2	64	M	6.0	pT3	DOD 9 m, generalization, retroperitoneal lymph nodes, liver, lung, bones
Case 3	69	F	3.0	pT1	AW 12
Case 4	76	M	22[b]	pT3	DOD 12
Case 5	45	M	2.8	pT1	AW 108, then LFU
Case 6	64	M	14.5	pT2	LFU
Case 7	14	M	12.5	pT2	DOD 36
Case 8	NA	M	NA	NA	LFU
Case 9	59	M	2.5	pT1	AW 108
Case 10	74	F	4.2	pT1	AW 132
Case 11	75	F	1.5	pT1	AW 10

DUD = death of unrelated disease.
DOD = death of disease.
AW = alive and well.
LFU = lost to follow up.
NA = not available.
[a] Associated with renal oncocytoma 3.0 cm.
[b] Sarcomatoid component.

pooled and templating and enrichment steps were performed using Hi-Q Template OT2 200 Kit. Sequencing was performed on a 316v2 chip using Hi-Q Sequencing kit according to manufacturer's protocols aiming to obtain minimum of 100 000 reads per sample. Signal processing, mapping and quality control was performed with Torrent Suite v.5.0. CNVs were called and visualized using Ion Reporter v5.2 using low-pass whole-genome aneuploidy workflow. The Median of the Absolute values of all Pairwise Differences (MAPD) score filter was set to 0.3. The called CNVs passing the confidence filter (≥1) were annotated using ISCN cytogenetic coordinates and sequence positions using Hg19 genome assembly and reported in the Table 4. The aneuploidies of gonosomes were adjusted manually regarding the sex of the patient. For each sample several detected CNVs were confirmed by FISH using enumeration probes as described elsewhere [19].

2.5. Mutation analysis of MLH1, MSH2 and MSH6 genes

Mutation analysis of the MLH1, MSH2 and MSH6 genes was performed using PCR and Sanger sequencing as previously described in Kacerovska et al. 2016 [20]. Whole coding sequences (including exon-intron junctions) of the MLH1, MSH2 and MSH6 genes were obtained and compared to the appropriate reference sequences.

2.6. Microsatellite instability (MSI) analysis

Five mononucleotide markers (BAT-25, BAT-26, NR-21, NR-24, and MONO-27) were analyzed using the "MSI Analysis System" kit (Promega, Madison, WI) according to the manufacturer's instructions. The PCR products were separated by capillary electrophoresis using ABI 3130XL Genetic Analyzer (Applied Biosystems), and the output data were analyzed with GeneMapper software (Applied Biosystems).

2.7. MLH1 promoter methylation analysis

To perform methylation analysis, the bisulfite conversion ("EZ DNA Methylation-Gold Kit;" Zymo Research, Burlington, ON, Canada) was followed by the methylation-specific PCR targeting the MLH1 promoter according to Chan et al. [21].

2.8. BRAF V600E mutation analysis

Presence of the BRAF V600E mutation status was tested using the real-time PCR kit Cobas® 4800 BRAF V600 Mutation Test (Roche; Mannheim, Germany) according to the manufacturer's instructions.

3. Results

3.1. Clinicopathologic data

Clinical and pathologic data were available for 10 of 11 cases and are summarized in Tables 1 and 2. The patients were predominantly males (73%) with male to female ratio of 3:1. Average age was 59 years (range 14–76). One half of all tumors were at pT1 stage. The mean size of tumors was 7 cm (range 1–22 cm).

Table 2
Morphological data on Warthin-like papillary renal cell carcinoma.

Case No.	ISUP grade	Foamy macrophages	Architectural pattern[a]	TIL abundance[b]	Cell layers	Nuclear pseudostr.[c]	Necrosis
Case 1	2	+	P	++	SI	+	−
Case 2	2	−	S/P/T	+++	MU	−	+++
Case 3	2	−	P/T	+++	SI	+	+
Case 4	4	−	P	+++	SI	+	+
Case 5	3	−	P	++	SI	+++	−
Case 6	2	−	T	++	SI	+	−
Case 7	3	−	P/T	++	SI	++	−
Case 8	2	+	S/P	++	MU	−	−
Case 9	3	−	P/S	+++	SI	+	+
Case 10	2	+	S/TA	++	SI	+	−
Case 11	2	−	P	+++	SI	−	−

SI – single cell layer; MU – multiple cell layers.
[a] Architectural pattern: P-papillary, S-solid, T-tubular.
[b] TIL - tumor infiltrating lymphocytes: abundance was assessed both on HE and CD3, CD5, and CD20 stained slides, in reference to index case which was designated as +++.
[c] Nuclear pseudostratification was assessed as negative (−), sparse (+), moderate (++), prominent (+++), in reference to index case.

Fig. 1. On cross section the tumors were mostly brown to grey, compact, and well-circumscribed.

In cases when gross description was available (8 of 11 cases), the tumors were brown to grey, compact, and well-circumscribed (Fig. 1). Grossly visible necroses or hemorrhages were not reported.

Follow up information was available for 9/11 patients. Follow up period ranged from 1 to 132 months (median range 47.6 months). In 6 patients, there were no records about aggressive behavior or disease progression. However, 3 patients died of disease 9–36 months after resection. Metastatic spreading was documented to lymph nodes, liver, lung and bones. Sarcomatoid tumor differentiation was present in one case with a lethal outcome.

3.2. Morphologic characteristics

Basic morphologic characteristics are summarized in Table 2. Most of the tumors showed papillary growth pattern in more than 60% of tumor volume (Fig. 2). However, tubular and solid/compressed papillary components were also present in smaller volume percentages, in the majority of the cases (Fig. 3). The tumors were composed of medium to large eosinophilic cells, most of them had visible nucleoli at high magnification, corresponding to ISUP grade 2 (Fig. 4). Two cases were ISUP grade 3 and one was grade 4. Nuclear pseudostratification was present in 8/11 (Fig. 5A), however it was not prominent in the majority of cases (Fig. 5B). Foamy macrophages were seen in 3/11 cases (Fig. 6 and Table 2). Prominent feature in all cases was moderate to strong stromal inflammatory infiltration, predominantly composed of lymphocytes (Fig. 7A and B). The stroma was mostly loose, located within papillary tufts and also in some cases within areas with tubulocystic architecture. Desmoplastic stroma was not seen in any of the cases. Necrotic foci were present in 4/11 cases.

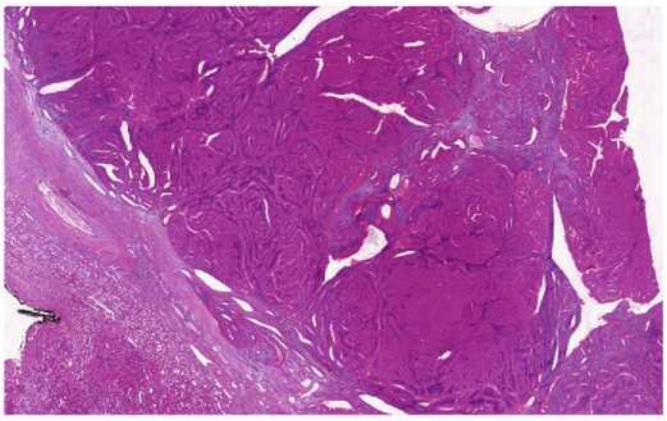

Fig. 3. Tubular and solid components. These were also present in smaller volume percentages in the majority of cases.

One WPRCC contained in addition to the papillary architecture, oncocytic cells and dense lymphoid stroma, a large component showing nondescript spindle cell sarcomatoid differentiation. Clinically, this tumor had an aggressive course and caused patient's death.

3.3. Immunohistochemical examinations

The results of the immunohistochemistry evaluation are summarized in Table 3. Briefly, the tumor cells were positive for PAX-8 (11/11, 100%), MIA (11/11, 100%) (Fig. 8A and B), vimentin (10/11, 91%) and OSCAR (11/11, 100%); variable for AMACR (10/11, 91%), CK7 (5/11, 54%) (Fig. 9 A + B), EMA (5/11, 45%), CD10 (7/11, 63%), and AE1/3 (4/11, 36%); mostly negative for carboanhydrase 9 (0/11, 0%), CD117

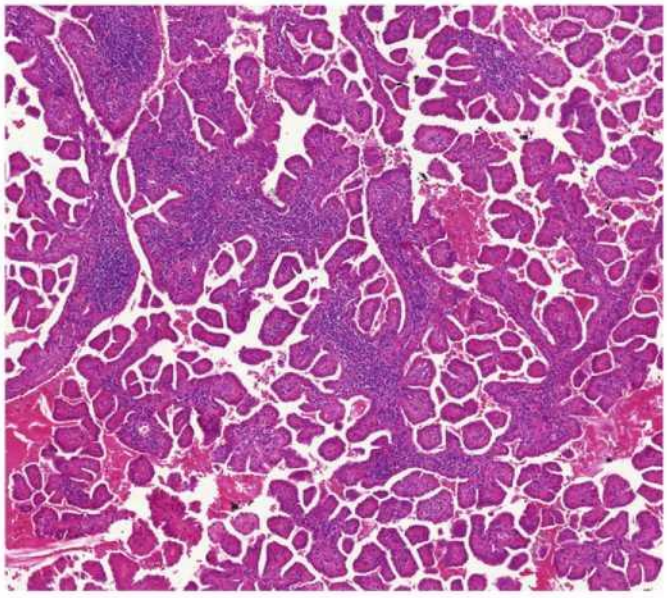

Fig. 2. Papillary growth pattern. It was seen in more than 60% of tumor volume in most tumors.

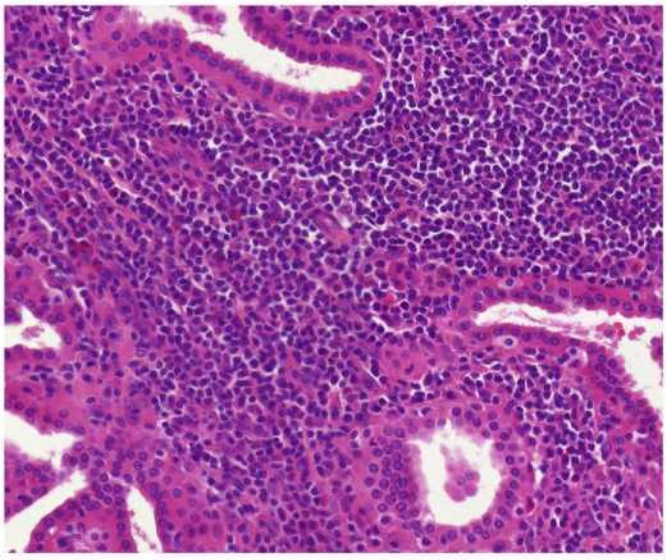

Fig. 4. Medium to large eosinophilic cells. Most of these cells had visible nucleoli at high magnification and corresponded to ISUP grade 2.

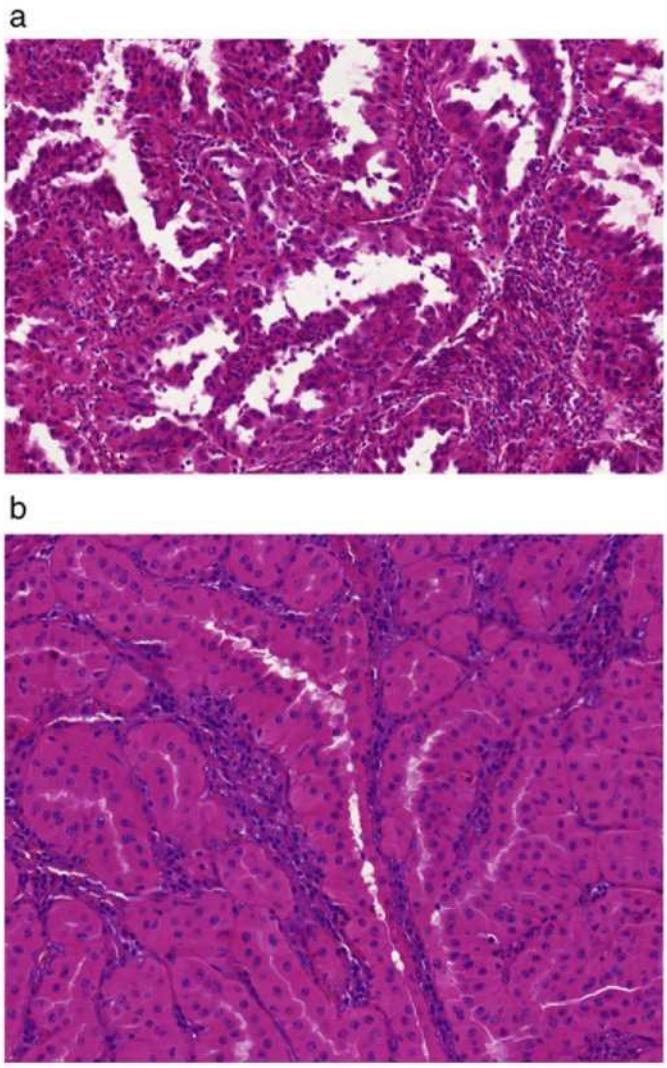

Fig. 5. Nuclear pseudostratification. It was present in 8/11 (A), however it was not prominent in the majority of cases (B).

(0/11, 0%), CK20 (1/11, 9%) and TTF-1 (0/11, 0%). DNA mismatch repair proteins (MLH1, MSH2, MSH6, PMS2) were retained in all cases except one case that exhibited a loss of MSH2 and MSH6 proteins (case no. 4).

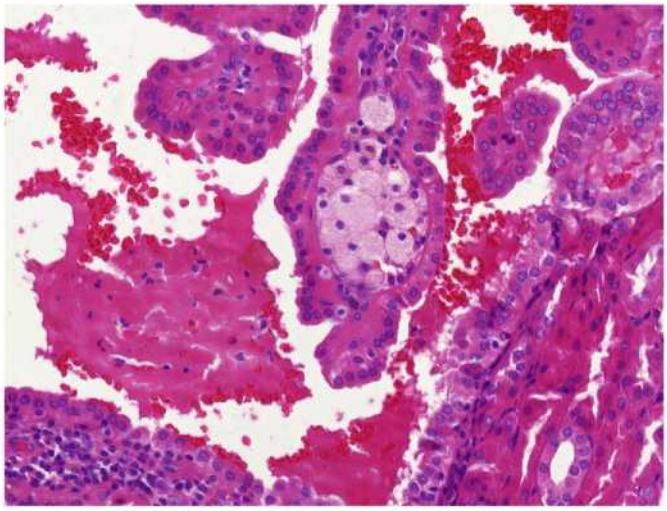

Fig. 6. Foamy macrophages. These cells were seen in 3/11 cases.

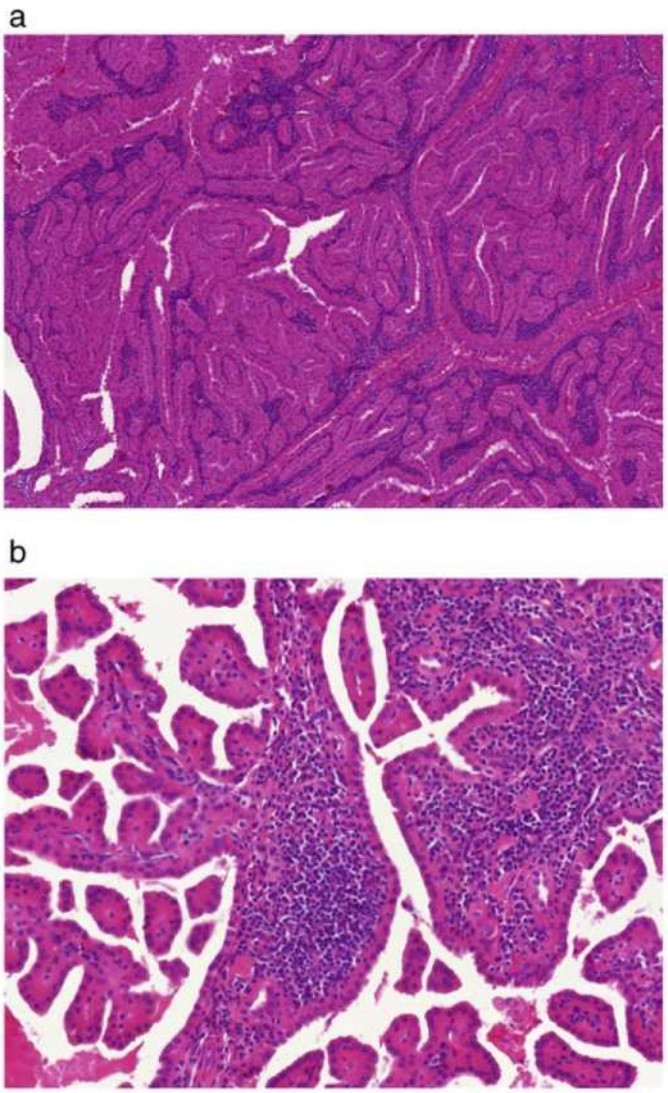

Fig. 7. A + B: lymphoid infiltration of the stroma. Moderate to strong stromal lymphoid infiltration was seen in all tumors.

TILs consisted of both B and T cells, mostly CD5 and CD3 positive, while in two cases CD20 positive lymphocytes were predominant.

3.4. Molecular genetic analysis

Nine cases produced good quality libraries and were successfully sequenced, while the remaining two samples were not analyzable. No CNV were found in four samples. The remaining five samples showed great variability in detected CNV ranging from loss of one chromosome to complex genome rearrangements including gains and losses of various parts of chromosomes as summarized in Table 4 and visualized in Fig. 10. Only one of the cases showed gain of chromosomes 7 and 17 (among the other aberrations). The range and quality of every detected CNV is summarized in Table 5.

Analyses of MMS and *BRAF V600E* were performed in one case (case 4), due to the loss of immunohistochemical reactivity with MSH2 and MSH6.

In the DNA purified from FFPE sample no microsatellite instability (MSI), no aberrant methylation of MLH1 promoter and no mutations in MLH1, MSH2 and MSH6 genes were found. Also *BRAF V600E* mutation was absent.

Table 3
Immunohistochemistry profile of Warthin-like papillary renal cell carcinoma.

Case No.	AMACR	PAX-8	Vimentin	MIA	CD10	CD117	CANH9	CK7	CK20	OSCAR	AE1/AE3	EMA	TTF-1	MSH2	MSH6	MLH1	PMS2
Case 1	+++	+++	+++	+++	+	−	−	−	−	+++	−	−	−	+++	+++	+++	+++
Case 2	−	+++	+++	+++	±	−	−	++	−	+++	+++	∓	−	+++	+++	+++	+++
Case 3	+++	+++	+++	+++	++	−	−	+++	−	+++	+++	+++	−	+++	+	+++	+++
Case 4	++	+++	−	+++	++	−	−	+	−	+++	−	+++	−	−	−	+++	+++
Case 5	+++	+++	++	+++	+++	−	−	−	−	+++	−	−	−	+++	+	+++	+++
Case 6	+++	++	+++	+++	++	−	−	−	−	+++	−	−	−	+++	++	+++	+++
Case 7	+++	+++	+++	+++	−	−	−	−	−	+	−	++	−	+++	+++	+++	+++
Case 8	+++	+++	+++	+++	++	−	−	+	−	+++	−	+	−	+++	+++	+++	+++
Case 9	+++	+++	+++	+++	++	−	−	−	+++	+++	−	−	−	+++	+	+++	+++
Case 10	+++	+++	+++	+++	−	−	−	+	−	+	+	−	−	+++	+++	+++	+++
Case 11	++	+++	+++	+++	−	−	−	+++	−	+++	+++	+++	−	+++	+++	+++	+++
	10/11 (91%)	11/11 (100%)	10/11 (91%)	11/11 (100%)	7/11 (63%)	0/11 (0%)	0/11 (0%)	6/11 (54%)	1/11 (9%)	11/11 (100%)	4/11 (36%)	5/11 (45%)	0/11 (0%)	10/11 (91%)	10/11 (91%)	11/11 (100%)	11/11 (100%)

Intensity and percentage of positive tumor cells were scored as: negative (−) if no staining or less than 5% staining was observed; weakly positive (+), if focal positivity seen in up to 25% of tumor cells; moderate (++), if positivity observed in 25–50% of tumor cells; diffuse (+++), if more than 50% of tumor cells positive. AMACR – alpha-methylacyl-CoA racemase; CANH9 – carboanhydrase 9; MIA – antimitochondrial antigen; MSH2, MSH6, PMS2, MLH1 – DNA mismatch repair enzymes/proteins.

4. Discussion

There are ongoing debates over the PRCC classification. Traditionally these carcinomas have been classified morphologically as type 1 and type 2. However, many cases of PRCC show only a part of the diagnostic criteria or overlapping morphology between both of the types. Results of immunohistochemical analyses are also more compact for type 1 PRCC and rather variable for type 2 PRCC [2]. Recent large multicentric studies from The Cancer Genome Atlas group and Marsaud et al. reported the genetic profile of large number of PRCCs and found that type 1 and type 2 are genetically distinct entities, but type 2 tumors may further be genetically subdivided into three groups [10,11].

Herein we report the clinicopathologic, morphological, immunohistochemical and molecular genetic profile of a distinct variant of renal carcinoma, showing predominantly papillary architecture, oncocytic cytology, and abundant tumor infiltrating lymphocytes, resembling benign Warthin's tumors of the parotid gland.

A series of so-called oncocytic PRCC (OPRCC) and several case reports of these tumors were previously published [4,13,22-25]. All of the studies reported similar morphological characteristics of the tumors, which are arranged mostly in papillary, but also tubular and solid architecture, with deeply eosinophilic cells, arranged in a single layer or in multiple layers, in some cases with pseudostratification. Nuclei are described mostly as bland and round, however, tumors with a nuclear grade 3 were also reported. Necrosis is recorded rarely. Foamy macrophages were occasionally present [13,25].

Our cohort of WPRCC was composed of tumors with similar morphology, however there were some substantial differences. The most striking feature was the presence of dense lymphocytic infiltration of the stroma within core of the papillae or stroma interspersed among tubular component. OPRCC are described mostly as tumors without pseudostratification [25,26], however this feature is mentioned in some papers [4,25]. In WPRCC series nuclear pseudostratification was detected in 8 cases, whereas in 2 cases was prominent and in 6 cases focal.

An interesting finding in our study was that of 10 cases with available follow-up data, 3 had an aggressive clinical course. Furthermore, one tumor with characteristic morphology (papillary architecture, oncocytic cells and dense lymphoid stroma) was associated with sarcomatoid differentiation. Remaining 2 aggressive cases were graded as grade 2 and 3 according ISUP grading system. Of note, the tumor with grade 2 was staged as pT3 according to the TNM 2009.

Immunohistochemical profile of OPRCCs has been reported in several studies [4,13,27]. In the current study, we found the immunoprofile of WPRCC almost identical to previously reported immunoprofile of OPRCC. However, vimentin was diffusely positive in 91% of cases in the current study, while it was variable in the OPRCC. WPRCCs were diffusely positive for AMACR, PAX-8, vimentin, MIA, and OSCAR, variably for cytokeratin AE1/AE3, CK7, CD10, EMA. Tumors were negative for carboanhydrase 9, CD117, CK20 and TTF-1.

Copy number variation analysis was successful in 9/11 cases. No numerical chromosomal aberrations were found in 4 tumors. The remaining 5 cases revealed variable chromosomal gains and losses. Such CNV variability is known in chromophobe RCC, in which, besides frequently encountered multiple loses, variable CNV pattern has been documented [19,28,29]. Only 1 of these 5 cases showed, among other chromosomal abnormalities, a polysomy of chromosomes 7 and 17, which is believed to be characteristic for PRCC. Given significant morphologic and genetic heterogeneity of the PRCC, even within type 2 category, these results are not too surprising. Recent large study from The Cancer Genome Atlas group identified genomic profile of PRCC, concluding that type 1 and 2 PRCC are distinctly different entities, and that type 2 PRCC is a heterogeneous disease with multiple distinct subgroups [10]. These results were also supported by previous studies comprising fewer cases [4,11,13,30,31].

The role of TILs is currently investigated by numerous research groups. Present data suggest that specific TIL phenotypes may have prognostic, predictive, or therapeutic value, however, this is yet to be clarified [17,32]. TIL and peritumoral lymphocytes are commonly found in carcinomas associated with Lynch syndrome (LS). LS is a hereditary cancer syndrome caused by mutations in DNA mismatch repair (MMR) proteins, resulting in deficient DNA repair machinery, eventually leading to a hypermutational phenotype and development of neoplasms in other organs. It is believed that renal cell carcinoma (in contrast to urothelial carcinoma of the renal pelvis) is not associated with LS. To find out whether WPRCC with its TILs could be associated with LS, we analyzed immunoreactivity of four MMR proteins, namely the MSH2, MSH6, PMS2, and MLH1. Except one case, we found in all tumors moderate to strong nuclear expression of investigated proteins, both in the tumor tissue and adjacent normal kidney tissue. In case with lost of MSH2 and MSH6 staining, microsatellite instability (MSI) and methylation of MLH1 promoter analyses, as well as mutations analysis in MLH1, MSH2 and MSH6 genes and *BRAF V600E* mutation were performed, which showed no abnormalities. Our results suggest no relationship between TILs in WPRCC and Lynch syndrome, and possibly, exclude the involvement of investigated MMR genes in tumorigenesis of WPRCC. The expression of MMR proteins was previously evaluated in clear cell RCC [33,34], but this is a first report of such in this unusual variant of PRCC.

Diagnostic features of WPRCC are not highly specific, and that several entities should be considered in the differential diagnosis. The most important one is a metastasis. Oncocytic variant of papillary thyroid

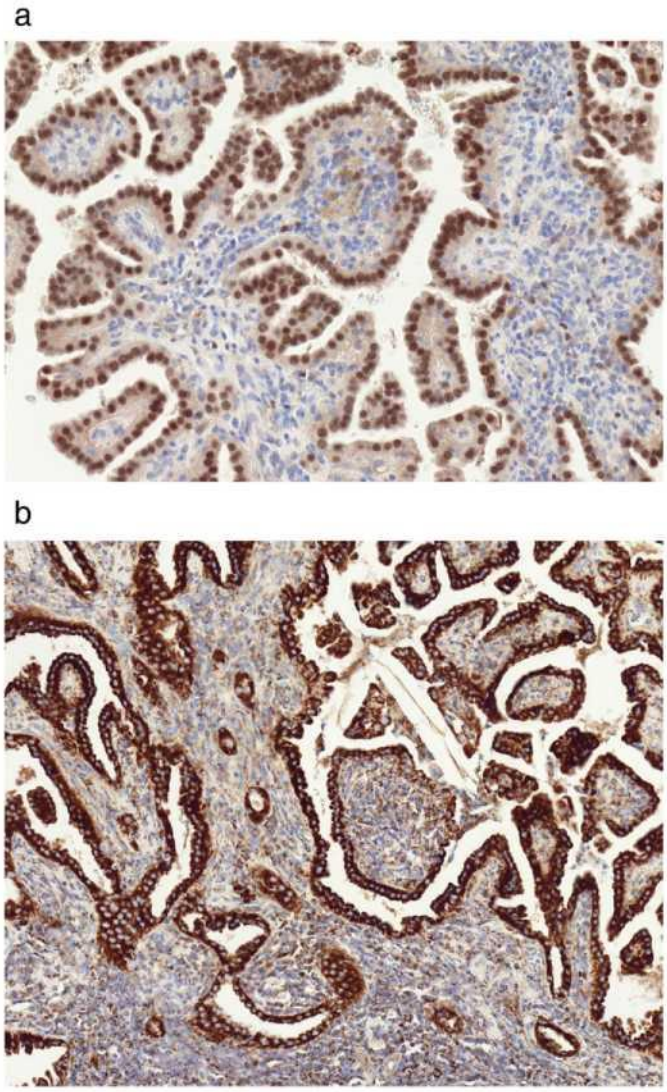

Fig. 8. Immunohistochemistry for PAX8 (A) and antimitochondrial antigen (B)·These immunostainings were positive in n all cases.

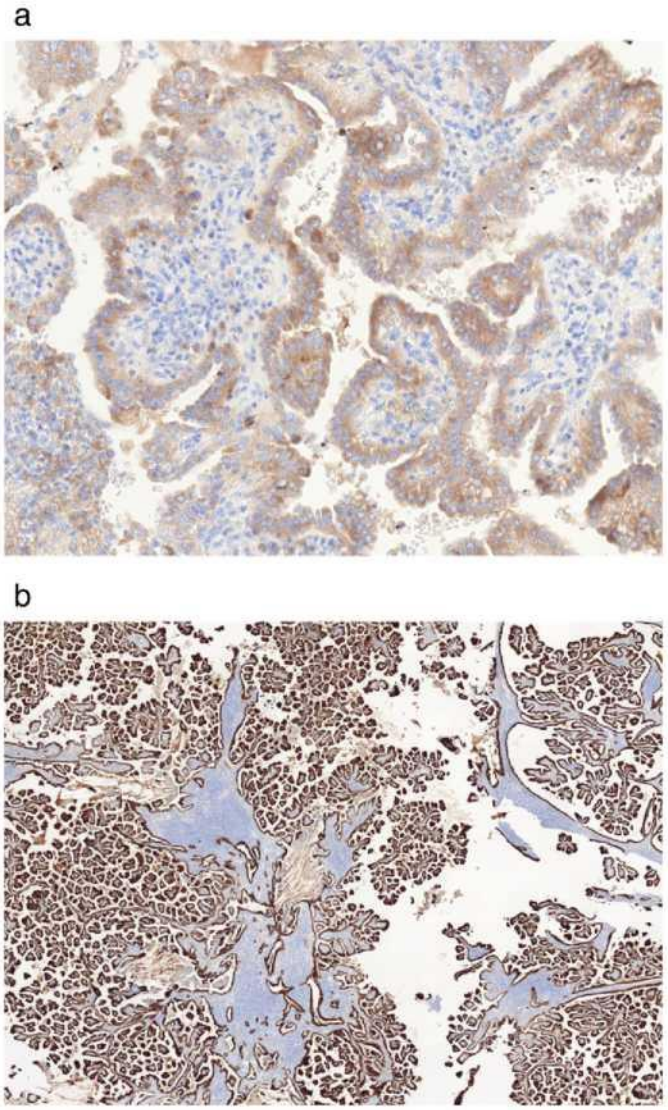

Fig. 9. Immunohistochemistry for AMACR (A) and CK 7 (B). All but one case (case 2) were positive for AMACR, 6 cases were immunoreactive for CK 7.

carcinoma with lymphocytic stroma (Warthin-like variant) is a rare tumor, generally reported to have a favorable prognosis but it may show aggressive clinical behavior [35]. The possibility of a renal metastasis of such a tumor was excluded in our series both clinically and by the fact that TTF-1 was negative in all tumors.

All eosinophilic subtypes of RCC may be considered in the differential diagnosis of Warthin-like PRCC. Oncocytoma and chromophobe RCC may rarely present with architecture mimicking PRCC, however true papillae are not part of the morphologic spectrum of these tumors [2]. Lymphocytic infiltrate in these tumors would be a highly unusual morphologic feature as well.

Another morphologically similar, but much more aggressive entity to be excluded is hereditary leiomyomatosis and renal cell carcinoma (HLRCC)-associated RCC/fumarate hydratase-deficient RCC [2,36,37]. This tumor can be papillary/tubulocystic, composed of eosinophilic cells with high grade nuclei and prominent deep red nucleoli. These tumors are characterized by mutation of the *fumarate hydratase gene* (*FH*). Oncocytic characteristics of cell population in these tumors are not mentioned in the literature. In contrast to HLRCC-associated RCC, we were not able to find typical large nuclei with red nucleoli and perinucleolar halo resembling cytomegalovirus inclusions. Moreover prominent TILs are not described in kidney tumors related to hereditary leiomyomatosis [37]. MiT family translocation carcinomas (namely spectrum of Xp11.2 RCC) may also be considered in the differential diagnosis, as they have papillary growth pattern, and may show areas composed of eosinophilic

Table 4
Summary of copy number variations of chromosomes.

Case No.	Gains	Loses
Case 1	None	None
Case 2	5	1, 3, Y
Case 3	None	None
Case 4	None	None
Case 5	NA	NA
Case 6	None	None
Case 7	None	1, 14, 18, 22
Case 8	1, 2, 5, 21	1, 3, 14, 15, Y
Case 9	7, 8, 12, 17	None
Case 10	None	x
Case 11	NA	NA

NA – not analyzable.

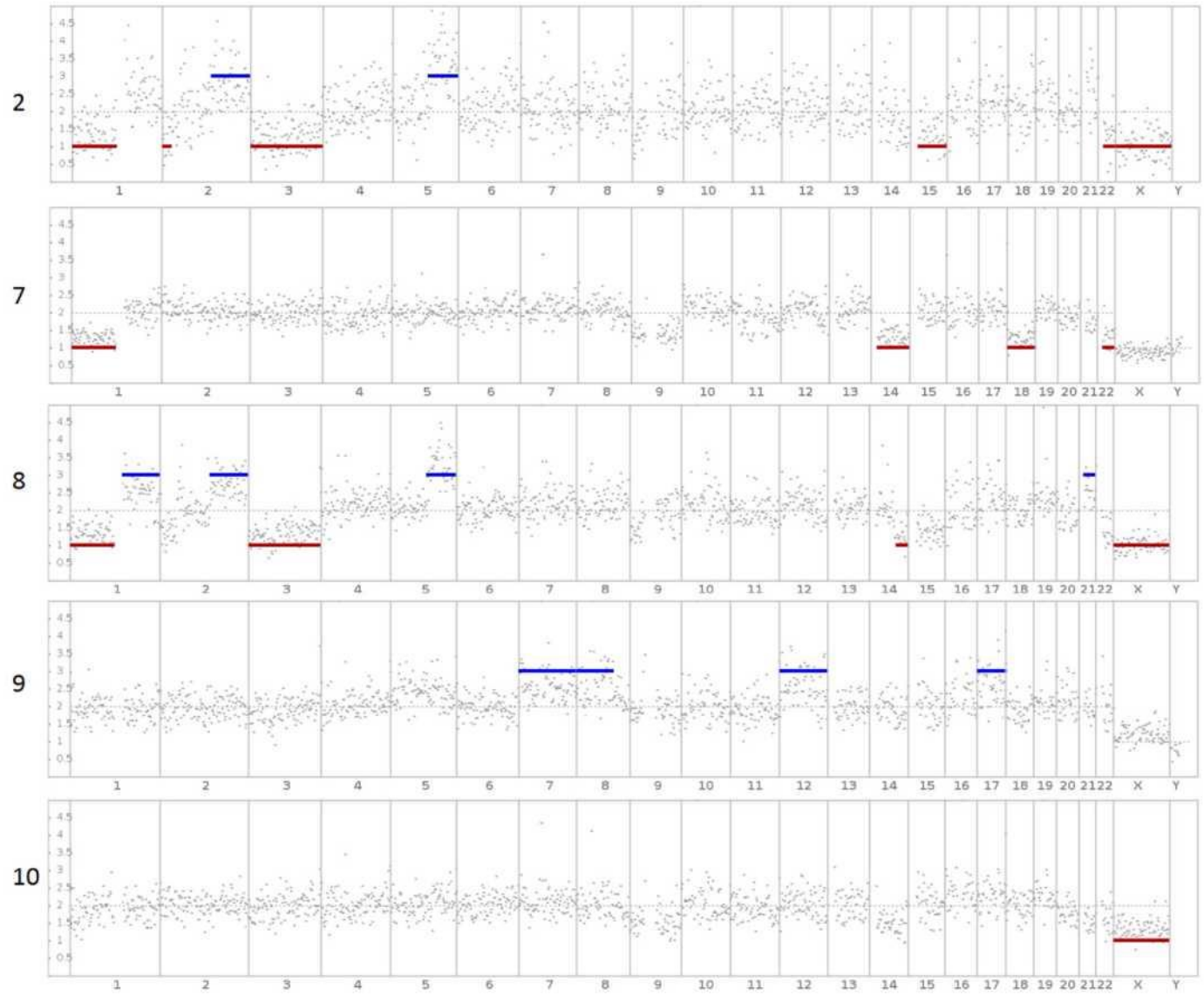

Fig. 10. Chromosome aberration patterns. CNV ranged from loss of one chromosome to complex genome rearrangements including gains and losses of various parts of chromosomes.

cells. Our cases were uniformly composed of oncocytic cells and did not show hyaline bodies, typical microcalcifications and areas with larger pale/clear cells [2].

Tubulocystic RCC may also be considered in the differential diagnosis, mainly because some of our cases did not display CNV. However, our cases differed from tubulocystic RCC by predominantly papillary architecture. No single case from our series showed a predominant tubulocystic growth pattern [38-40].

Succinate dehydrogenase-deficient RCC (SC-RCC) can be in the differential diagnosis as it includes tumors composed of vacuolated eosinophilic to clear cells with inconspicuous nucleoli, usually with a solid growth pattern, but rarely/less frequently showing a tubular or even papillary pattern. This tumor is characterized by the presence of cells with bubbly appearing eosinophilic cytoplasm. In addition to morphological differences, SC-RCC has different imunohistochemical and molecular hallmarks [2,41].

RCC in acquired cystic disease of the kidney (ACDK) is observed exclusively in patients with end-stage renal disease. All our patients had normal renal function, no one was dialyzed or had transplant kidney. Histologically, a variety of RCC types can be found in ACDK patients, including RCC with papillary and tubulopapillary architectures. The tumor cells always have acidophilic cytoplasm with oncocytic features and prominent nucleoli [2]. The presence of mostly abundant oxalate crystalloids is considered to be a typical morphologic feature. We were not able to find oxalate crystals in our cases.

In summary, we analyzed a cohort of PRCCs with oncocytic morphology and dense lymphoid stroma. While the immunohistochemical profile was consistent with PRCC, molecular genetic analysis revealed variable chromosomal abnormalities, indicating that they do not belong to neither type 1, nor type 2 PRCC. Nevertheless, due to the mophological resemblance to the OPRCC, we believe that WPRCC can be considered as part of the spectrum of this variant of papillary renal cell carcinoma group. Since 3/11 cases of WPRCC appeared to have metastatic potential, additional cases need to be studied to elucidate the true malignant potential of these tumors.

Conflict of interest

All authors declare no conflict of interest.

Table 5
Details of detected copy number variations.

Case No.	chr No.	ISCN	Hg19	Copies	Confidence
2	1	1p36.33p11.2	521368-120697156	1	10.02
	2	2p25.3p23.3	10000-25207815	1	1.50
	2	2q22.1q37.3	137858809-243102476	3	2.66
	3	3p26.3q29	60000-197962430	1	27.37
	5	5q21.1q35.3	99536286-180905260	3	13.43
	15	15q11.2q26.3	23564853-102521392	1	8.91
	22	22q11.1q13.33	16847850-50364777	1	5.59
	X	Xp22.33q28	2699520-154931044	1	57.92
7	1	1p36.33p11.2	521368-120697156	1	23.06
	14	14q11.1q32.33	19020000-107289540	1	11.64
	18	18p11.32q23	10000-78017248	1	12.69
	22	22q11.1q13.33	16847850-50364777	1	2.65
8	1	1p36.33p11.2	521368-120697156	1	12.12
	1	1q21.1q44	144810724-248908210	3	4.95
	2	2q22.1q37.3	139830771-243102476	3	14.84
	3	3p26.3q29	60000-197962430	1	24.09
	5	5q21.1q35.3	101498825-180905260	3	35.77
	14	14q24.3q32.33	75191525-107289540	1	1.22
	21	21q11.2q22.3	14338129-48119895	3	2.39
	X	Xp22.33q28	2699520-154931044	1	104.37
9	7	7p22.3q36.3	282484-159128663	3	11.13
	8	8p23.3q22.2	10000-100736467	3	5.95
	12	12p13.33q24.33	145739-133841895	3	8.85
	17	17p13.3q25.3	396626-81195210	3	6.32
10	X	Xp22.33q28	2699520-154931044	1	20.43

chr = chromosome, ISCN = International System for Human Cytogenetic Nomenclature.

Acknowledgement

We would like to thank our friend Ivan Damjanov, MD, PhD (University of Kansas), for all his critical and constructive comments and his assistance with editing of the manuscript.

References

[1] Kuroda N, Hess O, Zhou M. New and emerging renal tumour entities. Diagn Histopathol 2016;22:47–56.
[2] Moch H, Cubilla AL, Humphrey PA, Reuter VE, Ulbright TM. The 2016 WHO classification of tumours of the urinary system and male genital organs-part a: renal, penile, and testicular tumours. Eur Urol 2016;70:93–105.
[3] Moch H, Humphrey PA, Ulbright TM, Reuter VE. WHO classification of tumours of the urinary system and male genital organs. 4th ed. Lyon: IARC; 2016.
[4] Hes O, Brunelli M, Michal M, Cossu Rocca P, Hora M, Chilosi M, et al. Oncocytic papillary renal cell carcinoma: a clinicopathologic, immunohistochemical, ultrastructural, and interphase cytogenetic study of 12 cases. Ann Diagn Pathol 2006;10:133–9.
[5] Hes O, Condom Mundo E, Peckova K, Lopez JI, Martinek P, Vanecek T, et al. Biphasic squamoid alveolar renal cell carcinoma: a distinctive subtype of papillary renal cell carcinoma? Am J Surg Pathol 2016;40:664–75.
[6] Ulamec M, Skenderi F, Trpkov K, Kruslin B, Vranic S, Bulimbasic S, et al. Solid papillary renal cell carcinoma: clinicopathologic, morphologic, and immunohistochemical analysis of 10 cases and review of the literature. Ann Diagn Pathol 2016;23:51–7.
[7] Pivovarcikova K, Peckova K, Martinek P, Montiel DP, Kalusova K, Pitra T, et al. "Mucin"-secreting papillary renal cell carcinoma: clinicopathological, immunohistochemical, and molecular genetic analysis of seven cases. Virchows Arch 2016;469:71–80.
[8] Klatte T, Said JW, Seligson DB, Rao PN, de Martino M, Shuch B, et al. Pathological, immunohistochemical and cytogenetic features of papillary renal cell carcinoma with clear cell features. J Urol 2011;185:30–5.
[9] Ross H, Martignoni G, Argani P. Renal cell carcinoma with clear cell and papillary features. Arch Pathol Lab Med 2012;136:391–9.
[10] Cancer Genome Atlas Research N, Linehan WM, Spellman PT, Ricketts CJ, Creighton CJ, Fei SS, et al. Comprehensive molecular characterization of papillary renal-cell carcinoma. N Engl J Med 2016;374:135–45.
[11] Marsaud A, Dadone B, Ambrosetti D, Baudoin C, Chamorey E, Rouleau E, et al. Dismantling papillary renal cell carcinoma classification: the heterogeneity of genetic profiles suggests several independent diseases. Genes Chromosomes Cancer 2015;54:369–82.
[12] Bigot P, Bernhard JC, Gill IS, Vuong NS, Verhoest G, Flamand V, et al. The subclassification of papillary renal cell carcinoma does not affect oncological outcomes after nephron sparing surgery. World J Urol 2016;34:347–52.
[13] Xia QY, Rao Q, Shen Q, Shi SS, Li L, Liu B, et al. Oncocytic papillary renal cell carcinoma: a clinicopathological study emphasizing distinct morphology, extended immunohistochemical profile and cytogenetic features. Int J Clin Exp Pathol 2013;6:1392–9.
[14] Lefevre M, Couturier J, Sibony M, Bazille C, Boyer K, Callard P, et al. Adult papillary renal tumor with oncocytic cells: clinicopathologic, immunohistochemical, and cytogenetic features of 10 cases. Am J Surg Pathol 2005;29:1576–81.
[15] Ishibashi K, Ito Y, Masaki A, Fujii K, Beppu S, Sakakibara T, et al. Warthin-like mucoepidermoid carcinoma: a combined study of fluorescence in situ hybridization and whole-slide imaging. Am J Surg Pathol 2015;39:1479–87.
[16] Yeo MK, Bae JS, Lee S, Kim MH, Lim DJ, Lee YS, et al. The Warthin-like variant of papillary thyroid carcinoma: a comparison with classic type in the patients with coexisting Hashimoto's thyroiditis. Int J Endocrinol 2015;2015:456027.
[17] Festino L, Botti G, Lorigan P, Masucci GV, Hipp JD, Horak CE, et al. Cancer treatment with anti-PD-1/PD-L1 agents: is PD-L1 expression a biomarker for patient selection? Drugs 2016;76:925–45.
[18] van Dongen JJ, Langerak AW, Bruggemann M, Evans PA, Hummel M, Lavender FL, et al. Design and standardization of PCR primers and protocols for detection of clonal immunoglobulin and T-cell receptor gene recombinations in suspect lymphoproliferations: report of the BIOMED-2 concerted action BMH4-CT98-3936. Leukemia 2003;17:2257–317.
[19] Sperga M, Martinek P, Vanecek T, Grossmann P, Bauleth K, Perez-Montiel D, et al. Chromophobe renal cell carcinomas—chromosomal aberration variability and its relation to Paner grading system: an array CGH and FISH analysis of 37 cases. Virchows Archiv 2013;463:563–73.
[20] Kacerovska D, Drlik L, Slezakova L, Michal M, Stehlik J, Sedivcova M, et al. Cutaneous sebaceous lesions in a patient with MUTYH-associated polyposis mimicking Muir-Torre syndrome. Am J Dermatopathol 2016;38:915–23.
[21] Chan AO, Broaddus RR, Houlihan PS, Issa JP, Hamilton SR, Rashid A. CpG island methylation in aberrant crypt foci of the colorectum. Am J Pathol 2002;160:1823–30.
[22] Matsuoka T, Ichikawa C, Fukunaga A, Yano T, Sugino Y, Okada T, et al. Two cases of oncocytic papillary renal cell carcinoma. Hinyokika kiyo Acta Urol Jpn 2016;62:187–91.
[23] Masuzawa N, Kishimoto M, Nishimura A, Shichiri Y, Yanagisawa A. Oncocytic renal cell carcinoma having papillotubular growth: rare morphological variant of papillary renal cell carcinoma. Pathol Int 2008;58:300–5.
[24] Mai KT, Kohler DM, Robertson SJ, Belanger EC, Marginean EC. Oncocytic papillary renal cell carcinoma with solid architecture: mimic of renal oncocytoma. Pathol Int 2008;58:164–8.
[25] Kunju LP, Wojno K, Wolf Jr JS, Cheng L, Shah RB. Papillary renal cell carcinoma with oncocytic cells and nonoverlapping low grade nuclei: expanding the morphologic spectrum with emphasis on clinicopathologic, immunohistochemical and molecular features. Hum Pathol 2008;39:96–101.
[26] Kim JY. Oncocytic papillary renal cell carcinoma in the background of renal adenomatosis: a case report. Int J Surg Pathol 2016.
[27] Han G, Yu W, Chu J, Liu Y, Jiang Y, Li Y, et al. Oncocytic papillary renal cell carcinoma: a clinicopathological and genetic analysis and indolent clinical course in 14 cases. Pathol Res Pract 2017;213:1–6.
[28] Krill-Burger JM, Lyons MA, Kelly LA, Sciulli CM, Petrosko P, Chandran UR, et al. Renal cell neoplasms contain shared tumor type-specific copy number variations. Am J Pathol 2012;180:2427–39.
[29] Brunelli M, Eble JN, Zhang S, Martignoni G, Delahunt B, Cheng L. Eosinophilic and classic chromophobe renal cell carcinomas have similar frequent losses of multiple chromosomes from among chromosomes 1, 2, 6, 10, and 17, and this pattern of genetic abnormality is not present in renal oncocytoma. Mod Pathol 2005;18:161–9.
[30] Durinck S, Stawiski EW, Pavia-Jimenez A, Modrusan Z, Kapur P, Jaiswal BS, et al. Spectrum of diverse genomic alterations define non-clear cell renal carcinoma subtypes. Nat Genet 2015;47:13–21.
[31] Kovac M, Navas C, Horswell S, Salm M, Bardella C, Rowan A, et al. Recurrent chromosomal gains and heterogeneous driver mutations characterise papillary renal cancer evolution. Nat Commun 2015;6:6336.
[32] Massari F, Santoni M, Ciccarese C, Santini D, Alfieri S, Martignoni G, et al. PD-1 blockade therapy in renal cell carcinoma: current studies and future promises. Cancer Treat Rev 2015;41:114–21.
[33] Yoo KH, Won KY, Lim SJ, Park YK, Chang SG. Deficiency of MSH2 expression is associated with clear cell renal cell carcinoma. Oncol Lett 2014;8:2135–9.
[34] Petersson F, Sima R, Sperga M, Kazakov DV, Michal M, Hora M, et al. Lymphocyte-rich renal cell carcinoma: an unusual histomorphologic manifestation of a tumor that is not part of lynch syndrome. Appl Immunohistochem Mol Morphol 2011;19:519–27.
[35] Gross M, Eliashar R, Ben-Yaakov A, Weinberger JM, Maly B. Clinicopathologic features and outcome of the oncocytic variant of papillary thyroid carcinoma. Ann Otol Rhinol Laryngol 2009;118:374–81.
[36] Smith SC, Trpkov K, Chen YB, Mehra R, Sirohi D, Ohe C, et al. Tubulocystic carcinoma of the kidney with poorly differentiated foci: a frequent morphologic pattern of fumarate hydratase-deficient renal cell carcinoma. Am J Surg Pathol 2016;40:1457–72.
[37] Trpkov K, Hes O, Agaimy A, Bonert M, Martinek P, Magi-Galluzzi C, et al. Fumarate hydratase-deficient renal cell carcinoma is strongly correlated with fumarate hydratase mutation and hereditary leiomyomatosis and renal cell carcinoma syndrome. Am J Surg Pathol 2016;40:865–75.
[38] Tran T, Jones CL, Williamson SR, Eble JN, Grignon DJ, Zhang S, et al. Tubulocystic renal cell carcinoma is an entity that is immunohistochemically and genetically distinct from papillary renal cell carcinoma. Histopathology 2016;68:850–7.
[39] Ulamec M, Skenderi F, Zhou M, Kruslin B, Martinek P, Grossmann P, et al. Molecular genetic alterations in renal cell carcinomas with tubulocystic pattern: tubulocystic renal cell carcinoma, tubulocystic renal cell carcinoma with heterogenous component and familial leiomyomatosis-associated renal cell carcinoma. clinicopathologic and molecular genetic analysis of 15 cases. Appl Immunohistochem Mol Morphol 2016;24:521–30.
[40] Banerjee I, Yadav SS, Tomar V, Yadav S, Talreja S. Tubulocystic renal cell carcinoma: a great imitator. Rev Urol 2016;18:118–21.
[41] Kuroda N, Yorita K, Nagasaki M, Harada Y, Ohe C, Jeruc J, et al. Review of succinate dehydrogenase-deficient renal cell carcinoma with focus on clinical and pathobiological aspects. Pol J Pathol 2016;67:3–7.

1.2.6 "Mucin"-secreting papillary renal cell carcinoma: clinicopathological, immunohistochemical, and molecular genetic analysis of seven cases

Mucín a mucínu podobný materiál je typicky součástí mucinózního tubularního a vřetenobuněčného RCC (MTS RCC), ale vzácně též může být zastižen i u PRCC. V rámci studie bylo blíže morfologicky, histochemicky, imunohistochemicky a molekulárně-geneticky představeno 7 případů obsahujících extracelulární a/nebo intracelulární mucinózní/mucínu podobný materiál.

Všechny případy vykazovaly predominantně papilární architektoniku a mucín/mucínu podobný materiál byl přítomen u jednoho případu extracelulárně, ve třech případech intracelulárně a u třech případů kombinovaně intra- i extracelulárně. Klinická data byla dostupná u všech pacientů (pět mužů a jedna žena, věkové rozmezí 61-78 let). Velikost tumorů se pohybovala v rozměrů 3-5 cm (průměr 3,8 cm). Follow-up byl dostupný u 5/7 pacientů (v trvání 2-4 roky). Jeden pacient zemřel na nádorový rozsev. Všechny tumory měly pozitivní reakci pro AMACR, vimentin a OSCAR; CK7 bylo pozitivní v 4/7 tumorů. Mucikarmín byl pozitivní ve všech případech, PAS v šesti tumorech a Alciánová modř ve třech případech. Pět tumorů bylo pozitivní v MUC1, žádný nebyl pozitivní pro MUC2, MUC4, nebo MUC6. Cytogenetická analýza byla provedena u čtyř případů - zisk chromozomů 7 a 17 detekován ve dvou tumorech, zisk chromozomu 17 u jednoho případu a ztráta heterozigozity 3p (LOH3p) společně s polyzomií 7 a 17 byla prokázána u jednoho z tumorů.

PRCC s produkcí mucínu je raritní variantou PRCC s metastatickým potenciálem.

Virchows Arch (2016) 469:71–80
DOI 10.1007/s00428-016-1936-7

ORIGINAL ARTICLE

"Mucin"-secreting papillary renal cell carcinoma: clinicopathological, immunohistochemical, and molecular genetic analysis of seven cases

Kristyna Pivovarcikova[1] · Kvetoslava Peckova[1] · Petr Martinek[1] · Delia Perez Montiel[2] · Kristyna Kalusova[3] · Tomas Pitra[3] · Milan Hora[3] · Faruk Skenderi[4] · Monika Ulamec[5] · Ondrej Daum[1] · Pavla Rotterova[1] · Ondrej Ondic[1] · Magdalena Dubova[1] · Romuald Curik[1] · Ana Dunatov[6] · Tomas Svoboda[7] · Michal Michal[1] · Ondrej Hes[1,8]

Received: 28 December 2015 / Revised: 9 March 2016 / Accepted: 28 March 2016 / Published online: 12 April 2016

Abstract Mucin and mucin-like material are features of mucinous tubular and spindle renal cell carcinoma (MTS RCC) but are rarely seen in papillary renal cell carcinoma (PRCC). We reviewed 1311 PRCC and identified 7 tumors containing extracellular and/or intracellular mucinous/mucin-like material (labeled as PRCCM). We analyzed these using morphological, histochemical, immunohistochemical, and molecular genetic methods (arrayCGH, FISH). Clinical data were available for six of the seven patients (five males and one female, age range 61–78 years). Follow-up was available for four patients (2–4 years); one patient died of widespread metastases. Tumor size ranged from 3 to 5 cm (mean 3.8). Of all cases, histological architecture showed a predominantly papillary pattern. Mucin or mucin-like was extracellular in one, intracellular in three, and both intra/extracellular in three cases. All tumors were positive for AMACR, vimentin, and OSCAR, while CK7 was positive in four. Mucicarmine stain was positive in all cases, PAS in six and Alcian blue in three cases. Five tumors were positive for MUC 1, but none were positive for MUC 2, MUC 4, or MUC 6. In only four cases, genetic analysis could be performed. Gain of chromosomes 7 and 17 was found in two cases; gain of 17 only was found in one case. Loss of heterozygosity of 3p was found in one case together with polysomy of chromosomes 7 and 17. No abnormalities of *VHL*, *fumarate dehydrogenase*, and *TFE3* genes were detected. We conclude that PRCCM is a rare but challenging subtype of RCC that deserves to be further studied. In all the tumors, the mucin-like material was found in those stained with mucicarmin, but other conventional and immunohistochemical stains did not reveal consistent features of a single mucin. The molecular-genetic profile of these tumors was most consistent with that of typical papillary RCC, although one case had mixed genetic features of papillary and clear RCC. PRCCM has metastatic potential, as evidenced by one case with widespread metastases. It remains to be determined whether PRCCM represents a unique tumor subtype, deserving to be distinguished from other subtypes of PRCC.

Keywords Kidney · Papillary renal cell carcinoma · Mucin · Mucin-like secretion · Immunohistochemistry · Array CGH · FISH

✉ Ondrej Hes
hes@medima.cz

1 Department of Pathology, Medical Faculty, Charles University and Charles University Hospital Plzen, Alej Svobody 80, 304 60 Pilsen, Czech Republic

2 Department of Pathology, Instituto Nacional de Cancerologia, Mexico City, Mexico

3 Department of Urology, Medical Faculty, Charles University and Charles University Hospital Plzen, Prague, Czech Republic

4 Department of Pathology, University Hospital Sarajevo, Sarajevo, Bosna and Hercegovina

5 Pathology Department, Clinical Hospital Center, Sestre milosrdnice, Zagreb, Croatia

6 Department of Pathology, University Hospital Split, Split, Croatia

7 Department of Oncology, Medical Faculty, Charles University and Charles University Hospital Plzen, Prague, Czech Republic

8 Biomedical Centre, Faculty of Medicine in Plzen, Charles University in Prague, Plzen, Czech Republic

Introduction

Interstitial mucin is an almost constant feature of mucinous tubular and spindle RCC (MTS RCC) [1]. Other renal cell

tumors with mucin production, including mucinous papillary renal cell carcinoma (PRCC), renal papillary adenoma (RPA), renal oncocytoma (RO), and clear cell RCC (CCRCC), are rare, and most of them have been reported in the literature as case reports or a short series of cases. Mucin deposits in MPRCC, RPA, and CCRCC have been described as intracytoplasmic and intraluminal [2–5]. In RO, mucin was described in the lumen of scattered tubules but not intracytoplasmic [6].

Mucicarmine, an empirical stain for mucin and mucin-like material, has been occasionally used by pathologists to exclude renal origin in case of a papillary carcinoma with unknown primary [7]. However, rare cases of mucicarmine-positive papillary renal cell carcinomas have been reported. We therefore decided to determine how common mucicarmine-positive PRCC are and whether or not they represent a distinct clinicopathological entity. To this end, we reviewed 1311 PRCC in our files and identified 7 cases that were mucicarmine positive. This paper presents characteristics of these tumors.

Material and methods

Ten renal tumors matching keywords "unclassified, papillary, mucin, renal cell carcinoma" were retrieved out of 1311 PRCC from the Plzen Tumor Registry. All cases were reviewed by two pathologists (KPi, OH), who compared the features with the index cases. Finally, 7 cases were selected. There were 1–13 blocks available for each case; 1–2 representative blocks of each case were selected for immunohistochemical and molecular genetic study.

Tissue for light microscopy had been fixed in 4 % formaldehyde and embedded in paraffin using routine procedures. Tissue sections (4 μm) were cut and stained with hematoxylin and eosin (H&E). As special staining techniques for mucin, we used mucicarmine, Periodic Acid-Schiff (PAS), and Alcian blue at pH 2.5.

Immunohistochemical staining was performed using primary antibodies against the following antigens: racemase/AMACR (13H4, monoclonal, DAKO, Glostrup, Denmark, 1:200), carbonic anhydrase IX (rhCA9, 303123, monoclonal, RD Systems, Abingdon, GB, 1:100), vimentin VM (D9, monoclonal, NeoMarkers, Westinghouse, CA, 1:1000), MUC 1 (Ma695, monoclonal, Leica, Newcastle, UK, 1:200), MUC 5 AC (CLH2, monoclonal, Leica, 1:400), MUC 2 (Ccp58, monoclonal, Novocastra,Newcastle upon Tyne, UK, 1:400), MUCIN 4 (8G7, monoclonal, Santa Cruz Biotechnology, Dallas, TX, 1:50), MUC 6 (CLH5, monoclonal, Novocastra, 1:300), OSCAR (OSCAR, 1:500, Covance, Herts, UK, 1:500), PAX-8 (polyclonal rabbit, Cell Marque, Rocklin, CA, 1:25), CDX2 (CDX2-88, monoclonal, BioGenex, San Ramon, CA, 1:150), cytokeratin 7 (OV-TL12/30, monoclonal, DakoCytomation, Carpenteria, CA, 1:200), cytokeratin 20 (Ks20.8, monoclonal, DakoCytomation, 1:100), and cytokeratin (AE1-AE3, monoclonal, BioGenex, 1:1000). Bound antibodies were visualized using a supersensitive streptavidin-biotin-peroxidase complex (Biogenex). Appropriate positive controls were employed.

DNA extraction

DNA from macro-dissected formalin-fixed paraffin-embedded (FFPE) tissue was extracted using a QIAsymphony DNA Mini Kit (Qiagen, Hilden, Germany) on an automated system (QIAsymphony SP, Qiagen) according to the manufacturer's supplementary protocol for FFPE samples (purification of genomic DNA from FFPE tissue using the QIAamp DNA FFPE Tissue Kit and Deparaffinization Solution). Samples were then purified using Qiaquick kit (Qiagen) and eluted in EB buffer. Concentration and purity of isolated DNA was measured using NanoDrop ND-1000 (NanoDrop Technologies Inc., Wilmington, DE, USA). DNA integrity was examined by amplification of control genes in multiplex PCR [8].

Array comparative genomic hybridization

CytoChip Focus Constitutional (BlueGnome Ltd., Cambridge, UK) array was used for array comparative genomic hybridization (aCGH) analysis. It uses BAC technology and covers 143 regions of known significance with 1 Mb spacing across a genome. Probes are spotted in triplicate. First, 400 ng of DNA was labeled using a Fluorescent Labeling System (BlueGnome Ltd., Cambridge, UK). The procedure included Cy3 labeling of a test sample and Cy5 labeling of a reference sample. Commercially produced reference of the opposite sex was used when no reference sample was available (MegaPool Reference DNA Male/Female, Kreatech Diagnostics, Amsterdam, Netherlands). The labeled reference and the test sample were mixed, dried, and hybridized overnight at 47 °C using Arrayit hybridization cassette (Arrayit Corporation, California, U.S.A.). Post-hybridization washing was done using SSC buffers with increasing stringency. Dried microarrays were scanned with InnoScan 900 (Innopsys, France) at a resolution of 5 μm. Scanned images were analyzed and quantified by BlueFuse Multi software (BlueGnome Ltd., Cambridge, UK). The software uses Bayesian algorithms to generate intensity values for each Cy5 and Cy3 labeled spot on the array according an appropriate gal file. Cutoff values for log 2 ratio are preset to −0.3 for loss and to 0.3 for gain by BlueFuse software. All genomic coordinates were based on the March 2009 assembly of the reference genome GRCh37.

Fluorescent in situ hybridization (FISH)

FFPE tissue sections (4 μm) were placed onto a positively charged glass slide. The target area, corresponding to what was marked on a H&E stained slide, was circled with a diamond pen. The section was routinely deparaffinized, incubated in the 1× Target Retrieval Citrate Solution (DAKO, Glostrup, Denmark; pH 6 for 40 min at 95 °C) then cooled in the same solution (20 min at room temp). The slide was washed in deionized water and digested in protease solution with Pepsin (0.5 mg/ml in 0.01 M HCl; Sigma Aldrich, St. Louis, MO, USA) at 37 °C for 15 min. The slide was then immersed in deionized water for 5 min, dehydrated in a series of ethanol solutions (70, 85, and 96 %, 2 min each), and air-dried. Fluorescent in situ hybridization (FISH) probes CEP 7 Spectrum Orange (D7Z1), CEP 17Spectrum Orange, CEP X (DXZ1) Spectrum Green/CEP Y (DYZ3), and Spectrum Orange (Vysis/Abbott Molecular, Des Plaines, Illinois) were mixed with water and hybridization buffers according to the manufacturer's protocol. The slide was incubated in a ThermoBrite instrument (StatSpin/Iris Sample Processing, Westwood, Massachusetts) with codenaturation (85 °C for 8 min) and hybridization (37 °C for 16 h). Post-hybridization wash was performed in 2× SSC/0.3 % NP-40 solution (72 °C for 2 min). The section was counterstained with DAPI I (Vysis) and stored in the dark at −20 °C until examined. FISH signals were assessed using an Olympus BX51 fluorescence microscope. Scoring of aneuploidy was performed by counting the number of fluorescent signals in 100 randomly selected, non-overlapping tumor cell nuclei. The slide was independently enumerated by two observers (PG, TV). Cutoff values were set for each probe as shown in previous study [9].

Results

Clinical data were available for six of the seven cases (Table 1). These included five males and one female, age range 61 to 78 years (median 74 years, mean 71.17 years). Tumor size ranged from 3 to 5 cm in the greatest dimension (median 3.5 cm, mean 3.8 cm). One tumor was found in the left kidney and two in the right kidney; no information about laterality was available for four cases. On gross section, the tumors were yellowish to gray-white to grayish-brown, with visible hemorrhages in two cases.

Follow-up was available for four patients (range 2 to 4 years, mean 2.75 years, median 2.5 years). One patient died of disease 4 years after diagnosis despite treatment (sunitinib). One patient died of colorectal adenocarcinoma 2 years after diagnosis. Two patients are alive and well without signs of recurrence or metastasis, although for one patient, only basic and limited information was available. Other patients were lost to follow-up.

Histological findings

The histopathological features are summarized in Table 2. All seven cases showed at histological examination a papillary pattern architecture (Fig. 1). In two cases, a prominent tubulopapillary component (cases 4 and 5) was noted (Fig. 2). Cases 2 and 3 contained smaller areas with a solid pattern. Bluish to eosinophilic mucin-like material was present to a variable extent in all cases (Fig. 3a, b). This was only extracellular in one case; in three cases, it was only intracellular; and in three cases, it was present both intracellularly and extracellularly in H&E-stained sections.

Extracellular material presented as a bluish to eosinophilic deposit of mucin-like material in the interstitium between tumor cells or within papillary stalks. Intracellular material presented as a mucin-like substance in the cytoplasm as larger or smaller clear vacuoles. Some of these cells had the features of signet-ring cells (Fig. 4a, b) and they were present in five cases. In all cases, mucin-like material was positive for mucicarmine (Fig. 5), and in six cases, it was PAS positive (Fig. 6). In three cases, the cells were reactive with Alcian blue, and this was designated as PAS and Alcian blue co-staining. The intracellular mucin-like material was positive either for mucicarmine or for PAS in two of the cases containing cells with signet-ring

Table 1 Basic clinicopathological data

Case	Sex	Age (years)	Size (cm)	Site	Stage	Color	Follow-up
1	F	78	3 × 2 × 1.5	NA	pT1a (TNM09)	NA	NA
2	M	77	3 × 3.5 × 1.5 and 2 × 1.5 × 1	Right	pT1a (TNM09)	Ochroid	2 years, AW
3	M	76	3.5 × 2.5 × 3	Right	pT1 (TNM09)	Yellowish	Dead of disease 4 years after dg.
4	M	63	Diameter 5	NA	NA	NA	NA
5	NA	NA	NA	NA	NA	NA	NA
6	M	61	3 × 3.7 × 4	NA	NA	Gray-white	3 years, A, no information about health condition
7	M	72	NA	Left	NA	Grayish-brown	Dead 2 years after dg.—other malignant disease

M male, *F* female, *NA* not available, *AW* alive and well, *A* alive

Table 2 Histopathological features

Case	Papillary	Tubulopapillary	Solid	Extracellular mucin-like secretion	Intracellular mucin-like secretion	Signet-ring morphology	Hibernoma-like changes	Psammoma bodies	Siderophages	Foamy macrophages	Giant cells	Heamorrhage	Fuhrman grade (ISUP)	Type
1	+	–	–	+ (intraluminal)	+	+	–	–	–	–	–	–	2	1
2	+	–	+ (10 %)	+ (papillary stroma)	+	–	–	–	–	+	–	+	2	1
3	+	–	+ (20 %)	–	+	+	+	+	+	+	+	+	4	NOS
4	+	+ (80 %)	–	+ (papillary stroma)	–	–	–	–	–	+	–	–	2	1
5	+	+	–	+ (intraluminal)	+	+	–	–	–	+	–	–	3	NOS
6	+	–	–	–	+	+	–	–	+	+	+	+	3	2
7	+	–	–	–	+	+	+	–	+	+	+	+	3	2

+ = present, – = absent, *NOS* not otherwise specified

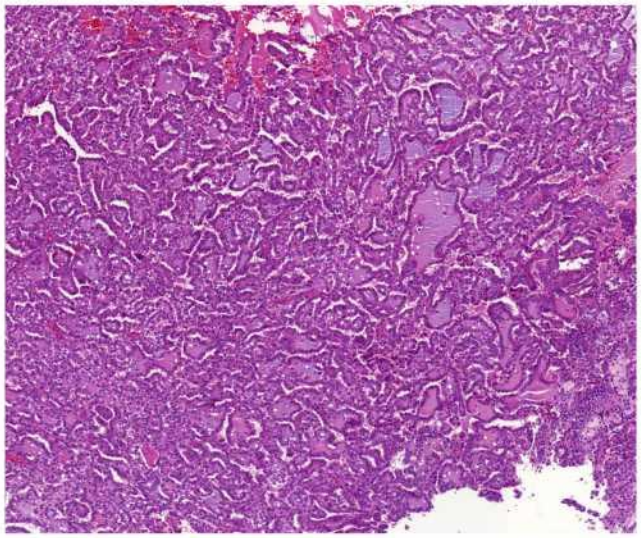

Fig. 1 All 7 cases were arranged in papillary pattern

morphology. In three of the cases, cells with signet-ring morphology did not react with mucicarmine nor PAS. Four tumors contained hemorrhagic areas. Foamy macrophages were found in six cases. Hemosiderophages were observed in three cases and in two cases (cases 3 and 7) clear cell-like areas, containing cells with foamy cytoplasm and microvacuolated appearance resembling macrophages or hibernoma cells (Fig. 7). These tumors both contained also giant multinucleated neoplastic cells.

In addition to these morphological features, we found a focus with epithelial cells in pseudorosette formation in case 3, numerous extracellular eosinophilic globules, and larger pools of eosinophilic material in case 5 and in case 6 abundant giant multinucleated cells and foamy macrophages.

Nuclear grades according to the "Fuhrman (ISUP) nucleolar" grading system was 4 (one case), 3 (three cases), and 2 (three cases). No relationship or direct connection with renal pelvis or calyces was seen.

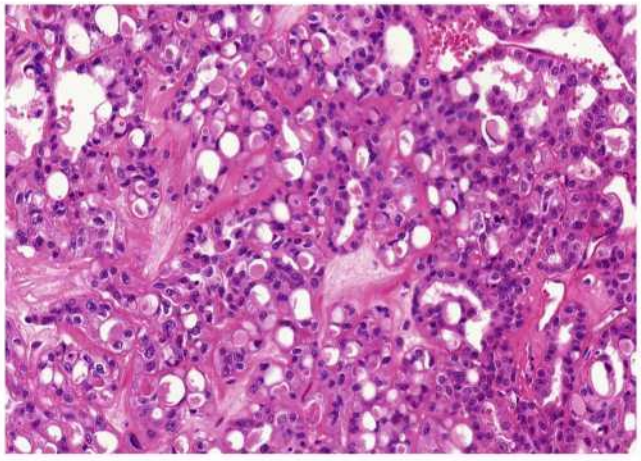

Fig. 2 Focus of tubulopapillary architecture was noted in 2 cases

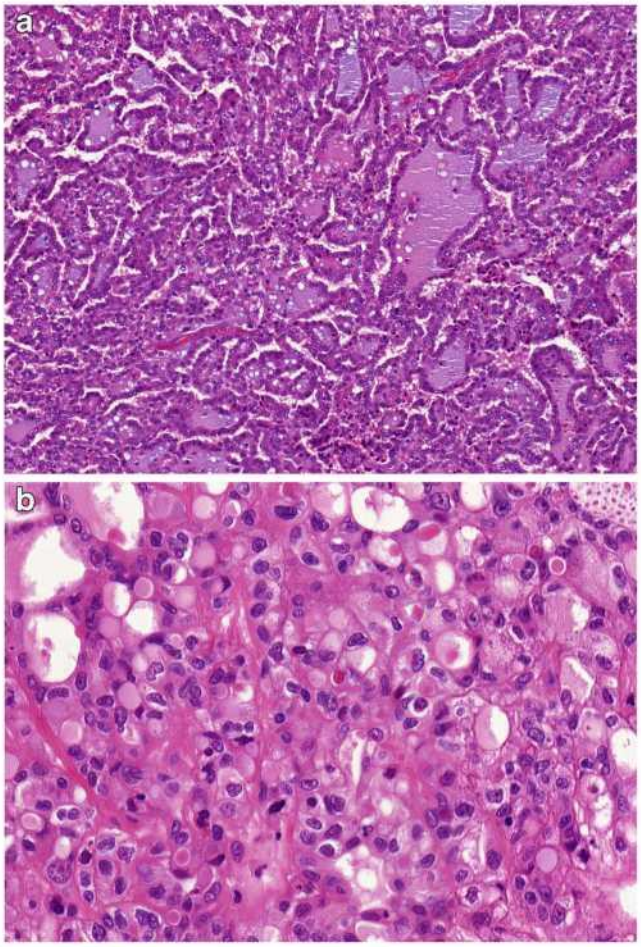

Fig. 3 Bluish to eosinophilic mucin-like secretion was variably present in all cases in the intersticium (**a**) or in intracellular vacuoles (**b**)

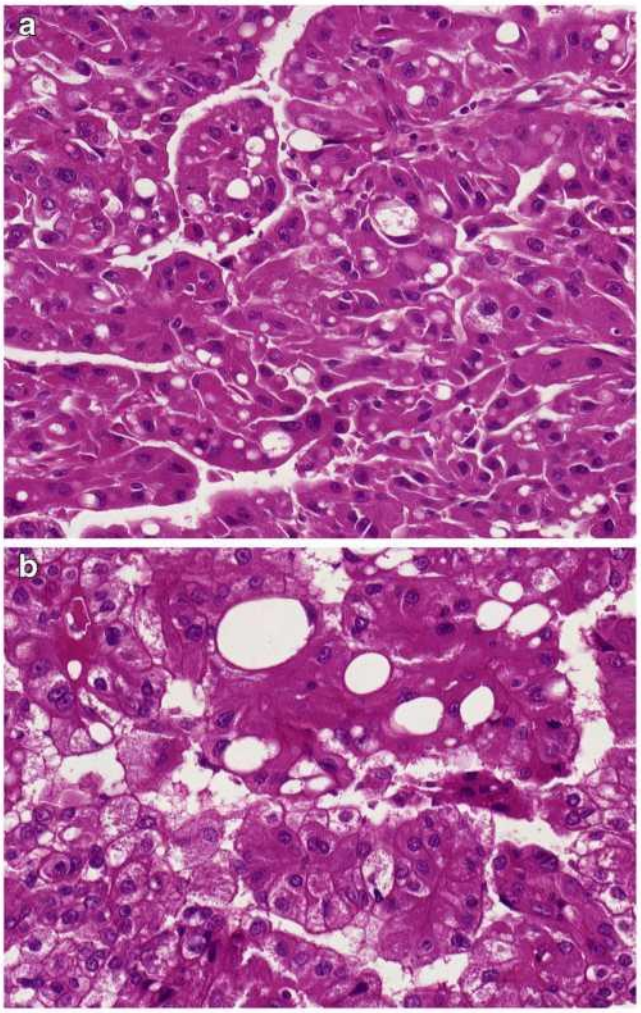

Fig. 4 As intracellular production was considered presence of the same material within cytoplasm in form of larger or smaller vacuoles. Some such cells reached the shape and characteristics of signet-ring cells (**a+b**)

Immunohistochemical analysis

Results of immunohistochemical examination are summarized in Table 3. All tumors were positive for AMACR, vimentin, and OSCAR. Keratin AE1-AE3 was diffusely positive in five tumors. CK 7 was diffusely positive in three (Fig. 8), focally in one case, and was negative in three cases. CK 20 was focally moderately positive in one tumor (CK 7 was negative in this case). Carbonic anhydrase IX was focally moderately positive in one case. PAX 8 was positive in six tumors, five strongly and diffuse, one focally. All tumors were negative for CDX2.

Mucin-like deposits were examined using a panel of antibodies against different MUC antigens (Table 4). MUC 1 was diffusely strongly positive in two cases and focally in three cases (two strongly and one moderately) (Fig. 9). None of the tumors were reactive for MUC 2, MUC 4, and MUC 6. Two cases were weakly positive for MUC 5 AC.

Molecular genetic analysis

Results of molecular genetic analyses are summarized in Table 5. Array CGH analysis was performed on one case (case

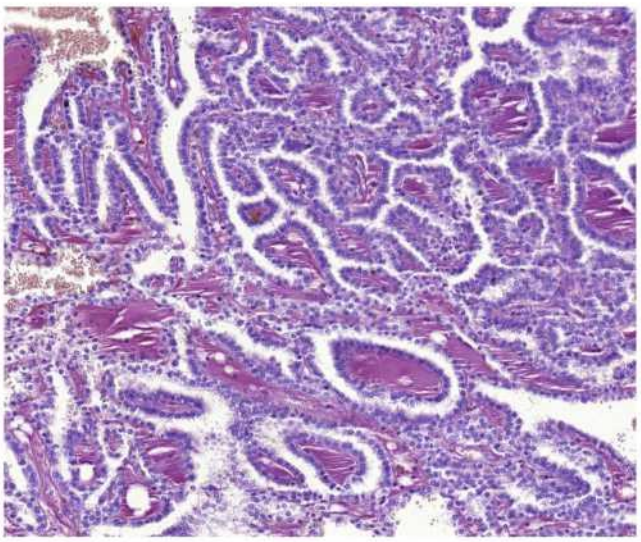

Fig. 5 Interstitial mucin-like material was positive for mucicarmin

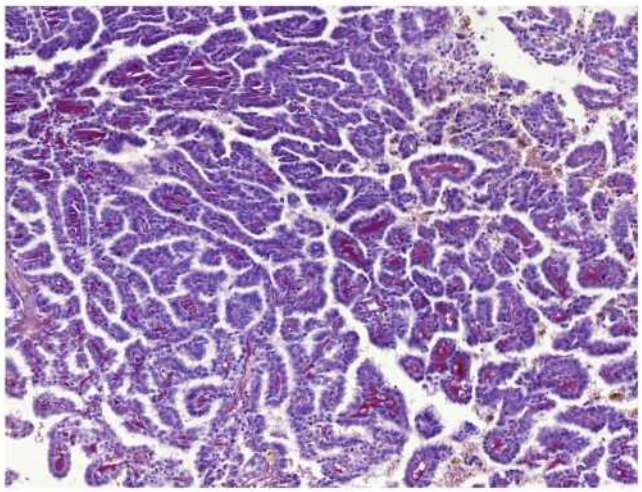

Fig. 6 The same interstitial deposition was positive for PAS

2), which showed gain of chromosomes 7, 16, and 17 and loss of chromosome Y. FISH was performed on four cases. Polysomy of chromosomes 7 and 17 was found in two cases. In one case, polysomy of only chromosome 17 was present. One case (case 1) was disomic for both chromosomes 7 and 17. Loss of heterozygosity (LOH) of chromosome 3p was assessed in five cases and was positive in one case (case 5), which also showed polysomy of chromosomes 7 and 17. In none of the six cases analyzed were mutations found in the *VHL* gene. We found no methylation of *VHL* gene promoter in the six cases analyzed.

Discussion

RCC with mucin or mucin-like secretion was initially published in 1963 by Foster and Levine [10], who reported Mayer's mucicarmine positive material in 2 out of 71 renal cell carcinomas. Their description unfortunately does not allow any conclusion as to the histological type according to current classifications [11]. Grignon et al. [12] described an RCC with luminal and cytoplasmic presence of mucin, reactive with Mayer's mucicarmine and Alcian blue. The documentation allows to conclude that this tumor was a papillary RCC with mucin/mucin-like secretion [12].

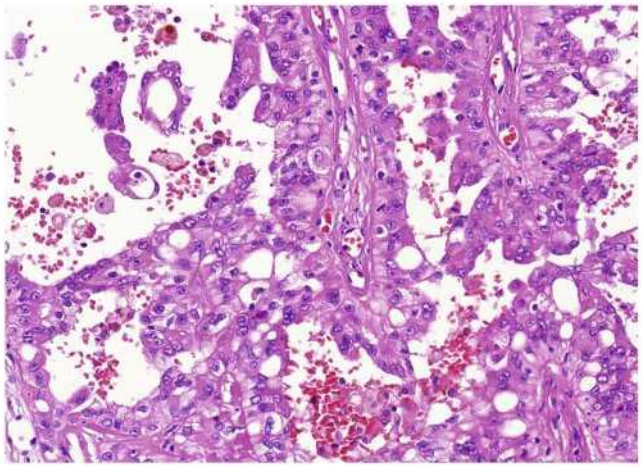

Fig. 7 Focally, cells had foamy cytoplasm and microvacuolated appearance resembling macrophages or hibernoma cells

The term "mucin" encompasses a large family of glycoproteins expressed by many normal and neoplastic cell types. Two main classes are distinguished: membrane-bound and secreted or gel forming [13]. Mucin can be stained empirically with mucicarmine, historically regarded as highly sensitive [14]. Recent studies correlating the results of mucicarmine staining with immunohistochemical staining for various antigens specific for individual mucin subtypes are lacking. Staining with PAS and Alcian blue might be more sensitive as they cover both neutral and acidic mucins, produced by epithelial or mesenchymal cells. However, these stains lack specificity as they also bind to other substances such as glycosylated proteins.

Of the MUC family, only MUC1 is expressed in normal epithelial cells of the kidney. MUC2, a secreted gel-forming mucin, is typically secreted by goblet cells of the gastrointestinal and respiratory tract [15]. MUC4 is a transmembrane glycoprotein, which provides a protective layer of mucus to epithelial cells of the intestine, airways, and mammary ducts [16]. MUC5AC is found mainly in the mucosal layer of the stomach, while MUC6 is located principally in gastric pyloric glands [17]. MUC 1 is expressed in convoluted distal tubules and in collecting ducts in normal renal tissue, with a polar apical distribution [18–20]. Leroy et al. reported that MUC1 is expressed in 54 % of PRCC. They found that MUC1 is predominantly expressed in type 1 PRCC and only rarely in type 2 PRCC [21].

The most frequent type of renal cell carcinoma with mucin production is MTS RCC, which is composed of tubules, many of which are elongated and merge into cord-like structures with transitions into spindle cells. Weakly basophilic mucin is present at least focally in most tumors [22], located mostly in the interstitium, and a proper term for such a finding would be myxoid rather than mucinous. Fine et al. mapped the histologic spectrum of MTS RCC and documented cases of MTS RCC without conspicuous extracellular mucin in H&E-stained sections [23]. However, scant mucinous material within cellular areas has been reported in these "mucin-poor" MTS RCC [24].

Our cases were completely different from MTS RCC. Tumors from our series lacked typical dual architecture; tubules lined by cuboidal cells were not encountered nor a spindle cell component with characteristic myxoid changes in the stroma. Immunohistochemical staining does not distinguish between PRCC and MTS RCC because of an overlapping

Table 3 Immunohistochemical examination

Case	AMACR	CANH9	VIM	OSCAR	AE1/3	PAX8	CK7	CK20	CDX2
1	+++	–	+++	+++	++	+++	++	–	–
2	+++	++ Foc.	+++	+++	++	+++	+++	–	–
3	+++	–	+++	+++	++	+++	+++ Foc.	–	–
4	++	–	+++	+++	+++	+++	+++	–	–
5	+++	–	+++	+++	+++	+++	–	–	–
6	++	–	+++	+	–	++ Foc.	–	–	–
7	+++	–	++	+	–	–	–	++ Foc.	–

Foc. = < 50 % cells staining, – = negative, + = weak positivity, ++ = moderate positivity, +++ = strong positivity, *AMACR* racemase, *CANH9* carbonic anhydrase, *AE1/3* cytokeratin AE1-AE3, *vim* vimentin

marker profile. However, a molecular genetic profile might help to differentiate between these entities. We have documented gain of chromosomes 7, 16, and 17 and loss of chromosome Y using array CGH analysis, confirmed subsequently by FISH. The pattern of these numerical chromosomal aberrations is not compatible with that of MTS RCC, which shows disomy of chromosomes 7 and 17 and chromosomal loss, notably of chromosomes 1, 4, 6, 8, 9, 13, 14, 15, and 22, regardless of grade [23].

Mucin production has been described in three primary papillary RCCs, which showed eosinophilic cuboidal to columnar cells and extensive luminal or intracytoplasmic acid mucin deposition, including sulphomucins as indicated by mucicarmine, Alcian blue (at pH 2.5), and high-iron diamine staining. Furthermore, foam cells (in two cases), hemosiderin, and siderophages (in two cases), calcification (in one case), and an incomplete fibrous capsule were described [2] [3]. Mucin production has also been reported in four papillary adenomas. Mucin was of acid type, as indicated by mucicarmine, Alcian blue (at pH 2.5), and Mowry's colloidal iron staining, intracellular in numerous scattered tumor cells in two cases, focal luminal in one case, and mixed intracellular and luminal in another case [4].

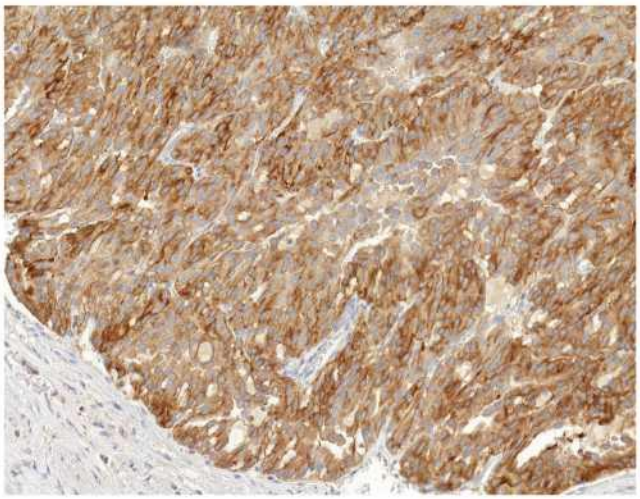

Fig. 8 CK 7 was diffusely positive in three cases

In this study, all tumors were classified as PRCC. Morphological and immunohistochemical features were mostly compatible with type 1 PRCC; however, some morphologic variability was noted [25]. All tumors expressed AMACR, vimentin, and OSCAR while four cases expressed CK 7. Architecture was predominantly papillary, even in CK 7-negative tumors. CK 7-negative PRCC has been reported notably by Langner et al. who described variable CK 7 reactivity in renal cell carcinoma subtypes, including PRCC [9]. Morphology and marker expression pattern (coexpression of AMACR, vimentin, and CK 7-among others) of our case 1 was typical of PRCC. However, for PRCC disomy of chromosomes 7, 17, and Y is unusual. Case 5 showed polysomy of chromosomes 7 and 17, supernumerary chromosome X, and LOH3p, compatible with both PRCC and clear cell RCC but morphology was consistent with PRCC. The marker expression pattern (CK 7 and carbonic anhydrase IX both negative) in this case was unusual for PRCC. We used morphology as ultimate criterion and considered the case as PRCC. Two more cases were not entirely typical of PRCC (cases 6 and 7) because they were negative for CK 7. Genetic analysis could not be performed on case 7 due to low quality of DNA. In case 6, status of the *VHL* gene (mutations, LOH3p, and methylation status) was normal but it showed loss of chromosome Y, which fits with PRCC. However, analysis of chromosomes 7 and 17 failed because of low-quality DNA.

We introduced the term "mucin-like" instead of "mucinous" because of the results of immunohistochemical staining for MUC antigens. The MUC antigens most commonly expressed in human mucinous carcinomas are MUC1, MUC2, MUC4, MUC5AC, and MUC6. Lack of expression of these antigens raises questions as to specificity of traditional stains (mucicarmine, PAS, Alcian blue) used to detect mucin. Reports on mucin deposits in tumors based only on traditional stains should be interpreted with caution when the results are not corroborated by immunohistochemistry. In all our cases, in H&E-stained sections, mucin-like material was present. Mucin-like material was

Table 4 Mucin staining

Case	Mucicarmine	Periodic Acid Schiff	Alcian blue	MUC1	MUC2	MUC4	MUC5AC	MUC6
1	+	++	−	+++ Foc.	−	−	−	−
2	+++ Foc.	+	+	+++ Foc.	−	−	+	−
3	+ Foc.	++	−	++ Foc.	−	−	−	−
4	+	−	+	+++	−	−	−	−
5	+	++	+	+++	−	−	+ Foc.	−
6	+ Foc.	+ Foc.	−	−	−	−	−	−
7	+ Foc.	+ Foc.	−	−	−	−	−	−

Foc. = < 50 % cells staining, − = negative, + = weak positivity, ++ = moderate positivity, +++ = strong positivity

intracytoplasmic in six cases, extracellular (intraluminal or in the stroma) in four cases. The interstitial myxoid changes were exclusively found in the core of papillae. Areas with diffuse myxoid changes which are seen in MTS RCC were absent. In five cases, we found cells with signet-ring morphology. Signet-ring cells are tumor cells with intracytoplasmic mucin that displaces the nucleus and their presence favors a diagnosis of signet-ring cell carcinoma regardless of site [26]. In two of our cases, mucicarmine or PAS-positive cells with signet-ring morphology were found which we considered as signet-ring cells. In three other cases, the cells with signet-ring morphology were negative for mucicarmine and PAS.

In the differential diagnosis of MTS RCC, several entities should be considered.

1. Hereditary leiomyomatosis renal cell carcinoma syndrome-associated renal cell carcinoma (HLRCC) arises in patients with a germline mutation in the *fumarate hydratase* (*FH*) gene. These tumors often have a papillary architecture but can be tubulopapillary, cribriform, or solid [22]. Even though the morphology of our tumors was not entirely compatible with HLRCC, we tested four cases for *FH* gene mutation but all of them showed a wild type *FH* gene.
2. Val-Bernal described a case of RO, composed of typical oncocytes in a predominantly tubular pattern and scattered tubules containing basophilic mucin (positive with Alcian blue at pH 2.5 and Mayer's mucicarmin), in the lumen but not intracytoplasmic. Immunohistochemistry was not reported. Tumor cells did not show gain of chromosomes 7 and 17 [6]. Our cases differed from RO in terms of morphology and marker profile, being mostly papillary and with expression of different markers. Chromosomal analysis with polysomy of chromosomes 7 and 17 supports our diagnosis of RCC. An oncocytic variant of PRCC has been reported but with morphologic characteristics different from our cases.
3. Val-Bernal also reported extracellular mucin within alveoli in CCRCC but only occasionally in the cytoplasm of neoplastic cells [24]. The mucin stained with Mayer's mucicarmine, Alcian blue-PAS (at pH 2.5), and Mowry's colloidal iron. Staining with Alcian blue at pH 0.4 indicated the presence of strongly acidic sulphated mucosubstances [5]. Our cases showed characteristic papillary architecture without clear cell elements. The marker profile was typical of PRCC only in four cases, with coexpression of vimentin and AMACR even in CK 7-negative tumors. Moreover, *VHL* was not mutated and its promoter not methylated. LOH of 3p was observed in one out of five analyzable cases. The latter case showed polysomy of chromosomes 7 and 17 and an unusual XXY pattern of sex chromosomes.

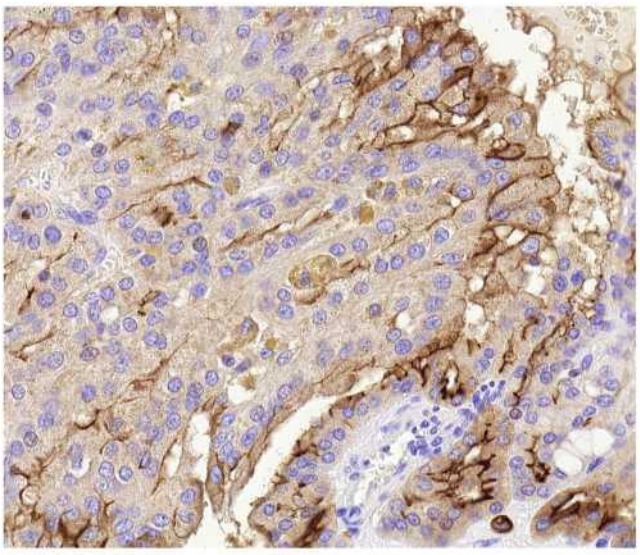

Fig. 9 MUC 1 was diffusely strongly positive in two cases and focally in three cases

Mucin/mucin-like secretion along with papillary architecture is more common in urothelial carcinomas (UC). Primary adenocarcinoma, UC with signet-ring cells, UC with gland-like lumina, and colonic types (villous

Table 5 Results of molecular genetic analyses

Case	Array CGH	LOH3p	TFE3F	TFEBF	VHL	VHLM	FISH 7	FISH16	FISH17	FISH Y	FH
1	NA	–	–	NA	–	–	D	–	D	XY	–
2	+7, +16, +17, −Y	–	–	NA	–	–	P	P	P	−Y	–
3	NA	NP	–	NA	–	–	NA	NA	NA	−Y	NA
4	NA	–	–	–	–	–	D	NA	P	−Y	–
5	NA	+	NA	NA	–	–	P	NA	P	XXY	NA
6	NA	–	NA	NA	–	–	NA	NA	NA	−Y	–
7	NA	NA	NA	NA	NA	NA	NA	NA	NA	NA	NA

− = negative, + = positive, *NA* not analyzable, *NP* not performed, − *Y* loss of chromosome Y, *VHL VHL* mutation, *VHLM VHL* methylation, *FH fumarate hydratase gene* mutation, *P* polysomy, *D* disomy

adenomas, villous carcinomas) are not extremely rare subtypes, and several reports have been published of such tumors in the whole urinary tract [27] [28]. Morphology of UC can be polymorphic and histochemical features and marker profile may vary. Glandular differentiation is observed in less than 10 % of urothelial carcinomas, usually in the form of small tubular or gland-like spaces in conventional urothelial carcinoma [29] [30]. Less frequently, foci similar to colonic-type adenocarcinoma can be found in otherwise typical UC and, rarely, a signet-ring cell or a mucinous component [31]. Primary adenocarcinoma is extremely rare in the renal pelvis, while at approximately 2 % of primary epithelial malignancies in the urinary bladder [6,8]. This entity includes primary bladder adenocarcinoma (non-urachal adenocarcinoma) and urachal carcinoma. Primary bladder adenocarcinoma develops in transitional epithelium through gradual changes (intestinal metaplasia) initiated by chronic inflammation [32]. Urachal carcinoma is less common than non-urachal adenocarcinoma of the bladder and arises from urachal remnants [10] [33]. Colonic-type villous adenoma and adenocarcinoma of the urinary tract are rare. Villous adenoma is characterized by papillary structures covered by columnar mucinous epithelium, as in colonic villous adenoma. Often an infiltrating adenocarcinoma coexists, which emphasizes the need to adequate sampling of any lesion diagnosed by biopsy as villous adenoma [28]. Our cases were located in the renal cortex or paracortex, without any connection with pelvic-calyceal system. No signs of urothelial differentiation were found, marker pattern was also unlike UC. One case was focally positive for CK 20 but not for CK 7.

The patient of case 7 died of metastatic colorectal carcinoma. In this case, the architecture of renal tumor was papillary, without tubules or dirty necrosis. Although the renal tumor was focally positive for CK 20, it also expressed vimentin and AMACR, which would be extremely unusual for metastasis of colorectal adenocarcinoma.

Conclusions

1. PRCCs with mucin/mucin-like secretion are rare (<0.5 % of all PRCC), and defining their morphology, immunohistochemical, and molecular genetic profile remains a challenge.
2. Mucicarmine-positive secretion does not rule out a diagnosis of PRCC.
3. A genuine mucin nature of the secreted material still needs to be confirmed by immunohistochemical analysis. Whether what is secreted in these PRCC cases is mucin or mucin-like remains to be clarified.
4. In the differential diagnosis of RCC with mucin/mucin-like secretion, in addition to tumors originating in renal parenchyma, also, lesions of urothelial origin should be considered, as they are more often mucicarmine positive.
5. PRCCs with mucin/mucin-like secretion have metastatic potential.

Acknowledgments The authors thank Dr. Ivan Damjanov for his help with the editing of our paper and for the constructive discussion.

Compliance with ethical standards The study was approved by local Ethics Committee (Medical Teaching Hospital and Medical School of Charles University in Plzen).

Funding The study was supported by the Charles University Research Fund (project number P36), by the project CZ.1.05/2.1.00/03.0076 from European Regional Development Fund, and by SVV 260283.

Conflict of interest The authors declare no conflict of interest.

References

1. Hes O, Hora M, Perez-Montiel DM, Suster S, Curik R, Sokol L, Ondic O, Mikulastik J, Betlach J, Peychl L, Hrabal P, Kodet R, Straka L, Ferak I, Vrabec V, Michal M (2002) Spindle and cuboidal renal cell carcinoma, a tumour having frequent association with nephrolithiasis: report of 11 cases including a case with hybrid conventional renal cell carcinoma/spindle and cuboidal renal cell carcinoma components. Histopathology 41:549–555

2. Val-Bernal JF, Gomez-Roman JJ, Vallina T, Villoria F, Mayorga M, Garcia-Arranz P (1999) Papillary (chromophil) renal cell carcinoma with mucinous secretion. Pathol Res Pract 195:11–17
3. Val-Bernal JF, Mayorga M, Garcia-Arranz P, Gomez-Roman JJ (1998) Mucin secretion in papillary (chromophil) renal cell carcinoma. Am J Surg Pathol 22:1037–1040
4. Val-Bernal JF, Pinto J, Gomez-Roman JJ, Mayorga M, Villoria F (2001) Papillary adenoma of the kidney with mucinous secretion. Histol Histopathol 16:387–392
5. Val-Bernal JF, Salcedo W, Val D, Parra A, Garijo MF (2013) Mucin-secreting clear cell renal cell carcinoma. A rare variant of conventional renal cell carcinoma. Ann Diagn Pathol 17:226–229
6. Val-Bernal JF, Val D, Garijo MF (2011) Mucin-producing renal oncocytoma. An undescribed variant of oncocytoma. Pathol Res Pract 207:271–274
7. A Renshaw, Fine needle aspiration of the kidney, In: Bostwick D, Cheng L. (eds) Urologic Surgical Pathology (2st ed), (2008) 196–213.
8. van Dongen JJ, Langerak AW, Bruggemann M, Evans PA, Hummel M, Lavender FL, Delabesse E, Davi F, Schuuring E, Garcia-Sanz R, van Krieken JH, Droese J, Gonzalez D, Bastard C, White HE, Spaargaren M, Gonzalez M, Parreira A, Smith JL, Morgan GJ, Kneba M, Macintyre EA (2003) Design and standardization of PCR primers and protocols for detection of clonal immunoglobulin and T-cell receptor gene recombinations in suspect lymphoproliferations: report of the BIOMED-2 Concerted Action BMH4-CT98–3936. Leukemia 17:2257–2317
9. Sperga M, Martinek P, Vanecek T, Grossmann P, Bauleth K, Perez-Montiel D, Alvarado-Cabrero I, Nevidovska K, Lietuvietis V, Hora M, Michal M, Petersson F, Kuroda N, Suster S, Branzovsky J, Hes O (2013) Chromophobe renal cell carcinoma–chromosomal aberration variability and its relation to Paner grading system: an array CGH and FISH analysis of 37 cases. Virchows Archiv: Int J Pathol 463:563–573
10. Gopalan A, Sharp DS, Fine SW, Tickoo SK, Herr HW, Reuter VE, Olgac S (2009) Urachal carcinoma: a clinicopathologic analysis of 24 cases with outcome correlation. Am J Surg Pathol 33:659–668
11. Foster EA, Levine AJ (1963) Mucin production in metastatic carcinomas. Cancer 16:506–509
12. Grignon DJ, Ro JY, Ayala AG (1988) Primary mucin-secreting adenocarcinoma of the kidney. Archiv Pathol Laboratory Med 112:847–849
13. Fowler J, Vinall L, Swallow D (2001) Polymorphism of the human muc genes. Front Biosci J Virtual Library 6:D1207–D1215
14. Lauren PA, Sorvari TE (1969) The histochemical specificity of mucicarmine staining in the identification of epithelial mucosubstances. Acta Histochem 34:263–272
15. Gum JR Jr, Hicks JW, Toribara NW, Siddiki B, Kim YS (1994) Molecular cloning of human intestinal mucin (MUC2) cDNA. Identification of the amino terminus and overall sequence similarity to prepro-von Willebrand factor. J Biol Chem 269:2440–2446
16. Jonckheere N, Van Seuningen I (2010) The membrane-bound mucins: from cell signalling to transcriptional regulation and expression in epithelial cancers. Biochimie 92:1–11
17. Ho SB, Shekels LL, Toribara NW, Kim YS, Lyftogt C, Cherwitz DL, Niehans GA (1995) Mucin gene expression in normal, preneoplastic, and neoplastic human gastric epithelium. Cancer Res 55:2681–2690
18. Cao Y, Karsten U, Zerban H, Bannasch P (2000) Expression of MUC1, Thomsen-Friedenreich-related antigens, and cytokeratin 19 in human renal cell carcinomas and tubular clear cell lesions. Virchows Archiv Int J Pathol 436:119–126
19. Kraus S, Abel PD, Nachtmann C, Linsenmann HJ, Weidner W, Stamp GW, Chaudhary KS, Mitchell SE, Franke FE, el Lalani N (2002) MUC1 mucin and trefoil factor 1 protein expression in renal cell carcinoma: correlation with prognosis. Human Pathol 33:60–67.
20. Leroy X, Copin MC, Devisme L, Buisine MP, Aubert JP, Gosselin B, Porchet N (2002) Expression of human mucin genes in normal kidney and renal cell carcinoma. Histopathology 40:450–457
21. Leroy X, Zini L, Leteurtre E, Zerimech F, Porchet N, Aubert JP, Gosselin B, Copin MC (2002) Morphologic subtyping of papillary renal cell carcinoma: correlation with prognosis and differential expression of MUC1 between the two subtypes. Modern Pathol Off J United States Canadian Acad Pathol Inc 15:1126–1130
22. Srigley JR, Delahunt B, Eble JN, Egevad L, Epstein JI, Grignon D, Hes O, Moch H, Montironi R, Tickoo SK, Zhou M, Argani P, Panel IRT (2013) The International Society of Urological Pathology (ISUP) Vancouver Classification of renal Neoplasia. Am J Surg Pathol 37:1469–1489
23. Peckova K, Martinek P, Sperga M, Montiel DP, Daum O, Rotterova P, Kalusova K, Hora M, Pivovarcikova K, Rychly B, Vranic S, Davidson W, Vodicka J, Dubova M, Michal M, Hes O (2015) Mucinous spindle and tubular renal cell carcinoma: analysis of chromosomal aberration pattern of low-grade, high-grade, and overlapping morphologic variant with papillary renal cell carcinoma. Ann Diagn Pathol 19:226–231
24. Fine SW, Argani P, DeMarzo AM, Delahunt B, Sebo TJ, Reuter VE, Epstein JI (2006) Expanding the histologic spectrum of mucinous tubular and spindle cell carcinoma of the kidney. Am J Surg Pathol 30:1554–1560
25. Delahunt B, Eble JN (1997) Papillary renal cell carcinoma: a clinicopathologic and immunohistochemical study of 105 tumors. Modern Pathol Off J United States and Canadian Acad Pathol Inc 10:537–544
26. Sung CO, Seo JW, Kim KM, Do IG, Kim SW, Park CK (2008) Clinical significance of signet-ring cells in colorectal mucinous adenocarcinoma. Modern Pathol Off J United States and Canadian Acad Pathol Inc 21:1533–1541
27. Alvarado-Cabrero D, Perez-Montiel O (2008) Hes, Multicystic urothelial carcinoma of the bladder with gland-like lumina and with signet-ring cells. A case report. Diagn Pathol 3:36
28. Seibel JL, Prasad S, Weiss RE, Bancila E, Epstein JI (2002) Villous adenoma of the urinary tract: a lesion frequently associated with malignancy. Hum Pathol 33:236–241
29. Lopez-Beltran L (2006) Cheng, histologic variants of urothelial carcinoma: differential diagnosis and clinical implications. Hum Pathol 37:1371–1388
30. Black PC, Brown GA, Dinney CP (2009) The impact of variant histology on the outcome of bladder cancer treated with curative intent. Urol Oncol 27:3–7
31. Amin MB (2009) Histological variants of urothelial carcinoma: diagnostic, therapeutic and prognostic implications. Modern Pathol Off J United States and Canadian Acad Pathol Inc 22(Suppl 2):S96–S118
32. Thomas DG, Ward AM, Williams JL (1971) A study of 52 cases of adenocarcinoma of the bladder. Br J Urol 43:4–15
33. Paner GP, Barkan GA, Mehta V, Sirintrapun SJ, Tsuzuki T, Sebo TJ, Jimenez RE (2012) Urachal carcinomas of the nonglandular type: salient features and considerations in pathologic diagnosis. Am J Surg Pathol 36:432–442

1.2.7 Biphasic Squamoid Alveolar Renal Cell Carcinoma: A Distinctive Subtype of Papillary Renal Cell Carcinoma?

Pro tuto studii bylo vyhledáno 21 bifazických skvamo-alveolárních renálních karcinomů (BSARCC), které byly podrobně analyzovány z hlediska morfologie, imunohistochemie a molekulárně genetických změn (pomocí array comparative genomic hybridization/aCGH a FISH).

Tumory pocházely od 11 mužů a 10 žen, pacienti byli ve věkovém rozmezí od 53 do 79 let. Tumory měly 1,5 až 16 cm v největším průměru. Následný průběh onemocnění vedl k rozvoji metastáz celkem v 5 případech. U všech tumorů byla zastižena dvojí populace buněk: malé neoplastické buňky s malým množstvím cytoplazmy většinou tvořící alveolární struktury a větší skvamoidní buňky s objemnou cytoplazmou a vezikulárními jádry uspořádané v kompakní hnízda (tyto tvořily od 10% do 80% nádorové tkáně). U 9/21 případů byly dále zastiženy i dobře formované papilární okrsky. Ve všech případech byla zastižena emperipoéza a všechny případy reagovaly pozitivně v CK7, EMA, vimentinu a cyclinu D1. aCGH a FISH prokázaly mnohotné numerické chromozomální změny včetně zisku chromosomů 7 a 17.

Nádory mikroskopicky vykazovaly spektrum morfologického vzhledu, avšak u všech tumorů byla konstantně prokázána přítomnost emperipoézy a skvamoidních buněk. Prokázáné cytogenetické znaky u těchto tumorů (zisk chromozomů 7 a 17) společně se zastiženým imunohistochemickým profilem a morfologií tumorů naznačují, že BSARCC je součástí spektra PRCC. U některých BSARCC bylo klinicky pozorováno agresivní chování. Jedná se o první deskriptivní studii této jednotky.

Biphasic Squamoid Alveolar Renal Cell Carcinoma

A Distinctive Subtype of Papillary Renal Cell Carcinoma?

Ondrej Hes, MD, PhD, Enric Condom Mundo, MD, PhD,†‡ Kvetoslava Peckova, MD,* Jose I. Lopez, MD,§ Petr Martinek, PhD,* Tomas Vanecek, PhD,* Giovanni Falconieri, MD,‖ Abbas Agaimy, MD,¶ Whitney Davidson, MD,# Fredrik Petersson, MD, PhD,** Stela Bulimbasic, MD, PhD,†† Ivan Damjanov, MD, PhD,# Mireya Jimeno, MD,‡‡ Monika Ulamec, MD, PhD,§§ Miroslav Podhola, MD, PhD,‖‖ Maris Sperga, MD,¶¶ Maria Pane Foix, MD,†‡ Ksenya Shelekhova, MD, PhD,## Kristyna Kalusova, MD,*** Milan Hora, MD, PhD,*** Pavla Rotterova, MD, PhD,* Ondrej Daum, MD, PhD,* Kristyna Pivovarcikova, MD,* and Michal Michal, MD**

Abstract: Biphasic squamoid alveolar renal cell carcinoma (BSARCC) has been recently described as a distinct neoplasm. Twenty-one cases from 12 institutions were analyzed using routine histology, immunohistochemistry, array comparative genomic hybridization (aCGH) and fluorescence in situ hybridization. Tumors were removed from 11 male and 10 female patients, whose age ranged from 53 to 79 years. The size of tumors ranged from 1.5 to 16 cm. Follow-up information was available for 14 patients (range, 1 to 96 mo), and metastatic spread was found in 5 cases. All tumors comprised 2 cell populations arranged in organoid structures: small, low-grade neoplastic cells with scant cytoplasm usually lining the inside of alveolar structures, and larger squamoid cells with more prominent cytoplasm and larger vesicular nuclei arranged in compact nests. In 9/21 tumors there was a visible transition from such solid and alveolar areas into papillary components. Areas composed of large squamoid cells comprised 10% to 80% of total tumor volume. Emperipolesis was present in all (21/21) tumors. Immunohistochemically, all cases were positive for cytokeratin 7, EMA, vimentin, and cyclin D1. aCGH (confirmed by fluorescence in situ hybridization) in 5 analyzable cases revealed multiple numerical chromosomal changes including gains of chromosomes 7 and 17 in all cases. These changes were further disclosed in 6 additional cases, which were unsuitable for aCGH. We conclude that tumors show a morphologic spectrum ranging from RCC with papillary architecture and large squamoid cells to fully developed BSARCC. Emperipolesis in squamoid cells was a constant finding. All BSARCCs expressed CK7, EMA, vimentin, and cyclin D1. Antibody to cyclin D1 showed a unique and previously not recognized pattern of immunohistochemical staining. Multiple chromosomal aberrations were identified in all analyzable cases including gains of chromosomes 7 and 17, indicating that they are akin to papillary RCC. Some BSARCCs were clinically aggressive, but their prognosis could not be predicted from currently available data. Present microscopic, immunohistochemical, and molecular genetic data strongly support the view that BSARCC is a distinctive and peculiar morphologic variant of papillary RCC.

Key Words: kidney, biphasic squamoid alveolar renal cell carcinoma, papillary renal cell carcinoma, immunohistochemistry, aCGH, FISH

(*Am J Surg Pathol* 2016;40:664–675)

From the Departments of *Pathology; ***Urology, Charles University, Medical Faculty and Charles University Hospital Plzen; ‖Department of Pathology, Charles University, Medical Faculty and Charles University Hospital Hradec Kralove, Czech Republic; †Department of Pathology, Bellvitge University Hospital, Bellvitge Biomedical Research Institute (IDIBELL); ‡Department of Pathology and Experimental Therapeutics, University of Barcelona School of Medicine; ‡‡Department of Pathology, Consorci Sanitari Integral, Barcelona; §Department of Pathology, Cruces University Hospital, Biocruces Research Institute, University of the Basque Country, Barakaldo, Spain; ‖Department of Pathology, University of Trieste, Trieste, Italy; ¶Department of Pathology, University Hospital Erlangen, Erlangen, Germany; #Department of Pathology, The University of Kansas School of Medicine, Kansas City, KS; **Department of Pathology, National University Health System, Singapore, Singapore; ††Department of Pathology, Clinical Hospital Center Zagreb; §§"Ljudevit Jurak" Pathology Department, Clinical Hospital Center "Sestre milosrdnice", Zagreb, Croatia; ¶¶Department of Pathology, East University, Riga, Latvia; and ##Department of Pathology, Petrov's Research Institute of Oncology, St Petersburg, Russia.

Conflicts of Interest and Source of Funding: Supported by the Charles University Research Fund (project number P36) and by the project CZ.1.05/2.1.00/03.0076 from European Regional Development Fund (O.H.). The authors have disclosed that they have no significant relationships with, or financial interest in, any commercial companies pertaining to this article.

Correspondence: Ondrej Hes, MD, PhD, Department of Pathology, Charles University, Medical Faculty and Charles University Hospital Plzen, Alej Svobody 80, 304 60 Pilsen, Czech Republic (e-mail: hes@medima.cz).

Three years ago we reported 2 renal cell carcinomas (RCCs) that we thought had unique and previously unrecognized histopathologic features.[1] We named that neoplasm descriptively as a biphasic alveolo-squamoid renal cell carcinoma (BSARCC). Unique to this tumor

were organoid structures composed of centrally located solid nests of large squamoid cells surrounded in an alveolar manner by smaller cuboidal and flattened cells reminiscent of dilated tubules or cysts. The squamoid cells had vesicular large nuclei, which were surrounded by eosinophilic cytoplasm with distinct cell borders. The alveolar cells were smaller and mostly cuboidal displaying a high nuclear to cytoplasmic ratio.[1] The clinicopathologic significance of these histopathologic data was not addressed, and thus we decided to assemble a much larger number of similar cases.

In the present paper we present 20 additional cases of this tumor type, providing evidence that BSARCCs are histogenetically closely related to papillary RCC (PRCC). Clinical follow-up shows that some of these cases had an adverse outcome. We hope that our study will stimulate other uropathologists to review their databases and further contribute to the characterization of BSARCC as a clinicopathologic entity.

MATERIALS AND METHODS

A search algorithm including the keywords "unclassified, squamoid, squamous, glomeruloid" was used to identify renal tumors from the Plzen Tumor Registry and multiple other institutional archives and consult files of the other authors. All cases were reviewed by 3 pathologists (O.H., K.Pe., M.M.) and compared with the index case to identify matching features. One or more hematoxylin and eosin stained slides were available for review in all cases (1 to 23 slides/case). Altogether 21 cases were identified from a total of 18,500 cases. Three cases have already been published previously and were included into the present study (cases 7, 14, and 15). These cases are marked by the sign § in Table 1.[1,2]

Light Microscopy

Tissue for light microscopy had been fixed in 4% formaldehyde and embedded in paraffin using routine procedures. Sections of 5 μm thickness were cut and stained with hematoxylin and eosin.

Immunohistochemistry

A relatively broad panel of antibodies was used for complex analysis of tumors with apparently dual population. All staining analyses were performed in 1 institution (University Hospital Plzen). The immunohistochemical study was performed using a Ventana Benchmark XT automated stainer (Ventana Medical System Inc., Tucson, AZ).

The following primary antibodies were used: epithelial membrane antigen (EMA) (E29, monoclonal; DakoCytomation, Carpinteria, CA; 1:1000), cytokeratins (AE1-AE3, monoclonal; BioGenex, San Ramon, CA; 1:1000), CK5/6 (D5/16B4, monoclonal; DakoCytomation; 1:100), CD10 (56C6; Novocastra, Burlingame, CA; 1:20), cytokeratin 7 (OV-TL12/30, monoclonal;

TABLE 1. Basic Clinicopathologic Data

Case	Sex	Age	Size (cm)	Side	Follow-up (mo)	Squamoid Area-extend in %	Emperipolesis
1	M	65	10×9.5×7	R	24, AWD*	10	Yes
2	M	57	6×5×4	UN	ND	20	Yes
3	F	60	10.5	L	29, DOD	20	Yes
4	F	53	3.2	R	1, DUN†	10	Yes
5	F	70	UN	UN	UN	40	Yes
6	M	66	3.5	R	6, AWD, then ND‡	10	Yes
7§	F	54	3	R	72, AW, then ND	100 (minimal papillary focus)	Yes
8	F	54	1.9×1.4×2	R	24, AW	40	Yes
9	M	63	3.5	UN	UN	60	Yes
10	M	57	3	UN	ND	45	Yes
11	F	79	4.5	UN	ND	30	Yes
12	F	70	2.9×1.7×1.5	R	18, AW	30	Yes
13	F	62	2.8×1.9×2	L	13, AW	35	Yes
14§	M	55	2	R	48, AW, then DUN¶	30	Yes
15§	F	54	2.2	R	96, AW, then DUN#	20	Yes
16	M	46	1.5	R	UN	40	Yes
17	M	60	2	R	24, AW	40	Yes
18	M	78	16.0	L	45, DOD**	45	Yes
19	M	53	3.0	R	6, AWD‡	5	Yes
20	M	65	5	UN	ND	30	Yes
21	F	72	6	L	3, AW	40	Yes

*pT3, pN2; lymph nodes paracaval (TNM 09)
†Dead of hemorrhagic shock 3 weeks after surgery, 18 years on hemodialysis.
‡6 months after nephrectomy, multiple bilateral lung metastases, lymph node metastases.
§Previously published cases [1,2]
Ductal invasive carcinoma of breast treated 1 year before nephrectomy.
¶Dead of small cell carcinoma of the lung
#Dead of cholangiogenic carcinoma of the liver.
**Metastases in mediastinal lymph nodes.
AW indicates alive and well; AWD, alive with disease; DOD, dead of disease; DUN, dead of unrelated condition; F, female; L, left; M, male; ND, not documented; R, right; UN, unknown.

FIGURE 1. Grossly, tumors are solid.

FIGURE 3. Some tumors were solid, firm with whitish color.

DakoCytomation; 1:200), cytokeratin 20 (M7019, monoclonal; DakoCytomation; 1:100), racemase/AMACR (P504S, monoclonal; Zeta, Sierra Madre, CA; 1:50), vimentin (D9, monoclonal; NeoMarkers, Westinghouse, CA; 1:1000), parvalbumin (PA-235, monoclonal; Sigma Aldrich, St Luis, MO; 1:500), Ki-67 (MIB1, monoclonal; Dako, Glostrup, Denmark; 1:1000), c-kit (CD117, polyclonal, Dako, Glostrup, Denmark, 1:300), CD10 (monoclonal, Sp67; Ventana, RTU), E-cadherin (12H6, monoclonal; Zymed, San Francisco, CA; 1:200), carbonic anhydrase IX (rhCA9, monoclonal; RD systems, Abingdon, GB; 1:100), p63 (4A4, monoclonal; Ventana, Tucson, AZ, RTU), p53 (DO-7, monoclonal; DakoCytomation; 1:30), antimelanosome (HMB45, monoclonal; DakoCytomation; 1:200), TFE3 (polyclonal; Abcam; 1:100), cathepsin K (3F9, monoclonal; Abcam; 1:100), WT1 (GF-H2, monoclonal; DakoCytomation; 1:150), TTF-1 (SPT24, monoclonal; Novocastra, Newcastle, UK; 1:400), antibody against cyclin D1-M 30 (M30 monoclonal; Lobome, Enzo Life Sciences, Ann Arbor, MI; 1:100), bcl-2 (monoclonal, 124; Cell Marque, Rocklin, CA; 1:100), cyclin D1 (SP4-R, monoclonal; Cell Marque; 1:100), (SP4-R, monoclonal; Ventana, RTU), (polyclonal; NeoMarkers, Fremont, CA; 1:100), and PAX-8 (polyclonal; Cell Marque; 1: 25). The primary antibodies were visualized using the supersensitive streptavidin-biotin-peroxidase complex (BioGenex). Appropriate positive controls were used.

FIGURE 2. Color ranges from whitish to tan/brown. Tan color of the gross section seen on a formalin-fixed tissue/specimen.

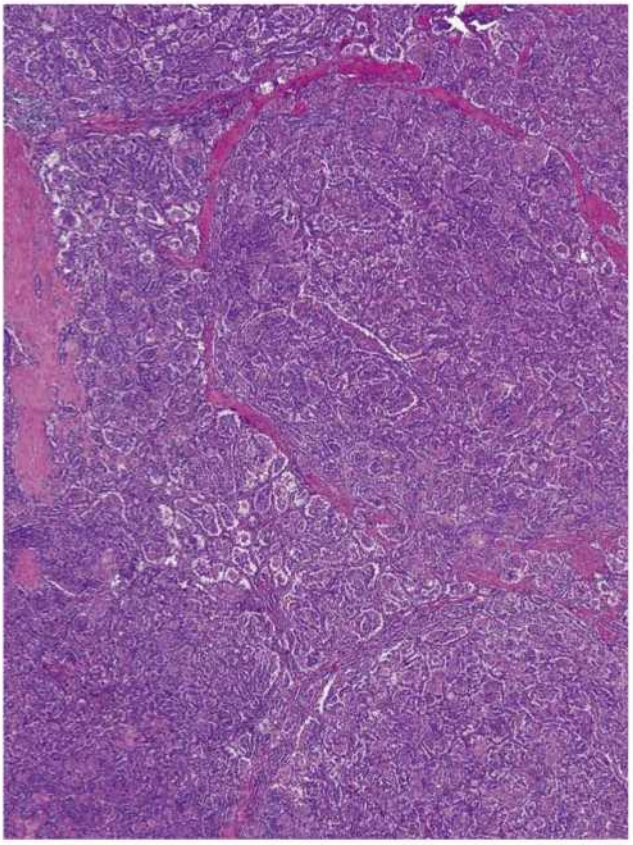

FIGURE 4. Well-developed BSARCC in which squamoid cells forming the majority of the tumors mass.

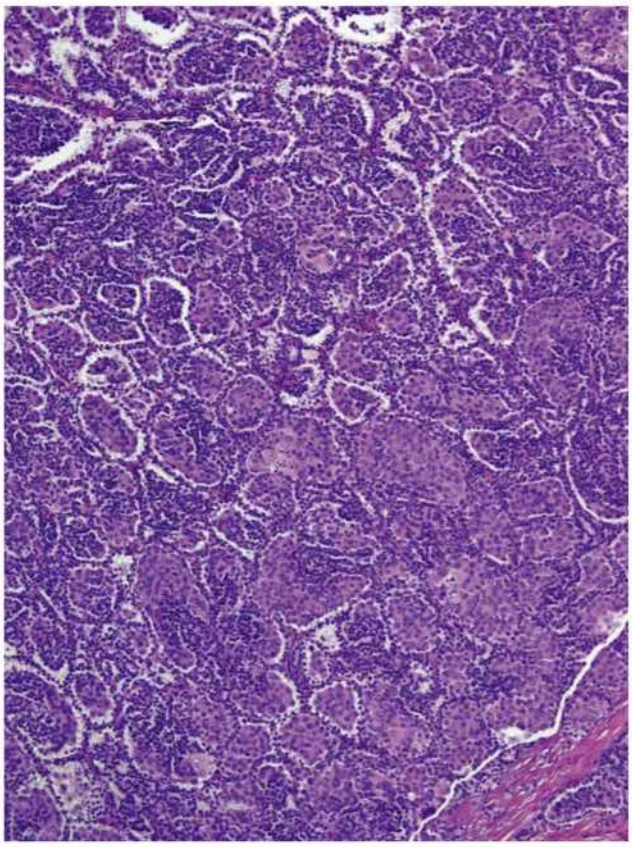

FIGURE 5. Solid-alveolar pattern of BSARCC is clearly seen.

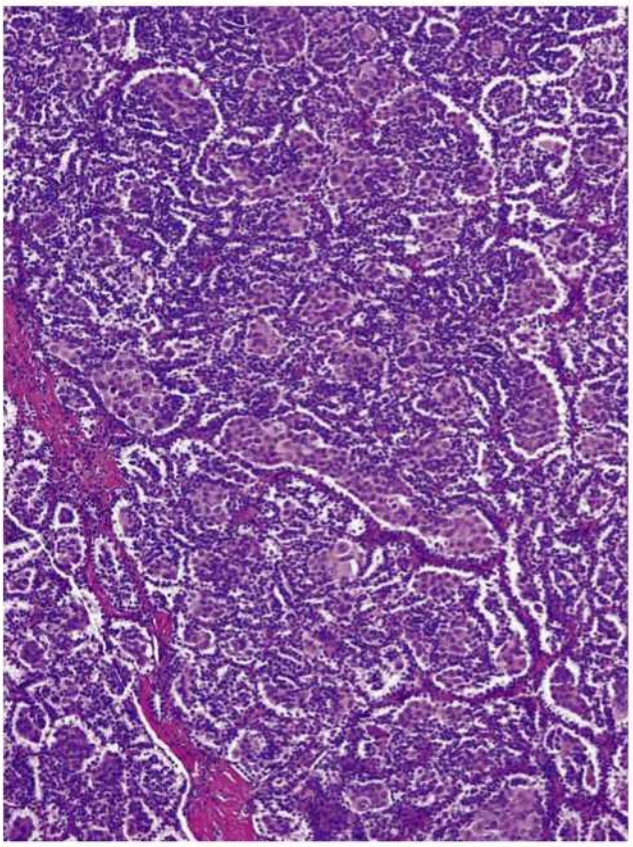

FIGURE 6. Squamoid areas surrounded by smaller cells with scant cytoplasm.

DNA Extraction

DNA from macrodissected formalin-fixed paraffin-embedded (FFPE) tissue was extracted using a QIAsymphony DNA Mini Kit (Qiagen, Hilden, Germany) on automated system (QIAsymphony SP, Qiagen) according to the manufacturer's supplementary protocol for FFPE samples (purification of genomic DNA from FFPE tissue using the QIAamp DNA FFPE Tissue Kit and Deparaffinization Solution). Samples were then purified using Qiaquick kit (Qiagen) and eluted in EB buffer (Qiagen). Concentration and purity of isolated DNA was measured using NanoDrop ND-1000 (NanoDrop Technologies Inc., Wilmington, DE). DNA integrity was examined by amplification of control genes in a multiplex polymerase chain reaction.[3]

Array Comparative Genomic Hybridization

Five cases (no 3, 9, 12, 13, 14) were suitable for analysis using array comparative genomic hybridization (aCGH).

CytoChip Focus Constitutional (BlueGnome Ltd, Cambridge, UK) array was used for aCGH analysis. It uses BAC technology and covers 143 regions of known significance with 1 Mb spacing across a genome. Probes are spotted in triplicates. First, 400 ng of DNA was labeled using the Fluorescent Labeling System (BlueGnome Ltd). The procedure included Cy3 labeling of a test sample and Cy5 labeling of a reference sample. Commercially produced reference of opposite sex was used in cases in which no reference sample was available (MegaPool Reference DNA Male/Female, Kreatech Diagnostics, Amsterdam, Netherlands). The labeled reference and the test sample were mixed, dried, and hybridized overnight at 47°C using Arrayit hybridization cassette (Arrayit Corporation, CA). Posthybridization washing was done using SSC buffers with increasing stringency. Dried microarray was scanned with InnoScan 900 (Innopsys, France) at a resolution of 5 μm. Scanned image was analyzed and quantified by BlueFuse Multi software (BlueGnome Ltd). The software uses Bayesian algorithms to generate intensity values for each Cy5 and Cy3 labeled spot on the array according an appropriate.gal file. Cutoff values for log 2 ratio are preset to −0.3 for loss and to 0.3 for gain by BlueFuse software.

Fluorescence In Situ Hybridization

Eleven cases were suitable for fluorescence in situ hybridization (FISH) analysis. A 4-μm-thick FFPE tissue section was placed onto a positively charged slide. The target area was circled with a diamond pen according to the corresponding hematoxylin and eosin–stained slide. The slide was routinely deparaffinized, incubated in the ×1 Target Retrieval Solution Citrate pH 6 (Dako) for 40 minutes at 95°C, then cooled for 20 minutes at room

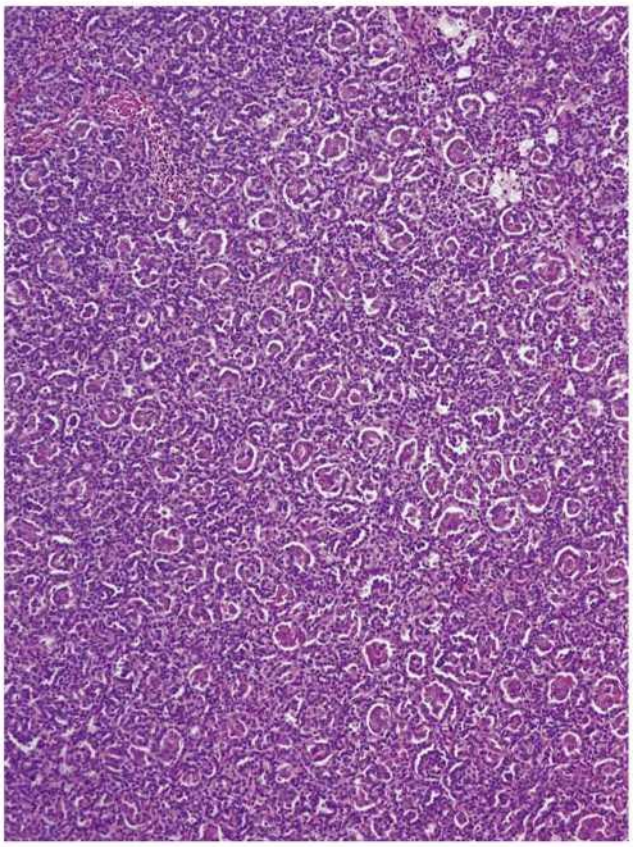

FIGURE 7. Scanning, low-power magnification shows RCC with papillary architecture comprising areas composed of large squamoid cells.

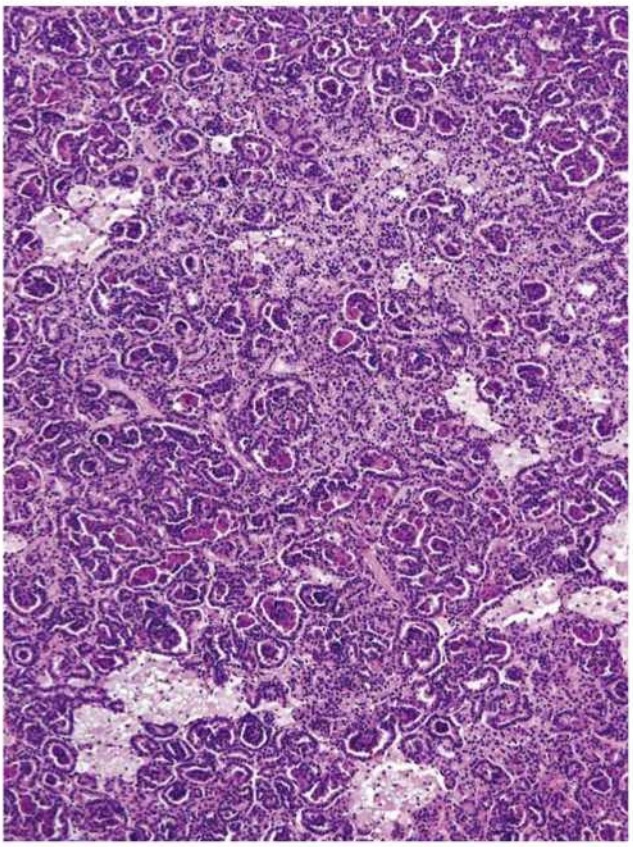

FIGURE 8. In some areas, foci of foam cells are present.

temperature in the same solution. The slide was washed in deionized water and digested in protease solution with pepsin (0.5 mg/mL) (Sigma Aldrich) in 0.01 M HCl at 37°C for 15 minutes. The slide was then immersed in deionized water for 5 minutes, dehydrated in a series of ethanol solutions (70%, 85%, and 96% for 2 min each) and air-dried. FISH probes CEP 7 Spectrum Orange (D7Z1), CEP 17 Spectrum Orange, CEP X (DXZ1) Spectrum Green/CEP Y (DYZ3) Spectrum Orange (Vysis/Abbott Molecular, Des Plaines, IL) were mixed with water and hybridization buffers according to manufacturer's protocol. The slide was incubated in a ThermoBrite instrument (StatSpin/Iris Sample Processing, Westwood, MA) with codenaturation at 85°C for 8 minutes and hybridization at 37°C for 16 hours. Posthybridization wash was performed in 2×SSC/0.3% NP-40 solution at 72°C for 2 minutes. The slide was counterstained with DAPI I (Vysis) and stored in the dark at −20°C until examined. FISH signals were assessed using an Olympus BX51 fluorescence microscope. Scoring of aneuploidy was performed by counting the number of fluorescent signals in 100 randomly selected, nonoverlapping tumor cell nuclei. The slide was independently enumerated by 2 observers (P.M., T.V.). Cutoff values were set for each probe as shown in previous study.[4]

RESULTS

The clinicopathologic features of 21 cases of BSARCC are summarized in Table 1. Eleven of the patients were male and 10 were female; their ages ranged from 53 to 79 years (mean, 61.57 y). Tumor size ranged from 1.5 to 16 cm in greatest dimension (mean, 4.63 cm; median, 3.1 cm). All cases were solitary lesions. Follow-up data were available for 14/21 patients, with follow-up period ranging from 1 to 96 months (mean, 29.21 mo; median, 24 mo); metastatic spread was confirmed in 5 cases.

Three patients were alive with disease (lymph node involvement and bilateral lung metastases) after periods ranging from 6 to 24 months. However, 1 patient from this group (lung and lymph node metastases) was lost to follow-up 6 months after nephrectomy. Two patients died of widespread metastatic disease 29 and 45 months status post nephrectomy. Six patients were alive and well 3 to 72 months after diagnosis, whereas another 3 patients were without evidence of disease at 1, 48, and 96 months after surgery but died of unrelated diseases or conditions.

On gross examination the tumors were described as solid with color varying from whitish to tan or light brown (Figs. 1–3). Small areas of hemorrhage were reported in 4 cases with grossly visible necrotic foci noted in a single case.

All tumors were composed of a distinctly dual cell population. The first contained relatively uniform, small, low-grade neoplastic cells with scant cytoplasm. Such

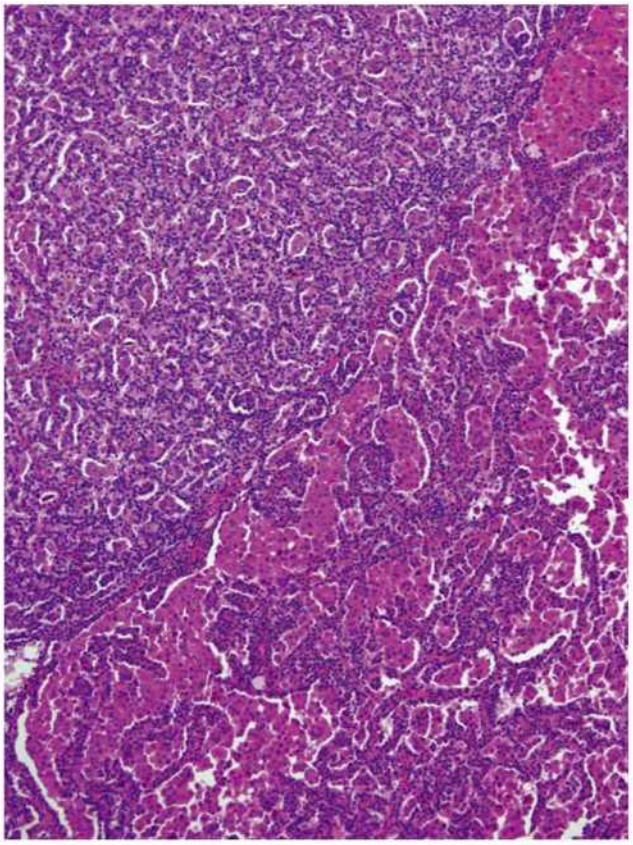

FIGURE 9. Transition between areas composed nearly exclusively of large squamoid cells and an area of more typical PRCC.

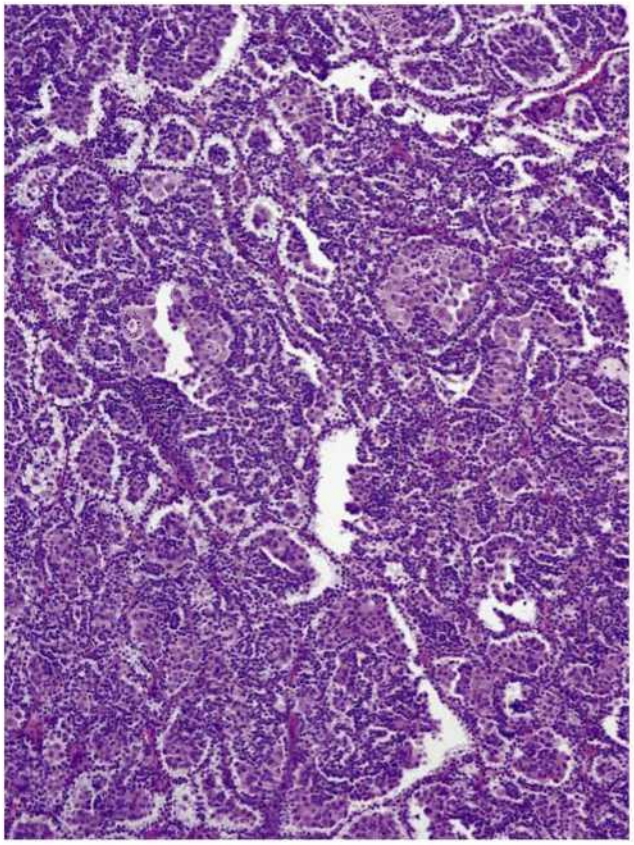

FIGURE 10. Emperipolesis was present in 21/21 tumors. This was found in large cells within squamoid areas. Scanning low-power magnification showing numerous foci of emperipolesis within squamoid areas.

small cells with scant cytoplasm had mostly round slightly elongated nuclei, resembling those of normal lymphocytes. These cells were arranged in rows forming alveolar-like structures, reminiscent of dilated tubules, microcystic structures, or Bowman capsular spaces. Alveolar spaces were often attached to the vascular septa contributing to their walls. Alveolar cells were separated by a slit space from the solid nests composed of larger squamoid cell, which formed the second cell population of all tumors. This second population was made up of large cells containing voluminous pink cytoplasm and large nuclei with prominent nucleoli. These eosinophilic cells were arranged in solid islands, forming the centers of alveolar structures and often revealing retraction artifacts, most likely related to the biphasic cell populations that were so closely intermixed. A retraction from the walls of the alveoli formed by smaller cells with scant cytoplasm may be seen in Figures 4–6. Neither the keratin pearls nor the intercellular bridges observed in true squamous epithelium were noted in any case. Large squamoid cells formed between 5% and 100% of the total tumor volume. Small foci of necrosis were identified on histologic examination in 3/21 cases, and a larger necrotic area was seen in just 1 case. Rare psammoma bodies were present in 7 tumors.

A visible transition from areas with a papillary pattern containing groups of large squamoid cells (Figs. 7, 8) to a fully developed solid-alveolar pattern was seen in 9 tumors (Fig. 9). These former areas were characterized by the presence of well-developed papillae and tubules all lined by mostly cuboidal low-grade epithelial cells with round nuclei. Focally, tubulopapillary formations with glomeruloid morphology were also noted.

Of particular note was the presence of emperipolesis, a highly unusual phenomenon among renal cell tumors. It was easily identified in all 21 cases. Emperipolesis was present only in large squamoid cells and was a very prominent feature within solid squamoid islands in some cases (Figs. 10–12). In fact, it was a conspicuous morphologic feature in a majority of the cases.

One case (case 3) included metastatic neoplastic tissue from multiple foci on the peritoneal surface and omentum. The metastatic deposits showed a mostly solid-alveolar pattern with large squamoid cells (Fig. 13), rare psammoma bodies (Fig. 14), and absent emperipolesis.

Immunohistochemical data are summarized in Table 2. One of the cases were not available for immunohistochemical examination. All analyzable tumors were positive for CK7 (Fig. 15), EMA, and vimentin in

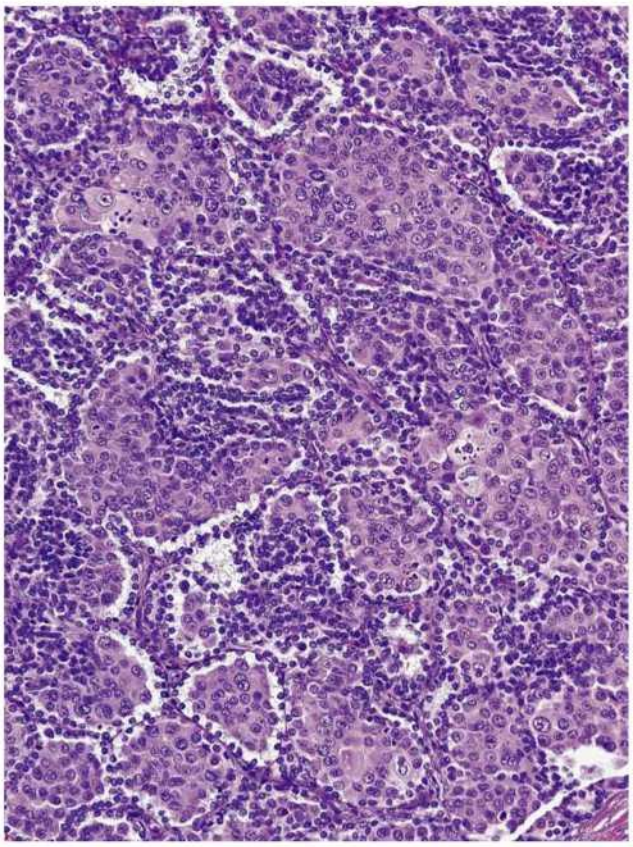

FIGURE 11. High-power magnification of squamoid cells with emperipolesis.

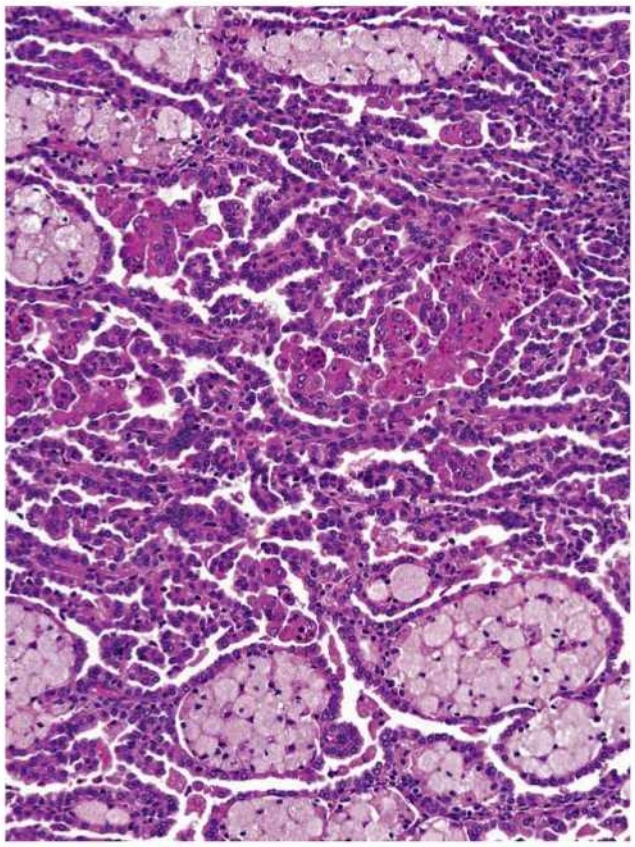

FIGURE 12. Similar to Figure 10. Emperipolesis in squamoid cells seen with foam cell macrophages intermingled among large squamoid cells.

both types of neoplastic cells. Nineteen of 21 cases were positive for cytokeratin AE1-AE3, and racemase (AMACR). All large squamoid cells expressed cyclin D1. There were no major differences among all 3 different antibodies against cyclin D1 (2 monoclonal and 1 polyclonal) (Figs. 16, 17). Large squamoid cells weakly expressed M30. All tumors were completely negative for TTF1, TFE 3, HMB45, and parvalbumin. Nineteen of 21 tumors were negative for CK 20, and 17/21 were negative for CD117 with documented positivity being focal, weak, and within the small-cell component.

Molecular-Genetic Data

Complete results of molecular genetic analyses, that is, aCGH and FISH, are summarized in Table 3. All analyzed samples (11/21) showed gains of chromosomes 7 and 17 (Fig. 18). Four of 5 analyzed male samples showed loss of chromosome Y. Additional gains of chromosome 20 were found in 3 of 5 analyzable cases using aCGH. Further chromosomal numerical changes including gain of chromosomes 16 and 12, loss of chromosome 21, and a loss of Xp22.33 were found in a single case.

DISCUSSION

Two cases of the so-called biphasic alveolo-squamoid renal carcinoma were reported in 2013.[1] Subsequently, 3 additional cases of the same tumor type were published in an abstract form in 2014.[1,2] The described tumors were composed of a distinctly dual cell population in which the larger tumor cells displayed squamoid features and formed round well-demarcated solid alveolar areas that, in large part, were surrounded by smaller neoplastic cells. Since publication of the above-mentioned paper, we have collected 20 additional cases from 12 institutions worldwide. In case 1 from Petersson et al's[1] paper, there was a very small, inconspicuous focus of papillary formation within the tumor. However, there were no other distinctive features to suggest the diagnosis of PRCC. Still we thought that the link of BSARCC and PRCC deserves to be explored.

PRCC is the second most frequently diagnosed RCC and is usually defined as a tumor derived from renal tubular epithelium with either papillary or tubule-papillary architecture. PRCC has traditionally been divided into 2 types. Type 1 PRCCs are mostly papillary, wherein the papillae are covered by cells with nuclei arranged in a single cell layer. The cells are relatively uniform with scant, pale, or basophilic cytoplasm and round nuclei. Type 2 is more polymorphic. Pseudostratification of nuclei is the key feature distinguishing type 2 from type 1 PRCC. PRCC type 2 usually has a higher nuclear grade, and cytoplasm is frequently eosinophilic.[5–7] A so-called

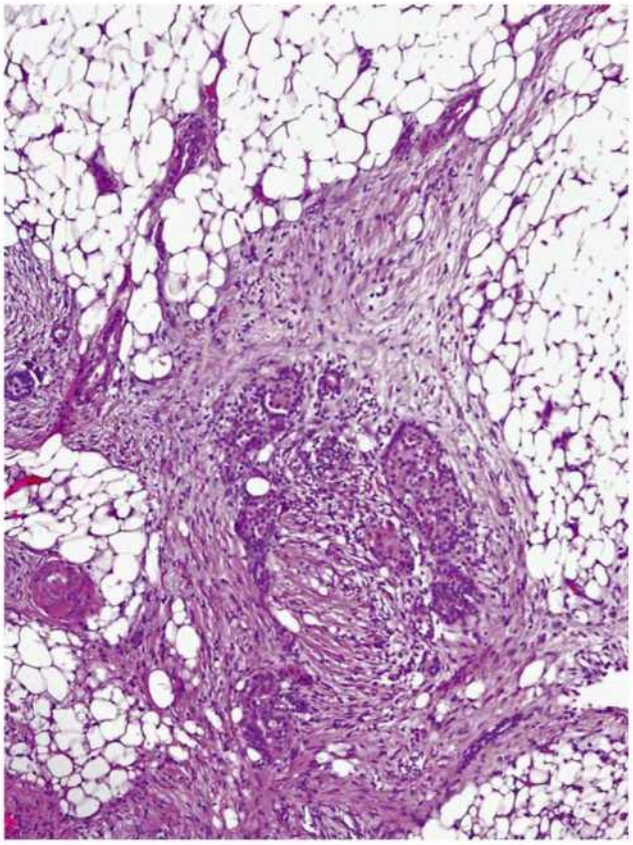

FIGURE 13. The metastatic deposits displayed a mostly solid alveolar pattern with large squamoid cells.

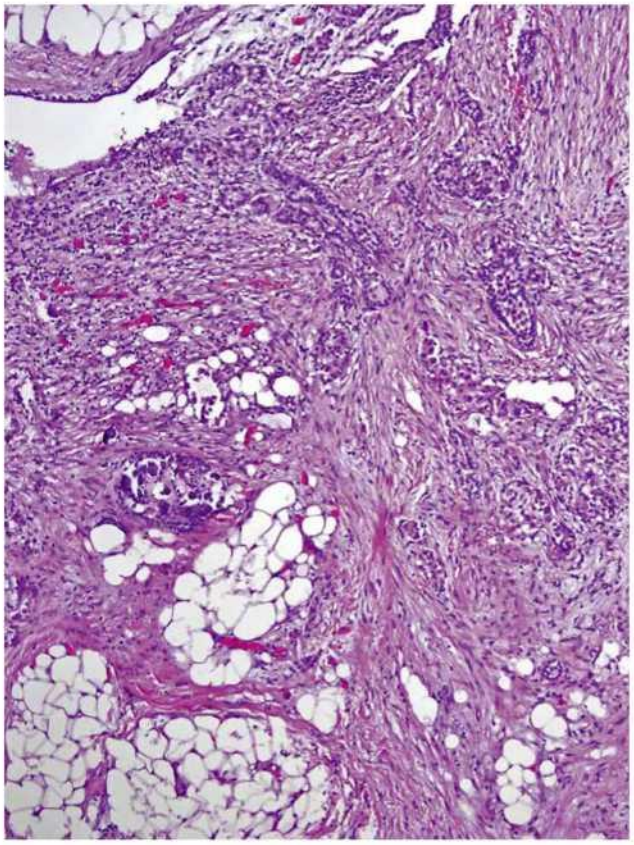

FIGURE 14. Rare psammoma bodies were present in metastases.

oncocytic variant of PRCC has also been described in the literature. These tumors are composed of cells with eosinophilic oncocytic cytoplasm, usually without pseudostratification of nuclei.[7–9] Some PRCCs are not easy to characterize as type 1, type 2, or oncocytic, and in such cases the diagnosis of PRCC, not otherwise specified, is usually established.

The fact that 10/21 cases of BSARCC exhibited components of classical PRCC suggests that BSARCC may be closely related to PRCC, or it may be a variant thereof with a peculiar and unusual morphology. The identified papillary component in these tumors was mostly compatible with type 1 PRCC according to Delahunt classification[5]; most papillae were covered by a single layer of smaller cells that had regular nuclei and scant cytoplasm.

In some areas the compression of papillae leads to the formation of tubulopapillary structures. Groups of larger, more pleomorphic cells with eosinophilic cytoplasm were found with such a pattern in the background. These larger cells displayed the same squamoid features seen in classical BSARCC and were immunohistochemically positive for cyclin D1. These transitional areas were either intermingled with areas exhibiting a more prominent biphasic pattern and with large areas of squamoid cells showing prominent emperipolesis or the transition between both patterns was in some cases more abrupt. PRCC with large eosinophilic cells like the cases reported herein has been described in the literature previously. It is shown in Sternberg's Diagnostic Pathology textbook (page 1982, figure 42.20).[10] The same type of PRCC is illustrated for example in the paper written by Mantoan Padilha et al.[11] We believe that so-called PRCC with formation of glomeruloids could be an early stage and BSARCC late stage of 1 neoplastic lesion and that we can consider such morphology as opposite ends of the same morphologic spectrum.

FISH analysis showed gains of chromosomes 7 and 17 in all 11 analyzable cases. Loss of chromosome Y was detected in 4 of 5 male cases, which is in line with patterns found in PRCC.[12,13] aCGH revealed some additional chromosomal changes, the most frequent being gain of chromosome 20. Case 2, which has been presented by Petersson et al[1] revealed a different chromosomal aberration pattern (losses on chromosomes 2, 5, 6, 9, 12, 15,16, 17, 18, and 22, including biallelic loss of the CDKN2A locus, and gains on chromosomes 1, 5, 11, 12, and 13). This case, after careful reevaluation of all available blocks and materials, was excluded from the current study and was rediagnosed as unclassified RCC. Hence, the pattern of chromosomal numerical aberrations was very uniform in all analyzable cases in our current study and was fully compatible with a diagnosis of PRCC.[7,14]

TABLE 2. Results of Immunohistochemical Examinations

Case	CANH	MIB1/hpf	TTF1	WT1	Cath	TFE3	HMB45	p53	p63	AE1/3	EMA	CK7
1	+	2-3 SC 5-6 LC	−	−	−	−	−	−	−	−	+	foc
2	−	0-1 SC 3-4 LC	−	−	−	−	−	−	−	+ − +	− +	− −
3	−	0-1 SC 4-6 LC	−	−	−	−	−	+ LC	−	+ + foc	+ foc	+
4	+	0-1	−	−	−	−	−	−	−	+ +	+ foc	+
5	NP	NP	NP	NP	NP	NP	NP	NP	NP	NP	NP	NP
6	+ +	0-1 SC 2-3 LC	−	−	−	−	−	−	−	+ +	+	+
7	+	0-2	−	−	−	−	−	+ LC	−	+ + foc	+	+
8	+ +	0-1	−	− foc.	−	−	−	−	−	+ − + foc	− + −	− − +
9	+ +	0-1	−	−	−	−	−	−	−	+ +	+	+
10	+ +	0 SC 1-2 LC	−	−	−	−	−	−	−	+ +	+	+
11	+ +	0 SC 1-2 LC	−	−	−	−	−	−	−	+ − +	− + −	− − +
12	−	0-1	−	−	−	−	−	−	−	+ + foc	+	+
13	−	0 SC 3-6 LC	−	−	−	−	−	−	−	+ +	+	+
14	−	0-1	−	−	−	−	−	−	−	+ − +	− + −	− − +
15	−	0-1	−	−	−	−	−	−	−	+ − +	− + −	− − +
16	+ + LC	1-2 SC 4-7 LC	−	foc.	−	−	−	+	foc	+ +	+	+
17	−	0-1	−	−	+ − foc	−	−	+ foc	−	+ − +	− + −	− − +
18	−	0-1 SC 5-7 LC	−	−	−	−	−	+ LC	−	+ − +	− + −	− − +
19	−	0–1	−	−	−	−	−	−	−	+ +	+	
20	−	0-1	−	−	−	−	−	+ foc	−	+ − +	− + −	− − +
21	−	0-1 SC, 2-3 LC	−	−	−	−	−	−	−	+ −	− + −	− −

− − + indicates strong positivity; + −, intermediate positivity; −, weak positivity; −, negative; AE1/3, AE1-AE3; CANH, carbonic anhydrase 9; cath, cathepsin K; E-cadh, E-cadherin; foc, focal; hpf, high-power field (×400); LC, large cells (squamoid); NP, not performed; parval, parvalbumin; SC, small cells; vim, vimentin.

Like in previous reports, we were not able to identify definitive morphologic proof of full squamous differentiation by light microscopy (intercellular bridges and/or keratin pearl formation) in any case.[1] Immunohistochemically, the absence of nuclear expression of p63 and only focal positivity with CK5/6 in 3/21 cases is in line with the light microscopic impression of "squamoid" rather than true squamous differentiation.

The presence of emperipolesis within the large squamoid cells is a very interesting phenomenon. Emperipolesis is defined as the presence of a non-neoplastic cell within the cytoplasm of another cell. An example of an entity featuring prominent emperipolesis is Rosai Dorfman disease.[15] Although the presence of emperipolesis is well recognized in several different tumorous entities, it is a highly unusual finding within RCCs. Emperipolesis was noted in all 21 cases and was a very prominent feature in some tumors. Staining with cyclin D1 proved helpful in revealing cells with emperipolesis, and such positivity was found exclusively in the large squamoid cell areas. Interestingly, cyclin D1 immunostaining has also proven helpful in disclosing cells with emperipolesis in cases of myxoinflammatory fibroblastic sarcomas.[16] *Cyclin D1/PRAD 1*, a cell cycle-related gene mapped to chromosome 11q13, has been found to be amplified in some breast cancers, certain squamous cell carcinomas of the head and neck and esophagus, several different lymphomas, etc.[17] Expression of cyclin D1 in RCCs has only recently been studied; Leroy et al[18] described overexpression of cyclin D1 in clear cell PRCC. Lima et al[19] looked at the prognostic significance of cyclin D1 expression in RCCs and concluded that high expression is associated with favorable prognosis. In addition, cyclin D1 has been used as part of the immunohistochemical panel for distinguishing between chromophobe RCC (CHRCC), clear cell RCC, and renal oncocytoma.[20] It seems that cyclin D1 positivity is one of the characteristic features of BSARCC; however, expression of cyclin D1 is not a specific diagnostic marker for BSARCC.

Differential Diagnosis

Squamoid differentiation described in all the 21 tumors of this series is one of the defining morphologic features of BSARCC. Generally speaking, squamous differentiation in RCC occurs extremely rarely. If ever found it should raise the possibility that particular tumor might be of urothelial origin. There have been several reports describing urothelial carcinoma within the kidney displaying squamous or squamoid features and even typical morphology of squamous carcinoma.[21–26] The present tumors differ, however, from such urothelial carcinomas: they were located inside the kidney parenchyma, and none of them was related to the urothelium of the renal pelvis or calices. No urothelial carcinoma in situ or urothelial dysplasia was detected in any of the current 21 cases. Thus we have excluded the possibility that the squamoid differentiation in BSARCC was related to squamous metaplasia of the urothelium.

Further evidence supporting the above interpretation was derived from the immunohistochemical data. Coexpression of CK7 and CK20 was noted within some large cells of the squamoid component in 1 case (case 7), but the small cells were completely negative for CK20. The vast majority of analyzable tumors were negative for CK20 in both cell components. Finally, we are not aware of any urothelial lesions with such a distinctly biphasic population of neoplastic cells in an organoid arrangement as seen in these renal tumors. Moreover, the cases with well-preserved

TABLE 2. *(continued)*

CyclinD1	CK20	CK5/6	CD10	AMACR	E-cadh	vim	Parval	CD117	M30	bcl2	PAX8
+ + +	–	–	+ + +	+ +	–	+ + + foc	–	–	+ +	foc.	+ +
+ + +	–	–	–	+ + +	–	+ +	–	–	+ +	–	+
+ + +	–	–	+ foc	+ + +	+ foc.	+ + +	–	–	+ +	–	+ dif
+ + +	–	–	–	+ + +	+ foc.	+ + + foc	–	–	+ + +	–	–
NP	NP	NP	NP	NP	NP	NP	NP	NP	NP	NP	NP
+ + +	–	–	–	+ + +	–	+ + +	–	–	+ + +	–	–
+ + +	+ + foc LC	+ +	–	+ + +	–	+ + +	–	–	+ + +	+ SC	+ +
+ + +	–	–	–	+ + +	+ + foc.	+ + +	–	–	+ + +	–	+ dif.
+ + +	–	+ +	–	+ + +	+ + + foc.	+ + +	–	–	+	–	–
+ + + –	–	–	–	–	+ foc.	+ + +	–	–	+ + +	–	+ dif.
+ + +	–	–	–	+ + +	–	+ + +	–	–	+ + foc.	+	+
+ + +	–	+ +	–	+ + +	+ + foc.	+ + + foc	–	–	+ + +	–	+ foc.
+ + +	–	–	–	+ + +	+ + + foc.	+ + +		–	+ + +	+ + +	+ +
+ + +	–	–	–	+ + +	+ foc.	+ + +	–	–	+ + foc.	+ dif.	+ dif
+ + +	–	–	–	+ + +	+ foc.	+ + +	–	+	+ + +	–	+ + +
+ + +	–	–	+ foc + +	+ + +	+ +	+ + +	–	+ + foc SC	+ + +	+ foc.	+ + foc
+ + +	–	–	–	+ + +	+ + foc	+ + +	–	+ foc SC	+ + +	+	+ + +
+ + +	–	–	+ + foc	+ + +	+ + SC + + + LC	+ + +	–	–	+ + dif	–	+
+ + +	–	–	–	+ +	– SC + LC	+ + +	–	–	+ + + dif.	–	–
+ + +	–	–	–	+ + +	–	+ + +	–	–	Foc +	+ foc	+ +
+ + +	–	–	–	+ +	foc. +	+ + +	–	–	–	–	+ +

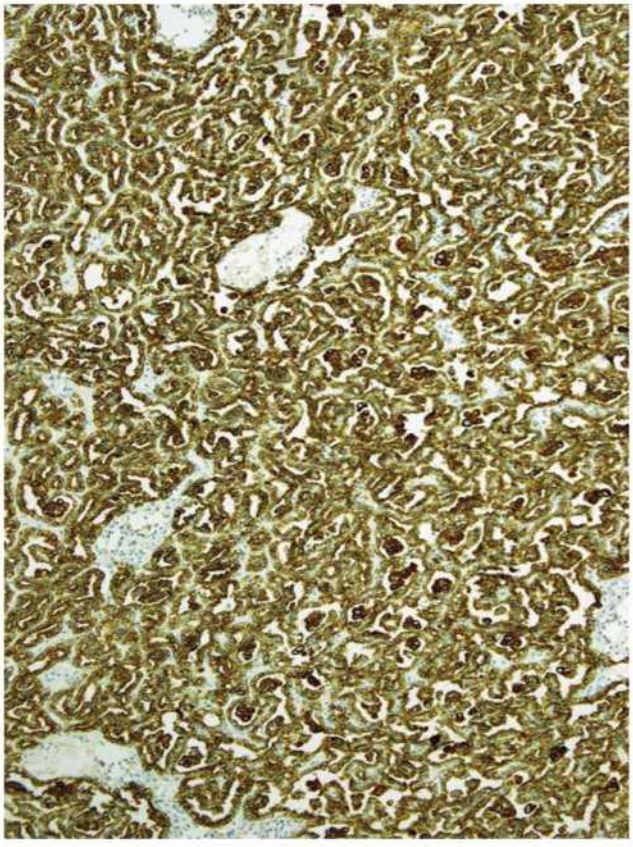

FIGURE 15. All tumors were positive for cytokeratin 7.

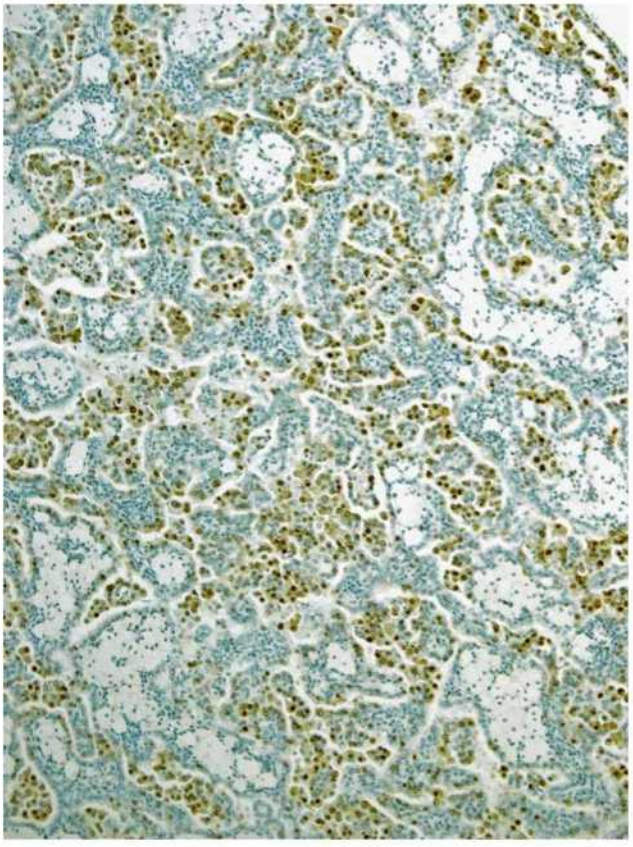

FIGURE 16. All large, squamoid cells expressed cyclin D1, reacting with both monoclonal antibodies (DAB-positive cells are brown).

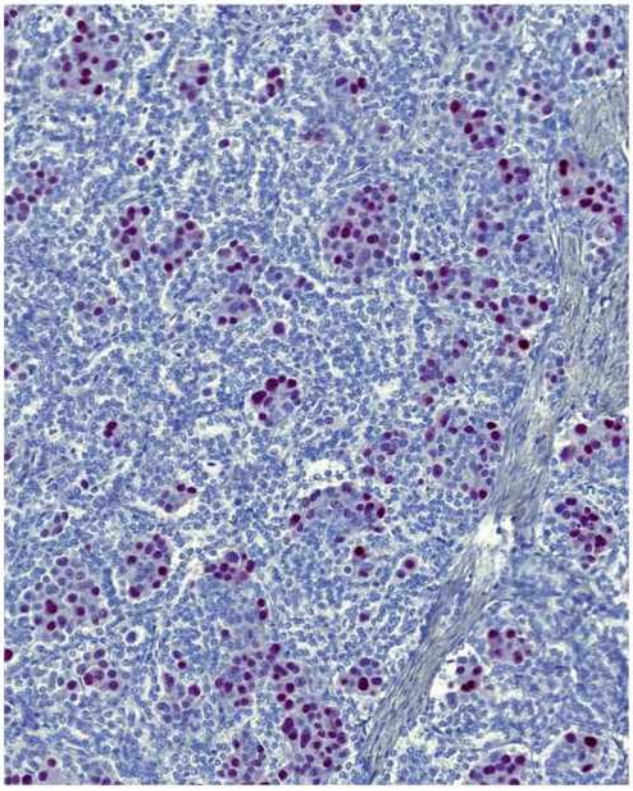

FIGURE 17. Squamoid cells were also positive with polyclonal antibody against cyclin D1 (alkaline phosphatase–positive cells are red).

DNA submitted to aCGH showed gains of chromosomes 7 and 17, which is suggestive of a connection to PRCC rather than urothelial carcinoma.

TABLE 3. Results of aCGH and FISH Analysis

Case	Sex	aCGH Result	CEP 7	CEP 17	CEP XY
1	M	NA	NA	NA	NA
2	M	NA	NA	NA	NA
3	F	+7, +17, +20, −21	P	P	XX
4	F	NA	P	P	XX
5	F	NA	NA	NA	NA
6	M	NA	NA	NA	NA
7	F	NA	P	P	XX
8	F	+7, +16, +17	P	P	XX
9	M	NA	NA	NA	NA
10	M	+7, +17, −Xp22.33, X-	P	P	X-
11	F	+7, +12, +17, +20	P	P	XX
12	F	+7, +17, +20	P	P	XX
13	F	NA	NA	NA	NA
14	M	NA	NA	NA	NA
15	F	NA	NA	NA	XX
16	M	NA	P	P	X-
17	M	NA	NA	NA	NA
18	M	NA	P	P	XY
19	M	NA	P	P	X-
20	M	NA	P	P	X-
21	F	NA	NA	NA	NA

CEP indicates centromeric probe; F, female; M, male; NA, not analyzable; P, polysomy; X-, loss of chromosome Y.

FIGURE 18. Gains of chromosomes 7 and 17 and losses of chromosomes 21 (variable) and Y were detected by aCGH analysis.

Squamous differentiation has been reported in RCC, but it seems to be a very rare phenomenon. Practically all RCCs with such morphology reported in the literature were CHRCCs with sarcomatoid transformation.[27–29] The cases presented here differ from CHRCC not only by morphology but also by their immunohistochemical and chromosomal profiles. There are 2 main variants of CHRCC that have been recognized: classical and eosinophilic.[30] Microscopically, these tumors are described as mostly solid or solid alveolar. However, the morphologic spectrum has been expanded to include microcystic, oncocytoma-like, adenomatoid, and tumors with neuroendocrine differentiation, and papillary arrangements.[31–37] There were no leaf-like cells or small eosinophilic cells present within the included tumors, and we were not able to identify raisinoid nuclei with perinuclear clearing typical of CHRCC. The sarcomatoid transformation seen in some CHRCCs has not been seen in our cases. The immunohistochemical profile of these cases differed from that of CHRCC. In this respect it is most important to note that CD117 was negative in 17/21 cases, and vimentin was positive in all analysable cases, which excludes the diagnosis of CHRCC. CD117 was only weakly positive within a small cell population of the 2 cases not counted above. CHRCCs are usually further characterized by multiple chromosomal losses of chromosomes 1, 2, 6, 10, 13, 17, and 21 in both classic and eosinophilic CHRCC.[30] Other studies also report numerical gains of chromosomes 4, 7, 15, 19, and 20,[4,38,39] but the significance of these findings is still a topic of discussion. The molecular genetic findings in all analyzed cases in this paper are completely different from the profiles identified in CHRCCs.

From the available clinical data, it is evident that BSARCC has metastatic potential. The morphology of the metastatic neoplasms did not differ significantly from that of the primary tumors, and it could be possible, albeit difficult, to recognize this unique pattern within a metastatic lesion even without information about the morphology of the primary tumor.

REFERENCES

1. Petersson F, Bulimbasic S, Hes O, et al. Biphasic alveolosquamoid renal carcinoma: a histomorphological, immunohistochemical, molecular genetic, and ultrastructural study of a distinctive morphologic variant of renal cell carcinoma. *Ann Diagn Pathol*. 2012;16:459–469.
2. Coromias Cishek A, Gonzalez M, Caamano V, et al. Biphasic alveolo-squamoid renal cell carcinoma (BASRC): light and immunohistochemical study of 3 cases. *Virchows Arch*. 2014;465(suppl 1):S157.
3. Van Dongen JJ, Langerak AW, Bruggemann M, et al. Design and standardization of PCR primers and protocols for detection of clonal immunoglobulin and T-cell receptor gene recombinations in suspect lymphoproliferations: report of the BIOMED-2 Concerted Action BMH4-CT98-3936. *Leukemia*. 2003;17:2257–2317.
4. Sperga M, Martinek P, Vaneeck T, et al. Chromophobe renal cell carcinoma—chromosomal aberration variability and its relation to Paner grading system: an array CGH and FISH analysis of 37 cases. *Virchows Arch*. 2013;463:563–573.
5. Delahunt B, Eble JN. Papillary renal cell carcinoma: a clinicopathologic and immunohistochemical study of 105 tumors. *Mod Pathol*. 1997;10:537–544.
6. Delahunt B, Eble JN, McCredie MR, et al. Morphologic typing of papillary renal cell carcinoma: comparison of growth kinetics and patient survival in 66 cases. *Hum Pathol*. 2001;32:590–595.
7. Srigley JR, Delahunt B, Eble JN, et al. The International Society of Urological Pathology (ISUP) Vancouver Classification of Renal Neoplasia. *Am J Surg Pathol*. 2013;37:1469–1489.
8. Lefevre M, Couturier J, Sibony M, et al. Adult papillary renal tumor with oncocytic cells: clinicopathologic, immunohistochemical, and cytogenetic features of 10 cases. *Am J Surg Pathol*. 2005;29:1576–1581.
9. Hes O, Brunelli M, Michal M, et al. Oncocytic papillary renal cell carcinoma: a clinicopathologic, immunohistochemical, ultrastructural, and interphase cytogenetic study of 12 cases. *Ann Diagn Pathol*. 2006;10:133–139.
10. Mills SE, Greenson JK, Hornick JL, et al, eds. *Sternberg's Diagnostic Surgical Pathology*, 6 ed. Philadelphia: Wolters Kluwer; 2015:2703.
11. Mantoan Padilha M, Billis A, Allende D, et al. Metanephric adenoma and solid variant of papillary renal cell carcinoma: common and distinctive features. *Histopathology*. 2013;62:941–953.
12. Kovacs G, Fuzesi L, Emanual A, et al. Cytogenetics of papillary renal cell tumors. *Genes Chromosomes Cancer*. 1991;3:249–255.
13. Jiang F, Richter J, Schraml P, et al. Chromosomal imbalances in papillary renal cell carcinoma: genetic differences between histological subtypes. *Am J Pathol*. 1998;153:1467–1473.
14. Eble JN, Sauter G, Epstein JI, et al. *WHO Classification of Tumours Tumours of the Urinary System and Male Genital Organs Pathology and Genetics*. Lyon: IARC Press; 2004:359.
15. Foucar E, Rosai J, Dorfman R. Sinus histiocytosis with massive lymphadenopathy (Rosai-Dorfman disease): review of the entity. *Semin Diagn Pathol*. 1990;7:19–73.
16. Michal M, Kazakov DV, Hadravsky L, et al. High-grade myxoinflammatory fibroblastic sarcoma: a report of 23 cases. *Ann Diagn Pathol*. 2015;19:157–163.
17. Zhang SY, Caamano J, Cooper F, et al. Immunohistochemistry of cyclin D1 in human breast cancer. *Am J Clin Pathol*. 1994;102:695–698.
18. Leroy X, Camparo P, Gnemmi V, et al. Clear cell papillary renal cell carcinoma is an indolent and low-grade neoplasm with overexpression of cyclin-D1. *Histopathology*. 2014;64:1032–1036.
19. Lima MS, Pereira RA, Costa RS, et al. The prognostic value of cyclin D1 in renal cell carcinoma. *Int Urol Nephrol*. 2014;46:905–913.
20. Zhao W, Tian B, Wu C, et al. DOG1, cyclin D1, CK7, CD117 and vimentin are useful immunohistochemical markers in distinguishing chromophobe renal cell carcinoma from clear cell renal cell carcinoma and renal oncocytoma. *Pathol Res Pract*. 2015;211:303–307.
21. Mardi K, Kaushal V, Sharma V. Rare coexistence of keratinizing squamous cell carcinoma with xanthogranulomatous pyelonephritis in the same kidney: report of two cases. *J Cancer Res Ther*. 2010;6:339–341.
22. Bhaijee F. Squamous cell carcinoma of the renal pelvis. *Ann Diagn Pathol*. 2012;16:124–127.
23. Zainuddin MA, Hong TY. Primary renal adenosquamous carcinoma. *Urol Ann*. 2010;2:122–124.
24. Terada T. Synchronous squamous cell carcinoma of the kidney, squamous cell carcinoma of the ureter, and sarcomatoid carcinoma of the urinary bladder: a case report. *Pathol Res Pract*. 2010;206:379–383.
25. Holmang S, Lele SM, Johansson SL. Squamous cell carcinoma of the renal pelvis and ureter: incidence, symptoms, treatment and outcome. *J Urol*. 2007;178:51–56.
26. Perez-Montiel D, Wakely PE, Hes O, et al. High-grade urothelial carcinoma of the renal pelvis: clinicopathologic study of 108 cases with emphasis on unusual morphologic variants. *Mod Pathol*. 2006;19:494–503.
27. Mete O, Kilicaslan I, Ozcan F, et al. Sarcomatoid chromophobe renal cell carcinoma with squamous differentiation. *Pathology*. 2007;39:598–599.
28. Viswanathan S, Desai SB, Prabhu SR, et al. Squamous differentiation in a sarcomatoid chromophobe renal cell carcinoma: an unusual case report with review of the literature. *Arch Pathol Lab Med*. 2008;132:1672–1674.
29. Husain AEBJ, Trpkov K. Composite chromophobe renal cell carcinoma with sarcomatoid differentiation containing osteosarcoma, chondrosarcoma, squamous metaplasia and associated collecting duct carcinoma: a case report. *Anal Quant Cytopathol Histopathol*. 2014;36:235–240.
30. Brunelli M, Eble JN, Zhang S, et al. Eosinophilic and classic chromophobe renal cell carcinomas have similar frequent losses of multiple chromosomes from among chromosomes 1, 2, 6, 10, and 17, and this pattern of genetic abnormality is not present in renal oncocytoma. *Mod Pathol*. 2005;18:161–169.
31. Hes O, Vaneeck T, Perez-Montiel DM, et al. Chromophobe renal cell carcinoma with microcystic and adenomatous arrangement and pigmentation: a diagnostic pitfall. Morphological, immunohistochemical, ultrastructural and molecular genetic report of 20 cases. *Virchows Arch*. 2005;446:383–393.
32. Dundr P, Pesl M, Povysil C, et al. Pigmented microcystic chromophobe renal cell carcinoma. *Pathol Res Pract*. 2007;203:593–597.
33. Parada DD, Pena KB. Chromophobe renal cell carcinoma with neuroendocrine differentiation. *APMIS*. 2008;116:859–865.
34. Kuroda N, Tamura M, Hes O, et al. Chromophobe renal cell carcinoma with neuroendocrine differentiation and sarcomatoid change. *Pathol Int*. 2011;61:552–554.
35. Kuroda N, Liyama T, Moriki T, et al. Chromophobe renal cell carcinoma with focal papillary configuration, nuclear basaloid arrangement and stromal osseous metaplasia containing fatty bone marrow element. *Histopathology*. 2005;46:712–713.
36. Ohe C, Kuroda N, Keiko M, et al. Chromophobe renal cell carcinoma with neuroendocrine differentiation/morphology: a clinicopathological and genetic study of three cases. *Hum Pathol*. 2014;1:31–39.
37. Kuroda N, Tanaka A, Yamaguchi T, et al. Chromophobe renal cell carcinoma, oncocytic variant: a proposal of a new variant giving a critical diagnostic pitfall in diagnosing renal oncocytic tumors. *Med Mol Morphol*. 2013;46:49–55.
38. Vieira J, Henrique R, Ribeiro FR, et al. Feasibility of differential diagnosis of kidney tumors by comparative genomic hybridization of fine needle aspiration biopsies. *Genes Chromosomes Cancer*. 2010;49:935–947.
39. Tan MH, Wong CF, Tan HL, et al. Genomic expression and single-nucleotide polymorphism profiling discriminates chromophobe renal cell carcinoma and oncocytoma. *BMC Cancer*. 2010;10:196.

1.2.8 Cystic and necrotic papillary renal cell carcinoma: prognosis, morphology, immunohistochemical, and molecular-genetic profile of 10 cases

V literatuře lze dohledat relativně konfliktní údaje o prognostickém významu přítomnosti nekrózy v PRCC a obecně bývá přítomnost nekrózy uváděna jako negativní prognostický znak. V této studii bylo hodnoceno celkem 10 rozsáhle nekrotických PRCC, v tradiční klasifikaci PRCC se jednalo o PRCC typ 1.

Tumory pocházely od 8 mužů a 2 žen, věkový průměr pacientů byl 62,6 let (rozmezí 32-85 let) a tumory měřily od 6 do 14 cm. Všichni pacienti v rámci dlouhodobého sledování (v rozmezí 0,5 – 14 let) vykazovali neagresivní průběh onemocnění (tj. bez recidiv a metastáz). Nádory byly makroskopicky sférické, cystické, opouzdřené fibrózní kapsulou a vyplněné hemoragickým/nekrotickým obsahem. Vitální nádorová tkáň (odpovídající morfologicky PRCC typ 1) byla přítomna jen v minimálním množství a to jako tenký lem vystýlající vnitřní povrch cystické dutiny. Nádorové hmoty byly ve všech případech pozitivní v AMACR, OSCAR, CAM 5.2, HIF-2 a vimentinu. Polysomie chromozomů 7 a 17 byla prokázána v 5/9 analyzovatelných případů, u dvou případů byla zaznamenána dizomie chromozomů 7 a 17 a jeden případ měl polyzomii pouze chromozomu 17. Ztráta chromozomu Y byla zastižena u pěti tumorů (včetně jednoho případu s disomickým statusem chromozomů 7 a 17).

PRCC typ 1 se může prezentovat jako objemný nekrotický či hemoragicky změněný, cystický tumor s fibroleiomyomatózním pouzdrem. Všechny případy v naší studii vykazovaly neagresivní chování, proto usuzujeme, že objemné ložisko nekrózy nemusí nutně znamenat nepříznivý prognostický znak, zejména pokud se vyskytne v PRCC typ 1.

Annals of Diagnostic Pathology 26 (2017) 23–30

Contents lists available at ScienceDirect

Annals of Diagnostic Pathology

Cystic and necrotic papillary renal cell carcinoma: prognosis, morphology, immunohistochemical, and molecular-genetic profile of 10 cases☆,☆☆

Kvetoslava Peckova, MD[a], Petr Martinek, PhD[a], Kristyna Pivovarcikova, MD[a], Tomas Vanecek, PhD[a], Reza Alaghehbandan, MD[b], Kristyna Prochazkova, MD[c], Delia Perez Montiel, MD[d], Milan Hora, MD, PhD[c], Faruk Skenderi, MD[e], Monika Ulamec, MD, PhD[f], Pavla Rotterova, MD, PhD[g], Ondrej Daum, MD, PhD[a], Jiri Ferda, MD, PhD[h], Whitney Davidson, BS[i], Ondrej Ondic, MD[a], Magdalena Dubova, MD[a], Michal Michal, MD[a], Ondrej Hes, MD, PhD[a,*]

[a] Department of Pathology, Charles University, Medical Faculty and Charles University Hospital Plzen, Czech Republic
[b] Department of Pathology, University of British Columbia, Royal Columbian Hospital, Vancouver, Canada
[c] Department of Urology, Charles University, Medical Faculty and Charles University Hospital Plzen, Czech Republic
[d] Department of Pathology, Instituto Nacional de Cancerologia, Mexico City, Mexico
[e] Department of Pathology, University Clinical Center, Sarajevo, Bosnia and Herzegovina
[f] "Ljudevit Jurak" Pathology Department, Clinical Hospital Center "Sestre milosrdnice,", Zagreb, Croatia
[g] Biopticka Laborator, Plzen, Czech Republic
[h] Department of Radiodiology, Charles University, Medical Faculty and Charles University Hospital Plzen, Czech Republic
[i] Department of Pathology, The University of Kansas School of Medicine, Kansas City, KS

ARTICLE INFO

Keywords:
Kidney
Papillary renal cell carcinoma
Cystic
Necrosis
Necrotics
Molecular genetics

ABSTRACT

Conflicting data have been published on the prognostic significance of tumor necrosis in papillary renal cell carcinoma (PRCC). Although the presence of necrosis is generally considered an adverse prognostic feature in PRCC, we report a cohort of 10 morphologically distinct cystic and extensively necrotic PRCC with favorable biological behavior. Ten cases of type 1 PRCC with a uniform morphologic pattern were selected from the 19 500 renal tumors, of which 1311 were PRCCs in our registry. We focused on precise morphologic diagnosis supported by immunohistochemical and molecular-genetic analysis. Patients included 8 men and 2 women with an age range of 32–85 years (mean, 62.6 years). Tumor size ranged from 6 to 14 cm (mean, 9.4 cm). Follow-up data were available in 7 patients, ranging from 0.5 to 14 years (mean, 4 years). All tumors were spherical, cystic, and circumscribed by a thick fibrous capsule, filled with hemorrhagic/necrotic contents. Limited viable neoplastic tissue was present only as a thin rim in the inner surface of the cyst wall, consistent with type 1 PRCC. All cases were positive for AMACR, OSCAR, CAM 5.2, HIF-2, and vimentin. Chromosome 7 and 17 polysomy was found in 5 of 9 analyzable cases, 2 cases demonstrated chromosome 7 and 17 disomy, and 1 case showed only chromosome 17 polysomy. Loss of chromosome Y was found in 5 cases, including 1 case with disomic chromosomes 7 and 17. No *VHL* gene abnormalities were found. Papillary renal cell carcinoma type 1 can present as a large hemorrhagic/necrotic unicystic lesion with a thick fibroleiomyomatous capsule. Most cases showed a chromosomal numerical aberration pattern characteristic of PRCC. All tumors followed a nonaggressive clinical course. Large liquefactive necrosis should not necessarily be considered an adverse prognostic feature, particularly in a subset of type 1 PRCC with unilocular cysts filled with necrotic/hemorrhagic material.

1. Introduction

Papillary renal cell carcinoma (PRCC) accounts for 15% to 20% of renal carcinomas and is a heterogeneous disease with histologic subtypes and variations in clinical behavior and outcome. It is traditionally subclassified as type 1, which is a distinct entity (morphologically, immunohistochemically, and genetically), and type 2, which is composed of more heterogeneous group of diseases [1]. Grossly, PRCCs are usually well circumscribed and may contain foci of necrosis and

☆ Disclosure of Conflict of Interest: All authors declare no conflict of interest.

☆☆ The study was supported by the Charles University Research Fund (Project No. P36), by the Ministry of Health of the Czech Republic—Conceptual Development of Research Organization (Faculty Hospital in Pilsen, 00669806), and by SVV 260283.

* Corresponding author at: Department of Pathology, Charles University, Medical Faculty and Charles University Hospital Plzen, Alej Svobody 80, 304 60 Pilsen, Czech Republic.
E-mail address: hes@medima.cz (O. Hes).

http://dx.doi.org/10.1016/j.anndiagpath.2016.10.007
1092-9134/

hemorrhage. Nonetheless, unilocular cystic tumors within type 1 PRCC are rather uncommon.

We describe a cohort of PRCC, morphologically consistent with type 1 according to the Delahunt classification, which were large unilocular cystic tumors surrounded by thick-wall fibrous capsule and filled with hemorrhagic/necrotic contents, demonstrating long-term favorable clinical outcome [1,2]. The purpose of this study was to describe a unique subpopulation of type 1 PRCC with an unusual gross and histologic presentation (cystic lesion with necrotic content) to enhance our understating of the prognostic significance of tumor necrosis (TN) in these tumors.

2. Materials and methods

This study design was approved by local ethical committee (Charles University, Medical School Plzen).

Of 19 500 renal tumors and tumor-like lesions (including 1311 PRCCs) in the institutional and consultation files of the Sikl's Department of Pathology at Charles' University, Plzen, Czech Republic, 10 cases of cystic and largely necrotic type 1 PRCC were retrieved. The tissue had been fixed in neutral formalin, embedded in paraffin, 3- to 4-μm-thick sections were cut and stained with hematoxylin and eosin.

All tumors were large cystic lesions encapsulated by a thick, mostly fibrotic tissue. In 2 cases, the tumor capsule was histologically composed of so-called phenomenon inflammatory pseudotumor, for which one of them has already been reported [3]. Cysts were filled with sanguinolent necrotic material, whereas viable neoplastic structures were identified only in the inner surface of the cyst wall. Cases were further examined by immunohistochemistry and analyzed by molecular-genetic methods.

2.1. Immunohistochemistry

The immunohistochemical study was performed using a Ventana Benchmark XT automated stainer (Ventana Medical System, Inc, Tucson, AZ). The following primary antibodies were used: cytokeratin AE1/3 VM (AE1/AE3/PCK26, monoclonal; Ventana-Roche, Mannheim, Germany, RTU), wide-spectrum keratin (OSCAR, monoclonal, 1:2000; Covance, Princetown, NJ), cytokeratin (CAM 5,2 monoclonal, 1:200; Becton-Dickinson, San Jose, CA), racemase/AMACR (P504S, monoclonal, 1:50; Zeta, Sierra Madre, CA), vimentin (D9, monoclonal, 1:1000; Neomarkers, Westinghouse, CA), carbonic anhydrase IX (rhCA9, monoclonal, 1:100; RD Systems, Abingdon, GB), CD31 (JC70A, monoclonal, 1:50; DakoCytomation, Glostrup, Denmark), CD34 (QBEnd-10, monoclonal, 1:100; DakoCytomation), c-kit (CD 117, polyclonal; DakoCytomation, RTU), cathepsin K (monoclonal, 3F9, 1:100; Abcam, Cambridge, UK), PAX-8 (polyclonal rabbit, 1:25; Cell Marque–Medac/RNDr. A. Manthey, Rocklin, CA), TFE3 (polyclonal, 1:100; Abcam), HIF-1α (ESEE122, 0.5:150; Abcam), HIF-2α (ep190b, 1:30; Abcam), and phospho-mTOR (Ser2448, 1:80; Cell Signaling Technology, Danvers, MA). Appropriate positive and negative controls were used.

2.2. Molecular-genetic study

2.2.1. Fluorescence in situ hybridization methods

Four-micrometer-thick section was placed onto a positively charged slide. Hematoxylin and eosin–stained slide was examined for the cell counting area determination.

The unstained slide was routinely deparaffinized and incubated in the 1× Target Retrieval Solution Citrate pH 6 (Dako, Glostrup, Denmark) for 40 minutes at 95°C and subsequently cooled for 20 minutes at room temperature in the same solution. The slide was washed in deionized water for 5 minutes and digested in protease solution with Pepsin (0.5 mg/mL; Sigma-Aldrich, St Louis, MO) in 0.01 M HCl at 37°C for 20 minutes. The slide was then placed into deionized water for 5 minutes, dehydrated in a series of ethanol solution (70%, 85%, and 96% for 2 minutes each), and air-dried. Probes for aneuploidy detection of chromosomes 7 and 17 (Vysis/Abbott Molecular, Des Plaines, IL; see Table 1) were mixed with water and LSI/WCP (Locus-Specific Identifier/Whole Chromosome Painting) Hybridization buffer (Vysis) in a 1:2:7 ratio. An appropriate amount of probe mix was applied on the specimen, covered with a glass coverslip and sealed with a rubber cement. The slide was incubated in the ThermoBrite instrument (StatSpin/Iris Sample Processing, Westwood, MA) with co-denaturation parameters 85°C for 8 minutes and hybridization parameters 37°C for 16 hours. Rubber-cemented coverslip was then removed and the slide was placed in a posthybridization wash solution (2× SSC/0.3% NP-40) at 72°C for 2 minutes. The slide was air-dried in the dark, counterstained with DAPI (Vysis), coverslipped and immediately examined.

2.2.2. Fluorescence in situ hybridization interpretation

The section was examined with an Olympus BX51 fluorescence microscope (Olympus Corporation, Tokyo, Japan) using a ×100 objective and filter sets Triple Band Pass (DAPI/SpectrumGreen/SpectrumOrange) and Single Band Pass (SpectrumGreen/SpectrumOrange). Scoring of aneuploidy was performed by counting the number of fluorescent signals in 100 randomly selected nonoverlapping tumor cell nuclei. The slide was independently enumerated by 2 observers (OH and PG). Monosomy and polysomy for studied chromosomes were defined as the presence of one signal per cell in greater than 45% and 3 and more signals in greater than 10% (mean + 3 SD in normal nonneoplastic control tissues), respectively.

2.2.3. DNA extraction and bisulfite DNA conversion

DNA for molecular-genetic investigation was extracted from formalin-fixed, paraffin-embedded tissue. Several 5-μm-thick sections were placed on the slides. Hematoxylin and eosin–stained slides were examined for identification of neoplastic tissue. Subsequently, neoplastic tumor and nonneoplastic tissue from unstained slides were scraped and DNA was isolated by the NucleoSpin Tissue Kit (Macherey-Nagel, Düren, Germany).

Bisulfite conversion of DNA was carried out using EZ DNA Methylation–Gold Kit (DNA input 500 ng; Zymo Research, Orange, CA).

All procedures were performed according to the manufacturer's protocols.

2.3. VHL gene analysis

Mutation analysis of exons 1, 2, and 3 of the *VHL* gene was performed using polymerase chain reaction (PCR) and direct sequencing. Polymerase chain reaction was carried out using primers shown in Table 2. The reaction conditions were as follows: 12.5 μL of HotStar Taq PCR Master Mix (Qiagen, Hilden, Germany), 10 pmol of each primer, 100 ng of template DNA, and distilled water up to 25 μL. The amplification program consisted of denaturation at 95°C for 15 minutes and then 40 cycles of denaturation at 95°C for 1 minute, annealing at 55°C for 1 minute, and extension at 72°C for 1.5 minute for all amplicons. The program was finished by 72°C incubation for 7 minutes.

The PCR products were checked on 2% agarose gel electrophoresis.

Successfully amplified PCR products were purified with magnetic particles Agencourt AMPure (Agencourt Bioscince Corporation, A Beckman Coulter Company, Beverly, MA), both side sequenced using Big Dye Terminator Sequencing kit (Applied Biosystems, Foster City, CA) and purified with magnetic particles Agencourt CleanSEQ (Agencourt Bioscince Corporation) all according to the manufacturer's protocol, and subsequently run on an automated sequencer ABI Prism 3130xl (Applied Biosystems) at a constant voltage of 13.2 kV for 20 minutes. All samples were analyzed in duplicates. Analyses of positive samples were repeated.

Table 1
Clinicopathologic data

Case	Age (y)	Sex	Size (cm)	Follow-up (y)	Follow-up (clinical information)
1	40	M	6 × 5.5 × 3.5	0.5	Open resection; pT1b. AW, without recurrency
2	67	F	6.5 × 5.5 × 5.5	2	Right kidney resection; pT1b; duplicate malignancy-brest cancer. AW, without recurrency
3	67	M	9 × 7.5 × 4	NA	NA
4	37	M	NA	NA	NA
5	65	F	9 × 7 × 6	4	AW
6	83	M	14 × 11.5 × 7	0.5	Nephrectomy with appendectomy; pT2. Epidermoid lung carcinoma. Died in 2008 of lung carcinoma. No autopsy
7	69	M	9 × 11 × 11	14	Nephrectomy with appendectomy; AW, without progression
8	85	M	9.5 × 7.5 × 5	NA	NA
9	32	M	NA	4	Marsupialization of "renal cyst"; pT2. Died in 2007 of hepatic failure. No autopsy
10	81	M	10 × 8 × 4	3	Nephrectomy. Died 3 y later of unknown causes. Suspect malignant tumor diagnosed from needle biopsy.

Abbreviations: AW, alive and well; F, female; M, male; NA, not available.

2.3.1. Analysis of VHL promoter methylation

Detection of promoter methylation was carried out via methylation-specific PCR as described by Herman et al [4]. Briefly, 100 ng of DNA or 2 μL of converted DNA was added to reaction consisted of 12.5 μL of HotStar Taq PCR Master Mix (Qiagen), 10 pmol of forward and reverse primer (Table 3), and distilled water up to 25 μL. The amplification program comprised denaturation at 95°C for 14 minutes and then 40 cycles of denaturation at 95°C for 1 minute, annealing at 60°C for 1 minute, and extension at 72°C for 1 minute. The program was finished by incubation at 72°C for 7 minutes.

The PCR products were checked on 2% agarose gel electrophoresis.

A patient with known *VHL* mutation and fully methylated HeLa cell DNA were used as a positive control for *VHL* mutation analysis and promoter methylation analysis, respectively. As a negative control, randomly selected healthy donor blood was used.

3. Results

3.1. Clinical features

Clinicopathologic data of the patients under study are summarized in Table 1. Of 10 patients, 8 were men and 2 were women, with age ranging from 32 to 85 years (mean, 62.6 years; median, 67 years). The tumor size ranged from 6 to 14 cm (mean, 9.4 cm; median, 9.3 cm). Follow-up data were available for 7 patients and ranged from 5 months to 14 years (mean, 4 years; median, 3 years). Three patients died of conditions unrelated to renal tumor progression (ie, lung cancer and hepatic failure). The remaining 7 patients were alive and well without disease progression or metastasis at the time of study.

3.2. Gross and microscopic findings

Grossly, tumors were large, with size up to 14 cm in greatest dimension (case 6). The tumors grew expansively, were well demarcated, and did not invade into adjacent structures (Fig. 1A + B). All tumors presented as unilocular cystic mass encapsulated by thick whitish fibrous tissue. The inner surface of the capsule was mainly covered by a very thin layer of brownish friable tissue, and the whole cyst was usually filled with hemorrhagic and necrotic material (Fig. 2). No grossly identifiable neoplastic tissue was noted within the entire tumor.

Microscopically, all cases showed similar basophilic morphologic appearance with low-grade nuclear features consistent with type 1 PRCC. In most cases, there was only very limited amount of viable neoplastic tissue present lining the inner surface the cyst (Fig. 3A + B). This residual viable neoplastic tissue focally formed short papillae/tubulopapillary structures mostly lined by a single-cuboidal or low-columnar epithelial cells with scant cytoplasm and relatively uniform nuclei (Fig. 4A + B). Occasionally, more complex papillary structures were encountered. Histologic grade 2 was found in 8 cases, 3 in 2 cases (International Society of Urological Pathology [ISUP] nucleolar grading).

All tumors were well circumscribed, with a prominent fibrous capsule showing a thickness up to 2 cm. In 2 cases (cases 9 and 10), the capsule wall comprised rather cellular tissue composed mostly of fibroblasts with focally dense lymphocytic infiltration. Such a phenomenon was morphologically consistent with the diagnosis of inflammatory pseudotumor (Fig. 5A + B). Cysts were filled with hemorrhagic and necrotic material.

3.3. Immunohistochemistry

The immunohistochemical findings are summarized in Table 2. All of the examined tumors were diffusely positive for AMACR, OSCAR, CAM 5.2, anti–HIF-2 and vimentin (Fig. 6). CD117 and anti HIF-1 were weakly positive. MIA was diffusely positive in 9/10 cases, and in one case (case 8) the positivity was focal. 7 of 10 tumors diffusely reacted with PAX 8, and the remaining 3 cases were focally positive. There was no expression of CANH and TFE3 in any case. Expression of CD34, CD31, mTor, Cathepsin K, and AE1-AE3 was variable. ALK-1 was negative both in pseudocapsules and in the neoplastic tissue in all cases.

3.4. Molecular-genetic findings

Findings of molecular-genetic analyses are summarized in Table 3. Tumors were analyzed for chromosomal copy number variation using array comparative genomic hybridization (aCGH) and fluorescence in

Table 2
Immunohistochemical findings

Case	CD117	CD31	CD34	Cath	AMACR	OSCAR	Vim	AE 1/3	CAM 5.2	MIA	TFE 3	CANH	PAX 8	Anti–HIF-1	Anti–HIF-2	mTOR	ALK 1[a]
1	+	−	−	−	+++	+++	+++	foc +++	++	+++	−	−	+++	+	+++	foc +++	−
2	+	+	+	−	+++	+++	+++	foc ++	++	+++	−	−	++	+	+++	foc +++	−
3	+	+	+	−	+++	+++	+++	foc +++	++	+++	−	−	++	+	+++	foc +++	−
4	+	+	−	−	+++	+++	+++	+++	+++	+++	−	−	+++	++	+++	foc +++	−
5	+	+	+	−	+++	+++	+++	foc +++	+++	+++	−	−	+++	+	+++	+	−
6	+	+	−	−	+++	+++	+++	+++	++	+++	−	−	++	++	+++	−	−
7	+	−	−	−	+++	+++	+++	foc +++	++	+++	−	−	foc +++	+	+++	foc +++	−
8	+	+	+	+	+++	+++	+++	+++	++	foc +++	−	−	foc +++	++	+++	foc +++	−
9	+	+	+	−	+++	+++	+++	+++	++	+++	−	−	foc +++	++	+++	foc ++	−
10	+	+	+	+	+++	+++	+++	foc ++	++	+++	−	−	+++	+	+++	+	−

Abbreviations: Cath, cathepsin K; foc, focally; Vim, vimentin; −, negative; +, weakly positive; ++, moderately positive; +++, strongly positive.
[a] Assessed in the capsule only.

Table 3
Molecular-genetic analyses

Case	Sex	aCGH	CEP 7	CEP 17	CEP XY	LOH 3p	VHL	VHLM
1	M	+9,+12,+20,−Y	D	D	X-	Neg	Neg	Neg
2	F	+12,+13,+16,+17,−21	D	P	XX	Neg	Neg	Neg
3	M	No changes	NA	NA	NA	Neg	Neg	Neg
4	M	NP	P	P	X-	NA	NA	Neg
5	F	NP	NP	NP	NP	NP	NP	NP
6	M	+7,+17	P	P	X-	Neg	Neg	Neg
7	M	+(7pter-7q22.1),+17,−Y	P	P	X-	NA	Neg	Neg
8	M	No changes	D	D	XY	Neg	Neg	Neg
9	M	+2,+3,+7,+12,+16,+17,+20,+21,+22	P	P	XY	Neg	Neg	Neg
10	M	NP	P	P	X-	NA	Neg	Neg

situ hybridization. Seven cases were analyzable by aCGH. Chromosome 7 and 17 polysomy was found in 5 cases (Fig. 7). No chromosomal numerical aberrations were found in 2 cases. In case 1, both chromosomes 7 and 17 were disomic with loss of chromosome Y detected by aCGH and subsequently confirmed by fluorescence in situ hybridization. Polysomies of chromosomes 9, 12, and 20 were found in the same tumor (case 1). Case 2 exhibited gains of chromosomes 12, 13, 16, and 17; chromosome 21 was monosomic and chromosome 7 was disomic.

No *VHL* gene abnormalities including mutations, hypermethylation of *VHL* promoter, and loss of heterozygosity of 3p locus were found in analyzable cases (Table 3).

4. Discussion

It has been evident since the so-called Heidelberg classification in 1997 that renal tumors represent a highly heterogeneous group of neoplasms not only morphologically but also from molecular-genetic perspectives [5]. In the 2004 World Health Organization classification of genitourinary tumors, 4 new subtypes of renal tumors were introduced [6]. In the 2012 ISUP Vancouver Renal Tumor Classification, further 5 new renal tumors were included and 3 more were recognized as "emerging" renal tumors [6]. The recent 2016 World Health Organization classification fully accepts the proposals of the 2012 ISUP Vancouver classification and one of the "emerging entities," succinate dehydrogenase deficient renal cell carcinoma (RCC), has been added as a new entity [7]. It is evident from these ever-evolving classifications that the morphologic and genetic variability of renal tumors are enormous and that one can reasonably anticipate different clinical outcomes in particular tumor types. Therefore, prognostic criteria and predictor factors can play a crucial role in providing individual risk profiles with a suitable aftercare conception [8]. It would be challenging to apply prognostic morphologic criteria to RCCs owing to vast tumor heterogeneity and the diverse biological pathways that exist in various tumors [8,9].

Type 1 PRCC is currently considered a distinct entity with relative uniform gross, histologic, and immunohistochemical features as well as similar molecular-genetic profile. Our cohort is constituted of a homogenous subset of type 1 PRCC presenting with large unilocular cystic necrotic tumors.

Papillary renal cell carcinoma, the second most common RCCs, was initially classified as 2 morphologic groups of so-called type 1 and type 2 by Delahunt and Eble [2]. Papillary renal cell carcinomas are generally immunoreactive for vimentin, cytokeratins AE1-AE3, CAM5.2, high-molecular-weight cytokeratins, EMA, CD10, and AMACR. Type 1 PRCC is more frequently positive for CK7. Genetic abnormalities in PRCC most commonly include trisomy/polysomy of chromosomes 7, 12, 16, 17, and 20 and loss of the Y chromosome. Several studies have

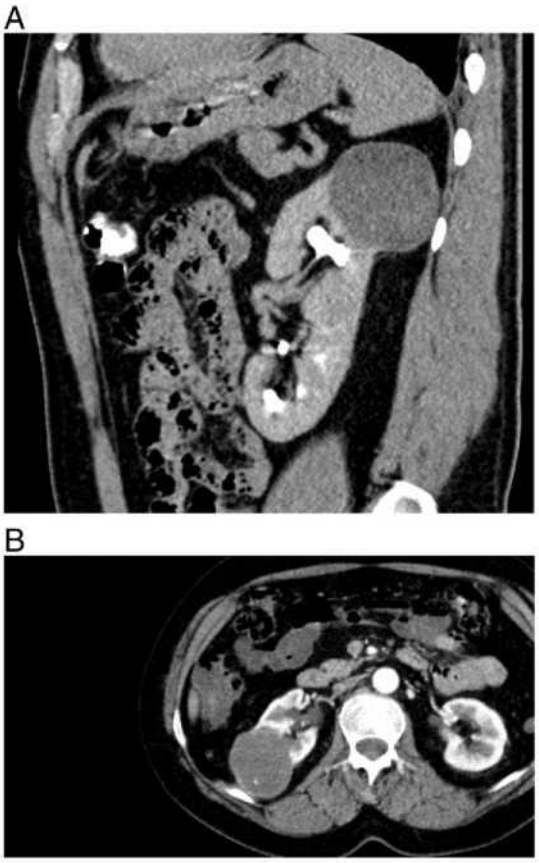

Fig. 1. (A) Case 2. Postcontrast computed tomography (CT), excretory phase, sagittal section. A round-shape tumor of the upper pole of the left kidney. Postcontrast density 17-61 HU. Necrotic center of the tumor is clearly visible. (B) Case 3. Postcontrast CT, arterial phase, axial section. Tumor of the right kidney, round shape with large central necrosis, postcontrast density 25-68 HU.

Fig. 2. Thick-walled cyst with thin, mostly necrotic rim of neoplastic tissue on the inner surface.

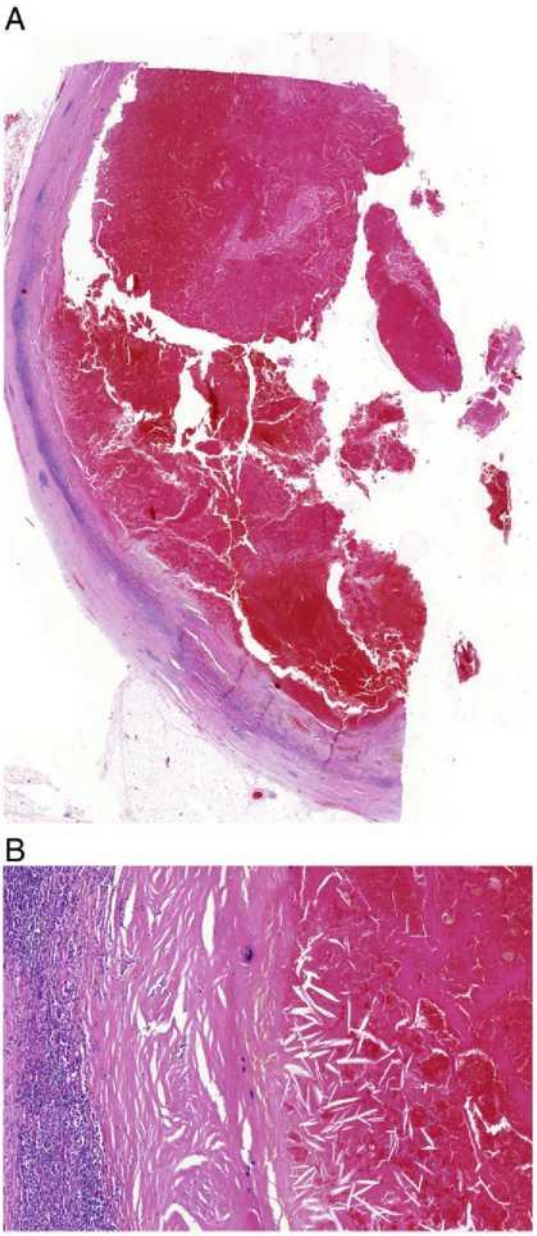

Fig. 3. (A + B) A limited amount of the vital neoplastic tissue lined the inner wall of the cyst. (A) Scanning magnification showing a large portion of thick-walled cyst. (B) Large areas of inner surface of the cyst were covered by necrotic material only.

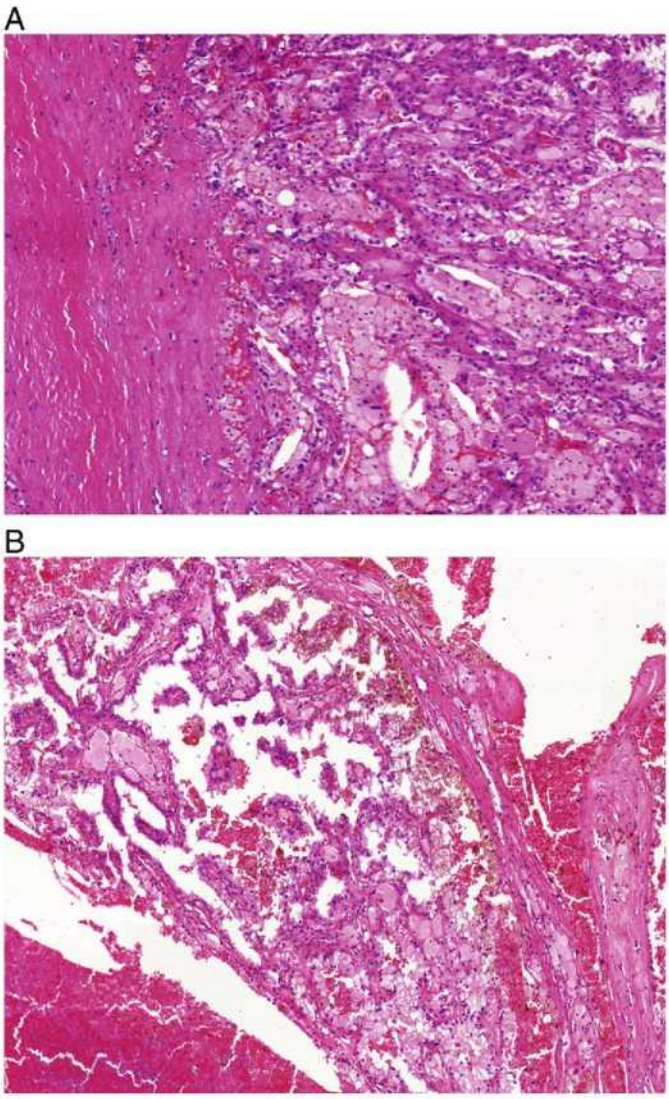

Fig. 4. Viable neoplastic tissue focally formed tubulopapillary (A) or short papillary (B) structures mostly lined by single-cuboidal or low-columnar epithelial cells with scant cytoplasm and uniform nuclei.

suggested genetic differences between type 1 (morphologically basophilic) and type 2 (morphologically eosinophilic) subtypes [6].

The increasing number of reported cases and the development of new diagnostic techniques have demonstrated that PRCC, as a group, is more diverse morphologically and genetically than previously thought.

Papillary renal cell carcinomas sometimes display overlapping morphologic features of type 1 and type 2, which can pose significant diagnostic difficulties in differentiating between the 2 types [10]. Several distinct variants of PRCC that are different from type 1 and type 2 have been described in the literature [11-14]. It should be noted that types 1 and 2 PRCCs are shown to be clinically and biologically distinct. Alterations in the MET pathway are associated with type 1, and activation of the NRF2-ARE pathway is described with type 2 [15]. Type 1 tumors often harbor gains of chromosomes 7p and 17p, whereas type 2 tumors contain an allelic imbalance of one or more chromosomes, namely, chromosomes 1p, 3p, 5, 6, 8, 9p, 10, 11, 15, 18, and 22 [6,15].

In our study, we attempted to assemble a uniform cohort of PRCC tumors that were consisted of large cystic necrotic/hemorrhagic tumors encapsulated by thick fibrous tissue. Morphologically and immunohistochemically, all lesions corresponded with type 1 PRCC. We noted that the tumors contained only scarce amounts of viable neoplastic tissue, mainly in the inner surface of the cyst wall, with most of tumor volume consisting of necrotic sanguinolent material.

The molecular-genetic profile was also expectedly consistent with type 1 PRCC (in 5/9 analyzable cases). Two of our cases demonstrated disomy in chromosomes 7 and 17, but also showed additional chromosomal abnormalities. Gains of chromosomes 9, 12, and 20 were found in 1 case (case 1), with a second case (case 6) exhibiting normal chromosome 7 and 17 status as well as disomy of all other chromosomes.

The prognosis of RCCs in general is attributed to several clinical and pathological factors such as symptomatic cancer, TNM classification, histologic grade, and presence/absence of a sarcomatoid differentiation [22]. The presence of TN has also been proposed repeatedly as an independent prognostic factor. Tumor necrosis appears to represent an interesting parameter in prognostic assessment owing to its easy and reproducible identification in routine histopathologic examination. However, there are several conflicting aspects that challenge the notion

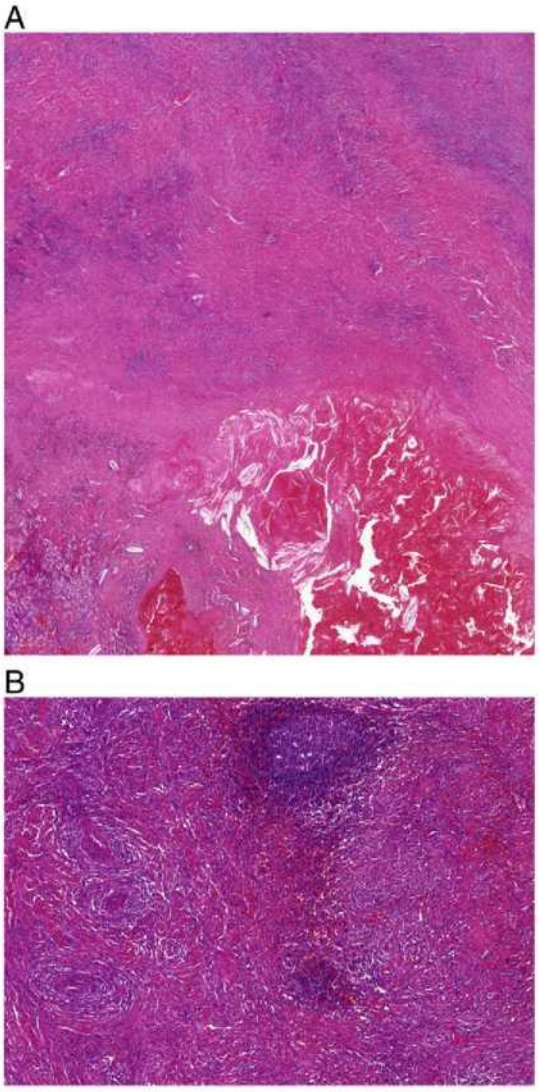

Fig. 5. Thick capsule resembling inflammatory pseudotumor was present in 2 cases. Scanning magnification (A) and detailed view (B).

of TN as a prognostic parameter. First, the prognostic significance of necrosis in RCCs remains controversial because the studies published to date have shown conflicting results [9,16,17]. This may be explained by the fact that no uniform consensus on assessing TN exists. Some researchers evaluate necrosis from gross specimens only [16,18], whereas others use radiologic or microscopic findings [9,17,19]. Klatte et al suggested that classification based solely on the presence or absence of necrosis is unsatisfactory. Conversely, they recommended a scoring system based on the extent of necrosis as a part of every pathological examination [33]. However, this concept is not currently accepted as part of standard reporting.

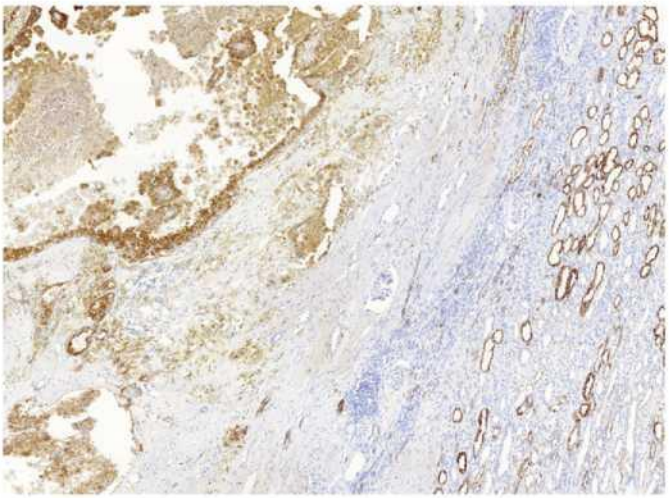

Fig. 6. All tumors were positive for AMACR.

Although TN is often reported as an adverse prognostic factor, its significance is only well established in clear cell RCC [6,20-22]. Furthermore, according to a recently proposed grading system for clear cell RCC, only coagulative-type necrosis is considered as a significant prognostic marker. It should be noted that no such criteria have been established for PRCC. Coagulative-type necrosis is characterized by preserved architecture of dead tissues and firm texture, with neoplastic cells showing no nuclei with limited structural damage, giving the appearance of so-called "ghost cells."

On the other hand, liquefactive necrosis is characterized by digestion of the dead cells resulting in transformation of the tissue into a liquid viscous mass [23]. We consider the necrosis within our cohort to be liquefactive type, as a substantial part of the tumor was transformed into a liquid viscous, largely hemorrhagic mass in all cases.

Considering that PRCCs are composed of a diverse and heterogeneous group of tumors, the determination of prognostic factors would even be more difficult to ascertain. The situation is further complicated by the fact that the incidence of PRCC is much lower than that of clear cell RCC, and a relatively limited number of studies dealing with prognostic factors in PRCC have been published [24]. One of the strengths of our series is that all the cases were uniformly and exclusively composed of type 1 PRCC according to Delahunt classification. It is worth noting that studies assessing clinical outcomes in PRCC may have generated inconsistent conclusions simply due to heterogeneous nature of PRCCs. Hence, numerous researchers have made an effort to determine the most useful method of histologic assessment in establishing meaningful prognostic factors. Onishi et al [25] studied clinicopathologic features of 42 PRCCs and their influence on prognosis. They suggested that the presence or absence of foam cells, pseudocapsule, solid architecture, cytologic appearance, stage, and nuclear grade were meaningful prognostic factors. In addition, they observed that the prognosis of patients with PRCC was similar to those with clear cell RCC. They did not include TN among the list of prognostic parameters, assuming that TN simply indicates poor tumor vascularization and that would be clinically irrelevant. However, because PRCC refers to a rather diverse heterogenous group of tumors and no further subclassifications of PRCC were provided by the authors, it would be difficult to determine which prognostic factors would have been attributed to different types of PRCC. Several other studies also reached a similar conclusion to that of Onishi et al, not considering TN to be an adverse prognostic parameter in PRCC [9,25-28]. In contrast, a number of studies reported TN to be associated with an adverse clinical course. In this regard, it is thus understandable that some researchers have designated TN as an adverse prognostic factor for PRCC [24,29-32].

However, it is of note that the subclassifying of PRCC into the type 1 and type 2 was not taken into consideration in some of these studies [8,26,28,33,34], whereas it was included in others [9,16,29,31]. For this reason, it is unclear whether it would be possible to compare the results from studies dealing with such a heterogeneous cohort of tumors. For instance, some PRCCs (ie, familiar leiomyomatosis associated [papillary] RCC) are clinically aggressive tumors, and that it would be inappropriate to objectively assess the prognostic value of TN in PRCCs without further subtyping.

This study is one of its kind to address this issue in an objective fashion. In our series of 10 largely necrotic type 1 PRCCs, none of the tumors demonstrated an aggressive or metastatic behavior. However, we would like to point out that our study has no ambition to establish prognostic criteria for type 1 PRCC or to evaluate presence/absence of

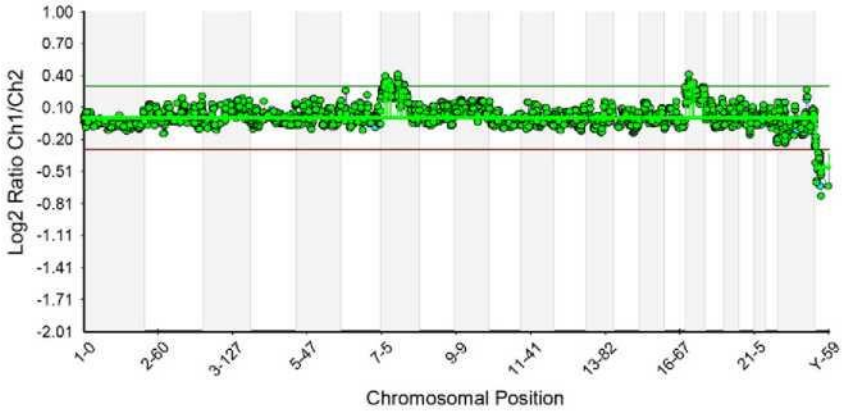

Fig. 7. Array CGH profile of case 7 revealing gains on chromosomes 7 (7pter-7q22.1) and 17, and a loss of chromosome Y.

necrosis as an adverse/ambivalent prognostic feature. The aim of this study was to describe a subpopulation of type 1 PRCC characterized by uniform, albeit unusual gross and histologic features.

An interesting phenomenon was documented in cases 9 and 10 of our series where the tumor capsule was composed of fibrous tissue, indistinguishable from inflammatory pseudotumor histologically. Therefore, it is very important to carefully examine the capsule and to distinguish myofibroblastic proliferation from sarcomatoid differentiation or even from sarcoma arising in an inflammatory pseudotumor. Inflammatory pseudotumors may express ALK-1 and cytokeratin immunostains, which can be helpful in differentiating ambiguous entities [33,34]. Neither ALK-1 nor cytokeratins showed a positive reaction in any tumor capsule in our series including the above-mentioned 2 cases. The capsules reminiscent of inflammatory pseudotumor in the above-mentioned cases exhibited identical immunohistochemical reaction against ALK-1 and cytokeratins as tumors with a "simple" fibrous capsule.

According to some authors, the presence of a fibromuscular pseudocapsule is rather characteristic of and more prominent in clear cell RCC, less frequently present in chromophobe RCC, and rarely in PRCC [34]. Fibromuscular pseudocapsules are characterized by a complex architecture including both connective tissue and smooth muscle fibers with thicker capsules sometimes containing vasculopathy. The presence of a pseudocapsule may be helpful to resolve diagnostic difficulties in challenging cases. The core biopsy specimen from patients with a high Bosniak type might be composed predominantly of fibromuscular tissue and only scant tumor fragments [34]. This kind of biopsy finding should lead to recommend additional tissue sampling. The designation of such a specimen as a nonrepresentative or even nonneoplastic biopsy should be considered with caution. According to some authors, radiologic and/or pathologic presence of a pseudocapsule/fibromuscular tissue may raise suspicion for RCC, with a higher probability of clear cell type [34]. The cases described in our study clearly show that a thick pseudocapsule can also be found in low-grade PRCC type 1.

5. Conclusions

Type 1 PRCC can present as a large unicystic lesion with necrotic/hemorrhagic content and surrounded by thick fibroleiomyomatous capsule. Most of our cases contained a chromosomal numerical aberration pattern characteristic of PRCC. All tumors followed a nonaggressive clinical course. Large liquefactive necrosis should not necessarily be considered an adverse prognostic feature, at least in a subset of type 1 PRCC with unilocular necrotic cystic presentation. Adequate tissue sampling in such tumors is crucial to arrive at accurate diagnosis, because most of these tumors contain limited viable neoplastic tissue lining the inner cyst wall.

Abbreviations: CEP, centromeric enumeration probe; F, female; LOH 3p, loss of heterozygosity of chromosome 3p; M, male; NA, not analyzable; Neg, negative; NP, not performed; P, polysomy; VHL, mutation analysis of VHL; VHLM, methylation of VHL; X-, loss of chromosome Y

References

[1] Moch H, Humphrey PA, Ulbright TM, Reuter VE. WHO classification of tumours of the urinary system and male genital organs; 2016.
[2] Delahunt B, Eble JN. Papillary renal cell carcinoma: a clinicopathologic and immunohistochemical study of 105 tumors. Mod Pathol 1997;10:537–44.
[3] Hes O, Hora M, Havlicek F, Chudacek Z, Klecka J, Michal M. Papillary renal cell carcinoma surrounded by unusual fibrotic reaction resembling inflammatory pseudotumour—a case report. Cesk Patol 2004;40:112–6.
[4] Herman JG, Graff JR, Myohanen S, Nelkin BD, Baylin SB. Methylation-specific PCR: a novel PCR assay for methylation status of CpG islands. Proc Natl Acad Sci U S A 1996;93:9821–6.
[5] Kovacs G, Akhtar M, Beckwith BJ, Bugert P, Cooper CS, Delahunt B, et al. The Heidelberg classification of renal cell tumours. J Pathol 1997;183:131–3.
[6] Srigley JR, Delahunt B, Eble JN, Egevad L, Epstein JI, Grignon D, et al. The International Society of Urological Pathology (ISUP) Vancouver classification of renal neoplasia. Am J Surg Pathol 2013;37:1469–89.
[7] Agaimy A. Succinate dehydrogenase (SDH)–deficient renal cell carcinoma. Pathologe 2016;37:144–52.
[8] Pflanz S, Brookman-Amissah S, Roigas J, Kendel F, Hoschke B, May M. Impact of macroscopic tumour necrosis to predict survival of patients with surgically resected renal cell carcinoma. Scand J Urol Nephrol 2008;42:507–13.
[9] Sengupta S, Lohse CM, Leibovich BC, Frank I, Thompson RH, Webster WS, et al. Histologic coagulative tumor necrosis as a prognostic indicator of renal cell carcinoma aggressiveness. Cancer 2005;104:511–20.
[10] Allory Y, Ouazana D, Boucher E, Thiounn N, Vieillefond A. Papillary renal cell carcinoma. Prognostic value of morphological subtypes in a clinicopathologic study of 43 cases. Virchows Arch 2003;442:336–42.
[11] Argani P, Netto GJ, Parwani AV. Papillary renal cell carcinoma with low-grade spindle cell foci: a mimic of mucinous tubular and spindle cell carcinoma. Am J Surg Pathol 2008;32:1353–9.
[12] Cantley R, Gattuso P, Cimbaluk D. Solid variant of papillary renal cell carcinoma with spindle cell and tubular components. Arch Pathol Lab Med 2010;134:1210–4.
[13] Hes O, Brunelli M, Michal M, Cossu Rocca P, Hora M, Chilosi M, et al. Oncocytic papillary renal cell carcinoma: a clinicopathologic, immunohistochemical, ultrastructural, and interphase cytogenetic study of 12 cases. Ann Diagn Pathol 2006;10:133–9.
[14] Val-Bernal JF, Gomez-Roman JJ, Vallina T, Villoria F, Mayorga M, Garcia-Arranz P. Papillary (chromophil) renal cell carcinoma with mucinous secretion. Pathol Res Pract 1999;195:11–7.
[15] Linehan WM, Spellman PT, Ricketts CJ, Creighton CJ, Fei SS, Davis C, et al. Comprehensive molecular characterization of papillary renal-cell carcinoma. N Engl J Med 2016;374:135–45.
[16] Leibovitch I, Lev R, Mor Y, Golomb J, Dotan ZA, Ramon J. Extensive necrosis in renal cell carcinoma specimens: potential clinical and prognostic implications. Isr Med Assoc J 2001;3:563–5.
[17] Zubac DP, Bostad L, Gestblom C, Kihl B, Seidal T, Wentzel-Larsen T, et al. Renal cell carcinoma: a clinicopathological follow-up study after radical nephrectomy. Scand J Urol Nephrol 2007;41:191–7.
[18] Sabo E, Boltenko A, Sova Y, Stein A, Kleinhaus S, Resnick MB. Microscopic analysis and significance of vascular architectural complexity in renal cell carcinoma. Clin Cancer Res 2001;7:533–7.
[19] Tollefson MK, Thompson RH, Sheinin Y, Lohse CM, Cheville JC, Leibovich BC, et al. Ki-67 and coagulative tumor necrosis are independent predictors of poor outcome for patients with clear cell renal cell carcinoma and not surrogates for each other. Cancer 2007;110:783–90.

[20] Delahunt B. Advances and controversies in grading and staging of renal cell carcinoma. Mod Pathol 2009;22(Suppl. 2):S24–36.
[21] Delahunt B, Bethwaite PB, Nacey JN. Outcome prediction for renal cell carcinoma: evaluation of prognostic factors for tumours divided according to histological subtype. Pathology 2007;39:459–65.
[22] Delahunt B, Bethwaite PB, Miller RJ, Sika-Paotonu D, Srigley JR. Re: Fuhrman grade provides higher prognostic accuracy than nucleolar grade for papillary renal cell carcinoma: T. Klatte, C. Anterasian, J. W. Said, M. de Martino, F. F. Kabbinavar, A. S. Belldegrun and A. J. Pantuck. *J Urol* 2010;183:2143-2147. J Urol 2011;185:356–7 [author reply 357-358].
[23] Kumar V, Abbas AK, Fausto N, Aster JC. Robbins and Cotran pathologic basis of diseases. , 3–42 Philadelpia: Saunders Elsevier; 2010.
[24] Sukov WR, Lohse CM, Leibovich BC, Thompson RH, Cheville JC. Clinical and pathological features associated with prognosis in patients with papillary renal cell carcinoma. J Urol 2012;187:54–9.
[25] Onishi T, Ohishi Y, Goto H, Suzuki M, Miyazawa Y. Papillary renal cell carcinoma: clinicopathological characteristics and evaluation of prognosis in 42 patients. BJU Int 1999;83:937–43.
[26] Moch H, Gasser T, Amin MB, Torhorst J, Sauter G, Mihatsch MJ. Prognostic utility of the recently recommended histologic classification and revised TNM staging system of renal cell carcinoma: a Swiss experience with 588 tumors. Cancer 2000;89:604–14.
[27] Kim H, Cho NH, Kim DS, Kwon YM, Kim EK, Rha SH, et al. Renal cell carcinoma in South Korea: a multicenter study. Hum Pathol 2004;35:1556–63.
[28] Cheville JC, Lohse CM, Zincke H, Weaver AL, Blute ML. Comparisons of outcome and prognostic features among histologic subtypes of renal cell carcinoma. Am J Surg Pathol 2003;27:612–24.
[29] Fu Z, Sun L, Huang Y, Zhang J, Zhang Z, Wang L, et al. A type 2 papillary renal cell carcinoma presenting as an intracystic necrotic lesion: a case report. Mol Clin Oncol 2013;1:318–20.
[30] Pichler M, Hutterer GC, Chromecki TF, Pummer K, Mannweiler S, Zigeuner R. Presence and extent of histological tumour necrosis is an adverse prognostic factor in papillary type 1 but not in papillary type 2 renal cell carcinoma. Histopathology 2013;62:219–28.
[31] Pichler M, Hutterer GC, Chromecki TF, Jesche J, Kampel-Kettner K, Rehak P, et al. Histologic tumor necrosis is an independent prognostic indicator for clear cell and papillary renal cell carcinoma. Am J Clin Pathol 2012;137:283–9.
[32] Klatte T, Remzi M, Zigeuner RE, Mannweiler S, Said JW, Kabbinavar FF, et al. Development and external validation of a nomogram predicting disease specific survival after nephrectomy for papillary renal cell carcinoma. J Urol 2010;184:53–8.
[33] Chan JK, Cheuk W, Shimizu M. Anaplastic lymphoma kinase expression in inflammatory pseudotumors. Am J Surg Pathol 2001;25:761–8.
[34] Roquero L, Kryvenko ON, Gupta NS, Lee MW. Characterization of fibromuscular pseudocapsule in renal cell carcinoma. Int J Surg Pathol 2015;23:359–63.

1.2.9 Papillary renal cell carcinoma with prominent spindle cell stroma - tumor mimicking mixed epithelial and stromal tumor of the kidney: Clinicopathologic, morphologic, immunohistochemical and molecular genetic analysis of 6 cases

Papilární renální karcinom je dobře prostudovanou jednotkou skupiny RCC a současná literatura kromě tradičního PRCC typ 1 prezentuje množství různých subtypů PRCC. V této práci byla popsána série šesti případů PRCC s papilárním, mikropapilárním a/nebo tubulopapilárním způsobem růstu a prominujícím vřetenitým stromatem, připomínající stroma u smíšeného epiteliálního a stromálního tumoru ledviny (MEST) či sarkomatoidního karcinomu. U těchto nádorů byly v rámci studie podrobně analyzovány klinické, morfologické, imunohistochemické a molekulárně genetické znaky.

Ve všech případech se jednalo o pacienty muže, ve věkovém rozmezí 44-98 roků (průměr 65,3 let, medián 65,5 roků). Velikost tumorů se pohybovala v rozmezí 2,4-11,4 cm (průměr 5,8 cm, medián 4,5 cm). Follow-up data byla dostupná u čtyř pacientů - v délce trvání 3 - 96 měsíců (průměr 42,75 měsíců, medián 36 měsíců). Epiteliální komponenta tumoru byla nejčastěji představována cylindrickými buňkami s eosinofilní cytoplazmou a nukleárním gradem 2 a 3 (ISUP/WHO). U všech případů jsme zaznamenali přítomnost kompaktní stromální komponenty sestávající z vřetenitých buněk, bez maligní mezenchymální heterologní komponenty. Tumory byly bez přítomnosti atypických mitóz a klasické mitózy byly přítomny jen vzácně (jak v epiteliální tak stromální komponentě). Epitelová komponenta imunohistochemicky vykazovala pozitivitu v CK7, AMACR a vimentinu ve všech šesti případech a zároveň byla negativní v TFE3, HMB45, desminu, CD34 a aktinu. Stromální komponenta reagovala pozitivně ve vimentinu, aktinu a fokálně v CD34 a naopak negativní byla v CK7, AMACR, TFE3, HMB45 a desminu. Estrogenové a progesteronové receptory byly kompletně negativní a exprese FH a SDHB byla zachována ve všech případech. Proliferační index byl sotva detekovatelný ve stromální komponentě a jen nízký v epiteliální komponentě (dosahoval rozmezí 0 až 5% pozitivních buněk na pole velkého zvětšení – HPF). Chromozomální numerické variace/cytogenetický status byly různé ve všech případech, bez jednoznačně pozorovatelných typických a specifických cytogenetických charakteristik a u tumorů a též bez přítomnosti mutace v genech *CDKN2A, BAP1, MET*. Obě komponenty tumoru (jak epiteliální tak stromální) neobsahovaly Müllerián skou diferenciaci, což bylo potvrzeno i imunohistochemicky.

Touto prací popsaný PRCC, připomínající MEST (MEST-like PRCC), je patrně odlišnou variantou PRCC, která MEST napodobuje. Prezentovaná studie dále obohacuje heterogenní spektrum PRCC o novou morfologickou variantu.

Annals of Diagnostic Pathology 44 (2020) 151441

Contents lists available at ScienceDirect

Annals of Diagnostic Pathology

journal homepage: www.elsevier.com/locate/anndiagpath

Original Contribution

Papillary renal cell carcinoma with prominent spindle cell stroma - tumor mimicking mixed epithelial and stromal tumor of the kidney: Clinicopathologic, morphologic, immunohistochemical and molecular genetic analysis of 6 cases

Joanna Rogala[a,b], Fumiyoshi Kojima[c], Reza Alaghehbandan[d], Abbas Agaimy[e], Petr Martinek[a], Ondrej Ondic[a], Monika Ulamec[f], Maris Sperga[g], Kvetoslava Michalova[a], Kristyna Pivovarcikova[a], Tomáš Pitra[h], Milan Hora[h], Ivan Ferak[i], Jana Marečková[a], Michal Michal[a], Ondrej Hes[a,*]

[a] Department of Pathology, Charles University, Medical Faculty and Charles University Hospital Plzen, Czech Republic
[b] Department of Pathology, Regional Specialist Hospital Wroclaw, Poland
[c] Department of Human Pathology, Wakayama Medical University, Wakayama, Japan
[d] Department of Pathology, Faculty of Medicine, University of British Columbia, Royal Columbian Hospital, Vancouver, BC, Canada
[e] Department of Pathology, University of Erlangen, Erlangen, Germany
[f] "Ljudevit Jurak" Pathology Department, Clinical Hospital Center "Sestre milosrdnice", Pathology Department, Medical University, Medical Faculty Zagreb, Croatia
[g] Department of Pathology, Riga Stradin's University, Riga, Latvia
[h] Department of Urology, Charles University, Medical Faculty and Charles University Hospital Plzen, Czech Republic
[i] Department of Pathology, Agel Laboratory, Novy Jicin, Czech Republic

ARTICLE INFO

Keywords:
Kidney
Papillary renal cell carcinoma
MESTK-like
Sarcomatoid-like

ABSTRACT

Papillary renal cell carcinoma (PRCC) is currently a well-studied type of RCC. In addition to PRCC type 1, there are a number of other subtypes and variants of PRCCs which have been reported. We describe a series of 6 PRCCs with papillary, micropapillary and/or tubulopapillary architecture and prominent spindle cell stroma, resembling stroma in mixed epithelial and stromal tumor of the kidney (MESTK) or sarcomatoid RCC.

Clinicopathologic, morphologic, immunohistochemical and molecular features were analyzed.

All patients were males with an age range of 44–98 years (mean 65.3, median 65.5 years). Tumor size ranged from 2.4–11.4 cm (mean 5.8, median 4.5 cm). Follow-up data were available for 4 patients, ranging from 3 to 96 months (mean 42.75, median 36 months). Epithelial cells were mostly cylindrical with eosinophilic cytoplasm, showing nuclear grade 2 and 3 (ISUP/WHO).

In all cases, loose to compact prominent stroma composed of spindle cells, without malignant mesenchymal heterologous elements was detected. No atypical mitoses were found, while typical mitoses were rare in both epithelial and stromal components.

Epithelial cells were positive for CK7, AMACR, and vimentin in all cases, while negative for TFE3, HMB45, desmin, CD34, and actin. The stroma was positive for vimentin, actin and focally for CD34, while negative for CK7, AMACR, TFE3, HMB45, and desmin. Estrogen and progesterone receptors were completely negative. FH and SDHB expression was retained in all analyzable cases. Proliferative index was barely detectable in stromal component and low in epithelial component, ranging 0 to 5% positive stained cells/high power field.

Copy number variation was variable with no distinct pattern. No mutations in *CDKN2A*, *BAP1*, *MET* were detected.

PRCC with MESTK-like features is a distinct variant of PRCC mimicking MESTK. Our findings add to the body of literature on ever expanding variants of PRCCs. Both epithelial and stromal components lacked true Müllerian features, which was also proven by immunohistochemistry.

* Corresponding author at: Department of Pathology, Medical Faculty and Charles University Hospital Plzen, Alej Svobody 80, 304 60 Pilsen, Czech Republic.
E-mail address: hes@medima.cz (O. Hes).

https://doi.org/10.1016/j.anndiagpath.2019.151441

1. Introduction

Papillary renal cell carcinoma (PRCC) is the second most common type of renal cell carcinoma. PRCC is traditionally classified according to the 2016 World Health Organization (WHO) Classification of Genitourinary Tumors into type 1 and type 2 [1]. However, studies published recently have shown more evidence emphasizing heterogeneity within this group of tumors, particularly the so-called type 2.

A number of PRCC variants were described recently in the literature such as oncocytic, solid, mucin secreting, biphasic squamoid, Warthin–like, and PRCC with reverse polarity [2-8]. All these variants are mostly defined by using morphologic and immunohistochemical features and they are more close to (at least in part variant of) type 1 PRCC. However even at the molecular genetic level, there are substantial differences among tumors classified generally as PRCC. The so-called type 2 PRCC seems to be rather composed of a group of tumors sharing papillary architecture than a uniform and distinct entity.

In this study, we analyzed clinicopathologic, morphologic, immunohistochemical, and molecular features of 6 unusual PRCC with papillary and/or tubulopapillary architecture and with prominent spindle cell stroma resembling mixed epithelial and stromal tumor of the kidney (MESTK).

2. Material and methods

2.1. Case selection and routine microscopy

Index case was sent to one of the authors (OH) for second opinion. Later we searched several institutional archives for cases, using the key words: renal cell, papillary, stroma-rich, sarcomatoid-like, MESTK-like, and spindle cell. The final review and case selection for the study was carried out by 2 pathologists (JR and OH) resulting in inclusion of 6 cases meeting the study criteria. Clinicopathologic and follow-up data were collected using the available medical records from the participating institutions. The tissue was fixed in 4% formalin, embedded in paraffin using routine procedures. 2 um thin sections were cut and stained with hematoxylin and eosin.

2.2. Immunohistochemistry

All immunohistochemistry (IHC) stains except for PBRM1 were performed in one laboratory (University Hospital Plzen), using a Ventana Benchmark XT automated stainer (Ventana Medical System, Inc., Tucson, AZ, USA). The following primary antibodies were used: CK7 (OV-TL12/30, monoclonal, DakoCytomation, 1:200), CK20 (M7019, monoclonal, DakoCytomation, 1:100), alpha-methylacyl-CoA-racemase (AMACR) (P504S, monoclonal, Zeta, Sierra Madre, CA, 1:50), vimentin (D9, monoclonal, NeoMarkers, Westinghouse, CA, 1:1000), Ki67 (MIB1, monoclonal, Dako, Glostrup, Denmark, 1:1000), anti-melanosome (HMB45, monoclonal, DakoCytomation, 1:200), TFE3 (polyclonal, Abcam, Cambridge, UK, 1:100), desmin (D33, monoclonal, DakoCytomation, 1:2500), actin S (1A4, Cell Marque, Rocklin, CA, RTU), CD34 (QBEnd-10, monoclonal, Dako, 1:100) and fumarate hydratase (J13, monoclonal, Santa Cruz, Dallas, TX, 1:3000). PBRM1 was stained in the Pathology Department, University Hospital Erlangen, Germany using a fully automated system ("Benchmark XT System", Ventana Medical Systems Inc., 1910 Innovation Park Drive, Tucson, Arizona, USA) and a primary anti-PBRM1 monoclonal antibody retrieved from Atlas Antibodies AB, SE-168 69 Bromma, Sweden (clone CLO331, dilution, 1: 50). The primary antibodies were visualized using a supersensitive streptavidin-biotin-peroxidase complex (BioGenex). Internal biotin was blocked by standard protocol used by Ventana Benchmark XT automated stainer (hydrogen peroxide based). Appropriate positive and negative controls were also used. The immunohistochemical evaluation was based on the staining percentage of cells: focal positive < 50%, diffuse positive > 50%, negative (−) 0%.

2.3. DNA extraction

Tumor areas of the formalin-fixed paraffin-embedded (FFPE) samples were determined using hematoxylin-eosin stained slides and macro dissected. DNA from FFPE tumor tissue was extracted using QIAsymphony DNA Mini Kit (Qiagen, Hilden, Germany) on an automated extraction system (QIAsymphony SP; Qiagen) according to manufacturer's supplementary protocol for FFPE samples. Concentration and purity of isolated DNA were measured using NanoDrop ND-1000 and DNA integrity was examined by amplification of control genes in a multiplex polymerase chain reaction (PCR). Only samples that were able to produce at least 400 bp long amplicons were used for low pass whole genome sequencing.

2.4. Low pass whole genome sequencing

SurePlex DNA amplification system (Illumina, San Diego, CA) was used to generate DNA template from tumor samples. Amplification is highly representative, which makes the resulting product suitable for copy number variation detection. The library of all samples was prepared using Nextera DNA Sample Prep Kit (Illumina, San Diego, CA) and was sequenced on MiSeq sequencer, copy-number variant analysis was performed using BlueFuse Multi software with the Veriseq plugin (Illumina, San Diego, CA). Following quality control filters for valid samples were set: minimum 1 million reads per sample, average quality score and average alignment score > 30, and overall noise < 0,3. Thresholds for CNV calling were set based on a group of samples with known CNVs, that were validated using array CGH and fluorescence in-situ hybridization. The percentage of tumor in the DNA sample was considered, when calling the lower frequency CNVs and thresholds for CNVs were set individually for each case typically the copy number was 1.5 for loss and 2.5 for gain. CNVs spanning less than the whole length of a chromosome arm were not called. Selected CNVs were confirmed by FISH as described previously [9]. The more complex changes are written out in the table description. Gonosomes were excluded from the analysis. CNV detection using low pass whole genome sequencing was proven to produce similar results as in fresh frozen tissue [10].

2.5. Targeted sequencing

The DNA part of TruSight Tumor 170 kit (Illumina) was used to analyze DNA mutations in CDKN2A, BAP1, and MET genes. The quality control (QC) of the input DNA was performed using Infinium HD FFPE QC Kit (Illumina), only samples with a Ct value < 5 were used for analysis. Library preparation was performed according to manufacturer's instructions and the libraries were sequenced on NextSeq 500. The quality of resulting data was controlled for median insert size (larger than 79 base pairs) and the percentage of bases, covered > 100× had to be at least 95%. Additionally, regions of interest were checked for minimal coverage of 100×. The variants were called using dedicated app for TruSight Tumor 170 kit, and then annotated and filtered using Variant Interpreter both on Illumina's cloud portal Basespace. The filters kept only non-synonymous variants that passed variant QC, had allelic frequency > 0.05, and had population frequency from ExAC database < 0.01. The remaining subset of variants was checked visually, and suspected artefactual variants were excluded.

3. Results

Six patients were included in this study. Detailed clinical data with follow up were available for 4 patients (Table 1). All patients were male with age range 44 to 98 years (mean 65.3, median 65.5 years). Tumor size ranged from 2.4–11.4 cm (mean 5.8 median 4.5 cm). Pathologic stage was pT1 in 3 cases (case 1, 5, and 6), pT2 in 1 (case 4), and pT3 in 2 cases (case 2 and 3). One patient initially presented with regional lymph node metastasis (case 4). Unfortunately, no further information

Table 1
Clinicopathological data.

Case no.	Sex	Age (years)	Tumor size-diameter (cm)	Stage	Grade	F/U time (months)	F/U
1	M	72	2.9	pT1a	2	12	AD[a]
2	M	44	6	pT3, No	2	96	AWD
3	M	98	9	pT3	3	LE	LE
4	M	47	11.4	pT2, N1	3	LE	LE
5	M	59	2.4	pT1a	2	60	AWD
6	M	72	3	pT1a	2	3	AWD

M, Male; Grade, according to the WHO/ISUP grading system; F/U, follow up; LE, Lost of evidence; AWD, Alive without evidence of disease; AD, Alive with disease; p TNM according to the 8th Edition, AJCC Staging Manual 2017.
[a] Uncertain findings by ultrasonography-suspect recurrence.

about clinical course was available for this particular patient.

Follow up data were available (for 4 patients), ranging from 3 to 96 months (mean 42.75, median 36 months). No records concerning aggressive behavior were found in 3 patients (case 2, 5 and 6). In one patient (case 1) ultrasonographic examination revealed suspicious residual lesion in the area of previous surgery. However, no biopsy was performed to further verify this finding.

Main morphologic characteristics are summarized in Table 2. All tumors were well demarcated, with one tumor demonstrating thick fibrous pseudocapsule (case 5). In two cases (case 2 and 3) renal sinus fat involvement by the tumor was documented. In 1 case (Case 3) lymphovascular invasion was also noted. The architecture was papillary and tubulopapillary (Fig. 1A+B). Micropapillation was detected in 5/6 cases (at least focally) (Fig. 2). However, true prominent micropapillae were not recognized. Papillae were lined by cuboidal to cylindrical neoplastic cells, with variable amount of eosinophilic cytoplasm (Fig. 3). Case 4 showed mostly pale cytoplasm, however no typical clear cell areas were identified. Nuclear grade was 2 in four cases (cases 1, 2, 5 and 6), while the remaining two cases showed grade 3 (case 3 and 4), according to Fuhrman (ISUP/WHO modification).

Necrosis in epithelial component was present in 2 cases (case 4 and 5). Mitotic activity was relatively low: no mitoses were found in 2 cases (case 2 and 5), 1 mitosis/10 HPF in 1 case (case 1) and up to 5 mitoses/10 HPF in 2 cases (case 3 and 4). No atypical mitotic figures were noted. Stroma was composed of uniform spindle cells resembling those of the Müllerian type stroma. The density of the spindle cell elements was variable, ranging from weak to dense (Fig. 4A+B). No smooth muscle differentiation was found. Foamy macrophages and psammoma bodies were present in all but one case (case 2). No necrosis or mesenchymal heterologous elements were found. Mitotic activity was absent.

Results of immunohistochemical examination are summarized in Tables 3A and 3B, separately for epithelial and stromal component. All tumors showed uniform strong and diffuse positivity for CK7, AMACR, and vimentin in the epithelial component (Fig. 5A+B). HMB45, TFE3, desmin, CD34, and actin were negative in the epithelial cells. Fumarate hydratase (FH) staining was retained in all cases. PBRM1 was positive (retained) in 5/6 cases (Fig. 6). In one case, both epithelial and stromal components were negative, as well as adjacent non-neoplastic tissues. This case was interpreted as non-analyzable. Stromal component was invariably positive for actin and vimentin. CD34 was positive in vessel wall within the stromal component, while stromal cells were negative. Estrogen and progesterone receptors were negative in both epithelial and stromal components. The Ki67 proliferation index was low in epithelial component and nearly absent in stromal component.

Numerical chromosomal aberration pattern of the analyzed cases is summarized in Table 4. Five cases were analyzable, copy number variation pattern was variable (multiple gains and losses of whole chromosomes or chromosomal arms were detected). In one case (case 4) multiple losses and gains were detected. Gain of chromosome 12 and loss of chromosome 18 were documented in 1 case (case 2). Multiple losses were documented in 1 case (case 5). One case had no detectable chromosomal numerical aberrations (case 1). No *CDKN2A*, *BAP1*, or *MET* gene abnormalities were found (Table 4).

4. Discussion

PRCC is a group of kidney tumors characterized mostly by papillary and/or tubulopapillary architecture. Type 1 PRCC is considered to represent a distinct entity with uniform characteristic morphologic, immunohistochemical, and molecular genetic features. The so-called type 2 is defined according to the WHO 2016 by presence of epithelial cells with abundant eosinophilic cytoplasm, high nuclear grade and nuclear pseudostratification [1]. However, immunohistochemical profile of so-called type 2 is rather variable as well as the molecular genetic profile. In fact, recent studies have shown that the so-called type 2 PRCC represents several distinct variants or subtypes of RCC sharing predominantly a papillary pattern [11,12].

Several studies describing unusual morphologic forms of PRCC, together with immunohistochemical and genetic profiles have been recently published in the literature. Such tumors significantly differ from type 1 and type 2 PRCC. The most frequently discussed variant is oncocytic PRCC (OPRCC), which is one of the provisional entities in the latest WHO classification [1]. OPRCC is relatively poorly understood entity without a precise or reproducible definition. In addition to OPRCC, a number of other PRCC variants have been documented, including Warthin-like PRCC, solid PRCC, biphasic squamoid PRCC, "mucin" secreting PRCC, PRCCs with clear cells, and papillary renal neoplasm with reverse polarity [3,5-8,13,14]. Immunohistochemical profile and molecular genetic features of above-mentioned variants of PRCC are variable and mostly are not consistent with type 1 or type 2 PRCC. Such variants represent a highly heterogeneous group of tumors, which share papillary or tubulopapillary architecture. Cytological features are different as well as immunohistochemical profile. Further, it is now evident that previous known historic "landmark" of chromosomal

Table 2
Morphological data.

Case	ISUP grade	Architectural pattern (a)	Foamy macrophages (b)	Psammoma bodies (c)	Necrosis (d)	Capsule	Stromal cellularity (e)	Type of epithelial cells (f)	Mitoses stroma	Mitoses epithelium
1	2	P	+	+	−	−	+	Cb	1/10HPF	1/10 HPF
2	2	P	+	−	−	−	++	Cb	−	−
3	3	T-P	+++	++	−	−	+++	Cl	−	5/10 HPF
4	3	T-P	++	++	+F	−	++	Cl	−	5/10HPF
5	2	P	++	+	+	+	+	Cl	−	−
6	2	P	+	−	+F	+	+	Cl	−	1/10HPF

a) architectural pattern: P-papillary, T-P -tubulo-papillary; b) foamy macrophages were assessed as absent (−), sparse (+), moderate (++), prominent (+++), c) psammoma bodies were assessed as absent (−), sparse (+), moderate (++), prominent (+++); d) necrosis was assessed as + (present), − (absent) F- focal; e) stromal cellularity was assessed as: sparse (+), moderate (++), prominent (+++); f) type of epithelial cells lining papillae were assessed as Cl- columnar, Cb-cuboidal; HPF high power field, absent mitoses (−).

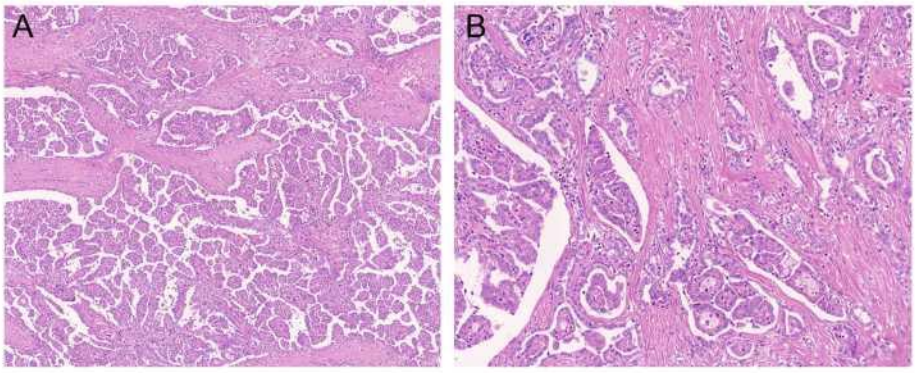

Fig. 1. The architecture was papillary (A) and tubulopapillary (B) in all cases.

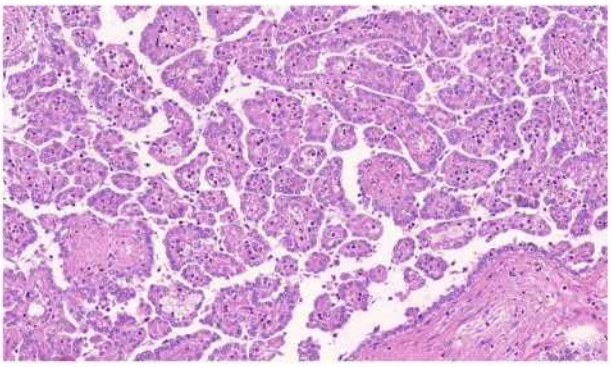

Fig. 2. Micropapillation was at least focally detected in majority of cases. No true prominent micropapillary areas were found.

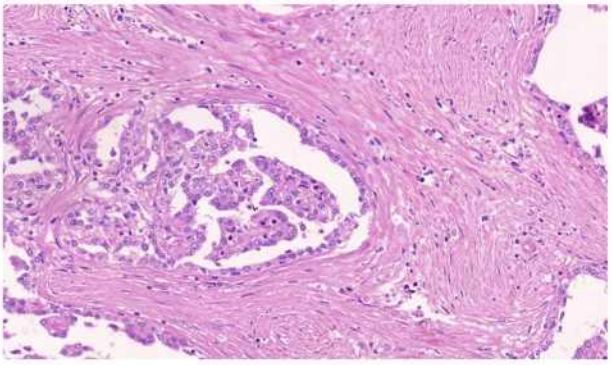

Fig. 3. Papillae or tubules were lined by cuboidal to cylindrical cells with variable amount of eosinophilic cytoplasm.

copy number variation pattern for PRCC - trisomy/polysomy of chromosomes 7 and 17 - is not a consistent finding in the ever expanding heterogeneous "PRCC" group [15]. In fact, it is not surprising that within such a heterogeneous group of tumors, all being lumped under the PRCC diagnostic umbrella, new variants/subtypes are still emerging.

Müllerian type stroma is a feature typically found in mixed epithelial and stromal tumor of the kidney (MESTK) [1,16-18]. Less prominent Müllerian type stroma is seen in subepithelial zones of cysts within so-called angiomyolipoma with epithelial cyst (AMLEC) [19]. Müllerian stroma is characterized by a loose to dense population of bland spindle cells, which immunohistochemically express estrogen and/or progesterone receptors. Similar type of stroma can also be found in other extra-renal tumors such as mucinous cystic neoplasm of the pancreas and mucinous cystadenoma of the liver [20]. Focal luteinization and corpus albicans-like changes may be seen, regardless of the tumor location, as a reactive change secondary to damaged stroma [21].

Tumors in our series are distinct owing to the architecture and the presence of prominent stroma resembling Müllerian type stroma. However, in a closer look, stroma in our cases differs in many aspects from stroma known as Müllerian type stroma. The stromal component in our cases was rather cellular despite the fact that it was slightly variable between the cases (dense to loose cellularity), but overall showed low grade morphologic features and was relatively uniform. No conspicuous mitotic activity, necrosis, or sarcomatous differentiation was documented. Also, epithelial component lacked features typically seen in MESTK. The neoplastic cells were relatively uniform, cuboidal to cylindrical. No intracytoplasmic vacuoles or ciliated epithelium were identified within our series. There were no true Müllerian structures (within stromal and epithelial component), which was further supported by immunohistochemistry.

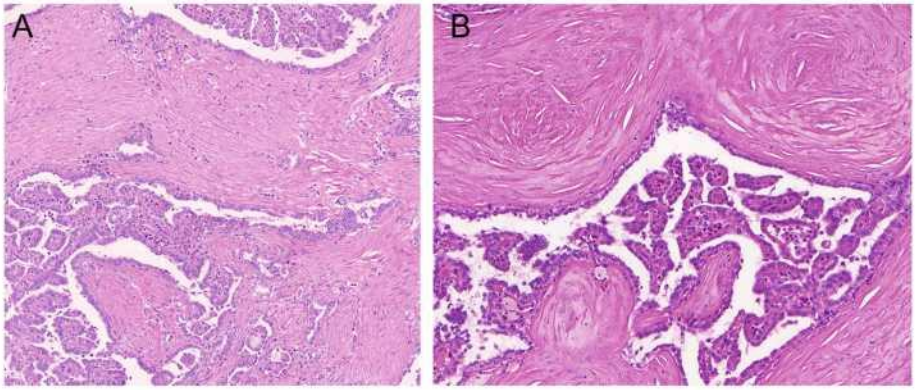

Fig. 4. Stroma was composed of uniform spindle cells resembling those in Müllerian type of stroma (panel A). Density of spindle cell elements was variable, ranged from weak to dense. Panel B shows weakly cellular parts of stroma.

Table 3A
Results of immunohistochemical examination-epithelial component.

Case	CK7	AMACR	vim	TFE3	HMB45	Desmin	CD34	Ki67	Actin	FH	ER	PR	PBMR1
1	+++	++++	+++	–	–	–	–	2–4/HPF	–	ret	–	–	ret
2	+++	+++	+++	–	–	–	–	0–2/HPF	–	ret	–	–	ret
3	++/foc +++	+++	+++	–	–	–	–	4–8/HPF	–	ret	–	–	ret
4	++	+++	++	–	–	–	–	0–1/HPF	–	ret	–	–	ret
5	+++	+++	+++	–	–	–	–	4–7/HPF	–	ret	–	–	NA
6	+++	+++	+++	–	–	–	–	0–4/HPF	–	ret	–	–	ret

Abbreviations: foc, focally positive; ret, expression retained; + weakly positive, ++ moderately positive, +++ strongly positive; vim, vimentin; FH, fumarate hydratase; ER, estrogen receptor; PR, progesterone receptor; NA, not analyzable; HPF, High Power Field.

Table 3B
Results of immunohistochemical examination-stromal component.

Case	CK7	AMACR	vim	TFE3	HMB45	desmin	CD34	Ki67	Actin	FH	ER	PR	PBMR1
1	–	–	foc +++[a]	–	–	–	foc +++[a]	0–1/HPF	++	ret	–	–	ret
2	–	–	foc +++[a]	–	–	–	foc +++[a]	0–1/HPF	++	ret	–	–	ret
3			+++	–	–	–	foc +++[a]	0–2/HPF	+++	ret	–	–	ret
4	–	–	++/foc +++[a]	–	–	–	foc +++[a]	0–1/HPF	+++	ret	–	–	ret
5	–	–	foc +++[a]	–	–	–	foc +++[a]	0–1/HPF	+++	ret	–	–	NA
6	–	–	foc ++	–	–	–	foc +++[a]	0	+++	ret	–	–	ret

Abbreviations: foc, focally positive; ret., + weakly positive, ++ moderately positive, +++ strongly positive, ret expression retained, vim vimentin, FH fumarate hydratase, ER estrogen receptor, PR progesterone receptor, NA not analyzable, HPF, High Power Field.
[a] Vessels.

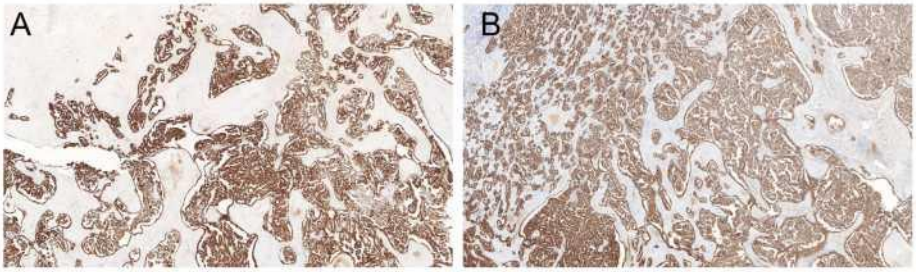

Fig. 5. Epithelial component was positive diffusely for CK7 (A) and AMACR (B).

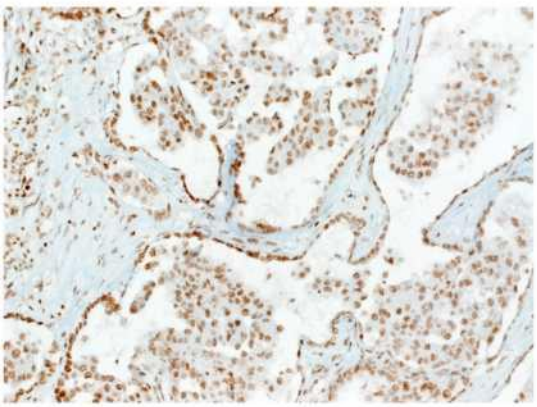

Fig. 6. Immunoreactivity for PBMR1 was retained in all analyzable cases.

Immunohistochemical profile of tumors in current series did not substantially differ (despite heterogeneity of PRCC as a group) from majority of PRCC variants. Co-expression of AMACR, CK7, and vimentin is considered as a relatively characteristic immunoprofile for PRCC. Immunohistochemical examination failed to confirm estrogen or progesterone receptor positivity both within stromal and epithelial components.

Morphologic features along with immunohistochemical profile strongly suggest the diagnosis of an unusual variant of PRCC.

At molecular genetic level, we were able to successfully analyze

Table 4
Summary of genetic analyses.

Case	Gains (chromosome)	Losses (chromosome)	*CDKN2A, BAP1, MET* mutations
1	None	None	Negative
2	12	18	Negative
3	16	None	Negative
4	1q,3q,12,17	1p,2q,3p, 9, 11q,13,21,22	Negative
5	None	6,9p,15q,22	Negative
6	NP	NP	Negative

Abbreviation: NP, not performed.

CNV pattern in 5/6 cases. CNV pattern was rather variable with multiple losses and gains. Polysomy of chromosomes 7 and 17 was detected, however not in a "characteristic" combination (i.e. trisomy or polysomy of both chromosome 7 and 17) seen in type 1 PRCC. This further supports the fact that trisomy/polysomy of chromosomes 7 and 17 is not a constant genetic feature in majority of PRCC subtypes [12,15].

Recent molecular studies confirmed that type 1 PRCC is a distinct entity, while type 2 PRCC is rather a heterogeneous group of renal tumors with predominantly papillary architecture. Type 1 PRCC is characterized by altered *MET* gene or increased chromosome 7 and 17 copy number. The Cancer Genomic Atlas Network study on the so-called type 2, and a group of unclassified PRCCs showed a heterogeneous genetic profile in 3 clusters: 1) *CDKN2A* altered PRCCs, 2)

Table 5
Differential diagnosis.

	Architecture	Epithelial component	Stroma	Immunohistochemistry	Molecular genetic features	Biological behavior
PRCC with MESTK-like stroma	P/T-P	Low to high grade, clear to eosinophilic cytoplasm	Fibroleiomyomatous	CK7, AMACR, vim (+) ER, PR (−)	Variable	Malignant
MESTK	T-C/S	Flat, hobnailed, cuboidal, columnar, urothelial-like, clear cell	Fibroleiomyomatous and true Müllerian stroma	ER, PR (+)	No specific alteration	Indolent
Sarcomatoid RCC	Variable	High-grade epithelial cells with clear to eosinophilic cytoplasm (if any epithelial elements present)	Malignant, high grade spindle cells, possible heterogeneous mesenchymal differentiation	Variable cytokeratin positivity	Variable	Malignant
Clear cell papillary RCC	P/T-P	Low-grade epithelial cells with clear cytoplasm	Fibroleiomyomatous	CK 7, CANH 9 (cup shaped pattern) (+); CD10, AMACR (−)	Lack of *VHL* gene abnormalities	Indolent
RCC with prominent leiomyomatous stroma	N/T	Low-grade epithelial cells with clear cytoplasm	Leiomyomatous	CANH 9, vim (+); CK 7, AMACR, CD10 variable(+)	Lack of *VHL* gene abnormalities Chr.7, 17 gain-variable	Indolent
AMLEC	TC/S	Benign/entrapped epithelium	Leiomyomatous and true Müllerian stroma	ER, PR,CD10, HMB-45, Melan-A(+)	Possible mutation in *TSC 1/ TSC 2*	Indolent
FH deficient RCC	P/TP, variable	Eosinophilic cytoplasm, high grade CMV inclusion-like deep red nucleoli	Fibrous, hyalinized	FH (−), 2SC (−) CK7 (−)	Mutation/LOH of *FH* gene	Malignant, aggressive
TCEB1 mutated renal cell carcinoma	S/T	Low-grade epithelial cells with clear cytoplasm	Fibromuscular	CANH 9(+), CK7 freq(+)	Mutations in *TCEB1* gene, lack of *VHL* gene abnormalities	Indolent

Abbreviations: RCC, renal cell carcinoma; PRCC, papillary renal cell carcinoma; MESTK, mixed epithelial and stromal tumor; AMLEC, angiomyolipoma with epithelioid cyst; FH, fumarate hydratase; P-papillary; T-P, Tubulo-papillary; T-C, Tubulo-cystic; N, Nested; S, Solid; T, Tubular; ER estrogen receptor, PR progesterone receptor, CANH9, carbonic anhydrase 9; +, positive; −, negative; freq, frequently.

SETD2, *BAP1* and *PBRM1* mutated PRCCs, and 3) CpG Island Methylator Phenotype associated tumors [11,22].

We analyzed *CDKN2A*, *BAP1*, *MET* genes in this study, and no mutations were found in our cases. It should be noted that the above-listed molecular classification has not been fully validated, and as such it seems that our tumors were not entirely compatible with at least 2 proposed groups. *PBRM1* was analyzed using immunohistochemistry. All analyzable cases (5/6) showed retained expression which is a strong surrogate for absence of inactivating or truncating *PBRM1* mutations. This suggests that it is unlikely that MESTK-like PRCC belongs to *BAP1* and *PBRM1* mutated PRCC subgroup proposed by Saleeb et al. [11].

From differential diagnostic point of view (Table 5), sarcomatoid differentiation within RCC should be taken into consideration.

"Sarcomatoid RCC" could be a diagnostic pitfall particularly on limited material, however clinical presentation and imaging studies may assist in resolving the matter. Patients with sarcomatoid RCC often present at an advanced stage with large tumor with infiltrative borders and necrosis. Morphologically, growth pattern is usually mosaic of original epithelial RCC component and solid sarcomatoid areas. Mitotic activity is usually brisk with atypical mitotic figures, as well as prominent necrotic foci. Heterologous mesenchymal neoplastic elements such as differentiation toward osteosarcoma, chondrosarcoma or other types of sarcomas can also be found [26]. Immunohistochemically, positivity of sarcomatoid spindle cell component for keratin cocktail AE1/AE3 or OSCAR, Cam5.2 or EMA can vary from focal to diffuse. Adequate sampling and basic immunohistochemical examination usually help to resolve the problematic differential diagnosis. The so-called RCC with prominent leiomyomatous stroma and/or RCC with *TFEB1* mutation should also be considered in the differential diagnosis, given prominent voluminous stroma an essential part of morphologic picture of such tumors [23-25]. However, the stromal component is less cellular in these tumors, compared to our cases. Moreover, stroma in RCC with prominent leiomyomatous stroma and/or RCC with *TFEB1* mutation is voluminous and rather fibroleiomyomatous, frequently with conspicuous leiomyomatous component. The architectural pattern in our cases is much complex. Further, the epithelial component of both RCC with prominent leiomyomatous stroma and *TFEB1*mutated RCC is nearly identical to low-grade clear cell RCC (arranged in nested/tubular pattern with clear voluminous cytoplasm) [23-25]. Papillary pattern is not documented in these RCCs. Low-grade spindle cell elements were described within clear cell RCC. However these cells were obviously epithelial origin and they did not represent stromal component [26]. Clear cell papillary RCC is another RCC with more or less prominent fibroleiomyomatous stroma that can enter into the differential diagnosis. Clear cell papillary RCC was first described as renal angioleiomyomatous tumor (RAT), owing to the presence of prominent leiomyomatous stroma, bland epithelial component and benign clinical course [27-28]. Subsequently, discussion about the relation of RAT and clear cell papillary renal cell carcinoma were held, which led to reserve the term RAT for cases with significant amount of stroma, while clear cell papillary RCC for cases with less prominent stroma [29]. Finally, both subtypes (stroma rich and cases with less prominent stroma) were proposed to be unified under –the term clear cell papillary RCC [1,30]. Stroma in clear cell papillary RCC is different in many aspects from the cases described herein. In clear cell papillary RCC, the stroma is mostly leiomyomatous, less cellular, and mostly without conspicuous spindle cell population. Further, the epithelial component of clear cell papillary RCC is different from our cases. Clear cell papillary RCC is composed of clear cell elements, different from pale eosinophilic cells in our tumors. Moreover, epithelial cells are arranged mostly in tubulopapillary pattern, wrapped in a delicate capillary network [30,31]. No capillary network around tubulary or tubulopapillary structures was noted, no elongated tubulary spaces (so-called "shark" smiles) or epithelial lining with nuclei orientated away from the basement membrane (so-called" piano keys") were noticed in any case in the current series. All such features are typical but not specific for clear cell papillary RCC.

In summary, we described a series of 6 distinct and uniform PRCCs with MESTK-like stroma. Further investigations of morphology and underlying molecular alterations will help us properly categorize subgroups within PRCC and, hence, may result in adequate clinical management and the development of more effective forms of therapy.

Funding

The study was supported by the Charles University Research Fund (project number Q39) and by the project Institutional Research Fund of University Hospital Plzen (Faculty Hospital in Plzen- FNPl 00669806).

Declaration of competing interest

All authors declare no conflict of interest.

References

[1] Moch H, Humphrey PA, Ulbright TM, R VE. WHO classification of tumours of the urinary system and male genital organs. IARC Lyon; 2016.
[2] Hes O, Brunelli M, Michal M, Cossu Rocca P, Hora M, Chilosi M, et al. Oncocytic papillary renal cell carcinoma: a clinicopathologic, immunohistochemical, ultrastructural, and interphase cytogenetic study of 12 cases. Ann Diagn Pathol 2006 Jun;10(3):133–9. (PubMed PMID: 16730306).
[3] Hes O, Condom Mundo E, Peckova K, Lopez JI, Martinek P, Vanecek T, et al. Biphasic squamoid alveolar renal cell carcinoma: a distinctive subtype of papillary renal cell carcinoma? Am J Surg Pathol 2016 May;40(5):664–75. (PubMed PMID: 26999503).
[4] Mantoan Padilha M, Billis A, Allende D, Zhou M, Magi-Galluzzi C. Metanephric adenoma and solid variant of papillary renal cell carcinoma: common and distinctive features. Histopathology 2013 Feb 4;62(6):941–53.
[5] Ulamec M, Skenderi F, Trpkov K, Kruslin B, Vranic S, Bulimbasic S, et al. Solid papillary renal cell carcinoma: clinicopathologic, morphologic, and immunohistochemical analysis of 10 cases and review of the literature. Ann Diagn Pathol 2016 Aug;23:51–7. (PubMed PMID: 27209513).
[6] Pivovarcikova K, Peckova K, Martinek P, Montiel DP, Kalusova K, Pitra T, et al. "Mucin"-secreting papillary renal cell carcinoma: clinicopathological, immunohistochemical, and molecular genetic analysis of seven cases. Virchows Arch 2016 Jul;469(1):71–80. (PubMed PMID: 27072821).
[7] Skenderi F, Ulamec M, Vanecek T, Martinek P, Alaghehbandan R, Foix MP, et al. Warthin-like papillary renal cell carcinoma: clinicopathologic, morphologic, immunohistochemical and molecular genetic analysis of 11 cases. Ann Diagn Pathol 2017 Apr;27:48–56. (PubMed PMID: 28325361).
[8] Al-Obaidy KI, Eble JN, Cheng L, Williamson SR, Sakr WA, Gupta N, et al. Papillary renal neoplasm with reverse polarity: a morphologic, immunohistochemical, and molecular study. Am J Surg Pathol 2019 Aug;43(8):1099–111. (PubMed PMID: 31135486).
[9] Sperga M, Martinek P, Vanecek T, Grossmann P, Bauleth K, Perez-Montiel D, et al. Chromophobe renal cell carcinoma—chromosomal aberration variability and its relation to Paner grading system: an array CGH and FISH analysis of 37 cases. Virchows Arch 2013 Oct;463(4):563–73. (PubMed PMID: 23913167).
[10] Munchel S, Hoang Y, Zhao Y, Cottrell J, Klotzle B, Godwin AK, et al. Targeted or whole genome sequencing of formalin fixed tissue samples: potential applications in cancer genomics. Oncotarget 2015 Sep 22;6(28):25943–61. (PubMed PMID: 26305677. Pubmed Central PMCID: 4694877).
[11] Saleeb RM, Brimo F, Farag M, Rompre-Brodeur A, Rotondo F, Beharry V, et al. Toward biological subtyping of papillary renal cell carcinoma with clinical implications through histologic, immunohistochemical, and molecular analysis. Am J Surg Pathol 2017 Dec;41(12):1618–29. (PubMed PMID: 28984673).
[12] Akhtar M, Al-Bozom IA, Al HT. Papillary renal cell carcinoma (PRCC): an update. Adv Anat Pathol 2019 Mar;26(2):124–32. (PubMed PMID: 30507616).
[13] Trpkov K, Athanazio D, Magi-Galluzzi C, Yilmaz H, Clouston D, Agaimy A, et al. Biphasic papillary renal cell carcinoma is a rare morphological variant with frequent multifocality: a study of 28 cases. Histopathology 2018 Apr;72(5):777–85. (PubMed PMID: 29119638).
[14] Petersson F, Sperga M, Bulimbasic S, Martinek P, Svajdler M, Kuroda N, et al. Foamy cell (hibernoma-like) change is a rare histopathological feature in renal cell carcinoma. Virchows Arch 2014 Aug;465(2):215–24. (PubMed PMID: 24903672).
[15] Pitra T, Pivovarcikova K, Alaghehbandan R, Hes O. Chromosomal numerical aberration pattern in papillary renal cell carcinoma: review article. Ann Diagn Pathol 2019 Jun;40:189–99. (PubMed PMID: 29454759).
[16] Michal M, Syrucek M. Benign mixed epithelial and stromal tumor of the kidney. Pathol Res Pract 1998;194(6):445–8. (PubMed PMID: 9689654).
[17] Michal M. Benign mixed epithelial and stromal tumor of the kidney. Pathol Res Pract 2000;196(4):275–6. (PubMed PMID: 10782473).
[18] Michal M, Hes O, Bisceglia M, Simpson RH, Spagnolo DV, Parma A, et al. Mixed epithelial and stromal tumors of the kidney. A report of 22 cases. Virchows Arch 2004 Oct;445(4):359–67. (PubMed PMID: 15322873).
[19] Fine SW, Reuter VE, Epstein JI, Argani P. Angiomyolipoma with epithelial cysts (AMLEC): a distinct cystic variant of angiomyolipoma. Am J Surg Pathol 2006 May;30(5):593–9. (PubMed PMID: 16699313).
[20] Quigley B, Reid MD, Pehlivanoglu B, Squires 3rd MH, Maithel S, Xue Y, et al. Hepatobiliary mucinous cystic neoplasms with ovarian type stroma (so-called "hepatobiliary cystadenoma/cystadenocarcinoma"): clinicopathologic analysis of 36 cases illustrates rarity of carcinomatous change. Am J Surg Pathol 2018 Jan;42(1):95–102. (PubMed PMID: 29016404).
[21] Michal M, Hes O. Corpora albicantia-like bodies in extraovarian lesions. Int J Surg Pathol 2004 Jul;12(3):298. (PubMed PMID: 15306946).
[22] Cancer Genome Atlas Research N, Linehan WM, Spellman PT, Ricketts CJ, Creighton CJ, Fei SS, et al. Comprehensive molecular characterization of papillary renal-cell carcinoma. N Engl J Med 2016 Jan 14;374(2):135–45. (PubMed PMID: 26536169. Pubmed Central PMCID: 4775252).
[23] Peckova K, Grossmann P, Bulimbasic S, Sperga M, Perez Montiel D, Daum O, et al. Renal cell carcinoma with leiomyomatous stroma—further immunohistochemical and molecular genetic characteristics of unusual entity. Ann Diagn Pathol 2014 Oct;18(5):291–6. (PubMed PMID: 25175809).
[24] Petersson F, Martinek P, Vanecek T, Pivovarcikova K, Peckova K, Ondic O, et al. Renal cell carcinoma with leiomyomatous stroma: a group of tumors with indistinguishable histopathologic features, but 2 distinct genetic profiles: next-generation sequencing analysis of 6 cases negative for aberrations related to the VHL gene. Appl Immunohistochem Mol Morphol 2018 Mar;26(3):192–7. (PubMed PMID: 29084058).
[25] Hakimi AA, Tickoo SK, Jacobsen A, Sarungbam J, Sfakianos JP, Sato Y, et al. TCEB1-mutated renal cell carcinoma: a distinct genomic and morphological subtype. Mod Pathol 2015 Jun;28(6):845–53. (PubMed PMID: 25676555. Pubmed Central PMCID: 4449825).
[26] Tanas Isikci O, He H, Grossmann P, Alaghehbandan R, Ulamec M, Michalova K, et al. Low-grade spindle cell proliferation in clear cell renal cell carcinoma is unlikely to be an initial step in sarcomatoid differentiation. Histopathology 2018 Apr;72(5):804–13. (PubMed PMID: 29194709).
[27] Michal M, Hes O, Havlicek F. Benign renal angiomyoadenomatous tumor: a previously unreported renal tumor. Ann Diagn Pathol 2000 Oct;4(5):311–5. (PubMed PMID: 11073338).
[28] Tickoo SK, dePeralta-Venturina MN, Harik LR, Worcester HD, Salama ME, Young AN, et al. Spectrum of epithelial neoplasms in end-stage renal disease: an experience from 66 tumor-bearing kidneys with emphasis on histologic patterns distinct from those in sporadic adult renal neoplasia. Am J Surg Pathol 2006 Feb;30(2):141–53. (PubMed PMID: 16434887).
[29] Srigley JR, Delahunt B, Eble JN, Egevad L, Epstein JI, Grignon D, et al. The International Society of Urological Pathology (ISUP) Vancouver classification of renal neoplasia. Am J Surg Pathol 2013 Oct;37(10):1469–89. (PubMed PMID: 24025519).
[30] Hes O, Comperat EM, Rioux-Leclercq N. Clear cell papillary renal cell carcinoma, renal angiomyoadenomatous tumor, and renal cell carcinoma with leiomyomatous stroma relationship of 3 types of renal tumors: a review. Ann Diagn Pathol 2016 Apr;21:59–64. (PubMed PMID: 26897641).
[31] Michal M, Hes O, Nemcova J, Sima R, Kuroda N, Bulimbasic S, et al. Renal angiomyoadenomatous tumor: morphologic, immunohistochemical, and molecular genetic study of a distinct entity. Virchows Arch 2009 Jan;454(1):89–99. (PubMed PMID: 19020896).

1.3 Karcinom ledviny asociovaný se syndromem familiární leiomyomatózy a karcinomem ledvin/fumarát hydratáza deficientní renální karcinom

(komentář 3 publikací)

Programmed death-1 (PD-1) receptor/PD-1 ligand (PD-L1) expression in fumarate hydratase-deficient renal cell carcinoma.
Alaghehbandan R, Stehlik J, Trpkov K, Magi-Galluzzi C, Condom Mundo E, Pane Foix M, Berney D, Sibony M, Suster S, Agaimy A, Montiel DP, Pivovarcikova K, Michalova K, Daum O, Ondic O, Rotterova P, Dusek M, Hora M, Michal M, Hes O.
Ann Diagn Pathol. 2017 Aug;29:17-22.

Fumarate hydratase deficient renal cell carcinoma: Chromosomal numerical aberration analysis of 12 cases.
Pivovarcikova K, Martinek P, Grossmann P, Trpkov K, Alaghehbandan R, Magi-Galluzzi C, Pane Foix M, Condom Mundo E, Berney D, Gill A, Rychly B, Michalova K, Rogala J, Pitra T, Micsik T, Polivka J, Hora M, Tanas Isikci O, Skalova S, Mareckova J, Michal M, Hes O.
Ann Diagn Pathol. 2019 Feb 10;39:63-68

Fumarát hydratáza deficientní renální karcinom a jemu podobný renální karcinom: Komparativní studie 23 geneticky testovaných případů.
Pivovarčíková K, Martínek P, Trpkov K, Alaghehbandan R, Magi-Galluzzi C, Mundo EC, Berney D, Suster S, Gill A, Rychlý B, Michalová K, Pitra T, Hora M, Michal M, Hes O.
Cesk Patol 2019;55(4):244-249

Fumarát hydratáza deficientní renální karcinom (FHRCC) je v současné době preferovaný název pro tumor ve WHO 2016 [24] označený pojmem renální karcinom asociovaný s hereditární leiomyomatozou a renálním karcinomem (hereditary leiomyomatosis and renal cell carcinoma-associated renal cell carcinoma/HLRCC) [45]. Jedná se o renální neoplázii známou pro svou vysokou agresivitu a možnou syndromovou a hereditární asociaci. Oproti původním dohadům je však evidentní, že nádor se u pacientů může objevovat i sporadicky a bez syndromové asociace, proto je dnes spíše upřednostňován právě název FHRCC.

Jednotka je definována přítomností alterace genu pro *fumarát hydratázu (FH)* [42, 49] a pouze průkaz této genetické změny je absolutním kritériem pro stanovení diagnózy - vždy je tak nutné provést molekulárně genetické vyšetření s průkazem abnormalit genu *FH* (chromozom 1q43). Ačkoli v posledních letech v různých studiích proběhly četné pokusy morfologicky [23] a imunohistochemicky [43] definovat tyto nádory a nastavit diagnostický algoritmus tak, aby co největší množství FHRCC bylo možno diagnostikovat i bez použití genetických metod, všechny studie nakonec vedly k identickým závěrům – bez genetického průkazu přítomnosti/absence *FH* abnormalit diagnózu FHRCC nelze spolehlivě stanovit ani vyloučit.

V současné době víme, že morfologické spektrum této neoplázie je široké, dříve typicky udávaný morfologický znak (přítomnost objemných jader s prominentními tmavě červenými „inklusními“ jadérky s perinukleolárním projasněním) sice bývá přítomen, může však být přítomen jen fokálně a může se též vyskytovat i u jiných renálních neoplázií,

nabízejících se v diferenciální diagnóze. V úvodu velké naděje vkládané do imunohistochemického barvení protilátkou proti FH (výpadek exprese v tumoru a pozitivní vnitřní kontrola v přilehlé non-neoplastické tkáni) se též postupně ukázaly jako liché - bylo prokázáno, že barvení může vykazovat vzácně ztrátu exprese i u jiných nádorů než u FHRCC [31] (možná jako následek fixačních artefaktů) a zároveň bylo zjištěno, že ne všechny FHRCC mají výpadek imunohistochemického barvení FH (některé genetické alterace v genu *FH* patrně vedou k formaci nefunkčního či inkompletního proteinu, který však poskytuje epitop pro imunohistochemickou reakci a tím pozitivitu barvení protilátkou proti FH). Další slibně se jevící marker (imunohistochemická protilátka proti 2-sukcynocysteinu/2SC) sice u FHRCC prokázal vysokou sensitivitu, ale nízkou specificitu [43]. Zároveň se jedná o protilátku, která není komerčně dostupná a její interpretace a uvedení do rutinního chodu laboratoře je vzhledem k nízké frekvenci těchto tumorů a tedy jejímu raritnímu užití velmi komplikované.

V posledních letech se však stále jasněji ukazuje, že kombinace různých morfologických vzhledů a růstových vzorců v jednou nádoru (tedy výrazná nádorová heterogenita), by mohla být klíčem k rozpoznání suspektních případů vhodných pro genetické testování *FH* [25, 31]. Je důležité aktivně pomýšlet a pátrat po této jednotce při diagnostice těžko klasifikovatelných renálních neoplázií a ani low-grade vzhled nádoru diagnózu FHRCC nevylučuje [40].

1.3.1 Programmed death-1 (PD-1) receptor/PD-1 ligand (PD-L1) expression in fumarate hydratase-deficient renal cell carcinoma

Pro účely studie bylo vybráno 13 FHRCC, u nichž byla vyšetřena expresse PD1 a PD-L1. Nádory byly nabarveny imunohistochemickou protilátkou PD-1 a PD-L1, analyzována byla reaktivita v nádorových buňkách a v tumor infiltrujících lymfocytech (TILs). Přítomnost PD-1/PD-L1 mRNA byla dále vyšetřena pomocí qPCR.

Imunohistochemicky, všech 13 FHRCC bylo PD-1 negativní v buňkách nádoru. Tumor infiltrující lymfocyty reagovaly pozitivně v PD-1 v 1/13 FHRCC, slabě pozitivně v 3/13 a 9/13 FHRCC bylo negativní. Exprese PD-L1 v nádorových buňkách byla zastižena ve 2/13 tumorů, slabě v 7/13 FHRCC a kompletně negativní bylo barvení v 4/13 případů. V imunohistochemickém průkazu PD-L1 byly TILs slabě imunoreaktivní v 5/13 případů a negativní v 8/13 FHRCC. qPCR potvrdilo výsledky barvení PD-1 ve 3/4 pozitivních případů (PD-1 imunohistochemická pozitivita TILs) a dále prokázalo pozitivitu dalších 3 imunohisochemicky negativních případů. U 9 imunohistochemicky PD-L1 pozitivních FHRCC (pozitivita nádorových buněk), PD-L1 mRNA byla prokázána u 7/9 případů. Dále qPCR prokázalo pozitivitu i u 1 případu s imunohistochemicky negativní expresí PD-L1 v nádorových buňkách, ale slabou expresí PD-L1 v TILs.

Většina FHRCC imunohistochemicky neexprimuje PD-1/PD-L1, což bylo potvrzeno i molekulární analýzou. Exprese PD-1/PD-L1 u FHRCC by teoreticky mohla předurčovat část tumorů, které by mohly profitovat z imunoterapie. Pro definitivní závěry jsou však nutné další klinické a klinicko-patologické studie.

Annals of Diagnostic Pathology 29 (2017) 17–22

Contents lists available at ScienceDirect

Annals of Diagnostic Pathology

journal homepage: www.elsevier.com/locate/anndiagpath

Programmed death-1 (PD-1) receptor/PD-1 ligand (PD-L1) expression in fumarate hydratase-deficient renal cell carcinoma☆,☆☆,☆☆☆

Reza Alaghehbandan[a], Jan Stehlik[b], Kiril Trpkov[c], Cristina Magi-Galluzzi[d], Enric Condom Mundo[e], Maria Pane Foix[e], Daniel Berney[f], Mathilde Sibony[g], Saul Suster[h], Abbas Agaimy[i], Delia Perez Montiel[j], Kristyna Pivovarcikova[b], Kvetoslava Michalova[b], Ondrej Daum[b], Ondrej Ondic[b], Pavla Rotterova[b], Martin Dusek[b], Milan Hora[k], Michal Michal[b], Ondrej Hes[b,*]

[a] Department of Pathology, Faculty of Medicine, University of British Columbia, Royal Columbian Hospital, Vancouver, BC, Canada
[b] Department of Pathology, Charles University, Medical Faculty and Charles University Hospital Plzen, Czech Republic
[c] Calgary Laboratory Services, University of Calgary, Calgary, AB, Canada
[d] Robert J. Tomsich Pathology and Laboratory Medicine Institute, Cleveland Clinic, Cleveland, OH, USA
[e] Department of Pathology, Bellvitge Biomedical Research Institute (IDIBELL), Barcelona, Spain
[f] Bart's Cancer Center, London, United Kingdom
[g] Hospital Cochin, Paris, France
[h] Department of Pathology, Medical College Wisconsin, Milwaukee, WI, USA
[i] Department of Pathology, University Erlangen, Germany
[j] Department of Pathology, Instituto Nacional de Cancerologia, Mexico City, Mexico
[k] Department of Urology, Charles University, Medical Faculty and Charles University Hospital Plzen, Czech Republic

ARTICLE INFO

Keywords:
Kidney
Fumarate hydratase-deficient renal cell carcinoma
Programmed death-1 (PD-1) receptor
PD-1 ligand (PD-L1) receptor

ABSTRACT

Fumarate hydratase-deficient renal cell carcinoma (FH-RCC) is a rare and aggressive tumor affecting mostly younger patients. This is the first study to assess the expression of programmed death-1 (PD-1) receptor/PD-1 ligand (PD-L1) in FH-RCC.

Formalin-fixed paraffin-embedded samples from 13 FH-RCCs collected in an international multi-institutional study, were evaluated by immunohistochemistry (IHC) for PD-1/PD-L1 reactivity in tumor cells and tumor infiltrating lymphocytes (TILs). PD-1/PD-L1 expression was further evaluated by qPCR.

By IHC, PD-1 was negative in tumor cells in all 13 cases. PD-L1 was positive in tumor cells in 2/13 cases, weak positive in 7/13, and negative in 4/13 cases, respectively. In TILs, PD-1 was positive in 1/13, weak positive in 3/13, and negative in 9/13 cases. In TILs, PD-L1 was weak positive by IHC in 5/13, and negative in 8/13 cases, respectively. qPCR confirmed the result for 2 of 3 IHC weak positive PD-1 samples. Of 7 IHC weak positive samples (in tumor cells), PD-L1 mRNA was detected in all 7 tumors.

The majority of FH-RCCs did not express PD-1/PD-L1 by IHC, which was confirmed by molecular analysis. PD-1/PD-L1 expression in FH-RCC is restricted to a proportion of cases which may benefit from targeted therapies.

1. Introduction

Renal cell carcinomas (RCCs) are a heterogeneous group of neoplasms, representing approximately 3% of all human malignant tumors [1]. RCCs currently appear to be one of the most therapy-resistant malignancies, responding poorly to radiotherapy and chemotherapy. Recent data indicate that antibody blockade of immune checkpoints can enhance antitumor immunity [2,3], which has led investigators to redirect their focus on new immunotherapeutic strategies and novel treatment approaches [4]. In fact, targeted immunotherapy has shown

☆ The study was supported by the Charles University Research Fund (project number P36) and by the project FN 00669806 (Ondrej Hes).
☆☆ All authors declare no conflicts of interest.
☆☆☆ A preliminary version of this study was presented as a poster presentation at the March 2017 United States and Canadian Academy of Pathology (USCAP) Meeting in St. Antonio, TX, USA.
* Corresponding author at: Department of Pathology, Medical Faculty and Charles University Hospital Plzen, Alej Svobody 80, 304 60 Pilsen, Czech Republic.
E-mail address: hes@medima.cz (O. Hes).

http://dx.doi.org/10.1016/j.anndiagpath.2017.04.007

great promise and currently represents an area of active research and increased interest. The programmed death-1/programmed death-ligand 1(PD-1/PD-L1) axis inhibition by targeted-antibodies represents a promising mechanism to stimulate the anti-tumor activity of the immune system in several malignancies. Targeting immune checkpoint inhibitors results in inhibitory interruption of the cross-talk between the tumor and immune cells, which has recently been approved for therapy in RCC, with promising clinical activity [5].

Fumarate hydratase-deficient renal cell carcinoma (FH-RCC) is a rare and particularly aggressive tumor, affecting mostly younger patients [6-8]. It is caused by inactivating germline mutation in the *Fumarate Hydratase* (*FH*) gene, located at 1q42.3-q43. The *FH* gene codes for an enzyme involved in the tricarboxylic acid cycle, which hydrates fumarate to form malate [9-15]. FH-RCC also occurs in a syndromic setting as part of hereditary leiomyomatosis and renal cell carcinoma syndrome (HLRCC), which is a rare autosomal dominant disorder characterized by inherited predisposition to uterine and cutaneous leiomyomas and RCCs.

In light of the resurgence of cancer immunotherapy and increasing demand for new and effective targeted treatments for RCCs, we conducted this study, which is the first of its kind, to assess the expression of PD-1/PD-L1 (both by immunohistochemistry and qPCR) in FH-RCCs.

2. Materials and methods

An institutional Ethics Review was obtained for the study (EK LF and FN Plzen).

2.1. Case identification

As a part of an international multi-institutional collaborative effort, we collected and evaluated 13 FH-RCCs, for which *FH* mutation status was confirmed. Clinicopathologic and follow-up data were documented on all cases, using medical chart review and contacting the primary pathologists. All 13 cases were previously published (shown in Table 1) [6,16].

Tissues for light microscopy were fixed in 4% formaldehyde and embedded in paraffin using routine procedure. Sections 5 μm thick were cut from tissue blocks and stained with hematoxylin and eosin (H & E).

2.2. Histologic quantification of tumor-infiltrating lymphocytes (TILs)

TILs were qualitatively scored using a histologic intensity score on representative whole sections of 13 FH-RCCs; TILs included both lymphocytes and macrophages. TILs location was recorded as peritumoral, intratumoral, or both. TILs intensity was scored as none (0), mild (1; rare TIL; < 5% of tumor area), moderate (2; focal infiltrate; 5%–50% of tumor area), and diffuse (3; diffuse infiltrate; > 50% of tumor area) [17,18]. In addition, the presence or absence of peritumoral lymphoid aggregates, defined as a collection of approximately 50 lymphoid cells, was recorded as absent (0), focal (1; rare, isolated aggregates of lymphoid cells), present (2; multiple lymphoid aggregates), and well developed (3; present with well-developed germinal centers).

2.3. Immunohistochemical analysis

IHC was performed using a Ventana Benchmark XT automated stainer (Ventana Medical System, Inc., Tucson, AZ, USA) on formalin fixed, paraffin embedded tissue. Following primary antibodies were employed: PD-1 (polyclonal, RD systems, Minneapolis, MN, dilution 1:100), PD-L1 (rabbit monoclonal, E1L3N, Cell Signaling, Danvers, MA, dilution 1:25), CD3 (mouse monoclonal, clone PS1, catalog no. ORG-8982; Leica Microsystems, Bannockburn, IL, dilution 1:50), CD8 (mouse monoclonal, clone C8/C8144B, catalog no. 760-4250; Cell Marque, Rocklin, CA, dilution 1:50), and FoxP3 (mouse monoclonal, clone 236A/E7, catalog no. 14-4777-80, dilution 1:50; eBioscience; San Diego, CA). The immunostains were performed individually (i.e. no dual labeling) on serial unstained sections. The primary antibodies were visualized using the supersensitive streptavidin-biotin-peroxidase complex (Biogenex). Appropriate positive controls were used. T lymphocytes were considered tumor infiltrating if they were located within one high-power field (HPF; × 40) of carcinoma cells. CD3 and CD8 positivity was defined as membranous lymphocyte staining, and FoxP3 positivity was defined as any nuclear lymphocyte staining.

2.4. Quantification of PD-1/PD-L1 staining in tumors and TILs

Immunohistochemical staining for PD-1/PD-L1 was performed in one laboratory (Charles University Hospital Plzen). PD-1/PD-L1 immunoreactivity (membranous or cytoplasmic) in tumor cells and TILs were assessed and scored as follows: moderate to strong staining (2 to 3 +) in > 5% of cells was considered 'positive', 1–5% positive cells of any intensity was 'weak positive' (1 +), and no staining was 'negative' (0). All cases were scored by one pathologist (R.A.); those with a positive or borderline PD-1 and/or PD-L1 score were independently reviewed by another pathologist (O.H.) and final score was reached by consensus.

2.5. Molecular Evaluation of PD-1/PD-L1

RNA from 13 tumor and 3 non-tumor tissue samples was extracted and treated by DNase according to the manufacturer's instructions using the RecoverAll Total Nucleic Acid Isolation Kit (Ambion, Austin, TX, USA). cDNA was synthesized using the Transcriptor First Strand cDNA Synthesis Kit (RNA input 2 μg) (Roche Diagnostics, Mannheim, Germany).

Each PCR reaction consisted of 3.5 μL of sterile PCR water, 10 μL of "iQ SYBR Green Supermix" (Bio-Rad Laboratories, Alfred Nobel Drive, Hercules, CA, USA), 0.75 μL of each primer (10 μmol/L) and 5 μL of cDNA. All amplifications were carried out on a Bio-Rad CFX96 Real-Time System C1000 Thermal Cycler instrument using following program: initial denaturation/Taq activation step at 94 °C for 5 min, then 45 amplification cycles (95 °C for 20 s, 60 °C for 30 s, and 72 °C for 30 s), then melting analysis (from 65 °C to 95 °C, each step 0.5 °C for 5 s). For detection of PD-1 mRNA following primers were used: PD1-F1 5′-GCGGCCAG-GATGGTTCTTAG-3′ and PD1-R1 5′-CCTTCGGTCACCACGAGCA-3′. For detection of PD-L1 mRNA following primers were used: PDL1-F1 5′-TATGGTGGTGCCGACTACAAGC-3′ and PDL1-R1 5′-AGGTGACT-GGATCCACAACCAA-3′. Simultaneously, housekeeping gene PPIA mRNA was detected in each sample using primers PPIA-F1 5′-GTGTTCTTCGACATTGCCGTC-3′ and PPIA-R1 5′-TGCTGTCTTT-GGGACCTTGTCT-3′. To prevent amplification of genomic DNA, all primer pairs were designed to anneal specifically to exons on both sides of very long intron (min. 2.5 kb). Specifity and sizes of PCR products were confirmed by 2% agarose gel electrophoresis and Sanger sequencing (PD-1 = 84 bp, PD-L1 = 94 bp, PPIA = 84 bp).

Bio-Rad CFX Manager IVD original software (version 1.6) was used for data analysis. Expression ratio (R) of target (PD-1 and PD-L1) mRNA to housekeeping PPIA mRNA was calculated for each sample using Delta Delta method according to Pffafl [19].

3. Results

3.1. Clinicopathologic findings

The clinicopathological characteristics of 13 FH-RCC cases are summarized in Table 1. Mean patient age was 55.9 years (range 24–65 years), with 8 males and 5 females. Average tumor size was 9.8 cm (range 0.9–18 cm).

Table 1
Clinicopathological characteristics of 13 FH-RCC cases.

Case no.	Age (years)	Sex	Size (cm)	FU (months)	Confirmed HL/ leiomyomas	Pattern	Clin Pres
1[a]	44	M	7	108 AWD	–	TC	pT2a M: pleura, mediastinum
2[a]	60	M	8	7 AWD	–	P, TC, C	pT2a M: -
3[a]	50	F	10.9	18 DOD	–	P	pT2a M: NA
4[a]	52	M	14	18 AWD	–	Sol, sarc	pT4 M: lungs, mediastinum
5[a]	62	M	10	114 AWD	–	P, C, TP	pT2 M: -
6[a]	42	M	10	18 DOD	–	P, T, C	pT2 M: -
7[a]	51	F	Multiple 1.4, 1.0, 1.6, 0.6 multiple	46 AWD	–	P, TC	pT1a M: -
8[a]	52	F	Multiple 0.9, 0.6, 0.3, 0.9, 0.2, 0.4	Recidive of patient case 7	–	P	pT1a M: -
9[a]	45	F	7	24 DOD	–	P, T	pT3a M: peritoneum, retroperitoneum
10[a]	54	M	14	96 AW	–	T	pT2 M: -
11[a]	61	M	12.5	12 DOD	–	P, Sol, Sarc	pTx M: retroperitoneum, mediastinum lymph nodes, lungs, bones
12[b]	24	F	Bilateral 2.3 and 13.0	192 AW	+	Sol, Cri, C	pT2 M: -
13[a]	65	M	18	3 DOD	–	Sarc, TC	pT3a M: liver, lungs, spleen, bones at presentation

Abbreviations: M = male, F = female, FU = follow up, HL = signs of hereditary leiomyomatosis, Clin Prs = Clinical presentation: pT stage (TNM 09), metastases, M = metastasis, NA = not available, P = papillary, TC = tubulocystic, TP = tubulopapillary, T = tubulary, sol = solid, sarc = sarcomatoid, Cri = cribriform, C = cystic, + = present, – = absent, UNK = unknown, DOD = death of disease, AWD = alive with disease, AW = alive and well.

[a] Case previously published [6].

[b] Case previously published [16].

Only one of 13 cases (case #12) was identified as having an association with HLRCC syndrome [16]. In remaining patients or their kindred, the presence of cutaneous and uterine leiomyomas was not documented, as well as familial history of syndromic features. Information about stage was available in 12/13 patients. Stage pT3a was observed in 2 patients, while most patients were staged as pT2 (7 patients). Stage pT4 was documented in 1 patient, and stage pT1a in 2 patients. Information on follow up was available for all patients.

After a mean follow-up of 54.7 months (median 105, range 3–192 months), 5 patients were dead of disease, and 5 had disease progression with evidence of either local recurrence or subsequent development of regional or distant metastases. One of these patients showed signs of disease regression after sunitinib treatment (case no 1) and is alive with stable disease 108 months after surgery.

Histologically, FH-RCC tumors showed variable and different architectural growth patterns (Figs. 1 and 2), which were frequently found in combination (Table 1). Papillary pattern was most commonly present (Fig. 1). Three cases showed sarcomatoid differentiation. All cases demonstrated at least focal macronucleoli with perinucleolar clearing (halos), which in some cases were ubiquitous (Fig. 3).

All 13 tumors contained TILs, which were distributed in both peritumoral and intratumoral location in 11/13 cases, and predominantly peritumoral in 2/13 cases. 3 of 13 cases showed TILs with diffuse (3 +) intensity, while the majority of tumors (6/13) demonstrated mild (1 +) TILs intensity. In one case peritumoral lymphoid aggregates with germinal centers (3 +) were present, while the majority of tumors showed none or rare isolated lymphoid aggregates (7/13).

3.2. Immunohistochemical findings

The results of immunohistochemical examinations are summarized in Tables 2 and 3. Approximately 50–95% of TILs were CD3 positive T cells. CD8 immunostain showed 5–30% staining of TILs in 6/13 cases, while in the remaining of 7 cases, 40–90% of TILs were positive for CD8. FoxP3 was positive in only 1–5% of TILs in 10/13 cases; in the remaining 3 cases, FoxP3 was positive in 10–50% of TILs, respectively.

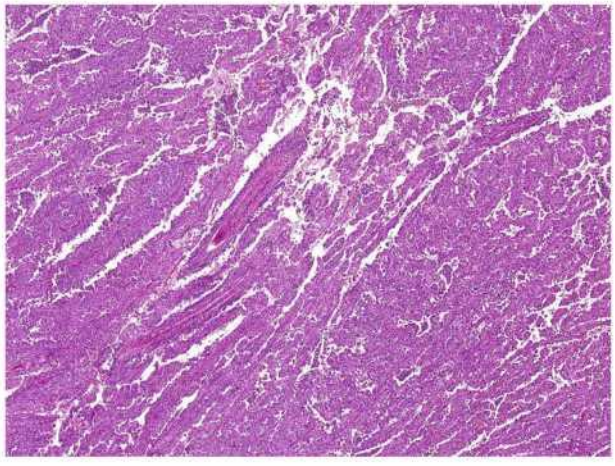

Fig. 1. FH-RCC tumor with predominant papillary growth pattern.

In the tumor cells, PD-1 was negative in all 13 cases. PD-L1 was positive in 2/13, weak positive in 7/13, and negative in 4/13 cases, respectively (Table 3). Fig. 4 shows strong membranous staining of the tumor cells by PD-L1.

In TILs, PD-1 was positive in 1/13, weak positive in 3/13, and negative in 9/13 cases. PD-L1 was weak positive in 5/13, and negative in 8/13 cases (Table 3). Fig. 5 illustrates TILs positive staining for PD-1.

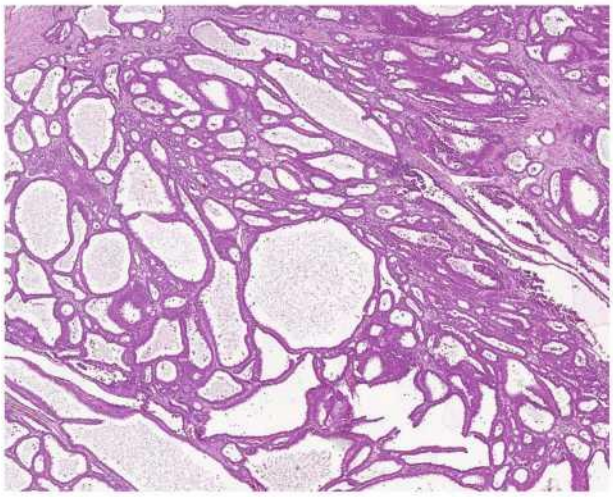

Fig. 2. FH-RCC tumor with predominant tubolocystic growth pattern.

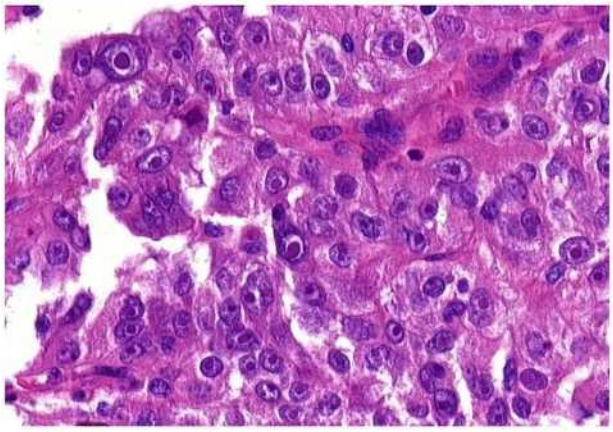

Fig. 3. FH-RCC tumor shows macronucleoli with perinucleolar clearing (halos).

Table 3
Results of PD-1 and PD-L1 expression in tumor cells and TILs by IHC and qPCR.

	PD-1			PD-L1		
Case no.	Tumor	TILs	qPCR	Tumor	TILs	qPCR
1	−	−	−	−	−	−
2	−	+	+	+	−	++
3	−	++	++	+	+	++
4	−	+	−	+	+	++
5	−	+	+	−	+	++
6	−	−	−	−	−	−
7	−	−	+	+	−	++
8	−	−	+	+	−	++
9	−	−	−	++	+	−
10	−	−	−	++	−	−
11	−	−	+	+	−	++
12	−	−	−	−	−	−
13	−	−	−	+	+	++

Abbreviations: TILs = tumor infiltrating lymphocytes, (−) negative, (+) weak positive, (++) positive.

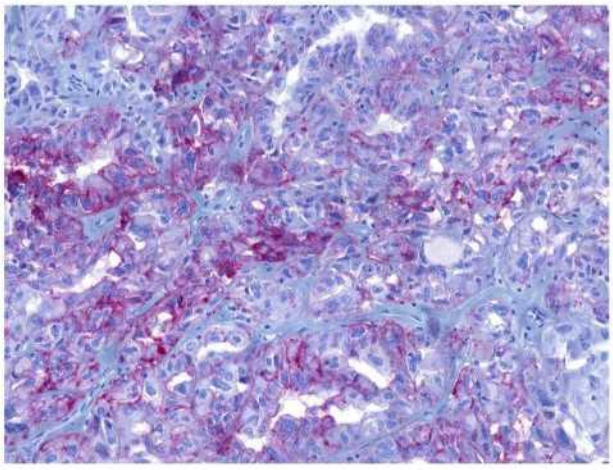

Fig. 4. PD-L1 strong membranous staining of the tumor cells.

3.3. qPCR molecular findings

All 13 cases were examined using qPCR method for both PD-1 and PD-L1 (Table 3). qPCR confirmed the PD-1 positivity in 1 and weak positivity in 5 cases, while the negative IHC result was confirmed in the remaining 7 cases. It should be noted that qPCR confirmed the result for 1 IHC positive PD-1 sample, and also for 2 of 3 weak positive samples (in TILs). No mRNA levels were detected in the third weak positive case. In 9 IHC negative PD-1 cases (in TILs), qPCR confirmed the absence of PD-1 expression in 6, while 3 showed only weak PD-1 mRNA expression.

On the other hand, PD-L1 was positive in 8 tumors by IHC while negative in 5 cases using qPCR. PD-L1 mRNA was detected in all 7 IHC weak positive samples (in tumor cells). 3 PD-L1 negative samples were confirmed by qPCR. Of note, 2 IHC PD-L1 positive cases tested negative for qPCR.

Table 2
Histologic quantification of TILs and related IHC results.

Case no.	TIL distribution	TIL intensity	PLA	CD3	CD8	FOXP3
1	Peritumoral	2	2+	NA	90%	5%
2	Both peritumoral and intratumoral	1	1+	70%	30%	1%
3	Both peritumoral and intratumoral	3	2+	95%	50%	1%
4	Both peritumoral and intratumoral	2	2+	70%	30%	1%
5	Both peritumoral and intratumoral	2	2+	70%	50%	1%
6	Both peritumoral and intratumoral	1	0	80%	30%	40%
7	Both peritumoral and intratumoral	2	3+	90%	10%	5%
8	Peritumoral	1	1+	95%	5%	1%
9	Both peritumoral and intratumoral	3	2+	80%	50%	10%
10	Both peritumoral and intratumoral	1	1+	50%	40%	5%
11	Both peritumoral and intratumoral	1	1+	70%	30%	1%
12	Both peritumoral and intratumoral	3	1+	50%	40%	50%
13	Both peritumoral and intratumoral	1	0	80%	40%	1%

Abbreviations: PLA = peritumoral lymphoid aggregate, TIL = tumor infiltrating lymphocyte.
NA = not available (false negative result, most likely as a result of fixation artifact).

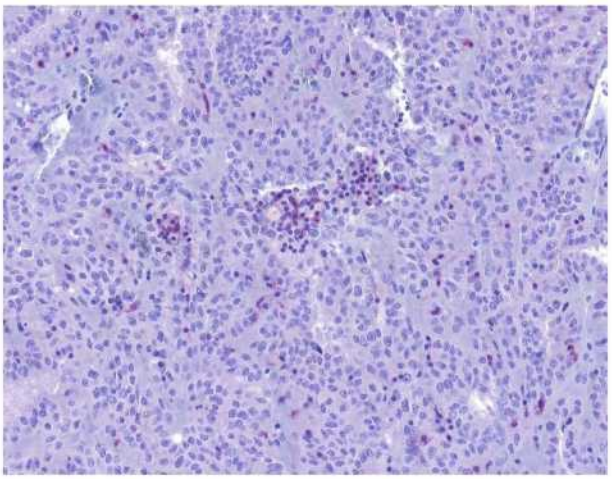

Fig. 5. PD-1 positive staining of tumor infiltrating lymphocytes (TILs).

4. Discussion

FH-deficient RCC is a very rare and aggressive renal malignancy that can be seen in both sporadic and hereditary settings (i.e. HLRCC-associated RCC) [6-8]. They mainly occur in younger patients showing aggressive clinical behavior, and adverse morphologic features. These tumors are characterized by predominant papillary architecture with invariable presence of macronucleoli, at least focally [6-8], however the architecture is variable and frequently multiple growth patterns are combined. HLRCC-associated RCC, the syndromic type of FH-RCC defined by both mutational analysis and clinical history, was initially included in the 2004 WHO classification of renal neoplasms as a presumed hereditary counterpart of papillary RCC [20]. With subsequent data highlighting the aggressive behavior of renal carcinoma associated with HLRCC syndrome and recognizing its morphologic spectrum, HLRCC–associated RCC was recognized as a distinct entity and a variant of RCC in the 2013 International Society of Urological Pathology (ISUP) Vancouver Classification of renal tumors, and it was included in the most recent 2016 WHO classification [21]. With recent studies on molecular characteristics of FH-RCCs, it became apparent that the term FH-RCC would be more appropriate, encompassing both sporadic (absence of features suggesting syndromic disease) and hereditary cases [6,8].

The association of immunological checkpoint markers PD-1/PD-L1 and the prognosis of various cancers and potential therapeutic implications have been a recent research hotspot. The interaction between PD-1 expressed on T cells and its ligand PD-L1 aberrantly expressed on tumor cells results in inhibition of the cellular immune response. In fact, several studies have identified an interesting correlation between tumor cell expression of PD-L1 and clear cell RCC (ccRCC) advanced grade, stage, and poor prognosis [22,23]. The Food and Drug Administration (FDA) also recently approved nivolumab, a monoclonal antibody directed against PD-1, in metastatic ccRCC [24]. It has been postulated that immune checkpoint inhibitors could also represent a therapeutic target in non-ccRCC [25,26], but so far very limited data are available on the role of immune checkpoint inhibitors and the expression patterns of PD-1/PD-L1 in other RCC subtypes. In this collaborative study, for the first time we assessed PD-1/PD-L1 expression patterns using both IHC and qPCR analysis in FH-RCC, which is a quite rare but extremely aggressive renal neoplasm.

We found that the majority of evaluated FH-RCCs were immunohistochemically negative for PD-1 in TILs (9/13). Of 9 negative PD-1 cases by IHC, 6 were confirmed as negative using the qPCR method. Overall, of 13 FH-RCCs, only 1 case was positive for PD-1 by qPCR, which suggests that IHC method of assessing PD-1 expression may not reflect the true PD-1 status. The expression of PD-1 has been linked with larger tumors, higher nuclear grade, and advanced tumor stage in cohorts mainly consisting of ccRCC [27,28]. In a recent study by Erlmeier et al. [5], 30.9% of chromophobe RCC were positive for PD-1 in TILs using IHC, but these findings were not further verified/confirmed by molecular analysis methods. In our study, 4/13 (30.8%) cases showed weak positive or strong positive PD-1 TIL expression using IHC, which is comparable to the reported frequency by Erlmeier et al. [5] in chromophobe RCC.

In this study, 8/13 (61.5%) tumors were positive for PD-L1 by qPCR. Immunohistochemically, the tumor cells were negative for PD-L1 in 4/13 cases while weak or strong positive in the remaining 9/13 cases. Out of 4 cases with negative tumoral PD-L1 expression by IHC, 3 were ultimately confirmed to be negative by qPCR. The rate of tumoral PD-L1 expression detected by qPCR in our study appears to be relatively higher than what has been previously reported in RCCs. It should be noted that qPCR method demonstrates the level of PD-1/PD-L1 expression in the entire tissue. In other words, this method does not distinguish between PD-1/PD-L1 expression in neoplastic cells, TILs, or even stromal component. Nonetheless, qPCR is currently a more sensitive method to determine PD-1/PD-L1 expression compared to IHC.

Thompson et al. were among the first to describe the PD-L1 expression in ccRCC, using only IHC method and without the qPCR confirmation [22]. In their study of 196 patients, PD-L1 expression by IHC was associated with more aggressive features such as higher TNM stage, tumor size or Fuhrman grade and increased risk of cancer-specific mortality [22]. In another study of 259 RCC patients, positive PD-L1 was seen in 59.1% of cases and was associated with similar factors [23]. In this study the correlation between PD-L1 expression and adverse prognostic factors has been identified with PD-L1 expression in both tumor cell membrane and TILs [23]. However the authors did not distinguish the PD-L1 positivity according to various RCC subtypes. Thus, it would be very difficult to compare their results with other more detailed studies [23]. In a recent study, Erlmeier et al. [5] reported that 14% of chromophobe RCC were positive for tumoral PD-L1 expression using IHC only. Choueiri et al. [25] found 10.9% positive PD-L1 (assessed only by IHC in tumor cells among non-ccRCC patients), 5.6% in chromophobe RCC, 10% in papillary RCC, 30% in Xp11.2 translocation RCC and 20% in collecting duct carcinoma. Further, a recent Japanese study by Motoshina et al. [29] showed that PD-L1 was expressed in tumor cells (by IHC only) in 29% of papillary RCCs. The authors found no statistical differences in PD-L1 expression between type 1 and type 2 papillary RCCs (22% vs. 36%). Of note, a recent comprehensive molecular analysis of papillary RCCs demonstrated that type 2 papillary RCC is a heterogeneous groups consisted of at least three subtypes based on molecular and phenotypic features [30].

In addition to tumor cells, we assessed PD-L1 expression in TILs and found PD-L1 to be weakly positive in 5/13. Choueiri et al. [25] found PD-L1 positivity in TILs in 56.4% of non-ccRCC patients, 36.1% in chromophobe RCC, 60% in papillary RCC, 90% in Xp11.2 translocation RCC, and 100% in collecting duct carcinoma. The authors concluded that in non-ccRCC, patients with positive PD-L1 tumors appeared to have worse clinical outcomes, although only PD-L1 positivity in tumor cells (not TILs) was associated with higher tumor stage and grade. The notion of PD-L1 positivity in tumor cells and poor prognostic factors is consistent with our findings of high rate of positive PD-L1 expression in tumor cells in FH-RCC, which is an aggressive subtype of RCC, generally associated with poor prognosis (regardless of their PD1/PD-L1 expression status). However, we are not able to draw any definite conclusion on the PD-1/PD-L1 expression status as a prognostic factor in these tumors, due to the small sample size of the evaluated cohort.

No morphologic features were associated with PD-1/PD-L1 positive cases in this study, and no association between PD-1/PD-L1 expression was found in the tumor cells and TILs. It is worth noting that in contrast to other malignancies, neither PD-1 nor PD-L1 positivity in ccRCC has been clearly linked to the response to immune checkpoint inhibition. So

far it has been unclear what role immune checkpoint inhibitors play in non-ccRCC.

One of the strengths of this study is that all evaluated FH-RCC cases were genetically tested for *FH* mutation and that no non-cc-RCC mimickers were included in the analysis. We also utilized a qPCR method, in addition to the IHC, to evaluate and confirm the PD-1/PD-L1 expression. Most of the previous studies assessing PD-1/PD-L1 status expression in RCCs used only IHC.

This study has several limitations. First, despite the international multi-institutional collaborative effort, we had a small sample size, mainly due to the rarity of FH-RCC. Second, the issue of intratumoral heterogeneity, which is well known in RCCs [31], may have impaired the IHC and the molecular analysis. Third, given the samples were collected via an international collaboration, we may have been subjected to potential pre-analytical factors (i.e., cold ischemic time, fixation time, etc.), which may have impacted the IHC interpretations. Fourth, PD-1/PD-L1 IHC interpretation itself can be challenging, given the intimate association of the neoplastic cells and the immune components in many cases. To address this, all cases with a positive or borderline PD-1 and/or PD-L1 IHC score were independently reviewed by a second pathologist. All these factors illustrate the limitation of using IHC-based tumor PD-L1 expression as an exclusive biomarker for selection of cases for cancer immunotherapy. Of note, several studies have demonstrated that only cell membrane-expressed PD-L1 has biological significance [3,32]. In this study all positive IHC-based PD-L1 cases showed membranous staining, but in some cases cytoplasmic staining was also observed. Therefore, it may seem more reasonable to analyze the correlations between membrane PD-L1 protein, rather than intracellular PD-L1 protein or mRNA, and the clinical outcomes. IHC-based detection of PD-L1 has also limitations because of its subjectivity in determining a true "positive" tumor PD-L1 staining [32]. Further, IHC-based detection of PD-L1 has its own technical issues, and the results may not accurately reflect the real PD-L1 expression status, because various PD-L1 antibody clones utilized in different studies can result in variable PD-L1 expression and interpretation [5,17,18,23,25,27].

In summary, we found that PD-1/PD-L1 expression in FH-RCCs, as in other non-ccRCCs, is restricted to a proportion of cases [22,27]. Nonetheless, targeted-therapies may be beneficial in the positive PD-1/PD-L1 FH-RCC tumors, provided the expression is confirmed by IHC and molecular testing. Further assessment in larger cohorts is warranted to ascertain the relevance of PD-1/PD-L1 in FH-RCC.

References

[1] Kang MJ, Kim KM, Bae JS, et al. Tumor-infiltrating PD1-positive lymphocytes and FoxP3-positive regulatory T cells predict distant metastatic relapse and survival of clear cell renal cell carcinoma. Transl Oncol 2013;6:282–9.

[2] Messai Y, Gad S, Noman MZ, et al. Renal cell carcinoma programmed death-ligand 1, a new direct target of hypoxia-inducible factor-2 alpha, is regulated by von Hippel-Lindau gene mutation status. Eur Urol 2016;70:623–32.

[3] Pardoll DM. The blockade of immune checkpoints in cancer immunotherapy. Nat Rev Cancer 2012;12:252–64.

[4] Sznol M, Chen L. Antagonist antibodies to PD-1 and B7-H1 (PD-L1) in the treatment of advanced human cancer. Clin Cancer Res 2013;19:1021–34.

[5] Erlmeier F, Hartmann A, Autenrieth M, et al. PD-1/PD-L1 expression in chromophobe renal cell carcinoma: an immunological exception? Med Oncol 2016;33:120.

[6] Trpkov K, Hes O, Agaimy A, et al. Fumarate hydratase-deficient renal cell carcinoma is strongly correlated with fumarate hydratase mutation and hereditary leiomyomatosis and renal cell carcinoma syndrome. Am J Surg Pathol 2016;40:865–75.

[7] Chen YB, Brannon AR, Toubaji A, et al. Hereditary leiomyomatosis and renal cell carcinoma syndrome-associated renal cancer: recognition of the syndrome by pathologic features and the utility of detecting aberrant succination by immunohistochemistry. Am J Surg Pathol 2014;38:627–37.

[8] Smith SC, Trpkov K, Chen YB, et al. Tubulocystic carcinoma of the kidney with poorly differentiated foci: a frequent morphologic pattern of fumarate hydratase-deficient renal cell carcinoma. Am J Surg Pathol 2016;40:1457–72.

[9] Alam NA, Rowan AJ, Wortham NC, et al. Genetic and functional analyses of FH mutations in multiple cutaneous and uterine leiomyomatosis, hereditary leiomyomatosis and renal cancer, and fumarate hydratase deficiency. Hum Mol Genet 2003;12:1241–52.

[10] Kiuru M, Launonen V, Hietala M, et al. Familial cutaneous leiomyomatosis is a two-hit condition associated with renal cell cancer of characteristic histopathology. Am J Pathol 2001;159:825–9.

[11] Kiuru M, Lehtonen R, Arola J, et al. Few FH mutations in sporadic counterparts of tumor types observed in hereditary leiomyomatosis and renal cell cancer families. Cancer Res 2002;62:4554–7.

[12] Launonen V, Vierimaa O, Kiuru M, et al. Inherited susceptibility to uterine leiomyomas and renal cell cancer. Proc Natl Acad Sci U S A 2001;98:3387–92.

[13] Tomlinson IP, Alam NA, Rowan AJ, et al. Germline mutations in FH predispose to dominantly inherited uterine fibroids, skin leiomyomata and papillary renal cell cancer. Nat Genet 2002;30:406–10.

[14] Toro JR, Nickerson ML, Wei MH, et al. Mutations in the fumarate hydratase gene cause hereditary leiomyomatosis and renal cell cancer in families in North America. Am J Hum Genet 2003;73:95–106.

[15] Varol A, Stapleton K, Roscioli T. The syndrome of hereditary leiomyomatosis and renal cell cancer (HLRCC): the clinical features of an individual with a fumarate hydratase gene mutation. Australas J Dermatol 2006;47:274–6.

[16] Lehtonen HJ, Blanco I, Piulats JM, et al. Conventional renal cancer in a patient with fumarate hydratase mutation. Hum Pathol 2007;38:793–6.

[17] Cimino-Mathews A, Thompson E, Taube JM, et al. PD-L1 (B7-H1) expression and the immune tumor microenvironment in primary and metastatic breast carcinomas. Hum Pathol 2016;47:52–63.

[18] Taube JM, Klein A, Brahmer JR, et al. Association of PD-1, PD-1 ligands, and other features of the tumor immune microenvironment with response to anti-PD-1 therapy. Clin Cancer Res 2014;20:5064–74.

[19] Pfaffl MW. A new mathematical model for relative quantification in real-time RT-PCR. Nucleic Acids Res 2001;29:e45.

[20] Eble JN, S G, Epstein JI, Sesterhenn IA. Pathology and genetics of tumours of the urinary system and male genital organs World Health Organization. Geneva: World Health Organization; 2004.

[21] Srigley JR, Delahunt B, Eble JN, et al. The International Society of Urological Pathology (ISUP) Vancouver classification of renal neoplasia. Am J Surg Pathol 2013;37:1469–89.

[22] Thompson RH, Gillett MD, Cheville JC, et al. Costimulatory B7-H1 in renal cell carcinoma patients: indicator of tumor aggressiveness and potential therapeutic target. Proc Natl Acad Sci U S A 2004;101:17174–9.

[23] Krambeck AE, Thompson RH, Dong H, et al. B7-H4 expression in renal cell carcinoma and tumor vasculature: associations with cancer progression and survival. Proc Natl Acad Sci U S A 2006;103:10391–6.

[24] Motzer RJ, Escudier B, McDermott DF, et al. Nivolumab versus everolimus in advanced renal-cell carcinoma. N Engl J Med 2015;373:1803–13.

[25] Choueiri TK, Fay AP, Gray KP, et al. PD-L1 expression in nonclear-cell renal cell carcinoma. Ann Oncol 2014;25:2178–84.

[26] Ciccarese C, Brunelli M, Montironi R, et al. The prospect of precision therapy for renal cell carcinoma. Cancer Treat Rev 2016;49:37–44.

[27] Abbas M, Steffens S, Bellut M, et al. Do programmed death 1 (PD-1) and its ligand (PD-L1) play a role in patients with non-clear cell renal cell carcinoma? Med Oncol 2016;33:59.

[28] Thompson RH, Dong H, Lohse CM, et al. PD-1 is expressed by tumor-infiltrating immune cells and is associated with poor outcome for patients with renal cell carcinoma. Clin Cancer Res 2007;13:1757–61.

[29] Motoshima T, Komohara Y, Ma C, et al. PD-L1 expression in papillary renal cell carcinoma. BMC Urol 2017;17:8.

[30] Cancer Genome Atlas Research N, Linehan WM, Spellman PT, et al. Comprehensive molecular characterization of papillary renal-cell carcinoma. N Engl J Med 2016;374:135–45.

[31] Gerlinger M, Catto JW, Ormtoft TF, et al. Intratumour heterogeneity in urologic cancers: from molecular evidence to clinical implications. Eur Urol 2015;67:729–37.

[32] Wang X, Teng F, Kong L, Yu J. PD-L1 expression in human cancers and its association with clinical outcomes. Onco Targets Ther 2016;9:5023–39.

1.3.2 Fumarate hydratase deficient renal cell carcinoma: Chromosomal numerical aberration analysis of 12 cases

S hereditární leiomyomatózou a renálním karcinomem asociovaný renální karcinom/fumarát hydratáza deficientní renální karcinom je agresivní renální neoplázie s morfologickým spektrem, definovaná molekulárně geneticky přítomností mutace/LOH ve *FH* genu. V rámci této studie jsme vyšetřovali chromozomální numerický aberační status (CNV) v FHRCC/HLRCC za pomoci arrayCGH analýzy a low pass whole genome sekvenování.

Genetická analýza byla úspěšně provedena celkem u 12 případů. Nejčastěji detekované chromozomální aberace byly kompletní či parciální ztráta chromozomu 4 (5/12 případů), ztráta chromozomu 15 (4/12 případů) a chromozomů 9, 13 a 14 (každá v 3/12 případů). Dále byl v případech zastižen kompletní či parciální zisk chromozomu 17 (u 4/12 případů). Ve 4 případech nebyla zastižena žádná ze sledovaných numerických chromozomálních alterací.

Chromozomální numerický aberační patern/status v rámci entity FHRCC/HLRCC je velmi variabilní a neposkytuje použitelný diagnostický nástroj pro tuto malignitu. Imunohistochemická barvení a zejména molekulárně genetické hodnocení *FH* genu (mutace/LOH) zůstává zlatým standardem pro identifikaci FHRCC/HLRCC.

Annals of Diagnostic Pathology 39 (2019) 63–68

Contents lists available at ScienceDirect

Annals of Diagnostic Pathology

journal homepage: www.elsevier.com/locate/anndiagpath

Fumarate hydratase deficient renal cell carcinoma: Chromosomal numerical aberration analysis of 12 cases

Kristyna Pivovarcikova[a], Petr Martinek[a], Petr Grossmann[a], Kiril Trpkov[b], Reza Alaghehbandan[c], Cristina Magi-Galluzzi[d], Maria Pane Foix[e], Enric Condom Mundo[e], Daniel Berney[f], Anthony Gill[g], Boris Rychly[h], Kvetoslava Michalova[a], Joanna Rogala[i], Tomas Pitra[j], Tamas Micsik[k], Jiri Polivka[l], Milan Hora[j], Ozlem Tanas Isikci[m], Sarka Skalova[a], Jana Mareckova[a], Michal Michal[a], Ondrej Hes[a,*]

[a] Department of Pathology, Charles University in Prague, Faculty of Medicine in Plzeň, University Hospital Plzen, Pilsen, Czech Republic
[b] Calgary Laboratory Services and University of Calgary, Calgary, AB, Canada
[c] Department of Pathology, Faculty of Medicine, University of British Columbia, Royal Columbian Hospital, Vancouver, BC, Canada
[d] Department of Pathology, School of Medicine, University of Alabama, Birmingham, AL, USA
[e] Department of Pathology, Bellvitge Biomedical Research Institut (IDIBELL), Bellvitge University Hospital, University of Barcelona School of Medicine, L'Hospitalet de Llobregat, Barcelona, Spain"
[f] Bart's Cancer Center, London, United Kingdom
[g] Cancer Diagnosis and Pathology Group, Kolling Institute of Medical Research and University of Sydney, Sydney, NSW, Australia
[h] Department of Pathology, Cytopathos, Bratislava, Slovakia
[i] Department of Pathology Regional Specialist Hospital, Wroclaw, Poland
[j] Department of Urology, Charles University in Prague, Faculty of Medicine in Plzeň, Pilsen, Czech Republic
[k] 1st Department of Pathology and Experimental Cancer Research, Semmelweis University, Budapest, Hungary
[l] Department of Histology and Embryology, Charles University in Prague, Faculty of Medicine in Plzeň, Pilsen, Czech Republic
[m] Department of Pathology, Ankara Training and Research Hospital, Ankara, Turkey

ARTICLE INFO

Keywords:
Kidney
Fumarate hydratase deficient renal cell carcinoma
Chromosomal numerical aberration pattern

ABSTRACT

Hereditary leiomyomatosis and renal cell carcinoma-associated renal cell carcinoma (HLRCC)/fumarate hydratase deficient renal cell carcinoma (FHRCC) is defined by molecular genetic changes (mutation/LOH in fumarate hydratase (*FH*) gene). We investigated chromosomal numerical aberration pattern (CNV) in FHRCC/HLRCC using array comparative genomic hybridization analysis and low pass whole genome sequencing. Genetic analysis was successfully completed in 12 tumors. Most common chromosomal aberrations detected were a complete or partial loss of chromosome 4 (5/12 cases), chromosome 15 (4/12 cases), and chromosomes 9, 13, and 14 (each in 3/12 cases), as well as a complete or partial gain of chromosome 17 (in 4/12 cases). No chromosomal losses or gains were detected in 4 cases. Copy number variation pattern in FHRCC/HLRCC appears to be highly variable and does not provide a useful diagnostic tool in identifying these cases. Immunohistochemical staining and especially molecular genetic evaluation of *FH* gene mutations/LOH remain the gold standard in identifying FHRCC/HLRCC.

1. Introduction

Molecular genetic features have become an integral part of modern classifications of renal tumors. Chromosomal aberration status, mutations of particular genes, loss of heterozygosity (LOH), and hypermethylation are frequently utilized even in routine differential diagnostic processes. However, recently published data seem to confirm that chromosomal numerical aberration pattern in renal cell carcinomas (RCCs) is rather more complex and variable than initially thought.

Hereditary leiomyomatosis and renal cell carcinoma-associated renal cell carcinoma (HLRCC)/fumarate hydratase deficient renal cell carcinoma (FHRCC) is one of recently recognized tumors defined by a molecular genetic change. The diagnostic hallmark of HLRCC/FHRCC is the mutation/LOH of the fumarate hydratase (*FH*) gene. Although HLRCC/FHRCC has variable morphology, papillary/tubular

* Corresponding author at: Department of Pathology, Medical Faculty and Charles University Hospital Plzen, Alej Svobody 80, 304 60 Pilsen, Czech Republic.
E-mail address: hes@biopticka.cz (O. Hes).

https://doi.org/10.1016/j.anndiagpath.2019.02.008

architectural pattern is the most frequently identified in the literature. The presence of large nuclei with prominent dark red nucleoli and perinucleolar clearing have been considered as helpful morphologic clue. However, even these morphologic features are not consistently present, and are not pathognomonic only for HLRCC/FHRCC [1]. In addition to the morphologic features, immunohistochemical stains including antibodies against fumarate hydratase (FH) and 2-succinocysteine (2SC) can also be helpful. It should be noted that there are several challenges concerning immunohistochemistry evaluation, given 2SC is not yet commercially available, and there are difficulties in the interpretation of these stains.

Two nomenclatures are used for renal tumors associated with impaired *FH* gene - hereditary leiomyomatosis and renal cell carcinoma-associated renal cell carcinoma (HLRCC) and fumarate hydratase deficient renal cell carcinoma (FHRCC). The term HLRCC is used for syndromic patients - HLRCC is characterized by germline mutations of the *FH* gene, autosomal dominant heredity and concurrent presence of cutaneous and/or uterine leiomyomas. The onset of renal tumor, uterine/cutaneous leiomyomas can be seen within several years and synchronous presence of renal tumor together with leiomyomas is not seen frequently. This syndrome was first reported in two families from Finland in 2001 [2]. The term FHRCC is recommended for tumors with suggestive morphology, typical immunophenotype (FH negativity, 2-succinocysteine [2SC] positivity) in the setting of uncertain clinical and family history and unknown genetic status. FHRCC also allows designation of cases that might represent apparently sporadic forms, harbouring somatic (not germline) alterations in the *FH* gene [3-5]. In fact, with recent studies on molecular characteristics of FHRCC, it became apparent that the term FHRCC would be more appropriate, encompassing both sporadic (absence of features suggesting syndromic disease) and hereditary cases.

HLRCC/FHRCC was initially included in the WHO 2004 classification, not as separate entity but as a presumed familiar counterpart of papillary renal cell carcinoma (PRCC) type 2 [6]. Currently, HLRCC is recognized as a separate entity and variant of RCC in the 2012 International Society of Urological Pathology (ISUP) Vancouver Classification of renal tumors, and it was included in the most recent 2016 WHO classification [7,8]. In general, PRCC is believed to be characterized (in addition to other abnormalities) by trisomy/polysomy of chromosomes 7 and 17 and a loss of chromosome Y in male patients [8]. However, recently published papers showed much more variable genetic profile [9-31]. The aim of this study was to investigate the chromosomal numerical aberration pattern (CNV) in FHRCC/HLRCC, and to compare it with CNV pattern typically associated with PRCC. To the best of our knowledge, only one study dealing with CNV pattern in FHRCC/HLRCC has been previously published [32].

2. Material and methods

Fourteen cases of FHRCC were collected from 9 institutions: Medical Faculty and Charles University Hospital Plzen (Plzen, Czech Republic), Calgary Laboratory Services and University of Calgary (Calgary, Canada), Robert J. Tomsich Pathology and Laboratory Medicine Institute - Cleveland Clinic (Cleveland, USA), Bellvitge Biomedical Research Institute (Barcelona, Spain), Bart's Cancer Center (London, UK), Medical College Wisconsin (Milwaukee, USA), Royal North Shore Hospital - University of Sydney (Sydney, Australia), Cytopathos (Bratislava, Slovakia), and Semmelweis University (Budapest, Hungary).

All cases were confirmed FHRCC, with genetically detected mutation/LOH of the *FH* gene. We did not determine, if the *FH* gene mutation was germline or somatic, therefore the term FHRCC was used. The majority of cases were published in 2 previous studies; 9/14 cases were reported in a clinicopathologic, morphologic, immunohistochemical and molecular-genetic study, and 13/14 cases were included in a study examining PD1 and PDL1 expression [4,33]. The material for the latter study was available in 12 cases, and only these cases were included in the presented study.

2.1. DNA extraction

Tumor areas of the formalin-fixed paraffin-embedded (FFPE) samples were determined using hematoxylin-eosin stained slides and macro dissected. DNA from FFPE tumor tissue was extracted using QIAsymphony DNA Mini Kit (Qiagen, Hilden, Germany) on an automated extraction system (QIAsymphony SP; Qiagen) according to manufacturer's supplementary protocol for FFPE samples. Concentration and purity of isolated DNA were measured using NanoDrop ND-1000 and DNA integrity was examined by amplification of control genes in a multiplex polymerase chain reaction (PCR).

2.2. Low pass whole genome sequencing

SurePlex DNA amplification system (Illumina, San Diego, CA) was used to generate DNA template from tumor samples. Amplification is highly representative, which makes the resulting product suitable for copy number variation detection. The library of all samples was prepared using Nextera DNA Sample Prep Kit (Illumina, San Diego, CA) and was sequenced on MiSeq sequencer, copy-number variant analysis was performed using BlueFuse Multi software with the Veriseq plugin (Illumina, San Diego, CA). Following quality control filters for valid samples were set: minimum 1 million reads per sample, average quality score and average alignment score > 30, and overall noise < 0.3. Thresholds for CNV calling were set based on a group of samples with known CNVs, that were validated using array CGH and fluorecence in-situ hybridization. The percentage of tumor in the DNA sample was considered, when calling the lower frequency CNVs and thresholds for CNVs were set individually for each case typically the copy number was 1.5 for loss and 2.5 for gain. CNVs spanning less than the whole length of a chromosome arm were not called. FISH as described previously [34] was used for confirmation of cohort of 5 analyzed cases (results not shown). The more complex CNV changes are listed in the table. Aberrations on gonosomes were excluded from the results. CNV detection using low pass whole genome sequencing was proven to produce similar results as in fresh frozen tissue [35].

3. Results

Twelve tumors from 11 patients were included in this study (case 2 is a recurrence of patient/case 1). Clinical data were available for all 11 patients (and all 12 tumors) (Table 1). The study cohort included 8 males and 3 females, age range 24 to 65 years (median 51 years, mean 50.1 years). Tumor size ranged from 0.9 to 18 cm in greatest dimension (median 8 cm, mean 8.9 cm). Pathologic staging included pT1 in 2 cases, pT2 in 6, and pT3 in 3 cases. No information about stage was available in one case.

Follow-up data were available for all 11 patients (range 3 to192 months, mean 57.2 months, median 24 months). Five patients had metastatic disease. Five patients died of disease 3–24 months post-surgery. No records concerning aggressive behavior were found in 2 patients.

The morphologic characteristics are summarized in Table 1. Most of the tumors (8/12) showed papillary growth pattern (at least focally) (Fig. 1), while 4 did not demonstrate any papillary architecture (Fig. 2a). Papillary architecture was found to be mixed with other growth patterns (i.e., tubular, cribriform, cystic, tubulocystic, solid and sarcomatoid) in the majority of cases (Fig. 2B), only two cases were pure papillary. Macronucleoli were found in all 12 cases (at least focally) (Fig. 3).

Low pass whole genome sequencing was successful in all 12 tumors. There were 61 chromosomal aberrations detected. The CNV's included 31 gains and 30 individual losses of whole chromosomes or parts of

Table 1
Clinical data and histopathologic features of FHRCC.

Case	Age (years)	Sex	Size (cm)	Follow-up (months)	Current status	Stage (AJCC/UICC2009)	Pattern
Case 1[a]	51	F	Multiple 1.4, 1.0, 1.6, 0.6	46	AWD (see case 2)	pT1a, M0	Papillary, tubulocystic
Case 2[a]	52	F	Multiple 0.9, 0.6, 0.3, 0.9, 0.2, 0.4	After 46 months, recurrent multiple lesions identified	Recurrence of case 1	pT1a, M0	Papillary
Case 3[a]	44	M	7	108	AWD	pT2a, M1	Tubulocystic
Case 4[a]	45	F	7	24	DOD	pT3a, M1	Papillary, tubular
Case 5[a]	42	M	10	18	DOD	pT2, M0	Papillary, tubular, cystic
Case 6[a]	65	M	18	3	DOD	pT3a, M1	Sarcomatoid, tubulocystic
Case 7[a]	60	M	8	114	AWD	pT2, M0	Papillary, cystic, tubulopapillary
Case 9[a]	60	M	8	7	AWD	pT2a, M0	Papillary, tubulocystic, cystic
Case 11[a]	54	M	14	96	ANED	pT2, M0	Papillary
Case 12[a]	61	M	12.5	12	DOD	pTx, M1	Papillary, solid, sarcomatoid
Case 13[a]	24	F	Multiple 2.3 and 13	192	ANED	pT2, M0	Solid, cribriform, cystic
Case 14	45	M	6.5	9	DOD	pT3a, M1	Tubulocystic

M male, *F* female, *NA* not available, *AWD* alive with the disease, *DOD* death of the disease, *ANED* alive and no evidence of disease.
[a] Cases already published [4,33].

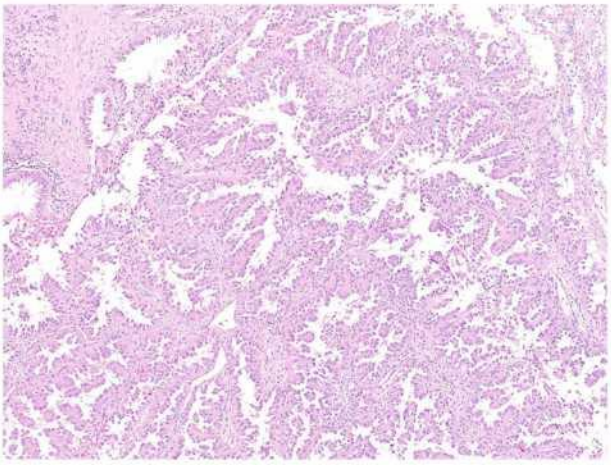

Fig. 1. FHRCC arranged in papillary pattern. Such cases were suggested to be familiar counterpart of so-called PRCC type 2 in previous WHO 2004 Classification of Genitourinary Tumors.

chromosomal arms (Table 2, Fig. 4). There were 42 unique changes. Most commonly detected chromosomal aberrations were a complete or partial loss of chromosomes 4 (found in 5/12 cases) loss of chromosome 15 (in 4/12 cases), and gain of chromosome 17 (4/12), followed by complete or partial loss of chromosome 9, 13, and 14 (in 3/12 cases). No chromosomal losses or gains were detected in 4 cases. The findings regarding losses and gains in individual cases are summarized in Table 3.

4. Discussion

HLRCC/FHRCC was recently defined as a tumor with variable architectural, cytological and clinical features. Historically, in earlier publications including the WHO 2004 classification, the tumor was described as displaying typically PRCC type 2 histology [2,6,32,36,37]. As the evidence accumulated in the literature, it became evident that the morphologic spectrum of these tumors is much wider than originally suggested. HLRCC/FHRCC includes tumors with predominantly papillary or tubulocystic architecture, usually mixed with other growing patterns representing multiplicity of patterns (cystic, tubular, tubulopapillary, tubulocystic, solid) [4,38-40]. Additionally, other RCC phenotypes have been described within the HLRCC/FHRCC entity, including collecting duct carcinoma [36,38,40-42], clear cell RCC [37,43,44], Wilms tumor [45], tubulocystic RCC [5], unclassified

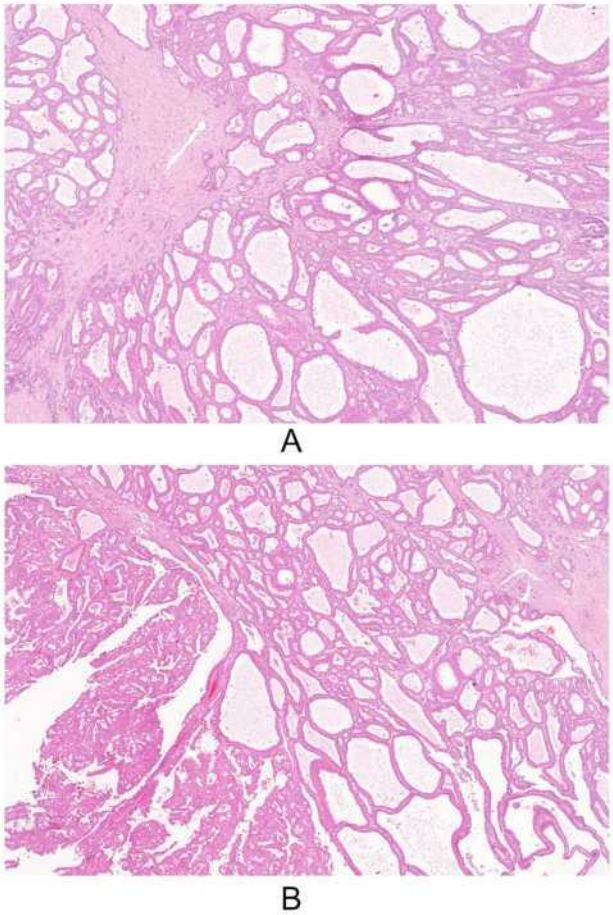

Fig. 2. Pure tubulocystic pattern is not frequently seen. Similar cases are always challenging (A). Mixed architecture is considered to be more characteristic (B).

oncocytic tumor [36,46], and even oncocytic type of RCC resembling SDH-deficient RCC [47]. In fact, HLRCC/FHRCC is a distinct histomolecular entity, which may have been previously labelled as unclassified high-grade RCC [4], PRCC type 2, tubulocystic with dedifferentiated foci, and collecting duct carcinoma. The most important histologic feature of these neoplasms seems to be the presence of a large nucleus with a prominent, inclusion-like eosinophilic nucleolus, surrounded by a clear halo [39]. However, with the current insight into the variable morphologic features associated with HLRCC/FHRCC, it is apparent

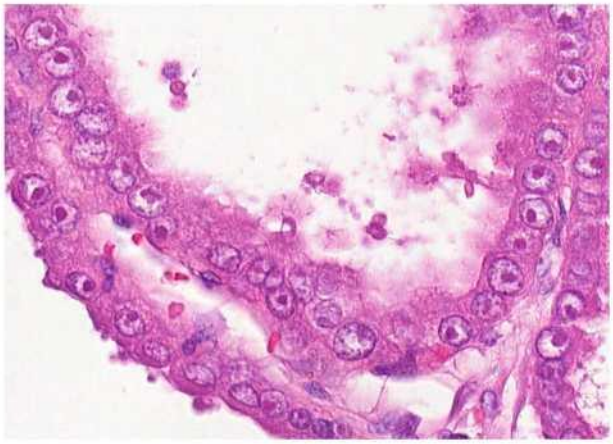

Fig. 3. Deep red macronucleoli with perinucleolar clearing were considered as specific for FHRCC, however they can be present in other renal cell carcinomas.

that the macronucleoli are not constant and specific morphologic feature of these tumors. A combined negative immunohistochemical staining for FH, and strong positive staining for 2SC is used as a useful ancillary tool, which strongly correlate with *FH* gene alterations and morphology compatible with HLRCC/FHRCC [1,4].

In this study, our tumors demonstrated a morphologically non-homogeneous spectrum. In fact, only two cases demonstrated pure papillary architectural growth pattern, while the majority (8 tumors) displayed mixed architectures, of which 6 cases exhibited only focal papillary areas, and 4 cases did not have any papillary foci.

The most frequent chromosomal gain in this study was the gain of chromosome 17 (4/12 cases). Only two cases demonstrated concurrent gains of chromosomes 7 and 17 (as typically seen in PRCC). A broad spectrum of individual gains was detected in the tumor cohort that included chromosomes 2, 3, 7, 10, 13, 15, 16, and 17 more than once. Losses of whole chromosomes or their parts were almost the same frequency as gains in our cohort (30 chromosomal losses, resp. 31 chromosomal gains). The most frequent loss was found in chromosome 4 (5/12 patients), followed by chromosome 15 (4/12 patients), and chromosomes 9, 13, 14 (each in 3/12 patients). Other less frequent individual chromosomal losses were recorded on chromosomes 1, 8, and 18 (each in 2/12 patients).

There was only one previous study that examined the CNV in FHRCC/HLRCC. Koski et al. studied 11 genetically confirmed HLRCCs and attempted to identify the specific chromosomal copy number changes characteristic of HLRCC. All tumors included in their study were morphologically defined as type 2 PRCC, according to the 2004 WHO classification. Array CGH analysis was successful in all 11 cases and showed that the most frequent changes were gains of chromosomes 2, 7, and 17 and losses in 13q12.3-q21.1, 14, 18, and X. They were able to confirm the gain of 17q and losses of 13q, 14q, 18p, and X at a frequency of 38% [32]. Copy number variation pattern in our study was also highly variable, which is similar to what was reported by Koski et al.

In light of the recent evidence, HLRCC/FHRCC is no longer considered part of the PRCC spectrum. PRCC represents a highly heterogeneous group of tumors with broad morphological spectrum and distinct immunohistochemical profile. In fact, CNV pattern of PRCC is much more complex than traditionally thought. Of all PRCC subtypes, PRCC type 1 seems to be the most genetically uniform group, while other types show different degrees of heterogeneity [48]. Nonetheless, the gains of chromosomes 7 and 17 are the most common findings even in PRCC type 2 (reported in 31%–69% for chromosome 7, and 50%–69% for chromosome 17). Other frequent chromosomal changes in PRCC type 2 include a polysomy of chromosomes 12, 16 and 20. Loss of gonosome Y was described in 64–90% male cases of PRCC type 2. Other chromosomal gains described with enormous variability in a small percentage of cases include gains of chromosomes 1, 2, 3, 4, 5, 6, 8, 9, 13, 18, 19 and 22, as well as losses of chromosomes 1, 2, 3, 4,5, 6, 7, 8, 9, 10, 12, 13, 14, 15, 17, 18, 19, 20, 21, 22, and X [10,12,19,22,25,26,48].

On the basis of the current knowledge, we believe that CNV in HLRCC/FHRCC partially overlaps with the CNV described in PRCC. Considering the wide spectrum of numerical aberrations in PRCC, it is not surprising that there is a partial overlap of CNV in HLRCC/FHRCC and PRCC. Nonetheless, we were not able to identify a characteristic CNV associated with FHRCC/HLRCC, which may provide either diagnostic utility or clinical significance in routine practice.

5. Conclusions

Copy number variation pattern in FHRCC/HLRCC appears to be highly variable. The analyzable samples in this study showed complex copy number variations, affecting mainly chromosomes 4, 9, 13, 14, 15, and 17.

Our findings suggest that FHRCC/HLRCC is one of the most heterogeneous renal tumors from histologic and chromosomal perspectives. It demonstrates a variable morphology and the immunohistochemical evaluation can be challenging, CNV does not provide a useful diagnostic tool in identifying these cases. Immunohistochemical staining and especially molecular genetic evaluation of *FH* gene mutations/LOH remain the gold standard in identifying FHRCC/HLRCC.

Table 2
Molecular genetic analyses.

Case	FH mutation analysis	Low pass whole genome sequencing CNVs
Case 1	c.698G > A p.(Arg233His)	−1, −4, −13, −14, −15
Case 2	c.698G > A p.(Arg233His)	−1p, −14, +15
Case 3	c.911_917delCTTTTGT p.(Phe305Leufs*22)	−4, −9, −15, +17
Case 4	c.805delA p.(Ile269fs*15)	Neg.
Case 5	c.395_398delTAAAT p.(Leu132*)	Neg.
Case 6	c.1189G > A p.(Gly397Arg) + LOH	+3, −4, −8p, −9, −13, −15, −18q
Case 7	c.174_177dupTGAAA p.(Leu60*)	−4q, −6q, −8p, −9, −13, −14, −15, −17p, −18q, −20p, −22
Case 9	c.496G > T p.(Gly166*)	+2, −3q, +4, +7, +10q, −16, +17
Case 11	c.239dupA p.(Ile81Aspfs*14)	-4q, +13q, +16q, +17
Case 12	c.589A > T p.(Ile197Phe) + LOH	Neg.
Case 13	c.1118A > G p.Asn373Ser	Neg.
Case 14	c.[(698G > T(;)1098_1099insTT)]/p.[(Arg233Leu(;)Ile367LeufsTer7)]	+1q, +2, +3, +5p, +6, +7, +8, +9, +10, +11, +12, +13, +15, +16, +17, +18, +19, +20, +21, +22

Neg. no loss or gain detected.

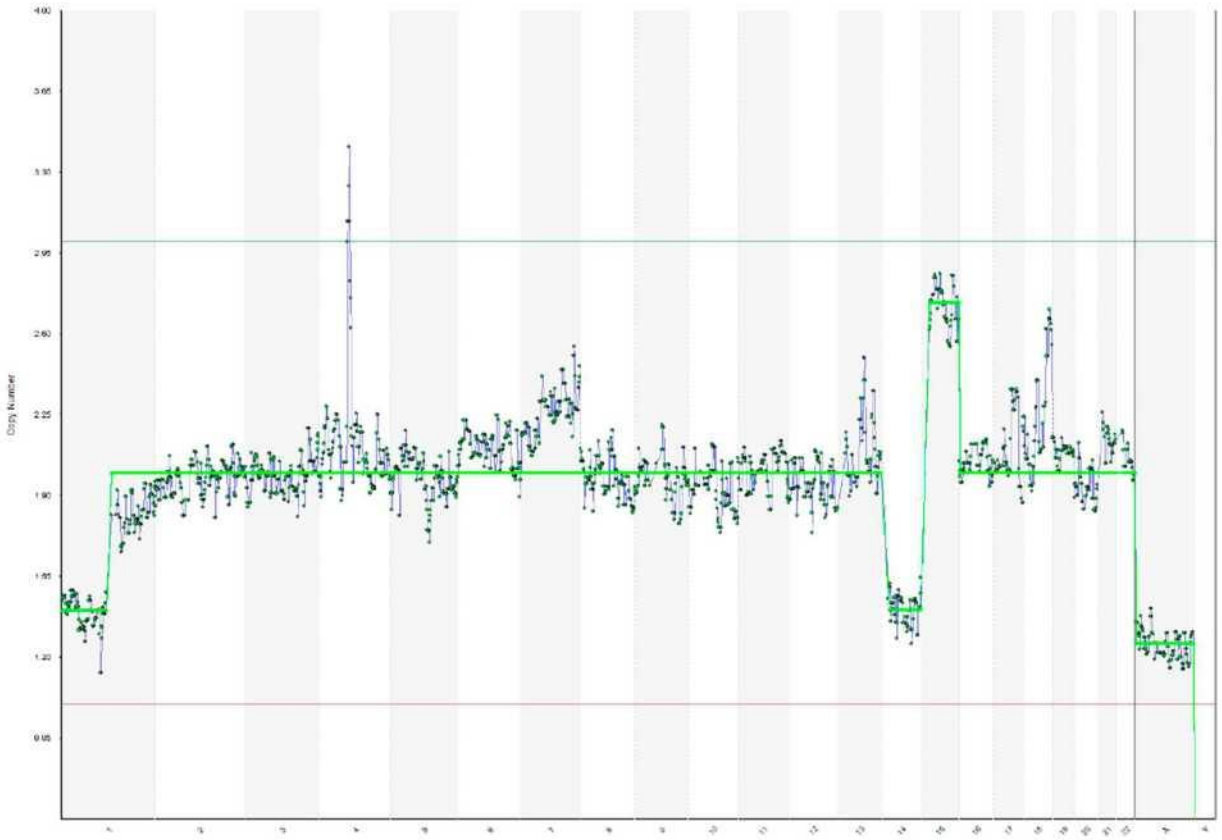

Fig. 4. Chromosomal numerical aberration pattern (CNV) chart of case 2. X axis - numbers of chromosomes, Y axis copy number.

Table 3
Summary of CNV pattern.

Case	Gains	Losses
Case 1	Neg.	−1, −4, −13, −14, −15
Case 2	+15	−1p, −14
Case 3	+17	−4, −9, −15
Case 4	Neg.	Neg.
Case 5	Neg.	Neg.
Case 6	+3	−4, −8p, −9, −13, −15, −18q
Case 7	Neg.	−4q, −6q, −8p, −9, −13, −14, −15, −17p, −18q, −20p, −22
Case 9	+2, +4, +7, +10q, +17	−3q, −16
Case 11	+13q, +16q, +17	−4q
Case 12	Neg.	Neg.
Case 13	Neg.	Neg.
Case 14	+1q, +2, +3, +5p, +6, +7, +8, +9, +10, +11, +12, +13, +15, +16, +17, +18, +19, +20, +21, +22	Neg.

Neg. - negative.

Disclosure of conflict of interest

All authors declare no conflict of interest.

Funding

The study was supported by the Charles University Research Fund (project number Q39), by Institutional Research Fund FN 00669806, and by Biobank Research on Telemedical Approaches for Human Biobanks in a European Region, Bavarian-Czech University Agency (BTHA).

References

[1] Muller M, Guillaud-Bataille M, Salleron J, et al. Pattern multiplicity and fumarate hydratase (FH)/S-(2-succino)-cysteine (2SC) staining but not eosinophilic nucleoli with perinucleolar halos differentiate hereditary leiomyomatosis and renal cell carcinoma-associated renal cell carcinomas from kidney tumors without FH gene alteration. Mod Pathol 2018;31(6):974–83.
[2] Launonen V, Vierimaa O, Kiuru M, et al. Inherited susceptibility to uterine leiomyomas and renal cell cancer. Proc Natl Acad Sci U S A 2001;98(6):3387–92.
[3] Smith S, Trpkov K, Mehra R, et al. Is Tubulocystic carcinoma with dedifferentiation a form of HLRCC/fumarate hydratase-deficient RCC? In. Mod Pathol 2015;260A.
[4] Trpkov K, Hes O, Agaimy A, et al. Fumarate hydratase-deficient renal cell carcinoma is strongly correlated with fumarate hydratase mutation and hereditary Leiomyomatosis and renal cell carcinoma syndrome. Am J Surg Pathol 2016;40(7):865–75.
[5] Smith SC, Trpkov K, Chen YB, et al. Tubulocystic carcinoma of the kidney with poorly differentiated foci: a frequent morphologic pattern of fumarate hydratase-deficient renal cell carcinoma. Am J Surg Pathol 2016;40(11):1457–72.
[6] Eble JN. Sauter G. Epstein JI: Sesterhenn IA. World Health Organization Classification of Tumours Pathology and Genetics Tumours of the Urinary System and Male Genital Organs. IARC Press Lyon; 2004.
[7] Srigley JR, Delahunt B, Eble JN, et al. The International Society of Urological Pathology (ISUP) Vancouver classification of renal neoplasia. Am J Surg Pathol 2013;37(10):1469–89.
[8] Moch H. Humphrey PA. Ulbright TM: Reuter VE. WHO classification of tumours of the urinary system and male genital organs. IARC Press Lyon; 2016.
[9] Renshaw AA, Zhang H, Corless CL, et al. Solid variants of papillary (chromophil) renal cell carcinoma: clinicopathologic and genetic features. Am J Surg Pathol 1997;21(10):1203–9.
[10] Jiang F, Richter J, Schraml P, et al. Chromosomal imbalances in papillary renal cell carcinoma: genetic differences between histological subtypes. Am J Pathol 1998;153(5):1467–73.
[11] Fuzesi L, Gunawan B, Bergmann F, et al. Papillary renal cell carcinoma with clear cell cytomorphology and chromosomal loss of 3p. Histopathology 1999;35(2):157–61.
[12] Gunawan B, von Heydebreck A, Fritsch T, et al. Cytogenetic and morphologic typing of 58 papillary renal cell carcinomas: evidence for a cytogenetic evolution of type 2 from type 1 tumors. Cancer Res 2003;63(19):6200–5.
[13] Salama ME, Worsham MJ, DePeralta-Venturina M. Malignant papillary renal tumors with extensive clear cell change: a molecular analysis by microsatellite analysis and fluorescence in situ hybridization. Arch Pathol Lab Med 2003;127(9):1176–81.

[14] Lefevre M, Couturier J, Sibony M, et al. Adult papillary renal tumor with oncocytic cells: clinicopathologic, immunohistochemical, and cytogenetic features of 10 cases. Am J Surg Pathol 2005;29(12):1576–81.
[15] Hes O, Brunelli M, Michal M, et al. Oncocytic papillary renal cell carcinoma: a clinicopathologic, immunohistochemical, ultrastructural, and interphase cytogenetic study of 12 cases. Ann Diagn Pathol 2006;10(3):133–9.
[16] Kunju LP, Wojno K, Wolf Jr. JS, et al. Papillary renal cell carcinoma with oncocytic cells and nonoverlapping low grade nuclei: expanding the morphologic spectrum with emphasis on clinicopathologic, immunohistochemical and molecular features. Hum Pathol 2008;39(1):96–101.
[17] Gobbo S, Eble JN, Grignon DJ, et al. Clear cell papillary renal cell carcinoma: a distinct histopathologic and molecular genetic entity. Am J Surg Pathol 2008;32(8):1239–45.
[18] Park BH, Ro JY, Park WS, et al. Oncocytic papillary renal cell carcinoma with inverted nuclear pattern: distinct subtype with an indolent clinical course. Pathol Int 2009;59(3):137–46.
[19] Antonelli A, Tardanico R, Balzarini P, et al. Cytogenetic features, clinical significance and prognostic impact of type 1 and type 2 papillary renal cell carcinoma. Cancer Genet Cytogenet 2010;199(2):128–33.
[20] Petersson F, Bulimbasic S, Hes O, et al. Biphasic alveolosquamoid renal carcinoma: a histomorphological, immunohistochemical, molecular genetic, and ultrastructural study of a distinctive morphologic variant of renal cell carcinoma. Ann Diagn Pathol 2012;16(6):459–69.
[21] Xia QY, Rao Q, Shen Q, et al. Oncocytic papillary renal cell carcinoma: a clinicopathological study emphasizing distinct morphology, extended immunohistochemical profile and cytogenetic features. Int J Clin Exp Pathol 2013;6(7):1392–9.
[22] Yu W, Zhang W, Jiang Y, et al. Clinicopathological, genetic, ultrastructural characterizations and prognostic factors of papillary renal cell carcinoma: new diagnostic and prognostic information. Acta Histochem 2013;115(5):452–9.
[23] Mantoan Padilha M, Billis A, Allende D, et al. Metanephric adenoma and solid variant of papillary renal cell carcinoma: common and distinctive features. Histopathology 2013;62(6):941–53.
[24] Zhang Y, Yong X, Wu Q, et al. Mucinous tubular and spindle cell carcinoma and solid variant papillary renal cell carcinoma: a clinicopathologic comparative analysis of four cases with similar molecular genetics datum. Diagn Pathol 2014;9:194.
[25] Kovac M, Navas C, Horswell S, et al. Recurrent chromosomal gains and heterogeneous driver mutations characterise papillary renal cancer evolution. Nat Commun 2015;6:6336.
[26] Marsaud A, Dadone B, Ambrosetti D, et al. Dismantling papillary renal cell carcinoma classification: the heterogeneity of genetic profiles suggests several independent diseases. Genes Chromosomes Cancer 2015;54(6):369–82.
[27] Hes O, Condom Mundo E, Peckova K, et al. Biphasic Squamoid alveolar renal cell carcinoma: a distinctive subtype of papillary renal cell carcinoma? Am J Surg Pathol 2016;40(5):664–75.
[28] Pivovarcikova K, Peckova K, Martinek P, et al. "mucin"-secreting papillary renal cell carcinoma: clinicopathological, immunohistochemical, and molecular genetic analysis of seven cases. Virchows Arch 2016;469(1):71–80.
[29] Peckova K, Martinek P, Pivovarcikova K, et al. Cystic and necrotic papillary renal cell carcinoma: prognosis, morphology, immunohistochemical, and molecular-genetic profile of 10 cases. Ann Diagn Pathol 2017;26:23–30.
[30] Han G, Yu W, Chu J, et al. Oncocytic papillary renal cell carcinoma: a clinicopathological and genetic analysis and indolent clinical course in 14 cases. Pathol Res Pract 2017;213(1):1–6.
[31] Skenderi F, Ulamec M, Vanecek T, et al. Warthin-like papillary renal cell carcinoma: Clinicopathologic, morphologic, immunohistochemical and molecular genetic analysis of 11 cases. Ann Diagn Pathol 2017;27:48–56.
[32] Koski TA, Lehtonen HJ, Jee KJ, et al. Array comparative genomic hybridization identifies a distinct DNA copy number profile in renal cell cancer associated with hereditary leiomyomatosis and renal cell cancer. Genes Chromosomes Cancer 2009;48(7):544–51.
[33] Alaghehbandan R, Stehlik J, Trpkov K, et al. Programmed death-1 (PD-1) receptor/PD-1 ligand (PD-L1) expression in fumarate hydratase-deficient renal cell carcinoma. Ann Diagn Pathol 2017;29:17–22.
[34] Sperga M, Martinek P, Vanecek T, et al. Chromophobe renal cell carcinoma–chromosomal aberration variability and its relation to Paner grading system: an array CGH and FISH analysis of 37 cases. Virchows Arch 2013;463(4):563–73.
[35] Munchel S, Hoang Y, Zhao Y, et al. Targeted or whole genome sequencing of formalin fixed tissue samples: potential applications in cancer genomics. Oncotarget 2015;6(28):25943–61.
[36] Toro JR, Nickerson ML, Wei MH, et al. Mutations in the fumarate hydratase gene cause hereditary leiomyomatosis and renal cell cancer in families in North America. Am J Hum Genet 2003;73(1):95–106.
[37] Vocke CD, Ricketts CJ, Merino MJ, et al. Comprehensive genomic and phenotypic characterization of germline FH deletion in hereditary leiomyomatosis and renal cell carcinoma. Genes Chromosomes Cancer 2017;56(9):484–92.
[38] Wei MH, Toure O, Glenn GM, et al. Novel mutations in FH and expansion of the spectrum of phenotypes expressed in families with hereditary leiomyomatosis and renal cell cancer. J Med Genet 2006;43(1):18–27.
[39] Merino MJ, Torres-Cabala C, Pinto P, Linehan WM. The morphologic spectrum of kidney tumors in hereditary leiomyomatosis and renal cell carcinoma (HLRCC) syndrome. Am J Surg Pathol 2007;31(10):1578–85.
[40] Grubb 3rd RL, Franks ME, Toro J, et al. Hereditary leiomyomatosis and renal cell cancer: a syndrome associated with an aggressive form of inherited renal cancer. J Urol 2007;177(6):2074–80.
[41] Alam NA, Rowan AJ, Wortham NC, et al. Genetic and functional analyses of FH mutations in multiple cutaneous and uterine leiomyomatosis, hereditary leiomyomatosis and renal cancer, and fumarate hydratase deficiency. Hum Mol Genet 2003;12(11):1241–52.
[42] Chen YB, Brannon AR, Toubaji A, et al. Hereditary leiomyomatosis and renal cell carcinoma syndrome-associated renal cancer: recognition of the syndrome by pathologic features and the utility of detecting aberrant succination by immunohistochemistry. Am J Surg Pathol 2014;38(5):627–37.
[43] Lehtonen HJ, Blanco I, Piulats JM, et al. Conventional renal cancer in a patient with fumarate hydratase mutation. Hum Pathol 2007;38(5):793–6.
[44] Harris M, Wallace J, Winship I, et al. Hereditary renal cell carcinoma: the clue can be in the skin. Intern Med J 2009;39(12):e12–3.
[45] Badeloe S, van Spaendonck-Zwarts KY, van Steensel MA, et al. Wilms tumour as a possible early manifestation of hereditary leiomyomatosis and renal cell cancer? Br J Dermatol 2009;160(3):707–9.
[46] Li Y, Reuter VE, Matoso A, et al. Re-evaluation of 33 'unclassified' eosinophilic renal cell carcinomas in young patients. Histopathology 2018;72(4):588–600.
[47] Smith SC, Sirohi D, Ohe C, et al. A distinctive, low-grade oncocytic fumarate hydratase-deficient renal cell carcinoma, morphologically reminiscent of succinate dehydrogenase-deficient renal cell carcinoma. Histopathology 2017;71(1):42–52.
[48] Pitra T, Pivovarcikova K, Alaghehbandan R, Hes O. Chromosomal numerical aberration pattern in papillary renal cell carcinoma: review article. Ann Diagn Pathol 2017. [Epub ahead of print].

1.3.3 Fumarát hydratáza deficientní renální karcinom a jemu podobný renální karcinom: Komparativní studie 23 geneticky testovaných případů

Pro účely této morfologické studie bylo z plzeňského registru nádorů vyhledáno a opětovně hodnoceno 23 renálních neoplázií suspektních z diagnózy FHRCC (na podkladě morfologie tumorů). U všech případů byla provedena molekulárně genetická analýza (průkaz mutace/LOH genu pro *FH*), morfologické hodnocení (architektonika, cytologické znaky) a základní imunohistochemické barvení (FH).

Genetické vyšetření prokázalo alteraci ve *FH* genu u 13 případů (případy finálně diagnostikované jako FHRCC), u 10 případů nebyla detekována žádná alterace *FH* genu (FH-like RCC). Tumory s geneticky potvrzenou diagnózou FHRCC měly heterogenní architektoniku kombinující různé růstové vzorce ve většině případů (9/13). Ve všech případech FHRCC byla zastiženy prominentní jadérka, u 10 případů i perinukleolární projasnění. Imunohistochemický průkaz FH byl proveden u 7 FHRCC, u 6/7 případů bylo barvení negativní, avšak 1/7 FHRCC vykazoval silnou difúzní reaktivitu. Skupina FH-like RCC byla více uniformní v architektonice, pouze jeden případ kombinoval různé růstové varianty. Všechny případy FH-like RCC měly prominentní jadérka a perinukleolární projasnění bylo zastiženo v 8/10 případů. Osm FH-like RCCs bylo pozitivní v imunohistochemickém průkazu FH, dva případy však vykazovaly kompletní negativitu.

Z výsledků je patrné, že čistě na podkladě morfologie či imunohistochemického vyšetření je zcela nemožné odlišit FHRCC od nádorů, které FHRCC jen napodobují (FH-like RCC). Diagnostika těchto lézí se tak zcela opírá o molekulárně genetické vyšetření *FH* genu. Typicky u FHRCC popisované morfologické znaky (prominentní eosinofilní jadérka s perinukleolarním projasněním) jsou často nacházeny i u jiných renálních neoplázií.

Fumarate hydratase deficient renal cell carcinoma and fumarate hydratase deficient-like renal cell carcinoma: Morphologic comparative study of 23 genetically tested cases

Kristýna Pivovarčíková[1], Petr Martínek[1], Kiril Trpkov[2], Reza Alaghehbandan[3], Cristina Magi-Galluzzi[4], Enric Condom Mundo[5], Daniel Berney[6], Saul Suster[7], Anthony Gill[8], Boris Rychlý[9], Květoslava Michalová[1], Tomáš Pitra[10], Milan Hora[10], Michal Michal[1], Ondřej Hes[1]

[1] Department of Pathology, Charles University in Prague, Faculty of Medicine in Plzeň, Pilsen, Czech Republic
[2] Calgary Laboratory Services and University of Calgary, Calgary, AB, Canada
[3] Department of Pathology, Faculty of Medicine, University of British Columbia, Royal Columbian Hospital, Vancouver, BC, Canada
[4] Robert J. Tomsich Pathology and Laboratory Medicine Institute, Cleveland Clinic, Cleveland, OH, USA
[5] Department of Pathology, Bellvitge Biomedical Research Institute (IDIBELL), Barcelona, Spain
[6] Bart's Cancer Center, London, United Kingdom
[7] Department of Pathology, Medical College Wisconsin, Milwaukee, WI, USA
[8] Royal North Shore Hospital, University of Sydney, Sydney, NSW, Australia
[9] Department of Pathology, Cytopathos, Bratislava, Slovakia
[10] Department of Urology, Charles University in Prague, Faculty of Medicine in Plzeň, Pilsen, Czech Republic

SUMMARY

Hereditary leiomyomatosis and renal cell carcinoma-associated renal cell carcinoma (HLRCC)/ fumarate hydratase deficient renal cell carcinoma (FHRCC) is an aggressive tumor defined by molecular genetic changes - alteration in fumarate hydratase (*FH*) gene. The morphologic spectrum of HLRCC/FHDRCC is remarkably variable. The presence of large nuclei and prominent dark red inclusion-like nucleoli and perinucleolar clearing are considered as helpful morphologic clue. We selected 23 renal neoplasms primarily based on their morphologic features suspicious for HLRCC/FHDRCC. Morphological, basic immunohistochemical, and genetic analysis was performed. The tumors were divided in two groups according to the molecular genetic findings. The first group included 13 tumors with detected *FH* mutation/LOH (compatible with diagnosis FHRCC), and the second group included 10 tumors without *FH* mutation/LOH (FH-like RCCs). In the FHRCC group, the vast majority of cases (9/13) had mixed morphology with different architectural growth patterns. All cases showed prominent macronucleoli, and perinucleolar clearing was found in 10/13 cases. Immunohistochemically, 6/7 FHRCC cases were negative for FH antibody, while one case showed strong diffuse FH reactivity. The FH-like RCC group showed more uniform architectural growth pattern. All 10 tumors had prominent macronucleoli, and perinucleolar clearing was present in 8/10 cases. Eight FH-like RCC cases showed diffuse strong positivity for FH, although 2 cases were completely negative for FH. It is evident that neither morphologic feature nor immunohistochemical analysis can be reliably used in routine practice for the diagnosis of HLRCC/FHRCC. In suspected cases, the diagnosis of HLRCC/FHRCC can be confirmed by molecular-genetic testing for *FH* mutation. It should be noted that the traditionally described morphologic features of HLRCC/FHRCC (prominent eosinophilic macronuclei with perinucleolar halos) can frequently be seen in other renal neoplasms.

Keywords: fumarate hydratase – HLRCC – renal cell carcinoma

Fumarát hydratáza deficientní karcinom z renálních buněk a jemu podobný karcinom z renálních buněk: Komparativní studie 23 geneticky testovaných případů

SOUHRN

S hereditární leiomyomatózou a renálním karcinomem asociovaný renální karcinom (HLRCC)/ fumarát hydratáza deficientní renální karcinom (FHRCC) je agresivní tumor definovaný na základě přítomnosti molekulárně genetické změny – alterace genu pro fumarát hydratázu (FH). Morfologické spektrum těchto neoplázií je široké, avšak přítomnost objemných jader s prominentními tmavě červenými „inklusními" jadérky a s perinukleolárním projasněním byla dlouho považována za důležitý morfologický diagnostický znak. Z Plzeňského registru nádorů bylo vyhledáno a opětovně hodnoceno 23 renálních neoplázií suspektní z FHRCC, primárně na podkladě morfologie. U všech případů byla provedena molekulárně genetická analýza (průkaz mutace/LOH genu pro fumarát hydratázu), detailní morfologické hodnocení (architektonika, cytologické znaky) a základní imunohistochemické barvení (FH). Genetické vyšetření prokázalo alteraci v FH genu u 13 případů (FHRCC), u 10 případů nebyla detekována žádná alterace *FH* genu (FH-like RCC). Tumory s geneticky potvrzenou diagnózou FHRCC měly heterogenní architektoniku kombinující různé růstové vzorce ve většině případů (9/13). Ve všech případech FHRCC byly zastiženy prominentní jadérka, u 10 případů i perinukleolární projasnění. Imunohistochemický průkaz protilátkou FH byl proveden u 7 FHRCC, u 6/7 případů bylo barvení negativní, avšak 1/7 FHRCC vykazoval silnou difúzní reaktivitu. Skupina FH-like RCC byla více uniformní v architektonice, pouze jeden případ kombinoval různé růstové varianty. Všechny případy FH-like RCC měly prominentní jadérka a perinukleolární projasnění bylo zastiženo v 8/10 případů. Osm FH-like RCCs bylo pozitivní v imunohistochemickém průkazu FH, dva případy však vykazovali kompletní negativitu. Z výsledků je patrné, že čistě na podkladě morfologie či imunohistochemického vyšetření je zcela nemožné odlišit FHRCC od nádorů, které FHRCC jen napodobují (FH-like RCC). Diagnostika těchto lézí se tak zcela opírá o molekulárně genetické vyšetření FH genu. Typicky u FHRCC popisované morfologické znaky (prominentní eosinofilní jadérka s perinukleolárním projasněním) jsou často nacházeny i u jiných renálních neoplázií.

Klíčová slova: fumarát hydratáza – HLRCC – renální karcinom

Cesk Patol 2019; 55(4): 244–249

✉ ***Correspondence address:***
Kristýna Pivovarčíková, MD, PhD
Department of Pathology
Medical Faculty and Charles University Hospital Plzen
Alej Svobody 80, 304 60 Pilsen
Czech Republic
e-mail: pivovarcikovak@fnplzen.cz

Hereditary leiomyomatosis and renal cell carcinoma-associated renal cell carcinoma (HLRCC) is an aggressive tumor defined by molecular genetic changes, namely mutation in fumarate hydratase (*FH*) gene. It has been recently proposed that renal tumors associated with impaired *FH* gene to be named fumarate hydratase deficient renal cell carcinoma (FHRCC). The term HLRCC is used for patients with germline mutation of *FH* gene, autosomal dominant heredity and syndromic presentation with

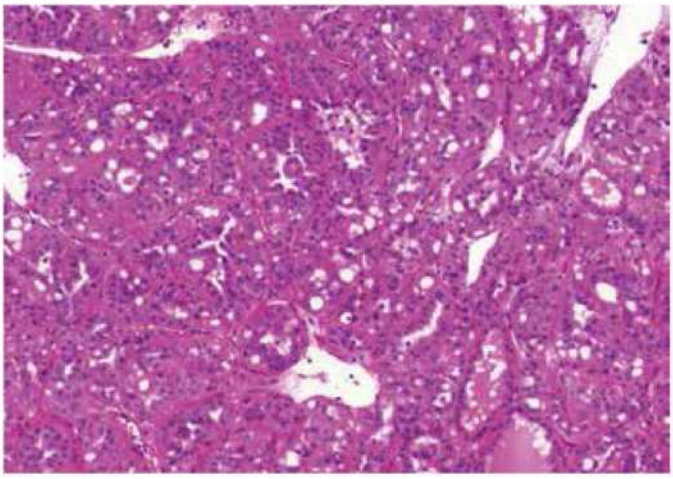

Fig. 1. Cribriform pattern in case of renal cell carcinoma mimicking FHRCC (FH-like RCC). HE 100x

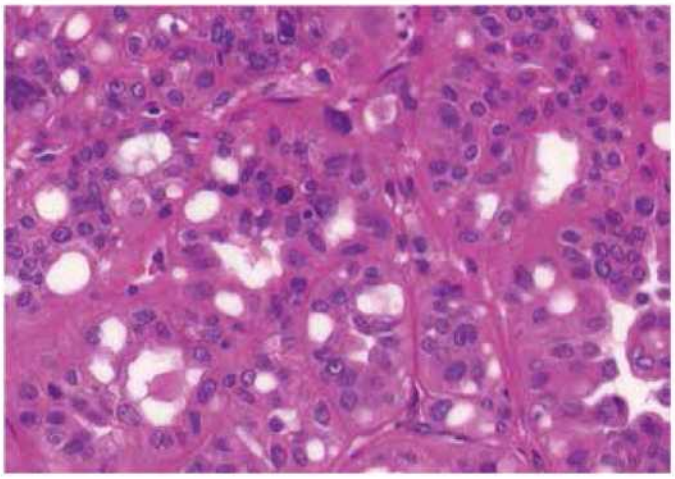

Fig. 2. Deep red macronucleoli and perinucleolar clearing in same case, showed in Figure 1. HE 400x

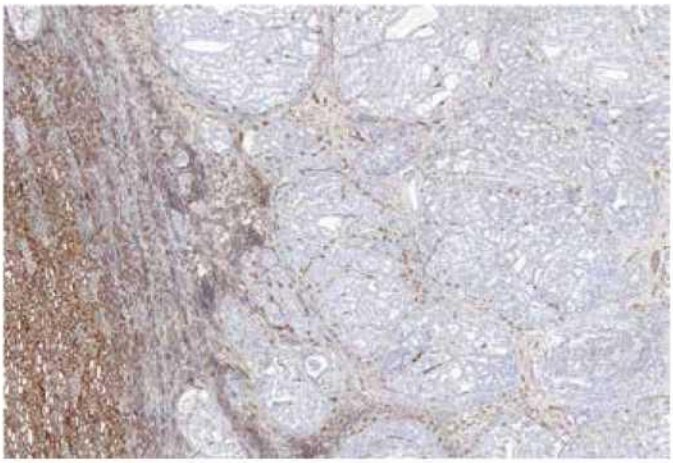

Fig. 3. Renal cell carcinoma mimicking FHRCC (no mutation/LOH of *FH gene* detected) with negative immunohistochemical staining for FH. 40x

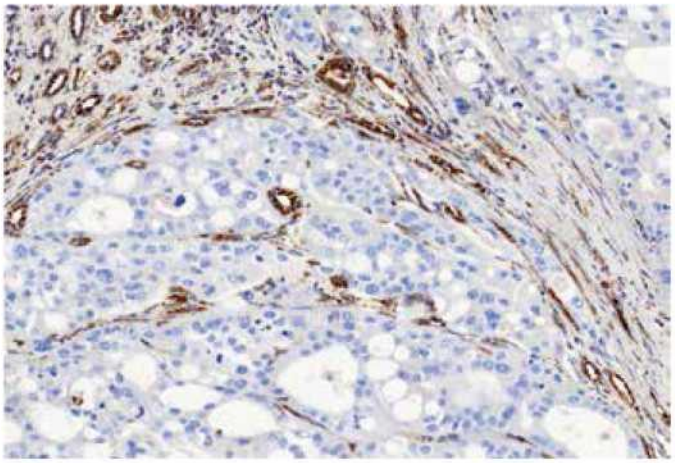

Fig. 4. Immunohistochemical staining for FH – detail. 200x

concurrent presence of cutaneous and/or uterine leiomyomas (1, 2). On the other hand, the term FHRCC is recommended for tumors with suggestive morphology and typical immunophenotype in the setting of uncertain clinical and family history and unknown genetic status. FHRCC also allows designation of cases that might represent apparently sporadic forms, harboring somatic (not germline) alterations in the *FH* gene (3-5). Overall, HLRCC/FHRCC is a distinct histomolecular entity.

The morphologic spectrum of HLRCC/FHRCC is remarkably variable, with various architectural and histologic features being reported in the literature (4-19). Immunohistochemical examination can be helpful in the diagnosis of these tumors with combined negative staining for fumarate hydratase (FH) and strong positive staining for 2-succinocysteine (2SC), demonstrating good sensitivity and excellent specificity (4, 20). Nonetheless, molecular genetic testing for *FH* mutation/LOH still remains the gold standard for the diagnosis of HLRCC/FHRCC.

While HLRCC/FHRCC is one of the most challenging renal tumors in routine practice, its detection can have a significant impact on family members and potentially the patient. Thus, pathologists should be aware of this entity, given its highly variable morphology and difficult immunohistochemical evaluation, to be able to identify suspect cases to be genetically tested.

In this study, we compared morphologic, immunohistochemical and molecular-genetic features between FHRCC (confirmed cases) and FH-like RCC tumors (suspicious cases).

MATERIAL AND METHODS

Case identification

Twenty three tumors suspect for FHRCC primarily based on morphology were identified in the Plzen Tumor Registry out of 26,000 renal neoplasms. Nine cases in this study were previously published (4), and 13 cases were included which were previously published by our group (21). All cases were reviewed by two Urologic Pathologists (KP and OH). Tissues for light microscopy were fixed in 4% formaldehyde and embedded in paraffin using routine procedure. Sections 4 μm thick were cut from tissue blocks and stained with hematoxylin and eosin (H&E). There were 1 to 48 tissue blocks (median 1) for each case. However all original HE slides were reviewed and evaluated. One representative block was selected for immunohistochemical and molecular–genetic studies (usually block with internal positive control of non-neoplastic renal parenchyma).

Tumors were divided in two groups after molecular genetic analysis. The first group included 13 tumors with detected *FH* mutation/LOH (compatible with diagnosis FHRCC), and the second group included 10 tumors without *FH* mutation/LOH (these cases are hereafter referred as FH-like RCC).

Architectural patterns, and morphologic features including the presence of prominent macronucleoli and perinucleolar clearing were analyzed in all 23 tumors. Macronucleoli were described as a prominent dark red inclusion-like nucleoli, and

a perinucleolar clearing was defined as an clear area between the nucleus and the cytoplasm (as seen by light microscopy at high magnification). Different growing patterns were detected in the tumors (papillary, tubulary, solid, cribriform, sarcomatoid, multicystic), every architectural pattern representing more than 5% of the whole tumor mass were count into definitive architectural results.

Immunohistochemistry

The immunohistochemical analysis was performed using a VentanaBenchMark ULTRA (Ventana Medical System, Inc., Tucson, Arizona), FH antibody (J-13, Santa Cruz Biotechnology, dilution 1:3000) was used. Appropriate positive controls were included.

Molecular genetic testing

All cases demonstrating suspicious morphology for FHRCC underwent molecular evaluation for *FH* gene mutation status by Sanger sequencing and loss of heterozygosity studies on DNA extracted from macrodissected FFPE tissue. We also evaluated 10 cases with retained *FH* expression for *FH* mutation, as a negative control group. Previously described custom primer sets were used for Sanger sequencing, and the whole coding sequence including exon-intron junctions was sequenced using primers designed to produce short amplicons suitable for degraded formalin fixed DNA(22). Loss of heterozygosity studies were performed using a previously described set of 6 polymorphic short tandem repeat markers (D1S517, D1S2785, D1S180, AFM214xe11, D1S547, and D1S2842), surrounding the *FH* gene (22).

RESULTS

Fumarate hydratase renal cell carcinoma group (FH RCC group)

FHRCC cohort included 13 tumors from 12 patients. Patients were 8 males and 4 females, with age range of 24-65 years (mean 50.8 years). Tumor size ranged from 0.9-18 cm (mean 9.6 cm).

Molecular genetic analysis confirmed the presence of *FH* mutation/LOH in all 13 cases (Table 1).

Histologic assessment showed mixed patterns in majority of cases (9/13 cases). Pure papillary architecture was detected only in 3/13 cases. Sarcomatoid differentiation was identified in 2/13 tumors. Cytoplasm of the neoplastic cells were bright eosinophilic in 9/13 cases, and weak to scant eosinophilic in four cases. All 13 tumors had prominent macronucleoli (focally in 4 tumors). Perinucleolar clearing was found in 10/13 (focally in 7 tumors).

Material for seven tumors was available for immunohistochemical examination with FH antibody (7/13). Negative staining for FH was found in six cases (with presence of an appropriate positive internal control in adjacent non-neoplastic renal parenchyma), while one case showed strong diffuse FH reactivity (this case demonstrated genetically *FH* mutation c.1118A>G p.Asn373Ser).

Fumarate hydratase-like renal cell carcinoma group (FH-like RCC group)

Five males and five females with age range of 21-82 years (mean 62.4 years) were included in this group. Tumor size ranged from 2.6-11 cm (mean 7.5 cm).

No mutations/LOH of *FH* gene was identified in these 10 cases.

All 10 cases were considered suspicious for FHRCC based on morphology. These tumors were purely papillary in 4 cases, tubulopapillary in 4 cases, tubular in one case, and combined tubulo-cystic and cribriform in one case. Cytoplasm of the neoplastic cells was bright eosinophilic in 8/10 cases, while only focally in two cases. All 10 tumors had prominent macronucleoli (in one case only focally), and perinucleolar clearing was present in 8/10 cases (in 2 cases focally).

Immunohistochemistry showed diffuse strong positivity for FH in 8 cases, which was confirmed by the absence of *FH* mutations. Although 2 cases were completely negative for FH by immunohistochemistry (with an appropriate positive internal control), we were unable to demonstrate *FH* mutations in these cases.

Finally, all these 10 cases were classified as papillary renal cell carcinoma (PRCC), according to the current WHO classification (2). Two cases fulfilled the criteria for diagnosis PRCC type 1, and 8 tumors were classified as PRCC not otherwise specified (NOS).

DISCUSSION

In early publications, even in WHO 2004, the HLRCC/FHRCC was described as displaying typically PRCC type 2 histology (6,9). In recent years, the morphologic spectrum of HLRCC/FHRCC has expanded. It is now evident that the histologic appearance of this tumor is nearly unpredictable. HLRCC/FHRCC includes tumors with predominantly papillary or tubulocystic architecture, usually mixed with other growing patterns (cystic, tubulary, tubulopapillary, tubulocystic, solid). Sometimes, these tumors can closely mimic other renal neoplastic entities – e.g. collecting duct carcinoma, clear cell RCC, tubulocystic RCC, unclassified oncocytic tumor, or even oncocytic type of RCC resembling SDH-deficient RCC (4,5,7,8,10-13,15-19).

Historically, the presence of large nuclei, prominent dark red inclusion-like nucleoli and perinucleolar clearing were considered as helpful morphologic clue (11). However, it is now recognized that even these morphologic features are not consistently present. Recent study by Muller´s group clearly showed that these histologic features are not distinctive for HLRCC/FHRCC. They compared pathological features and imunohistochemical profile (FH/2SC immunohistochemistry) of 24 renal cell carcinomas from proven *FH* mutations carriers and 12 PRCC type 2 from patients without *FH* mutations. In this study, they reported the presence of prominent eosinophilic macronuclei with perinucleolar clearing in 58% PRCC type 2 from patients with no *FH* germline mutation. Further, they concluded that multiplicity of architectural patterns, rhabdoid/sarcomatoid components and combined FH/2SC staining can differentiate HLRCC from type 2 PRCC with efficient *FH* gene (20).

We investigated 23 renal tumors with suspicious histology for HLRCC/FHRCC. The vast majority of these cases were send to us by experienced uropathologists, either for a second opinion or for a molecular-genetic study. The histology was indeed suggestive of FHRCC in all cases, with predominantly papillary growth, often mixed with other patterns, prominent macronuclei (23/23), and perinucleolar clearing (18/23). The *FH* mutation/LOH was confirmed genetically in 13 cases. Four of the 13 genetically proven FHRCC in our cohort showed uniform architecture (3 with papillary and one with tubulocystic pattern), while 9 FHRCCs demonstrated mixed architectural patterns. On the other hand, the tumors that resembled FHRCC (FH-like RCC) were more architecturally uniform. Only one FH-like RCC had mixed growth pattern. Our study along with Muller's study clearly showed that the multiplicity of architectural patterns in conjunction with pertinent immunohistochemical profile may help differentiate HLRCC/FHRCC from PRCC. It should be noted

Table 1. FH deficient RCC and FH deficient-like RCC - Basic clinical data and results of morphologic, immunohistochemical a molecular-genetic study.

Case	Age (years)	Sex	Size (cm)	*FH* mutation	Pattern	Cytoplasm	Macronucleoli	Perinucleolar clearing	FH - IHC	Final diagnosis
Case 1	51	F	Multiple 1.4, 1.0, 1.6, 0.6	c.698G>A p.(Arg233His)	Papillary, tubulocystic, cribriform	eosin	+	+	NP	FHRCC
Case 2**	52	F	Multiple 0.9, 0.6, 0.3, 0.9, 0.2, 0.4	c.698G>A p.(Arg233His)	Papillary	eosin	+ (foc.)	+ (foc.)	NP	FHRCC
Case 3	44	M	7	c.911_917delCTTTTGT p.(Phe305Leufs*22)	Tubulocystic	Scant, Weak eosin	+	+ (foc.)	-	FHRCC
Case 4	45	F	7	c.805delA p.(Ile269fs*15)	Papillary, tubulary	eosin	+ (foc.)	+ (foc.)	NP	FHRCC
Case 5	42	M	10	c.395_398delTAAAT p.(Leu132*)	Papillary, tubulary, cystic	eosin	+	+ (foc.)	NP	FHRCC
Case 6	65	M	18	c.1189G>A p.(Gly397Arg) + LOH	Sarcomatoid, tubulocystic	Scant, eosin	+	-	-	FHRCC
Case 7	60	M	8	c.174_177dupTGAAA p.(Leu60*)	Papillary, cystic, tubulopapillary	eosin	+	-	-	FHRCC
Case 8	50	F	10.9	c.139C>T p.(Gln47Ter) + LOH	Papillary	eosin	+ (foc.)	+ (foc.)	NP	FHRCC
Case 9	60	M	8	c.496G>T p.(Gly166*)	Papillary, tubulocystic, cystic	Weak, eosin	+	+	-	FHRCC
Case 10	52	M	14	c.1385_1390+6del	Solid, sarcomatoid	eosin	+	-	NP	FHRCC
Case 11	54	M	14	c.239dupA p.(Ile81Aspfs*14)	Papillary	eosin	+	+ (foc.)	-	FHRCC
Case 12	61	M	12.5	c.589A>T p.(Ile197Phe) + LOH	Solid-papillary, tubulocystic	eosin	+	+	-	FHRCC
Case 13	24	F	Multiple 2.3 and 13	c.1118A>G p.Asn373Ser	Tubulary, multicystic	Scant, eosin	+ (foc.)	+ (foc.)	+++	FHRCC
Case 14	35	M	11	Neg.	Tubulopapillary	eosin	+	-	+++	PRCC NOS (oncocytic)
Case 15	81	F	4.2	Neg.	Papillary compressed	Weak eosin	+	+	++	PRCC NOS
Case 16	72	F	2.6	Neg.	Tubulocystic, cribriform	eosin	+	+ (foc.)	-	PRCC NOS
Case 17	21	F	5.5	Neg.	papillary	eosin	+	+	-	PRCC NOS (with mucin-like)
Case 18	50	M	10.1	Neg.	papillary	Weak eosin	+	+	+++	PRCC NOS (with clear cell changes)
Case 19	80	M	11	Neg.	tubulopapillary	Weak eosin	+	+	+++	PRCC NOS (solid)
Case 20	62	M	6.4	Neg.	tubulary	eosin	+	+	+++	PRCC NOS
Case 21	67	F	8.5	Neg.	papillary	eosin*	+ (foc.)	-	+++	PRCC type 1
Case 22	74	F	4.2	Neg.	tubulopapillary	eosin	+	+ (foc.)	+++	PRCC type 1
Case 23	82	M	11	Neg.	tubulopapillary	eosin	+	+	+++	PRCC NOS

Yellow block FHdeficient RCC, *green block* FHdeficient-like RCC, *M* male, *F* female, *Neg.* negative, *eosin*eosinophilic, *largedepositsofhemosiderin, *foc.*focally, +present, - absent, *NP* not performed, ** recurrence of case 1, *FH-IHC* immunohistochemical examination with FH antibody

that prominent macronucleoli and perinucleolar clearing are not very specific for this type of neoplasia, and as such it should not be used as a determining criteria for the diagnosis of HLRCC/FHRCC.

Immunohistochemistry can be a useful diagnostic tool in these tumors. Concurrent negative staining for FH and positive staining for 2SC should demonstrate a very good sensitivity and specificity for detecting HLRCC/FHRCC (4). Unfortunately, 2SC immunohistochemistry is still not commercially available. In this study, we found that separate immunohistochemistry for FH, although useful as a screening test, is not 100% sensitive and specific. We identified 2 cases which showed negative FH reactivity by immunohistochemistry, in which we could not confirm a mutation/LOH of the *FH* gene by molecular-genetic tests (FH-like RCCs). Concurrently, immunohistochemical staining with FH antibody reached the sensitivity of 86% in our FHRCC/HLRCC cases. Other recently published study determined that single use of FH antibody shows specificity of 100% but sensitivity of 87.5% (20). This illustrates the limitations of the immunohistochemistry screening for FH in suspicious cases with overlapping histomorphologic patterns. In our view, all morphologically suspicious cases should be evaluated for *FH* gene mutations to separate the true HLRCC/FHRCC from their mimickers, regardless of the FH immunohistochemistry findings.

It is evident that neither morphologic feature nor immunohistochemical analysis can solely be used in routine practice for the diagnosis of HLRCC/FHRCC. Yet morphology and immunohistochemistry could aid and be used as a further screening tool in detecting suspicious cases for genetic testing.

CONCLUSIONS

Our findings showed that it was virtually impossible to separate genuine HLRCC/FHRCC from cases that demonstrate morphologic similarities (FH-like RCC) solely based on morphologic features. Considering the limitations of immunohistochemistry, analysis of *FH* gene is currently the only reliable method for distinguishing HLRCC/FHRCC from their mimickers. Traditionally described histologic features of HLRCC/FHRCC (prominent eosinophilic macronuclei with perinucleolar halos) are frequently found in other renal neoplasms.

FUNDING

The study was supported by the Charles University Research Fund (project number Q39) and by Institutional Research Fund FN 00669806.

CONFLICT OF INTEREST

The authors declare that there is no conflict of interest regarding the publication of this paper.

REFERENCES

1. **Srigley JR, Delahunt B, Eble JN, Egevad L, Epstein JI, Grignon D, et al.** The International Society of Urological Pathology (ISUP) Vancouver Classification of Renal Neoplasia. *Am J Surg Pathol* 2013; 37(10): 1469-1489.
2. **Moch H, Humphrey PA, Ulbright TM, Reuter VE**. WHO classification of tumours of the urinary system and male genital organs. Lyon: IARC; 2016.
3. **Smith S, Trpkov K, Mehra R, Divatia M, Hes O, Menon S, et al.** Is Tubulocystic Carcinoma With Dedifferentiation a form of HLRCC/Fumarate Hydratase-Deficient RCC? United States and Canadian Academy of Pathology (USCAP) - 104th Annual Meeting, Boston, MA, March 21-27, 2015. *Mod Pathol* 2015; 95 (Suppl 1): 260A.
4. **Trpkov K, Hes O, Agaimy A, Bonert M, Martinek P, Magi-Galluzzi C, et al.** Fumarate Hydratase-deficient Renal Cell Carcinoma Is Strongly Correlated With Fumarate Hydratase Mutation and Hereditary Leiomyomatosis and Renal Cell Carcinoma Syndrome. *Am J Surg Pathol* 2016; 40(7): 865-875.
5. **Smith SC, Trpkov K, Chen YB, Mehra R, Sirohi D, Ohe C, et al.** Tubulocystic Carcinoma of the Kidney With Poorly Differentiated Foci: A Frequent Morphologic Pattern of Fumarate Hydratase-deficient Renal Cell Carcinoma. *Am J Surg Pathol* 2016; 40(11): 1457-1472.
6. **Launonen V, Vierimaa O, Kiuru M, Isola J, Roth S, Pukkala E, et al**. Inherited susceptibility to uterine leiomyomas and renal cell cancer. *Proc Natl Acad Sci U S A* 2001; 98(6): 3387-3392.
7. **Alam NA, Rowan AJ, Wortham NC, Pollard PJ, Mitchell M, Tyrer JP, et al.** Genetic and functional analyses of FH mutations in multiple cutaneous and uterine leiomyomatosis, hereditary leiomyomatosis and renal cancer, and fumarate hydratase deficiency. *Hum Mol Genet* 2003; 12(11): 1241-1252.
8. **Toro JR, Nickerson ML, Wei MH, Warren MB, Glenn GM, Turner ML, et al.** Mutations in the fumarate hydratase gene cause hereditary leiomyomatosis and renal cell cancer in families in North America. *Am J Hum Genet* 2003; 73(1): 95-106.
9. **Eble JN, Sauter G, Epstein JI, Sesterhenn IA.** World Health Organization Classification of Tumours Pathology and Genetics Tumours of the Urinary System and Male Genital Organs. IARC Press Lyon. 2004.
10. **Wei MH, Toure O, Glenn GM, Pithukpakorn M, Neckers L, Stolle C, et al.** Novel mutations in FH and expansion of the spectrum of phenotypes expressed in families with hereditary leiomyomatosis and renal cell cancer. *J Med Genet* 2006; 43(1): 18-27.
11. **Merino MJ, Torres-Cabala C, Pinto P, Linehan WM**. The morphologic spectrum of kidney tumors in hereditary leiomyomatosis and renal cell carcinoma (HLRCC) syndrome. *Am J Surg Pathol* 2007; 31(10): 1578-1585.
12. **Grubb RL, 3rd, Franks ME, Toro J, Middelton L, Choyke L, Fowler S, et al.** Hereditary leiomyomatosis and renal cell cancer: a syndrome associated with an aggressive form of inherited renal cancer. *J Urol* 2007; 177(6): 2074-2080.
13. **Lehtonen HJ, Blanco I, Piulats JM, Herva R, Launonen V, Aaltonen LA.** Conventional renal cancer in a patient with fumarate hydratase mutation. *Hum Pathol* 2007; 38(5): 793-796.
14. **Koski TA, Lehtonen HJ, Jee KJ, Ninomiya S, Joosse SA, Vahteristo P, et al.** Array comparative genomic hybridization identifies a distinct DNA copy number profile in renal cell cancer associated with hereditary leiomyomatosis and renal cell cancer. *Genes Chromosomes Cancer* 2009; 48(7): 544-551.
15. **Harris M, Wallace J, Winship I, Hale L, Gardner M**. Hereditary renal cell carcinoma: the clue can be in the skin. *Intern Med J* 2009; 39(12): e12-13.
16. **Chen YB, Brannon AR, Toubaji A, Dudas ME, Won HH, Al-Ahmadie HA, et al.** Hereditary leiomyomatosis and renal cell carcinoma syndrome-associated renal cancer: recognition of the syndrome by pathologic features and the utility of detecting aberrant succination by immunohistochemistry. *Am J Surg Pathol* 2014; 38(5): 627-637.
17. **Smith SC, Sirohi D, Ohe C, McHugh JB, Hornick JL, Kalariya J, et al.** A distinctive, low-grade oncocytic fumarate hydratase-deficient renal cell carcinoma, morphologically reminiscent of succinate dehydrogenase-deficient renal cell carcinoma. *Histopathology* 2017; 71(1): 42-52.
18. **Vocke CD, Ricketts CJ, Merino MJ, Srinivasan R, Metwalli AR, Middelton LA, et al.** Comprehensive genomic and phenotypic characterization of germline FH deletion in hereditary leiomyomatosis and renal cell carcinoma. *Genes Chromosomes Cancer* 2017; 56(6): 484-492.
19. **Li Y, Reuter VE, Matoso A, Netto GJ, Epstein JI, Argani P.** Re-evaluation of 33 'unclassified' eosinophilic renal cell carcinomas in young patients. *Histopathology* 2018; 72(4): 588-600.
20. **Muller M, Guillaud-Bataille M, Salleron J, Genestie C, Deveaux S, Slama A, et al.** Pattern multiplicity and fumarate hydratase (FH)/S-(2-succino)-cysteine (2SC) staining but not eosinophilic nucleoli with perinucleolar

halos differentiate hereditary leiomyomatosis and renal cell carcinoma-associated renal cell carcinomas from kidney tumors without FH gene alteration. *Mod Pathol* 2018; 31(6): 974-983.

21. **Alaghehbandan R, Stehlik J, Trpkov K, Magi-Galluzzi C, Condom Mundo E, Pane Foix M, et al.** Programmed death-1 (PD-1) receptor/PD-1 ligand (PD-L1) expression in fumarate hydratase-deficient renal cell carcinoma. *Ann Diagn Pathol* 2017; 29: 17-22.
22. **Martinek P, Grossmann P, Hes O, Bouda J, Eret V, Frizzell N, et al.** Genetic testing of leiomyoma tissue in women younger than 30 years old might provide an effective screening approach for the hereditary leiomyomatosis and renal cell cancer syndrome (HLRCC). *Virchows Arch* 2015; 467(2): 185-191.

OSOBNÍ SDĚLENÍ

Spomienka na emeritného primára MUDr. Petra Kosseya, CSc.

V júli 2019 si slovenská obec patológov a spolupracujúcich klinikov, najmä onkológov pripomenula nedožité 100. výročie narodenia prim. MUDr. Petra Kosseya, CSc., zakladateľa slovenskej onko-patológie.

Peter Kossey sa narodil 14. júla 1919 v Kopašneve, okr. Chust (Podkarpatská Rus) na území vtedajšieho Československa (tč. Zakarpatská oblasť Ukrajiny) v rodine grécko-katolíckeho farára a učiteľky. Detstvo prežil v Strážskom v okrese Michalovce. Stredoškolské štúdium absolvoval na reálnom gymnáziu v Užhorode, kde roku 1938 maturoval. Štúdium medicíny začal na Karlovej univerzite v Prahe, avšak po vyhlásení Protektorátu Čiech a Moravy v r. 1939 pokračoval vo svojich štúdiách na Lekárskej fakulte Semmelweisovej univerzity v Budapešti, kde v septembri 1944 promoval. Po promócii narukoval do maďarskej armády, spočiatku slúžil vo vojenskej nemocnici v Budapešti, ale napokon bol odvelený do vojenského tábora v Nemecku, kde sa v apríli 1945 dostal do amerického zajatia, odkiaľ sa vrátil domov v novembri 1945. V decembri 1945 nastúpil ako sekundárny lekár štátnej nemocnice v Lučenci, kde pôsobil dva roky. Medzitým v apríli 1947 nostrifikoval svoj lekársky diplom na Univerzite Komenského v Bratislave. V rokoch 1947-1953 bol asistentom na Patologicko-anatomickom ústave LFUK v Bratislave, kde sa venoval aj pedagogickej činnosti - viedol praktické cvičenia, prednášal a skúšal medikov. Bol spoluautorom učebných textov i vysokoškolskej učebnice patológie (Základy všeobecnej patologickej anatómie). V rokoch 1953-1974 vykonával funkciu histopatológa na Výskumnom onkologickom ústave, kde sa venoval patológii experimentálnych zvierat a hlbšie patológii ľudských nádorov. V roku 1968 obhájil kandidátsku dizertačnú prácu „Patomorfológia a diferenciálna diagnostika fibrocystických onemocnení kostí", v roku 1970 získal špecializáciu II. stupňa z patologickej anatómie. Založil oddelenie onko-patológie, prvé oddelenie klinickej patológie na Slovensku. V rokoch 1974-1989 vykonával funkciu prednostu Oddelenia klinickej patológie a cytológie Ústavu klinickej onkológie (ÚKO) v Bratislave. Absolvoval niekoľko študijných pobytov doma i v zahraničí, aktívne sa zúčastnil viacerých vedeckých konferencií a kongresov doma i v zahraničí, ako aj pracovných zasadaní WHO v Ženeve ako člen expertnej skupiny pre testikulárne nádory. V rokoch 1978-1981 pôsobil na expertíze v Kuwaite. Ako samostatne pracujúci lekár pracoval na plný úväzok do veku 75 rokov (1994) a do 80 rokov (do 1999) ešte na polovičný úväzok.

Bohatá bola jeho spolupráca s akademikom Viliamom Thurzom, prvým riaditeľom Ústavu experimentálnej onkológie SAV, spolupráca na výskumných úlohách s viacerými klinickými pracoviskami vtedajšieho ÚKO. Dlhoročná bola aj spolupráca s akademikom Jánom Červeňanským, prednostom vtedajšej Ortopedickej kliniky v Bratislave a akademikom Vladimírom Zvarom, prednostom vtedajšej Urologickej kliniky v Bratislave.

Venoval sa diagnostike celého spektra nádorových ochorení, pôsobil ako onko-patológ, konzultant prakticky pre celé Slovensko. Stal sa priekopníkom histopatologickej diagnostiky najmä kostných nádorov, lymfómov, nádorov prsníka a testikulárnych nádorov na Slovensku.

S manželkou Vierou, ktorá pôsobila ako u pacientov veľmi obľúbená praktická lekárka, vychovali 7 detí, z ktorých najstaršie dve dcéry pokračovali v „šľapajách" rodičov ako lekárky.

K jeho záľubám patrila predovšetkým vážna hudba, pravidelne navštevoval abonentné koncerty Slovenskej filharmónie a kupoval gramofónové platne s vážnou hudbou. Rád sa učil cudzie jazyky, hovoril dobre po anglicky, nemecky, rusky, ukrajinsky, poľsky i maďarsky a čiastočne aj po francúzsky a arabsky.

Dr. Peter Kossey, CSc. zomrel 19. septembra 2002 v Bratislave.

Vážený pán primár, chcem sa Vám v mene Vašich bývalých spolupracovníkov, kolegov, i rodinných priateľov, ktorým ste odovzdávali kus seba, poďakovať a vysloviť presvedčenie, že ostávate natrvalo v našich spomienkach a srdciach.

Prof. MUDr. Dalibor Ondruš, DrSc.

1.4 MiT rodina translokačního renálního karcinomu, současný pohled

Molecular-genetic analysis is essential for accurate classification of renal carcinoma resembling Xp11.2 translocation carcinoma.
Hayes M, Peckova K, Martinek P, Hora M, Kalusova K, Straka L, Daum O, Kokoskova B, Rotterova P, Pivovarcikova K, Branzovsky J, Dubova M, Vesela P, Michal M, Hes O.
Virchows Arch. 2015 Mar;466(3):313-22.

Aggressive and nonaggressive translocation t(6;11) renal cell carcinoma: comparative study of 6 cases and review of the literature.
Peckova K, Vanecek T, Martinek P, Spagnolo D, Kuroda N, Brunelli M, Vranic S, Djuricic S, Rotterova P, Daum O, Kokoskova B, Vesela P, Pivovarcikova K, Bauleth K, Dubova M, Kalusova K, Hora M, Michal M, Hes O.
Ann Diagn Pathol. 2014 Dec;18(6):351-7.

TFE3-Fusion Variant Analysis Defines Specific Clinicopathologic Associations Amog Xp11 Translocation Cancers.
Pivovarcikova K, Grossmann P, Alaghehbandan R, Sperga M, Michal M, Hes O.
Am J Surg Pathol. 2017 Jan;41(1):138-140

MiT rodina translokačního renálního karcinomu (MITF RCC) je skupina renálních neoplázií, která svým názvem zastřešuje renální karcinomy s přeskupením/rearanží některého ze členů MiT rodiny transkripčních faktorů, zejména genů *TFE3* a *TFEB* [24].

Xp11 translokační RCC (též někdy označovaný *TFE3* rearanžovaný RCC) je nádor definovaný přítomností genové fúze *TFE3* s širokým spektrem genů partnerských (nejčastěji s geny *PRCC, ASPSCR1, SFPQ*, je však popsáno i mnoho jiných partnerů) [4]. Xp11 translokační RCC má popisované morfologické spektrum, histologický vzhled může být s různými fúzními partnery významně heterogenní [3, 7]. Typicky však bývá Xp11 translokační RCC popisován jako papilárně uspořádaný tumor ze světlých buněk s přítomností psammomakalcifikací [34]. Genetické vyšetření (break-apart FISH) je nejspolehlivějším nástrojem při diagnostice těchto tumorů [32]. V současné době však víme, že i toto vyšetření má při diagnostice Xp11 translokačního RCC své limity a ve specifických případech je třeba k jeho hodnocení přistupovat s obezřetností – u některých fúzních partnerů dochází k paracentrické inverzi v oblasti Xp11, která je pomocí break-apart FISH obtížně detekovatelná [6]. Imunohistochemické vyšetření protilátkou TFE3 je problematické, zatíženo relativně významnou chybovostí, funkčnost imunohistochemického průkazu je patrně podmíněna a závisí na dobré fixaci tkáně.

TFEB rearanžovaný RCC je stejně jako předchozí jednotka definován přítomností genové fúze, tentokráte však postihující gen *TFEB*, typicky a nejčastěji s fúzním partnerem *MALAT1* (proto byla tato neoplázie dříve označován též jako t(6;11) RCC [24]). Popsáno je ovšem i spektrum jiných alternativních fúzních partnerů (např. *COL21A1, ACTB, EWSR1, CLTC* a další [52]). Pro TFEB rearanžovaný RCC je typický bifazický vzhled s většími epiteloidními buňkami na periferii nádorových hnízd a klastry menších buněk okolo hyalinního materiálu v centru [24] (vytváří tak vzhled tzv. pseudorozet). Tumory však mohou mít i zcela odlišný histologický vzhled, překrývný se spektrem Xp11 translokačního karcinomu [39], ale i např. CCRCC, PRCC a jiných renálních tumorů [52]. U *TFEB* rearanžovaných tumorů translokace v genu *TFEB* typicky vede k overexpresi TFEB

s možností imunohistochemické detekce (jaderná pozitivita), toto imunohistochemické barvení je však též zatíženo rizikem fixačních artefaktů. Současně s overexpresí TFEB u těchto neoplázií charakteristicky dochází k aberantní expresi některých melanomových markerů (HMB45 a Melan A) [5]. Pro definitivní stanovení diagnózy je nutné provést FISH vyšetření s průkazem translokace v *TFEB* genu. I u *TFEB* rearanžovaného RCC však byly popsány paracentrické inverze vedoucí k „negativnímu" výsledku FISH vyšetření a potenciálně tak k stanovení nesprávné diagnózy při stanovení rearanže genu *TFEB* [52].

Recentní doporučení GUPS pak dále doporučují specificky odlišovat v této skupině neoplázií ještě *TFEB* amplifikovaný RCC. To je zcela racionální přístup, neboť bylo prokázáno, že nádory s amplifikací *TFEB* genu jsou asociovány s agresivním chováním [5, 27]. V literatuře jsou popsány *TFEB* amplifikované RCC jak s konkurentně přítomnou translokací, tak i bez ní. I u těchto tumorů dochází k overexpresi TFEB a aberantní expresi Melan A a HMB45. Tumory mohou být morfologicky variabilní, histologicky však ne zcela odlišné od TFEB rearanžovaných RCC. V podstatném se však *TFEB* rearanžovaný RCC a TFEB amplifikovaný RCC liší - tumory se chovají agresivně (high-stage onemocnění s rozvojem metastáz) a statisticky postihují starší populaci. Proto je důležité u tumorů suspektních z diagnózy *TFEB* rearanžovaného či *TFEB* amplifikovaného RCC vždy současně vyšetřovat nikoliv pouze přítomnost translokace *TFEB* (break-apart FISH), ale též vyšetřit i eventuální přítomnost enumerace genu *TFEB* v tumoru.

1.4.1 Molecular-genetic analysis is essential for accurate classification of renal carcinoma resembling Xp11.2 translocation carcinoma

Tato studie prezentuje 20 renálních neoplázií (vybraných z celkem 17 500 archivních případů plzeňského registru nádorů), u nichž na základě morfologie vyvstalo podezření z diagnózy Xp11.2 translokačního RCC. Pouze v devíti případech (9/20) byla pomocí FISH analýzy potvrzena translokace genu *TFE3*. Tato studie se pak blíže zaměřila na zbylých 11 případů bez molekulárně-geneticky prokázané translokace genu *TFE3*. Materiál dostupný pro další studii byl u devíti zbylých tumorů (9/11). U těchto případů byla provedena detailní morfologická a imunohistochemická analýza, molekulárně genetické vyšetření se zaměřením na abnormality genu *VHL* a status chromozomů 7 a 17.

Morfologické spektrum bylo různorodé, šest tumorů vykazovalo směs buněk s eosinofilní a vodojasnou cytoplazmou vytvářející tubulární, acinární a papilární okrsky. Jeden případ měl vyloženě high-grade morfologii kombinující epiteloidní, vřetenité a sarkomatoidní okrsky. Dále byl zaznamenán případ se solidními, tubulárními a papilárními okrsky obsahující vřetenité buňky a celkově tak připomínající tzv. "mucinous tubular and spindle cell carcinoma" a případ s dyskohezivními hnízdy velkých epiteloidních histiocytoidních buněk na pozadí denzního lymfoplasmocytárního infiltrátu. Nádory byly difúzně AE1/3 pozitivní v 3/9 případů a CK7 pozitivní pouze u 1/9 tumorů. PAX8 a CD10 reaktivita byla prokázána u 8/9 tumorů, AMACR a vimentim byly pozitivní u 7/9 případů a katepsin K ve dvou případech. Imunohistochemický průkaz TFE3 prokázal jadernou expresi u 2/9 případů, jeden z těchto případů vykazoval cytogeneticky polysomii chromozomu 7 a druhý polysomii chromozomu 17; oba byly bez *VHL* abnormalit a finálně tak byly diagnostikovány jako RCC "unclassifiable". U 3/7 imunohistochemicky i FISH TFE3 negativních tumorů byla prokázána polyzomie chromozomů 7/17 a současně i abnormality genu *VHL*, tyto tumory pak byly definitivně klasifikovány jako kombinované CCRCC/PRCC. Dále jeden imunohistochemicky i FISH „TFE3 negativní" tumor cytogeneticky vykazoval normální status chromozomů 7 a 17, ale přítomna byla LOH3p (abnormalita genu *VHL*), tumor byl definitivně označen jako CCRCC. Jeden imunohistochemicky i FISH „TFE3 negativní" tumor s polyzomií 7/17 a normálním statusem *VHL* byl definitivně klasifikován jako PRCC a dva tumory s dizomií 7 a 17 a bez prokázaných abnormalit *VHL* byly označeny jako RCC "unclassifiable".

Xp11.2 translokační RCC je morfologicky vysoce heterogenní tumor, zlatým diagnostickým standardem pro správnou diagnózu je provedení molekulárně-genetické analýzy translokace genu *TFE3*.

Virchows Arch (2015) 466:313–322
DOI 10.1007/s00428-014-1702-7

ORIGINAL ARTICLE

Molecular-genetic analysis is essential for accurate classification of renal carcinoma resembling Xp11.2 translocation carcinoma

Malcolm Hayes · Kvetoslava Peckova · Petr Martinek · Milan Hora · Kristyna Kalusova · Lubomir Straka · Ondrej Daum · Bohuslava Kokoskova · Pavla Rotterova · Kristyna Pivovarčikova · Jindrich Branzovsky · Magdalena Dubova · Pavla Vesela · Michal Michal · Ondrej Hes

Received: 21 August 2014 / Revised: 26 October 2014 / Accepted: 1 December 2014 / Published online: 28 December 2014

Abstract Xp11.2-translocation renal carcinoma (TRCC) is suspected when a renal carcinoma occurs in young patients, patients with a prior history of exposure to chemotherapy and when the neoplasm has morphological features suggestive of that entity. We retrieved 20 renal tumours (from 17,500 archival cases) of which morphology arose suspicion for TRCC. In nine cases, TFE3 translocation was confirmed by fluorescence in situ hybridisation analysis. In 9 of the remaining 11 TRCC-like cases (7 male, 4 female, aged 22–84 years), material was available for further study. The morphological spectrum was diverse. Six tumours showed a mixture of cells with eosinophilic or clear cytoplasm in tubular, acinar and papillary architecture. One case was high grade with epithelioid, spindle cell and sarcomatoid areas. Another showed tubular, solid, and papillary areas and foci containing spindle cells reminiscent of mucinous tubular and spindle cell carcinoma. The third showed dyscohesive nests of large epithelioid and histiocytoid cells in a background of dense lymphoplasmacytic infiltrate. By immunohistochemistry, keratin AE1/AE3 was diffusely positive in three tumours, while CK7 strongly stained one tumour and another focally and weakly. CD10 and Pax8 were expressed by eight, AMACR and vimentin by seven, CA-IX by four and TFE3 and cathepsin K by two tumours. Of the two TFE3-positive tumours, one showed polysomy of chromosome 7 and the other of 17; they were *VHL* normal and diagnosed as unclassifiable RCC. Of the seven TFE3-negative tumours, three showed polysomy of 7/17 and *VHL* abnormality and were diagnosed as combined clear cell RCC/papillary RCC. One TFE3-negative tumour with normal 7/17 but LOH 3p (*VHL* abnormality) was diagnosed as clear cell RCC. One TFE3-negative tumour with polysomy 7/17 but normal *VHL* was diagnosed as papillary RCC, and two with normal chromosomes 7/17 and *VHL* gene were considered unclassifiable. As morphological features and IHC are heterogeneous, TRCC-like renal tumours can only be sub-classified accurately by multi-parameter molecular-genetic analysis.

Keywords Translocation · Renal cell carcinoma · TFE3 · Xp11 · FISH · Molecular genetics · MiTF · Immunohistochemistry

M. Hayes
Department of Pathology, BC Cancer Agency and Clinical Professor of Pathology, University of British Columbia, Vancouver, Canada

K. Peckova · P. Martinek · O. Daum · B. Kokoskova · P. Rotterova · K. Pivovarčikova · J. Branzovsky · M. Dubova · P. Vesela · M. Michal · O. Hes (✉)
Department of Pathology, Medical Faculty, Charles University and Charles University Hospital Plzen, Alej Svobody 80, 304 60 Plzen, Czech Republic
e-mail: hes@medima.cz

M. Hora · K. Kalusova
Department of Urology, Medical Faculty, Charles University and Charles University Hospital Plzen, Plzen, Czech Republic

L. Straka
Klinicka Patologia Presov, Presov, Slovak Republic

Introduction

Translocation-associated renal cell carcinoma (TRCC) resulting from Xp11.2 (TFE3) translocation was recognised first in paediatric and young adult patients [30, 41]. Subsequently TRCC was documented in older adults, and its frequency in the adult population is probably underestimated [8, 13, 20, 25, 48]. While TRCC has a favourable prognosis in children, these neoplasms may be aggressive in adults [24, 27, 31, 40].

Several variants of TRCC with translocation of TFE3 to different partner genes are now described [1, 2, 6, 7, 17, 42,

43]. The more common partners are *ASPL* and *PRCC* genes. TFE3 translocation also occurs in other neoplasms including alveolar soft-part sarcoma and some forms of PEComa [3, 22, 47]. TRCC involving the closely related *TFEB gene*, which is also part of the MiTF gene family, is rarer than TFE3-TRCC but has a similar clinical presentation and may have overlapping morphology [4, 9, 18, 38]. The two variants of MiTF-TRCC lack a familial history and are not multifocal, in contrast to renal cancers of the hereditary CCRCC syndrome associated with chromosome 3 translocations, and the hereditary PRCC associated with c-MET mutations [46].

Renal carcinoma occurring in a child, or in a patient exposed to chemotherapy for an earlier cancer, suggests the possibility of TRCC. Morphological studies of TRCC delineated an association with histological features that include a mixed papillary and alveolar architecture, a mixture of cells with clear and eosinophilic cytoplasm and clear cells with abundant voluminous cytoplasm. Presence of blood lakes, psammoma bodies, stromal hyaline globules and eosinophilic cytoplasmic inclusions are additional features described in TRCC. None of these morphological features is specific for TRCC, and some of the features depend on the precise translocation partner of the *TFE3 gene* fusion. Demonstration of the TFE3 translocation is the defining characteristic of TRCC. This is best demonstrated by break-apart fluorescence in situ hybridisation (FISH) [32]. Over-expression of the TFE3 protein can be shown by immunohistochemistry, but the test requires careful calibration and adherence to strict standards of fixation and controls to avoid false results. Furthermore, TRCC has relatively specific immunohistochemical and gene expression profiles that assist in its distinction from CRCC and PRCC [5, 14, 38].

The present study was performed on a group of 20 renal neoplasms selected for their unusual morphology or clinical presentation, which were considered suspicious for TRCC. Having excluded the bona fide cases of TFE3-TRCC by FISH testing, the remaining nine TRCC-like cases with adequate material were studied further in an attempt to classify them in terms of the currently accepted Vancouver classification. This exercise entailed the development of an investigative algorithm for future recommendation.

Materials and methods

Twenty tumours suspect for TRCC based mostly on morphological features were identified in the Plzen archive of 17,500 renal neoplasms. Haematoxylin and eosin-stained (H&E) glass slides and formalin-fixed paraffin embedded blocks were retrieved, and the pathology reports and clinical records were studied to obtain demographic and follow-up data of the patients and for gross descriptions of the tumours. In addition to the original archival slides, standard 4-μm sections were cut from formalin-fixed, paraffin-embedded blocks selected from the tumours. These were stained with H&E for light microscopic examination using standard methodology and spare sections were cut for IHC. The number of blocks per case ranged from 3 to 30.

All H&E-stained sections and IHC stains were reviewed by three authors of this paper (MH, KP and OH).

The immunohistochemical study was performed using a Ventana Benchmark XT automated stainer (Ventana Medical System, Inc., Tucson, AZ, USA). Antibodies against CK7 (monoclonal, OV-TL 12/30, 1:200, Dako, Glostrup, Denmark), pan keratin (polyclonal, AE1-AE3/PCK26, RTU, Ventana-Roche), CD10 (monoclonal, 56C6, 1:20, Novocastra, Burlingame, CA, USA), AMACR (monoclonal, 13H4, 1:200, Dako), TFE3 (polyclonal, Abcam, 1:100, Cambridge, UK), vimentin (D9, monoclonal, Neomarkers, Westinghouse, CA, USA, 1:1000), CA-IX (monoclonal, 303123, 1:100, RD systems, Minneapolis, MN, USA), cathepsin K (monoclonal, 3F9, Abcam, 1:100), PAX-8 (polyclonal, Abcam, Cambridge, UK, 1:100) and anti-melanosome (monoclonal, HMB45, DakoCytomation, 1:200) were applied to all cases. Selected cases were also stained for S-100 protein (polyclonal, DakoCytomation, 1:400), wide spectrum keratin (OSCAR, monoclonal, Covance, Princetown, NJ, 1:2000), cytokeratin 20 (M7019, monoclonal, DakoCytomation, 1:100) and cytokeratin (CAM 5,2 monoclonal, Becton-Dickinson, San Jose, CA, USA, 1:200) as part of their initial diagnostic work-up.

For each case, 3–30 blocks were available; for immunohistochemical study, 1–2 selected blocks were used per case.

Molecular genetic study

FISH analysis was performed for *TFE3* break and for enumeration of chromosomes X, Y, 7 and 17. The FISH procedure using centromeric probes for chromosomes 7 and 17 was described in paper of Petersson et al. [34]. The same technique of analysis and cut-off setting was used with probes CEP X/CEP Y (VYSIS/Abbott Molecular, Des Plaines, IL, USA) and ZytoLight® SPEC TFE3 Dual Color Break Apart Probe (ZytoVision GmbH, Bremerhaven, Germany). Monosomy and polysomy for chromosomes X and Y was defined as the presence of one signal per cell in >45 % and three and more signals in >10 % of cells, respectively. The cut-off value for TFE3 break was set to more than 10 % of nuclei with break signals. Mutation analysis of the *VHL* gene and loss of heterozygosity for chromosome 3p region (LOH3p) were studied by PCR and sequencing and fragmentation analysis, respectively. Methylation of the promoter of the VHL gene was analysed by methylation-specific PCR. All these methods were thoroughly described in paper of Petersson et al. [34].

Results

Clinical and gross findings

The patients, six male and three female, ranged in age from 43 to 84 years, 7 exceeding 50 years of age (Table 1). Tumour size ranged from 2.6 to 13 cm with six cases equal to or exceeding 5 cm in greatest dimension. Six cases were stage pT1 according TNM 09, two cases pT2 and one pT3. Four were from the left kidney and five from the right kidney. Most tumours were tan coloured with areas of brown, yellow to tan (Fig. 1a), white or grey with occasional, grossly visible necroses (Fig. 1b).

Follow-up was available in six cases. This ranged from 1 to 3 years. One patient died 1 year after diagnosis, and the other five patients are alive and well.

Histological findings

Three tumours had a prominent tubulopapillary architecture admixed with some solid nests of cells (Fig. 2a, b). Two tumours had a predominantly nested and alveolar pattern with alveolar spaces filled with eosinophilic secretions reminiscent of thyroid follicles (Fig. 3). One of these tumours contained small foci with a papillary architecture. Blood lakes were prominent in these two tumours and were seen focally in six other tumours. These two tumours and one of the neoplasms with a tubulopapillary architecture contained abundant clear cells with voluminous cytoplasm, prominent lateral cell borders and irregular apical cytoplasmic borders (so-called "blister" cells; Fig. 4). Such cells were seen focally in three other tumours. A population of cells with abundant eosinophilic (oncocyte-like) cytoplasm was also present in four of these tumours and predominated in two of the neoplasms (Fig. 5). One tumour with a nested and alveolar architecture mostly resembled CCRCC but had focal papillary architecture and some cells with eosinophilic granular cytoplasm (Fig. 6). Three of the above tumours contained varying numbers of psammoma bodies and one demonstrated prominent eosinophilic hyaline cytoplasmic inclusion bodies. None showed extracellular hyaline nodules of the type descried in some cases of TRCC. These six tumours were within the classically described morphological spectrum of TFE3-TRCC. Nuclei were Fuhrman grade 2 in three tumours and grade 3 in the other 3 tumours. Necrosis was seen in four of the six tumours.

Three tumours had unusual morphology. One unusual tumour exhibited a mixture of compressed tubules, papillary structures and spindle cells associated with a myxoid stroma that in places resembled the mucinous tubular and spindle cell renal carcinoma. Other areas had a so-called "solid papillary" pattern. The spindle cells in this neoplasm had eosinophilic cytoplasm imparting a myoid appearance. Nuclei were predominantly grade 2, but focally nuclei were highly pleomorphic; grade 3–4 and necrosis was identified in several foci (Fig. 7). Mitoses were scanty and not atypical. Therefore, in our opinion, this tumour did not represent sarcomatoid carcinoma but was too atypical to be considered mucinous tubular and spindle cell renal carcinoma. The second showed poorly cohesive nests of large plump polygonal cells some with abundant eosinophilic cytoplasm imparting a histiocytoid and rhabdoid appearance. Some cells showed peripheral clearing and vacuolation of their cytoplasm resembling that seen in Touton giant cells. In many areas, the neoplastic cells were overrun by numerous lymphocytes and plasma cells simulating a lymphoepithelial carcinoma or recalling the morphology of Hashimoto's thyroiditis. The third unusual tumour was composed predominantly of markedly atypical spindle cells arranged in poorly cohesive nests lying within a background of myxoid collagen imparting a sarcomatoid appearance. Focally, the spindle cell component was associated with intercellular eosinophilic matrix resembling osteoid. Elsewhere, this neoplasm showed poorly cohesive nests of large epithelioid cells with large vesicular nuclei containing macronucleoli suggesting melanoma or alveolar soft-part sarcoma. This

Table 1 Clinicopathologic data

Case	Sex	Age	Site	Size (cm)	pT TNM09	Color	Follow-up
1	M	51	Left	13	pT2	Yellowish	NA
2	M	80	Left	10×6×3	pT3a	Tan to brown	DOD 1 year after dg
3	F	60	Right	6×4×3	pT1b	Whitish	3 years AW
4	F	75	Right	2.6×2×2	pT1a	Gray to tan	1 year AW
5	F	84	Left	Diam. 5	pT1b	Gray to tan	NA
6	M	57	Right	2.5×2.7×2.9	pT1a	Yellowish	2 years AW
7	M	48	Right	9×8×7	pT2	Brownish-yellow	NA
8	M	72	Left	5×4.5×3.5	pT1b	Tan to brow	1 year AW, CRI, HT
9	M	43	Right	5.5×4.5×3	pT1b	Tan	1 year AW

M male, *F* female, *NA* not available, *DOD* dead of disease, *AW* alive and well, *CRI* chronic renal insufficiency, *HT* hypertension, *dg* diagnosis

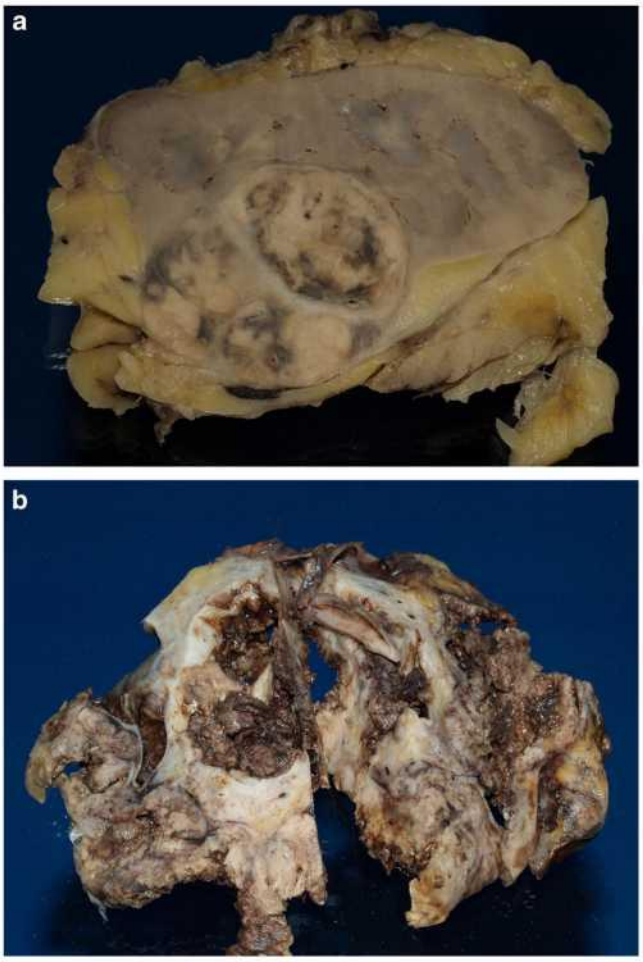

Fig. 1 Tumours were mostly yellow to tan on gross section (**a**) with foci of grossly visible necrosis (**b**)

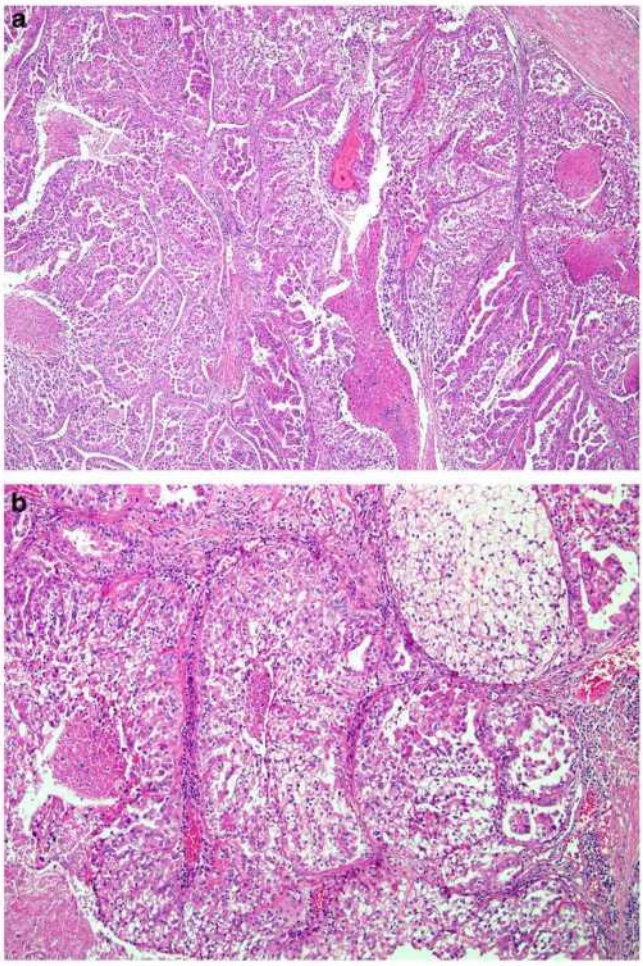

Fig. 2 Some tumours had a prominent tubulopapillary architecture admixed with solid nests of cells admixed with solid nests of cells(**a**, **b**)

tumour contained extensive necrosis, numerous mitoses and some atypical mitoses. It was invasive into perinephric fat and exhibited extensive lymphovascular invasion. This tumour was initially considered to potentially fall within the spectrum of ASPL-TFE3 or TFEB-TRCC and required exclusion of metastatic melanoma.

Immunohistochemical analysis

Results of the immunohistochemical analysis are listed in Table 2. None of the tumours showed an immunoprofile diagnostic of any particular type of RCC. Importantly, TFE3 was positive in two tumours neither of which was strongly positive for cathepsin K. A third tumour was initially interpreted as positive for TFE3 but presence of staining in adjacent benign tissues prompted repeat of the stain, which was negative. None of the tumours was positive for HMB45. Cathepsin K was positive in two tumours but one showed only weak focal staining. The latter tumour was positive for TFE3 by IHC but not FISH (Fig. 8). All but one of the nine TRCC-like tumours were positive for CD10, seven were positive for vimentin and four for carbonic anhydrase-IX (CA-IX). Seven were positive for AMACR. Keratin AE1/AE3 was diffusely positive in three tumours and was negative in six. CK7

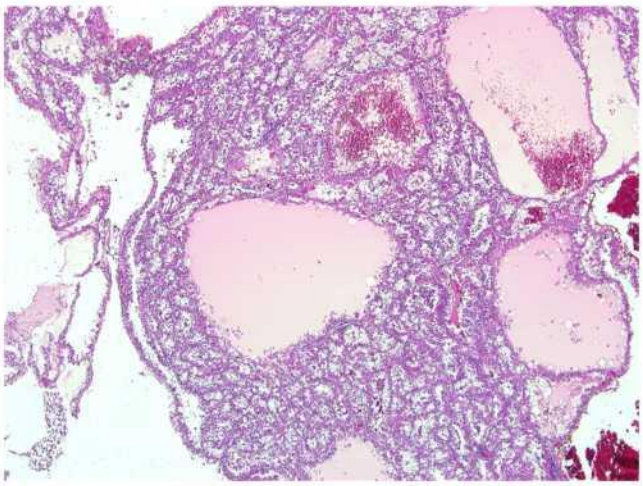

Fig. 3 Two tumours had a predominantly nested and alveolar pattern with alveolar spaces filled with eosinophilic secretions reminiscent of thyroid follicles

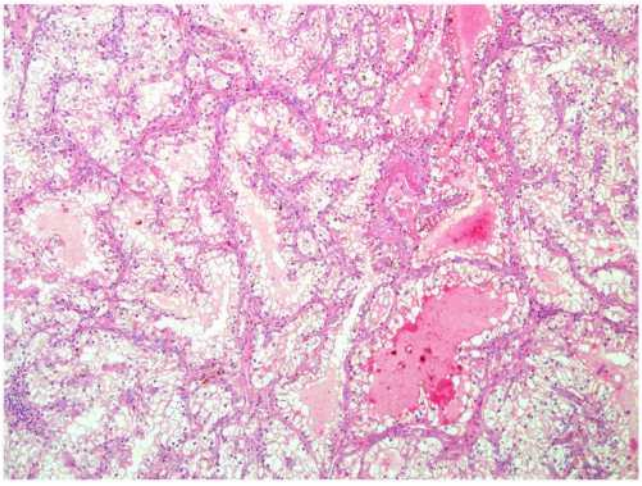

Fig. 4 Tumours with tubulopapillary architecture contained abundant clear cells with voluminous cytoplasm, prominent lateral cell borders and irregular apical cytoplasmic borders (so-called "blister" cells)

strongly stained one tumour, was weakly and focally positive in 1 and was negative in six cases. Pax 8 was positive in all but one case.

Molecular and cytogenetic analysis

One TFE3-negative tumour (case 8) showed normal copy numbers of 7,17 and LOH 3p (*VHL* abnormality) (Table 3). This tumour was diagnosed as clear cell RCC (CCRCC). One TFE3-negative tumour (case 1) with polysomy 7 and 17 but normal *VHL* status was diagnosed as papillary RCC (PRCC). Two TFE3-negative tumours (cases 4 and 6) had a normal complement of chromosomes 7 and 17 and no abnormality of the *VHL* gene. These tumours were considered unclassifiable. Three TFE3-negative tumours (cases 5, 7 and 9) that showed both polysomy of 7 and 17 and *VHL* abnormality were regarded as composite or combined CRCC/PRCC (unclassifiable). One of the two TFE3-IHC positive tumours (cases 2 and 3) showed only polysomy 7 and the other only polysomy 17, and both were negative for *VHL* gene abnormalities. These were also regarded as unclassifiable RCC.

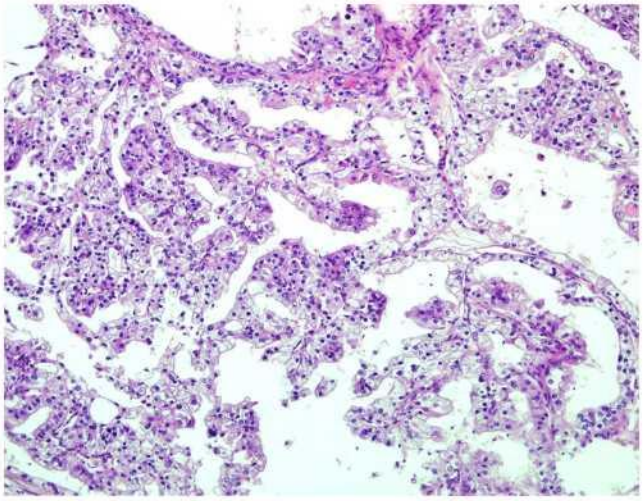

Fig. 6 One tumour with a nested and alveolar architecture mostly resembled CCRCC but had focal papillary architecture and some cells with eosinophilic granular cytoplasm

Discussion

RCCs associated with TFE3 gene fusions are relatively rare tumours in adults but comprise approximately 30–50 % of renal cell carcinomas in children. There is an established association between TRCC and prior exposure to chemotherapy [14, 39]. The rarity of TRCC cases in our archive could be explained by the fact that a large majority of the renal neoplasms in the archive were obtained from hospitals concentrating on adult clinical practice (age of the patients is over 18 years). TFE3 translocation can occur to several different

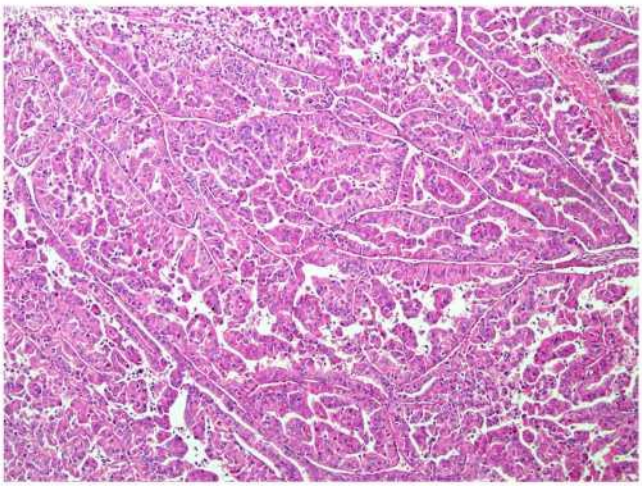

Fig. 5 A population of cells with abundant eosinophilic cytoplasm was also present in four of these tumours

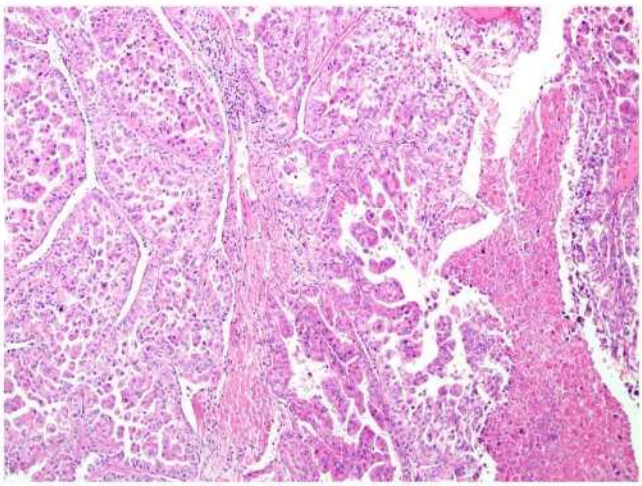

Fig. 7 Areas of necrosis were noted in the vicinity of papillary and micropapillary structures

Table 2 Immunohistochemical examination

Case:	TFE3	CANH9	CD10	Vim	AMACR	Cathep.	HMB45	AE1–AE3	CK7	Pax8
1	–	–	+++	+++	++	–	–	–	–	++
2	+++	–	++ foc	+++	–	–	–	–	+ foc	–
3	+++	–	+++ foc	+++	–	+ foc	–	–	–	+
4	–	–	++ foc	–	+++	+++	–	–	–	+
5	–	–	–	+++	+++	–	–	++	–	+
6	–	++ foc	+++	+++	+++	–	–	–	–	++
7	–	++ foc	+++	–	+++ foc	–	–	+++	–	++
8	–	++ foc	+++	+++	+++	–	–	++	+++	+
9	–	+++	+++	+++	+++ foc	–	–	–	–	+

foc=<25 % cells staining

CANH9 carbonic anhydrase IX, *Vim* Vimentin, *AMACR* alpha-methylacyl-CoA racemase, *Cathep.* cathepsin K, (–) negative, (+) weak, (++) moderate, (+++) strong

partner genes including *ASPL*, *PRCC*, *PSF*, *CLTC*, *NonO*, and others not yet fully clarified [7, 8, 10, 11, 19]. Prior to the recognition of translocation carcinomas of the kidney, most of these tumours were classified in the categories of clear cell renal cell carcinoma and papillary renal cell carcinoma [15, 35, 37]. Young age at presentation is one of the main indicators of a possible translocation-associated renal carcinoma and prompts the pathologist to consider such a diagnosis. However, since classical CCRCC and PRCC comprise the most common renal neoplasms in adults, the possibility of TRCC is seldom considered in that age group so the incidence of TFE3 translocation carcinomas in adults aged >50 years is not known but is likely underestimated. Recent studies have shown that TRCC occurs in younger adults who typically present a higher clinical stage than in paediatric patients. The more aggressive behaviour of TRCC in adults may also be explained by the progressive acquisition of chromosomal copy number alterations [33]. The importance of recognising TRCC is increasing in the era of potential targeted therapy [23, 28].

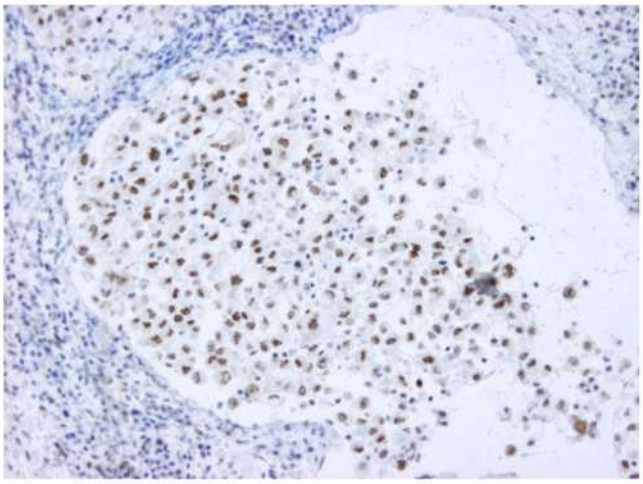

Fig. 8 Strong nuclear TFE3 positivity was noted in two tumours

At the time of initial description, TRCC was noted to have mostly papillary architecture and to be composed of cells with voluminous clear cytoplasm. Additional histological pointers to possible TRCC include an admixture of cells with clear and eosinophilic cytoplasm, presence of psammoma bodies and hyaline stromal globules [2, 44]. However, larger studies have expanded the histological profile to include mixed solid, nested, alveolar and papillary patterns such that accurate distinction from CCRCC and PRCC is impossible based only on morphology [1, 45]. The cells may have clear or eosinophilic cytoplasm, which may or may not be voluminous. Rare cases of TRCC contain melanin, express melanocytic markers by immunohistochemistry and exhibit a morphology that overlaps with PEComa, melanoma and even alveolar soft part sarcoma [3]. Different variants of TFE3 translocation were thought to result in different morphological appearances, but cases with overlapping morphological features were described later. Furthermore, a closely related form of TRCC involving the TFEB gene, another member of the MiTF gene family, was likewise initially thought to have a distinctive morphology but more experience with larger numbers of cases has shown morphological overlap with the more common TFE3 neoplasms and the more usual variants of renal carcinoma [8, 14, 18].

Immunohistochemical analysis may be helpful in differentiating TRCC from PRCC in that TRCC is negative or only weakly and focally positive for keratins and EMA, and is negative for racemase (AMACR) [1, 2, 12, 14]. Similar to clear cell carcinoma, TRCC is positive with the antibody to vimentin and strongly positive with CD10. However, vimentin staining is patchy in TRCC but diffuse in CCRCC, and TRCC is negative for carbonic anhydrase-9 (CA-IX). Positive nuclear staining for TFE3 protein and cytoplasmic staining for cathepsin K have been regarded as specific for

Table 3 Results of molecular and cytogenetic analyses

Case	TFE3 ba	CEP 7	CEP 17	X/Y	LOH3p	Mut VHL	Methyl VHL	Diag
1	Neg	Polysomy[a]	Polysomy[a]	4~5X/0Y; 2X/1Y[b]	Neg	Neg	Neg	PRCC
2	Neg	Polysomy	Disomy	NA	NA	Neg	NA	UNC
3	Neg	Disomy	Polysomy[a]	NP	Neg	Neg	Neg	UNC
4	Neg	Disomy	Disomy	NP	Neg	Neg	Neg	UNC
5	Neg	Polysomy[a]	Polysomy[a]	NP	Pos	Neg	Neg	CRCC/PRCC
6	Neg	Disomy	Disomy	2X/1Y	Neg	Neg	Neg	UNC
7	Neg	Polysomy	Polysomy	2X/2Y	Pos	Pos[c]	Neg	CRCC/PRCC
8	Neg	Disomy	Disomy	2X/0Y	Pos	Neg	Neg	CCRCC
9	Neg	Polysomy[a]	Polysomy[a]	Neg	Pos	Pos[d]	Neg	CRCC/PRCC

Pos positive, *Neg* negative, *NA* not analysable, *NP* not performed, *PRCC* papillary renal cell carcinoma, *UNC* unclassified renal cell carcinoma, *CRCC* clear cell renal cell carcinoma, *Mut VHL* mutation of *VHL gene, Methyl VHL* methylation status of *VHL gene*, *Diag* diagnosis

[a] Polysomy in large nuclei only

[b] Gain X, loss Y (4~5X/0Y) in large nuclei; gain X (2X/1Y) in small nuclei

[c] Somatic mutation c.504_508del/p.Leu168GlnfsTer3

[d] Somatic mutation c.393C>G/p.Asn131Lys

TRCC [5, 29, 38], but false positive and negative results have been reported in several studies not all of which have been explained on the basis of technical problems [21]. Indeed, it seems that over-expression of wild-typeTFE3 protein transcript may occur as a result of up-regulation of the normal gene, or as the result of increased gene copy number due to polysomy or amplification particularly in high grade CCRCC and in carcinomas with sarcomatoid and cystic features [26, 48]. Similarly, positive immunostains for melanocytic markers such as HMB45 may be seen in some variants of TFE3-TRCC, in the TFEB-TRCC and in PEComas [14, 16].

In the present study of 20 cases of RCC in which there was a suspicion of TRCC, nine cases were confirmed as X11.2-TRCC by break-apart FISH analysis. The remaining TRCC-like carcinomas showed a diverse morphology that precluded definite classification of these tumours on morphological grounds. Thus, many showed a mixture of papillary and CCRCC patterns. Seven cases contained clear cells with voluminous cytoplasm, so-called "blister" cells, a well-known feature of TRCC. IHC was also contradictory to the morphology in many cases, again suggesting possible TRCC. Of five cases exhibiting a predominantly papillary architecture, only one was strongly positive for CK7 and that tumour was also positive for CA-IX, a marker of CCRCC. Those tumours with morphology similar to CCRCC were all positive for AMACR, a marker of PRCC. The sarcomatoid tumour with morphology suggestive of melanoma or APSL-TFE3 TRCC posed a diagnostic challenge. It was positive for TFE3 by IHC, negative for HMB45 and showed only focal weak staining for cathepsin K. Although the stain for Pax-8 was negative, there was no clinical history of prior cutaneous melanoma or other visceral malignancy. Furthermore, metastatic melanoma was excluded by negative immunostaining for S-100 protein and diffusely positive staining for wide spectrum keratin (OSCAR). Positive immunostaining for TFE3 in the absence of the translocation has been described previously in sarcomatoid and other high-grade RCCs sometimes explained by gene polysomy or amplification [26]. Because of the contradictory morphological and immunohistochemical profiles of these TRCC-like neoplasms, we conclude that molecular/genetic analysis is the most reliable method extant to classify this group of unusual renal tumours.

The final molecular/genetic diagnosis did not correlate exactly with the histomorphology and immunoprofile in some cases (Table 4). In the case diagnosed as CCRCC on the basis of isolated abnormality of the *VHL* locus, the histology showed a prominent papillary architecture and alveolar nests with a micropapillary pattern within them. Immunostains for CK7 and AMACR were strongly positive. However, CA-IX was also positive. The case diagnosed as PRCC on the basis of polysomy of chromosomes 7 and 17 in the absence of *VHL* abnormality had prominent papillary architecture but showed a predominance of clear cells with voluminous vacuolated cytoplasm suggesting TRCC. On IHC, the tumour was negative for CK7 and positive for CD10 and vimentin. However, the stain for AMACR was positive. One of the three tumours diagnosed as combined PRCC–CCRCC on the basis of morphology, immunohistochemical examination and polysomy of chromosomes 7 and 17 and *VHL* abnormality showed a combined papillary, tubular and nested architecture and a predominance of cells with eosinophilic cytoplasm and scanty clear cells. One PRCC–CCRCC did not contain papillary structures and had a morphology most consistent with CCRCC but with clear cells showing voluminous cytoplasm suggesting TRCC. The third PRCC–CCRCC was the unusual tumour with a solid papillary pattern and areas of spindle cells in a mucinous

Table 4 Summary of unusual features

Molecular category	Case	Unusual features
CRCC	8	Papillary architecture AMACR and CK 7 strongly positive
PRCC	1	Clear cells with voluminous cytoplasm Glassy hyaline intra-cytoplasmic globules CK 7 negative
Combined PRCC-CCRCC	5, 7, 9	Spindle cell component and myxoid stroma and no alveolar or solid nest patterns in 1 case Papillary pattern absent in 1 case Very scanty clear cell component in 2 cases CK 7 negative in all AMACR positive in all CA-IX positive in 2 cases
Unclassifiable NOS	4, 6 2 3	2 cases had mixed PRCC and CCRCC morphology. Both contained clear cells with voluminous cytoplasm CK 7 negative but AMACR and cathepsin K positive Strong TFE3 positivity (by IHC), not confirmed by FISH

CRCC clear cell renal cell carcinoma, *PRCC* papillary renal cell carcinoma, *NOS* not otherwise specified, *IHC* Immunohistochemistry

stroma described above. By IHC, all three tumours were negative for CK7, positive for AMACR, and two were positive for CA-IX.

The study reported herein confirms the conclusion of other workers [36] that cytogenetic analysis is preferable to morphology and immunostains for TFE3 and cathepsin K in the diagnosis of TRCC. Furthermore, when TRCC-like tumours are selected on the basis of histological changes that do not conform to those classically described for other subtypes of RCC, immunohistochemistry is shown to be especially unreliable in further classifying these unusual renal neoplasms.

In conclusion, the molecular/genetic algorithm used herein is recommended for tumours with a TRCC-like morphology. This algorithm could also be applied in the investigation of unclassifiable RCC. Firstly, break-apart FISH analysis for TFE3 is performed and true cases of X11.2 translocation separated out. Next, numerical analysis of chromosomes 7 and 17 is performed together with thorough investigation of the status of the *VHL* gene on chromosome 3p using PCR for mutation analysis and LOH and methylation-specific PCR for the methylation analysis of the promoter region of the *VHL* gene. This enables true CCRCC and PRCC to be separated from the tumours that have combined features of CCRCC–PRCC. The remainder of unclassifiable RCCs may contain rare cases of TFEB–TRCC. These tumours are usually positive for cathepsin K and melanocytic markers on immunohistochemistry and can be confirmed by break-apart FISH analysis for the t(6;11) TFEB translocation [9]. Further, such unclassifiable cases may benefit from whole genome sequencing studies. Molecular features are indeed one of the characteristics useful for classification of unusual renal tumours. However, in group of TRCC and TRCC-like cases, it seems that they play a key role in the differential diagnostic process.

Acknowledgements The study was supported by the Charles University Research Fund (project number P36), by the project by the project CZ.1.05/2.1.00/03.0076 from European Regional Development Fund and by Ministry of Health, Czech Republic—conceptual development of research organization (Faculty Hospital in Pilsen—FNPl, 00669806).

Conflict of interest All authors declare no conflict of interest.

References

1. Argani P, Antonescu CR, Couturier J, Fournet JC, Sciot R, Debiec-Rychter M, Hutchinson B, Reuter VE, Boccon-Gibod L, Timmons C, Hafez N, Ladanyi M (2002) PRCC-TFE3 renal carcinomas: morphologic, immunohistochemical, ultrastructural, and molecular analysis of an entity associated with the t(X;1)(p11.2;q21). Am J Surg Pathol 26:1553–1566
2. Argani P, Antonescu CR, Illei PB, Lui MY, Timmons CF, Newbury R, Reuter VE, Garvin AJ, Perez-Atayde AR, Fletcher JA, Beckwith JB, Bridge JA, Ladanyi M (2001) Primary renal neoplasms with the ASPL-TFE3 gene fusion of alveolar soft part sarcoma: a distinctive tumor entity previously included among renal cell carcinomas of children and adolescents. Am J Pathol 159:179–192. doi:10.1016/S0002-9440(10)61684-7
3. Argani P, Aulmann S, Illei PB, Netto GJ, Ro J, Cho HY, Dogan S, Ladanyi M, Martignoni G, Goldblum JR, Weiss SW (2010) A distinctive subset of PEComas harbors TFE3 gene fusions. Am J Surg Pathol 34:1395–1406. doi:10.1097/PAS.0b013e3181f17ac0

4. Argani P, Hawkins A, Griffin CA, Goldstein JD, Haas M, Beckwith JB, Mankinen CB, Perlman EJ (2001) A distinctive pediatric renal neoplasm characterized by epithelioid morphology, basement membrane production, focal HMB45 immunoreactivity, and t(6;11)(p21.1;q12) chromosome translocation. Am J Pathol 158:2089–2096. doi:10.1016/S0002-9440(10)64680-9
5. Argani P, Hicks J, De Marzo AM, Albadine R, Illei PB, Ladanyi M, Reuter VE, Netto GJ (2010) Xp11 translocation renal cell carcinoma (RCC): extended immunohistochemical profile emphasizing novel RCC markers. Am J Surg Pathol 34:1295–1303. doi:10.1097/PAS.0b013e3181e8ce5b
6. Argani P, Ladanyi M (2005) Translocation carcinomas of the kidney. Clin Lab Med 25:363–378. doi:10.1016/j.cll.2005.01.008
7. Argani P, Lui MY, Couturier J, Bouvier R, Fournet JC, Ladanyi M (2003) A novel CLTC-TFE3 gene fusion in pediatric renal adenocarcinoma with t(X;17)(p11.2;q23). Oncogene 22:5374–5378. doi:10.1038/sj.onc.1206686
8. Argani P, Olgac S, Tickoo SK, Goldfischer M, Moch H, Chan DY, Eble JN, Bonsib SM, Jimeno M, Lloreta J, Billis A, Hicks J, De Marzo AM, Reuter VE, Ladanyi M (2007) Xp11 translocation renal cell carcinoma in adults: expanded clinical, pathologic, and genetic spectrum. Am J Surg Pathol 31:1149–1160. doi:10.1097/PAS.0b013e318031ffff
9. Argani P, Yonescu R, Morsberger L, Morris K, Netto GJ, Smith N, Gonzalez N, Illei PB, Ladanyi M, Griffin CA (2012) Molecular confirmation of t(6;11)(p21;q12) renal cell carcinoma in archival paraffin-embedded material using a break-apart TFEB FISH assay expands its clinicopathologic spectrum. Am J Surg Pathol 36:1516–1526. doi:10.1097/PAS.0b013e3182613d8f
10. Armah HB, Parwani AV (2010) Xp11.2 translocation renal cell carcinoma. Arch Pathol Lab Med 134:124–129. doi:10.1043/2008-0391-RSR.1
11. Armah HB, Parwani AV, Surti U, Bastacky SI (2009) Xp11.2 translocation renal cell carcinoma occurring during pregnancy with a novel translocation involving chromosome 19: a case report with review of the literature. Diagn Pathol 4:15. doi:10.1186/1746-1596-4-15
12. Bazille C, Allory Y, Molinie V, Vieillefond A, Cochand-Priollet B, Cussenot O, Callard P, Sibony M (2004) Immunohistochemical characterisation of the main histologic subtypes of epithelial renal tumours on tissue-microarrays. Study of 310 cases. Ann Pathol 24:395–406
13. Bruder E, Moch H (2004) [Pediatric renal cell carcinoma] Der Pathologe 25:324–327. doi:10.1007/s00292-004-0699-0
14. Camparo P, Vasiliu V, Molinie V, Couturier J, Dykema KJ, Petillo D, Furge KA, Comperat EM, Lae M, Bouvier R, Boccon-Gibod L, Denoux Y, Ferlicot S, Forest E, Fromont G, Hintzy MC, Laghouati M, Sibony M, Tucker ML, Weber N, Teh BT, Vieillefond A (2008) Renal translocation carcinomas: clinicopathologic, immunohistochemical, and gene expression profiling analysis of 31 cases with a review of the literature. Am J Surg Pathol 32:656–670. doi:10.1097/PAS.0b013e3181609914
15. Cao Y, Paner GP, Perry KT, Flanigan RC, Campbell SC, Picken MM (2005) Renal neoplasms in younger adults: analysis of 112 tumors from a single institution according to the new 2004 World Health Organization classification and 2002 American Joint Committee on Cancer Staging System. Arch Pathol Lab Med 129:487–491. doi:10.1043/1543-2165(2005)129<487:RNIYAA>2.0.CO;2
16. Chang IW, Huang HY, Sung MT (2009) Melanotic Xp11 translocation renal cancer: a case with PSF-TFE3 gene fusion and up-regulation of melanogenetic transcripts. Am J Surg Pathol 33:1894–1901. doi:10.1097/PAS.0b013e3181ba7a5f
17. Clark J, Lu YJ, Sidhar SK, Parker C, Gill S, Smedley D, Hamoudi R, Linehan WM, Shipley J, Cooper CS (1997) Fusion of splicing factor genes PSF and NonO (p54nrb) to the TFE3 gene in papillary renal cell carcinoma. Oncogene 15:2233–2239. doi:10.1038/sj.onc.1201394
18. Davis IJ, Hsi BL, Arroyo JD, Vargas SO, Yeh YA, Motyckova G, Valencia P, Perez-Atayde AR, Argani P, Ladanyi M, Fletcher JA, Fisher DE (2003) Cloning of an Alpha-TFEB fusion in renal tumors harboring the t(6;11)(p21;q13) chromosome translocation. Proc Natl Acad Sci U S A 100:6051–6056. doi:10.1073/pnas.0931430100
19. Dijkhuizen T, van den Berg E, Wilbrink M, Weterman M, GeurtsvanKessel A, Storkel S, Folkers RP, Braam A, de Jong B (1995) Distinct Xp11.2 breakpoints in two renal cell carcinomas exhibiting X;autosome translocations. Gene Chromosome Cancer 14:43–50
20. Eble JN, Sauter G, Epstein JI, Sesterhenn I, WHO Classification of Tumours (2004) Tumours of the urinary system and male genital organs. Pathology and genetics. IARC Press, Lyon
21. Gaillot-Durand L, Chevallier M, Colombel M, Couturier J, Pierron G, Scoazec JY, Mege-Lechevallier F (2013) Diagnosis of Xp11 translocation renal cell carcinomas in adult patients under 50 years: interest and pitfalls of automated immunohistochemical detection of TFE3 protein. Pathol Res Pract 209:83–89. doi:10.1016/j.prp.2012.10.013
22. Hodge JC, Pearce KE, Wang X, Wiktor AE, Oliveira AM, Greipp PT (2014) Molecular cytogenetic analysis for TFE3 rearrangement in Xp11.2 renal cell carcinoma and alveolar soft part sarcoma: validation and clinical experience with 75 cases. Mod Pathol 27:113–127. doi:10.1038/modpathol.2013.83
23. Hora M, Urge T, Travnicek I, Ferda J, Chudacek Z, Vanecek T, Michal M, Petersson F, Kuroda N, Hes O (2014) MiT translocation renal cell carcinomas: two subgroups of tumours with translocations involving 6p21 [t (6; 11)] and Xp11.2 [t (X;1 or X or 17)]. SpringerPlus 3:245. doi:10.1186/2193-1801-3-245
24. Klatte T, Streubel B, Wrba F, Remzi M, Krammer B, de Martino M, Waldert M, Marberger M, Susani M, Haitel A (2012) Renal cell carcinoma associated with transcription factor E3 expression and Xp11.2 translocation: incidence, characteristics, and prognosis. Am J Clin Pathol 137:761–768. doi:10.1309/AJCPQ6LLFMC4OXGC
25. Komai Y, Fujiwara M, Fujii Y, Mukai H, Yonese J, Kawakami S, Yamamoto S, Migita T, Ishikawa Y, Kurata M, Nakamura T, Fukui I (2009) Adult Xp11 translocation renal cell carcinoma diagnosed by cytogenetics and immunohistochemistry. Clin Cancer Res: Off J Am Assoc Cancer Res 15:1170–1176. doi:10.1158/1078-0432.CCR-08-1183
26. Macher-Goeppinger S, Roth W, Wagener N, Hohenfellner M, Penzel R, Haferkamp A, Schirmacher P, Aulmann S (2012) Molecular heterogeneity of TFE3 activation in renal cell carcinomas. Mod Pathol: Off J U S Can Acad Pathol Inc 25:308–315. doi:10.1038/modpathol.2011.169
27. Malouf GG, Camparo P, Molinie V, Dedet G, Oudard S, Schleiermacher G, Theodore C, Dutcher J, Billemont B, Bompas E, Guillot A, Boccon-Gibod L, Couturier J, Escudier B (2011) Transcription factor E3 and transcription factor EB renal cell carcinomas: clinical features, biological behavior and prognostic factors. J Urol 185:24–29. doi:10.1016/j.juro.2010.08.092
28. Malouf GG, Camparo P, Oudard S, Schleiermacher G, Theodore C, Rustine A, Dutcher J, Billemont B, Rixe O, Bompas E, Guillot A, Boccon-Gibod L, Couturier J, Molinie V, Escudier B (2010) Targeted agents in metastatic Xp11 translocation/TFE3 gene fusion renal cell carcinoma (RCC): a report from the Juvenile RCC Network. Ann Oncol: Off J Eur Soc Med Oncol / ESMO 21:1834–1838. doi:10.1093/annonc/mdq029
29. Martignoni G, Pea M, Gobbo S, Brunelli M, Bonetti F, Segala D, Pan CC, Netto G, Doglioni C, Hes O, Argani P, Chilosi M (2009) Cathepsin-K immunoreactivity distinguishes MiTF/TFE family renal translocation carcinomas from other renal carcinomas. Mod Pathol: Off J U S Can Acad Pathol Inc 22:1016–1022. doi:10.1038/modpathol.2009.58

30. Meloni AM, Sandberg AA, Pontes JE, Dobbs RM Jr (1992) Translocation (X;1)(p11.2;q21). A subtype of renal adenocarcinomas. Cancer Genet Cytogenet 63:100–101
31. Meyer PN, Clark JI, Flanigan RC, Picken MM (2007) Xp11.2 translocation renal cell carcinoma with very aggressive course in five adults. Am J Clin Pathol 128:70–79. doi:10.1309/LR5G1VMXPY3G0CUK
32. Mosquera JM, Dal Cin P, Mertz KD, Perner S, Davis IJ, Fisher DE, Rubin MA, Hirsch MS (2011) Validation of a TFE3 break-apart FISH assay for Xp11.2 translocation renal cell carcinomas. Diagn Mol Pathol: Am J Surg Pathol B 20:129–137. doi:10.1097/PDM.0b013e31820e9c67
33. Pan CC, Sung MT, Huang HY, Yeh KT (2013) High chromosomal copy number alterations in Xp11 translocation renal cell carcinomas detected by array comparative genomic hybridization are associated with aggressive behavior. Am J Surg Pathol 37:1116–1119. doi:10.1097/PAS.0b013e318293d872
34. Petersson F, Grossmann P, Hora M, Sperga M, Montiel DP, Martinek P, Gutierrez ME, Bulimbasic S, Michal M, Branzovsky J, Hes O (2013) Renal cell carcinoma with areas mimicking renal angiomyoadenomatous tumor/clear cell papillary renal cell carcinoma. Hum Pathol. doi:10.1016/j.humpath.2012.11.019
35. Ramphal R, Pappo A, Zielenska M, Grant R, Ngan BY (2006) Pediatric renal cell carcinoma: clinical, pathologic, and molecular abnormalities associated with the members of the mit transcription factor family. Am J Clin Pathol 126:349–364. doi:10.1309/98YE9E442AR7LX2X
36. Rao Q, Williamson SR, Zhang S, Eble JN, Grignon DJ, Wang M, Zhou XJ, Huang W, Tan PH, Maclennan GT, Cheng L (2013) TFE3 break-apart FISH has a higher sensitivity for Xp11.2 translocation-associated renal cell carcinoma compared with TFE3 or cathepsin K immunohistochemical staining alone: expanding the morphologic spectrum. Am J Surg Pathol 37:804–815. doi:10.1097/PAS.0b013e31827e17cb
37. Renshaw AA, Zhang H, Corless CL, Fletcher JA, Pins MR (1997) Solid variants of papillary (chromophil) renal cell carcinoma: clinicopathologic and genetic features. Am J Surg Pathol 21:1203–1209
38. Smith NE, Illei PB, Allaf M, Gonzalez N, Morris K, Hicks J, Demarzo A, Reuter VE, Amin MB, Epstein JI, Netto GJ, Argani P (2014) t(6;11) renal cell carcinoma (RCC): expanded immunohistochemical profile emphasizing novel RCC markers and report of 10 new genetically confirmed cases. Am J Surg Pathol 38:604–614. doi:10.1097/PAS.0000000000000203
39. Srigley JR, Delahunt B, Eble JN, Egevad L, Epstein JI, Grignon D, Hes O, Moch H, Montironi R, Tickoo SK, Zhou M, Argani P, Panel IRT (2013) The International Society of Urological Pathology (ISUP) Vancouver classification of renal neoplasia. Am J Surg Pathol 37:1469–1489. doi:10.1097/PAS.0b013e318299f2d1
40. Sukov WR, Hodge JC, Lohse CM, Leibovich BC, Thompson RH, Pearce KE, Wiktor AE, Cheville JC (2012) TFE3 rearrangements in adult renal cell carcinoma: clinical and pathologic features with outcome in a large series of consecutively treated patients. Am J Surg Pathol 36:663–670. doi:10.1097/PAS.0b013e31824dd972
41. Tomlinson DC, L'Hote CG, Kennedy W, Pitt E, Knowles MA (2005) Alternative splicing of fibroblast growth factor receptor 3 produces a secreted isoform that inhibits fibroblast growth factor-induced proliferation and is repressed in urothelial carcinoma cell lines. Cancer Res 65:10441–10449. doi:10.1158/0008-5472.CAN-05-1718
42. Tonk V, Wilson KS, Timmons CF, Schneider NR, Tomlinson GE (1995) Renal cell carcinoma with translocation (X;1). Further evidence for a cytogenetically defined subtype. Cancer Genet Cytogenet 81:72–75
43. Weterman MA, Wilbrink M, Geurts van Kessel A (1996) Fusion of the transcription factor TFE3 gene to a novel gene, PRCC, in t(X;1)(p11;q21)-positive papillary renal cell carcinomas. Proc Natl Acad Sci U S A 93:15294–15298
44. Winarti NW, Argani P, De Marzo AM, Hicks J, Mulyadi K (2008) Pediatric renal cell carcinoma associated with Xp11.2 translocation/TFE3 gene fusion. Int J Surg Pathol 16:66–72. doi:10.1177/1066896907304994
45. Wu A, Kunju LP, Cheng L, Shah RB (2008) Renal cell carcinoma in children and young adults: analysis of clinicopathological, immunohistochemical and molecular characteristics with an emphasis on the spectrum of Xp11.2 translocation-associated and unusual clear cell subtypes. Histopathology 53:533–544. doi:10.1111/j.1365-2559.2008.03151.x
46. Yan BC, Mackinnon AC, Al-Ahmadie HA (2009) Recent developments in the pathology of renal tumors: morphology and molecular characteristics of select entities. Arch Pathol Lab Med 133:1026–1032. doi:10.1043/1543-2165-133.7.1026
47. Zhong M, De Angelo P, Osborne L, Keane-Tarchichi M, Goldfischer M, Edelmann L, Yang Y, Linehan WM, Merino MJ, Aisner S, Hameed M (2010) Dual-color, break-apart FISH assay on paraffin-embedded tissues as an adjunct to diagnosis of Xp11 translocation renal cell carcinoma and alveolar soft part sarcoma. Am J Surg Pathol 34:757–766. doi:10.1097/PAS.0b013e3181dd577e
48. Zhong M, De Angelo P, Osborne L, Paniz-Mondolfi AE, Geller M, Yang Y, Linehan WM, Merino MJ, Cordon-Cardo C, Cai D (2012) Translocation renal cell carcinomas in adults: a single-institution experience. Am J Surg Pathol 36:654–662. doi:10.1097/PAS.0b013e31824f24a6

1.4.2 Aggressive and nonaggressive translocation t(6;11) renal cell carcinoma: comparative study of 6 cases and review of the literature

t(6;11) RCC je považován za vzácný a většinou neagresivní tumor. Kritéria odlišující agresivní od neagresivních t(6;11) RCCs však nejsou zcela jasně stanovena.

V rámci studie bylo vyhledáno celkem šest t(6;11) RCC, které byly analyzovány morfologicky a za užití imunohistochemie a molekulárně-genetických metod. Pět případů t(6;11) RCCs se chovalo neagresivně, jeden z analyzovaných tumorů však měl jasně agresivní potenciál/průběh onemocnění. Agresivní tumor pocházel od 77-ti leté pacientky, která zemřela 2,5 měsíce po stanovení diagnózy, tumor byl objemný (v největším rozměru měřil 12 cm). Neagresivní t(6;11) renální karcinomy pocházely od tří žen a 2 mužů, jejichž věk se pohyboval v rozmezí 15 - 54 let a tumory měřily od 3 do 14 cm v největším rozměru. Všechny tumory byly dobře ohraničeny, vykazovaly solidní a alveolární architektoniku s ojedinělými tubuly a pseudorozetami. Agresivní t(6;11) renální karcinom byl současně i rozsáhle nekrotický a fokálně vykazoval pseudopapilární okrsky lemované bizarními polymorfními buňkami. Mitózy byly přítomny relativně vzácně, ale zaznamenány ve všech šesti případech. Všechny tumory byly imunohistochemicky pozitivní v barvení HMB45, Melan A, Katepsin K a cytokeratinech. Pozitivita CD117 byla prokázána jak u 4/5 neagresivních t(6;11) RCC, tak i v primárním agresivním t(6;11) RCC i jeho metastatických ložiscích. Celkem u 4/5 neagresivních t(6;11) RCC jsme prokázaly imunoreaktivitu ve vimentinu, naopak vimentin byl negativní v agresivním t(6;11) RCC (v primárním tumoru i v metastáze). V 2/5 neagresivních t(6;11) RCC byla prokázána „pozitivita mTOR“. Translokace t(6;11)(*Alpha-TFEB*) nebo zlom v genu *TFEB* byly detekovány v 4/5 neagresivních t(6;11) RCC, agresivní t(6;11) RCC vykazoval amplifikaci lokusu *TFEB*. Ztráta části chromozomu 1 a chromozomu 22 byla zastižena v 1/5 neagresivních a i v případě agresivního t(6;11) RCC.

Závěry této práce lze shrnout do několika bodů: (1) agresivní varianta t(6;11) RCC se patrně vyskytuje ve starším věku v porovnání s indolentním t(6;11) RCC. (2) Nekróza byla přítomna pouze u agresivního t(6;11) RCC. (3) Amplifikace lokusu *TFEB* byla zastižena pouze u agresivního t(6;11) RCC, teoreticky by tak mohla značit agresivní chování u této nádorové jednotky.

Annals of Diagnostic Pathology 18 (2014) 351–357

Contents lists available at ScienceDirect

Annals of Diagnostic Pathology

Aggressive and nonaggressive translocation t(6;11) renal cell carcinoma: comparative study of 6 cases and review of the literature

Kvetoslava Peckova, MD [a], Tomas Vanecek, PhD [a], Petr Martinek, MSc [a], Dominic Spagnolo, MD [b], Naoto Kuroda, MD [c], Matteo Brunelli, MD, PhD [d], Semir Vranic, MD, PhD [e], Slavisa Djuricic, MD, PhD [f], Pavla Rotterova, MD, PhD [a], Ondrej Daum, MD, PhD [a], Bohuslava Kokoskova, MD [a], Pavla Vesela, MD [a], Kristyna Pivovarcikova, MD [a], Kevin Bauleth, MD [a], Magdalena Dubova, MD [a], Kristyna Kalusova, MD [g], Milan Hora, MD, PhD [g], Michal Michal, MD [a], Ondrej Hes, MD, PhD [a,h,*]

[a] Department of Pathology, Faculty of Medicine, University Hospital Plzeň, Charles University, Pilsen, Czech Republic
[b] Department of Pathology, PathWest Laboratory Medicine WA, Nedlands, Australia
[c] Department of Diagnostic Pathology, Kochi Red Cross Hospital, Kochi, Japan
[d] Department of Pathology and Diagnostic, University of Verona, Verona, Italy
[e] Department of Pathology, Clinical Center of the University of Sarajevo, Sarajevo, Bosnia and Herzegovina
[f] Department of Pathology, Mother and Child Health Institute of Serbia, Belgrade, Serbia
[g] Department of Urology, Faculty of Medicine in Plzeň, Charles University in Prague, Pilsen, Czech Republic
[h] Biomedical Centre, Faculty of Medicine in Plzen, Charles University in Prague, Pilsen, Czech Republic

ARTICLE INFO

Keywords:
Kidney
Translocation renal cell carcinoma
t(6;11)
Aggressive
Nonaggressive
Immunohistochemistry
Molecular biology

ABSTRACT

t(6;11) renal cell carcinoma (RCC) has been recognized as a rare and mostly nonaggressive tumor (NAT). The criteria for distinguishing aggressive tumors (AT) from NATs are not well established. A total of 6 cases were selected for the study. Five cases of t(6;11) RCCs behaved nonaggressively, and 1 was carcinoma with aggressive behavior. The tumors were analyzed morphologically using immunohistochemistry and by molecular-genetic methods. The specimen of aggressive t(6;11) RCC was from a 77-year-old woman who died of the disease 2.5 months after diagnosis. The specimens of nonaggressive t(6;11) RCCs were from 3 women and 2 men whose ages range between 15 and 54 years. Follow-up was available in all cases (2.5 months-8 years). The tumor size ranged from 3 to 14 cm in nonaggressive t(6;11) RCC. In the aggressive carcinoma, the tumor size was 12 cm. All tumors (6/6) were well circumscribed. Aggressive t(6;11) RCC was widely necrotic. Six (100%) of 6 all tumors displayed a solid/alveolar architecture with occasional tubules and pseudorosettes. Pseudopapillary formations lined by bizarre polymorphic cells were found focally in the aggressive t(6;11) RCC case. Mitoses, though rare, were found as well. All cases (AT and NAT) were positive for HMB-45, Melan-A, Cathepsin K, and cytokeratins. CD117 positivity was seen in 4 of 5 NATs, as well as in the primary and metastatic lesions of the AT. mTOR was positive in 2 of 5 NATs and vimentin in 4 of 5 NATs. Vimentin was negative in the primary lesion of the AT, as well as in the metastasis found in the adrenal gland. Translocation t(6;11)(*Alpha-TFEB*) or *TFEB* break was detected in 4 of 5 NATs and in the AT case. Aggressive tumor showed amplification of *TFEB* locus. Losses of part of chromosome 1 and chromosome 22 were found in 1 of 5 NATs and in the AT. Conclusions: (1) Aggressive t(6;11) RCCs generally occur in the older population in comparison with their indolent counterparts. (2) In regard to the histologic findings in ATs, 3 of 5 so far published cases were morphologically not typical for t(6;11) RCC. Of the 3 cases, 2 cases lacked a small cell component and 1 closely mimicked clear cell–type RCC. (3) Necroses were only present in aggressive t(6;11) RCC. (4) Amplification of *TFEB* locus was also found only in the aggressive t(6;11) RCC.

1. Introduction

t(6;11) translocation renal cell carcinoma (t(6;11) (TRCC) has been recognized as a new entity by the International Society of Urological Pathology 2012 conference and has subsequently been considered as a part of MiT family translocation carcinomas [1]. Regrouping TFEB and TFE3 translocation carcinomas together under the category of "MiTF/TFE family translocation carcinomas" was first suggested by Argani and Ladanyi [2–4], because the reason for regrouping of t(6;11) RCC and Xp11 TRCCs was similar morphologic, immunohistochemical, and molecular-genetic features. Translocation involving *TFEB* and *TFE3* induces the overexpression of these proteins and can be specifically identified by immunohistochemistry, where nuclear

* Corresponding author. Department of Pathology, Faculty of Medicine, Charles University Hospital Plzeň, Charles University, Alej Svobody 80, 304 60 Pilsen, Czech Republic. Tel.: +420 377104643; fax: +420 377104650.
E-mail address: hes@medima.cz (O. Hes).

http://dx.doi.org/10.1016/j.anndiagpath.2014.10.002
1092-9134/

labeling for TFEB is specific to t(6;11) RCC and nuclear positivity of TFE3 is specific to Xp11.2 translocations. However, recent articles have shown the limited reliability of immunohistochemical evaluation of TFE3 protein [5].

Together with the TFEB and TFE3, MiT family also involves MITF and TFEC, all of which have overlapping transcriptional activities [6]. The variations of the clinicopathologic spectrum of these tumors have yet to be determined. Contrary to the Xp11.2 TRCCs, where aggressive clinical behavior has frequently been documented, the t(6;11) TRCC presented mostly with a nonaggressive clinical course, thus having come to be considered as indolent, usually low-stage and low-grade tumors [7–9].

Up to date, 49 cases of t(6;11) TRCC have been reported, most without signs of aggressive behavior. [5,10,11]. Only 4 cases with aggressive behavior have been reported thus far (8%) [11–14].

In our study, we have compared 5 nonaggressive tumors (NAT) with 1 previously unreported aggressive metastazing tumor (AT), using the morphology, immunohistochemistry, and molecular-genetic examinations. Extensive research of the literature written in English has been undertaken to elucidate all known facts about aggressive t(6;11) TRCC that have been described so far.

2. Materials and methods

Out of 17 700 renal tumors and tumor-like lesions in the institutional and consultation files of Sikl's Department of Pathology, Charles University, Plzen, Czech Republic, 6 cases of t(6;11) RCC were identified. Four cases have been reported [15,16], and 2 new unpublished cases (including 1 aggressive metastazing case) have been added. The tissues were fixed in neutral formalin and embedded in paraffin and were cut into 4 to 5 μm thin sections and stained with hematoxylin and eosin.

2.1. Immunohistochemistry

The immunohistochemical study was performed using a Ventana Benchmark XT automated stainer (Ventana Medical System, Inc, Tucson, Arizona) on formalin-fixed, paraffin-embedded tissue. The following primary antibodies were used: cytokeratins (CAM 5,2, monoclonal, 1:200; Becton-Dickinson, San Jose, California), AE1-AE3 (monoclonal, 1:1000; BioGenex, San Ramon, California), CD10 (56C6, 1:20; Novocastra, Burlingame, California), c-kit (CD 117, polyclonal, RTU; DakoCytomation, Glostrup, Denmark), racemase/AMACR (P504S, monoclonal, 1:50; Zeta, Sierra Madre, California), vimentin (D9, monoclonal, 1:1000; NeoMarkers, Westinghouse, California), anti-melanosome (HMB45, monoclonal, 1:200; DakoCytomation), PAX8 (polyclonal, 1:25; Cell Marque, Rocklin, California), cathepsin K (3F9, monoclonal, 1:100; Abcam, Cambridge, UK), S100 (polyclonal, 1:400; DakoCytomation), Melan-A (A103,monoclonal, RTU; DakoCytomation), TFE3 (monoclonal, MRQ-37, RTU; Cell Marque), tyrosinase (polyclonal, 1:100; NeoMarkers, Westinghouse, Fremont California), mTor (monoclonal, Ser 2448, 49F9, 1:50; Cell Signaling, Danvers, Massachusetts). The primary antibodies were visualized using the supersensitive streptavidin-biotin-peroxidase complex (BioGenex). Appropriate positive controls were used.

2.2. Molecular-genetic study

Detection of *Alpha-TFEB* genomic junction, *Alpha-TFEB* fusion transcript, and chromosomal numerical changes was performed by polymerase chain reaction (PCR; case 2), reverse transcriptase PCR (cases 2 and 6), and array comparative genomic hybridization (aCGH) (case 2), respectively. All these methods were described in Petersson et al [15]. Fluorescence in situ hybridization (FISH) analysis was performed in cases 1, 3, 4, 5, and 6 using break apart probe *TFEB* ba (6p21) consisting of BAC probes RP11-328M4 a RP11-533O20 (BlueGnome, Cambridge, UK). In cases 5 and 6, FISH analysis of chromosomal loci 1p36 and 22q was performed using probes 1p36/1q25 and LSI 22BCR (VYSIS/Abbott Molecular, Des Plaines, Illinois). The tumor areas of the specimens were examined with an Olympus BX51 fluorescence microscope using a ×100 objective and filter sets Triple Band Pass (DAPI/Spectrum Green/Spectrum Orange) and Single Band Pass (Spectrum Green, Orange, and Aqua). Scoring was performed by counting the number of fluorescent signals in 100 randomly selected, nonoverlapping tumor cell nuclei. The slide was independently enumerated by 2 observers (P.M. and T.V.). Cutoff values for monosomy were set at 35% and 37% for 1p36 and 22q probes, respectively, and for polysomy at 10% for both probes. Cutoff for *TFEB* ba probe was set at 10%.

3. Results

3.1. Clinical features

The basic clinicopathologic data are summarized in Table 1. Cases 1 to 4 have been already reported [15,16]. In brief, the patients were 4 women and 2 men (all Caucasian) with age ranging from 15 to 77 years (mean, 35.3 years; median, 23 years). Follow-up was available for all patients (ranging from 2.5 months to 8 years; mean, 3.37; median, 3 years). Clinical data from the 2 new patients were as follows:

Case 5: a 15-year-old boy was referred to the hospital because of a palpable painless swelling of the abdomen. No hematuria was detected. Radical nephrectomy was performed; no adjuvant oncologic treatment was administered.

Case 6: tumor was found in a 77-year-old women. The patient complained of increasing back pain and renal colic. Computed tomographic (CT) scan revealed a tumor of the left kidney measuring 16.5 × 12.3 × 16.7 cm. The patient died of disease 2.5 months after diagnosis with metastases to ipsilateral adrenal gland (histologically confirmed) and lung (determined using CT and positron emission tomography/CT scanning).

3.2. Pathological findings

3.2.1. Gross pathology

Nonaggressive tumors were well circumscribed, largely encapsulated, and displayed gray to tan cut surface with focal hemorrhage. Focal cystic change was present in 1 case. There were no grossly visible foci of necrosis. Tumor size ranged from 3 to 14 cm (median, 5 cm). In all cases, the tumors were confined to the kidney. Hence, there was no infiltration of the perirenal or sinusoidal fat, neither was there renal vein invasion.

Aggressive tumor was partially encapsulated, well circumscribed with voluminous, mostly centrally located hemorrhagic necrosis. Cut surface was brown. Tumor measured 12 × 11.5 × 9 cm (Fig. 1).

3.2.2. Morphology

3.2.2.1. Cases 1 to 5 (NATs). On low power, all tumors displayed a solid or solid/alveolar architecture. The tumors were mostly surrounded by a fibrous pseudocapsule. Although only focally, groups of entrapped

Table 1
Main clinicopathologic data

Case	Age (y)	Sex	Size (cm)	Clinical manifestation	Follow-up
1	22	M	3	Incidental finding	8 y AW, then LE
2	24	F	14	Palpable mass	3 y AW, then LE
3	20	F	9.5	Incidental finding	5 y AW, than LE
4	54	F	7	Increasing pain right hip (nephrectomy)	AW 3 y after dg, then LE
5	15	M	10	Palpable mass	AW 1 y
6	77	F	12	Increased back pain, renal colic	DOD 2.5 mo after dg

Abbreviations: M, male; F, female; AW, alive and well; LE, lost of evidence; DOD, dead of disease; dg, diagnosis.

Table 2
Results of immunohistochemical examinations: nonaggressive cases

Case	HMB45	Melan-A	TFE3	CD10	CD117	Tyros	mTor	CAM 5.2	AE1/AE3	Cath	Vim	PAX8	MIB1
1	+++	++	−	+	++	+	−	Foc ++	−	+++	+	−	1-2/hpf
2	+++	++	−	Foc +	++	Foc +	Foc+	++	++	+++	+	Foc weak+	1-2/hpf
3	+++	−	−	Foc +	−	+ −	Foc+	Foc+	−	+++	+	++	0-1/hpf
4	++ focal	++	−	0	Foc ++	Not done	−	−	−	+++	Not done	Foc +	0-1/hpf
5	+++	+++	−	Foc ++	Foc ++	Foc+	−	Foc ++	Foc ++	+++	+	Foc ++	5-8/hpf

Abbreviations: Cath, Cathepsin-K; MIB1, antibody against Ki-67 antigen; Tyros, tyrosinase; vim, vimentin; hpf, high-power field; foc, focal.
"+" = weak positivity; "++" = moderate positivity; "+++" = strong positivity; "−" = negative.

tubules at the edge of the tumor were found. Degenerative changes were noted in 2 of the 4 cases. Microscopic foci of necrosis and fibrosis were seen in cases 1 and 2. All tumors contained areas with discohesive neoplastic cells. Some of these areas displayed tubulary architecture, whereas other areas showed a more solid architecture. The pseudorosettes were present in all tumors (Fig. 2). These pseudorosettes were formed by smaller lymphocyte-like cells, grouped around collagenous spheres, formed by basement membrane material. The small lymphocyte-like cells had scanty cytoplasm and round nuclei (Fuhrman grade 1). The pseudorosettes frequently contained areas with signet ring–like change or conspicuous clear cell change. In some tumors (cases 1, 3, and 4), the pseudorosettes were already apparent at low magnification. In case 2, the pseudorosettes were less apparent and discernible only at higher magnification and after serial sectioning. In the same case, there were long branching narrow tubules that were already very conspicuous at low-power magnification. These tubules were rimmed by one row of neoplastic cells with granular cytoplasm, having the nuclei aligned on the basement membrane, thus giving these structures a resemblance to glandular epithelium. Infrequently, areas with solid growth and moderate atypia (corresponding to Fuhrman nucleolar grade 2 or rarely 3) were observed (Fig. 3). Most of the neoplastic cells had abundant eosinophilic, slightly granular, and sometimes "feathery" cytoplasm. Populations of larger cells with voluminous clear to slightly eosinophilic cytoplasm were present in all tumors. In 2 cases (cases 1 and 2), we found areas with hyalinization formed by basal membrane material. Mitotic figures were exceptionally rare in 1 case (case 2), and atypical mitoses were absent. In addition to the above-described morphologic characteristics, small foci with morphologic features strongly resembling another translocation associated renal tumor, the ASPL-TFE3 renal carcinoma (Xp11.2 group), were detected in 1 case (case 2). In this area, alveolar and tubulopapillary structures were lined by large cells having voluminous clear to slightly eosinophilic cytoplasm. The nuclei in these areas were Fuhrman nucleolar grade 3.

3.2.2.2. Case 6 (AT). Tumor was mostly solid to solid-alveolar, composed of larger eosinophilic cells with the occasional presence of lymphocytes in the interstitium (Fig. 4). There were voluminous necrotic and hemorrhagic areas. Occasionally, large tubules and pseudotubules were scattered through tumorous mass. Cells were mostly voluminous, weakly eosinophilic with "cloudy" appearance. Nuclei were of grade 2 and 3 according to Fuhrman nucleolar grade. Pseudorosettes were located mostly within large pseudotubules. Only few mitotic figures were noted, no atypical mitoses were encountered. Foci of pseudopapillary to papillary formations were rarely noted. Papillae were lined by large, bizarre polymorphic cells with Fuhrman nucleolar grade 3 and 4 (Fig. 5).

3.2.3. Immunohistochemistry

3.2.3.1. NATs (cases 1-5). The immunohistochemical findings of NATs are summarized in Table 2. All of them were diffusely positive for Cathepsin K, HMB-45 (Fig. 6A), and Melan-A. Vimentin was positive in all cases, although positivity was weak. Expression of cytokeratins CAM 5.2 and AE1-AE3 was variable (Fig. 6B). CD10 and tyrosinase were weakly and focally positive in 4 of 5. Two of 5 cases were weakly and focally immunoreactive for mTOR. Four of 5 NATs were positive strongly but focally for CD117. PAX8 immunoreactive pattern was variable with negative (1/5) to moderate positive staining (1/5). Mostly tumors were focally positive (3/5). There was no diffuse expression of TFE3 in any of the tumors.

3.2.3.2. AT (case 6). The complete results of immunohistochemical examinations of primary aggressive t(6;11) RCC and metastatic lesion are summarized in Table 3. Both showed a strong, diffuse immunoreactivity for HMB-45, Melan-A, and Cathepsin-K. CAM 5.2 and CD10 were moderately positive. CD117 was positive in both primary and metastatic lesions. PAX8 was focally positive in primary and metastatic tumor. The neoplastic cells did not express TFE3, tyrosinase, mTOR, AE1/AE3, and vimentin in both primary and metastatic tumor.

3.3. Molecular-genetic findings

Results of molecular-genetic findings are summarized in Table 4. *TFEB* gene rearrangement or *Alpha-TFEB* translocation was found in 5 of 6 cases. One was unanalyzable. In AT, *TFEB* gene break was accompanied by its amplification. In 2 of 3 analyzed cases, including AT, loss of 1p36 and 22q was also detected.

4. Discussion

t(6;11) TRCC is recognized mostly as a low-grade NAT. This is in contrast to Xp11.2 TRCC. Most of Xp11.2 TRCCs are considered to be highly aggressive, high-stage, and high-grade tumors [1,16].

There are no well-established prognostic criteria predicting biological behavior that are applicable for t(6;11) TRCC.

t(6;11) TRCC is usually described as neoplasm with a distinctive biphasic pattern, comprising larger and smaller epithelioid cells, with the latter often clustered around basement membrane material; however, the full spectrum of the morphologic appearances of the t(6;11) TRCC is probably more variable [17–19]. The t(6;11) TRCCs express Cathepsin K, HMB-45, Melan-A, and usually PAX8. Nuclear labeling for TFEB protein by IHC is supposed to be a sensitive and specific assay for

Table 3
Results of immunohistochemical examinations—aggressive case

	HMB45	Melan-A	TFE3	CD 10	CD 117	Tyros	mTor	CAM 5.2	AE1/AE3	Cath	Vim	PAX8	MIB1
Prim	+++	+++	0	++	Foc ++	0	0	++	0	+++	−	Foc +	0-5/hpf
Meta	+++	+++	0	Foc ++	Foc ++	0	0	++	0	+++	−	Foc +	8-12/hpf

Abbreviations: Cath, Cathepsin-K; MIB1, antibody against Ki-67 antigen; Tyros, tyrosinase; Vim, vimentin; hpf, high-power field; Prim, primary tumor; Meta, metastasis to suprarenal gland; foc, focal.
"+" = weak positivity; "++" = moderate positivity; "+++" = strong positivity; "−" = negative.

Table 4
Molecular-genetic analysis

Case	Numerical changes	Translocation		
	aCGH or FISH (1p36 and 22q probes)	FISH *TFEB* ba probe	RT-PCR *Alpha-TFEB*	PCR *Alpha-TFEB*
1	NP	NA	NP	NP
2[a]	Loss 1p35.1 to p36.21 (aCGH) Loss 22q (aCGH)	NP	Positive	Positive
3	NP	Positive	NP	NP
4	NP	Positive	NP	NP
5	Negative (FISH)	Positive	NP	NP
6	Loss 1p36 (FISH) Loss 22q (FISH)	Positive (amplification)	Positive	NP

Abbreviations: RT, reverse transcriptase; NP, not performed; NA, not analyzable.
[a] Translocation t(X;17) (ASPL-TFE3) was analyzed in case 2 with negative result.

these neoplasms; however, there are many false-positive/negative staining as a result of fixation, autolysis, and other steps related to the tissue processing [5,20]. Furthermore, CD117 was found to be another potential distinguishing marker between the t(6;11) TRCC and Xp11.2 TRCC. CD117 is usually positive in t(6;11) TRCC, but not positive in most of Xp11.2 TRCCs [11]. In our series, one of the NATs was negative for CD117. Generally, positivity for CD117 was moderate, but mostly focal. In the AT, focal membranous positivity for CD117 was noted both in the primary tumor and in metastasis. Immunoreactivity with PAX8 was highly variable (negative to moderately positive) in our cases.

Fluorescence in situ hybridization assay for *TFEB* gene break or PCR-based analysis for the presence of *Alpha-TFEB* fusion is currently available even for paraffin-embedded material, which seems a more robust technique than immunohistochemical examination [1,21].

t(6;11) TRCC has long been considered as NAT. Even so, the possible late recurrence, similar to the behavior reported of Xp11.2 TRCC, and metastatic potential have been observed. Up to date, 4 aggressive cases of t(6;11) TRCC have been reported. The overview of 4 aggressive t(6;11) TRCC described in the literature and summary of our new case is outlined in Table 5[11,14].

The first case was described by Martignoni et al [12] in 2005. The tumor was found in 42-year-old woman who presented with paratracheal and pleural metastases 3 years after the surgery. However, later the question was raised, whether this tumor was indeed t(6;11) TRCC, Xp11.2 TRCC, or an unusual variant of TRCC with overlapping features between Xp11.2 and t(6;11) TRCC (Dr. Guido Martignoni and Dr. Matteo Brunelli's personal communication).

The second aggressive case of t(6;11) TRCC was reported by Camparo et al [13] in 2008. The size of the tumor was 20 cm, and it

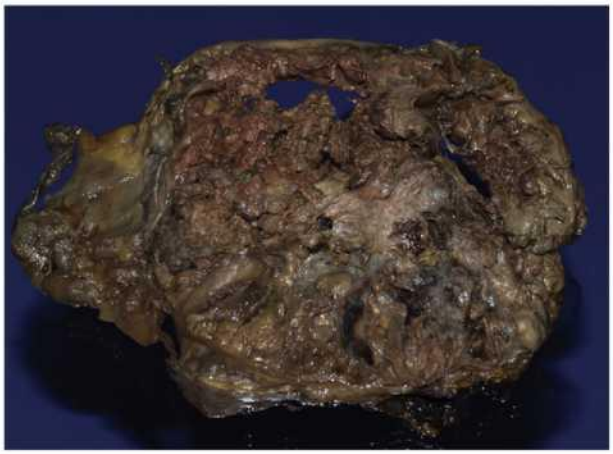

Fig. 1. Huge area of mostly centrally located necrosis was present on gross section of aggressive case.

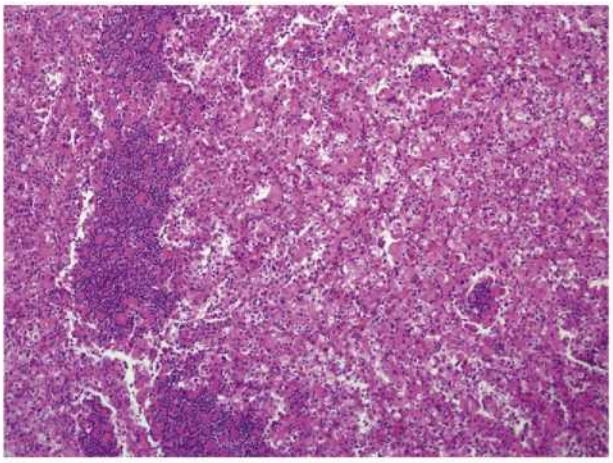

Fig. 2. In typical cases of nonaggressive cases, the pseudorosettes were formed by smaller lymphocyte-like cells grouped around collagenous spherules.

presented as an abdominal mass in a 36-year-old man who died after 3 months after the diagnosis with widespread metastatic disease.

Third malignant t(6;11) TRCC was described by Inamura et al [14] in 2012. A 37-year-old man had undergone a total nephrectomy in 1989. Eight years later, he presented with lung and mediastinal lymph node metastases. The renal tumor was originally diagnosed as clear cell-type RCC. Subsequently, he underwent a lymph node dissection and

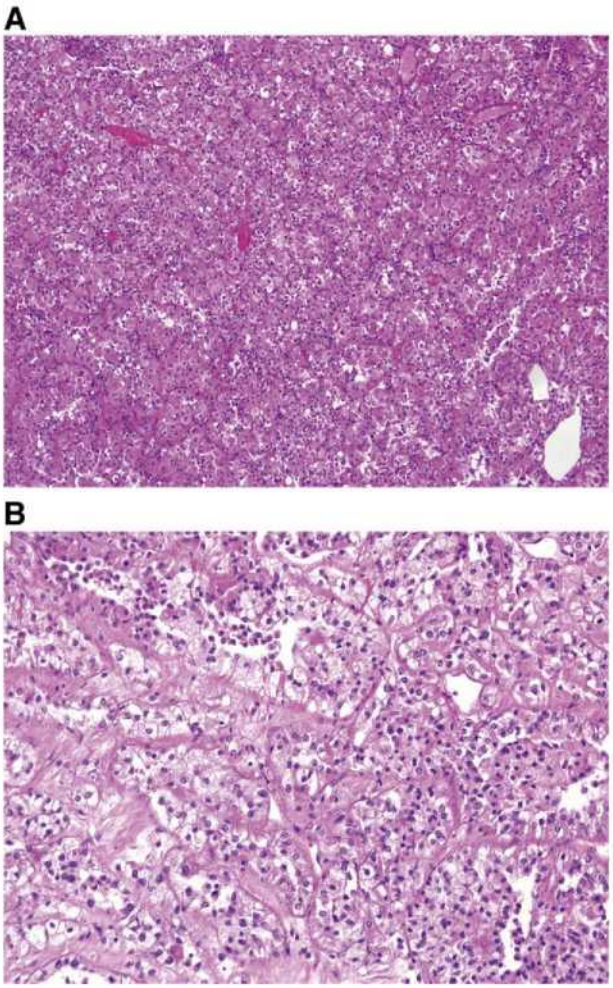

Fig. 3. Areas with solid growth and moderate atypia were observed both in nonaggressive cases (A) and in aggressive cases (B).

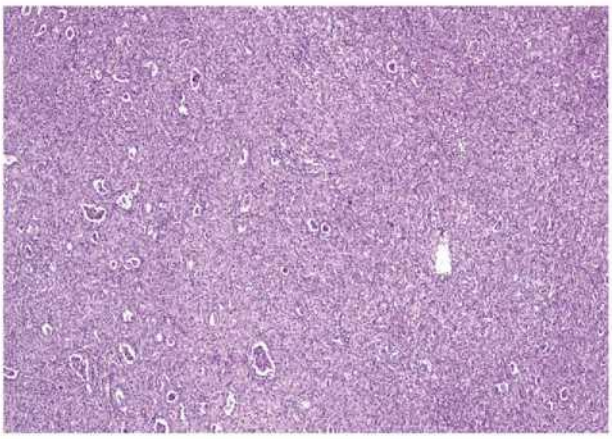

Fig. 4. Pseudorosettes in aggressive case were less conspicuous comparing with typical nonaggressive cases.

partial resection of the lung for the metastatic tumor measuring 4.5 cm. Karyotyping of the tumor revealed a t(6;11) (p21.1;q12 ~ 13) chromosomal rearrangement, a characteristic of the t(6;11) TRCC. Thirty months after second surgery, the patient died of multiple metastases to the lung and bone.

The fourth case was described by Smith et al [11] in January 2014. The tumor was found in a 34-year-old man. The patient developed rib metastasis 8 years after resection of the primary tumor.

The fifth case (currently described case) differs clinically from previously reported ATs mainly by age of the patient. The size of the tumor was relatively large; however, substantially larger NATs have been reported. Our patient died of disease 2.5 months after surgery.

Summarizing all available clinical data dealing with aggressive t(6;11) RCC cases, a few mutual characteristics have been observed. As regards clinicopathologic features, the aggressive t(6;11) TRCC appears to affect older population (mean, 45.2 years; median, 37 years) than nonaggressive cases (mean, 31.5 years; median, 30.5 years). Previously described ATs metastasized into the pleura (case 1), lung (cases 3 and 5), mediastinal lymph nodes (cases 1 and 3), bones (cases 3 and 4), and adrenal gland (case 5) (Fig. 7). The same 8-year interval between resection of the primary tumor and metastasis was observed in cases 3 and 4 (Table 5).

Size of the ATs was bigger (mean, 11.67 cm; median, 20 cm) than that of the NATs (mean, 7.43 cm; median, 4.75 cm).

Microscopic foci of necrosis were described in 1 nonaggressive case only [13]; however, it is not possible to get more information about presence/absence of necrotic foci from the previous literature. Grossly visible necrotic areas were present in 2 of 5 malignant tumors only.

Probably, the presence of grossly visible necrosis could be a possible adverse prognostic factor in t(6;11) TRCC. Mitotic figures were observed in 2 of 49 NATs and in 1 AT. However, presence/absence of mitotic activity has been seldom mentioned in the literature.

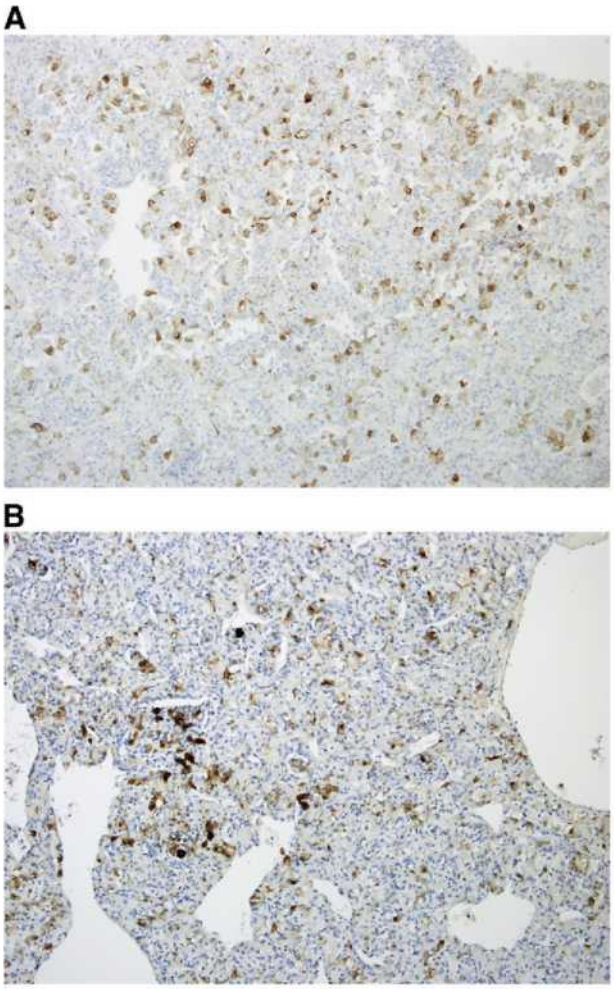

Fig. 6. All cases were positive for HMB45 (A) and cytokeratins (CAM 5.2 shown in case 2) (B).

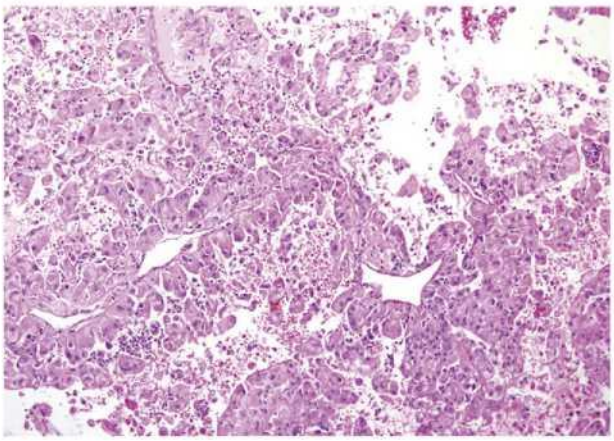

Fig. 5. In aggressive case, it was possible to find foci with papillary/pseudopapillary structures composed of bizarre atypical cells.

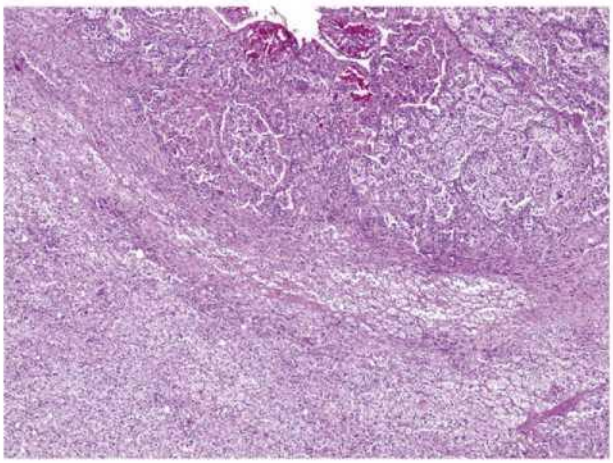

Fig. 7. Metastasis of t(6;11) RCC to the ipsilateral adrenal gland.

Table 5
Overview of the aggressive cases in the literature and current case

Case	Age (y)	Size (cm)	Necrosis	Vimentin	Mitoses	Atypical mitoses	TFEB rearrangement	Meta
Case 1: Martignoni et al Martignoni et al [12]	42	NA	None	+	None	None	NP	Paratracheal lymph nodes, pleura
Case 2: Camparo et al [13]	36	20	+ (5%)	+	Not known	Not known	NA	Not known (deceased)
Case 3: Inamura et al [14]	37	NA	Not known	+	Not known	Not known	+	Lung, mediastinal lymph node, bone
Case 4: Smith et al [11]	34	3	Not known	Not known	Not known	Not known	+	Rib
Case 5: currently described new case	77	12	+ (40%)	−	+	None	+	Adrenal gland and lung

Abbreviations: NP, not performed; NA, nonavailable; Meta, metastasis; y, years.
"+" = positive; "−" = negative.

Histologically, 2 ATs (cases 2 and 4; Table 5) lacked a small cell component. One AT (case 3; Table 5) showed features of unusual morphology for t(6;11) TRCC and was initially diagnosed as clear cell–type RCC. Morphology in the current aggressive case (case 5; Table 5) was compatible with the usual features of t(6;11) TRCC; however, some minor variations were noted (for further details, see the Results section). Papillary and pseudopapillary formations lined by high-grade cells were not described in any of NATs according to the literature. However, similar focal architecture has been described in 1 NAT but with low-grade neoplastic cells.

Aggressive tumor (case 5; Table 5) showed amplification of *TFEB* locus. No information about copy number changes of TFEB loci is mentioned in previous articles dealing AT; however, as this phenomenon was found in our set only in AT, it could be a genetic hallmark of aggressive t(6;11) RCC. Analysis of other ATs is, however, necessary to confirm this hypothesis.

Translocation t(6;11) (Alpha-TFEB) or *TFEB* break was detected in 4 NATs and 1 AT.

Losses of part of chromosomes 1 and 22 were found in our AT. However, identical findings were shown in nonaggressive case (case 2 in the original series) published previously [15]. Thus, chromosomal aberration pattern does not seem to predict/rule out potential aggressive behavior.

Regarding the histopathologic differential diagnosis, the morphology and immunohistochemical pattern of t(6;11) TRCC could mimic Xp11.2 TRCC. The most distinctive histologic pattern of the Xp11 TRCC is presence of both clear/eosinophilic cells, mostly papillary architecture and, in some cases, abundant psammoma bodies. However, Xp11.2 TRCCs can also produce pattern or unusual morphology mimicking other types of RCCs [22]. The biphasic morphologic variant with population of larger polygonal cells mixed with smaller cells clustering around hyaline material has been already described in Xp11.2 TRRCC. Such cases can simulate t(6;11) TRCC. On the other hand, the t(6;11) TRCC can mimic Xp11.2 TRCC as well [22]. The Xp11 TRCC is distinguished by chromosomal translocations with breakpoints involving the *TFE3*, which maps to the Xp11.2 locus. Differential diagnosis between both basic types of translocation carcinomas is complicated in difficult cases. Analysis of the morphology, together with immunohistochemical examination (TFE3, TFEB—if available, CD117, HMB-45, and Melan-A), should be supported by the molecular-genetic analysis.

Another tumor, which should be ruled out during the differential diagnostic process, is angiomyolipoma (AML), especially its epithelioid/oncocytic variety. Both t(6;11) TRCC and AML are positive for HMB-45 and Melan-A. It is important to note that some AMLs, as well as t(6;11) TRCC, may show only scattered HMB-45–positive cells. Angiomyolipoma is frequently composed, at least in part, of voluminous cells with slightly eosinophilic cloudy cytoplasm resembling in some aspects the neoplastic cells in t(6;11) TRCC. Angiomyolipoma frequently contains lipocytes, which are usually absent in t(6;11)-associated RCCs. Voluminous prominent vascular structures characteristic for AML could be present/absent in t(6;11) TRCC. Thus, it is not possible to use this morphologic feature for differential diagnosis. Moreover, the epithelioid variant of AML lacks usually lipocytic component (or it is inconspicuous), and vascular component could be less prominent [23]. The so-called oncocytic variant of AML is composed of large cells with voluminous eosinophilic cytoplasm arranged in solid arrangements [1,24]. Again, in unusual challenging cases, a good sampling is necessary and, in more difficult cases, analysis of translocation and/or TFEB protein performed by molecular-genetic techniques would be helpful.

5. Conclusions

We have compared all, to date reported, malignant cases of t(6;11) translocation carcinomas with one another and have tried to find some mutual features.

1. Aggressive t(6;11) RCCs generally occur in older population in comparison with their indolent counterparts.
2. In regard to the histologic findings in ATs, 3 of 5 cases were morphologically slightly different from nonaggressive t(6;11) RCC. Of the 3 cases, 2 cases lacked a small cell component and 1 closely mimicked clear cell–type RCC.
3. Grossly visible necroses were present in aggressive t(6;11) RCC only and could be potentially taken as a adverse prognostic factor.
4. Amplification of *TFEB* locus was also found only in aggressive t(6;11) RCC.

Further genetic and clinicopathologic investigations with additional new cases can further highlight this rare and peculiar variant of RCC.

Disclosure of conflict of interest

All authors declare no conflict of interest.

The study was supported by the Charles University Research Fund (project number P36) and by the project by the project CZ.1.05/2.1.00/03.0076 from European Regional Development Fund.

References

[1] Srigley JR, Delahunt B, Eble JN, Egevad L, Epstein JI, Grignon D, et al. The International Society of Urological Pathology (ISUP) Vancouver Classification of Renal Neoplasia. Am J Surg Pathol 2013;37(10):1469–89 [PubMed PMID: 24025519].
[2] Argani P, Ladanyi M. Recent advances in pediatric renal neoplasia. Adv Anat Pathol 2003;10(5):243–60 [PubMed PMID: 12973047].
[3] Argani P, Ladanyi M. Distinctive neoplasms characterised by specific chromosomal translocations comprise a significant proportion of paediatric renal cell carcinomas. Pathology 2003;35(6):492–8 [PubMed PMID: 14660099].
[4] Argani P, Ladanyi M. The evolving story of renal translocation carcinomas. Am J Clin Pathol 2006;126(3):332–4 [PubMed PMID: 16880145].
[5] Argani P, Yonescu R, Morsberger L, Morris K, Netto GJ, Smith N, et al. Molecular confirmation of t(6;11)(p21;q12) renal cell carcinoma in archival paraffin-embedded material using a break-apart TFEB FISH assay expands its clinicopathologic spectrum. Am J Surg Pathol 2012;36(10):1516–26 [PubMed PMID: 22892601].
[6] Medendorp K, van Groningen JJ, Schepens M, Vreede L, Thijssen J, Schoenmakers EF, et al. Molecular mechanisms underlying the MiT translocation subgroup of renal cell carcinomas. Cytogenet Genome Res 2007;118(2-4):157–65 [PubMed PMID: 18000366].
[7] Kuiper RP, Schepens M, Thijssen J, van Asseldonk M, van den Berg E, Bridge J, et al. Upregulation of the transcription factor TFEB in t(6;11)(p21;q13)-positive renal

cell carcinomas due to promoter substitution. Hum Mol Genet 2003;12(14):1661–9 [PubMed PMID: 12837690].
[8] Davis IJ, Hsi BL, Arroyo JD, Vargas SO, Yeh YA, Motyckova G, et al. Cloning of an Alpha-TFEB fusion in renal tumors harboring the t(6;11)(p21;q13) chromosome translocation. Proc Natl Acad Sci U S A 2003;100(10):6051–6 [PubMed PMID: 12719541. Pubmed Central PMCID: 156324].
[9] Geller JI, Argani P, Adeniran A, Hampton E, De Marzo A, Hicks J, et al. Translocation renal cell carcinoma: lack of negative impact due to lymph node spread. Cancer 2008;112(7):1607–16 [PubMed PMID: 18278810].
[10] Rao Q, Liu B, Cheng L, Zhu Y, Shi QL, Wu B, et al. Renal cell carcinomas with t(6;11)(p21;q12): a clinicopathologic study emphasizing unusual morphology, novel alpha-TFEB gene fusion point, immunobiomarkers, and ultrastructural features, as well as detection of the gene fusion by fluorescence in situ hybridization. Am J Surg Pathol 2012;36(9):1327–38 [PubMed PMID: 22895266].
[11] Smith NE, Illei PB, Allaf M, Gonzalez N, Morris K, Hicks J, et al. t(6;11) renal cell carcinoma (RCC): expanded immunohistochemical profile emphasizing novel RCC markers and report of 10 new genetically confirmed cases. Am J Surg Pathol 2014;38(5):604–14 [PubMed PMID: 24618616].
[12] Martignoni G, Tardarico R, Pea M, Pecciarini L, Gobbo S. t6;11 renal cell tumor. A clinicopathological study of two cases in adults. Mod Pathol 2005;18(Suppl 1):155A.
[13] Camparo P, Vasiliu V, Molinie V, Couturier J, Dykema KJ, Petillo D, et al. Renal translocation carcinomas: clinicopathologic, immunohistochemical, and gene expression profiling analysis of 31 cases with a review of the literature. Am J Surg Pathol 2008;32(5):656–70 [PubMed PMID: 18344867].
[14] Inamura K, Fujiwara M, Togashi Y, Nomura K, Mukai H, Fujii Y, et al. Diverse fusion patterns and heterogeneous clinicopathologic features of renal cell carcinoma with t(6;11) translocation. Am J Surg Pathol 2012;36(1):35–42 [PubMed PMID: 21959307].
[15] Petersson F, Vanecek T, Michal M, Martignoni G, Brunelli M, Halbhuber Z, et al. A distinctive translocation carcinoma of the kidney; "rosette forming," t(6;11), HMB45-positive renal tumor: a histomorphologic, immunohistochemical, ultrastructural, and molecular genetic study of 4 cases. Hum Pathol 2012;43(5):726–36 [PubMed PMID: 22051379].
[16] Hora M, Urge T, Travnicek I, Ferda J, Chudacek Z, Vanecek T, et al. MiT translocation renal cell carcinomas: two subgroups of tumours with translocations involving 6p21 [t(6;11)] and Xp11.2 [t(X;1 or X or 17)]. SpringerPlus 2014;3:245 [PubMed PMID: 24877033. Pubmed Central PMCID: 4032393].
[17] Argani P, Lae M, Hutchinson B, Reuter VE, Collins MH, Perentesis J, et al. Renal carcinomas with the t(6;11)(p21;q12): clinicopathologic features and demonstration of the specific alpha-TFEB gene fusion by immunohistochemistry, RT-PCR, and DNA PCR. Am J Surg Pathol 2005;29(2):230–40 [PubMed PMID: 15644781].
[18] Argani P, Lae M, Ballard ET, Amin M, Manivel C, Hutchinson B, et al. Translocation carcinomas of the kidney after chemotherapy in childhood. J Clin Oncol 2006;24(10):1529–34 [PubMed PMID: 16575003].
[19] Suarez-Vilela D, Izquierdo-Garcia F, Mendez-Alvarez JR, Miguelez-Garcia E, Dominguez-Iglesias F. Renal translocation carcinoma with expression of TFEB: presentation of a case with distinctive histological and immunohistochemical features. Int J Surg Pathol 2011;19(4):506–9 [PubMed PMID: 19687027].
[20] Martignoni G, Bonetti F, Chilosi M, Brunelli M, Segala D, Amin MB, et al. Cathepsin K expression in the spectrum of perivascular epithelioid cell (PEC) lesions of the kidney. Mod Pathol 2012;25(1):100–11 [PubMed PMID: 21874011].
[21] Zhong M, De Angelo P, Osborne L, Keane-Tarchichi M, Goldfischer M, Edelmann L, et al. Dual-color, break-apart FISH assay on paraffin-embedded tissues as an adjunct to diagnosis of Xp11 translocation renal cell carcinoma and alveolar soft part sarcoma. Am J Surg Pathol 2010;34(6):757–66 [PubMed PMID: 20421778].
[22] Argani P, Olgac S, Tickoo SK, Goldfischer M, Moch H, Chan DY, et al. Xp11 translocation renal cell carcinoma in adults: expanded clinical, pathologic, and genetic spectrum. Am J Surg Pathol 2007;31(8):1149–60 [PubMed PMID: 17667536].
[23] Nese N, Martignoni G, Fletcher CD, Gupta R, Pan CC, Kim H, et al. Pure epithelioid PEComas (so-called epithelioid angiomyolipoma) of the kidney: a clinicopathologic study of 41 cases: detailed assessment of morphology and risk stratification. Am J Surg Pathol 2011;35(2):161–76 [PubMed PMID: 21263237].
[24] Martignoni G, Pea M, Bonetti F, Brunelli M, Eble JN. Oncocytoma-like angiomyolipoma. A clinicopathologic and immunohistochemical study of 2 cases. Arch Pathol Lab Med 2002;126(5):610–2 [PubMed PMID: 11958671].

1.4.3 TFE3-Fusion Variant Analysis Defines Specific Clinicopathologic Associations Amog Xp11 Translocation Cancers

Dopis adresovaný editorovi časopisu „American Journal of Surgical Pathology“ reagující na sdělení autorů Argani a kol. publikované v červenci 2016 (původní práce autorů s názvem „TFE3-Fusion variant analysis defines specific clinicopathologic associations among Xp11 translocation cancers“ [7]).

V rámci zde prezentovaného dopisu editorovi jsme poskytli naše zkušenosti s jedním z raritních translokačních partnerů genu *TFE3*, genem *NONO* (též nazývaným *p54nrb*). V Plzeňském registru nádorů bylo tou dobou dostupných 41 Xp11 translokačních RCC, z nichž u 3 případů byla geneticky potvrzena přítomnost *NONO-TFE3* genové fúze. Tumory jsme detailně morfologicky a imunohistochemicky analyzovali a naše závěry porovnali s recentními daty publikovanými právě ve zmiňované původní práci Arganiho a kol [7].

Částečně i na podkladě námi zdokumentovaných dat je evidentní, že i přes velké množství popsaných morfologických variant Xp11 translokačního RCC je morfologické spektrum těchto lézí stále mnohem komplexnější a touto limitovanou sérií tří případů *NONO-TFE3* translokačních RCC jsme obohatili stále se rozšiřující morfologické spektrum.

TFE3-Fusion Variant Analysis Defines Specific Clinicopathologic Associations Among Xp11 Translocation CancersJanuary

To the Editor:

We read with great interest the article by Argani and colleagues "*TFE3*-Fusion variant analysis defines specific clinicopathologic associations among Xp11 translocation cancers" published in June 2016 volume of *American Journal of Surgical Pathology*. The authors studied 60 Xp11 translocation carcinomas using fluorescence in situ hybridization (FISH) to establish their *TFE3* fusion partner. Of 60 cases, 47 were Xp11 translocation renal cell carcinomas (RCCs). They identified, among others, 5 cases with NONO-TFE3 RCC and described theirs morphologic features. Tumors were characterized mostly by papillary architecture, with clear to weakly eosinophilic cytoplasm with subnuclear vacuoles leading to distinctive nuclear palisading.

Among 41 Xp11.2 (TFE3) translocation RCCs in our registry, we identified 3 cases of NONO-TFE3 RCC. Patients included 2 men and 1 woman, with an age range of 34 to 66 years (mean 49.7 y).

Two of our cases presented grossly as localized lesions, with a tumor size of 0.8 and 6 cm in greatest dimension. Histologically, they demonstrated papillary architecture, covered mostly by clear to eosinophilic neoplastic cells. Subnuclear vacuolization described by Argani and colleagues was at least focally noted in both cases. Both tumors had psammoma bodies and dystrophic calcifications (Fig. 1). The diagnosis of Xp11.2 translocation RCC was confirmed using FISH.

Our third case was particularly interesting with a tumor size of 2.3 cm in greatest dimension showing soft gray cut-surface (partial nephrectomy

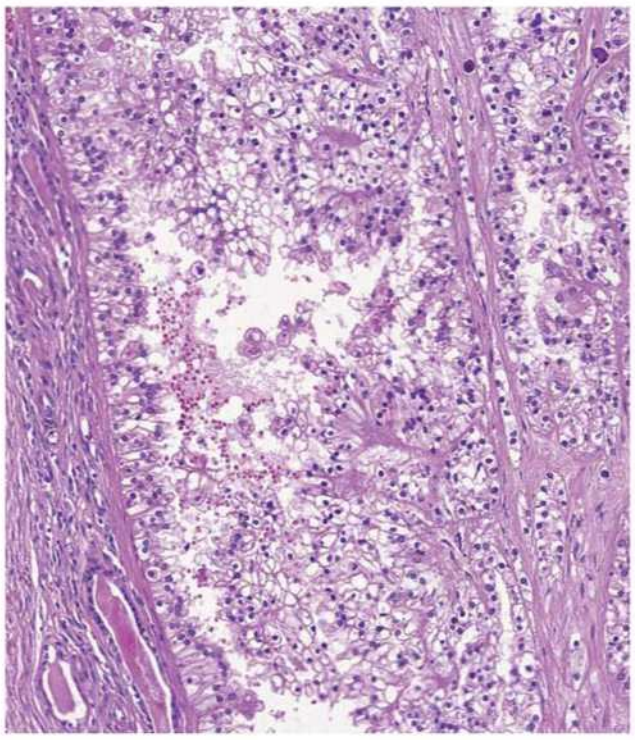

FIGURE 1. NONO-TFE3 translocation RCC (case 1) resembling cases described by Argani et al.[1]

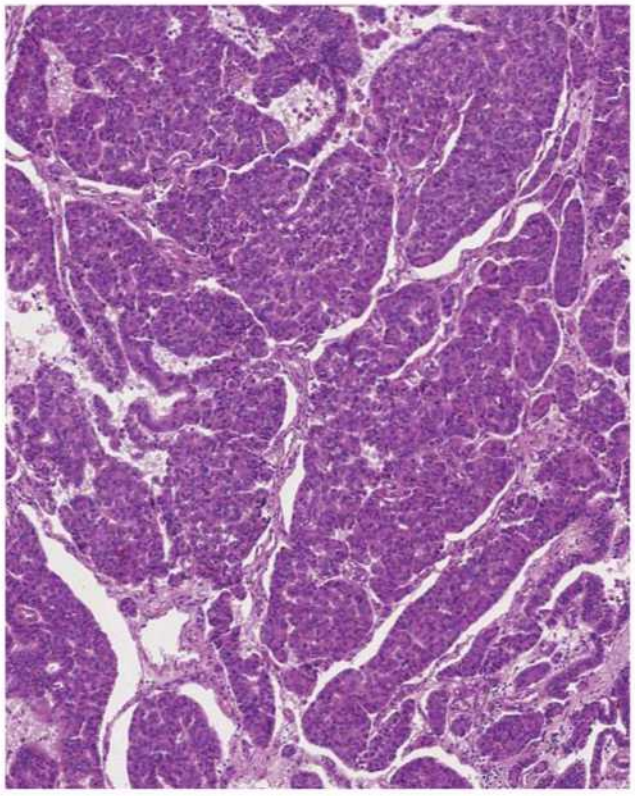

FIGURE 2. Overview of primary renal tumor (case 3) composed of eosinophilic cells with elongated polymorphic nuclei.

TABLE 1. Results of Immunohistochemical Examination of 3 NONO-TFE3 Cases

Case	Vim	AMACR	CAIX9	PAX 8	TFE3	CK 7	CD 10	HMB45	GATA 3	Cathepsin K
Case 1	Foc.	·	–	·	·	–	·	·	–	
Case 2	–	·	–	·	–	–	·	·	–	–
Case 3	–	–	–	–	–	–	–	–	–	–
Case 3—recurrent lesion	–	·	–	·	–	·	·	–	–	–

– indicates negative; ·, weak positivity; AMACR, racemase; *CAIX9*, carbonic anhydrase IX; Foc. < 50% cells staining; Vim, vimentin.

of the upper pole tumor with a pathologic stage of pT1a). Histologically, the tumor exhibited tubulopapillary architecture with small foci of necrosis. Neoplastic cells were eosinophilic and formed structures resembling a palisading pattern at the periphery of pseudotubular and papillary structures (Fig. 2). Nuclei were elongated with occasional nuclear grooves. Foci of dystrophic calcifications were also noted. Recurrent tumor (located within the lower portion of the renal medulla and protruding into the renal pelvis) was identified 4 months after resection by ultrasound examination during regular check-up. The tumor showed a similar architectural pattern to that seen in the primary lesion, with more pronounced palisading vaguely resembling urothelial carcinoma (UC).

Results of immunohistochemical examination of our 3 NONO-TFE3 cases are summarized in Table 1. All cases were positive for racemase, PAX 8, and CD10, while negative for carbonic anhydrase IX. Interestingly, 2 tumors were positive for HMB45. Vimentin was positive focally in 1 case, and TFE3 was positive in 2 cases as well as cathepsin K.

FISH analysis showed the break of *NONO* gene (using probe SureFISH Xq13.1 NONO BA) and the break of *TFE3* gene (using ZytoLight R SPEC TFE3 Dual-color Breakapart Probe) in all 3 primary tumors as well as the recurrent one. We also tested normal "nontumorous" tissue of the patient with recurrence, which showed no break of the *NONO* gene or the *TFE3* gene.

First 2 cases from our small series were very similar to the description provided by Argani and colleagues. They all were arranged in a predominantly papillary pattern. The neoplastic cells mostly showed voluminous clear to weakly eosinophilic cytoplasm. Subnuclear vacuolization resembled similar changes known from clear cell papillary RCC, which should be considered in the differential diagnosis. Both tumors had psammoma bodies and/or dystrophic calcifications. Results of FISH analyses were close to the results reported by Argani et al[1] and Clark et al.[2]

The third case was particularly interesting for several reasons. First, the architecture was more tubular than papillary. Second, the neoplastic cells were eosinophilic with relative scant cytoplasm (in comparison with previous cases), making an overall resemblance to UC. The early detection of the recurrent tumor in the renal medulla and pelvis was highly surprising in this case. It should be noted that we were unable to fully rule out the possibility that the tumor may have been initially present within the renal pelvis during the first surgery. Coincidence of RCC and UC has repeatedly been described in the literature; however, we are not aware of any UC harboring NONO-TFE3 translocation. On the basis of morphology and immunohistochemical examination, it was evident that recurrent tumor was of renal cell origin, despite its morphologic resemblance to UC. Of note, the recurrent lesion was located deep within the renal medulla, with no connection to the surface urothelium of the renal pelvis. Further, no urothelial dysplasia or UC was identified. Nontumorous tissue in this patient did not show genetic changes, that is, no break *NONO* gene or *TFE3* gene, and was used as a negative control. Similar case has been reported by Green et al[3] in 2013. Authors described Xp11 translocation RCC, which involved renal pelvis and simulated UC in several aspects.

Xp11 translocation RCCs are the most common translocation RCCs in adult population. In addition to typical Xp11.2 RCC with papillary architecture, mostly clear cells and frequent psammoma bodies, there are several other morphologic variants as well as tumors with different TFE3 fusion partners.[3–5] However many different morphologic variants of Xp11.2 translocation RCCs were described in the literature, we believe pathologic features of Xp11.2 translocation RCCs are much more complex than what is currently known. In our small series of 3 NONO-TFE3 RCCs, we enriched morphologic spectrum, which requires further investigations.

Kristyna Pivovarcikova, MD*
Petr Grossmann, PhD*
Reza Alaghehbandan, MD†
Maris Sperga, MD‡
Michal Michal, MD*
Ondrej Hes, MD, PhD*
*Department of Pathology, Medical Faculty, Charles University, Charles University Hospital Plzen, Plzen Czech Republic
†Department of Pathology, Faculty of Medicine, University of British Columbia Royal Columbian Hospital, Vancouver BC, Canada
‡Department of Pathology, East University, Riga, Latvia

Conflicts of Interest and Source of Funding: Supported by the Charles University Research Fund (project number P36) and by Institutional Research Fund FN 00669806. The authors have disclosed that they have no significant relationships with, or financial interest in, any commercial companies pertaining to this article.

REFERENCES

1. Argani P, Zhong M, Reuter VE, et al. TFE3-fusion variant analysis defines specific

clinicopathologic associations among Xp11 translocation cancers. *Am J Surg Pathol.* 2016;40:723–737.
2. Clark J, Lu YJ, Sidhar SK, et al. Fusion of splicing factor genes PSF and NonO (p54nrb) to the TFE3 gene in papillary renal cell carcinoma. *Oncogene.* 1997;15:2233–2239.
3. Green WM, Yonescu R, Morsberger L, et al. Utilization of a TFE3 break-apart FISH assay in a renal tumor consultation service. *Am J Surg Pathol.* 2013;37:1150–1163.
4. Argani P, Antonescu CR, Illei PB, et al. Primary renal neoplasms with the ASPL-TFE3 gene fusion of alveolar soft part sarcoma: a distinctive tumor entity previously included among renal cell carcinomas of children and adolescents. *Am J Pathol.* 2001;159:179–192.
5. Malouf GG, Monzon FA, Couturier J, et al. Genomic heterogeneity of translocation renal cell carcinoma. *Clin Cancer Res.* 2013;19:4673–4684.

Nuclear Bubbles (Nuclear Pseudo-Pseudoinclusions): A Pitfall in the Interpretation of Microscopic Sections From the Thyroid and Other Human Organs

To the Editor:

An intriguing artifact in histopathology consists of the presence of single or multiple nuclear vacuoles (referred herein as bubbles) resulting in a bubbly appearance of the nucleus. We have referred to them, tongue-in-cheek, as "pseudo-pseudoinclusions" to distinguish them from the bonafide nuclear "pseudoinclusions" resulting from an invagination of the nuclear membrane and regarded as a pretty reliable marker of papillary thyroid carcinoma.[1–3] The bubbles that are the subject of this communication are variously sized, colorless or pale grayish, and sometimes coalescent and multiple, resulting in an empty-like appearance of the nucleus, with loss of chromatin texture and margination of nucleoli. They may severely interfere with the identification of cell types and grading assessment, especially in lymphoid neoplasms,[1] and also in epithelial and mesenchymal tumors.[2–5]

These nuclear bubbles have been thought to be caused by incomplete fixation, dehydration, or clearing during tissue processing, or by an excessively high temperature during tissue processing, water bath, or sections drying.[1–3,6] We noted the occurrence of this artifact sporadically on slides routinely prepared in

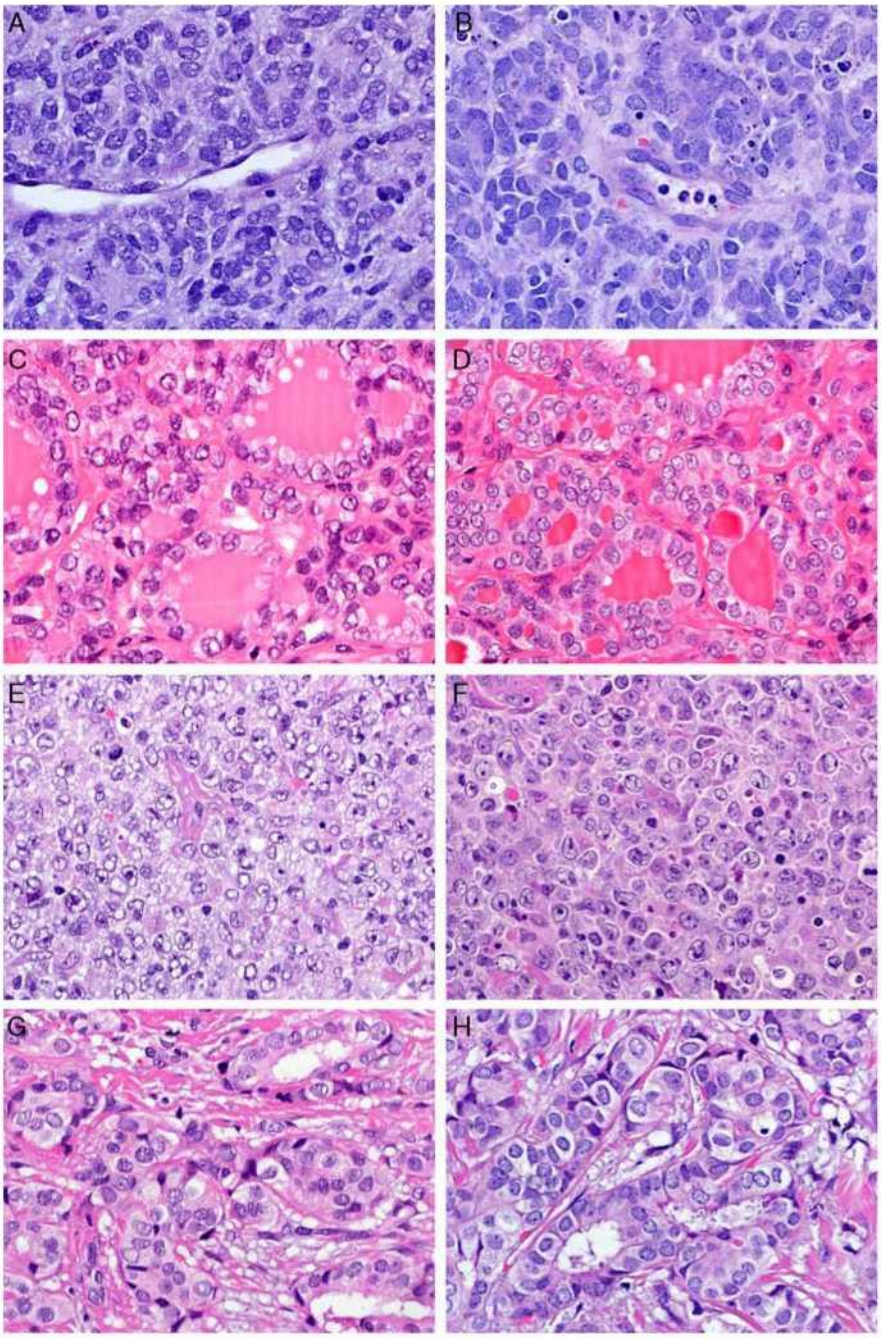

FIGURE 1. Pairs of images taken from the same tumor area on sections routinely dried (left) and dried following the fan procedure (right). A and B, Undifferentiated neoplasm. C and D, Thyroid papillary carcinoma, follicular variant (note that some "facts" are artifacts). E and F, Diffuse large B-cell lymphoma. G and H, Breast invasive ductal carcinoma (hematoxylin and eosin).

1.5 Světlobuněčný renální karcinom, inovativní pohled na tradiční jednotku

(komentář 5 publikací)

High-grade renal cell carcinoma with emperipolesis: Clinicopathological, immunohistochemical and molecular-genetic analysis of 14 cases.
Rotterova P, Martinek P, Alaghehbandan R, Prochazkova K, Damjanov I, Rogala J, Suster S, Perez-Montiel D, Alvarado-Cabrero I, Sperga M, Svajdler M, Michalova K, Pivovarcikova K, Daum O, Hora M, Dusek M, Ondic O, Stehlikova A, Michal M, Hes O.
Histol Histopathol. 2018 Mar;33(3):277-287

Low-grade spindle cell proliferation in clear cell renal cell carcinoma is unlikely to be an initial step in sarcomatoid differentiation.
Tanas Isikci O, He H, Grossmann P, Alaghehbandan R, Ulamec M, Michalova K, Pivovarcikova K, Montiel DP, Ondic O, Daum O, Prochazkova K, Hora M, Michal M, Hes O.
Histopathology. 2018 Apr;72(5):804-813

Papillary pattern in clear cell renal cell carcinoma: Clinicopathologic, morphologic, immunohistochemical and molecular genetic analysis of 23 cases.
Alaghehbandan R, Ulamec M, Martinek P, Pivovarcikova K, Michalova K, Skenderi F, Hora M, Michal M, Hes O.
Ann Diagn Pathol. 2018 Nov 22;38:80-86

Reactivity of CK7 across the spectrum of renal cell carcinomas with clear cells.
Gonzalez ML, Alaghehbandan R, Pivovarcikova K, Michalova K, Rogala J, Martinek P, Foix MP, Mundo EC, Comperat E, Ulamec M, Hora M, Michal M, Hes O.
Histopathology. 2019 Mar;74(4):608-617

Clear cell renal cell carcinoma with Paneth-like cells: Clinicopathologic, morphologic, immunohistochemical, ultrastructural, and molecular analysis of 13 cases.
Kojima F, Bulimbasic S, Alaghehbandan R, Martinek P, Vanecek T, Michalova K, Pivovarcikova K, Michal M, Hora M, Murata SI, Sugawara E, Rogala J, Limani R, Hes O.
Ann Diagn Pathol. 2019 Jun 3;41:96-101

Světlobuněčný renální karcinom je vůbec nejčastější renální neoplázií [24]. V tradičním pojetí stále zůstává nádorem typicky sestávajícím ze světlých buněk s jemnou a prominující vaskulární sítí. Současná literatura se však stále častěji zaměřuje i na jeho ne zcela „typické“ varianty a postupně se rozšiřující morfologické spektrum. Popsány byly CCRCC obsahující „syncytiální” obrovské buňky [50], low-grade vřetenité okrsky buněk [41], produkci hlenovitého materiálu [47], buňky obdobné buňkám Panethovým [20], high-grade okrsky s emperipoézou [35], či CCRCC s eozinofilními okrsky [26]. Histologické rozlišování variant a subklasifikace CCRCC na jednotlivé morfologické subtypy však patrně nemá v současné době klinická opodstatnění – nejsou dostupné studie hodnotící prognostický význam jednotlivých subtypů. Znalost morfologického spektra CCRCC patologem je však důležitá zejména pro správné určení definitivní diagnózy CCRCC.

Aktuální literatura se dále soustředí především na potenciálně užitečné prognostické a prediktivní markery/znaky CCRCC, možnosti terapeutického ovlivnění nádorů (včetně relativně módního užití imunoterapeutických agens) a genetické pozadí tumorů. Celkově však CCRCC zůstává tumorem s ne příliš terapeuticky ovlivnitelným průběhem a nejefektivnější léčbou kompletní chirurgickou resekcí.

1.5.1 High-grade renal cell carcinoma with emperipolesis: Clinicopathological, immunohistochemical and molecular-genetic analysis of 14 cases

Přítomnost emperipoézy byla popsána jako konstantní a patognomický morfologický znak bifazického skvamo-alveolárního RCC (BSARCC), ačkoliv raritně lze přítomnost emperipoézy vypozorovat i u některých high-grade RCC. Záměrem této studie bylo objektivně vyhodnotit incidenci emperipoézy u RCC a tyto tumory do detailu analyzovat pomocí imunohistochemie a molekulární genetiky.

Z registru nádorů bylo vyhledáno a opětovně hodnoceno celkem 14 high-grade RCC s prokázanou emperipoézou. Většina nádorů pocházela od pacientů, mužů (12/14 tumorů), jen ve dvou případech se jednalo u tumory vznikající u žen, věkové rozmezí pacientů se pohybovalo mezi 41 a 72 roky (průměr 58,6 let). Velikost nádorového ložiska byla průměrně 8,8 cm v největším rozměru (6 – 16,5 cm) a informace o dalším průběhu onemocnění byla dostupná u 8/14 pacientů (v délce trvání 0,5 – 10 let), z toho v šesti případech byl popsán rozvoj metastáz. Všechny tumory vykazovaly solidně-alveolární způsob růstu, fokálně s naznačeně pseudopapilárním vzhledem a obsahovaly velké buňky s bizarními jádry a eosinofilní "rhabdoid-like" cytoplazmou. Emperipoéza byla znakem vázaným na tyto objemné bizarní buňky. Tumory byly pozitivní v imunohistochemickém průkazu cytokeratinu OSCAR, CA IX, vimentinu, cyclinu D1, INI-1 a myoD1 a naopak negativní v melanocytárních markerech, CK7, myoglobinu, katepsinu K a TFE3. Genetické vyšetření prokázalo abnormality genu *VHL* v 6/9 analyzovatelných případů, z nichž dva současně vykazovaly i polyzomii chromozomů 7 a 17. Všechny nádory po korelaci morfologického vzhledu a výsledků imunohistochemických barvení byly klasifikovány jako CCRCC.

Emperipoéza je vzácný histomorfologický znak, který (kromě své typické přítomnosti u BSARCC) může být vzácně zaznamenán též u high-grade CCRCC, přičemž u většiny pacientů s touto morfologickou abnormalitou došlo k rozvoji metastatického onemocnění.

Histol Histopathol (2018) 33: 277-287

http://www.hh.um.es

Histology and Histopathology

From Cell Biology to Tissue Engineering

High-grade renal cell carcinoma with emperipolesis: Clinicopathological, immunohistochemical and molecular-genetic analysis of 14 cases

Pavla Rotterova[1,2], Petr Martinek[1], Reza Alaghehbandan[3], Kristyna Prochazkova[4], Ivan Damjanov[5], Joanna Rogala[6], Saul Suster[7], Delia Perez-Montiel[8], Isabel Alvarado-Cabrero[9], Maris Sperga[10], Marian Svajdler[1], Kvetoslava Michalova[1], Kristyna Pivovarcikova[1], Ondrej Daum[1], Milan Hora[4], Martin Dusek[1], Ondrej Ondic[1], Adela Stehlikova[1], Michal Michal[1] and Ondrej Hes[1,11]

[1]Department of Pathology, Charles University, Medical Faculty and Charles University Hospital Plzen, [2]Biopticka laborator Plzen, Czech Republic, [3]Department of Pathology, Faculty of Medicine, University of British Columbia, Royal Columbian Hospital, Vancouver, BC, Canada, [4]Department of Urology, Charles University, Medical Faculty and Charles University Hospital Plzen, Czech Republic, [5]Department of Pathology, University of Kansas, Kansas City, KS, USA, [6]Department of Pathology, Wojewódzki Szpital Specjalistyczny, Wrocław, Poland, [7]Department of Pathology, Medical College of Wisconsin, Milwaukee, WI, USA, [8]Department of Pathology, Instituto Nacional de Cancerologia, [9]Department of Pathology, Centro Medico, Mexico City, Mexico, [10]Department of Pathology, East University, Riga, Latvia and [11]Biomedical Centre, Faculty of Medicine in Plzen, Charles University in Prague, Plzen, Czech Republic

Summary, Emperipolesis has recently been described as a constant feature of "biphasic squamoid" papillary renal cell carcinoma (BPRCC). We also noticed this in some high-grade (HG) RCC, which promoted the present study to estimate the incidence of emperipolesis in RCCs and to describe them in further detail.

14 cases of HGRCC showing emperipolesis were retrieved from our registry. Microscopic examination of filed slides was supplemented with immunohistochemical and molecular-genetic analyses using paraffin embedded tissue.

12 of 14 patients were males with a mean age of 58.6 years (range 41-72 years). Tumor size ranged from 6-16.5 cm (mean of 8.8 cm). Follow up data were available for 8/14 patients (range 0.5-10 years). Metastases were documented in 6 cases. All tumors showed solid-alveolar growth patterns with focal pseudopapillary features, and were composed of large cells with bizarre nuclei and eosinophilic rhabdoid-like cytoplasm. Emperipolesis was a constant and prominent feature in large bizarre cells. All cases were positive for OSCAR, CANH 9, vimentin, cyclin D1, INI-1, and myoD1, while negative for melanocytic markers, CK 7, myoglobin, cathepsin K, and TFE3. *VHL* gene abnormalities were found in 6/9 analyzable cases, of which 2 demonstrated polysomy of chromosomes 7, 17.

Emperipolesis is a rare histomorphologic feature which can be seen not only in BPRCCs but also in highgrade CCRCCs. All RCC cases with prominent emperipolesis fulfilled both morphologic and immunohistochemical diagnostic criteria of high-grade CCRCC. The majority of patients with available follow up information developed metastases.

Key words: Kidney, Clear cell renal cell carcinoma, High-grade, Emperipolesis

Offprint requests to: Ondrej Hes, MD, PhD, Department of Pathology, Charles University, Medical Faculty and Charles University Hospital Plzen, Alej Svobody 80, 304 60 Pilsen, Czech Republic. e-mail: hes@medima.cz

DOI: 10.14670/HH-11-925

Introduction

Emperipolesis is defined as the presence of an intact cell within the cytoplasm of another cell. Rosai-Dorfman disease is the prototypic example of a pathologic condition for which emperipolesis is a prominent morphologic feature (Foucar et al., 1990). In studies of renal tumors, emperipolesis has been mentioned rather rarely and is considered a highly unusual phenomenon.

Emperipolesis has recently been described as a

constant feature of "biphasic squamoid" papillary renal cell carcinoma (BPRCC) (Petersson et al., 2012; Hes et al., 2016). Interestingly, it is always seen in the high grade component of these tumors. Emperipolesis has also been reported in series of clear cell renal cell carcinomas with multinucleated syncytial-type giant cells (Williamson et al., 2014). We thus hypothesized that emperipolesis might be a feature of high grade renal tumors.

The aim of this study was to estimate the incidence of emperipolesis in RCCs, and to describe this phenomenon in greater detail using morphological, immunohistochemical and molecular genetic analyses.

Materials and methods

Study design was approved by local ethical committee (Medical School Plzen, Charles University).

The Plzen Tumor Registry, including approximately 20,000 renal tumors and pseudotumors was electronically searched using key words "renal cell", "kidney", "carcinoma", "oncocytoma", "giant cells", "bizarre cells", and "emperipolesis". 65 cases met the search criteria, of which 14 cases of RCCs were found to have bizarre giant cells and emperipolesis. It should be noted that 26 cases of BPRCC were also identified in this search and were subsequently excluded from the study, given they were previously described in detail in other studies (Petersson et al., 2012, Hes et al., 2016).

Tissue for light microscopy was fixed in 10% buffered formalin, and embedded in paraffin using routine procedure. 4-5 μm thin sections were cut and stained with Hematoxylin and Eosin (H&E). Overall, 1-7 paraffin blocks were available for each case. All tumors were independently reviewed by two pathologists (P.R. and O.H.). Clinicopathological and follow-up data were collected using chart review at the participating institutions. Selected tissue blocks were further analyzed using immunohistochemistry, and molecular genetic methods.

Immunohistochemistry

The immunohistochemical study was performed using a Ventana Benchmark XT automated immunostainer (Ventana Medical System, Inc., Tucson, AZ, USA) on formalin fixed, paraffin embedded tissue. The following primary antibodies were employed: cytokeratins: CK 7 (OV-TL12/30, monoclonal, DakoCytomation, Glostrup, Denmark, 1:200), OSCAR (OSCAR, Covance, Herts, UK, 1:500), CAM5.2 (Ventana, RTU), AE1-AE3, monoclonal, BioGenex, San Ramon, CA, 1:1000), racemase/AMACR (P504S, monoclonal, Zeta, Sierra Madre, CA, 1:50), vimentin (D9, monoclonal, NeoMarkers, Westinghouse, CA, 1:1000), MART-1/melan A (A103, Ventana, RTU), anti-melanosome (HMB45, monoclonal, DakoCytomation, 1:200), Ki-67 (MIB1, monoclonal, Dako, Glostrup, Denmark, 1:1000), p53 (D-07, Ventana, RTU), human choriogonadotropin (polyclonal, Dako, 1:10000), myoglobin (polyclonal, ThermoScientific, Fremont, CA, 1:1000), MyoD1 (EP212, monoclonal, Cell Marque, Rocklin, CA, 1:50), INI-1 (MRQ-27 monoclonal, Ventana, RTU), cyclin D1 (SP4-R, monoclonal, Cell Marque, Rocklin, CA, 1:100), (polyclonal, NeoMarkers, Fremont, CA, 1:100), carbonic anhydrase 9 (rhCA9, monoclonal, RD systems, Abingdon, GB, 1:100), TFE3 (polyclonal, Abcam, 1:100), cathepsin K (3F9, monoclonal, Abcam, Cambridge, GB, 1:100), desmin (D33, monoclonal, Dako, 1:100), CD68 (KP1 monoclonal, Dako-Cytomation, 1:200). The primary antibodies were visualized using the supersensitive streptavidin-biotin-peroxidase complex (BioGenex). Appropriate positive controls were employed.

Molecular genetic analysis

Material used for molecular genetic analysis was formalin-fixed paraffin-embedded. Areas with bizarre cells showing emperipolesis were precisely identified and cut out from the tissue block using macrodissection. Low-grade areas composed of "classic" clear cell elements were not analyzed. DNA extraction, mutational analysis of *VHL* gene, detection of loss of heterozygosity of chromosome 3p, and hypermethylation of *VHL* gene were performed using methods described in a previous study (Ulamec et al., 2016) . Chromosomes 7, 9, 14, 15, and 17 were enumerated using fluorescent in-situ hybridization according to protocols reported previously (Sperga et al., 2013).

Array Comparative Genomic Hybridization (aCGH)

Microarray processing: Only samples meeting the required DNA quality (amplifiable fragment at least 400 base pairs long) were tested by aCGH. A SurePrint G3 Human CGH Microarray Kit, 8x60K (Agilent Technologies, CA, USA) with overall median probe spacing of 41 kilo bases was used for analysis. First, 400 ng of DNA was labeled using the SureTag Complete DNA Labeling Kit (Agilent). The procedure included Cy3 labeling of a test sample and Cy5 labeling of a reference sample. Commercially produced MegaPool Reference DNA Female (Kreatech Diagnostics, Amsterdam, Netherlands) was used as a reference material. The labeled specimens were mixed, dried and hybridized overnight at 47°C using Arrayit hybridization cassette (Arrayit Corporation, California, U.S.A.). Post-hybridization washing was done using SSC buffers with increasing stringency. Dried microarray was scanned with InnoScan 900 (Innopsys, France) at a resolution of 5 µm.

Image and Data analysis: Scanned images were analyzed and quantified by the Feature Extraction for CytoGenomics software (Agilent). Intensity values for each Cy5 and Cy3 labeled spot on the array were generated according an appropriate grid template in a

xml file. Minimum average absolute log ratio for deletion and amplification was set to more than 0.25. All genomic coordinates used for annotation are based on the March 2009 assembly of the reference genome GRCh37.

Results

Table 1 presents clinical information on 14 patients including 12 males and 2 females. Patient's age ranged from 41 to 72 years (mean 58.6, median 60 years). Tumor size varied from 6 to 16.5 cm (mean 8.8, median 6.5 cm). Follow up data (0.5-10 years, mean 4.3, median 10 years) were available in 8 of 14 patients. Metastases were documented in 6 cases. Four patients died of disease (0.5-10 years after diagnosis). One patient is alive with stable metastases to the lung 7 years post-surgery and one patient is alive 0.5 year after nephrectomy.

Gross description was available in 11/14 cases, showing non-capsulated tumors, mostly lobulated with tan to gray cut surface (Fig. 1). Necrotic areas were present in 6/11 cases.

Microscopically, all tumors showed solid-alveolar growth pattern with focal pseudopapillary features (Fig. 2). Foci of hemorrhage and necrosis were frequently encountered. The tumors were mostly composed of neoplastic cells with eosinophilic granular cytoplasm.

Table 1. Basic clinicopathological data.

Case	Sex (years)	Age	Size (cm)	Grade (ISUP)	Follow up (years)
1	M	69	6cm	4	ND
2	M	55	7.5x7x7	4	DOD 1.5, meta lung, liver
3	M	41	16.5x14.5x9	4	AW 0.5 Meta reg lymph nodes *-
4	M	60	8.5x4.5x4	2,4	AW 1
5	M	72	UNK	4	ND
6	F	52	9x6.5x6.5	4	Meta lung, kidney, liver, spleen, adrenals, DOD 2 *
7	M	60	9.5x6.5x8	4	Meta lung, AWD 7
8	M	62	Diam 7	4	ND
9	F	61	6x3.5x4.5	4	ND
10	M	64	13x10x10	4	Intrarenal meta, DOD 0.5
11	M	68	Diam 6.5	4	ND
12	M	54	Diam 6	4	Meta bone** DOD 10
13	M	51	Diam 10	4	AW 9
14	M	52	7.5x8.5x5	4	AW 7

M, male; F, female; Diam, diameter; Meta, metastasis; reg, regional; *, treated by Atzpodien protocol; **, treated by actinotherapy; *-, at the time of surgery; AW, alive and well; DOD, death of disease; AWD, alive with disease; ND, follow up not documented.

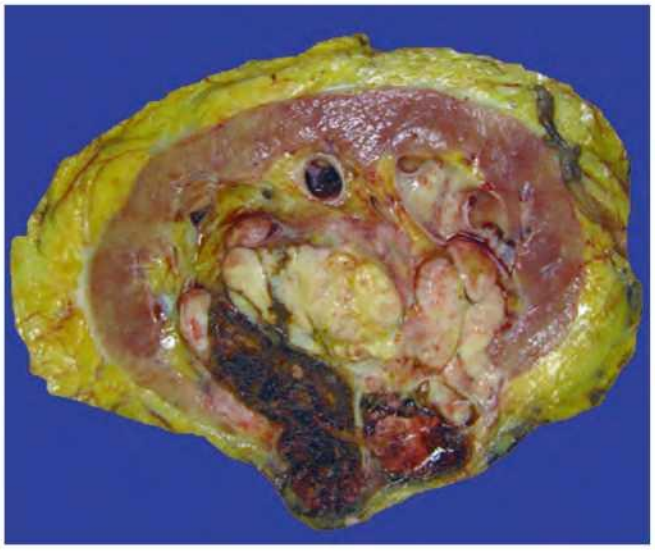

Fig. 1. Tumors were non-capsulated, mostly lobulated with tan to gray cut surface (case 4) and with grossly visible angioinvasion.

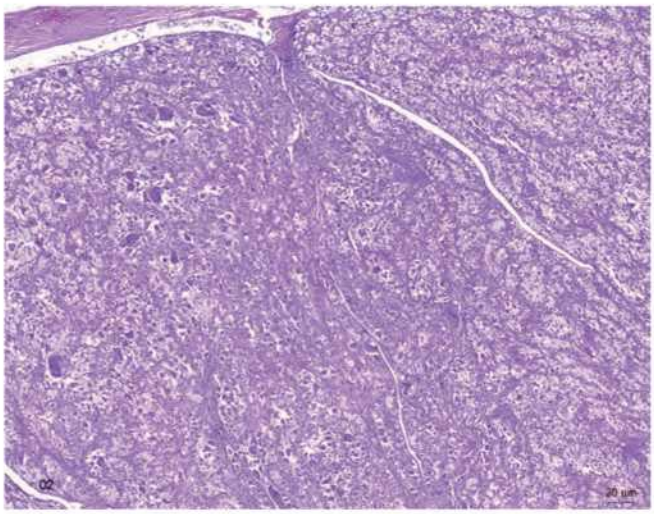

Fig. 2. Tumor with solid alveolar architecture composed of large clear to weakly eosinophilic high grade cells with scattered population of large bizarre multinucleated cells. x 40

Focally, smaller areas with clear cell elements were also noted (Fig. 3). In clear cells, numerous so-called glassy hyaline globules were seen (Fig. 4). This component was considered as low-grade clear cell RCC, which constituted less than 10% of tumor volume. In all cases, the tumor cells, at least focally, showed rhabdoid-like cytoplasmic changes. These cells had prominent nuclei with nucleoli and were considered as grade 4 (ISUP grading system). Large cells with bizarre nuclei (grade 4) and eosinophilic cytoplasm were also present in all cases (Fig. 5). These cells were characterized by

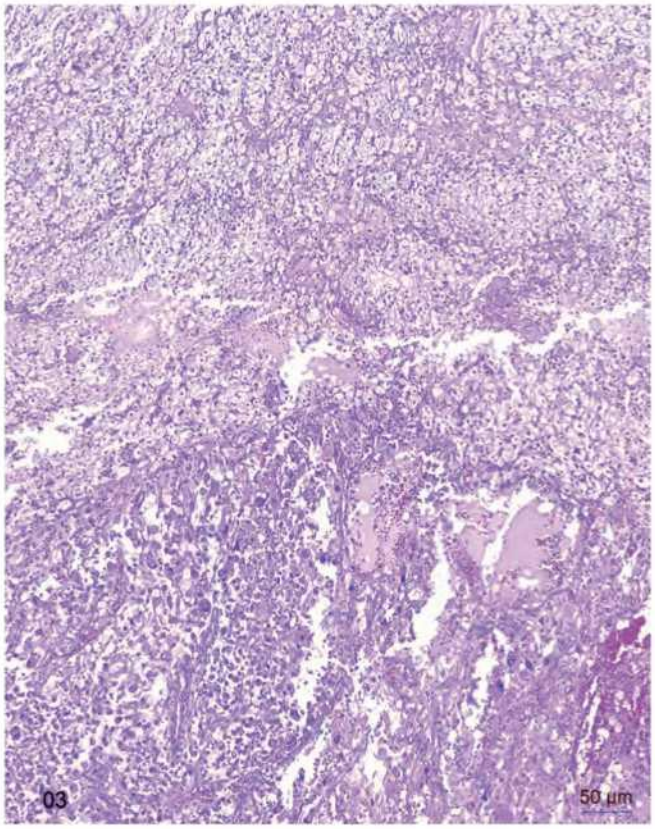

Fig. 3. Smaller areas with clear cell elements were present as well as areas with large bizarre pleomorphic cells with emperipolesis. x 100

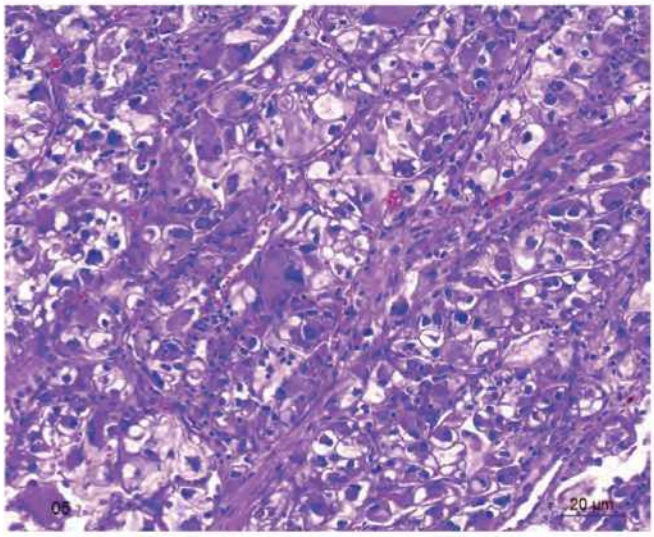

Fig. 5. Large high grade eosinophilic cells without emperipolesis. x 200

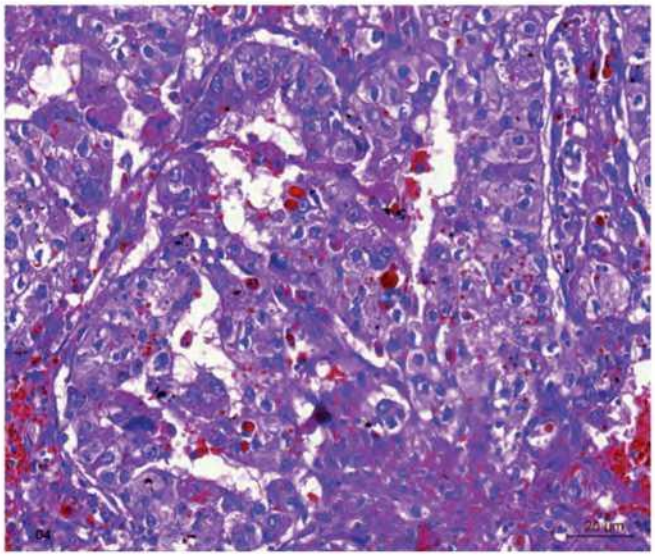

Fig. 4. So-called glassy hyaline globules are believed to be characteristic for clear cell RCC. x 200

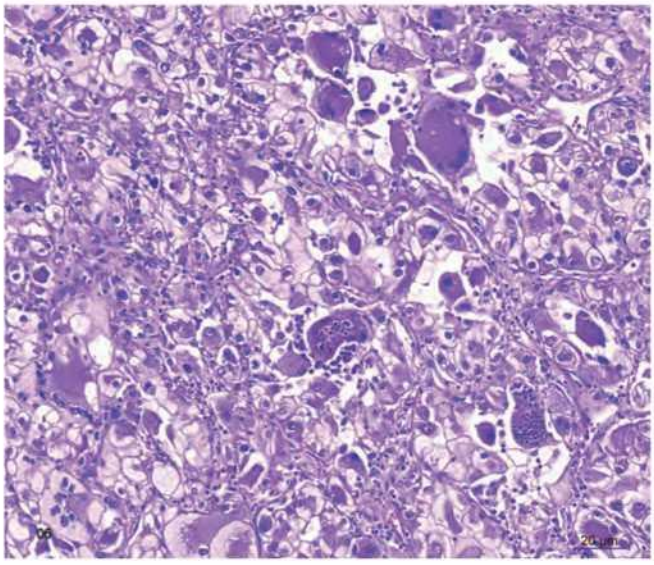

Fig. 6. Bizarre cells characterized by voluminous cytoplasm, numerous nuclei and presence of emperipolesis. x 200

voluminous cytoplasm with vacuoles, mostly numerous nuclei, and presence of emperipolesis (Fig. 6). Nuclei were arranged either at the periphery or centrally within the cell. Some large cells contained a single large nucleus with pink inclusion-like nucleolus (Fig. 7A,B). Lymphoid infiltrate was seen focally within neoplastic stroma. Mitotic figures including atypical mitoses were easily identified within high grade components.

The results of immunohistochemical examination are summarized in Table 2. All cases were positive for OSCAR, carbonic anhydrase 9 (CANH 9), vimentin, cyclin D1, INI-1, myoD1. Tumors were completely negative for melanocytic markers (Melan A, HMB45), CK 7, myoglobin, cathepsin K, and TFE3.

Cytokeratins (OSCAR, AE1-AE3) and CANH 9 were variably positive, with most intense staining in well differentiated areas, while weakly positive in large giant cells and in the neoplastic cells with rhabdoid-like features (Fig. 8). Large syncytial cells were positive mostly for cytokeratin OSCAR, while focally positive for CD68 (8/14) and negative for human choriogonadotropin. INI-1 was positive both in low-grade neoplastic elements, and in high-grade large bizarre cells. MyoD1 were only positive in rhabdoid-like

Table 2. Results of immunohistochemical examination.

	AE1-3	CAM	CK7	OSC	CANH	P53	Melan	HMB	hCG	CD68*	TFE	cath	myogl	desm	vim	cyclin M	Cyclin P	myo	INI
1	++	-	-	+++	++ mem, cyto	10%	-	-	-	Foc +	-	-	-	-	+++	++	++	+	+++
2	Foc ++	Foc +	-	+++	++ mem, cyto	-	-	-	-	Foc +	-	-	-	-	+++	+++	+++	++	++
3	-	Foc ++	-	Foc++	+++	-	-	-	-	Foc +	-	-	-	-	+++	+++ (HG area)	-	+++	+++
4	-	+	-	+++	+++	-	-	-	-	Foc +	-	-	-	-	+++	++	+	+	++
5	-	-	-	++	+++	10%	-	-	-	-	-	-	-	-	+++	+++	+++	++	++
6	-	-	-	Foc+++	++ mem, cyto	20%	-	-	-	Foc +	-	-	-	-	+++	+++	+++	Diff ++	+++
7	-	-	Foc ++	+++	+++ mem, cyto	SC	-	-	-	-	-	Foc++	-	-	+++	+++	+++	++	+++
8	++	-	-	+++	+++ mem, cyto	-	-	-	-	-	-	-	-	-	+++	-	+	-	++
9	-	-	-	Foc ++	+++ mem, cyto	15%	-	-	-	Foc +	-	-	-	-	+++	+++	++	++	++
10	Foc++	Foc++	Foc++	+++	+++ mem, cyto	SC	-	-	-	Foc +	-	-	-	-	+++	++	++	++	+++
11	-	-	-	++ foc+++	+++ mem, cyto	-	-	-	-	Foc +	-	-	-	-	+++	+++	+++	+	+++
12	-	-	-	++	+++ mem, cyto	-	-	-	-	-	-	-	Dot like foc	-	+++	+++	+++	+	+++
13	-	-	-	Dif + foc++	+++	70%	-	-	-	-	-	-	-	-	+++	+++	+++	+	++
14	-	Foc +	-	Dif +Foc +++	Dif +++	SC	-	-	-		-	-	-	-	+++	+++	+++	++	+++
	AE1-3	CAM	CK7	OSC	CANH	P53	Melan	HMB	hCG	CD68	TFE	cath	myogl	desm	vim	cyclin M	Cyclin P	myo	INI

SC, single cells; Foc, focal (less than 50%); Dif, diffuse (more then 50%); mem, membranous positivity; cyto, cytoplasmic positivity; -, negative; +, weak positivity; ++, moderate positivity; +++, strong positivity; *, syncytial cells; CAM, cytokeratin CAM 5.2; OSC, cytokeratin OSCAR; CANH, carbonic anhydrase 9; Melan, Melan A; HMB, HMB45; hCG, human choriogonadotropin; TFE, TFE3; cath, cathepsin K; myogl, myoglobin; desm, desmin; vim, vimentin; cyclin M, cyclin D1-monoclonal antibody; Cyclin P, cyclin D1-polyclonal antibody; myo, myoD1; INI, INI-1.

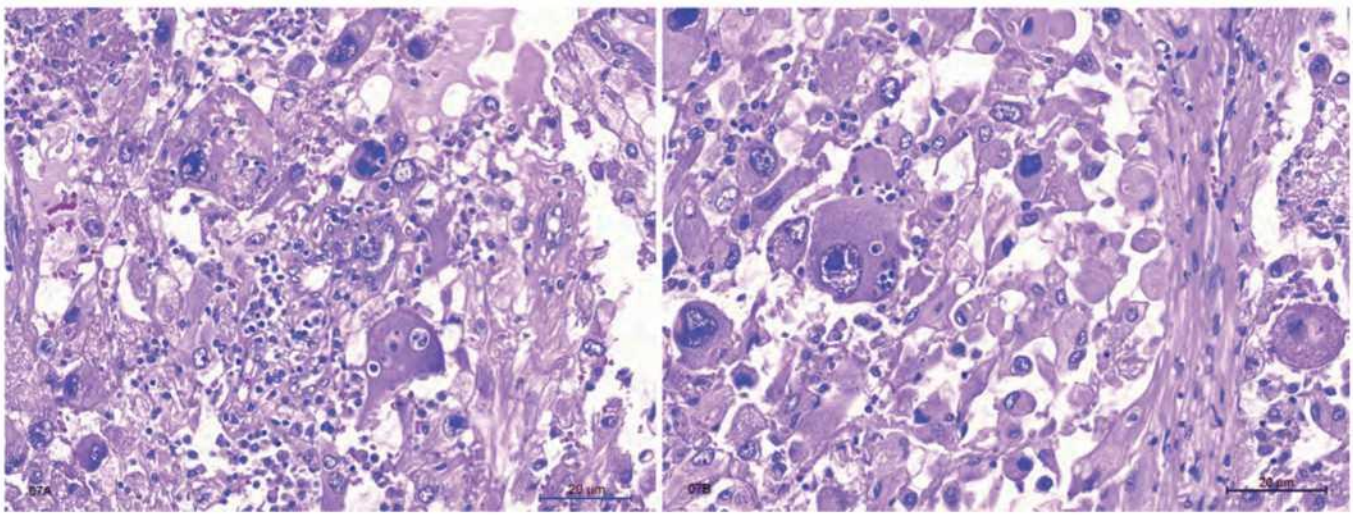

Fig. 7. A, B. Nucleolar inclusions present in some cells showing prominent emperipolesis. x 200

cells. No low-grade elements were positive for MyoD1. Cyclin D1 highlighted mostly large syncytial cells with emperipolesis (however, positivity was also noted in cells without emperipolesis) (Fig. 9).

The results of molecular genetic analyses are summarized in Tables 3 and 4. Aneuploidies of chromosomes 7, 9, 14, 15, and 17 were tested in 10 cases. Four cases had sufficient quality to be examined for copy number variations (CNV) across the whole genome using aCGH. Three cases showed complex CNVs repeatedly including chromosomes 1, 8, 9, and 14 (Fig. 10). A detailed list of detected CNVs is shown in Table 4. Overall multiple losses (n=15) and gains (n=9) were found in parts or whole chromosomes out of 107 chromosomes tested. Most losses were detected in chromosome 9. Two cases showed gains in

Table 3. Molecular-genetic analysis.

Case	Enu 7	Enu 9	Enu 14	Enu 15	Enu 17	#chr with CNV by aCGH	L3p	VHL	VHLM
1	D	M	M	D	D	-1, -9, +12, -14, -19, -22	-	-	-
2	D	P	D	NA	D	NA	NA	NA	NA
3	D	M	D	D	D	-1, +1, +3, +5,-5, +8,-9, -13	+	+	-
4	P	D	D	D	P	NA	+	-	-
5	NA	NA	NA	NA	NA	NA	NA	NA	NA
6	NA	NA	NA	NA	NA	NA	NA	NA	NA
7	D	D	D	NA	D	NA	NA	+	-
8	D	M	M	M	D	-1, -4, -8, -9, -14, -15, -18	+	+	-
9	NA	M	NA	NA	NA	NA	+	+	-
10	NA	NA	NA	NA	NA	NA	NA	NA	NA
11	NA	NA	NA	NA	NA	NA	NA	NA	NA
12	P	NA	P	NA	P	NA	+	-	-
13	D	D	D	D	D	No changes	-	-	-
14	D	D	NA	NA	NA	NA	-	-	-

Enu, chromosome enumeration FISH analysis; #chr with CNV by aCGH, list of chromosome numbers with copy number variations detected by aCGH (+=gain, -=loss, details in Table 4); L3p, loss of heterozygosity of chromosome 3p; VHL, mutation in *VHL* gene; VHLM, methylation status of *VHL* gene; D, disomy; M, monosomy; P, polysomy; +, present; -, absent; NA, non analyzable.

Table 4. Detailed list of CNVs detected using aCGH analysis.

case #	# chr	ISCN	Hg19	log ratio	p-value	CNV type
1	1	p36.33p35.1	759762-33607663	-0,304	3,412E-314	loss
	9	p24.3p13.1	271257-38490834	-0,274	2,11E-12	loss
	9	q21.11q34.13	71035346-135813928	-0,265	3,53E-11	loss
	12	q12q15	39268243-71002905	0,285	4,85E-292	gain
	14	p12q32.31	101028367-102000547	-0,531	3,85E-11	loss
3	1	p31.1p12	72207033-120185492	-0,266	1,81E-40	loss
	1	q21.1q44	144988715-249212668	0,272	4,900E-324	gain
	3	p14.3p11.1	56652175-90254062	0,555	4,900E-324	gain
	5	p15.33p11	207981-46100367	0,342	4,677E-319	gain
	5	q11.1q21.3	49690172-104823961	-0,292	0,00E+00	loss
	8	q11.1q24.3	47681335-146157954	0,306	4,900E-324	gain
	9	p24.1p23	8935512-9872132	-0,657	1,83E-36	loss
	9	p21.3	21978346-22241139	-0,586	4,94E-20	loss
	13	q11q34	19296544-114490071	-0,274	4,900E-324	loss
8	1	p36.33p34.3	2281640-38688668	-0,435	4,900E-324	loss
	4	q13.1q35.2	64967429-190767114	-0,405	4,900E-324	loss
	8	p23.3p11.1	221611-43333638	-0,414	4,900E-324	loss
	9	p24.3p13.1	271257-38490834	-0,458	4,900E-324	loss
	9	q21.11q34.13	71035346-135813928	-1,076	4,900E-324	loss
	9	p21.3	21805270-22416608	-0,420	6,70E-24	loss
	14	q11.2q32.33	20253739-107258824	-0,437	4,900E-324	loss
	15	q11.1q26.3	20603042-102465355	-0,283	4,900E-324	loss
	18	q11.1q23	18620055-77982126	-0,416	4,900E-324	loss

ISCN, cytological band description; Hg 19, chromosomal position based on Hg19 assembly; log ratio, average absolute log ratio; p-value, log likelihood that the called copy number state is not normal ploidy; chr, chromosome; CNV, copy number variation.

chromosomes 7 and 17 and in other cases several gains were found in chromosomes 3, 8, 9, and 14. *VHL* gene abnormalities were found in 6/9 analyzable cases. Two of the cases showing LOH3p also had gains in chromosomes 7 and 17.

Discussion

Emperipolesis is an unusual phenomenon known to occur in several diseases, including Rosai-Dorfman disease as a hallmark morphologic feature. This can also be seen in myeloproliferative disorders such as myeloid leukaemia, Hodgkin lymphoma and also in non-hematological malignancies and non-neoplastic conditions (Foucar et al., 1990; Nishie et al., 2006; Wang et al., 2014).

A cell engulfing another cell (so-called cellular cannibalism), in general, is a phenomenon observed in both benign and malignant neoplasms including breast carcinoma, giant cell carcinoma of lung, malignant melanoma, gastric adenocarcinoma, giant-cell tumor of the tendon sheath, gallbladder carcinoma, giant cell granuloma of the oral cavity, and oral squamous cell carcinoma (Jain, 2015). However, such a phenomenon is an exceedingly rare and unusual finding in renal neoplasms.

Emperipolesis in RCC was initially published in a case report (Shen and Wen, 2004), describing an aggressive clear cell renal cell carcinoma (CCRCC) with syncytial giant cells, and subsequently reported in a large series of 13 CCRCCs with syncytial cells and emperipolesis. In this tumor type, emperipolesis was present within large histiocytic-like giant cells with multiple or single nuclei and voluminous, finely granular cytoplasm (Shen and Wen, 2004; Williamson et al., 2014).

Histiocytic-like giant cells with syncytial (multinucleated) morphology have been described in few cases of mostly low-grade CCRCC. However, emperipolesis has never been documented in these papers (Lloreta et al., 2002; Berzal Cantalejo et al., 2004).

Another renal tumor type showing emperipolesis is BPRCC, which is believed to be a peculiar variant of papillary RCC. In these tumors, emperipolesis is present within large cells resembling squamoid cells, however their squamous origin has never been fully proven

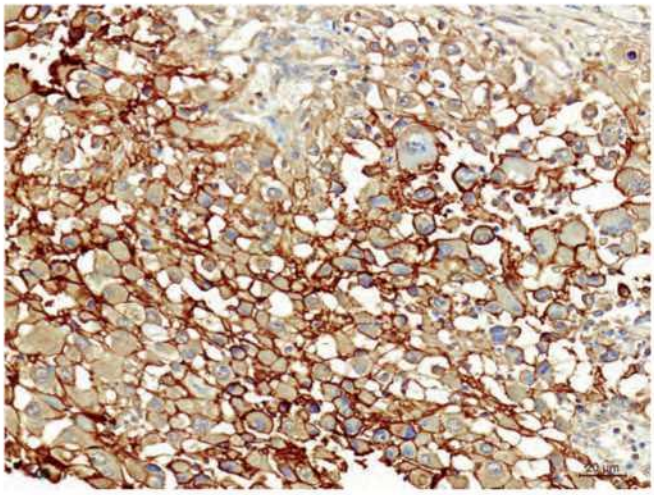

Fig. 8. All cases showed membranous positivity for carbonic anhydrase 9 (CANH 9). x 100

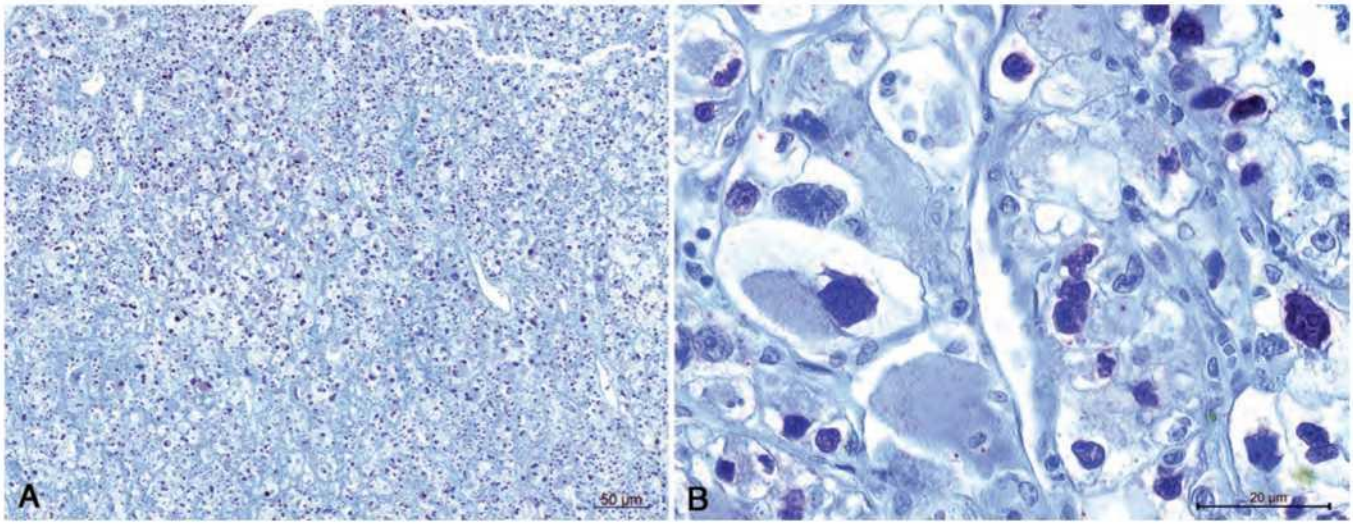

Fig. 9. A, B. Cyclin D1 nuclear positivity was noted in all 14 cases in large bizarre cells and also in smaller cells without emperipolesis. Scanning magnification **(A)**, detailed view **(B)**. A, x 100; B, x 400

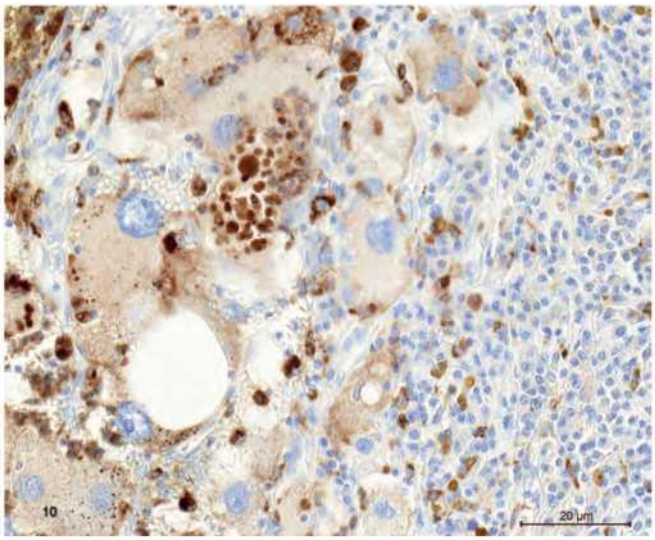

Fig. 10. CD68 was positive in large bizarre cells with emperipolesis. Positivity was strong and mostly cytoplasmic. x 200

(Petersson et al., 2012; Hes et al., 2016). The real nature of these cells is enigmatic, given renal neoplasms or even normal renal tissue do not contain squamous cells. It should be noted that squamoid cells differed from giant syncytial multinucleated cells described in CCRCC.

BPRCCs are characterized by a dual morphology and constant presence of emperipolesis. They show a solid to alveolar growth pattern. The dual morphology is composed of small cells similar to that seen in type 1 PRCC and larger high grade cells resembling squamous cells, which show emperipolesis. Tumors mostly displayed more or less prominent papillary component, sometimes with abrupt border to typical BPRCC (Hes et al., 2016). BPRCC are different from the subset of tumors included into the current study, hence no true papillary architectural pattern was seen in our series. Further, molecular genetic characteristics were different than those reported in BPRCC.

In this study, we attempted to estimate the frequency of emperipolesis in renal tumors and also to map the spectrum of the tumors manifesting such a morphologic feature. The estimated frequency was below 0.1% in all tumors from our registry. These tumors fell into two distinct RCC subtypes: BPRCCs (n=23) and high-grade CCRCCs (n=14). In all cases, emperipolesis did not seem to be restricted to syncytial giant cells, but was also present within large squamoid cells (in BPRCC). Nonetheless, in both tumor types emperipolesis occurred only within the high-grade component (no emperipolesis was found within low-grade neoplastic cells in either tumor types). In estimating the frequency of emperipolesis, we actively searched the tumor registry for all RCC cases with large giant bizarre cells. Yet we recognize that there might have been some RCCs with emperipolesis that were not recorded and ultimately captured through the search, although a unlikely possibility.

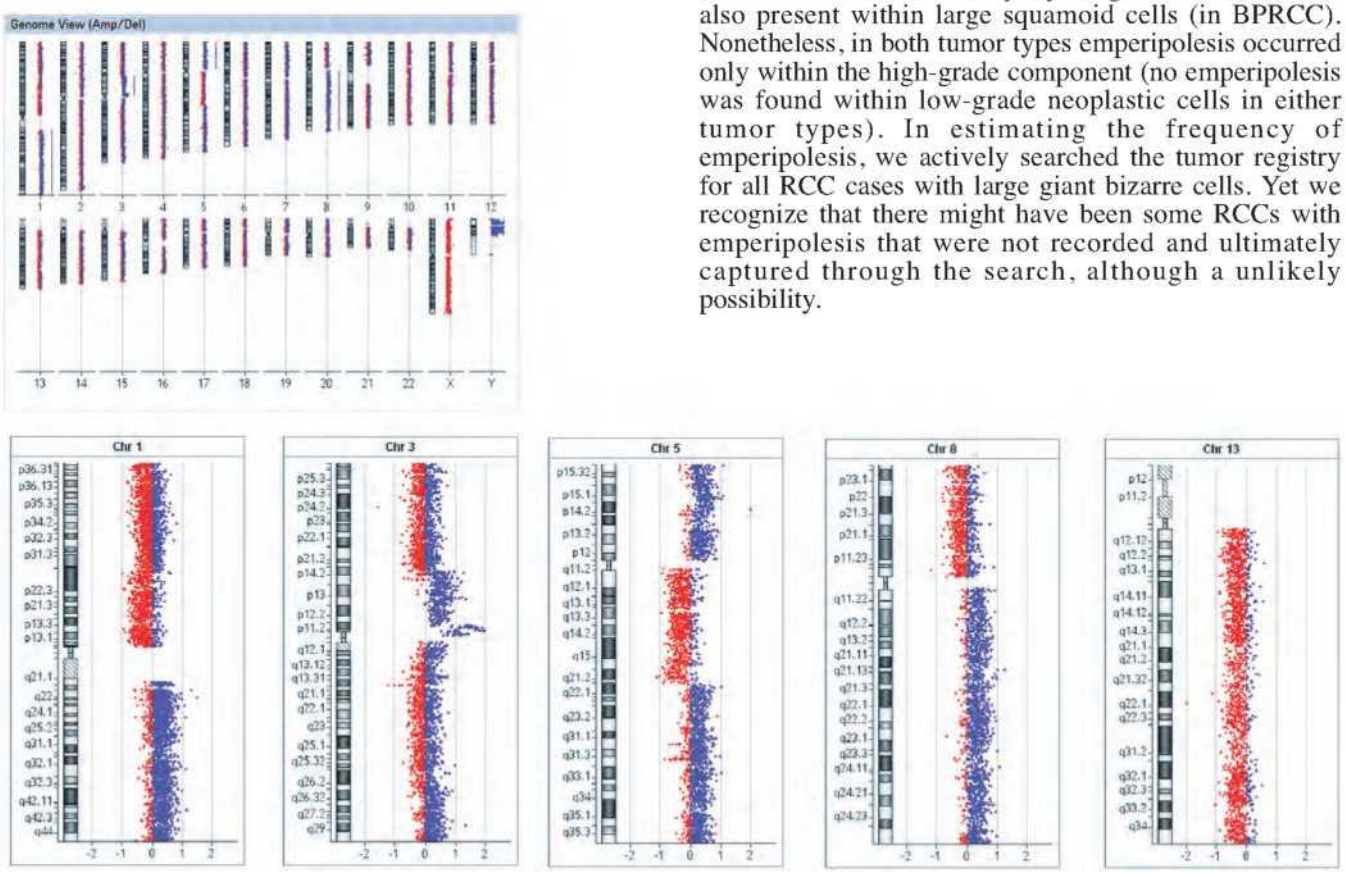

Fig. 11. ArrayCGH analysis in case 3 showed -1p, +1q, +3p14-p11, -5q111-q21, +8q, -13. LOH 3p and mutated *VHL* gene were also found in this case.

There were several unusual clinical aspects noted in this study including a high male predominance gender in our cases (12/14 cases). Similar distribution with male predominance was also reported in series of Williamson et al. (M:F=8:5) (Williamson et al., 2014). In this study we also documented an aggressive clinical behavior including 6 of 8 patients with known follow-up succumbed to metastatic disease (4/6 patients died of generalized dissemination of the tumor). However, aggressive clinical behavior as well as male predominance may reflect just high-grade and high-stage of examined tumors instead of emperipolesis. On the other hand, emperipolesis was always associated with high-grade areas and it was not found in low-grade areas.

In our series, we were able to find areas of typical "conventional" clear cell RCC merging with high-grade areas with bizarre cells. Glassy hyaline globules, which are considered rather typical for CCRCC, were present in such high-grade clear cells (Hes et al., 1998). No emperipolesis was found within low-grade component. Further, the immunoprofile was consistent with the diagnosis of high-grade CCRCC.

In this study, cyclin D1 immunostaining proved to be helpful in identifying neoplastic cells with emperipolesis. It should be noted that we, however, found such positivity in large bizarre cells without visible emperipolesis. *Cyclin D1/PRAD 1*, a cell cycle-related gene mapped to chromosome 11q13, has been found to be amplified in some breast cancers, certain squamous cell carcinomas of the head and neck, esophagus, several different lymphomas, and myxoinflammatory fibroblastic sarcomas. (Zhang et al., 1994; Michal et al., 2015). Expression of cyclin D1 in RCCs has only recently been studied by Leroy et al., who described overexpression of cyclin D1 in clear cell papillary RCC (Leroy et al., 2014). Lima et al., investigated the prognostic significance of cyclin D1 expression in RCCs and concluded that high expression is associated with favorable prognosis (Lima et al., 2014). However, based on our findings, all tumors were high-grade CCRCC with bizarre cells showing cyclin D1 immunoreactivity, which were not associated with favorable biologic behavior. It should be noted that cyclin D1 positivity is one of the characteristic features of BPRCC, although it is not a specific diagnostic marker for these tumors.

An interesting phenomenon found in this study was CD68 positivity of large bizarre syncytial neoplastic cells. This was also reported earlier as a feature of emperipolesis by Williamson et al. (2014). Of note, CD68, a histiocytic marker, can also be positive in epithelial cells. In RCCs an identical finding was described by Petersson et al., where CD68 positive cells were apparently epithelial in origin and were part of a neoplastic cell population of unusual papillary RCCs. CD68 can be present in all cell types rich in lyso-/endosomes and is not restricted to macrophages (Petersson et al., 2014).

All our cases displayed high grade morphologic features with rhabdoid/rhabdoid-like differentiation. Cells with so-called rhabdoid features in RCCs are usually defined as large epithelioid cells with large eccentric and vesicular nuclei and large paranuclear intracytoplasmic hyaline globules (Leroy et al., 2007; Sugimoto et al., 2016). According to some authors, these cells are distinct from so-called "rhabdoid-like" cells with large eccentric nucleolus and abundant eosinophilic cytoplasm without paranuclear globules that are usually seen in areas marked by discohesive growth. We noticed both cell types in our cases but we were not able to separate tumors with rhabdoid features from tumors with so-called "rhabdoid-like" only features (Sugimoto et al., 2016). It should be noted that we did not histologically identify any cross striations usually seen in neoplastic cells with "rhabdoid" differentiation. Further, the immunoprofile of these cells (i.e., desmin, myoglobin, MyoD1, and INI-1) was rather variable. Overall, we believe that finding of such cells may be related to morphologic variability of high-grade CCRCC rather than true rhabdoid differentiation.

INI1 immunoreactivity is absent in some primary rhabdoid tumors, such as pediatric rhabdoids tumors and rhabdoid tumors of the kidney. Medullary renal carcinoma is another example of renal tumors for which INI1 is referred as negative (Cheng et al., 2008). Overall, we believe that it would be difficult and rather inaccurate to use this marker as further evidence for rhabdoid or rhabdoid-like morphology in obvious RCCs.

The results of *VHL* gene analyses (mutation, LOH3p, methylation status of *VHL* gene) were in concordance with morphologic diagnosis of CCRCC. Six of 9 analyzable tumors showed *VHL* gene abnormalities. Interestingly, in 2 cases with LOH3p, polysomy of chromosomes 7 and 17, a hallmark of PRCC, was also found. Such cases with LOH3p, polysomy of chromosomes 7 and 17 may display an aberrant chromosomal numerical aberration pattern within CCRCC group (Petersson et al., 2013). The other interesting molecular-genetics finding was the fact that in two cases tested positive for LOH3p, aCGH deletion including the *VHL* locus 3p25.3 was not found. This can be explained by copy neutral loss of heterozygosity described as prevalent in CCRCC (Brugarolas, 2014). Four cases showed chromosome 9 losses, three of which were confirmed by aCGH to affect locus of the tumor suppressor *CDKN2A* (case 8 could be bi allelic loss). Small deleted regions including *CDKN2A* were found to be prevalent (53%) in a subset of CCRCCs in a large study by the Cancer Genome Atlas consortium in 2013. Overall, the diversity of detected molecular genetic features in our series is consistent with the prevalent CCRCC genetic patterns as they are described in large studies (Dordevic et al., 2012; Moore et al., 2012). Similar genetic heterogeneity has also been described in other RCC subtypes (Cancer Genome Atlas Research Network, 2016).

We believe it may not be possible to consider the

presence of emperipolesis as an independent prognostic feature in RCCs. First, the number of cases in our series is too small for statistically meaningful conclusion. Secondly, we did not have available low-grade CCRCC cases with emperipolesis to be included in the study for comparison purposes. Thus, the presence of emperipolesis within high-grade CCRCC seems to only illustrate another aspect of morphologic variability in high-grade RCCs. In other words, the aggressive behavior of such tumors may not be attributed to the presence of emperipolesis.

From a practical point of view, it is crucial to consider urothelial carcinoma (UC) as a mimicker and potential differential diagnosis in the settings of RCCs with emperipolesis. UC may well demonstrate several variable morphologic variants. UC with giant bizarre cells has been well known for years (Moch et al., 2016). There are several variations on this morphologic pattern, of which UC with syncytiotrophoblastic cells is worth mentioning. These tumors can be positive for human choriogonadotropin (hCG), although hCG negative UC with giant osteoclast-like cells, strongly resembling syncytiotrophoblastic cells, are also mentioned in the literature (Amin, 2009). We did not see any morphologic features or immunophenotypes similar to urothelial differentiation in our cases. Moreover, none of the tumors in our series showed any relation to urothelium, and further, they were negative for CK7 and positive (among other markers) for vimentin. Also, abnormalities in *VHL* gene would be quite an unusual feature for UC.

Another renal tumor which may be composed of large bizarre cells is RCC with sarcomatoid differentiation. It is possible to find unusual epithelial or epithelioid morphology within both epithelial and even sarcomatoid components (de Peralta-Venturina et al., 2001). We did not find true sarcomatoid differentiation within our tumors and all bizarre large cells with emperipolesis were of epithelial origin.

Rosai Dorfman disease is characterized by the presence of numerous histiocytic cells with large vesicular nuclei and abundant clear or weakly eosinophilic cytoplasm. Emperipolesis is almost exclusively found in these large cells (Foucar et al., 1990). Rosai Dorfman disease is mostly known to occur in lymph nodes, although it may also involve extranodal organs. A series of cases from the kidney and testis have recently been published (Wang et al., 2014). It should be noted that the large histiocytic cells with emperipolesis were very similar to those described in our cases. The majority of the lesions were composed of obviously epithelial renal cell carcinoma and large bizarre cells formed only a minor part of the tumor.

Conclusions

Emperipolesis is a rare histomorphologic feature which can be seen not only in BPRCCs but also in other RCCs, mostly high-grade CCRCCs. All RCC cases in this study with prominent emperipolesis fulfilled both morphologic and immunohistochemical diagnostic criteria of high-grade CCRCC, yet 2 tumors had the molecular-genetic features of both CCRCC and PRCC. Metastases were documented in 6/8 cases with available follow up information. We believe it would be very challenging to estimate the true incidence of RCCs with emperipolesis, but based on our tumor registry data, it seems that the incidence is somewhat below 0.1%.

Compliance with Ethical Standards: Study design has been approved by local ethical committee (Charles University, Medical School Plzen) LEK FN Plzeň.

Funding: The study was supported by the Charles University Research Fund (project number P36) and by the project FN 00669806.

Disclosure of Conflict of Interest: All authors declare no conflict of interest

References

Amin M.B. (2009). Histological variants of urothelial carcinoma: diagnostic, therapeutic and prognostic implications. Mod. Pathol. 22 (Suppl 2), S96-S118.

Berzal Cantalejo F., Sabater Marco V., Alonso Hernández S., Jiménez Peña R. and Martorell Cebollada M.A. (2004). Syncytial giant cell component: review of 55 renal cell carcinomas. Histol. Histopathol. 19, 113-118.

Brugarolas J. (2014). Molecular genetics of clear-cell renal cell carcinoma. J. Clin. Oncol. 32, 1968-1976.

Cancer Genome Atlas Research Network (2016). Comprehensive molecular characterization of papillary renal-cell carcinoma. N. Engl. J. Med. 374, 135-145.

Cheng J.X., Tretiakova M., Gong C., Mandal S., Krausz T. and Taxy J.B. (2008). Renal medullary carcinoma: rhabdoid features and the absence of INI1 expression as markers of aggressive behavior. Mod. Pathol. 21, 647-652.

de Peralta-Venturina M., Moch H., Amin M., Tamboli P., Hailemariam S., Mihatsch M., Javidan J., Stricker H., Ro J.Y. and Amin M.B. (2001). Sarcomatoid differentiation in renal cell carcinoma: a study of 101 cases. Am. J. Surg. Pathol. 25, 275-284.

Dordevic G., Matusan Ilijas K., Hadzisejdic I., Maricic A., Grahovac B. and Jonjic N. (2012). EGFR protein overexpression correlates with chromosome 7 polysomy and poor prognostic parameters in clear cell renal cell carcinoma. J. Biomed. Sci. 19, 40.

Foucar E., Rosai J. and Dorfman R. (1990). Sinus histiocytosis with massive lymphadenopathy (Rosai-Dorfman disease): review of the entity. Semin. Diagn. Pathol. 7, 19-73.

Hes O., Michal M., Sulc M., Kocova L., Hora M. and Rousarova M. (1998). Glassy hyaline globules in granular cell carcinoma, chromophobe cell carcinoma, and oncocytoma of the kidney. Ann. Diagn. Pathol. 2, 12-18.

Hes O., Condom Mundo E., Peckova K., Lopez J.I., Martinek P., Vanecek T., Falconieri G., Agaimy A., Davidson W., Petersson F., Bulimbasic S., Damjanov I., Jimeno M., Ulamec M., Podhola M., Sperga M., Pane Foix M., Shelekhova K., Kalusova K., Hora M., Rotterova P., Daum O., Pivovarcikova K. and Michal M. (2016). Biphasic squamoid alveolar renal cell carcinoma: A distinctive subtype of papillary renal cell carcinoma? Am. J. Surg. Pathol. 40, 664-675.

Jain M. (2015). An overview on cellular cannibalism with special reference to oral squamous cell carcinoma. Exp. Oncol. 37, 242-245.

Leroy X., Zini L., Buob D., Ballereau C., Villers A. and Aubert S. (2007). Renal cell carcinoma with rhabdoid features: an aggressive neoplasm with overexpression of p53. Arch. Pathol. Lab. Med. 131, 102-106.

Leroy X., Camparo P., Gnemmi V., Aubert S., Flamand V., Roupret M., Fantoni J.C. and Comperat E. (2014). Clear cell papillary renal cell carcinoma is an indolent and low-grade neoplasm with overexpression of cyclin-D1. Histopathology 64, 1032-1036.

Lima, M.S., Pereira R.A., Costa R.S., Tucci S., Dantas M., Muglia V.F., Ravinal R.C. and Barros-Silva G.E. (2014). The prognostic value of cyclin D1 in renal cell carcinoma. Int. Urol. Nephrol. 46, 905-913.

Lloreta J., Bielsa O., Munne A., Dominguez D., Keysers U., Gelabert A. and Serrano S. (2002). Renal cell carcinoma with syncytial giant cell component. Virchows Arch. 440, 330-333.

Michal M., Kazakov D.V., Hadravsky L., Kinkor Z., Kuroda N. and Michal M. (2015). High-grade myxoinflammatory fibroblastic sarcoma: a report of 23 cases. Ann. Diagn. Pathol. 19, 157-163.

Moch H., Humphrey P.A., Ulbright T.M. and Reuter V.E. (2016). WHO classification of tumours of the urinary system and male genital organs. IARC. Lyon.

Moore, L.E., Jaeger E., Nickerson M.L., Brennan P., De Vries S., Roy R., Toro J., Li H., Karami S., Lenz P., Zaridze D., Janout V., Bencko V., Navratilova M., Szeszenia-Dabrowska N., Mates D., Linehan W. M., Merino M., Simko J., Pfeiffer R., Boffetta P., Hewitt S., Rothman N., Chow W.H. and Waldman F. M. (2012). Genomic copy number alterations in clear cell renal carcinoma: associations with case characteristics and mechanisms of VHL gene inactivation. Oncogenesis 1, e14.

Nishie, M., Mori F., Houzen H., Yamaguchi J., Jensen P.H. and Wakabayashi K. (2006). Oligodendrocytes within astrocytes ("emperipolesis") in the cerebral white matter in hepatic and hypoglycemic encephalopathy. Neuropathology 26, 62-65.

Petersson, F., Bulimbasic S., Hes O., Slavik P., Martinek P., Michal M., Gomolcakova B., Hora M. and Damjanov I. (2012). Biphasic alveolosquamoid renal carcinoma: a histomorphological, immunohistochemical, molecular genetic, and ultrastructural study of a distinctive morphologic variant of renal cell carcinoma. Ann. Diagn. Pathol. 16, 459-469.

Petersson, F., Grossmann P., Hora M., Sperga M., Perez Montiel D. , Martinek P., Gutierrez M.E., Bulimbasic S., Michal M., Branzovsky J. and Hes O. (2013). Renal cell carcinoma with areas mimicking renal angiomyoadenomatous tumor/clear cell papillary renal cell carcinoma. Hum. Pathol. 44, 1412-1420.

Petersson, F., Sperga M., Bulimbasic S., Martinek P., Svajdler M., Kuroda N., Hora M., Simpson R., Tichy T., Peckova K., Branzovsky J., Pivovarcikova K., Rotterova P., Kokoskova B., Bauleth K., Martincok D., Nagy V., Michal M. and Hes O. (2014). Foamy cell (hibernoma-like) change is a rare histopathological feature in renal cell carcinoma. Virchows Arch. 465, 215-224.

Shen R. and Wen P. (2004). Clear cell renal cell carcinoma with syncytial giant cells: a case report and review of the literature. Arch. Pathol. Lab. Med. 128, 1435-1438.

Sperga, M., Martinek P., Vanecek T., Grossmann P., Bauleth K., Perez-Montiel D., Alvarado-Cabrero I., Nevidovska K., Lietuvietis V., Hora M., Michal M., Petersson F., Kuroda N., Suster S., Branzovsky J. and Hes O. (2013). Chromophobe renal cell carcinoma--chromosomal aberration variability and its relation to Paner grading system: an array CGH and FISH analysis of 37 cases. Virchows Arch. 463, 563-573.

Sugimoto M., Kohashi K., Kuroiwa K., Abe T., Yamada Y., Shiota M., Imada K., Naito S. and Oda Y. (2016). Renal cell carcinoma with rhabdoid-like features lack intracytoplasmic inclusion bodies and show aggressive behavior. Virchows Arch. 468, 357-367.

Ulamec M., Skenderi F., Zhou M., Kruslin B., Martinek P., Grossmann P., Peckova K., Alvarado-Cabrero I., Kalusova K., Kokoskova B., Rotterova P., Hora M., Daum O., Dubova M., Bauleth K., Slouka D., Sperga M., Davidson W., Rychly B., Perez Montiel D., Michal M. and Hes O. (2016). Molecular genetic alterations in renal cell carcinomas with tubulocystic pattern: Tubulocystic renal cell carcinoma, tubulocystic renal cell carcinoma with heterogenous component and familial leiomyomatosis-associated renal cell carcinoma. Clinicopathologic and molecular genetic analysis of 15 cases. Appl. Immunohistochem. Mol. Morphol. 24, 521-530.

Wang, C.C., Al-Hussain T.O., Serrano-Olmo J. and Epstein J.I. (2014). Rosai-Dorfman disease of the genito-urinary tract: analysis of six cases from the testis and kidney. Histopathology 65, 908-916.

Williamson, S.R., J. Kum B., Goheen M.P., Cheng L., Grignon D.J. and Idrees M.T. (2014). Clear cell renal cell carcinoma with a syncytial-type multinucleated giant tumor cell component: implications for differential diagnosis. Hum. Pathol. 45, 735-744.

Zhang S.Y., Caamano J., Cooper F., Guo X. and Klein-Szanto A.J. (1994). Immunohistochemistry of cyclin D1 in human breast cancer. Am. J. Clin. Pathol. 102, 695-698.

Accepted September 1, 2017

1.5.2 Low-grade spindle cell proliferation in clear cell renal cell carcinoma is unlikely to be an initial step in sarcomatoid differentiation

Vřetenobuněčná proliferace vyskytující se v rámci CCRCC může být často nesprávně považována za sarkomatoidní dediferenciaci tumoru. Low-grade vřetonobuněčná proliferace (LG-SCP) v rámci CCRCC byla popsána v roce 2001 a jedná se o jev, který ač není příliš častý, působí nemalé diagnostické obtíže (zejména v rámci hodnocení punkčních biopsií). Cílem této studie tak bylo popsat morfologické, imunohistochemické a molekulárně genetické charakteristiky CCRCC s LG-SCP. U těchto tumorů byla analyzována přítomnost morfologických a imunohistochemických znaků epiteliálně-mezenchymální tranzice/přechodu (EMT).

Z plzeňského registru nádorů čítajícího přes 21000 renálních tumorů bylo vyhledáno 11 CCRCC s LG-SCP a dále 10 případů "konvenčního" CCRCC a 10 případů typického sarkomatoidního CCRCC (kontrolní skupiny). CCRCC s LG-SCP byly resekovány od pěti mužů a pěti žen ve věkovém rozmezí 60 – 81 let (průměr 68,5 let) a průměrná velikost tumorů byla 7,1 cm (rozmezí 1,7 – 12 cm). Informace o dalším průběhu onemocnění byly dostupné u 9/10 pacientů (v průměrné délce trvání 44-78 měsíců), u tumorů nebylo dokumentováno agresivní chování. Okrsky LG-SCP tvořily cca 5-80% (průměr 32,3%) z celkového objemu nádorové masy a nekrotické či regresivně změněné okrsky byly fokálně pozorovány u všech tumorů (v rozsahu 5-30% tumorózní masy). LG-SCP byla čistě epiteliální, bez přítomnosti mitóz či známek mezenchymální diferenciace. Imunohistochemický profil LG-SCP byl konzistentní s diagnózou "konvenčního" CCRCC. Při porovnání se sarkomatoidním CCRCC, některé z markerů EMT byly v LG-SCP alterovány (včetně nižší exprese N-cadherinu a Zeb1 a vyšší exprese E-cadherinu). Při porovnání skupiny CCRCC s LG-SCP a "konvenčního" CCRCC však nebyly při expresi EMT zaznamenány výraznější rozdíly. Abnormality genu *VHL* byly ve skupině CCRCC s LG-SCP prokázány celkem v 6/11 případů.

Výsledky této studie tak ukazují, že LG-SCP v CCRCC mají srovnatelné imunohistochemické a molekulárně genetické charakteristiky jako "konvenční" CCRCC. Stejně tak exprese EMT markerů se u těchto dvou entit výrazně neliší. LG-SCP je tak patrně část morfologické heterogenity v rámci CCRCC a nepředstavuje iniciální stádium sarkomatoidní diferenciace. CCRCC s LG-SCP nevykazují agresivnější chování než "konvenční" CCRCC.

Histopathology

Histopathology 2018, **72**, 804–813. DOI: 10.1111/his.13447

Low-grade spindle cell proliferation in clear cell renal cell carcinoma is unlikely to be an initial step in sarcomatoid differentiation

Ozlem Tanas Isikci,[1] Huying He,[2] Petr Grossmann,[3] Reza Alaghehbandan,[4] Monika Ulamec,[5] Kvetoslava Michalova,[3] Kristyna Pivovarcikova,[3] Delia Perez Montiel,[6] Ondrej Ondic,[3] Ondrej Daum,[3] Kristyna Prochazkova,[7] Milan Hora,[7] Michal Michal[3] & Ondrej Hes[3]

[1]*Department of Pathology, Ankara Training and Research Hospital, Ankara, Turkey,* [2]*Department of Pathology, Peking University, Health Science Center, Beijing, China,* [3]*Department of Pathology, Charles University, Medical Faculty and Charles University Hospital Plzen, Plzen, Czech Republic,* [4]*Department of Pathology, Faculty of Medicine, University of British Columbia, Royal Columbian Hospital, Vancouver, BC, Canada,* [5]*Clinical Hospital Center Sestre Milosrdnice, Medical Faculty Zagreb, Zagreb, Croatia,* [6]*Department of Pathology, Instituto Nacional de Cancerologia, Mexico City, Mexico, and* [7]*Department of Urology, Charles University, Medical Faculty and Charles University Hospital Plzen, Plzen, Czech Republic*

Date of submission 4 July 2017
Accepted for publication 28 November 2017
Published online *Article Accepted* 1 December 2017

Tanas Isikci O, He H, Grossmann P, Alaghehbandan R, Ulamec M, Michalova K, Pivovarcikova K, Montiel D P, Ondic O, Daum O, Prochazkova K, Hora M, Michal M & Hes O
(2018) *Histopathology* **72**, 804–813. https://doi.org/10.1111/his.13447

Low-grade spindle cell proliferation in clear cell renal cell carcinoma is unlikely to be an initial step in sarcomatoid differentiation

Aims: Spindle cell proliferation within clear cell renal cell carcinoma (ccRCC) is usually considered as a sarcomatoid differentiation. Low-grade spindle cell proliferation (LG-SCP) in ccRCC was first described in 2001. This phenomenon is not common and can pose diagnostic challenges, particularly in core biopsies. The aim of this study was to describe morphological, immunohistochemical and molecular characteristics of ccRCCs with LG-SCP.

Methods and results: Eleven cases of ccRCC with LG-SCP were retrieved from approximately 21 000 renal tumours in our registry. Ten cases of conventional ccRCC and 10 cases of typical sarcomatoid ccRCC were included as control groups. Morphological and immunohistochemical characteristics of epithelial–mesenchymal transition (EMT) were analysed. Von Hippel–Lindau syndrome gene abnormalities were also analysed using molecular genetics. Among ccRCC with LG-SCP cases, there were five males and five females (clinical information was not available in one case) with a median age of 67 years (mean: 68.5, range: 60–81 years). Average tumour size was 7.1 cm (median:7.5, range:1.7–12 cm). Follow-up data were available in nine cases (mean: 44.78 months), with no aggressive behaviour seen. On average, LG-SCP areas constituted 5–80% of tumour volume (mean: 32.3%). Necrotic/regressed areas were seen in all cases ranging from 5% to 30%. LG-SCP was clearly epithelial, with no mitoses or any evidence of mesenchymal differentiation. Immunohistochemical profile of LG-SCP was consistent with 'conventional' ccRCC. Compared with sarcomatoid ccRCC, some EMT markers showed alteration in LG-SCP, including lower expression of N-cadherin and Zeb1 as well as higher expression of E-cadherin. However, there were no significant differences in EMT

Address for correspondence: O Hes MD, PhD, Department of Pathology, Medical Faculty and Charles University Hospital Plzen, Alej Svobody 80, 304 60 Pilsen, Czech Republic. e-mail: hes@medima.cz

markers between LG-SCP and conventional ccRCC. Abnormalities in *VHL* (mutations, LOH3p) were found in six of 11 cases.

Conclusions: Our findings showed that LG-SCP in ccRCC have comparable immunohistochemical and molecular characteristics to those seen in 'conventional' ccRCC. Further, immunohistochemical analysis of EMT markers showed that LG-SCP did not differ from 'conventional' ccRCC. We believe that LG-SCP is a part of morphological heterogeneity in ccRCCs and that they may not represent an initial stage of sarcomatoid differentiation. This is supported further by the fact that ccRCC with LG-SCP did not display more aggressive behaviour than 'conventional' ccRCC.

Keywords: clear cell renal cell carcinoma, EMT, immunohistochemistry, kidney, low grade spindle cells

Introduction

Kidney cancer is among the 10 most frequently diagnosed cancers in men and women in the United States, with more than an estimated 62 000 new cases in 2016.[1] Clear cell renal cell carcinoma (ccRCC), the most common subtype of RCCs, is a morphologically heterogeneous group of malignant neoplasms composed of cells with clear or eosinophilic cytoplasm. Several unusual histological findings, such as syncytial giant cells and mucin production, have been described in ccRCCs.[2–4] Sarcomatoid changes can occur in approximately 1–8% of various RCC subtypes, including ccRCCs. They are associated with aggressive clinical behaviour.[5] Spindle cell differentiation within RCCs is usually considered to be a high-grade feature consistent with sarcomatoid differentiation/changes. It is well known that sarcomatoid differentiation can present in several variable histological patterns (i.e. fibrosarcoma, osteosarcoma), even within a given tumour. Another renal tumour demonstrating spindle cell proliferation is mucinous tubular and spindle cell carcinoma (MTSCC). In this tumour, spindle cell component is mainly low-grade [usually International Society of Urological Pathology (ISUP) nuclear grade 2], although rarely high-grade spindle cell morphology consistent with sarcomatoid differentiation can occur. Low-grade spindle cell proliferation (LG-SCP) in ccRCC was described initially as 'focal spindled morphology' by de Peralta Venturina in 2001.[6] This phenomenon is not common, and can potentially pose diagnostic challenges in which it should not be diagnosed as sarcomatoid change in RCC. LG-SCP in ccRCCs is a poorly understood finding. and as such our aim was to explore and characterise further this unusual morphological phenomenon from an immunohistochemical and molecular genetics perspective. We hypothesised that LG-SCP in ccRCCs may not represent the so-called 'epithelial–mesenchymal transition (EMT)' process, which is the basis for sarcomatoid differentiation.

Materials and methods

An institutional Ethics Review was obtained for the study (E.K., L.F. and F.N. Plzen, Charles University, 3 February 2015).

The Plzen Tumor Registry (including approximately 21 000 RCCs) was searched electronically and 11 cases of ccRCCs with LG-SCP were selected and enrolled into the study. We defined LG-SCP as the areas composed of spindle cells with bland and small nucleus, showing scant cytoplasm, but lacking pleomorphism, atypical mitoses, high mitotic activity and necrosis. There were one to 11 paraffin blocks available for each case.

Two control groups, including 10 cases of sarcomatoid RCCs with high-grade nuclear features and 10 cases of conventional ccRCCs with low-grade nuclear features, were selected randomly to compare immunohistochemical profile pertinent to EMT between the study groups.

Tissues for light microscopy were fixed in 4% formaldehyde and embedded in paraffin using a routine procedure. Five-μm-thick sections were cut from the tissue blocks and were stained with haematoxylin and eosin (H&E).

All tumours were reviewed independently by two pathologists (O.T.I. and O.H.). Clinicopathological and follow-up data were collected using medical records available from each participating institution.

IMMUNOHISTOCHEMISTRY

The immunohistochemical study was performed using a Ventana Benchmark XT automated immunostainer (Ventana Medical System, Inc., Tucson, AZ, USA) on formalin-fixed, paraffin-embedded tissue. The following primary antibodies were employed: p63 (4A4, monoclonal; Ventana, Tucson, AZ, USA, RTU), vimentin (D9, monoclonal; NeoMarkers, Westinghouse, CA, USA, 1:1000), claudin 1 (polyclonal;

Invitrogen, Camarillo, CA, USA, 1:50), claudin 7 (CLDN7, monoclonal; LifeSpan BioSciences, Seattle, WA, USA, 1:100), E-cadherin (12H6, monoclonal; Zymed, San Francisco, CA, USA, 1:200), N-cadherin (6G11, monoclonal; Dako, Glostrup, Denmark, 1:50), zinc finger E-box-binding homeobox 1 (Zeb1) (polyclonal, Sigma, St Louis, MO, USA, 1:100), forkhead box protein 3 (FoxP3) (mAbcam 450, monoclonal, Abcam, Cambridge, UK, 1:20), secreted protein acidic and rich in cysteine (Sparc) (MM0557-8NJ8, monoclonal Abcam, 1:150) and Twist family BHLH transcription factor 1 (Twist) (10E4E6, monoclonal; Abcam, 1:600).

The primary antibodies were visualised using the supersensitive streptavidin–biotin–peroxidase complex (BioGenex, San Ramon, CA, USA). Appropriate positive controls were employed.

We evaluated immunohistochemical expression according to staining percentage and intensity as follows: negative (−), focal < 50%, diffuse > 50%, weak (+), moderate (++) and strong (+++) expression.

MOLECULAR GENETIC METHODS

Molecular methods of analysis of Von Hippel–Lindau syndrome (*VHL*) gene, *VHL* promoter methylation and 3p LOH (loss of heterozygosity) were described previously.[7]

DNA extraction and bisulphite DNA conversion

DNA for molecular genetic investigation was extracted from formalin-fixed, paraffin-embedded tissue. Several 5-μm-thick sections were placed on the slides. H&E-stained slides were examined for identification of neoplastic tissue. Subsequently, neoplastic tumour and non-neoplastic tissue from unstained slides was scraped and DNA was isolated by the NucleoSpin® Tissue Kit (Macherey-Nagel, Düren, Germany).

Bisulphite conversion of DNA was carried out using the EZ DNA Methylation–Gold Kit (DNA input 500 ng) (Zymo Research, Orange County, CA, USA). All procedures were performed according to the manufacturer's protocols.

VHL gene analysis

Mutation analysis of exons 1, 2 and 3 of the *VHL* gene was performed using polymerase chain reaction (PCR) and direct sequencing. PCR was carried out using primers shown in Supporting information, Table S1. The reaction conditions were as follows: 12.5 μl of HotStar Taq PCR Master Mix (Qiagen, Hilden, Germany), 10 pmol of each primer, 100 ng of template DNA and distilled water up to 25 μl. The amplification programme consisted of denaturation at 95°C for 14 min and then 40 cycles of denaturation at 95°C for 1 min, annealing at 60°C for 1 min and extension at 72°C for 1 min for all amplicons. The programme was finished by 72°C incubation for 7 min. The PCR products were checked on 2% agarose gel electrophoresis.

Successfully amplified PCR products were purified with magnetic particles Agencourt® AMPure® (Agencourt Bioscience Corporation, Beverly, MA, USA), both side sequenced using the Big Dye Terminator Sequencing kit (Applied Biosystems, Foster City, CA, USA) and purified with magnetic particles of Agencourt® CleanSEQ® (Agencourt Bioscience Corporation), all according to the manufacturer's protocol, and subsequently run on an automated sequencer ABI Prism 3130xl (Applied Biosystems) at a constant voltage of 13.2 kV for 20 min. All samples were analysed in duplicate. Analyses of positive samples were repeated.

Analysis of VHL promoter methylation

Detection of promoter methylation was carried out via methylation-specific PCR as described by Herman *et al.*[8] Briefly, 100 ng of DNA or 2 μl of converted DNA was added to reaction consisting of 12.5 μl of HotStar Taq PCR Master Mix (Qiagen), 10 pmol of forward and reverse primer (Supporting information, Table S2) and distilled water up to 25 μl. The amplification programme was the same as mentioned above. The PCR products were checked on 2% agarose gel electrophoresis.

A patient with a known *VHL* mutation and fully methylated HeLa cell DNA was used as a positive control for *VHL* mutation analysis and promoter methylation analysis, respectively. For negative control, randomly selected healthy donor blood was used.

3p LOH analysis

For LOH analysis of neoplastic tissue DNA, 10 short-tandem repeat (STR) markers, D3S666, D3S1270, D3S1300, D3S1581, D3S1597, D3S1600, D3S1603, D3S1768, D3S2338 and D3S3630, located on the short arm of chromosome 3 (3p), were chosen from the database (Gene Bank UniSTS). The primers are listed in Supporting information, Table S3. PCR conditions were the same as mentioned above. Successfully amplified PCR products were mixed with GeneScan™ 500 LIZ™ dye size standard (Applied Biosystems) and run on an automated genetic analyser ABI Prism 3130xl (Applied Biosystems) at a constant voltage of 15 kV for 20 min. A sample was

considered LOH-positive if the ratio of non-tumour DNA to tumour DNA was > 1.5 or < 0.66. All samples were analysed in duplicate.

STATISTICAL ANALYSIS

The values of continuous parameters were calculated as means ± standard deviation (SD). Fisher's exact test was used to compare categorical variables. The *t*-test and 95% confidence intervals (95% CI) were used to compare the mean values of various continuous variables in different groups. All tests were two-tailed, and $P < 0.05$ was considered statistically significant. All descriptive and inferential statistical analyses were carried out using the Statistical Package for the Social Sciences (SPSS), version 19.0 (Chicago, IL, USA).

Results

Basic clinicopathological data for patients in all three groups, ccRCCs with LG-SCP, ccRCCs with sarcomatoid differentiation and conventional ccRCCs are summarised in Table 1 and Supporting information, Tables S4 and S5.

The patients in ccRCCs with LG-SCP group were five males and five females (information on gender was not available in one patient). Patient age at diagnosis ranged from 60 to 81 years (median: 67, mean: 68.54 years). Tumour size ranged from 1.7 to 12 cm in greatest dimension (median: 5.25 cm, mean: 7.1 cm). Follow-up information was available in nine cases (range: 3–144 months, median: 36 months, mean: 44.8 months). Grossly, the tumours were solid, yellow–tan on the cut surface, with whitish areas and foci of haemorrhage and necrosis. The mean age of patients with ccRCC with LG-SCP was significantly higher than those in the sarcomatoid RCC group (68.5 versus 55.1 years, $P < 0.05$). No statistically significant difference was found between the mean age of patients in ccRCC with LG-SCP and conventional ccRCC (68.5 versus 61 years, $P > 0.05$). Further, no statistically significant differences were found between ccRCC with LG-SCP and the other two control groups (sarcomatoid RCC and conventional ccRCC) in terms of gender distribution, mean tumour size and pathological staging.

Table 1. Clinicopathological data of ccRCCs with LG-SCP cases

Case no.	Age (years)	Sex	Tm size (cm)	Stage	Status	F/U months
1	64	F	7	pT3a	AW	12
2	81	M	1.7	pT1	AW	144
3	75	F	8.5	pT3a	AW	4
4	67	NA	NA	NA	NA	NA
5	60	F	5	pT1b	AW	36
6	68	M	5.5	pT1b	NA	NA
7	75	M	8.5	NA	AW	36
8	64	M	4.8	pT1b	AW	3
9	61	F	8	pT3a	AW	48
10	77	M	12	PT3a	AW	108
11	62	F	10	pT3a	AW	12

ccRCC, Clear cell renal cell carcinoma; LG-SCP, Low-grade spindle cell proliferation; F, Female; M, Male; Tm, Tumour; AW, Alive without disease; NA, Not available; F/U, Follow up.

Morphological features of ccRCC cases with LG-SCP are shown in Table 2. Eight of 11 tumours showed clear cell cytoplasmic morphology, while the remaining three exhibited variable eosinophilic granular cytoplasmic changes (5, 50 and 80% of the tumours). In nine of 11 cases, areas of necrosis ranging from 5% to 30% were identified. Regressed and degenerative changes, including fibrosis and myxoid oedematous changes, were seen in seven cases extending from 5% to 30% of the total tumour volume. In all cases, uniform spindle cell areas, composed of cells with scant eosinophilic or clear cytoplasm showing low-grade nuclei, are noted (Figure 1A, B). The spindle cell components were occasionally present in nodular architecture (Figure 1C) or intermingled with conventional clear cells (Figure 1D, E). Spindle cells were also arranged in fascicles, whorls, palisading or streaming patterns. There were no prominent pleomorphic spindle cell elements, high mitotic activity or atypical mitoses. In four of 11 cases necrosis was present in close vicinity to the LG-SCP areas. The LG-SCP areas ranged from 5% to 80% of the total tumour volume and showed an ISUP nuclear grade 2.

Results of immunohistochemical examination of ccRCCs with LG-SCP are summarised in Table 3. Claudin 1 and p63 were negative in all tumour cells, including the LG-SCP and clear cell components. In LG-SCP areas, vimentin was positive in all cases (Figure 2A). E-cadherin was negative in two cases, while it was variably positive (focal to diffuse and weak to moderate) in nine cases (Figure 2B). N-cadherin was variably positive (focal to diffuse and weak to strong) in nine of 11 cases (Figure 2C). Zeb1 was focally and weakly positive in seven of 11 and moderately

Table 2. Histopathological findings of ccRCCs with LG-SCP

Case no.	Pure CC	Eos-gra diff %	SCP %	Necrosis %	Regression %	SCP (ISUP)	CC (ISUP)	Tumour including blocks
1	+	–	10	10	30	2	3	9
2	+	–	80	–	5	2	2	1
3	+	–	60	10	10	2	3	9
4	+	–	20	5	–	2	3	1
5	+	–	15	10	5	2	2	6
6	+	–	80	20	5	2	2	4
7	+	–	25	20	<5	2	2	2
8	+	–	5	10	<5	2	3	11
9	–	5	20	10	–	2	2	3
10	–	80	20	30	–	2	3	2
11	–	50	20	10	–	2	3	9

+, Present; –, Absent; CC, Clear cell areas; Eos-gra diff, Eosinophilic granular differentiation; SCP, Spindle cell proliferation areas; Regression, degenerative, regressive changes other than necrosis; ISUP, International Society of Urological Pathology; ccRCC, Clear cell renal cell carcinoma; LG-SCP, Low-grade spindle cell proliferation.

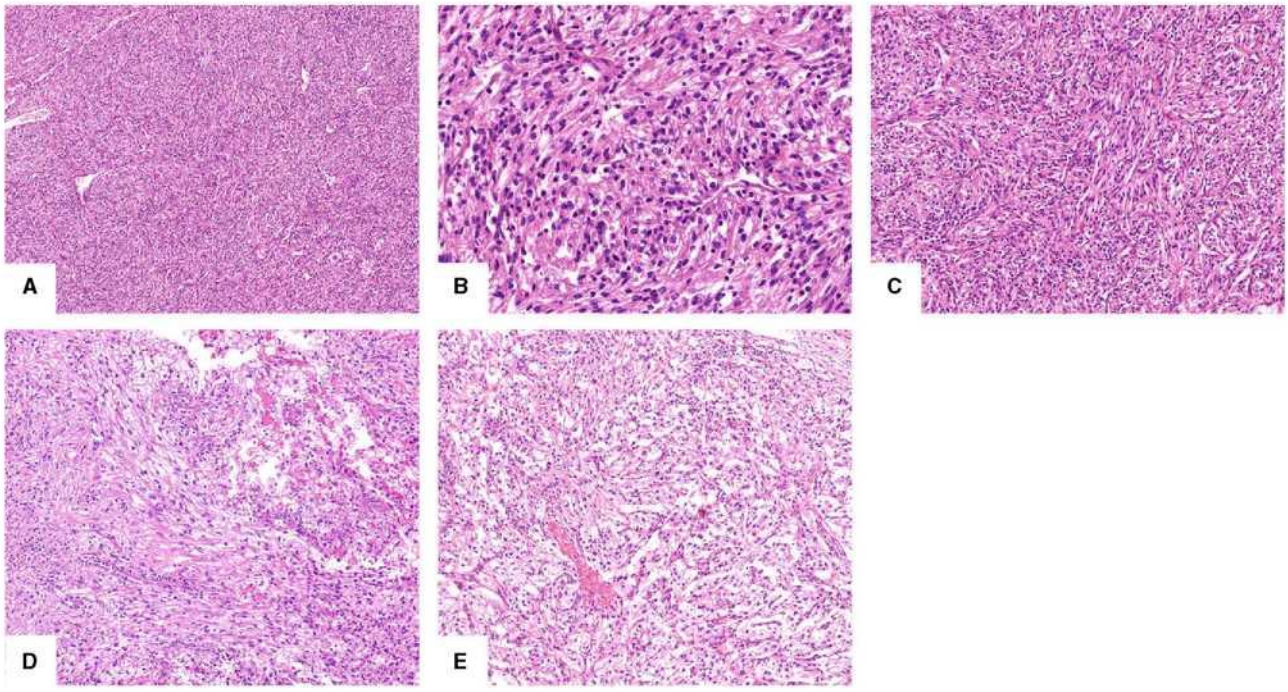

Figure 1. A, Low-grade spindle cell proliferation was characterized by elongated slender cells with small nuclei without marked cellular atypias. B, Higher magnification showing relative uniform low-grade nuclei. C, The spindle cell components were occasionally present in nodular architecture forming loose whorls. D, Low-grade spindle cell elements were intermingled with conventional clear cells. E, Low-grade spindle cell elements present as inconspicuous foci on clear cell background.

positive in one of 11 cases. FoxP3 was focally and weakly positive in six of 11 cases. Claudin 7 was diffusely and weakly cytoplasmic-positive in 10 cases (one case was not analysable). Sparc was weakly positive in seven of 11 and moderately positive in one of 11 cases. Twist was focally and weakly positive in

Table 3. Immunohistochemical staining results in ccRCCs with LG-SCP

Case no.	SC/CC	P63	VIM	E-CAD	N-CAD	Zeb1	FoxP3	CLA-1	CLA-7	Sparc	Twist
1	+/+	−/−	++/F+++	F+/++	++/++	F+/F+	−/−	−/−	+/+	F+/F+	−/−
2	+/+	−/−	+++/F++	+/++	+/++	F++/F+	F+/−	−/−	NA	−/−	−/−
3	+/+	−/−	+++/++	F+/++	+++/++	F+/F+	−/F+	−/−	+/+	F+/F+	−/−
4	+/+	−/−	+++/++	−/F+	+++/++	F+/F+	F+/F+	−/−	+/F+	F+/F+	−/−
5	+/+	−/−	+++/+++	F+/−	+/FM+++	F+/F+	F+/F+	−/−	+/F+	F+/F+	−/−
6	+/+	−/−	+++/F++	F++/+	+/F++	F+/−	F+/−	−/−	+/+	+/+	−/F+
7	+/+	−/−	F++/F+	++/F++	+++/+	−/−	−/−	−/−	+/+	F+/F+	F+/F+
8	+/+	−/−	+++/F+++	F+/++	−/−	F+/F+	F+/−	−/−	+/+	F+/−	−/F+
9	+/+	−/−	F+++/+++	+/++	−/+	−/+	−/+	−/−	+/−	−/F+	−/−
10	+/+	−/−	F+++/++	F++/+	FM+++/F+	−/−	−/−	−/−	+/F+	−/F+	F+/F+
11	+/+	−/−	++/F+	−/F+	++/++	F+/F+	F+/F+	−/−	+/+	F++/−	−/−

ccRCC, Clear cell renal cell carcinoma; LG-SCP, Low-grade spindle cell proliferation; SC/CC, Spindle cell areas/clear cell areas; F, Focal; D, Diffuse; FM, Focal mosaic; VIM, Vimentin; E-CAD, E-Cadherin; N-CAD, N-Cadherin; CLA-1, Claudin 1; CLA-7, Claudin 7; Zeb1, Zinc finger E-box-binding homeobox 1; Twist, Twist family BHLH transcription factor 1; Sparc, Secreted protein acidic and rich in cysteine; NA, Not analysable; F, Focal (positive under 50% of cells); −, Negative; +, Weak staining; ++, Moderate staining; +++, Strong staining; FoxP3, Forkhead box protein 3.

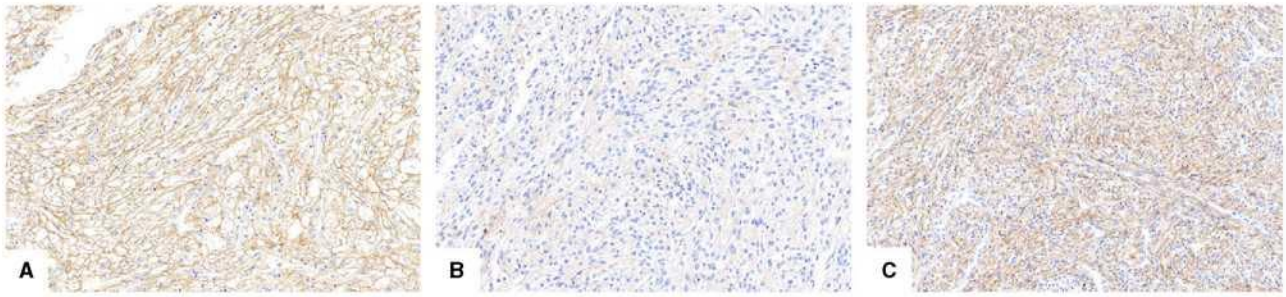

Figure 2. A, Low-grade spindle cells were diffusely strongly positive for vimentin. B, E-cadherin was variably positive (focal to diffuse and weak-moderate) in low-grade spindle cell component in majority of the cases. C, N-cadherin was mostly strong positive in nine of 11 cases with low-grade spindle cell component.

two of 11 cases. There were no significant differences between immunohistochemical findings of LG-SCP and 'classic' clear cell component within the same tumours ($P > 0.05$).

Results of immunohistochemical examination of ccRCCs with sarcomatoid differentiation are summarised in Supporting information, Table S6. Vimentin, Zeb1, claudin 7, Sparc and N-cadherin were variably positive in all cases. E-cadherin was negative in five of 10 cases. FoxP3 was focally and moderately positive in one, focally and weakly positive in six and negative in the remaining four cases. Claudin 1 was weakly positive in three of 10 cases. Twist was weakly positive in seven of 10 cases and p63 was weakly positive in one of 10 cases. Our analysis showed that there were no statistically significant differences between the IHC profile of sarcomatoid component and that of the LG-SCP group ($P > 0.05$).

The results of immunohistochemical examination of comparative conventional ccRCCs are summarised in Supporting information, Table S7. Vimentin, N-cadherin and claudin 7 were variably positive in all cases. E-cadherin was negative in five of 10 cases. Zeb1 and Sparc were focally to diffusely and weakly to moderately positive in nine of 10 and eight of 10 cases, respectively. FoxP3 was focally or diffusely weakly positive in seven of 10 and negative in three of 10 cases. Twist was focally and weakly positive in

Table 4. Results of molecular genetic analysis in ccRCCs with LG-SCP

Case no.	VHL	LOH3p	VHLm	
1	Neg	NA	Neg	
2	Neg	Neg	Neg	
3	Pos	Pos	Neg	c.320_327delGCCGCA TC/p.Arg107Profs*22
4	NA	NA	NA	
5	Pos	Neg	Neg	c.246_247delCG/p. Val83Argfs*49
6	Pos	Neg	Neg	c.439delA/p.Ile147Phefs*12
7	Pos	NA	Neg	c.463 + 2T>A/p.?
8	Neg	Neg	Neg	
9	Neg	Neg	Neg	
10	Pos	Neg	Neg	c.336_340 + 10del/p?
11	Neg	Neg	Neg	

ccRCC, Clear cell renal cell carcinoma; LG-SCP, Low-grade spindle cell proliferation; Pos, Positive; Neg, Negative; NA, Not analysable; VHL, Von Hippel–Lindau syndrome gene; LOH, Loss of heterozygosity; VHLm, VHL gene methylation status.

one case. Claudin 1 and p63 were negative in all cases. It should be noted that there were no statistically significant differences between immunohistochemical findings in conventional ccRCCs with either 'classic' clear cell or LG-SCP components in ccRCCs with LG-SCP ($P > 0.05$).

The results of molecular genetic testing are summarised in Table 4. In five of 11 ccRCC with LG-SCP cases, mutations of the *VHL* gene were disclosed. However, not all molecular genetic aspects, such as *VHL* gene mutations, methylation status of the *VHL* gene and LOH3p, were analysable due to the DNA quality.

Discussion

Sarcomatoid differentiation within carcinomas is a well-known phenomenon in various organs (i.e. lung, breast, gastrointestinal, etc.), including kidney. Sarcomatoid carcinoma is not a specific morphogenetic subtype of RCC but is considered as a pattern of dedifferentiation.[4,6,9,10] Sarcomatoid morphology may be found in any histological subtypes of RCC, including clear cell, papillary, chromophobe, collecting duct and other rare and unclassified subtypes, and is associated with an adverse outcome.[4,10] It should be noted that sarcomatoid differentiation is associated mainly with ccRCC, considering that clear cell is the most common subtype of RCC; however, some authors have considered chromophobe RCC, as a subtype of RCC, to be associated most frequently with sarcomatoid differentiation.[6,11] Sarcomatoid areas are composed of malignant mesenchymal-like elements or fully developed mesenchymal malignant tissue (either homologous or heterologous) juxtaposed or intermingling with neoplastic epithelial components. The diagnostic criteria of sarcomatoid differentiation would include spindle cells demonstrating high-grade features (i.e. necrosis or haemorrhage, brisk mitotic activity, atypical mitoses) in at least one low-power field. However, LG-SCP that is morphologically distinct from high-grade sarcomatoid changes can also be seen in RCCs.

In 2001, de Peralta Venturina *et al.* first described 'focal spindled morphology' in conventional RCCs. The authors found nine of 101 cases of ccRCCs with areas composed of 'focal spindled morphology' which were clearly different from typical sarcomatoid transformation, and suggested that such a finding should not be diagnosed as sarcomatoid differentiation.[6] Delahunt *et al.* described this phenomen as 'early spindle cell change' (ESCC) in ccRCC. The authors examined collagen expression in sarcomatoid RCCs, ccRCCs and ccRCCs with ESCC and found a similar distribution of collagen expression among sarcomatoid and ESCC, including ccRCCs. The authors proposed that such a morphology could be an early possible step towards the evolution of sarcomatoid differentiation.[12]

In this study, we suggest describing such a morphology as 'low-grade spindle cell proliferation', given that spindle cells showed low-grade nuclear features, and were morphologically very different from sarcomatoid change/differentiation (Supporting information, Table S7). Further, no areas with unequivocal mesenchymal transformation (benign or malignant) were found within tumours with LG-SCP.

In this study, we examined LG-SCP in ccRCCs morphologically, immunohistochemically and genetically in order to assess a possible relationship with EMT. We also included 10 cases of conventional ccRCC and 10 cases of ccRCC with unequivocal sarcomatoid differentiation to serve as control groups. Both control groups were similar to ccRCC with the LG-SCP group from a demographic and clinicopathological perspective.

EMT is a biological process in which epithelial cells gradually lose epithelial phenotype and gain a mesenchymal one, leading to spindle cell morphology,

increased motility, invasive capacity, high resistance to apoptosis and increased production of extracellular matrix proteins.[13] Morphological metamorphosis is followed by changes in the immunohistochemical profile of such cells. In this study, we used various important pertinent immunohistochemical stains in order to determine the possible presence of the EMT process (i.e. p63, vimentin, claudin 1, claudin 7, E-cadherin, N-cadherin, Zeb1, FoxP3, Sparc and Twist). Loss of E-cadherin immunostain and gain of N-cadherin positivity is considered to be a hallmark of EMT. Twist and Zeb1 are transcription factors that promote tumour invasion and metastasis by inducing EMT via down-regulation of E-cadherin.[14,15] SPARC is a secreted glycoprotein that modifies cell extracellular interactions during proliferation, and is related to increased motility.[16] FoxP3 is a transcription factor which is identified as a tumour suppressor gene. FoxP3 down-regulation is considered to play a role in EMT in neoplastic cells by inducing proliferation, migration and invasion capacity of tumour cells.[17] Claudins are suggested to be integral membrane proteins, responsible for maintaining epithelial cell polarity. Repression of p63, a transcription factor required for maintenance of epithelial cell differentiation, induces EMT.[18–20]

Morphologically, LG-SCP areas in our ccRCC cases appeared to derive directly from 'conventional' clear cell elements. There was a continual spectrum of gradually elongated clear cells to fully developed slender spindle cells with low-grade nuclei. Further, cytoplasmic characteristics of spindle cell proliferation were almost identical to that of the epithelial neoplastic component.

From an immunohistochemical viewpoint, some EMT markers showed alteration in LG-SCP, including reduced expression of N-cadherin and Zeb1 as well as increased expression of E-cadherin, compared to sarcomatoid ccRCCs (control group). Further, LG-SCP showed an almost identical immunoprofile to that of the clear cell epithelial element. In this study, we employed a second matched control group including 10 cases of ccRCC with no LG-SCP or sarcomatoid differentiation to examine further our hypothesis that the LG-SCP component has comparable immunohistochemical characteristics to those in conventional ccRCC. Immunohistochemical findings in the control group showed a similar immunoprofile to that observed in the ccRCCs with the LG-SCP group.

We also performed extensive analyses comparing the ccRCC group with the sarcomatoid RCC cohort in terms of immunohistochemical profiles. Essentially, the immunohistochemical profile of epithelial components of the two groups showed no statistically significant differences for all stains used in the study ($P > 0.05$). However, the immunoprofile of the sarcomatous component showed a slightly different pattern. The statistical differences in P63, Zeb1, claudin 1, claudin 7 and Sparc may be related to the epithelial–mesenchymal transitions reflected in some of these stains. We recognise that this should be interpreted with caution, as the sample sizes used in these groups are somewhat small.

We also utilised molecular–genetic testing concerning *VHL* gene abnormalities, including *VHL* gene mutation analysis, analysis of LOH3p and determination of the methylation status of the *VHL* gene to further support establishment of a diagnosis of ccRCC. Our findings showed abnormalities in the *VHL* gene (mutations and LOH3p) to be found in five of 11 cases, although we expected a higher frequency of *VHL* gene abnormalities. This could be due to the lack of a complete analysis. We were not able to analyse LOH3p in three cases and *VHL* gene mutation status and methylation status of the *VHL* gene in one case.

Overall, our morphological, immunohistochemical and genetic findings support our hypothesis that LG-SCP in ccRCCs may represent a morphological variation of 'conventional' ccRCC. Clinically, we did not observe aggressive behaviour associated with LG-SCP in ccRCCs. However, we recognised that the follow-up time-period in some of the cases may have been somewhat short (3–144 months, mean: 44.78). Conversely, in the control group (ccRCC with sarcomatoid differentiation), six of eight cases (with available follow-up information) showed metastatic spreading or dead of disease in a time-period ranging from 4 to 24 months from resection of the renal tumour.

This study faced a number of limitations. First, the sample size was somewhat small, which could be due to the rarity of LG-SCP in ccRCC, being under-recognised or possibly misdiagnosed as sarcomatoid differentiation. Secondly, we were not able to predict further development of the LG-SCP component if left *in vivo*. One of the strengths of the study was the inclusion of two matched control groups, ccRCCs with sarcomatoid differentiation and ccRCCs with no LG-SCP or sarcomatoid differentiation, for comparison purposes.

Spindle cell proliferation in kidney can present a broad range of differential diagnoses, including both benign and malignant lesions as well as primary and metastasis. The main differential diagnosis would include sarcomatoid RCC, MTSCC, AML and pseudoxanthogranulomatous pyelonephritis.

Lack of nuclear pleomorphism, atypia and high mitotic activity can help to differentiate LG-SCP in ccRCCs from sarcomatoid RCCs. Moreover, no heterologous mesenchymal element is associated with LG-SCP, while such a finding is relatively frequent in sarcomatoid RCCs.

MTSCC is a renal epithelial neoplasm composed of tubular formations merging with bland spindle cells and myxoid stroma. The spindle cell components in this neoplasm have mainly low-grade nuclear features, easily distinguishable from sarcomatoid changes.[4,21–25] LG-SCP in ccRCCs lack myxoid stroma and a biphasic pattern, which are characteristic of MTSCC. Also, the immunoprofile of LG-SCP differs from MTSCC and both tumour types are easily distinguishable.

AML is composed typically of fat, smooth muscle and vascular component. Rarely, AMLs can be spindle cell-rich and fat-poor, sometimes presenting a diagnostic challenge. All AML are positive for HMB45 and/or Melan A and such immunohistohemical examination can easily resolve differential diagnostic problems.

Pseudoxanthomatous pyelonephritis is a mainly non-capsulated, irregular destructive process within renal parenchyma. Histologically, it is composed of spindle cell elements, which are histiocytic in origin, admixed with multinucleated giant cells and prominent lymphocytic infiltration. All these features were absent in LG-SCP and the majority of cases would easily be diagnosed based on H&E examination.

Conclusions

Our findings show that LG-SCP in ccRCC have comparable immunohistochemical and molecular characteristics to those seen in 'conventional' ccRCC. Further, immunohistochemical analysis of EMT markers show that LG-SCP did not differ from 'conventional' ccRCC. We believe that LG-SCP is a part of morphological heterogeneity in ccRCCs, and they may not represent an initial stage of sarcomatoid differentiation. This is supported further by the fact that ccRCC with LG-SCP did not display more aggressive behaviour than 'conventional' ccRCC.

Acknowledgements

The study was supported by the Charles University Research Fund Progres (project number Q39) and the Institutional Research Fund of University Hospital Plzen, FN 00669806.

Conflicts of interest

All authors declare no conflicts of interest.

References

1. Choueiri TK, Motzer RJ. Systemic therapy for metastatic renal-cell carcinoma. *N. Engl. J. Med.* 2017; **376**: 354–366.
2. Williamson SR, Kum JB, Goheen MP, Cheng L, Grignon DJ, Idrees MT. Clear cell renal cell carcinoma with a syncytial-type multinucleated giant tumor cell component: implications for differential diagnosis. *Hum. Pathol.* 2014; **45**: 735–744.
3. Val-Bernal JF, Salcedo W, Val D, Parra A, Garijo MF. Mucin-secreting clear cell renal cell carcinoma. A rare variant of conventional renal cell carcinoma. *Ann. Diagn. Pathol.* 2013; **17**: 226–229.
4. Moch H, Cubilla AL, Humphrey PA, Reuter VE, Ulbright TM. The 2016 WHO classification of tumours of the urinary system and male genital organs – Part A: renal, penile, and testicular tumours. *Eur. Urol.* 2016; **70**: 93–105.
5. Kuroda N, Toi M, Hiroi M, Enzan EH. Review of sarcomatoid renal cell carcinoma with focus on clinical and pathobiological aspects. *Histol. Histopathol.* 2003; **18**: 551–555.
6. de Peralta-Venturina M, Moch H, Amin M *et al.* Sarcomatoid differentiation in renal cell carcinoma: a study of 101 cases. *Am. J. Surg. Pathol.* 2001; **25**: 275–284.
7. Peckova K, Grossmann P, Bulimbasic S *et al.* Renal cell carcinoma with leiomyomatous stroma – further immunohistochemical and molecular genetic characteristics of unusual entity. *Ann. Diagn. Pathol.* 2014; **18**: 291–296.
8. Herman JG, Graff JR, Myohanen S, Nelkin BD, Baylin SB. Methylation-specific PCR: a novel PCR assay for methylation status of CpG islands. *Proc. Natl Acad. Sci. USA* 1996; **93**: 9821–9826.
9. Cheville JC1, Lohse CM, Zincke H *et al.* Sarcomatoid renal cell carcinoma: an examination of underlying histologic subtype and an analysis of associations with patient outcome. *Am. J. Surg. Pathol.* 2004; **28**: 435–441.
10. Delahunt B, Cheville JC, Martignoni G *et al.* The International Society of Urological Pathology (ISUP) grading system for renal cell carcinoma and other prognostic parameters. *Am. J. Surg. Pathol.* 2013; **37**: 1490–1504.
11. Akhtar M, Tulbah A, Kardar AH, Ali MA. Sarcomatoid renal cell carcinoma: the chromophobe connection. *Am. J. Surg. Pathol.* 1997; **21**: 1188–1195.
12. Delahunt B, Bethwaite PB, McCredie MRE, Nacey JN. The evolution of collagen expression in sarcomatoid renal cell carcinoma. *Hum. Pathol.* 2007; **38**: 1372–1377.
13. Kalluri R, Weinberg RA. The basics of epithelial–mesenchymal transition. *J. Clin. Invest.* 2009; **119**: 1420–1428.
14. Zhang P, Sun Y, Ma L. ZEB1: at the crossroads of epithelial–mesenchymal transition, metastasis and therapy resistance. *Cell Cycle* 2015; **14**: 481–487.
15. Nieto MA, Huang RY-J, Jackson RA, Thiery JP. EMT: 2016. *Cell* 2016; **166**: 21–45.
16. Conant JL, Peng Z, Evans MF, Naud S, Cooper K. Sarcomatoid renal cell carcinoma is an example of epithelial–mesenchymal transition. *J. Clin. Pathol.* 2011; **64**: 1088–1092.
17. Wang X, Liu Y, Dai L *et al.* Foxp3 downregulation in NSCLC mediates epithelial–mesenchymal transition via NF-κB signaling. *Oncol. Rep.* 2016; **36**: 2282–2288.

18. Olsen JR, Oyan AM, Rostad K *et al.* p63 attenuates epithelial to mesenchymal potential in an experimental prostate cell model. *PLoS ONE* 2013; **8**: e62547.
19. Candi E, Agostini M, Melino G, Bernassola F. How the TP53 family proteins TP63 and TP73 contribute to tumorigenesis: regulators and effectors. *Hum. Mutat.* 2014; **35**: 702–714.
20. Yoh KE, Regunath K, Guzman A *et al.* Repression of p63 and induction of EMT by mutant Ras in mammary epithelial cells. *Proc. Natl Acad. Sci. USA* 2016; **113**: E6107–E6116.
21. Pillay N, Ramdial PK, Cooper K, Batuule D. Mucinous tubular and spindle cell carcinoma with aggressive histomorphology – a sarcomatoid variant. *Hum. Pathol.* 2008; **39**: 966–969.
22. Bulimbasic S, Ljubanovic D, Sima R *et al.* Aggressive high-grade mucinous tubular and spindle cell carcinoma. *Hum. Pathol.* 2009; **40**: 906–907.
23. Kuroda N, Hes O, Michal M *et al.* Mucinous tubular and spindle cell carcinoma with Fuhrman nuclear grade 3: a histological, immunohistochemical, ultrastructural and FISH study. *Histol. Histopathol.* 2008; **23**: 1517–1523.
24. Fine SW, Argani P, DeMarzo AM *et al.* Expanding the histologic spectrum of mucinous tubular and spindle cell carcinoma of the kidney. *Am. J. Surg. Pathol.* 2006; **30**: 1554–1560.
25. Farghaly H. Mucin poor mucinous tubular and spindle cell carcinoma of the kidney, with nonclassic morphologic variant of spindle cell predominance and psammomatous calcification. *Ann. Diagn. Pathol.* 2012; **16**: 59–62.

Supporting Information

Additional Supporting Information may be found in the online version of this article:

Table S1. PCR primers used in mutation analysis of the *VHL* gene and designed in Primer3 software

Table S2. PCR primers used in methylation status of the *VHL* gene.

Table S3. PCR primers used in LOH analysis of chromosome 3p.

Table S4. Clinicopathologic data of ccRCC cases with sarcomatoid differentiation.

Table S5. Clinicopathologic data of conventional ccRCCs cases (grade 1–2 Fuhrman/ISUP)

Table S6: Immunohistochemical staining results in ccRCCs with sarcomatoid differentiation.

Table S7. Immunohistochemical satining results in conventional ccRCCs

1.5.3 Reactivity of CK7 across the spectrum of renal cell carcinomas with clear cells

Imunoreaktivita cytokeratinu CK7 v rámci CCRCC je v současné literatuře popisována řadou relativně konfliktních výsledků. Proto bylo cílem této studie objektivně zhodnotit CK7 imunoreaktivitu v rámci vybraných renálních neoplázií sestávajících ze světlých buněk.

Za účelem komplexní analýzy bylo vybráno 75 případů renálních karcinomů/neoplázií, které byly pro účely studie rozděleny do pěti různých skupin (1. low-grade CCRCC, 2. high-grade CCRCC, 3. multicystická renální neoplázie nízkého maligního potenciálu/MCRNLMP, 4. CCRCC s cystickými změnami a 5. světlobuněčnému papilárnímu renálnímu karcinomu podobné tumory) a obarveny dvěma různými klony cytokeratinu CK7. Nejvyšší míry reaktivity CK7 bylo dosaženo ve skupinách low-grade CCRCC, MCRNLMP a světlobuněčnému papilárnímu renálnímu karcinomu podobných tumorech, s pozitivitou v rozmezí 60 až 93%.

CK7 imunoreaktivita v rámci CCRCC je variabilní a míra pozitivity je patrně závislá na gradu a architektonickém uspořádání tumoru.

Histopathology

Histopathology 2019, **74**, 608–617. DOI: 10.1111/his.13791

Reactivity of CK7 across the spectrum of renal cell carcinomas with clear cells

Manuel L Gonzalez,[1] Reza Alaghehbandan,[2] Krystina Pivovarcikova,[3] Kvetoslava Michalova,[3] Joanna Rogala,[4] Petr Martinek,[3] María P Foix,[5] Enric C Mundo,[5] Eva Comperat,[6] Monika Ulamec,[7] Milan Hora,[8] Michal Michal[3] & Ondrej Hes[3]

[1]*Department of Pathology, University of Kansas, Medical Center, Kansas City, Kansas, USA,* [2]*Department of Pathology, Faculty of Medicine, University of British Columbia, Royal Columbian Hospital, Vancouver, BC, Canada,* [3]*Department of Pathology, Charles University in Prague, Faculty of Medicine in Plzeň, Pilsen, Czech Republic,* [4]*Department of Pathology, University Hospital Wroclaw, Wroclaw, Poland,* [5]*Department of Pathology, Bellvitge Biomedical Research Institut (IDIBELL), Bellvitge University Hospital, University of Barcelona School of Medicine, L'Hospitalet de Llobregat, Barcelona, Spain,* [6]*Department of Pathology, Hospital Tenon, Paris, Sorbonne University, Paris, France,* [7]*'Ljudevit Jurak' Pathology Department, Clinical Hospital Center 'Sestre milosrdnice', Pathology Department, Medical University, Medical Faculty Zagreb, Zagreb, Croatia, and* [8]*Department of Urology, Charles University in Prague, Faculty of Medicine in Plzeň, Pilsen, Czech Republic*

Date of submission 20 August 2018
Accepted for publication 13 November 2018
Published online *Article Accepted* 16 November 2018

Gonzalez M L, Alaghehbandan R, Pivovarcikova K, Michalova K, Rogala J, Martinek P, Foix M P, Mundo E C, Comperat E, Ulamec M, Hora M, Michal M & Hes O

(2019) *Histopathology* **74**, 608–617. https://doi.org/10.1111/his.13791

Reactivity of CK7 across the spectrum of renal cell carcinomas with clear cells

Aims: Current available data on cytokeratin 7 (CK7) immunostaining pattern in the clear cell renal cell carcinoma (RCC) spectrum is conflicting. The aim of this study was to assess CK7 immunoreactivity within the spectrum of clear cell renal neoplasms, including clear cell RCC, multicystic renal neoplasm of low malignant potential and clear cell papillary RCC-like tumours.

Methods and results: We analysed two clones of CK7 and two tumour blocks for a total of 75 cases divided into five distinct groups: (i) low-grade clear cell RCC, (ii) high-grade clear cell RCC, (iii) multicystic renal neoplasm of low malignant potential, (iv) clear cell RCC with cystic changes and (v) clear cell papillary RCC-like tumours. We found the highest CK7 reactivity in low-grade clear cell RCC, multicystic renal neoplasm of low malignant potential and clear cell papillary RCC-like groups, ranging from 60% to 93%.

Conclusions: Our findings show that CK7 immunoreactivity in clear cell RCC is variable, and the extent of staining depends on the grade and architectural growth patterns of the tumours.

Keywords: clear cell renal cell carcinoma, cytokeratin 7, immunohistochemistry, kidney

Introduction

Renal tumours with clear cells form a broad spectrum, including clear cell renal cell carcinoma (CC-RCC), multicystic renal neoplasm of low malignant potential (MCRN-LMP), clear cell papillary renal cell carcinoma (CCP-RCC), translocation carcinomas and some papillary renal cell carcinomas (P-RCC).

There is considerable morphological overlap in the features that distinguish each one of these entities. For example, multicystic changes may be seen in low-grade CC-RCC, or some cases of 'conventional' CC-RCC may have morphological features resembling CCP-RCC (CCP-RCC-like).

Given the differences in prognosis and aggressiveness among the renal tumours with clear cell

Address for correspondence: O Hes, Department of Pathology, Medical Faculty and Charles University Hospital Plzen, Alej Svobody 80, 304 60 Pilsen, Czech Republic. e-mail: hes@medima.cz

morphology, an accurate diagnosis is important. Immunohistochemical profiling can be helpful in establishing the correct diagnosis. However, similar to morphological features, overlapping immunophenotypes exist, making interpretation difficult.

According to the latest edition of the World Health Organisation (WHO) classification of genitourinary tumours, CK7 positivity in CC-RCC is only seen in isolated cells in rare high-grade tumours.[1] In low-grade tumours, immunoreactivity for CK7 in clear cell tumours has also been described in areas around cystic changes.[1,2]

The current available data regarding distribution, frequency and intensity of CK7 positivity in CC-RCC are conflicting. The aim of this study was to assess CK7 immunoreactivity within the spectrum of CC-RCC, MCRN-LMP and CCP-RCC-like tumours.

Materials and Methods

An institutional Ethics Review was obtained for the study (EK, LF and FN Plzen, Charles University, 02.03.2015).

We created a study set of 75 cases divided into five distinct groups, including: (i) low-grade clear cell renal cell carcinoma (LGCC-RCC), (ii) grade III clear cell renal cell carcinoma (HGCC-RCC), (iii) multicystic renal neoplasm of low malignant potential (MCRN-LMP), (iv) clear cell renal cell carcinoma with cystic changes (CC-RCC) and (v) cases of CC-RCC mimicking clear cell papillary renal cell carcinoma (CCP-RCC-like).

The LGCC-RCC group was composed of cases of CC-RCC with WHO/International Society of Urological Pathology (ISUP) grades I or II, predominantly exhibiting a solid growth pattern. The HGCC-RCC group only included cases with WHO/ISUP grade III with a predominantly solid growth pattern. The MCRN-LMP group was defined as cases with cystic morphology. The cysts were lined by a single layer of tumour cells with abundant clear cytoplasm and small nuclei without nucleoli. All cases examined in this study were extensively sampled, with no obvious expansile growth pattern, solid nodule or back-to-back pattern. Immunohistochemistry was further used to support the diagnosis, as described previously (Table S1).[5] CC-RCCs with cystic changes were defined as cases of CC-RCC with cystic changes (up to 50% of the total tumour volume), which did not meet the diagnostic criteria for MCRN-LMP due to necrosis, vascular invasion or high nuclear grade (grades II or III). Cases were included in the CCP-RCC-like group if they had at least two histological features resembling CCP-RCC, such as clear cells, cystic, tubular or papillary patterns, apically situated nuclei and fibromuscular stroma or myoid metaplasia of the tumour capsule, but did not fulfil all the diagnostic criteria required for CCP-RCC. It should be noted that *VHL* gene analysis was performed in the CCP-RCC-like group in order to confirm the diagnosis of CC-RCC.

Tissue for light microscopy was fixed in 4% formaldehyde and embedded in paraffin using the routine procedure. Sections 2 μm thick were cut from tissue blocks and stained with haematoxylin and eosin (H&E).

For each case, two representative blocks were stained for CK7 with two different clones (OV-TL12/30, monoclonal; DakoCytomation, Carpinteria CA, USA/1:200 and SP52, monoclonal; Ventana Medical Systems, Tucson, AZ, USA, RTU). Immunohistochemical staining was performed using a Ventana Benchmark XT automated stainer (Ventana Medical Systems, Inc.).

For evaluation of immunohistochemical staining, the slides were initially scanned at ×100 magnification, followed by ×400 if positive. Any amount of membranous or cytoplasmic staining of the neoplastic cells was considered positive. The staining extent was divided into three groups: (i) 0%, (ii) 1–50% and (iii) 51–100%. The staining intensity was graded as weak (+) to strong (++++). Areas surrounding tumour necrosis were not included in the analysis. Non-neoplastic renal tissue was used as a positive internal control. All slides were evaluated independently by three pathologists (M.L.G., K.P. and O.H.).

Molecular Genetic Methods

DNA EXTRACTION AND BISULPHITE DNA CONVERSION

DNA for molecular genetic investigation was extracted from formalin-fixed, paraffin-embedded tissue. Several 5-μm-thick sections were placed on the slides. H&E-stained slides were examined for identification of neoplastic tissue. Subsequently, neoplastic tumour and non-neoplastic tissue from unstained slides were scraped and DNA was isolated by the QIAsymphony DSP AXpH DNA Kit (Qiagen, Hilden, Germany).

Bisulphite conversion of DNA was carried out using EZ DNA Methylation–Gold Kit (DNA input 500 ng) (Zymo Research, Irvine, CA, USA). All procedures were performed according to the manufacturer's protocols.

VHL GENE ANALYSIS

Mutation analysis of exons 1, 2 and 3 of the *VHL* gene was performed using polymerase chain reaction (PCR) and direct sequencing. PCR was carried out using primers shown in Table 1. The reaction conditions were as follows: 12.5 μl of HotStar Taq PCR Master Mix (Qiagen, Hilden, Germany), 10 pmol of each primer, 100 ng of template DNA and distilled water up to 25 μl. The amplification programme consisted of denaturation at 95°C for 14 min and then 40 cycles of denaturation at 95°C for 1 min, annealing at 60°C for 1 min and extension at 72°C for 1 min for all amplicons. The programme was finished by 72°C incubation for 7 min. The PCR products were checked on 2% agarose gel electrophoresis.

Successfully amplified PCR products were purified with magnetic particles Agencourt® AMPure® (Agencourt Bioscience Corporation, Beverly, MA, USA), both side-sequenced using Big Dye Terminator Sequencing kit (Applied Biosystems, Foster City, CA, USA) and purified with magnetic particles Agencourt® CleanSEQ® (Agencourt Bioscience Corporation), all according to the manufacturer's protocol, and subsequently run on an automated sequencer ABI Prism 3130xl (Applied Biosystems) at a constant voltage of 13.2 kV for 20 min. All samples were analysed in duplicate. Analyses of positive samples were repeated.

Table 1. Polymerase chain reaction (PCR) primers used in mutation analysis of the *VHL* gene

Gene/exon	Name	Primers (sequence 5′→3′)
VHL/exon 1	VHL e1-1	CGCGAAGACTACGGAGGT
	VHL e1-2	GTCTTCTTCAGGGCCGTA
	VHL e1-3	GAGGCAGGCGTCGAAGAG
	VHL e1-4	GCGATTGCAGAAGATGACCT
	VHL e1-5	GCCGAGGAGGAGATGGAG
	VHL e1-6	CCCGTACCTCGGTAGCTGT
	VHL e1-7	CCGTATGGCTCAACTTCGAC
	VHL e1-8	GCTTCAGACCGTGCTATCGT
VHL/exon 2	VHL e2-1	ACCGGTGTGGCTCTTTAACA
	VHL e2-2	TCCTGTACTTACCACAACAACCTT
VHL/exon 3	VHL e3-1	GCAAAGCCTCTTGTTCGTTC
	VHL e3-2	ACATTTGGGTGGTCTTCCAG
	VHL e3-3	CAGGAGACTGGACATCGTCA
	VHL e3-4C	CCATCAAAAGCTGAGATGAAAC

ANALYSIS OF VHL PROMOTER METHYLATION

Detection of promoter methylation was carried out via methylation-specific PCR, as described by Herman *et al.*[8] Briefly, 100 ng of DNA or 2 μl of converted DNA was added to the reaction consisting of 12.5 μl of HotStar Taq PCR Master Mix (Qiagen), 10 pmol of forward and reverse primer (Table 2) and distilled water up to 25 μl. The amplification programme was the same as mentioned above. The PCR products were checked on 2% agarose gel electrophoresis.

A patient with known *VHL* mutation and fully methylated HeLa cell DNA was used as a positive control for VHL mutation analysis and promoter methylation analysis, respectively. For negative control, a randomly selected healthy donor blood was used.

3P LOSS OF HETEROZYGOSITY ANALYSIS

For loss of heterozygosity (LOH) analysis of neoplastic tissue DNA, 10 STR (short tandem repeats) markers D3S666, D3S1270, D3S1300, D3S1581, D3S1597, D3S1600, D3S1603, D3S1768, D3S2338 and D3S3630 located on the short arm of chromosome 3 (3p) were chosen from the database (Gene Bank UniSTS). The primers are listed in Table 3. PCR conditions were the same as mentioned above. Successfully amplified PCR products were mixed with GeneScan™ 500 LIZ™ dye size standard (Applied Biosystems) and run on an automated genetic analyser ABI Prism 3130xl (Applied Biosystems) at a constant voltage of 15 kV for 20 min. A sample was considered LOH-positive if the ratio of non-tumour DNA to tumour DNA was >1.5 or <0.66. All samples were analysed in duplicate.

STATISTICAL ANALYSIS

The values of continuous parameters were calculated as means ± standard deviation (SD). Pearson's χ^2

Table 2. PCR primers used in methylation status of the *VHL* gene

Gene	Name	Primers (sequence 5′→3′)
VHL unmethylated	VHL-U-S	GTTGGAGGATTTTTTTGTGTATGT
VHL unmethylated	VHL-U-A	CCCAAACCAAACACCACAAA
VHL methylated	VHL-M-S	TGGAGGATTTTTTTGCGTACGC
VHL methylated	VHL-M-A	GAACCGAACGCCGCGAA

test was used for categorical variables. All tests were two-tailed, and $P < 0.05$ was considered statistically significant. All descriptive and inferential statistical analyses were carried out using the Statistical Package for the Social Sciences (SPSS), version 19.0 (Chicago, IL, USA).

Results

All basic clinicopathological data are summarised in Table 4. Five groups were chosen and included in the study as follows: LGCC-RCC (Figure 1), HGCC-RCC (Figure 2), MCRN-LMP (Figure 3), CC-RCC with cystic changes (Figure 4) and CCP-RCC-like CC-RCC (Figure 5). Each group consisted of 15 patients.

Immunohistochemical results in each study group are summarised in Tables 5–9. CK7 positivity rate was observed highest in LGCC-RCC (60–66%), MCRN-LMP (86–93%) and CCP-RCC-like CC-RCC groups (80%), while HGCC-RCCs (6%) and CC-RCCs with cystic changes (20–25%) demonstrated lowest rates of CK7 positivity. No statistically significant differences were found in CK7 positivity rates between the blocks examined in each group ($P > 0.05$). Further, the CK7 positivity rates between LGCC-RCC, MCRN-LMP and CCP-RCC-like CC-RCC groups were not statistically different ($P > 0.05$). A similar finding was observed regarding the CK7 positivity rate between HGCC-RCCs and CC-RCCs with cystic changes ($P > 0.05$).

The CK7 positivity rate was significantly higher in LGCC-RCCs ($P = 0.0052$), MCRN-LMP ($P < 0.0001$) and CCP-RCC-like CC-RCCs ($P = 0.0001$) than in HGCC-RCCs. Similarly, the CK7 positivity rate was overall statistically higher in MCRN-LMP ($P < 0.05$) and CCP-RCC-like CC-RCCs ($P < 0.05$) than in CCR-CCs with cystic changes. Comparing CK7 positivity in LGCC-RCCs and CC-RCCs with cystic changes, there were no statistically significant differences (which varied based on the chosen block and the antibody clone).

Table 3. PCR primers used in loss of heterozygosity (LOH) analysis of chromosome 3p

Marker	Name	Primers (sequence 5′→3′)
D3S666	D3S666-SK#15	CAAGGCATTAAAGTGGCCACGC
	D3S666-SK#16	GTTTGAACCAGTTTCCTACTGAG
D3S1270	D3S1270-F	TGGAACTGTATCAAAGGCTC
	D3S1270-R	TTGCATTAGNATTCTCCAGA
D3S1300	D3S1300SF	AGCTCACATTCTAGTCAGCCT
	D3S1300A	GCCAATTCCCCAGATG
D3S1581	D3S1581-F	CAGAACTGCCAAACCA
	D3S1581-R	GGGTAACAGGAGCGAG
D3S1597	D3S1597-F	AGTACAAATACACACAAATGTCTC
	D3S1597-R	GCAAATCGTTCATTGCT
D3S1600	D3S1600-F	ATCACCATCATCTGCCTGTC
	D3S1600-R	TGCTTGCCTTGGGATTTA
D3S1603	D3S1603-F	CCCTAACTCCACTTGAAAGC
	D3S1603-R	TCAGCGAACAGCAACAAAT
D3S1768	D3S1768SF	GGTTGCTGCCAAAGATTAGA
	D3S1768A	CACTGTGATTTGCTGTTGGA
D3S2338	D3S2338-F	GAAGCCAGCAGTTTCTC
	D3S2338-R	CTGTATTGTTTTCCAGGATAAG
D3S3630	D3S3630-F	AAGGGATAAGCTGCAAATCA
	D3S3630-R	ACCAAATACAATTCATGAGACCTGA

Table 4. Clinicopathological distribution of the 75 malignant clear cell renal tumours

Group	Sex (M, F)	Age* (mean ± SD)	Tumour size (cm) (mean ± SD)
Low-grade CC-RCC	12, 3	59.5 ± 9.6	3.6 ± 1.4
Grade III-CC-RCC	12, 3	62.7 ± 12.5	6.3 ± 2.9
MCRN-LMP	11, 4	55.3 ± 11.2	3.4 ± 1.3
CC-RCC with cystic changes	10, 5	57.4 ± 10	5.3 ± 2.6
Clear cell papillary-like RCC	12, 3	55.7 ± 12.6	5.3 ± 3.3
Total	75 (57, 18)		

CC-RCC, clear cell renal cell carcinoma; MCRN-LMP, multilocular cystic renal neoplasm of low malignant potential; M, male; F, female; SD, standard deviation.
*Years.

MOLECULAR GENETICS

Examination of *VHL* status was used to support the diagnosis of CC-RCC in cases with atypical morphology, i.e. CCP-RCC-like CC-RCC. All 15 cases from this group showed abnormalities in *VHL* gene (mutation, methylation or loss of 3p heterozygosity).

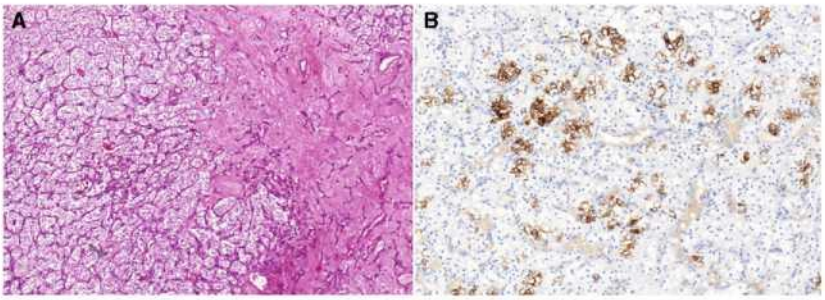

Figure 1. A, Group 1: low-grade clear cell renal cell carcinoma (haematoxylin and eosin). B, Immunohistochemical reaction showing strong focal positivity for cytokeratin (CK) 7.

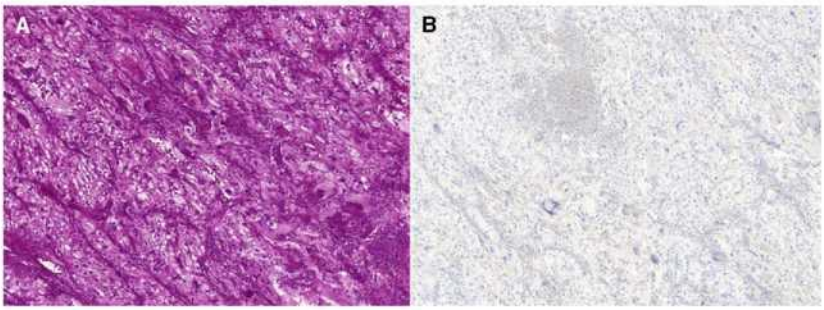

Figure 2. A, Group 2: high-grade clear cell renal cell carcinoma with giant multinucleated cells (haematoxylin and eosin). B, High-grade clear cell renal cell carcinomas were negative in 14 of 15 cases for cytokeratin (CK) 7.

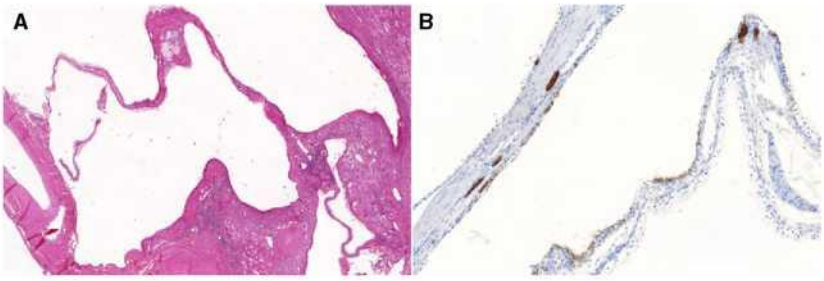

Figure 3. A, Group 3: multilocular cystic renal neoplasm of low malignant potential (haematoxylin and eosin). B, Cytokeratin (CK) 7 was diffusely positive in 10 of 15 cases, while in five of 15 cases positivity was focal.

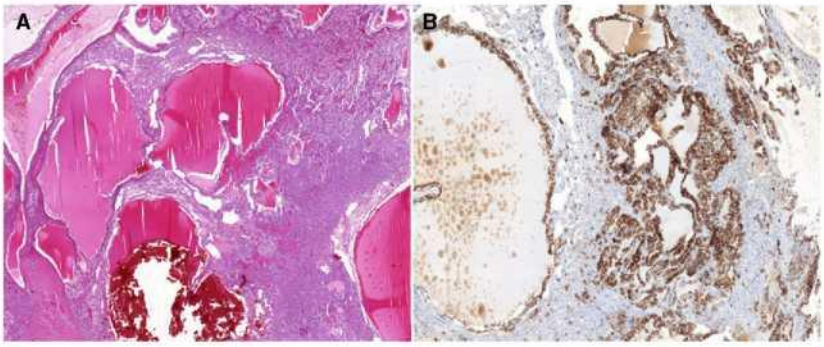

Figure 4. A, Group 4: clear cell renal cell carcinoma with cystic changes (haematoxylin and eosin). B, Clear cell renal cell carcinoma with cystic changes was diffusely strongly positive for cytokeratin (CK) 7 in one case, and three cases (of 15) were positive focally.

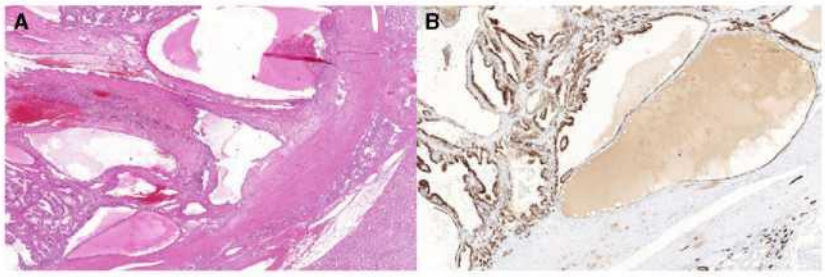

Figure 5. A, Group 5: low-grade clear cell renal cell carcinoma mimicking clear cell papillary renal cell carcinoma (haematoxylin and eosin). B, Low-grade clear cell renal cell carcinoma mimicking clear cell papillary renal cell carcinoma was diffusely positive for cytokeratin (CK) 7 in 11 of 15 cases, focally positive in one case, and three cases were negative for CK7.

Table 5. Reactivity of low-grade CC-RCC with two clones for cytokeratin 7

Case	Age*, sex	Size (cm)	CK7 (OV-TL12/30)	CK7 (SP52)
1	66, M	3.9	Focal ++	Focal +++
2	63, M	4.8	Focal +	Focal ++
3	55, M	4.5	–	–
4	63, F	3.0	Focal +++	Focal ++++
5	60, F	3.5	Focal ++	Focal ++
6	67, M	3.5	Focal +	Focal +++
7	44, M	2.5	Focal ++++	Focal ++++
8	71, F	4.0	–	–
9	63, M	4.2	Focal +	Focal +++
10	45, M	3.0	Focal ++	Focal +++
11	46, M	1.3	Focal +	Focal ++
12	76, M	3.5	Focal ++++	Focal ++++
13	66, M	3.5	Focal ++	Focal +++
14	56, M	1.7	Focal ++	Focal +++
15	52, M	7.5	–	–

Focal, 1–50% of tumour positive; diffuse, 51–100% of tumour positive. CK, cytokeratin; RCC, renal cell carcinoma; M, male; F, female; +, positive; –, negative.
*Years.

Table 6. Reactivity of high-grade CC-RCC with two clones for cytokeratin 7

Case	Age*, sex	Size (cm)	CK7 (OV-TL12/30)	CK7 (SP52)
16	71, M	11.5	–	–
17	61, M	8.0	–	–
18	41, M	5.5	–	–
19	62, M	6.8	–	–
20	78, F	4.5	–	–
21	61, M	7.0	–	–
22	65, M	3.7	–	–
23	67, M	6.5	–	–
24	61, F	5.5	–	–
25	64, M	11.5	–	–
26	31, F	8.0	–	–
27	66, M	5.2	–	–
28	78, M	2.0	–	–
29	74, M	8.0	–	–
30	60, M	1.5	Focal ++	Focal +++

Focal, 1–50% of tumour positive. CK, cytokeratin; RCC, renal cell carcinoma; M, male; F, female; +, positive; –, negative.
*Years.

Discussion

CC-RCC is a morphologically heterogeneous group of renal carcinomas with clear or eosinophilic cytoplasm that originates from the proximal convoluted tubule epithelium. The majority of cases are characterised by neoplastic cells with clear cytoplasm in nested, cystic or acinar growth patterns, interspersed with the intricate arborising vasculature. According to the literature, up to 70% of CC-RCCs bear abnormalities in the *VHL* gene (mutations, hypermethylation or LOH3p).[1]

CC-RCC tends to express low molecular weight cytokeratins. As the first paper describing CK7 expression in P-RCC and CC-RCC,[3] there has been a great deal of inconsistency in the extent and the intensity of CK7 immunoreactivity reported in CC-RCCs.

Table 7. Reactivity of multicystic renal neoplasm of low malignant potential with two clones for cytokeratin 7

Case	Age*, sex	Size (cm)	CK7 (OV-TL12/30)	CK7 (SP52)
31	60, M	1.2	Diffuse ++	Diffuse +++
32	50, F	2.5	Focal ++	Focal +
33	52, M	2.8	Diffuse +++	Diffuse ++++
34	73, M	3.4	Diffuse +++	Diffuse ++++
35	60, F	3.7	Diffuse +++	Diffuse ++++
36	59, M	4.8	Diffuse ++	Diffuse ++++
37	63, M	3.0	–	–
38	67, M	2.5	Diffuse +++	Diffuse ++++
39	33, M	5.0	Focal +	Focal +
40	36, M	3.0	Diffuse ++	Diffuse +++
41	32, F	3.9	Diffuse ++	Diffuse +++
42	75, M	2.5	Diffuse ++	Diffuse +++
43	46, M	5.0	Diffuse ++	Diffuse +++
44	43, M	5.8	–	–
45	80, F	2.4	Focal +	Focal +

Focal, 1–50% of tumour positive; diffuse, 51–100% of tumour positive. CK, cytokeratin; M, male; F, female; +, positive; –, negative.
*Years.

Table 8. Reactivity of CC-RCC with cystic changes with two clones for cytokeratin 7

Case	Age*, sex	Size (cm)	CK7 (OV-TL12/30)	CK7 (SP52)
46	45, M	5.8	–	–
47	57, M	1.0	–	–
48	46, M	2.6	–	–
49	62, F	4.8	–	–
50	62, F	6.0	–	–
51	73, M	4.0	–	–
52	70, M	7.5	–	–
53	56, F	3.4	Focal ++	Focal +++
54	56, F	6.1	–	–
55	56, M	8.5	–	–
56	36, F	1.8	Focal ++	Focal +++
57	57, M	4.7	–	–
58	78, M	9.5	Focal ++	Focal ++
59	52, M	9.5	–	–
60	55, M	5.1	Diffuse +++	Diffuse +++

Focal, 1–50% of tumour positive; diffuse, 51–100% of tumour positive. CK, cytokeratin; RCC, renal cell carcinoma; M, male; F, female; +, positive; –, negative.
*Years.

CC-RCCs are mostly considered to be CK7 negative tumours.[1] This is despite the fact that different studies reported a wide range of CK7 positivity (0–38%) in CC-RCCs.[3,5,11] Gatalica *et al.* and Liu *et al.* found positive CK7 staining in 24% and 11% ($n = 45$) cases of CC-RCCs in their studies, respectively. Conversely, Pradhan *et al.* reported CK7 negativity in CC-RCC in their study of 278 cases.[3,4,6–8] Similarly, most textbooks described CK7 reactivity in CC-RCC as negative in the majority of cases.[9–11] Williamson *et al.*[12] found CK7 positivity in 38% of CC-RCCs, using CC-RCC as a control group to compare with cases of MCRN-LMP (92%).

CCP-RCC is recognised as a distinct entity in the latest WHO classification of genitourinary tumours.[1] It is a renal epithelial neoplasm composed of low-grade clear epithelial cells arranged in tubules and papillae with predominantly linear nuclear alignment away from the basement membrane. Diffuse and strong CK7 positivity and carbonic anhydrase IX positivity in a cup-like distribution are characteristic.[1] The *VHL* gene in these tumours is usually referred to as normal, according to most studies.[1,16]

MCRN-LMP, previously known as multicystic CC-RCC, are low-grade tumours (WHO/ISUP grade I or II), composed entirely of cysts lined by a single layer of neoplastic cells with abundant clear cytoplasm. CK7 staining in these tumours has been reported as high as 92% (63% diffuse).[12]

In this study, we found CK7 immunoreactivity in 60–66% of LG CC-RCCs. Further, when examining different blocks or using two different clones, no statistically significant differences in CK7 positivity rates were found. Our CK7 positivity rate is certainly higher than those reported in other studies.[4,7,12] We would take a note of caution in this regard, given that most previous studies did not correlate the tumour grade with CK7 immunoreactivity. In contrast to the LGCC-RCC group, CK7 was only positive in 6% of HGCC-RCCs. Additionally, we found a significant statistical difference in CK7 positivity rate between the two cohorts (LGCC-RCCs versus HGCC-RCCs, $P = 0.0052$). It appears that CK7 immunoreactivity is well correlated with the tumour grade in CC-RCCs, with LGCC-RCC demonstrating more CK7

Table 9. Reactivity of clear cell papillary-like RCC with two clones for cytokeratin 7

Case	Age*, sex	Size (cm)	CK7 (OV-TL12/30)	CK7 (SP52)
61	60, M	9.0	Diffuse +++	Diffuse ++++
62	73, M	2.6	Diffuse ++	Diffuse +++
63	29, M	2.5	Diffuse +++	Diffuse ++++
64	68, M	5.0	Diffuse +++	Diffuse ++++
65	51, M	6.0	Diffuse +	Diffuse ++
66	61, M	7.0	Diffuse ++	Diffuse +++
67	66, M	7.0	Diffuse ++	Diffuse ++++
68	66, M	5.3	Diffuse +++	Diffuse +++
69	50, M	2.2	Diffuse +++	Diffuse ++++
70	39, M	5.3	Focal +++	Focal ++++
71	71, M	2.5	–	–
72	48, F	12	–	–
73	48, F	9.5	–	–
74	46, M	2.0	Diffuse +++	Diffuse +++
75	60, F	1.5	Diffuse +++	Diffuse ++++

Focal, 1–50% of tumour positive; diffuse, 51–100% of tumour positive. CK, cytokeratin; RCC, renal cell carcinoma; M, male; F, female; +, positive; –, negative.
*Years.

staining than the higher grade tumours. Such findings can have significant diagnostic implications, particularly in limited samples (i.e. core biopsies), as CC-RCCs are historically considered to be either CK7-negative or focally positive. For instance, based on these findings, one may be able to almost rule out the possibility of a HGCC-RCC in a core biopsy showing strong and diffuse CK7 positivity. It is important to emphasise that although CK7 immunoreactivity was strong in intensity in all LGCC-RCCs it was always variably focal, with no cases showing diffuse strong CK7 positivity.

CK7 was positive in 86–93% of MCRN-LMPs, which is similar to other studies. Williamson *et al.*[12] reported CK7 staining in MCRN-LMPs as high as 92% (63% diffuse). These neoplasms are low grade and also considered to have low malignant potential, and as such a high CK7 positivity rate seems to be related to the tumour grade.

In this study, we included a cohort of tumours which had histological features resembling CCP-RCC (i.e. clear cells, cystic/tubulopapillary patterns, apically located nuclei and fibromuscular stroma), yet did not fully meet the diagnostic criteria of CCP-RCC. In routine practice these tumours can be quite challenging. In most cases, proper and possibly extensive sampling will help to arrive at the accurate diagnosis, but in some other instances both immunohistochemistry (particularly CK7) and *VHL* gene testing would be necessary.[17,18] For this reason, we performed *VHL* gene analysis on all CCP-RCC-like tumours in order to confirm the diagnosis of CC-RCC.

We found 80% of CCP-RCC-like CC-RCCs to be CK7-positive. From a differential diagnostic point of view, CK7 is an important marker and its interpretation should be made with caution in such tumours. In general, diffusely CK7-positive tumours composed of clear cells should be approached carefully. Although a diffuse CK7 positivity in clear cell renal tumours points towards CCP-RCCs, such a staining pattern does not completely rule out the possibility that the tumour may belong to CC-RCC group. In scenarios where CK7 is positive but the morphology is not typical (regardless results of GATA 3 or CANH 9 immunohistochemical examinations), molecular genetic techniques would be helpful (i.e. *VHL* gene abnormalities).[16–18] However, CCP-RCC may be found in patients with VHL syndrome and, in such cases, there are germline mutations of *VHL* gene.[19] Further, focal albeit strong CK7 positivity does not rule out the diagnosis of CC-RCC. For instance, in this study, 12 of 15 cases showed strong CK7 positivity with at least one clone. It should be noted that the extent of CK7 positivity can potentially be misleading, particularly in limited samples such as core biopsies.

P-RCCs are a highly heterogeneous group of RCCs, traditionally divided into types 1 and 2. However, an increasing number of recent studies showed that P-RCC is more diverse than previously thought.[13–15] It seems that these tumours are composed of different subtypes of RCC sharing similar architectural growth pattern, but demonstrating variable immunoprofile and molecular genetic features. P-RCCs are characterised mainly by malignant epithelial cells forming variable proportions of papillae and tubules. Diffuse CK7 positivity has been reported for P-RCC in varying proportions, depending on the subtype.[1,3] In some, but not entirely rare, cases, P-RCC is composed of neoplastic cells with pale/clear cytoplasm, which are positive for CK7. The results of our study also showed that up to 80% of CCP-RCC-like CC-RCCs were CK7-positive. This is a crucial point that needs to be considered in the differential diagnosis between these two RCC types.

Other tumours which can display clear cell morphology are Mitf RCCs. Xp11.2 are composed mainly of clear cell or pale eosinophilic elements; however, architecture is usually papillary or tubulopapillary. There have been several cases of Xp11.2 described in the literature with more diverse morphology. In such cases, immunohistochemical reaction with TFE3, cathepsin K or fluorescence *in-situ* hybridisation (FISH) analysis can solve the differential diagnostic problem.[20,21]

Translocation t(6;11) RCCs are typically composed of large eosinophilic cells with formation of pseudorosettes. These tumours are immunoreactive for HMB45, Melan A and TFEB, and the diagnosis can be further confirmed by molecular genetic analysis of *TFEB* (break or protein expression).[22,23]

One of the limitations of this study was the relatively small sample size employed in each cohort. However, the study's strengths would include (i) the use of multiple tumour blocks to address possible tumour heterogeneity bias, (ii) the use of two different clones of CK7 antibody for precision and accuracy purposes, (iii) comparing different cohorts from a wide spectrum of clear cell renal neoplasms, (iv) having consistent and uniform tumours in each cohort and (v) testing and confirming *VHL* gene abnormalities in CCP-RCC-like CC-RCCs to avoid misdiagnosis.

Conclusions

Our findings show that CK7 immunoreactivity in CC-RCCs can be of variable pattern and the extent of staining depends on the grade and architecture of the tumours. LGCC-RCCs demonstrate a higher rate of CK7 positivity that is mainly focal and strong, while HGCC-RCCs are essentially negative for CK7. A majority of CCP-RCC-like CC-RCCs show some extent of CK7 reactivity. Our findings shed light on differential diagnostic work up of clear cell tumours, which should be particularly kept in mind in the interpretation of limited samples (i.e. core biopsy).

Acknowledgements

This study was supported by the Charles University Research Fund (project number Q39) and by the project FN 00669806 (Ondrej Hes). Informed, written consent was not required according to the local ethics committee. Studies were performed according to the Declaration of Helsinki. The procedures were approved by a local ethics committee (EK, LF and FN Plzen, Charles University, 02.03.2015).

Conflicts of interest

All authors declare no conflicts of interest.

References

1. Moch H, Humphrey PA, Ulbright TM, Reuter V. *WHO classification of tumours of the urinary system and male genital organs*. Lyon, France: International Agency for Research on Cancer, 2016.
2. Tan PH, Cheng L, Rioux-Leclercq N *et al.* Renal tumors: diagnostic and prognostic markers. *Am. J. Surg. Pathol.* 2011; **37**: 1518–1531.
3. Gatalica Z, Kovatich A, Miettinen M. Consistent expression of cytokeratin 7 in papillary renal-cell carcinoma. *J. Urol. Pathol.* 1997; **6**: 195–203.
4. Liu L, Qian J, Bostwick DG *et al.* Immunohistochemical analysis of chromophobe renal cell carcinoma, renal oncocytoma, and clear cell carcinoma: an optimal and practical panel for differential diagnosis. *Arch. Pathol. Lab. Med.* 2007; **131**: 1290–1297.
5. Srigley JR, Brimo F, Li G *et al.* Cystic clear cell papillary renal cell carcinoma: is it related to multilocular clear cell cystic neoplasm of low malignant potential? *Histopathology* 2016; **68**: 666–672.
6. Pradhan D, Kakkar N, Joshi K *et al.* Sub-typing of renal cell tumours: contribution of ancillary techniques. *Diagn. Pathol.* 2009; **4**: 21.
7. Skinnider BF, Folpe AL, Hennigar RA *et al.* Distribution of cytokeratins and vimentin in adult renal neoplasms and normal renal tissue: potential utility of a cytokeratin antibody panel in the differential diagnosis of renal tumors. *Am. J. Surg. Pathol.* 2005; **29**: 747–754.
8. Langner C, Wegscheider BJ, Zigeuner R *et al.* Keratin immunohistochemistry in renal cell carcinoma subtypes and renal oncocytomas: a systematic analysis of 233 tumors. *Virchows Arch.* 2004; **444**: 127–134.
9. Bostwick D, Cheng L. *Urologic surgical pathology*. 2nd ed. Maryland Heights, MI: Mosby Elsevier, 2008.
10. Amin MB, Grignon DJ, Srigley JR, Eble JN. *Urological pathology*. 1st ed. Alphen aan den Rijn, the Netherlands: Walters Kluwer, 2014.
11. Amin MB, McKenney JK, Tickoo S *et al. Diagnostic pathology: genitourinary*. 2nd ed. Salt Lake City, UT: AMIRSYS, 2010.
12. Williamson SR, Halat S, Eble JN *et al.* Multilocular cystic renal cell carcinoma: similarities and differences in immunoprofile compared with clear cell renal cell carcinoma. *Am. J. Surg. Pathol.* 2012; **36**: 1425–1433.
13. Linehan WM, Spellman PT, Ricketts CJ *et al.* Comprehensive molecular characterization of papillary renal-cell carcinoma. *N. Engl. J. Med.* 2016; **374**: 135–145.
14. Saleeb RM, Brimo F, Farag M *et al.* Toward biological subtyping of papillary renal cell carcinoma with clinical implications through histologic, immunohistochemical, and molecular analysis. *Am. J. Surg. Pathol.* 2017; **41**: 1618–1629.
15. Troxell ML, Higgins JP. Renal cell carcinoma in kidney allografts: histologic types, including biphasic papillary carcinoma. *Hum. Pathol.* 2016; **57**: 28–36.
16. Hes O, Compérat EM, Rioux-Leclercq N. Clear cell papillary renal cell carcinoma, renal angiomyoadenomatous tumor, and renal cell carcinoma with leiomyomatous stroma relationship of 3 types of renal tumors: a review. *Ann. Diagn. Pathol.* 2016; **21**: 59–64.

17. Williamson SR, Gupta NS, Eble JN *et al.* Clear cell renal cell carcinoma with borderline features of clear cell papillary renal cell carcinoma: combined morphologic, immunohistochemical, and cytogenetic analysis. *Am. J. Surg. Pathol.* 2015; **39**: 1502–1510.
18. Petersson F, Grossmann P, Hora M *et al.* Renal cell carcinoma with areas mimicking renal angiomyoadenomatous tumor/clear cell papillary renal cell carcinoma. *Hum. Pathol.* 2013; **44**: 1412–1420.
19. Williamson SR, Cheng L. Do clear cell papillary renal cell carcinomas occur in patients with von Hippel-Lindau disease? *Hum. Pathol.* 2015; **46**: 340–341.
20. Skala SL, Xiao H, Mehra R. Detection of 6 TFEB-amplified renal cell carcinomas and 25 renal cell carcinomas with MITF translocations: systematic morphologic analysis of 85 cases evaluated by clinical TFE3 and TFEB FISH assays. *Mod. Pathol.* 2018; **31**: 179–197.
21. Argani P, Zhong M, Antonescu CR *et al.* TFE3-fusion variant analysis defines specific clinicopathologic associations among Xp11 translocation cancers. *Am. J. Surg. Pathol.* 2016; **40**: 723–737.
22. Peckova K, Vanecek T, Hes O *et al.* Aggressive and nonaggressive translocation t(6;11) renal cell carcinoma: comparative study of 6 cases and review of the literature. *Ann. Diagn. Pathol.* 2014; **18**: 351–357.
23. Argani P, Reuter VE, Antonescu CR *et al.* TFEB-amplified renal cell carcinomas: an aggressive molecular subset demonstrating variable melanocytic marker expression and morphologic heterogeneity. *Am. J. Surg. Pathol.* 2016; **40**: 1484–1495.

Supporting Information

Additional Supporting Information may be found in the online version of this article:

Table S1. Reactivity of CCRCC with cystic changes with CANH 9 and GATA 3.

1.5.4 Clear cell renal cell carcinoma with Paneth-like cells: Clinicopathologic, morphologic, immunohistochemical, ultrastructural, and molecular analysis of 13 cases

Výskyt Panethovým buňkám podobných buněk (Paneth-like cells/PLC) byl dříve referován v různých orgánech (např. hepatobiliárním, genitourinárním a ženském genitálním traktu). V genitourinárním traktu byly PLC popsány v epididymis, močovém měchýři a prostatě. Cílem této práce bylo vyhodnotit výskyt PLC v CCRCC.

Z celkem 1378 CCRCC v našem nádorovém registru bylo vybráno 13 případů CCRCC s prominentními PLC (CCRCCPLC). Tumory byly studovány morfologicky, imunohistochemicky, ultrastrukturálně a za použití molekulárně-genetických metod. CCRCCPLC byly nejčastěji low-grade (12/13 CCRCCPLC). Imunohistochemický profil léze byl kompatibilní s klasickým CCRCC. Panethovým buňkám podobné buňky zaujímaly od 10 do 70% objemu nádorové masy (průměr 17,7%, medián 10%) a PLC neexprimovaly neuroendokrinní markery (chromogranin A, synaptofysin, CD56, INSM-1). Ultrastrukturálně PLC obsahovaly množství různě velikých vezikul ohraničených membránou a jejich ultrastrukturální morfologie tak byla kompatibilní se sekrečním typem buněk. Mutace *VHL* genu byla zastižena v 9/9 analyzovatelných případů, LOH3p byla detekována v 6/8 případů.

Panethovým buňkám podobné buňky mohou být variabilně přítomny v „klasických" CCRCC a to dokonce i v relativně velkém množství. Ultrastrukturálně, PLC mají atributy buněk sekrečních. Limitované dostupné poznatky o klinickém chovaní CCRCC obsahujících PLC neprokázaly u těchto tumorů asociaci s agresivním klinickým průběhem.

Annals of Diagnostic Pathology 41 (2019) 96–101

Contents lists available at ScienceDirect

Annals of Diagnostic Pathology

journal homepage: www.elsevier.com/locate/anndiagpath

Original Contribution

Clear cell renal cell carcinoma with Paneth-like cells: Clinicopathologic, morphologic, immunohistochemical, ultrastructural, and molecular analysis of 13 cases☆

Fumiyoshi Kojima[a], Stela Bulimbasic[b], Reza Alaghehbandan[c], Petr Martinek[d], Tomas Vanecek[d], Kvetoslava Michalova[d], Kristyna Pivovarcikova[d], Michal Michal[d], Milan Hora[e], Shin-ichi Murata[a], Emiko Sugawara[f], Joanna Rogala[d], Rinë Limani[g], Ondrej Hes[d,*]

[a] Department of Human Pathology, Wakayama Medical University, Wakayama, Japan
[b] Clinical Department of Pathology and Cytology, University Hospital Centre Zagreb, Croatia
[c] Department of Pathology, Faculty of Medicine, University of British Columbia, Royal Columbian Hospital, Vancouver, BC, Canada
[d] Department of Pathology, Charles University in Prague, Faculty of Medicine in Plzeň, Pilsen, Czech Republic
[e] Department of Urology, Charles University in Prague, Faculty of Medicine in Plzeň, Pilsen, Czech Republic
[f] Department of Pathology, Musashino Red Cross Hospital, Tokyo, Japan
[g] Institute of Pathology, Hospital and University Clinic Services of Kosovo, Prishtina, Kosovo

ARTICLE INFO

Keywords:
Kidney
Clear cell renal cell carcinoma
Paneth-like cells
Immunohistochemistry
Next generation sequencing

ABSTRACT

Clear cell renal cell carcinoma (CRCC) is well known for its intratumoral heterogeneity. Paneth-like cells (PLC) have been reported in variable organs (i.e., hepatobiliary, genitourinary, and female genital tract). In genitourinary system, it is possible to find PLCs in epididymis, urinary bladder and prostate. The objective of this study was to assess PLC in CRCCs 13 CRCCs with prominent PLC (CRCCPLC) were selected out of 1378 CRCCs in our registry. The tumors were analyzed using morphologic, immunohistochemical, ultrastructural, and molecular genetic methods.

CRCCPLCs were mostly of low histologic grade (12/13). Immunohistochemical profile was compatible with classic CRCC. PLC constituted 10 to–70% of the tumor volume (mean 17.7%, median 10%). PLCs did not express neuroendocrine markers (chromogranin, synaptophysin, CD56, INSM-1). Ultrastructurally, PLCs were filled by membrane bounded vesicles of various sizes and were compatible with secretory type of cells. *VHL* mutation was found in 9/9 cases, and LOH3p was found in 6/8 analyzable cases.

Conclusions: PLC morphology can variably be present in "classic" CRCC, even in a substantial proportion. Ultrastructurally, PLCs have all attributes of secretory cells. Preliminary follow up data showed that these tumors may not be associated with aggressive clinical behavior.

1. Introduction

Intratumor heterogeneity (ITH) is a well-established phenomenon in carcinogenesis extensively studied in many neoplasms including the genitourinary system. While intertumor heterogeneity is a well-known event in renal cell carcinomas (RCCs), ITH has been overlooked by urological pathologists for years. ITH of RCC was already demonstrated back in 1988 [1]. In routine practice, ITH in renal tumors can cause diagnostic discrepancies between core biopsy and resection specimens which could have prognostic/therapeutic implications, i.e. possible failure of targeted therapy [2]. In situation, when the tumor is insufficiently sampled, ITH may also be responsible for unpredictable aggressive clinical behavior that some RCCs display [2].

Paneth cells are located in normal mucosa of the duodenum and small intestine where they serve as a part of antimicrobial barrier of the gastrointestinal tract [3]. They can also be encountered in large bowel affected by chronic inflammatory processes [4]. Paneth-like cells (PLC), which are different from genuine Paneth cells, are cells with

☆ This study was supported by the Charles University Research Fund (project number Q39) and by the grant of Ministry of Health of the Czech republic-Conceptual Development of Research Organization (Faculty Hospital in Plzen- FNPl 00669806).

* Corresponding author at: Department of Pathology, Charles University, Medical Faculty and Charles University Hospital Plzen, Alej Svobody 80, 304 60 Pilsen, Czech Republic.
E-mail address: hes@medima.cz (O. Hes).

https://doi.org/10.1016/j.anndiagpath.2019.05.012

voluminous cytoplasm packed with eosinophilic granules [5]. PLCs have been reported in different organs including hepatobiliary tract, genitourinary system, and female genital tract [6-13]. Within the genitourinary system, PLCs occasionally occur in normal epididymis [8,9] or as a component of urinary bladder and prostate tumors [13,14]. With respect to renal tumors, presence of PLC is rarely mentioned in the literature [10]. In our experience, clear cell renal cell carcinoma (CRCC) can demonstrate scattered, easily overlooked PLCs. We assembled a cohort of 13 cases, where PLCs were prominent and conspicuous. The aim of this study was to characterize CRCC with prominent PLCs (CRCCPLC) using morphologic, immunohistochemical, ultrastructural, and molecular genetic methods.

2. Materials and methods

2.1. Study design

Of approximately 26,000 renal tumors and tumor-like renal lesions in the Plzen Tumor Registry, 1378 cases of CRCC were retrieved. Thirteen CRCCPLCs were subsequently selected for study.

2.2. Histological analyses

The tissues were fixed in neutral formalin, embedded in paraffin, cut into 2–4 μm thin sections and stained with Hematoxylin and Eosin (H& E). One to nine paraffin blocks were available for each case. All tumors were independently reviewed by two pathologists (FK and OH). Clinicopathologic and follow-up data were collected using medical records available from each participating institution.

2.3. Immunohistochemical analyses

The immunohistochemical study was performed using a Ventana Benchmark XT automated immunostainer (Ventana Medical System, Inc., Tucson, AZ, USA) on formalin fixed, paraffin embedded (FFPE) tissue. The following primary antibodies were employed: CK7 (OV-TL12/30, monoclonal, DakoCytomation, Glostrup, Denmark, 1:200), alpha-methylacyl-CoA-racemase (AMACR) (P504S, monoclonal, Zeta, Sierra Madre, CA, 1:50), vimentin (D9, monoclonal, NeoMarkers, Westinghouse, CA, 1:1000), Melan A (A103, monoclonal, Ventana, RTU), antimitochondrial antibody (MIA) (113–1, monoclonal, Biogenex, San Ramon, CA, 1:500), carbonic anhydrase IX (CAIX) (rhCA9, monoclonal, RD systems, Abingdon, GB, 1:100), CD10 (monoclonal 56C6, Leica, Newcastle, UK, 1:20), CD56 (1B6, monoclonal, Leica Biosystems, Newcastle, UK, 1:100), synaptophysin (polyclonal, LabVision, Fremont, CA, 1:350), chromogranin A (monoclonal, DAK-A3, DakoCytomation, 1:600), ISMN-1 (monoclonal, A-8, Santa Cruz, US, 1:1000). The primary antibodies were visualized using a supersensitive streptavidin-biotin-peroxidase complex (BioGenex). Internal biotin was blocked by standard protocol used by Ventana Benchmark XT automated stainer (hydrogene peroxide based). Appropriate positive and negative controls were employed. We regarded the result as positive findings if the intensity was more than mild, and evaluated the proportional score as follows: 0 negative, focal $< 50\%$; diffuse $\geq 50\%$.

2.4. Ultrastructural analyses

Electron microscopy evaluation was performed on five cases. Small pieces of paraffin-embedded tumor tissue with Paneth-like changes from 5 cases (No 3, 6, 8, 12, and 13) were de-paraffinized and further routinely processed for ultrastructural analysis. Semi-thin sections of epoxy embedded tissue were stained with toluidine blue and examined by light microscopy. Ultrathin sections from representative area were cut, stained with uranyl acetate and lead citrate, and examined with a JEOL (Tokyo, Japan) JEM 1400 Transmission Electronic Microscope using Olympus iTEM universal TEM imaging platform.

2.5. Molecular analyses

2.5.1. Mutational analyses

Sanger sequencing and methylation of *VHL* gene, and analysis of loss of heterozygosity (LOH) of locus 3p were performed using previously described methods [15].

2.5.2. Targeted next-generation sequencing

A panel of 271 cancer related genes (Comprehensive cancer panel, Qiagen, Hilden, Germany) were used to analyze tumor tissue samples. The samples were isolated using macro dissection from FFPE blocks. DNA was isolated using Qiagen DNA mini kit, and 250 ng of DNA was used to construct the library. Library was sequenced on Illumina's Nextseq 500, aiming at average coverage 350 x after deduplication of molecular barcodes to detect 10% allele frequency with 95% sensitivity. Variants were called using Qiagen's proprietary pipeline. Subsequently the variants were filtered using the calculated limit of detection for each sample. Furthermore the variants were annotated using The Genome Aggregation Database (GnomAD) [16] for population statistics and ClinVar database [17] or the relationships among variations and phenotypes. Variants more frequent than 1% in the GnomAD database were excluded as well as known benign variants according to the ClinVar database. The remaining subset was checked visually and suspected artefactual variants were excluded.

3. Results

3.1. Clinicopathological findings

Basic clinicopathologic data are summarized in Table 1. The patients were 10 males and 2 females, with age ranged from 25 to 74 years (median 61, mean 55.1). Detailed clinicopathologic data for one patient were not available. The tumor size ranged from 1.2 to 8.5 cm (mean 3.6). Eight patients were pT1a, 3 were pT1b, and 1 was pT2a according to TNM staging (8th edition of AJCC). Grossly, the tumors were mostly solid, yellow to tan, with occasionally foci of regressive changes or hemorrhage. Follow up data were available for 10 patients, ranged from 0.5 to 11 years. No metastatic disease or any clinical aggressive behavior was identified in any case. However, one patient with confirmed VHL syndrome had anamnesis of multiple CCRCCs (without PLC), and another patient underwent renal resection of contralateral CCRCC, 3 years prior to the current surgery (detailed information present in Table 1).

Microscopically, all CRCCPLCs were well-circumscribed, occasionally encircled by fibrous pseudocapsule. Tumors were arranged in mixed solid-alveolar, tubular, or cystic growth patterns. In two cases, prominent regressive changes were encountered. Tubular or cystic structures filled with eosinophilic proteinaceous fluid were prominent in 8 cases. Necrosis or lymphovascular invasion were not seen. All but one case showed low-grade histology (grade 1 or 2– according Fuhrman/ISUP grading system). PLCs were arranged in groups, formed conspicuous bright red areas (Fig. 1). Groups of PLC formed solid foci or lined tubular or pseudotubular structures (Fig. 2). Larger tubules had cystic appearance with prominent PLC lining (Fig. 3A and B). PLCs were large with cytoplasmic eosinophilic round granules (Fig. 4). Granules positively stained with diastase digestive Periodic-Schiff stain (d-PAS) with maximum intensity in the apical part of the cells.

Immunohistochemical findings are summarized in Table 2. Most CRCCPLCs were positive for vimentin, CAIX, CD10, AMACR, and MIA. Six of 13 CRCCPLCs showed focal positivity for CK7. All CRCCPLCs were negative for neuroendocrine (NE) markers, namely ISMN-1, chromogranin A, synaptophysin, and CD56.

Table 1
Clinicopathological findings of CRCCPLCs.

Case	Age	Sex	Tumor size[b] (cm)	Stage	Follow up (years)	PLCs (%)	Necrosis	LVI	ISUP	Growth pattern
1	61	m	3.0	1a	1AW	30	0	0	2	Tubular
2	71	m	8.5[b]	2a	LFU	20	0	0	3	Solid-tubular
3	65	f	4.5	1b	5AW	10	0	0	2	Solid alveolar
4	25	m	1.2	1a	2AW	10	0	0	2	Tubulocystic
5	NA	NA	NA	NA	NA	20	0	0	2	Solid-tubular
6	35	m	3.2	1a	11AW[c]	10	0	0	1	Tubulocystic
7	47	m	3	1a	5AW[d]	10	0	0	2	Solid alveolar
8	67	f	1.2	1a	4AW	10	0	0	2	Solid-tubular
9	62	m	6.5	1b	3AW	10	0	0	1	Solid alveolar with cyst
10	74	m	1.8	1a	LFU	10	0	0	1	Solid alveolar
11	49	m	5.5	1b	3AW	10	0	0	1	Tubular
12[a]	61	m	2.5	1a	3AW	10	0	0	2	Solid alveolar
13	44	m	2.5	1a	0.5 AW	70	0	0	2	Tubular

Abbreviation; NA, not available; m, male; f, female; AW, alive without disease; LE,; PLCs, Paneth-like cells; LVI, lymphovascular invasion; LFU, lost to follow up; ISUP, Fuhrman/ISUP grade.

[a] Von Hippel Lindau syndrome and multifocal tumor.

[b] Maximum diameter.

[c] Basalioma of chest and lipoma of the tight 8 years after nephrectomy.

[d] 3 years prior current surgery, contralateral resection of low grade clear cell renal cell carcinoma without Paneth-like cells.

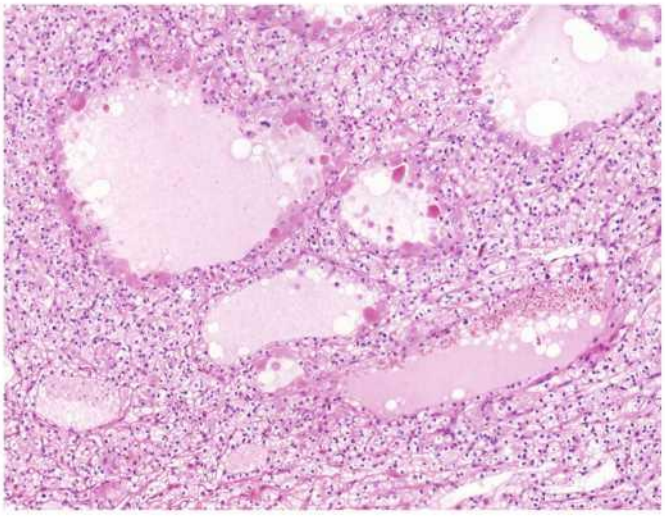

Fig. 1. PLCs were arranged in groups or tubules and formed conspicuous bright red areas. (For interpretation of the references to color in this figure legend, the reader is referred to the web version of this article.)

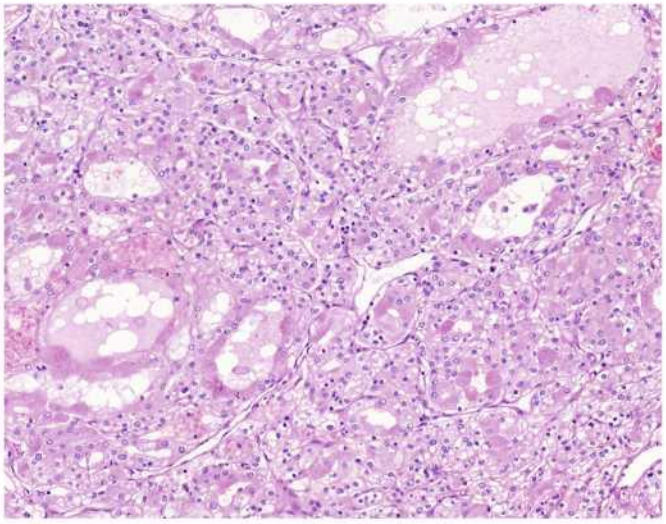

Fig. 2. Clear cell population is visible on the background with prominent PLCs growing in solid and tubular pattern.

3.2. Electron microscopical findings

Ultrastructural analysis revealed moderately preserved tumor tissue composed of large polygonal cells organized in solid nests and lining microcystic spaces. There were two types of cells with the first one type showing typical features of CRCC, i.e., abundant clear cytoplasm and irregular nuclei with occasional prominent nucleoli. Lipid droplets were dissolved during processing for light microscopy, leaving large pale spaces without other cytoplasmic structures. The second cell type, corresponding to PLCs seen on light microscopy, showed moderate amount of large cytoplasmic secretory granules, ranging from 1.45 to 2.85 μm in diameters (Fig. 5). Some of the granules were dispersed through cytoplasm, others located in upper, luminal part of the cell. Typical electron dense NE type granules, larger amount of glycogen particles or other specific structures were not found.

3.3. Molecular genetic findings

Eleven CRCCPLCs were selected for molecular genetic testing, of which nine samples were analyzable. The results of genetic analyses are shown in Table 3. The NGS sequencing of the mutation panel was successful in six cases; two cases did not meet the expected sequencing quality control and were reported as not analyzable. A total of 47 variants were found including variants in genes *ROS1* and *LRP1B* appearing more in two cases. The number of mutations per each case ranged from 1 to 16 (mean 7.83, median 6). In three cases with insufficient DNA quality for NGS, we performed Sanger sequencing of *VHL* gene, and further performed LOH analysis of chromosome locus 3p. Together we detected 9 *VHL* mutations and 6 LOH of locus 3p. No hypermethylation status of *VHL* promoter was detected in eight successfully analyzed cases. Two cases were not included in the molecular genetic studies due to insufficient amount of tissue material.

4. Discussion

CRCC is well-known for its high ITH. The spectrum of ITH is a broad, encompassing uniform CRCCs together with considerably morphologically and architecturally heterogenous cases [2,18]. It has been shown that ITH is an inherent process of tumorigenesis and it seems that it has become a major obstacle for the successful targeted therapy [19]. Hence, gross description and extensive sampling play a crucial role in the examination of CRCC. Multisite tumor sampling enhances

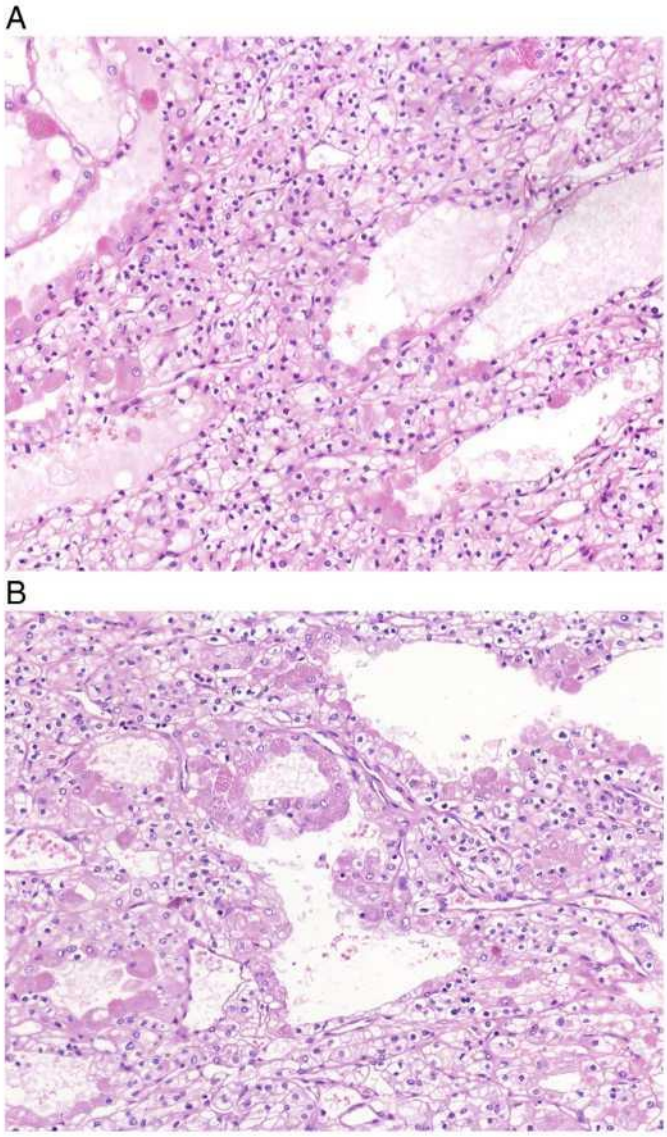

Fig. 3. PLCs formed cell lining of smaller cysts (A). Pseudostratification was noted in some cystic spaces (B).

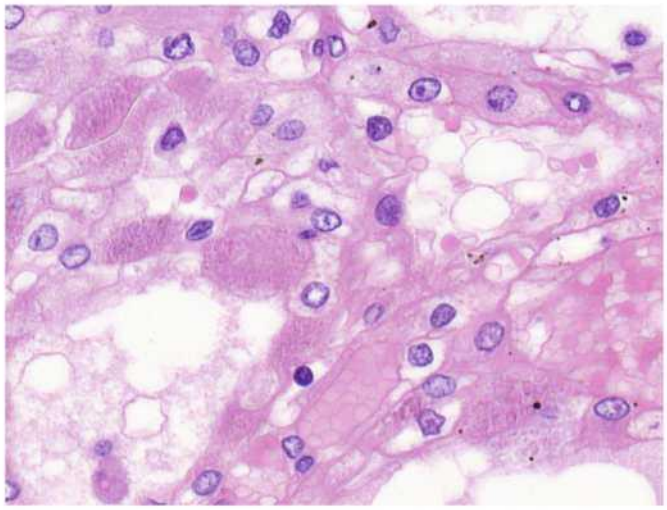

Fig. 4. PLCs were large cells with voluminous cytoplasm filled by intracytoplasmic eosinophilic round granules.

the detection of ITH at all different temporal stages of tumor evolution [20,21]. In this study we focused on CRCCs with unusual cytologic features represented by prominent voluminous neoplastic cells filled by fine eosinophilic droplets. Such cells remarkably resembled Paneth cells of the gastrointestinal tract. To the best of our knowledge, the presence of prominent and conspicuous PLC is to date undocumented phenomenon in CRCC. Genuine Paneth cells are considered as fully differentiated cell, located in the deep portion of a crypt in mucosa of gastrointestinal tract. Paneth cells contain defensin, lysozyme and phospholipase A2 within their cytoplasm [3]. Histochemically, the granules within Paneth cells are positive for PAS stain with or without diastase digestion as well as a1-antitrypsin [22]. Some reports documented that so-called intestinal type adenocarcinoma of urinary bladder, uterine cervix, ovary, and gallbladder may also contain Paneth cells [6,7,11,12]. Based on their almost identical appearance to intestinal adenocarcinoma, we supposed they are closely related to those in the small intestine.

The situation of Paneth cells in the prostate is different. It has been shown that cells resembling Paneth cells within prostatic adenocarcinoma contained NE granules [23]. Those cells were smaller and more uniform than PLCs documented in our series. Moreover, NE granules were mostly located in the sub-nuclear portion of the cell, similarly to genuine endocrine cells in the gastrointestinal tract. Interestingly, prostatic adenocarcinoma with Paneth cell-like NE differentiation has been reported to have a better prognosis than conventional acinar adenocarcinoma, equally graded as Gleason pattern 5 [24,25]. PLCs were morphologically and immunohistochemically distinct from NE cells and the tumors in our series did not show any apparent features of NE differentiation.

PLCs within CRCC were first reported by Krishnan and Truong in 2002 [10]. However, their study was focused on ultrastructure and no data about clinical, morphological, immunohistochemical, and molecular genetic features were provided. Most of our cases had tubular and cystic structure, and were morphologically compatible with classic CRCC. All but one case were low stage and low grade tumors. Based on our ultrastructural finding, it seems that granules within PLC were secretory granules. This finding is different from what Krishan and Truong concluded that granules in their cases were lysosomes. It is possible that Paneth-like granule is formed by variable constituents.

Besides PLC, another type of membrane bounding particles were described. So-called glassy hyaline globules occur in CRCC and some papillary RCCs. These globules are different in many aspects from granules found in PLCs [26]. Glassy hyaline globules are encountered mostly in tumors with high grade features (so-called "granular variant" of CRCC) and are located predominantly extracellularly. On the contrary, PLC in the current study were part of the low-grade tumors and were located exclusively in intracellular space. Another type of globules, so-called rhabdoid globules, was described within renal oncocytoma. Gatalica and Guarino documented such globules mainly in renal oncocytoma and in some RCCs (clear cell RCC, chromophobe RCC, or papillary RCC) [27,28]. Based on immunohistochemical and ultrastructural examinations, they suggested these globules were derived from basement membrane. The globules documented in renal oncocytoma were quite different from those of PLCs on the following points: location (extra vs intracytoplasmic), number (sparse vs frequent), size (large vs small in diameter), and shape (round vs lobulated).

Out of the kidneys, epididymis is another genitourinary organ where PLCs were described. In epididymis, the morphology of PLCs was similar to that documented by Krishnan and Truong in CRCC. Epididymal PLCs were filled with lysosomes [10]. Nistal et al. reported epididymal PLCs were positive for a1-antichymotrypsin and CD68, contrary to intestinal Paneth cells [9]. Shah et al. suggested a possible relationship between the presence of PLCs and epididymal obstruction [8]. Nistal et al. reported 9 cases of epididymis with prominent PLCs, co-occurring with testicular tumor without evidence of epididymal

Table 2
Immunohistochemical findings of CRCCPLCs.

Case	Vimentin	CA9	CD10	CK7	AMACR	ISMN1	Chromogranin a	Synaptophysin	CD56	MIA
1	f	f	d	f	d	0	0	0[a]	0[a]	d
2	f	d	d	0	d	0	0	0[a]	0[a]	d
3	f	d	d	0	f	0	0	0	0	d
4	d	d	d	f	d	0	0	0[a]	0[a]	d
5	d	0	d	d	d	0	0	0	0	d
6	d	d	f	d	d	0	0	0	0[a]	d
7	d	d	d	d	d	0	0	0	0	d
8	d	d	d	d	d	0	0	0[a]	0[a]	d
9	d	0	f	0	f	0	0	0	0	0
10	d	d	d	0	d	0	0	0	0	f
11	d	0	d	0	0	0	0	0[a]	0[a]	f
12	d	0	f	0	d	0	0	0	0	f
13	d	f	d	0	d	0	0	0	0	d

Abbreviation; f, focal; d, diffuse.
[a] Non-specific cytoplasmic granular staining.

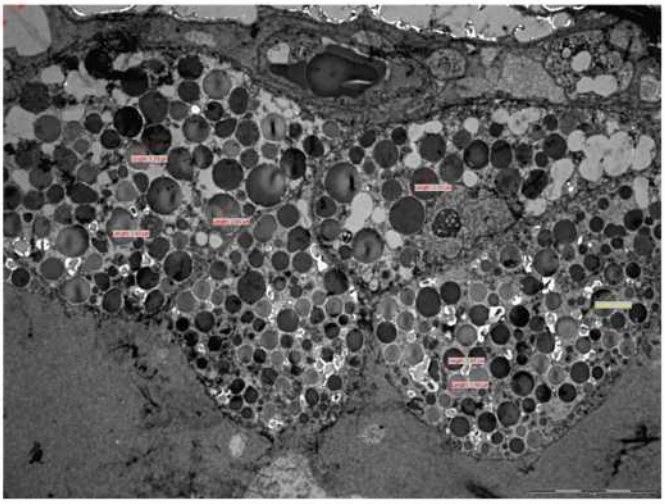

Fig. 5. PLCs showed moderate amount of large cytoplasmic secretory granules, ranging from 1.45 to 2.85 μm in diameters.

obstruction. They postulated that increase of endocytolytic activity for intraluminal fluid storage lead to formation of PLCs. CRCCPLCs in our series composed of dilated tubules or cystic structures containing eosinophilic fluid with PLCs distributed around such regions. These findings supported the theory of Nistal, et al. that excess fluid lead to formation of PLC.

As indicated earlier, all cases included in this study containing prominent areas of PLCs were low-grade. However, single PLC or small inconspicuous groups of PLCs can also be present in CRCCs with high grade morphologic features (grade 3 and 4). Such tumors characteristically show marked ITH and the distribution of PLCs is mainly in the low grade areas.

All 9 presented CRCCPLCs had *VHL* mutation and 6 had also LOH 3p, which are characteristic genetic features for CRCC. We found multiple mutations in other tested genes, only two genes (*ROS1, LRP1B*) were found mutated in two different cases. This does not significantly differ from the findings of combined studies of CRCCs that showed mutations in these genes to be present in 3.2 and 2.7%, respectively (datasets of 502 tested samples available via the cBioPortal) [29]. Since most of the gene mutations presented herein have already been reported in CRCC, we consider molecular features of CRCCPLCs compatible with the diagnosis of CRCC. Hypermethylation of VHL promoter was not found in the analyzed cases, which is consistent with the reported hypermethylation of 7% CRCC found in the Cancer Genome Atlas Research Network studies [30].

In the differential diagnosis, particularly in limited material (core biopsy), Xp11.2 translocation RCC should be considered. The morphology of Xp11.2 translocation RCCs can be variable, depending on many factors including fusion partner [31]. Translocation Xp11.2 RCC should be always considered within the differential diagnosis in case of tumor composed of clear cells mixed with voluminous eosinophilic cells. However, in our cases there were no psammoma bodies, prominent microcalcifications, papillary structures or fully developed papillae. Also, the vasculature was prominent in our cases, as it is characteristic for CRCC rather than for Xp11.2 translocation RCCs. In difficult cases an immunohistochemical panel (together with FISH) can

Table 3
Molecular genetic findings of CRCCPLCs.

Case #	HCCP	LOH3p	*VHL* methylation	*VHL* Sanger	*VHL* mutation
1	NP	NP	NP	NP	
2	8	+	−	NP	c.419del p.(Leu140ProfsTer19)
3	NP	+	−	+	c.256C > A p.(Pro86Thr)
4	1	−	−	NP	c.233A > T p.(Asn78Ile)
5	NP	NP	NP	NP	
6	4	+	−	NP	c.302 T > G p.(Leu101Arg)
7	4	+	−	NP	c.341-2dup p(?)
8	14	NP	NP	NP	c.563 T > A p.(Leu188Gln)
9	NP	NA	NA	NA	
10	NP	NA	NA	NA	
11	NA	+	−	+	c.296_333dup p.(Tyr112GlnfsTer60)
12	NA	+	−	+	c.349 T > C p.(Trp117Arg)
13	16	−	−	NP	c.611_612del p.(Glu204AlafsTer51)

Abbreviation; NA not analyzable, NP not performed, + positive, − negative, HCCP – Human Comprehensive Cancer NGS panel (with number of detected variants), LOH3p – loss of heterozygosity of chromosome 3p, *VHL* Sanger – Sanger sequencing of *VHL* gene.

aid in arriving at the accurate diagnosis. Metastatic carcinoma should also be included in the differential diagnosis.

In conclusion, we found that CRCCPLC do not have distinct clinical, immunohistochemical, and genetic features and that they are part of morphologic spectrum of usual low grade CRCC. The prognosis does not seem to be affected by the presence or absence of PLCs.

Declaration of Competing Interest

All authors declare no conflict of interest.

References

[1] Nordenson I, Ljungberg B, Roos G. Chromosomes in renal carcinoma with reference to intratumor heterogeneity. Cancer Genet Cytogenet 1988;32(1):35–41.
[2] Zaldumbide L, Erramuzpe A, Guarch R, Cortes JM, Lopez JI. Large (> 3.8 cm) clear cell renal cell carcinomas are morphologically and immunohistochemically heterogeneous. Virchows Arch 2015;466(1):61–6.
[3] Bevins CL, Salzman NH. Paneth cells, antimicrobial peptides and maintenance of intestinal homeostasis. Nat Rev Microbiol 2011;9(5):356–68.
[4] Tanaka M, Saito H, Kusumi T, Fukuda S, Shimoyama T, Sasaki Y, et al. Spatial distribution and histogenesis of colorectal Paneth cell metaplasia in idiopathic inflammatory bowel disease. J Gastroenterol Hepatol 2001;16(12):1353–9.
[5] Nevalainen TJ, Shah VI, de Peralta-Venturina M, Amin MB. Absence of group II phospholipase A2, a Paneth cell marker, from the epididymis. APMIS 2001;109(4):295–8.
[6] Albores-Saavedra J, Nadji M, Henson DE. Intestinal-type adenocarcinoma of the gallbladder. A clinicopathologic study of seven cases. Am J Surg Pathol 1986;10(1):19–25.
[7] Pallesen G. Neoplastic Paneth cells in adenocarcinoma of the urinary bladder: a first case report. Cancer 1981;47(7):1834–7.
[8] Shah VI, Ro JY, Amin MB, Mullick S, Nazeer T, Ayala AG. Histologic variations in the epididymis: findings in 167 orchiectomy specimens. Am J Surg Pathol 1998;22(8):990–6.
[9] Nistal M, Marino-Enriquez A, De Miguel MP. Granular changes (Paneth cell-like) in epididymal epithelial cells are lysosomal in nature and are not markers of obstruction. Histopathology 2007;50(7):944–7.
[10] Krishnan B, Truong LD. Renal epithelial neoplasms: the diagnostic implications of electron microscopic study in 55 cases. Hum Pathol 2002;33(1):68–79.
[11] Lee KR, Trainer TD. Adenocarcinoma of the uterine cervix of small intestinal type containing numerous Paneth cells. Arch Pathol Lab Med 1990;114(7):731–3.
[12] Bigelow B, Blaustein A. Paneth cells in a mucinous cystadenoma of the ovary: light and electron microscopic study. Gynecol Oncol 1978;6(4):391–4.
[13] Weaver MG, Abdul-Karim FW, Srigley J, Bostwick DG, Ro JY, Ayala AG. Paneth cell-like change of the prostate gland. A histological, immunohistochemical, and electron microscopic study. Am J Surg Pathol 1992;16(1):62–8.
[14] Chen YB, Epstein JI. Primary carcinoid tumors of the urinary bladder and prostatic urethra: a clinicopathologic study of 6 cases. Am J Surg Pathol 2011;35(3):442–6.
[15] Petersson F, Grossmann P, Hora M, Sperga M, Montiel DP, Martinek P, et al. Renal cell carcinoma with areas mimicking renal angiomyoadenomatous tumor/clear cell papillary renal cell carcinoma. Hum Pathol 2013;44(7):1412–20.
[16] Lek M, Karczewski KJ, Minikel EV, Samocha KE, Banks E, Fennell T, et al. Analysis of protein-coding genetic variation in 60,706 humans. Nature 2016;536(7616):285–91.
[17] Landrum MJ, Lee JM, Benson M, Brown GR, Chao C, Chitipiralla S, et al. ClinVar: improving access to variant interpretations and supporting evidence. Nucleic Acids Res 2018;46(D1). [D1062-D7].
[18] Lopez JI. Intratumor heterogeneity in clear cell renal cell carcinoma: a review for the practicing pathologist. APMIS 2016;124(3):153–9.
[19] Erramuzpe A, Cortes JM, Lopez JI. Multisite tumor sampling enhances the detection of intratumor heterogeneity at all different temporal stages of tumor evolution. Virchows Arch 2018;472(2):187–94.
[20] Lopez JI, Cortes JM. Multisite tumor sampling: a new tumor selection method to enhance intratumor heterogeneity detection. Hum Pathol 2017;64:1–6.
[21] Lopez JI, De Petris G. Discovering intratumor heterogeneity: the next frontier for pathologists. Pathologica 2017;109(2):110–3.
[22] Molmenti EP, Perlmutter DH, Rubin DC. Cell-specific expression of alpha 1-antitrypsin in human intestinal epithelium. J Clin Invest 1993;92(4):2022–34.
[23] Epstein JI, Amin MB, Beltran H, Lotan TL, Mosquera JM, Reuter VE, et al. Proposed morphologic classification of prostate cancer with neuroendocrine differentiation. Am J Surg Pathol 2014;38(6):756–67.
[24] Tamas EF, Epstein JI. Prognostic significance of paneth cell-like neuroendocrine differentiation in adenocarcinoma of the prostate. Am J Surg Pathol 2006;30(8):980–5.
[25] So JS, Gordetsky J, Epstein JI. Variant of prostatic adenocarcinoma with Paneth cell-like neuroendocrine differentiation readily misdiagnosed as Gleason pattern 5. Hum Pathol 2014;45(12):2388–93.
[26] Hes O, Michal M, Sulc M, Kocova L, Hora M, Rousarova M. Glassy hyaline globules in granular cell carcinoma, chromophobe cell carcinoma, and oncocytoma of the kidney. Ann Diagn Pathol 1998;2(1):12–8.
[27] Guarino M, Zuccoli E, Garda E, Cristofori E, Pallotti F, Nebuloni M, et al. Extracellular matrix globules in renal oncocytoma. Pathol Res Pract 2001;197(4). [245–52].
[28] Gatalica Z, Miettinen M, Kovatich A, McCue PA. Hyaline globules in renal cell carcinomas and oncocytomas. Hum Pathol 1997;28(4). [400–3e].
[29] Cerami E, Gao J, Dogrusoz U, Gross BE, Sumer SO, Aksoy BA, et al. The cBio cancer genomics portal: an open platform for exploring multidimensional cancer genomics data. Cancer Discov 2012;2(5):401–4.
[30] Comprehensive molecular characterization of clear cell renal cell carcinoma. Nature 2013;499(7456):43–9.
[31] Argani P, Zhong M, Reuter VE, Fallon JT, Epstein JI, Netto GJ, et al. TFE3-fusion variant analysis defines specific Clinicopathologic associations among Xp11 translocation cancers. Am J Surg Pathol 2016;40(6):723–37.

1.5.5 Papillary pattern in clear cell renal cell carcinoma: Clinicopathologic, morphologic, immunohistochemical and molecular genetic analysis of 23 cases

U CCRCC lze (ne zcela raritně) zastihnout papilární způsob růstu a tento nález představuje diagnostickou výzvu pro hodnotícího patologa. Cílem této studie bylo analyzovat CCRCC s predominantně papilárním růstem z morfologické, imunohistochemické a molekulárně-genetické (NGS) perspektivy.

Pro účely studie bylo vybráno celkem 23 CCRCC s papilární architektonikou, u nichž byla vyloučena diagnóza MiT translokačního RCC (užitím TFE3 imunohistochemického barvení). Průměrný věk pacientů byl 65,2 let (rozmezí 42-81 let) a 19/23 tumorů vzniklo u mužů. Velikost tumorů se pohybovala v rozmezí 1,6 -12,8 cm (medián 6,5 cm). Průměrný follow-up u pacientů trval 2,5 roku (v rozmezí délky trvání 1,5 – 9 roků), přičemž u čtyř případů bylo zaznamenáno agresivní chování, kdy 2 pacienti zemřeli na následky onemocnění, u 2 pacientů došlo k rozvoji metastáz. Okrsky s papilárním vzhledem představovaly průměrně od 40% do 100% nádorové masy. Imunohistochemický průkaz CK7 byl negativní v nonpapilárních okrscích ve většině případů (20/23) a jen fokálně pozitivní u 3/23 tumorů (13%). AMACR reagoval pozitivně/fokálně pozitivně v 17/23 případů v papilárních okrscích, v nonpapilárních okrscích byl pozitivní/fokálně pozitivní v 22/23 případech. Karbohydráza IX byla ve většině negativní jak v nonpapipárních, tak i papilárních okrscích (u 15/23, resp. 16/23 tumorů). Molekulární analýza u 15 analyzovatelných případů odhalila jako nejčastěji mutovaný gen *VHL* (v 9 případech), následovaný mutací v genu *PRBM1* (ve 2 případech) a 29 jinými variabilními mutacemi v různých genech.

Papilární růst u CCRCC není zcela vzácnou situací a v rámci zvažované diferenciální diagnózy je nutné odlišit zejména PRCC a MiTF RCC (TFE3 translokační RCC). Molekulárně-genetická analýza případů podpořila oprávněnost našeho přístupu, kdy nádory tohoto morfologického vzhledu byly klasifikovány jako morfologická varianta CCRCC.

Annals of Diagnostic Pathology 38 (2019) 80–86

Contents lists available at ScienceDirect

Annals of Diagnostic Pathology

journal homepage: www.elsevier.com/locate/anndiagpath

Papillary pattern in clear cell renal cell carcinoma: Clinicopathologic, morphologic, immunohistochemical and molecular genetic analysis of 23 cases

Reza Alaghehbandan[a], Monika Ulamec[b], Petr Martinek[c], Kristyna Pivovarcikova[c], Kvetoslava Michalova[c], Faruk Skenderi[d], Milan Hora[e], Michal Michal[c], Ondrej Hes[c,*]

[a] Department of Pathology, Faculty of Medicine, University of British Columbia, Royal Columbian Hospital, Vancouver, BC, Canada
[b] "Ljudevit Jurak" Pathology Department, Clinical Hospital Center "Sestre milosrdnice", Pathology Department, Medical University, Medical Faculty, Zagreb, Croatia
[c] Department of Pathology, Charles University, Faculty of Medicine in Plzeň, Pilsen, Czech Republic
[d] Department of Pathology, University of Sarajevo Clinical Center, Sarajevo, Bosnia and Herzegovina
[e] Department of Urology, Charles University, Faculty of Medicine in Plzeň, Pilsen, Czech Republic

ARTICLE INFO

Keywords:
Clear cell renal cell carcinoma
Papillary pattern
NGS

ABSTRACT

Clear cell renal cell carcinoma (ccRCC), the most common histologic subtype of RCCs, demonstrates a wide spectrum of morphologic features (i.e., low-grade spindle cell, syncytial giant cells, and mucin-producing cells). However, papillary growth pattern in ccRCCs is rather a rare finding, which can present challenges in differential diagnostic work up. The aim of this study was to investigate ccRCCs with predominant papillary features from morphologic, immunohistochemical and molecular genetic perspectives.

23 clear cell renal cell carcinomas with papillary architecture were selected. Tumors were evaluated morphologically, immunohistochemically, and molecularly by next-generation sequencing (NGS). The diagnosis of MiT family translocation RCC was excluded by TFE3 immunohistochemistry.

Mean age of patients was 65.2 years (range 42–81 years), and 19/23 were male. Tumor size ranged from 1.6 to 12.8 cm (median 6.5 cm). At a median follow-up of 2.5 years (range 1.5–9 years), 2 patients (8.7%) died of disease, 2 developed metastasis. Areas of papillary pattern accounted for approximately 40–100% of the tumor. CK7 was negative in non-papillary areas in majority of cases (20/23, 87%), and was only focally positive in 3/23 cases (13%). In papillary areas, AMACR was positive/focally positive in 17/23 (73.9%) cases and in the non-papillary areas it was positive/focally positive in 22/23 (95.6%) cases. CAIX was mainly negative in both non-papillary and papillary areas (15/23 [65%] and 16/23 [69.5%], respectively). Molecular analysis of 15 analyzable cases revealed the most frequently mutated gene to be *VHL* (in 9 cases), followed by *PRBM1* (in 2 cases) and 29 other different mutations in various genes.

Papillary growth pattern in ccRCC is not an uncommon situation. Papillary RCC with clear cells and MiT family (TFE3) translocation RCCs are the major differential diagnostic considerations in such scenarios. Our NGS molecular analysis supported classifying such tumors as a morphologic variant of ccRCC.

1. Introduction

Clear cell renal cell carcinoma (ccRCC) is the most common subtype of RCCs, representing approximately 65–70% of all adult renal carcinomas [1]. ccRCCs are architecturally and cytologically diverse including solid, alveolar, acinar, cystic growth patterns of neoplastic cells with clear and/or eosinophilic cytoplasm. High-grade ccRCCs usually composed of mixed neoplastic cells with clear and eosinophilic cytoplasm. In fact, tumor heterogeneity is a well-documented and known phenomenon in ccRCCs with various morphologic features such as low-grade spindle cell, syncytial giant cells, and mucin-producing cells [2-5]. The presence of mixed morphologic components in renal neoplasms in general and in ccRCCs in particular can be puzzling in routine practice, which can potentially lead to misdiagnosis [6].

It is well-known that ccRCCs can present with papillary architectural growth pattern although rarely. A number of studies since early 1990s studied and reported RCCs with clear cells and papillary features [7-10]. This finding is not rare and certainly can pose diagnostic

* Corresponding author at: Department of Pathology, Medical Faculty, Charles University Hospital Plzen, Alej Svobody 80, 304 60 Pilsen, Czech Republic.
E-mail address: hes@medima.cz (O. Hes).

https://doi.org/10.1016/j.anndiagpath.2018.11.004

1092-9134/

Table 1
Clinicopathologic data on patients with clear cell renal cell carcinoma with papillary architecture.

Case	Papillary (%)	Classic clear cell (%)	Necrosis (%)	No. block	Gender	Age	Size (cm) +	pTNM	Grade	Follow up (mon)
1	100	0	0	2	F	57	6	T3aNxMx	3	2 yrs AW, then LF
2	80	15	5	2	M	77	5.2	T1b	3	LF
3	60	40	0	3	M	62	8	T3a	3	3 yrs WA
4	70	30	0	2	M	74	7.5	T2NxM1[a]	3	1.5 yrs DOD
5	85	0	40	2	M	54	6.5	T1bNxMx	4	2.3 yrs DOD[b]
6	75	25	0	2	M	76	3.3	T1a	3	5 yrs AW
7	60	40	5	10	M	42	7.5	T3aNx	4	1.5 yrs AW
8	70	20	10	6	F	81	4.5	T3aN0Mx	3	AW 2 years
9	85	10	15	2	M	81.	7	T3b	3	LF
10	90	5	5	5	M	76	5,5	pT1b	2	LF
11	60	40	0	2	M	54	3	T1a	3	LF
12	60	20	20	6	M	64	8	T3bN0Mx	4	6 yrs AW, then LF
13	40	60	0	4	M	61	3.5	T1a	2	9 yrs AW
14	80	10	10	4	M	68	4	T1b	3	LF
15	95	5	0	4	F	58	4	pT1b	1	9 yrs AW[c]
16	70	25	5	3	M	48	9	pT3b	3	LF
17	70	30	3	1	M	69	3	pT1a	3	LF
18	80	20	0	1	M	56	1.6	pT1a	2	5 yrs AW[e]
19	100	0	0	1	M	67	8	pT2a	2	2 years AW[f]
20	75	5	50	2	M	67	12.5	pT3	2	2.5 yrs AW, then DotD[d]
21	70	30	0	1	F	65	4.5	pT1b	3	LF
22	50	50	10	11	M	74	8	pT3a	3	LF
23	60	20	20	5	M	63	12.8	pT3a	3	LF

DotD = dead of other disease, DOD = dead of disease, AW = alive and well, LF = lost to follow up, M = male, F = female, + = largest diameter, yr = year, yrs = years.

[a] Meta to lung, vertebra.
[b] Meta to brain, lung, lymph nodes, liver.
[c] Treated for breast carcinoma.
[d] Myocardial infarct.
[e] Followed for cataract.
[f] Surgery for cataract.

challenge in limited samples (i.e., renal core biopsies). The differential diagnosis would include two main RCC subtypes, namely papillary RCC and ccRCC with papillary features. The recent 2016 WHO (World Health Organization) classification included RCCs with clear cell features such as clear cell papillary RCC and MiT family translocation carcinomas (namely Xp11.2) [1]. This differential diagnosis can have potential therapeutic implications and as such it would be crucial to arrive in accurate diagnosis.

The purpose of this study was to investigate ccRCCs with predominant papillary features from morphologic, immunohistochemical and molecular genetic perspectives. It is our hope that findings of this study will shed light on better understanding of such neoplasms.

2. Materials and methods

An institutional Ethics Review was obtained for the study. Cases were selected and retrieved by searching both in-house and consultation files of Charles University Hospital, Plzen, Czech Republic, and the Royal Columbian Hospital, University of British Columbia, Canada.

Of 543 ccRCCs searched, 23 were selected which included ccRCCs with prominent papillary architecture (more than 40%). All cases were reviewed by two urologic pathologists (R.A. and O.H.). One or multiple blocks/slides were available for review in all cases (ranging from 1 to 11). Clinicopathologic and follow-up data were collected using medical chat review and contacting primary consulting pathologists in all cases. The diagnosis of MiT family translocation RCC was excluded by TFE3 immunohistochemistry.

Tissues for light microscopy were fixed in 4% formaldehyde and embedded in paraffin using a routine procedure. 5 μm thick sections were cut from the tissue blocks and were stained with hematoxylin and eosin.

2.1. Immunohistochemical studies

The immunohistochemical study was performed using a Ventana Benchmark XT automated stainer (Ventana Medical System, Inc., Tucson, AZ, USA). Immunochemical studies were carried out using a panel of antibodies including CK7 (OV-TL12/30, monoclonal, DakoCytomation, Carpinteria, CA, 1:200), racemase/AMACR (P504S, monoclonal, Zeta, Sierra Madre, CA, 1:50), vimentin (D9, monoclonal, NeoMarkers, Westinghouse, CA, 1:1000), carbonic anhydrase IX (rhCA9, monoclonal, RD systems, Abingdon, GB, 1:100), TFE3 (polyclonal, Abcam, Cambridge, UK, 1:100), and CD10 (monoclonal 56C6, Leica, Newcastle, UK, 1:20). Appropriate positive and negative controls were used.

2.2. NGS mutation analysis

A panel of 271 cancer related genes (Comprehensive Cancer Panel, Qiagen, Hilden, Germany) was used to analyze tumor tissue samples. The samples were isolated using macro dissection from FFPE blocks. DNA was isolated using Qiagen DNA mini kit, and 250 ng of DNA was used to construct the library. The QIAseq technology applies unique Molecular Identifiers (UMI) for more specific allele frequency determination as well as PCR error reduction. Technical duplicates and positive controls were used to establish quality control of the analysis parameters. Library was sequenced on Illumina's Nextseq 500, aiming at average coverage 350× after deduplication of molecular identifiers to detect 10% allele frequency with 95% sensitivity. Variants were called using Qiagen's proprietary pipeline. Subsequently the variants were filtered using the calculated limit of detection for each sample. Furthermore the variants were annotated using The Genome Aggregation Database (GnomAD) [11] for population statistics and ClinVar database [12] for the relationships among variations and phenotypes. Variants more frequent than 0.001% in the GnomAD database were excluded as well as known benign variants according to the

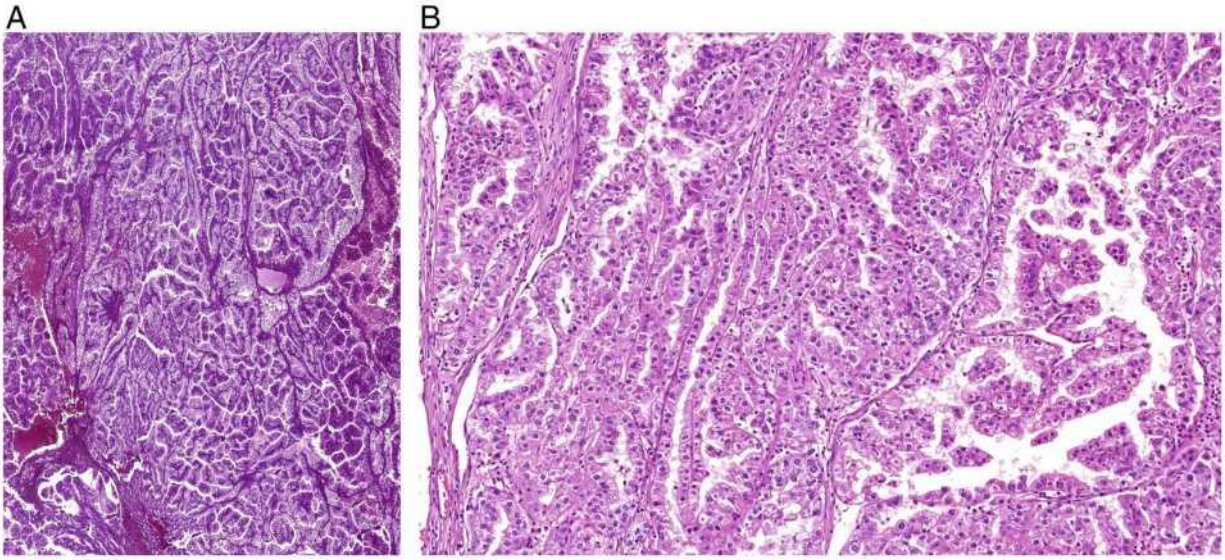

Fig. 1. a. Clear cell renal cell carcinoma with prominent papillary pattern.
b. Clear cell renal cell carcinoma with areas of compressed papillary structures.

ClinVar database. The remaining subset was checked visually, and suspected artefactual variants were excluded.

3. Results

Table 1 presents clinical and demographic information on 23 patients including 19 males and 4 females. Patient's age ranged from 42 to 81 years (mean 65.2, median 65 years). Tumor size varied from 1.6 to 12.8 cm (mean 6.3, median 6.5 cm). Follow up data (1.5–9 years, mean 3.9, median 2.5 years) were available in 13 of 23 patients. Eleven patients were staged as pT1, 2 patients pT2, and 10 patients pT3. Metastases were documented in 2 cases. Two patients died of disease (1.5 and 2.3 years after diagnosis).

Gross description was available in 13 cases, showing yellow golden masses with regressive changes, hemorrhages and foci of firm gray tissue on cut surface. Necrotic areas were present in 12 cases, ranging from 5 to 50% of the total tumor volume.

Microscopically, all tumors showed majority of neoplastic cells with predominantly clear cytoplasm, arranged mainly in alveolar, nested, and trabecular patterns, separated by fibrovascular septae. Areas of papillary pattern accounted for approximately 40–100% of the tumor (Fig. 1a–b). Papillae were lined by clear and/or eosinophilic neoplastic cells (Fig. 2a–b). Foamy macrophages were not observed. The ISUP/WHO histologic grade ranged 1–4 (Fig. 3a–c).

Results of immunohistochemical examination are summarized in Table 2. CK7 was negative in non-papillary areas in majority of cases (20/23, 87%), and was only focally positive in 3/23 cases (13%). In papillary areas, AMACR was positive/focally positive in 17/23 (73.9%) cases and in the non-papillary areas it was positive/focally positive in 22/23 (95.6%) cases. CAIX immunohistochemical stain was mainly negative in both non-papillary and papillary areas (15/23 [65%] and 16/23 [69.5%], respectively). On the other hand, vimentin was positive/focally positive in most cases in both non-papillary and papillary areas (20/23 [87%] and 18/23 [78.3%], respectively). CD10 immunohistochemical stain was consistently positive (either focal or diffuse) in non-papillary area (23/23, 100%), and similarly it was positive in 22/23 (95.6%) cases in the papillary area. TFE3 was negative in all 23 cases.

Fifteen of 23 samples were successfully sequenced (met the quality control standards) and as a result, a total of forty mutations were filtered (Table 3). Most frequently mutated gene was *VHL* (in 9 cases) followed by *PRBM1* (in 2 cases) and 29 other different mutations in various genes. Some samples with low DNA quality had unfavourable ratio of sequenced reads to UMI's and as such the limit of detection was increased. The details are listed in Table 4.

4. Discussion

ccRCC usually shows a solid, alveolar or acinar growth pattern, composed of clear or eosinophilic neoplastic cells. Tumor heterogeneity in renal neoplasms is a well-documented fact [6,13]. ccRCC, the most common subtype of RCCs, are no exception and can exhibit great variability in both architectural growth patterns and morphologic features. The morphologic features of ccRCCs can also be dependent on the tumor grade, with higher tumor grades demonstrating a mixture of clear cells and neoplastic cells with eosinophilic granular cytoplasm. In fact, our group recently described a rare subset of high grade ccRCCs with prominent emperipolesis [14]. These tumors showed focal pseudopapillary features with large cells with bizarre nuclei and eosinophilic rhabdoid-like cytoplasm [14]. In recent years, a number of rare morphologic variants of ccRCCs have been described, including mucin-secreting ccRCC, ccRCC with low-grade spindle cell proliferation, ccRCC with syncytial giant cell component, and ccRCCs with prominent emperipolesis [2,4,5,14,15].

From architectural point of view, although ccRCCs usually present in a solid growth pattern, cystic changes can frequently be seen. ccRCC with true papillary architecture is a rather rare variant but has previously been described [7-10,16]. According to the most recent World Health Organization (WHO) Classification of Genitourinary tumors, "focal" papillary areas can be seen in ccRCCs [17]. In reality, we and others have noticed that ccRCCs can have rather large papillary areas with well-formed true papillae [7-10,16]. In fact, the papillary area could constitute a substantial portion of the tumor as it is the case in our study with ccRCCs demonstrating between 40 and 100% papillary areas. This can simply present a diagnostic challenge in routine practice, particularly in limited samples, with the current understating that ccRCCs can have "focal" papillary areas [17]. The two most common differential diagnoses of RCCs with papillary architecture and clear cell morphology would include MiT family (TFE3) translocation RCC, and clear cell papillary RCC. Other rather less frequent differential diagnoses would include collision tumors, *fumarate hydratase*-deficient RCCs, and RCCs with leiomyomatous stroma [18]. It would be expected that such tumors might have been classified as PRCC, collision tumors, or even unclassified in the past [9,10]. However, with the current

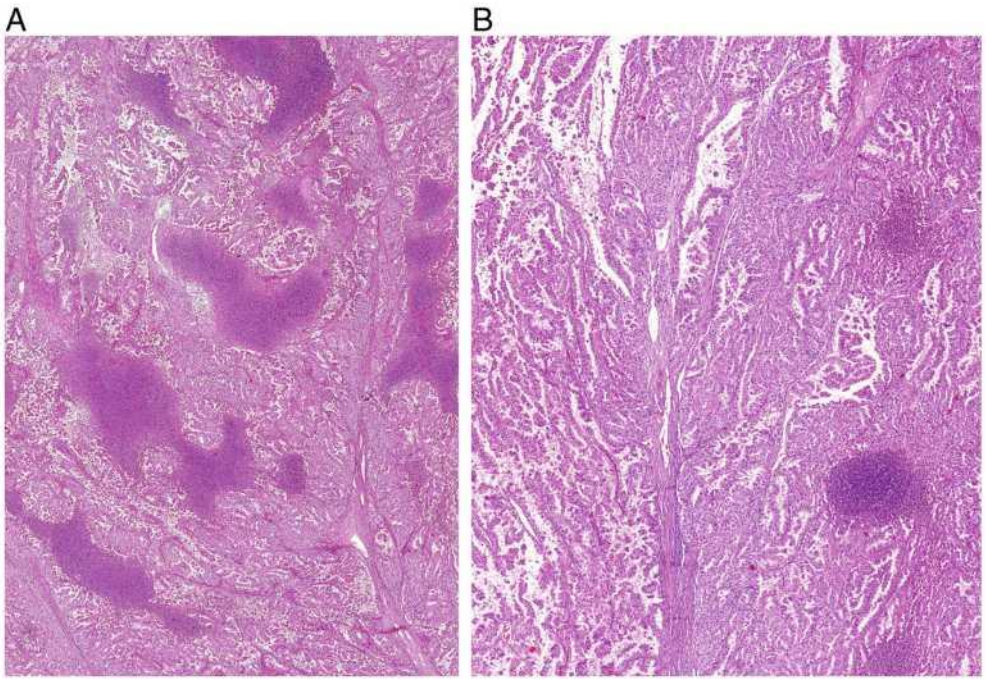

Fig. 2. a. Clear cell renal cell carcinoma with papillary pattern and extensive foci of necrosis.
b. Clear cell renal cell carcinoma with papillary architecture and small foci of necrosis.

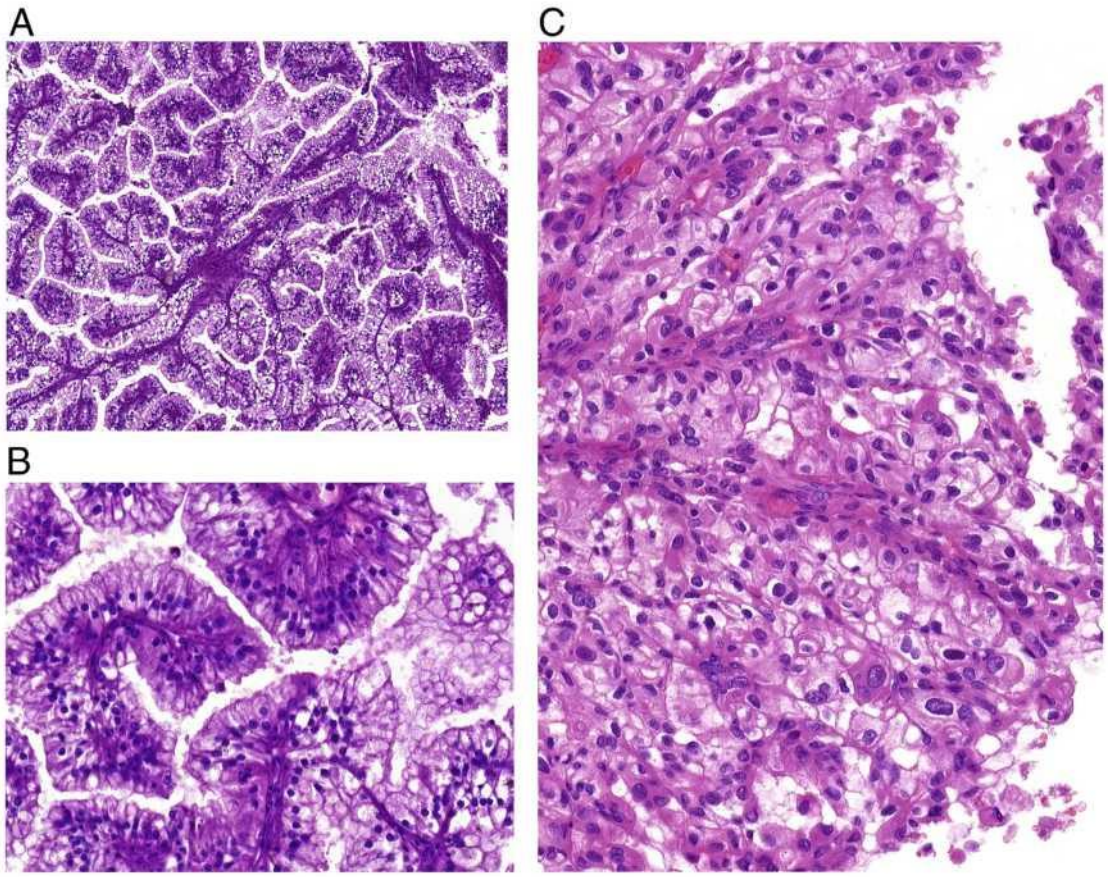

Fig. 3. a. Cytological features are identical to clear cell renal cell carcinoma, however demonstrating papillary architecture.
b. Clear cell renal cell carcinoma with papillary features showing grade 1 nuclear grade.
c. Clear cell renal cell carcinoma with papillary features showing grade 3 nuclear morphology.

Table 2
Results of immunohistochemistry on clear cell renal cell carcinoma with papillary architecture.

Case	CK7-cc	CK7-Pap	AMACR-cc	AMACR-Pap	CAIX-cc	CAIX-Pap	Vim-cc	Vim-Pap	CD10-cc	CD10-Pap	TFE3 cc/Pap
1	Neg.	Neg.	Neg.	Focal pos.	Neg.	Neg.	Focal pos.	Focal pos.	Pos.	Pos.	Neg.
2	Neg.	Neg.	Neg.	Focal pos.	Neg.	Neg.	Focal pos.	Focal pos.	Pos.	Pos.	Neg.
3	Neg.	Neg.	Focal pos.	Pos.	Pos.	Pos.	Pos.	Focal pos.	Pos.	Pos.	Neg.
4	Neg.	Focal pos.	Neg.	Focal pos.	Neg.	Neg.	Focal pos.	Focal pos.	Pos.	Pos.	Neg.
5	Neg.	Neg.	Focal pos.	Pos.	Neg.	Neg.	Focal pos.	Focal pos.	Focal pos.	Focal pos.	Neg.
6	Neg.	Neg.	Focal pos.	Focal pos.	Neg.	Neg.	Focal pos.	Focal pos.	Pos.	Pos.	Neg.
7	Neg.	Neg.	Focal pos.	Focal pos.	Focal pos.	Focal pos.	pos.	Pos.	Pos.	Pos.	Neg.
8	Focal pos.	Neg.	Pos.	Pos.	Neg.	Neg.	Focal pos.	Focal pos.	Pos.	Pos.	Neg.
9	Neg.	Neg.	Pos.	Pos.	Focal pos.	Neg.	Focal pos.	Neg.	Pos.	Pos.	Neg.
10	Neg.	Neg.	Focal pos.	Focal pos.	Neg.	Neg.	Focal pos.	Focal pos.	Pos.	Pos.	Neg.
11	Focal pos.	Neg.	Pos.	Focal pos.	Neg.	Neg.	pos.	Focal pos.	Pos.	Focal pos.	Neg.
12	Focal pos.	Pos.	Focal pos.	Focal pos.	Neg.	Neg.	Neg.	Neg.	Focal pos.	Pos.	Neg.
13	Neg.	Neg.	Focal pos.	Focal pos.	Pos.	Pos.	Pos.	Pos.	Pos.	Pos.	Neg.
14	Neg.	Neg.	Pos.	Pos.	Neg.	Neg.	pos.	Neg.	Pos.	Pos.	Neg.
15	Neg.	Neg.	Focal pos.	Focal pos.	Neg.	Neg.	Focal pos.	Focal pos.	Pos.	Neg.	Neg.
16	Neg.	Neg.	Focal pos.	Focal pos.	Neg.	Neg.	Neg.	Neg.	Pos.	Pos.	Neg.
17	Neg.	Neg.	Focal pos.	Focal pos.	Pos.	Pos.	Focal pos.	Focal pos.	Pos.	Focal pos.	Neg.
18	Neg.	Neg.	Neg.	Focal pos.	Neg.	Neg.	Pos.	Pos.	Pos.	Pos.	Neg.
19	Neg.	Neg.	Focal pos.	Pos.	Neg.	Neg.	Neg.	Neg.	Pos.	Pos.	Neg.
20	Neg.	Neg.	Pos.	Pos.	Neg.	Neg.	Focal pos.	Focal pos.	Pos.	Focal pos.	Neg.
21	Neg.	Focal pos.	Focal pos.	Focal pos.	Focal pos.[a]	Focal pos.[a]	Pos.	Pos.	Pos.	Pos.	Neg.
22	Neg.	Neg.	Neg.	Neg.	Pos.	Pos.	Pos.	Pos.	Pos.	Pos.	Neg.
23	Neg.	Neg.	Neg.	Focal pos.	Pos.	Pos.	Pos.	Pos.	Pos.	Focal pos.	Neg.

cc = classic clear cell area, Pap = papillary area, Neg. = negative, Pos. = positive, CAIX = carbonic anhydrase 9, vim = vimentin.
[a] Artefact/fixation.

Table 3
Summary of molecular genetic findings on analyzable clear cell renal cell carcinoma with papillary architecture.

Case	HCCP # mutations	LOD 95
1	NA	NA
2	7	0.1301
3	5	0.0949
4	5	0.1881
5	4	0.2144
6	1	0.3418
7	NA	NA
8	0	0.1961
9	1	0.4606
10	NA	NA
11	0	0.5108
12	NA	NA
13	3	0.1197
14	1	0.4389
15	NA	NA
16	2	0.192
17	3	0.192
18	2	0.1675
19	5	0.0575
20	1	0.1843

HCCP # mutations – human comprehensive cancer panel result with number of detected variants, LOD 95 – average 95th percentile estimated minimum detectible allele fraction, NA not analyzable.

knowledge and available ancillary testing such tumors can hopefully be correctly diagnosed.

MiT family (TFE3) translocation RCCs, mostly tumors associated with Xp11.2 translocation, demonstrate variable morphological features. These tumors are mostly arranged in papillary architecture with large, weakly eosinophilic or clear neoplastic cells with occasional psammoma bodies and eosinophilic hyaline nodules. Immunohistochemically, these tumors express TFE3 protein, albeit TFE3 break-apart fluorescence in situ hybridization assay is the most reliable method of detection [18]. Clear cell papillary RCC, the other main differential diagnosis, is easily recognizable morphologically, including tubopapillary architecture, variable presence of leiomyomatous stroma, "shark smiles," and apical "blister" feature and low-grade basally located nuclei. Unlike ccRCCs which are mostly CK7 negative/focally positive, these tumors are strongly and diffusely positive for CK7 [18].

Earlier studies including Fuzesi et al. [16] analyzed 3 cases of PRCC with clear cell morphology, using classic cytogenetics (standard G-banding techniques), which demonstrated loss of terminal 3p chromosomal segments with no trisomy 17 observed. Subsequently, Salama et al. [7] used fluorescence in situ hybridization (FISH) and microsatellite analysis to determine the genetic alterations in 7 malignant renal tumors with papillary architecture and extensive clear cell change. The authors concluded that because such tumors showed molecular changes identical to ccRCCs, such neoplasms should be classified as ccRCC [7]. Most recently, Jia et al. [19] examined 13 cases of RCCs with clear cytoplasm, high-grade nuclear features, and prominent papillary architecture from Memorial Sloan Kettering Cancer Center and TCGA papillary RCC public databases. The authors reported that molecular analysis of 8 cases revealed a *VHL* mutation and concurrent 3p loss in 7 of 8 cases, while no trisomy 7/17 or MET mutations were found. They concluded that molecular analysis of such neoplasms with clear cytoplasm and prominent papillary architecture showed characteristic molecular features of ccRCC and supports their classification as a rare morphologic variant of ccRCC.

In our study, the samples analyzed by NGS Comprehensive cancer panel showed large variety of variants with mostly unknown pathogenicity (Table 4). Most frequently mutated gene was *VHL* (in 9 cases) followed by *PRBM1* (in two cases) and 29 other different mutations in various genes. Five of the most commonly mutated genes in ccRCCs including *VHL*, *PRBM1*, *PTEN*, *PIK3CA*, and *KDM5C*, were mutated in our study group [20]. It should be noted that most of the low frequency samples were filtered out due to the insufficient limit of detection, which was caused by low quality of source DNA of many samples. The somatic status of the variants was confirmed by comparing tumor to normal tissue pairs. Of note, some variants had no known clinical implication/interpretation. Our molecular genetic findings are compatible with prior studies, particularly with Jia et al. [19], in which such tumors share characteristic molecular features of ccRCC and that they are best classified as a rare morphologic variant of ccRCC.

Table 4
Details of detected mutations on analyzable clear cell renal cell carcinoma with papillary architecture.

Case	pos	Variant frequency	Symbol	HGVSc	HGVSp	VEP dbSNP ID	Clinical significance
2	chr3:10188316	0.2197	*VHL*	NM_000551.3:c.461del	NP_000542.1:p.Pro154GlntsTer5	CM065515	Pathogenic
	chr3:52643374	0.2206	*PBRM1*	NM_181042.4:c.2522A > C	NP_851385.1:p.Gln841Pro	–	–
	chr4:66270158	0.1839	*EPHA5*	NM_001281765.2:c.1727T > A	NP_001268694.1:p.Ile576Asn	–	–
	chr9:139405209	0.4185	*NOTCH1*	NM_017617.3:c.2636G > A	NP_060087.3:p.Arg879Gln	rs368011392	Uncertain significance
	chr17:8109861	0.5329	*AURKB*	NM_001284526.1:c.637G > C	NP_001271455.1:p.Gly213Arg	rs149651741	–
	chr22:23655142	0.2306	*BCR*	NM_004327.3:c.3391T > C	NP_004318.3:p.Tyr1131His	–	–
	chrX:53245132	0.2439	*KDM5C*	NM_004187.3:c.807del	NP_004178.2:p.Thr270GlnfsTer2	–	Pathogenic
3	chr1:226253407	0.0966	*H3F3A*	NM_002107.4:c.179A > G	NP_002098.1:p.Glu60Gly	–	–
	chr3:10188308	0.2451	*VHL*	NM_000551.3:c.451_452delinsTG	NP_000542.1:p.Ile151Cys	COSM479175	–
	chr3:47098949	0.2118	*SETD2*	NM_014159.6:c.6325C > T	NP_054878.5:p.Arg2109Ter	COSM4970575, COSM4970576	Pathogenic
	chr10:89720679	0.0976	*PTEN*	NM_001304717.2:c.1349C > A	NP_001291646.2:p.Thr450Lys	rs398123329, CM109589, COSM35645, COSM5347081	Uncertain significance
	chr19:52714542	0.2068	*PPP2R1A*	NM_014225.5:c.300G > T	NP_055040.2:p.Glu100Asp	–	–
4	chr3:10183770	0.332	*VHL*	NM_000551.3:c.239G > A	NP_000542.1:p.Ser80Asn	rs5030805, CM961418, CM951273, CD951872, COSM30216, COSM3364919	–
	chr3:52595935	0.2424	*PBRM1*	NM_181042.4:c.4135del	NP_851385.1:p.Arg1379GlyfsTer5	COSM4119134, COSM4119135, COSM4119136	Pathogenic
	chr7:116339762	0.293	*MET*	NM_001127500.2:c.624T > G	NP_001120972.1:p.Asp208Glu	–	–
	chr19:15271577	0.485	*NOTCH3*	NM_000435.2:c.6862C > T	NP_000426.2:p.Pro2288Ser	rs551855907	–
	chrX:123210269	0.6429	*STAG2*	NM_001042749.1:c.2621A > T	NP_001036214.1:p.Tyr874Phe	–	–
5	chr3:10188196	0.2756	*VHL*	NM_000551.3:c.341-2A > T	–	CS071275, COSM14425, COSM17750, COSM30295	Pathogenic
	chr3:178936091	0.2899	*PIK3CA*	NM_006218.2:c.1633G > A	NP_006209.2:p.Glu545Lys	rs104886003, CM126692, COSM125370, COSM27133, COSM295672, COSM763	Pathogenic/likely pathogenic
	chr6:117647551	0.3696	*ROS1*	NM_002944.2:c.5393A > G	NP_002935.2:p.Asn1798Ser	–	–
	chr9:98009767	0.6316	*FANCC*	NM_000136.2:c.197C > T	NP_000127.2:p.Thr66Ile	rs762234072	–
6	chr2:46597010	0.4825	*EPAS1*	NM_001430.4:c.824G > A	NP_001421.2:p.Arg275His	rs759634197, COSM461020	–
9	chr7:6026906	0.5043	*PMS2*	NM_001322014.1:c.1490G > A	NP_001308943.1:p.Gly497Asp	rs199739859, COSM3412219	Conflicting interpretations of pathogenicity
13	chr1:65321324	0.4789	*JAK1*	NM_001321853.1:c.1516C > T	NP_001308782.1:p.Arg506Cys	rs61735631	Not provided
	chr2:178098806	0.15	*NFE2L2*	NM_006164.4:c.239C > G	NP_006155.2:p.Thr80Arg	COSM132857, COSM132861, COSM132964	–
	chr3:10183739	0.4194	*VHL*	NM_000551.3:c.208G > T	NP_000542.1:p.Glu70Ter	rs5030802, CM951268, CM984688, COSM1169478, COSM17711	Pathogenic
14	chr10:8111553	0.4444	*GATA3*	NM_001002295.1:c.1042C > T	NP_001002295.1:p.Leu348Phe	COSM4603687	–
16	chr3:10191508	0.6216	*VHL*	NM_000551.3:c.504_508del	NP_000542.1:p.Leu169GlnfsTer3	–	Pathogenic
	chr14:103363665	0.3125	*TRAF3*	NM_145725.2:c.887G > A	NP_663777.1:p.Cys296Tyr	–	–
17	chr3:10191546	0.2899	*VHL*	NM_000551.3:c.541_550del	NP_000542.1:p.Val181SerfsTer18	–	Pathogenic
	chr15:91346808	0.4231	*BLM*	NM_000057.2:c.3416G > C	NP_000048.1:p.Arg1139Pro	rs771776126, COSM5850071	Uncertain significance
	chr19:42791037	0.2751	*CIC*	NM_001304815.1:c.2909C > T	NP_001291744.1:p.Pro970Leu	–	–
18	chr3:10188252	0.3846	*VHL*	NM_000551.3:c.395A > C	NP_000542.1:p.Gln132Pro	CM994242, COSM17857	–
	chr3:69987012	0.7264	*MITF*	NM_198159.2:c.394C > A	NP_937802.1:p.Gln132Lys	rs201297175	–
19	chr3:10191572	0.2045	*VHL*	NM_000551.3:c.567del	NP_000542.1:p.Asp190ThrfsTer12	–	Pathogenic
	chr5:149433662	0.1211	*CSF1R*	NM_005211.3:c.2889G > C	NP_005202.2:p.Leu963Phe	–	–
	chr9:98222010	0.2051	*PTCH1*	NM_000264.3:c.2759A > C	NP_000255.2:p.Tyr920Ser	–	–
	chr12:46123671	0.1032	*ARID2*	NM_152641.2:c.52G > A	NP_689854.2:p.Ala18Thr	–	–
	chr16:89846345	0.5191	*FANCA*	NM_000135.2:c.1647G > C	NP_000126.2:p.Gln549His	–	–
20	chr16:2110710	0.4205	*TSC2*	NM_000548.4:c.1015G > A	NP_000539.2:p.Val339Ile	rs559727962, COSM368620	Uncertain significance

HGVSc - DNA level variant description, HGVSp - protein lever variant description, gnomAD AF – variant frequency found in the gnomAD database, dbSNP ID – identifier in NCBI dbSNP or COSMIC databases.

5. Conclusion

Papillary growth pattern in ccRCC is not uncommon and in fact it can constitute a substantial portion the tumor. Papillary RCC with clear cells and MiT family (TFE3/XP11.2) translocation RCCs are the major differential diagnostic considerations, which can be resolved with help of IHC and basic FISH testing. Our NGS molecular analysis supported classifying such tumors as a rare variant of ccRCC.

Disclosure of conflict of interest

All authors declare no conflict of interest.

Funding

The study was supported by the Charles University Research Fund (project number Q39) and by the project Institutional Research Fund of University Hospital Plzen (FN 00669806).

References

[1] Moch H, Cubilla AL, Humphrey PA, Reuter VE, Ulbright TM. The 2016 WHO classification of tumours of the urinary system and male genital organs-part A: renal, penile, and testicular tumours. Eur Urol 2016;70:93–105.
[2] Val-Bernal JF, Salcedo W, Val D, Parra A, Garijo MF. Mucin-secreting clear cell renal cell carcinoma. A rare variant of conventional renal cell carcinoma. Ann Diagn Pathol 2013;17:226–9.
[3] Williamson SR, Kum JB, Goheen MP, Cheng L, Grignon DJ, Idrees MT. Clear cell renal cell carcinoma with a syncytial-type multinucleated giant tumor cell component: implications for differential diagnosis. Hum Pathol 2014;45:735–44.
[4] Tanas Isikci O, He H, Grossmann P, Alaghehbandan R, Ulamec M, Michalova K, et al. Low-grade spindle cell proliferation in clear cell renal cell carcinoma is unlikely to be an initial step in sarcomatoid differentiation. Histopathology 2018;72:804–13.
[5] de Peralta-Venturina M, Moch H, Amin M, Tamboli P, Hailemariam S, Mihatsch M, et al. Sarcomatoid differentiation in renal cell carcinoma: a study of 101 cases. Am J Surg Pathol 2001;25:275–84.
[6] Lopez JI, Angulo JC. Pathological bases and clinical impact of intratumor heterogeneity in clear cell renal cell carcinoma. Curr Urol Rep 2018;19:3.
[7] Salama ME, Worsham MJ, DePeralta-Venturina M. Malignant papillary renal tumors with extensive clear cell change: a molecular analysis by microsatellite analysis and fluorescence in situ hybridization. Arch Pathol Lab Med 2003;127:1176–81.
[8] Diegmann J, Tomiuk S, Sanjmyatav J, Junker K, Hindermann W, von Eggeling F. Comparative transcriptional and functional profiling of clear cell and papillary renal cell carcinoma. Int J Mol Med 2006;18:395–403.
[9] Klatte T, Said JW, Seligson DB, Rao PN, de Martino M, Shuch B, et al. Pathological, immunohistochemical and cytogenetic features of papillary renal cell carcinoma with clear cell features. J Urol 2011;185:30–5.
[10] Haudebourg J, Hoch B, Fabas T, Cardot-Leccia N, Burel-Vandenbos F, Vieillefond A, et al. Strength of molecular cytogenetic analyses for adjusting the diagnosis of renal cell carcinomas with both clear cells and papillary features: a study of three cases. Virchows Arch 2010;457:397–404.
[11] Lek M, Karczewski KJ, Minikel EV, Samocha KE, Banks E, Fennell T, et al. Analysis of protein-coding genetic variation in 60,706 humans. Nature 2016;536:285–91.
[12] Landrum MJ, Lee JM, Benson M, Brown GR, Chao C, Chitipiralla S, et al. ClinVar: improving access to variant interpretations and supporting evidence. Nucleic Acids Res 2018;46:D1062–7.
[13] Gerlinger M, Catto JW, Orntoft TF, Real FX, Zwarthoff EC, Swanton C. Intratumour heterogeneity in urologic cancers: from molecular evidence to clinical implications. Eur Urol 2015;67:729–37.
[14] Rotterova P, Martinek P, Alaghehbandan R, Prochazkova K, Damjanov I, Rogala J, et al. High-grade renal cell carcinoma with emperipolesis: clinicopathological, immunohistochemical and molecular-genetic analysis of 14 cases. Histol Histopathol 2018;33:277–87.
[15] Faragalla H, Al-Haddad S, Stewart R, Yousef GM. The significance of florid giant cell component in renal cell carcinoma: a case report and review of the literature. Can J Urol 2010;17:5219–22.
[16] Fuzesi L, Gunawan B, Bergmann F, Tack S, Braun S, Jakse G. Papillary renal cell carcinoma with clear cell cytomorphology and chromosomal loss of 3p. Histopathology 1999;35:157–61.
[17] Moch H, Humphrey PA, Ulbright TM, Reuter VE. WHO Classification of Tumours of the Urinary System and Male Genital Organs. Lyon: IARC; 2016.
[18] Hes O, Comperat EM, Rioux-Leclercq N. Clear cell papillary renal cell carcinoma, renal angiomyoadenomatous tumor, and renal cell carcinoma with leiomyomatous stroma relationship of 3 types of renal tumors: a review. Ann Diagn Pathol 2016;21:59–64.
[19] Jia LJG, Al-Ahmadie H, Fine SW, Gopalan A, Sirintrapun SJ, Tickoo S, et al. Clear cell renal cell carcinoma with prominent papillary architecture: a rare morphologic variant supported by molecular evidence. Lab Invest 2018;98:353.
[20] Network CGAR. Comprehensive molecular characterization of clear cell renal cell carcinoma. Nature 2013;499:43–9.

1.6 Eosinofilní tumor s vakuolami (eosinophilic vacuolated tumor/EVT), nová jednotka

(komentář 1 publikace)

"High-grade oncocytic renal tumor": morphologic, immunohistochemical, and molecular genetic study of 14 cases.
He H, Trpkov K, Martinek P, Isikci OT, Maggi-Galuzzi C, Alaghehbandan R, Gill AJ, Tretiakova M, Lopez JI, Williamson SR, Montiel DP, Sperga M, Comperat E, Brimo F, Yilmaz A, Pivovarcikova K, Michalova K, Slouka D, Prochazkova K, Hora M, Bonert M, Michal M, Hes O.
Virchows Arch. 2018 Dec;473(6):725-738

Pojmem eosinofilní tumor s vakuolami (EVT) je doporučenými postupy GUPS [45] nově označována recentně popsaná renální neoplastická jednotka, která byla v úvodních studiích v literatuře popsána pod názvem "high-grade oncocytic tumor/HOT" [14] a "sporadic RCC with eosinophilic and vacuolated cytoplasm" [18]. Jedná se o tumor bez zdokumentovaného agresivního potenciálu, vykazující však paradoxně lehce matoucí high-grade morfologii.

Nádor je popisován jako tumor se solidní až "nested" architektonikou, fokálně s tubulocystickými okrsky, sestávající z objemných eosinofilních buněk s intracytoplazmatickými vakuolami. Jádra jsou oválná, s prominentními jadérky (odpovídá WHO/ISUP grade 3) a hladkou konturou. Buňky obsahují velké množství mitochondrií intracytoplazmaticky [37]. Tento vzhled tak řadí jednotku do široké skupiny diferenciálně diagnosticky obtížných eosinofilních, resp. onkocytických tumorů. Sekvenační analýza omezeného počtu těchto neoplázií prokázala mutace *TSC2* a *TSC1* genu a aktivační mutaci *MTOR* [18].

Jednotka, ač v literatuře při svém recentním popisu relativně mladá, patrně bude zahrnuta a zmíněna připravovanou WHO klasifikací.

1.6.1 „High-grade oncocytic renal tumor“: morphologic, immunohistochemical, and molecular genetic study of 14 cases

Skupina tzv. „onkocytických“ renálních tumorů patří v posledních letech k často studovaným nádorům. Stále častěji se na tomto poli v literatuře setkáváme se zcela novými provizorními jednotkami. Prezentovaná studie představuje a nově popisuje doposud nepopsanou nádorovou jednotku morfologicky odlišného high-grade oncocytického tumoru (HOT), dle současné WHO klasifikace jsou morfologicky identické tumory většinou klasifikovány jako renální karcinom „neklasifikovatelný/unclassified“. V multiinstitucionálních archivech bylo identifikováno 14 případů HOT, u kterých byla provedena detailní morfologická, imunohistochemická a molekulárně-genetická analýza.

Soubor zahrnoval tumory od 3 mužů a 11 žen, ve věkovém rozmezí 25 až 73 let (medián 50 let, průměr 49 let). Velikost tumorů se pohybovala mezi 1,5 – 7,0 cm v největším rozměru (medián 3 cm, průměr 3,4 cm), všechny tumory byly dle TMN (2017) pT1. U deseti pacientů byl dostupný „follow-up“ v průměrné délce trvání 28 měsíců (od 1 do 112 měsíců), všichni pacienti jsou dlouhodobě bez známek onemocnění, bez známek progrese. Mikroskopicky, tumory vykazovaly „nested“ či solidní a fokálně i tubulocystickou architektoniku a sestály z uniformních buněk s objemnou onkocytickou cytoplazmou. Četně byly zachyceny intracytoplasmatické vakuoly, avšak bez přítomnosti iregulárních (rozinkových) jader či perinukleárních projasnění (perinukleárních haló). U všech tumorů byla viditelná prominentní jadérka (odpovídaly tak grade 3 dle WHO/ISUP). Imunohistochemicky jsme prokázali pozitivitu AE1/3, CK18, PAX 8, MIA a SDHB ve všech 14 případech, CD117 vykazovalo pozitivitu u 9/14 případů, katepsin K v 13/14 případů a CD10 v 12/13 případů. Cytokeratin CK7 byl buď kompletně negativní či pouze fokálně pozitivní v 6/14 případů. Všechny tumory byly negativní v imunohistochemickém průkazu TFE3, HMB45, Melan A. Detailní výsledky molekulárně-genetických vyšetření jsou kompletně dostupné v přiložené publikaci. V žádném z případů genetické vyšetření nezastihlo translokaci genu TFEB či TFE3. arrayCGH u 3/9 tumorů neprokázala žádnou cytogenetickou abnormalitu, ve 3/9 případů byly detekovány ztráty chromozomu 19 (2x ztráta krátkého raménka (p) chromozomu 19, 1x ztráta celého chromozomu 19), u jednoho z případů konkurentně se ztrátou chromozomu 1. Dále cytogenetická studie prokázala ztrátu chromozomu 1 v 1/9 případů, ztrátu chromozomu 1 konkurentně se ziskem 19p v 1/9 tumorů a zisk chromozomu 5 společně se ztrátou 9q u 1/9 tumorů.

HOT je tumor s unikátní morfologií a vlastním imunofenotypem - tyto charakteristiky se u všech případů zdály relativně konzistentní a nesplňovaly diagnostická kritéria pro jiné dříve popsané eosinofilní renální tumory (RO, chromofóbní renální karcinom, MiTF RCC, SDH-deficientní renální karcinom a eosinofilní solidní a cystický renální karcinom). Dle našeho názoru by tak HOT měl být považován za novou renální neoplázii/jednotku.

Virchows Archiv (2018) 473:725–738
https://doi.org/10.1007/s00428-018-2456-4

ORIGINAL ARTICLE

"High-grade oncocytic renal tumor": morphologic, immunohistochemical, and molecular genetic study of 14 cases

Huiying He[1] · Kiril Trpkov[2] · Petr Martinek[3] · Ozlem Tanas Isikci[4] · Cristina Maggi-Galuzzi[5] · Reza Alaghehbandan[6] · Anthony J Gill[7,8,9] · Maria Tretiakova[10] · Jose Ignacio Lopez[11] · Sean R. Williamson[12] · Delia Perez Montiel[13] · Maris Sperga[14] · Eva Comperat[15] · Fadi Brimo[16] · Ali Yilmaz[2] · Kristyna Pivovarcikova[3] · Kveta Michalova[3] · David Slouka[17] · Kristyna Prochazkova[18] · Milan Hora[18] · Michael Bonert[19] · Michal Michal[3] · Ondrej Hes[3]

Received: 11 May 2018 / Revised: 29 August 2018 / Accepted: 10 September 2018 / Published online: 19 September 2018

Abstract

The spectrum of the renal oncocytic tumors has been expanded in recent years to include several novel and emerging entities. We describe a cohort of novel, hitherto unrecognized and morphologically distinct high-grade oncocytic tumors (HOT), currently diagnosed as "unclassified" in the WHO classification. We identified 14 HOT by searching multiple institutional archives. Morphologic, immunohistochemical (IHC), molecular genetic, and molecular karyotyping studies were performed to investigate these tumors. The patients included 3 men and 11 women, with age range from 25 to 73 years (median 50, mean 49 years). Tumor size ranged from 1.5 to 7.0 cm in the greatest dimension (median 3, mean 3.4 cm). The tumors were all pT1 stage. Microscopically, they showed nested to solid growth, and focal tubulocystic architecture. The neoplastic cells were uniform with voluminous oncocytic cytoplasm. Prominent intracytoplasmic vacuoles were frequently seen, but no irregular (raisinoid) nuclei or perinuclear halos were present. All tumors demonstrated prominent nucleoli (WHO/ISUP grade 3 equivalent). Nine of 14 cases were positive for CD117 and cytokeratin (CK) 7 was either negative or only focally positive in of 6/14 cases. All tumors were positive for AE1-AE3, CK18, PAX 8, antimitochondrial antigen, and SDHB. Cathepsin K was positive in 13/14 cases and CD10 was positive in 12/13 cases. All cases were negative for TFE3, HMB45, Melan-A. No *TFEB* and *TFE3* genes rearrangement was found in analyzable cases. By array CGH, complete chromosomal losses or gains were not found in any of the cases, and 3/9 cases showed absence of any abnormalities. Chromosomal losses were detected on chromosome 19 (4/9), 3 with losses of

✉ Ondrej Hes
hes@medima.cz

[1] Department of Pathology, Health Science Center, Peking University, Beijing, China

[2] Department of Pathology and Laboratory Medicine, Calgary Laboratory Services and University of Calgary, Calgary, AB, Canada

[3] Department of Pathology, Medical Faculty and Charles University Hospital Plzen, Alej Svobody 80, 304 60 Pilsen, Czech Republic

[4] Department of Pathology, Ankara Education and Research Hospital, Ankara, Turkey

[5] Robert J. Tomsich Pathology and Laboratory Medicine Institute, Cleveland Clinic, Cleveland, OH, USA

[6] Department of Pathology, Faculty of Medicine, University of British Columbia, Royal Columbian Hospital, Vancouver, BC, Canada

[7] Cancer Diagnosis and Pathology Group, Kolling Institute of Medical Research, Royal North Shore Hospital, St Leonards, NSW 2065, Australia

[8] University of Sydney, Sydney, NSW 2006, Australia

[9] NSW Health Pathology Department of Anatomical Pathology, Royal North Shore Hospital, St Leonards, NSW 2065, Australia

[10] Department of Anatomic Pathology, Harborview Medical Center, Seattle, WA, USA

[11] BioCruces Institute, Cruces University Hospital, University of the Basque Country (UPV/EHU), Barakaldo, Bizkaia, Spain

[12] Department of Pathology, Henry Ford Hospital, Detroit, MI, USA

[13] Department of Pathology, Instituto Nacional de Cancerologia, Mexico City, Mexico

[14] Department of Pathology, Riga Stradin's University, Riga, Latvia

[15] Sorbonne Université Service d'Anatomie et Cytologie Pathologiques Hôpital Tenon, HUEP, Paris, France

[16] Department of Pathology, McGill University, Montreal, QC, Canada

[17] Biomedicine Center, Charles University, Medical Faculty and Charles University Hospital Plzen, Prague, Czech Republic

[18] Department of Urology, Charles University, Medical Faculty and Charles University Hospital Plzen, Prague, Czech Republic

[19] Department of Pathology and Molecular Medicine, Faculty of Health Sciences, McMaster University, Hamilton, ON, Canada

the short arm (p) and 1 with losses of both arms (p and q). Loss of chromosome 1 was found in 3/9 cases; gain of 5q was found in 1/9 cases. On molecular karyotyping, 3/3 evaluated cases showed loss of heterozygosity (LOH) on 16p11.2-11.1 and 2/3 cases showed LOH at 7q31.31. Copy number (CN) losses were found at 7q11.21 (3/3), Xp11.21 (3/3), Xp11.22-11.21 (3/3), and Xq24-25 (2/3). CN gains were found at 13q34 (2/3). Ten patients with available follow up information were alive and without disease progression, after a mean follow-up of 28 months (1 to 112 months). HOT is a tumor with unique morphology and its IHC profile appears mostly consistent. HOT should be considered as an emerging renal entity because it does not meet the diagnostic criteria for other recognized eosinophilic renal tumors, such as oncocytoma, chromophobe renal cell carcinoma (RCC), TFE3 and TFEB RCC, SDH-deficient RCC, and eosinophilic solid and cystic RCC.

Keywords Kidney · Oncocytic · Chromophobe renal cell carcinoma · High grade · Oncocytoma · Hybrid · Immunohistochemistry · Molecular biology

Introduction

The spectrum of renal tumors composed of oncocytic or eosinophilic cells is broad. Renal oncocytoma and chromophobe renal cell carcinoma are recognized and well-defined tumors. Several other entities have also been widely discussed in the literature, including oncocytic papillary RCC (OPRCC), hybrid oncocytic/chromophobe tumors within the Birt-Hogg-Dubé (BHD) syndrome, renal oncocytosis, and sporadic cases with "hybrid" features of renal oncocytoma and chromophobe renal cell carcinoma [1–4]. Sporadic cases not associated with BHD syndrome, labeled "hybrid" renal oncocytoma/chromophobe renal cell carcinoma (HOCT), are currently considered a variant of chromophobe renal cell carcinoma, according to the ISUP Vancouver 2012 and WHO 2016 classifications [5] [6]. However, other oncocytic tumors exist with mixed and unusual morphology, that currently do not fit into any of the recognized categories and their diagnosis remains challenging [7].

In the current study, we describe a group of morphologically uniform tumors, composed predominantly of oncocytic cells with distinct cytoplasmic membranes, high-grade nuclei, and prominent intracytoplasmic vacuoles. This tumor type, to our knowledge, has not been previously reported.

Material and methods

Patients and tumors

After encountering several index cases in practice, we searched several institutional archives for additional examples, using the keywords oncocytic, eosinophilic, hybrid, chromophobe, unusual, high-grade, BHD-like, and translocation-like. The final review and case selection for the study was done by two pathologists (HH and OH). We excluded all tumors with papillary architecture, tumors associated with renal oncocytosis, BHD syndrome, succinate dehydrogenase (SDH)-deficient renal cell carcinoma (RCC), translocation t(6;11) RCC, and all tumors that did not satisfy the morphologic criteria. The final study cohort comprised 14 morphologically uniform cases that we labeled "high-grade oncocytic tumors" (HOT). One to 22 paraffin blocks were available for each case (main 6.25, median 12/blocks per case). Clinicopathologic and follow-up data were collected using the available medical records from the participating institutions.

Immunohistochemistry

Immunohistochemistry (IHC) stains were performed in one laboratory (University Hospital Plzen), using a Ventana Benchmark XT automated stainer (Ventana Medical System, Inc., Tucson, AZ, USA). The following primary antibodies were used: AE1-AE3 (monoclonal, BioGenex, San Ramon, CA, 1:1000), cytokeratin (CK) 8 (35betaH11, monoclonal, CellMarque, Rocklin, CA, 1: 400), CK18 (DC 10, monoclonal, DakoCytomation, Carpinteria CA, 1: 100), CK7 (OV-TL12/30, monoclonal, DakoCytomation, 1:200), CK20 (M7019, monoclonal, DakoCytomation, 1:100), alpha-methylacyl-CoA-racemase (AMACR) (P504S, monoclonal, Zeta, Sierra Madre, CA, 1:50), vimentin (D9, monoclonal, NeoMarkers, Westinghouse, CA, 1:1000), Ki67 (MIB1, monoclonal, Dako, Glostrup, Denmark, 1:1000), c-kit (CD117, polyclonal, Dako, 1:300), CD10 (Sp67, monoclonal, Ventana, RTU), anti-melanosome (HMB45, monoclonal, DakoCytomation, 1:200), Melan A (A103, monoclonal, Ventana, RTU), PAX 8 (MRQ-50, monoclonal, CellMarque, RTU), TFE3 (polyclonal, Abcam, Cambridge, UK, 1:100), cathepsin K (3F9, monoclonal, Abcam, 1:100), cyclin D1 (SP4-R, monoclonal, Cell Marque, 1:100), antimitochondrial antibody (113-1, monoclonal, Biogenex, 1:500), and SDHB (polyclonal, Sigma Aldrich, St. Luis, MO, 1:50). The primary antibodies were visualized using a supersensitive streptavidin-biotin-peroxidase complex (BioGenex). Internal biotin was blocked by standard protocol used by Ventana Benchmark XT automated stainer (hydrogene peroxide based). Appropriate positive and negative controls were also used. The immunohistochemical evaluation was based on the staining percentage of cells: focal positive < 50%, diffuse positive > 50%, negative (−) 0%,

Molecular genetic methods

DNA extraction

DNA was extracted from formalin-fixed paraffin-embedded (FFPE) tumor tissue using QIAsymphony DNA Mini Kit (QIAGEN, Hilden, Germany). We used an automated extraction system (QIAsymphony SP; QIAGEN), according to the manufacturer's supplementary protocol for FFPE samples (Purification of genomic DNA from FFPE tissue using the QIAamp DNA FFPE Tissue Kit and Deparaffinization Solution). The concentration and the purity of the isolated DNA was measured using NanoDrop ND-1000 (NanoDrop Technologies Inc., Wilmington, DE). DNA integrity was examined by amplification of control genes using a multiplex polymerase chain reaction (PCR).

Analysis of SDHB, SDHC, and SDHD gene mutation

Mutational analysis of complete CDS (CoDing Sequence) and exon-intron junctions of the SDHA, SDHB, and SDHC genes was performed using PCR and direct sequencing. Briefly, 100 ng DNA was added to a reaction mixture consisting of 12.5 μl of FastStart PCR Master (Roche Diagnostic, Mannheim, Germany), 10 pmol of forward and reverse primers (Table 1), and distilled water up to 25 μl. The amplification program consisted of denaturation at 95 °C for 9 min, 35 cycles of denaturation at 95 °C for 1 min, annealing 62 °C for 1 min, and extension at 72 °C for 1 min. The program was terminated by incubation at 72 °C for 7 min. The PCR products were separated by electrophoresis through a 2% agarose gel. Successfully amplified PCR products selected for sequencing analysis were purified with magnetic particles Agencourt AMPure (Agencourt Bioscience Corporation, A Beckman Coulter Company; Beverly, MA), both side sequenced using Big Dye Terminator Sequencing kit (Applied Biosystems) and purified with magnetic particles Agencourt CleanSEQ (Agencourt Bioscince Corporation, A Beckman Coulter Company), all according to the manufacturer's protocol. Samples were then run on an automated sequencer ABI Prism 3130xl (Applied Biosystems) at a constant voltage of 13.2 kV for 20 min. DNA sequences were compared with the reference sequence (http://www.ncbi.nlm.nih.gov) by the online program BLAST (http://blast.ncbi.nlm.nih.gov/Blast.cgi).

Array comparative genomic hybridization

Microarray processing Only samples meeting the required DNA quality (amplifiable fragment at least 400 base pairs long) were tested by array comparative genomic hybridization (aCGH). A SurePrint G3 Human CGH Microarray Kit, 8x60K (Agilent Technologies, CA, USA) with overall median probe spacing of 41 k bases was used for analysis. First, 400 ng of DNA was labeled using the SureTag Complete DNA Labeling Kit (Agilent). The procedure included Cy3 labeling of a test sample and Cy5 labeling of a reference sample. Commercially produced MegaPool Reference DNA of opposite sex than the sample (Kreatech Diagnostics, Amsterdam, Netherlands) was used as a reference material. The labeled specimen were mixed, dried, and hybridized overnight at 47 °C using Arrayit hybridization cassette (Arrayit Corporation, California, USA). Post-hybridization washing was done using SSC buffers with increasing stringency. Dried microarray was scanned with InnoScan 900 (Innopsys, France) at a resolution of 5 μm.

Image and data analysis Scanned image was analyzed and quantified by the Feature Extraction for CytoGenomics software (Agilent). Intensity values for each Cy5 and Cy3-labeled spot on the array were generated according to an appropriate grid template in the xml file. Minimum average absolute log ratio for deletion and amplification was set to more than 0.25. All genomic coordinates used for annotation are based on the March 2009 assembly of the reference genome GRCh37. Variations on sex chromosomes were artificially induced by using opposite se reference and were used only as an internal control and not included in the results.

Fluorescence in-situ hybridization

For the detection of *TFE3* and *TFEB* rearrangements, Zyto*Light*® SPEC TFE3 Dual Color Break Apart Probe (ZytoVision, Gmbh, Bremerhaven, Germany), and SureFish 6p21.1 *TFEB* break-apart (Agilent Technologies, Santa Clara, CA, USA) probe were used. All detected copy number variations were confirmed by corresponding fluorescence in-situ hybridization (FISH) probes: Zyto*Light*® SPEC 1p36/1q25 Dual Color Probe, Zyto*Light*® SPEC 19q13/19p13 Dual Color Probe, (both ZytoVision), and Vysis EGR1 (5q31) FISH Probe (Vysis/Abbott Molecular, IL, USA). The procedure was performed as described [8]. Before applying onto specimen, both probes for *TFEB* rearrangement (orange and green) were mixed with deionized water and LSI Buffer (Vysis/Abbott Molecular) in 1:1:1:7 ratio, and the probe for 5q31 enumeration was mixed with deionized water and LSI Buffer in 1:2:7 ratio. ZytoVision probes were factory premixed. The results were interpreted as described previously [9] [8].

Molecular karyotyping (whole-genome copy number analysis)

Molecular karyotyping was performed to identify candidate CN variations (amplification/deletion and loss-of-heterozygosity) from FFPE tissue blocks in three cases (cases 1–3). For the OncoScan assay, 5 mm sections from formalin-fixed and paraffin-embedded (FFPE) tissue blocks were utilized for DNA isolation. In brief, after the FFPE sections were deparaffinized

Table 1 *SDH* Primers

Gene	Exon number and direction	Sequence
SDHB	1-F	GGTCCTCAGTGGATGTAGGC
	1-R	TCTCTGAGGCTCCAGGACTC
	2-F	TCTGTTGTGCCAGCAAAATG
	2-R	TCTCCTTCAATAGCTGGCTTTC
	3-F	ATTCCGAAGGTGACCTGAGA
	3-R	AGCCCAACAGGAATGAAATG
	4-F	AGTATTTGGGGCAGGACTGA
	4-R	CCCCCATGCAAATAAAAACA
	5-F	AAGCTGAGGTGATGATGGAA
	5-R	CACACTCCTGGCAATCATCTT
	6-F	GTCTCTCCCGTCACAAGCTC
	6-R	CCTCAGAATGGCTGGCTTAC
	7-F	TGGCAGCTCAGCTAATCATC
	7-R	ACTTCTGGCGTGTCAGCTCT
	8-F	GGGTTTTCCCTTTCAGTTTCA
	8-R	TGCTGTATTCATGGAAAACCAA
SDHC	1-F	GCGTCACTTCCGTCCAGA
	1-R	CTGCCCAGGCACAGGATA
	2-F	TCTATCCCTTCACCCCTAAAAA
	2-R	AGCGAGACTCCGTCTCAAAA
	3-F	GATTACAGGCCTGAGCAACC
	3-R	CTGGCTCCAGAATCCTTCCT
	4-F	TTCCTTTTTAAAATTGTCTTTGTGTG
	4-R	TTCAAAGGAGGCGGAGACTA
	5-F	GCTGTGACAAGCTACTTGGTTTT
	5-R	AGTCTCCCCACTCCCTTCAC
	6-F	TGTCCTATTTACTGAAATTCCTTTTT
	6-R	CTGCTCCAAGGAGATCTGAAA
SDHD	1-F	GTGGGAATTGTCGCCTAAGT
	1-R	AGGCTACGCTAAGCACCTCA
	2-F	TCAGTCCTGTTAAAGGAGAGGTTC
	2-R	CTAGAGCCCAGAAAGCAGCA
	3-F	CATCAACTTTTATGAATCTGGTCCT
	3-R	CACAGCAAACAAACTGAGCA
	4-F	TTTTTGCAGCCAAGTTATCTGT
	4-R	GCAGAGGCAAAGAGGCATAC

with xylene and washed with ethanol, purification of genomic DNA was performed according to the protocol of the QIAamp DNA FFPE Tissue kit (Cat No. 56404, QIAGEN, Valencia, CA). The quality and concentration of double-strand DNA were determined using Nanodrop Spectrophotometer, Agilent Bioanalyzer, and the fluorescence-based Qubit dsDNA HS Assay Kit (Q32851). Genomic DNA was subjected to OncoScan FFPE MIP-based assay. The data were analyzed using the Nexus Express for OncoScan Copy Number software (Version 7.5; BioDiscovery, El Segunda, CA).

Results

Clinicopathologic findings

Clinicopathologic findings are summarized in Table 2. There were 3 men and 11 women, with median age of 50 years (mean 49; range 25 to 73 years). Tumor size ranged from 1.5 to 7.0 cm in greatest dimension (median 3, mean 3.4 cm). All tumors were stage pT1 (12—pT1a and 2—pT1b) and no invasion into the perinephric fat, renal sinus,

Table 2 Clinicopathologic features

Case	Age (years)	Gender	Size (cm)	Stage	Follow up (months)	Status
1	73	F	2.5	T1aN0M0	112	AW
2	59	F	1.5	T1aN0M0	76	AW
3	37	F	3.0	T1aN0M0	34	AW
4	36	F	2.4	T1aN0M0	14	AW
5	25	M	3.8	T1aN0M0	12	AW
6	31	F	7.0	T1bN0M0	12	AW
7	55	F	2.1	T1aN0M0	NA	NA
8	72	F	3.0	T1aN0M0	11	AW
9	54	F	3.2	T1aN0M0	NA	NA
10	37	F	3.1	T1aN0M0	12	AW
11	73	M	2.3	T1a, No, Mo	1	AW
12	54	M	2.6	T1a, N0, M0	NA	NA
13	46	F	4.6	T1a, N0, M0	15	AW
14	40	F	7.0	T1bNxMx	NA	NA

M male, *F* female, *NA* not available, *AW* alive and well

or renal vein branches was identified in any case. Follow-up was available for ten patients, ranging from 1 to 112 months (median 12, mean 28 months). Disease recurrences or metastases were not documented in any of the patients.

Gross and microscopic features

All tumors were circumscribed and appeared solid (Fig. 1a). In one case, focal cystic change was found grossly (Fig. 1b). The cut surface was tan-mahogany, gray, or dark brown and there was no gross evidence of necrosis or hemorrhage. The summary of histologic features is shown in Table 3. All tumors were well-circumscribed and lacked a dense fibrous peripheral capsule. Predominant architectural pattern was nested or solid, making up 60–95% of tumor in all cases. Nested growth pattern, set in the background of loose fibromatous stroma, as seen in renal oncocytoma, was found at least focally in 13/14 cases. Entrapped non-neoplastic renal tubules and prominent thick-walled vessels were present in all cases, particularly at the periphery of the tumor (Fig. 2). Only rare and limited foci of hemorrhage were noted. Focal tubulocystic pattern was present in all cases; only in one case it was dominant. The tubules were filled by serosanguinous fluid without foam cells. Limited foci of trabecular growth were present in 3/14 cases.

All tumors were composed of cells with voluminous cytoplasm, which was either eosinophilic (oncocytic) or clear. The

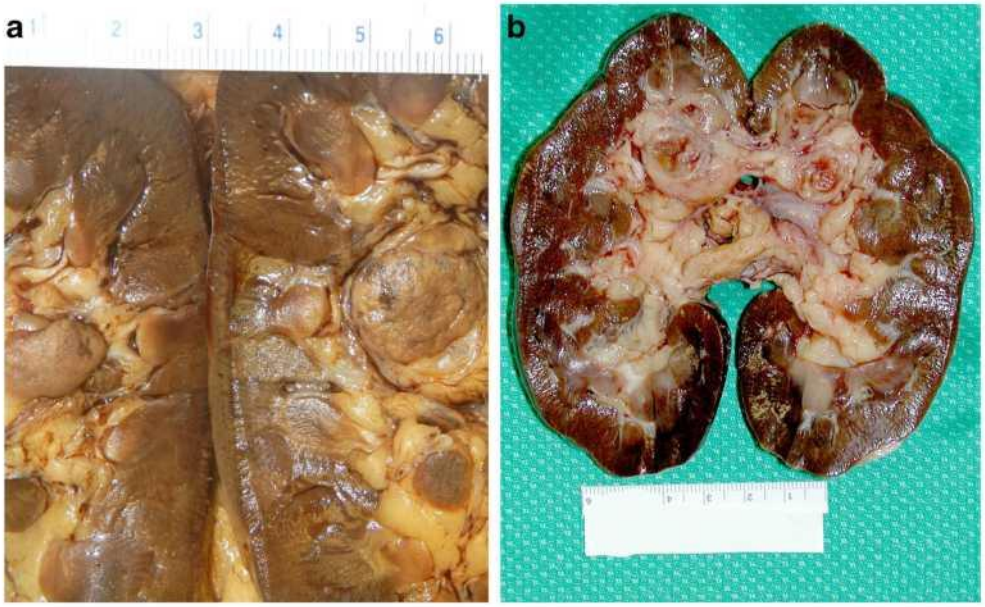

Fig. 1 **a** The tumors were all circumscribed, but unencapsulated solid masses, mostly tan to brown in cut section. **b** Central cystic change was documented in one case

Table 3 Morphologic features

Case	Growth pattern			Cytoplasm			Nuclei					Entrapped tubules	Thick wall vessels	Edematous stroma
	Nested (%)	Solid (%)	Tubulocystic (%)	Trabecular	Oncocytic (%)	Pale eosinophilic/clear (%)	Vacuoles	Wrinkled	Round	Grade				
1	35	60	5	0	70	30	+	–	+*	III		+	+	+
2	60	0	10	30	90	10	+	–	+	III		+	+	+
3	30	65	5	0	80	20	+	–	+	III		+	+	+
4	0	95	5	0	40	60	+	–	+	III		+	+	–
5	30	0	40	30	90	10	+	–	+	III		+	+	+
6	15	80	5	0	60	40	+	–	+	III		+	+	+
7	30	65	5	0	90	10	+	–	+*	III		+	+	+
8	95	0	5	0	80	20	+	–	+	III		+	+	+
9	30	60	10	0	90	10	+	–	+*	III		+	+	+
10	90	10	0	0	90	10	+	–	+	III		+	+	+
11	30	70	0	0	90	10	+	–	+	III		+	+	+
12	20	60	20	0	90	10	+	–	+	III		+	+	+
13	40	60	0	0	50	50	+	–	+*	III		+	+	+
14	10	90	0	0	30	70	+	–	+*	III		+	+	+

eosinophilic cells had variably granular cytoplasm and contained frequent and large cytoplasmic vacuoles or inclusions of flocculent eosinophilic material. Intracytoplasmic vacuoles were found in all 14 cases, but they were prominent in 6/14 cases. The cells with clear to pale cytoplasm were admixed with the eosinophilic cells; they showed mosaic-like pattern in one case (Fig. 3). The cell membranes were usually distinct and the nuclei were typically round, and less often oval to slightly elongated, demonstrating smooth nuclear contours. Slightly irregular nuclei or binucleation were encountered in some cases, but prominent nuclear irregularities, with "wrinkled" or "raisinoid" nuclei were not seen in any case. Conspicuous and enlarged nucleoli, corresponding to WHO/ISUP grade 3, were present in the majority of cells in all cases. Mitoses were encountered infrequently. An ambiguous biphasic cellular appearance was present in two cases, consisting of larger and smaller eosinophilic cells, which formed structures, vaguely resembling those seen in translocation t(6;11) RCC (Fig. 4). Scattered intratumoral lymphocytes were seen in 2/14 cases. Morphologic variation of all 14 cases is showed in composite figure (Fig. 5).

Immunohistochemistry findings

The results of IHC staining are summarized in Table 4. Positive CD117 was found in 9/14 cases. Eight of 14 cases were negative for CK7 (only occasional single cell was positive) and 6/14 were only focally positive. All tumors were positive for CK18 and AE1/AE3, PAX 8, and antimitochondrial antigen (MIA). Reactivity for cathepsin K was found in 13/14 cases and cyclin D1 showed mostly focal reactivity in all cases. CD10 was positive in 12/14 cases and AMACR was positive in 11/14 (in some cases, either focal or weak). SDHB was retained in all cases, typically demonstrating strong and diffuse reactivity (Fig. 6). All tumors were completely negative for TFE3, HMB45, and Melan-A; they were also negative for vimentin (although only rare, scattered cells were reactive in some cases).

Molecular genetic results

TFEB, SDHA, SDHB, and SDHC gene analysis

All analyzable cases were negative for a break in the *TFEB* and *TFE3* gene. All but one case were negative for *SDHB* variants or mutations. In one case (no. 13), the following *SDHB* variant was found: c.487 T > C (p.Ser163Pro). Online database review indicated that this represented a benign polymorphism (ref: https://www.ncbi.nlm.nih.gov/clinvar/variation/12792/ accessed February 25, 2018). The IHC for SDHB demonstrated retained positive staining in this case, further confirming this as an incidental benign polymorphism rather than a pathogenic mutation (Table 5).

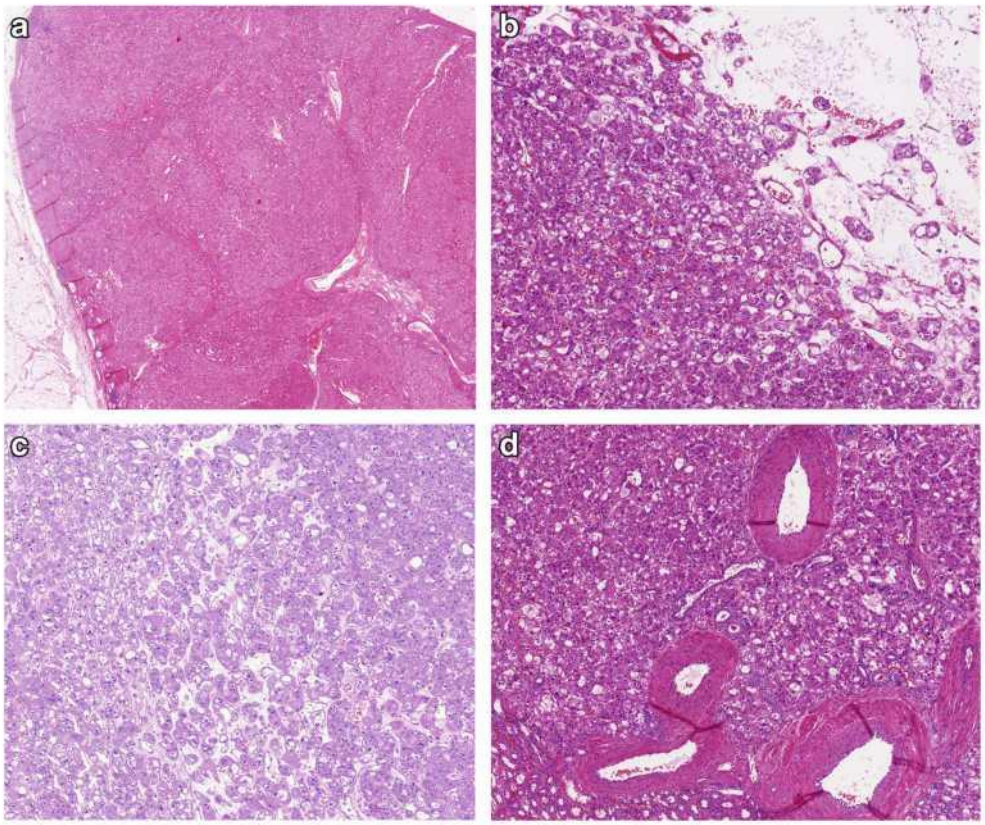

Fig. 2 **a** Tumors were well-circumscribed and lacked a thick fibrous capsule. **b** Predominant architectural pattern was nested or solid, at least focally set in background of loose fibromatous stroma. **c** In some cases, loose stroma with islets of neoplastic cells resembled those seen in renal oncocytoma. **d** Entrapped non-neoplastic renal tubules and prominent thick-walled vessels were present in all cases, particularly at the periphery of the tumor

All cases were negative for *SDHA*, *SDHC* variants, or mutations.

aCGH and molecular karyotype analysis

Of nine cases analyzable by aCGH, the most frequent CN losses were detected on chromosome 19 (4/9), with three cases showing losses of the short arm (p) and one demonstrating losses of both arms (p and q). The second most common CN alteration was the loss of chromosome 1 (3/9 cases); gain of chromosome 5q was found in 1/9 cases. Losses of chromosome 1 and gain of chromosome 5q were successfully confirmed by FISH. Multiple chromosomal or CN gains or losses, as seen for example in chromophobe renal cell carcinoma, were not found in any case. Due to the assay setup, the changes on gonosomes were not analyzable (Table 5).

Molecular karyotyping analysis was available in three cases (no. 1–3); they all showed diploid pattern without either complete chromosomal losses or gains. All three evaluated cases demonstrated loss of heterozygosity (LOH) on 16p11.2-11.1

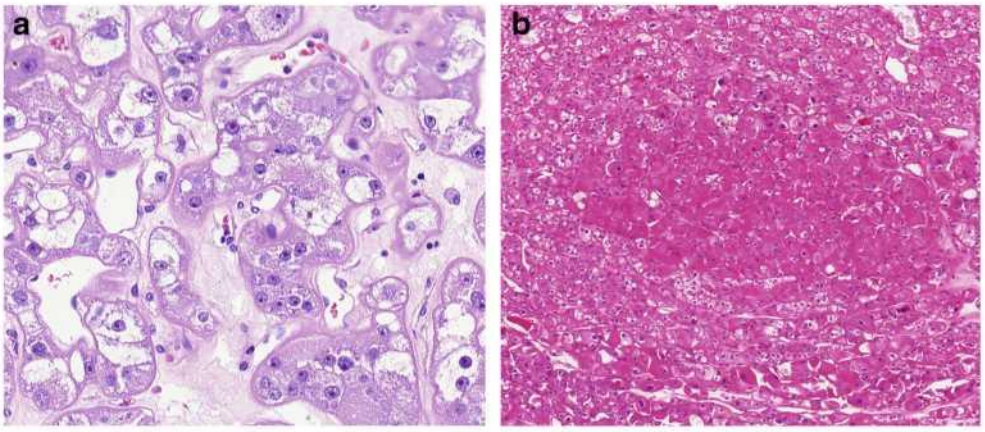

Fig. 3 **a** All tumors were composed of cells with voluminous cytoplasm, which was mostly oncocytic. **b** The oncocytic cells had variably granular cytoplasm and contained frequent and large cytoplasmic vacuoles or inclusions of flocculent eosinophilic material. **c** Intracytoplasmic vacuoles were found in all cases and were prominent in 6/14 cases. **d** The cells with clear to pale cytoplasm and oncocytic (eosinophilic) cells showed mosaic-like pattern in one case

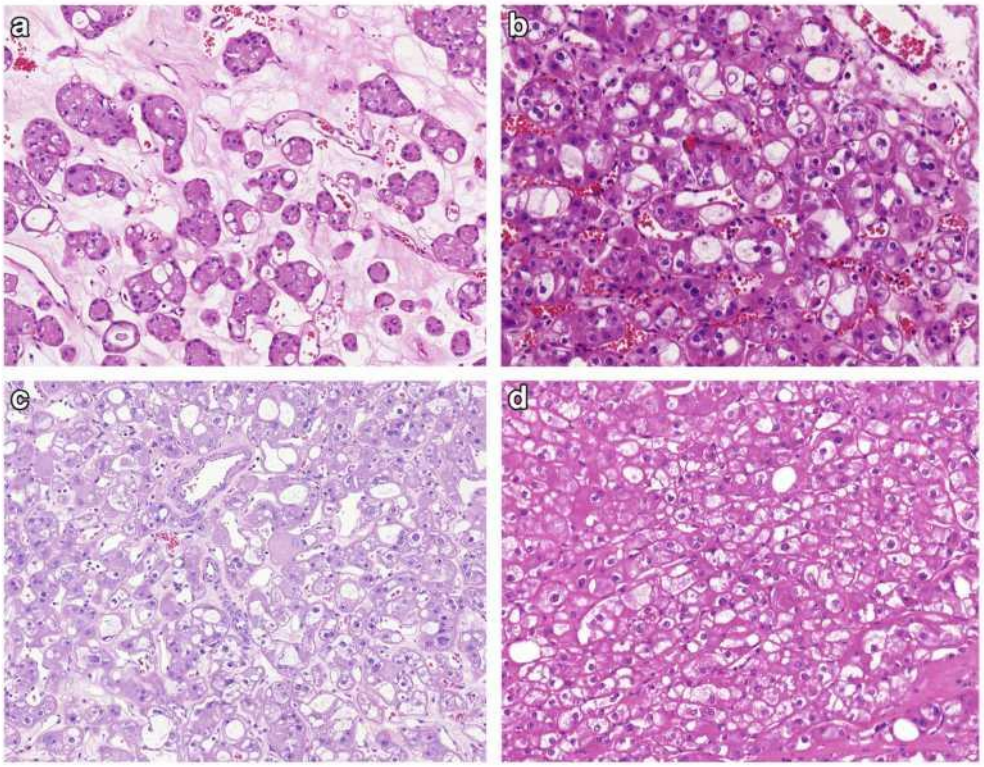

Fig. 4 **a**, **b** An ambiguous biphasic cellular appearance resembling translocation t(6;11) RCC was present in two cases

(3/3) and 2/3 cases showed LOH at 7q31.31. Copy number (CN) losses were found at 7q11.21 (3/3), Xp11.21 (3/3), Xp11.22-11.21 (3/3), and Xq24-25 (2/3). CN gains were found at 13q34 (2/3) (Table 6).

Discussion

For many years, we were aware of renal tumors that shared some morphologic features of renal oncocytoma and chromophobe renal cell carcinoma, as well as of HOCT. The tumors however, included in this study, show slightly different features than these three categories. The summary of the clinical, morphologic, IHC, and molecular genetic features of these tumors, which we designated "high-grade oncocytic" tumors (HOT), is shown in Table 7. HOT demonstrate a fairly uniform morphology and is composed of larger cells with eosinophilic granular cytoplasm with prominent cytoplasmic membranes. A significant component of the cells contain intracytoplasmic, frequently large vacuoles, resembling signet ring cell. A second cell component, often variable in size, demonstrates pale to clear cytoplasm. The nucleoli are typically enlarged and conspicuous, corresponding to WHO/ISUP grade 3. They often show prominent thick-walled vessels at the periphery, as well as entrapped non-neoplastic tubules. By IHC, most cases are positive for CD117, negative or focally positive for CK7, and are also positive for MIA, cathepsin K (13/14), and CD10 (12/14).

It can be argued that the cases included in the current series may fall in the broad category of the "hybrid" oncocytic tumors, because of their overlapping morphology with renal oncocytoma and chromophobe renal cell carcinoma and their indolent clinical course. We are fully aware of the ambiguities associated with the term "hybrid tumor," which is often used to designate tumors with overlapping features between renal oncocytoma and chromophobe renal cell carcinoma [7, 10]. Although cases included in this series share some morphologic and IHC similarities with and chromophobe renal cell carcinoma, they do not fit the established criteria of these entities.

One also has to be aware that there are morphologic variations of renal oncocytoma, which include predominant multicystic pattern, small cell variant—with or without pseudorosettes, and presence of numerous atypical bizarre cells [11, 12] [6]. Chromophobe renal cell carcinoma is characterized by solid sheets of cells with distinct or accentuated cell borders, perinuclear halos and frequent irregular ("rasinoid") nuclei. Two types of cells are typical for chromophobe renal cell carcinoma: large plant-like cells with mostly clear cytoplasm and smaller cells with eosinophilic cytoplasm, corresponding to the so-called classic and eosinophilic variants. Several chromophobe renal cell carcinoma morphologic subtypes were also described and include pigmented,

Fig. 5 Composite figure shows all described cases to allow to the readers ▶ to appreciate morphologic variations in between the cases. **a** case 1, **b** case 2, **c** case 3, **d** case 4, **e** case 5, **f** case 6, **g** case 7, **h** case 8, **i** case 9, **j** case 10, **k** case 11, **l** case 12, **m** case 13, **n** case 14

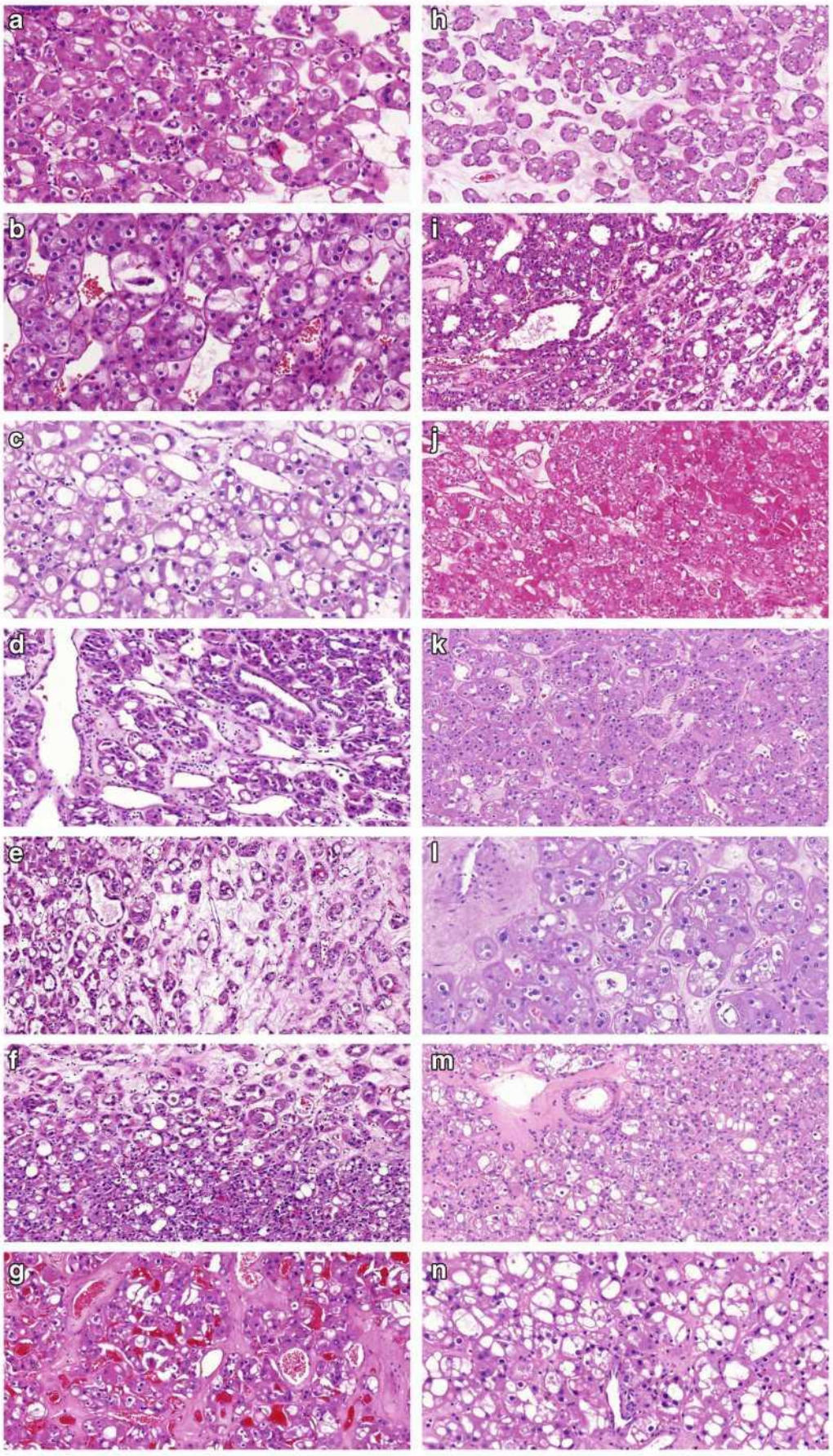
a
h
b
i
c
j
d
k
e
l
f
m
g
n

Table 4 Immunohistochemical analysis results

Case	CD117	CK7	CK20	AE1/AE3	CK8	CK18	Vimentin	CathepsinK	MIA	CyclinD1	SDHB	MelanA	HMB45	TFE3	Pax8	AMACR	CD10	Ki67
1	–	–	F+*	+	w+	+	–	–	+	F+	+	–	–	–	+	–	–	0–2/hpf
2	+	–	+	F+	+	+	–	+	+	F+	+	–	–	–	+	F +	+	0–1/hpf
3	+	F+	F+*	+	+	+	–	+	F+	+	+	–	–	–	+	–	+	3–5/hpf
4	–	F +	–	F+	–	+	–	+	F+	F+*	+	–	–	–		+	+	0–1/hpf
5	+	–	–	+	+	+	–	+	+	F+*	+	–	–	–	+	+	+	1–2/hpf
6	+	–	–	+	+	+	–	+	+	F+	+	–	–	–	+	F+	+	0–1/hpf
7	+	–	F+*	+	+	+	–	F+	+	F+	+	–	–	–	+	+	+	2–4/hpf
8	+	F+	–	+	+	+	–	+	+	F+	+	–	–	–	+	+	+	0–1/hpf
9	+	–	–	+	+	+	–	+	+	F+	+	–	–	–	+	w+	+	1–3/hpf
10	–	–	–	F+	+	+	–	+	+	F+	+	–	–	–	+	w+	+	0–1/hpf
11	–	F+	–	+	+	+	–	+	+	F+	+	–	–	–	+	F+	–	0–2/hpf
12	–	–	–	F+	F+	+	–	F+	+	+	+	–	–	–	+	+	+	1–3/hpf
13	+	F+	F+	F+	–	+	–	+	+	F+	+	–	–	–	+	+	+	2–4/hpf
14	+	F+	F+	+	–	+	–	+	+	F+	+	–	–	–	+	–	+	1–2/hpf

F focal (less than 50% of cells positive), + positive, – negative, *w* weak, * single cells, *MIA* antimitochondrial antibody, *SDHB* succinate dehydrogenaze B, *hpf* high power field

adenomatoid, multicystic, and chromophobe renal cell carcinoma with neuroendocrine differentiation (or with neuroendocrine-like differentiation) [13–16].

So-called "hybrid oncocytic tumor" (HOCT) is a rare tumor with overlapping morphology between renal oncocytoma and chromophobe renal cell carcinoma. Although HOCT may occur sporadically as a solitary neoplasm, it is more frequently encountered as a multifocal tumor either in association with renal oncocytosis or in patients with BHD syndrome [17–19] [20] [21]. All three HOCT groups share similar histological features, including a mixture of architectural and cytologic features which overlap those of renal oncocytoma and chromophobe renal cell carcinoma. According to the WHO classification of genitourinary tumors 2016, these tumors are currently considered either subtypes or peculiar variants of chromophobe renal cell carcinoma [5, 6]; there is also a debate how this terminology should be used in practice [7].

The main morphologic differences between cases we describe in this study as HOT and the tumors previously included in the HOCT spectrum include their prominent cytoplasmic membranes, intracytoplasmic vacuoles, thick-walled vessels, and the enlarged high-grade nuclei with prominent nucleoli. All tumors in this series were solitary and were not associated with oncocytosis or BHD syndrome. Great majority of the tumors were small (11/14 were less than 4 cm), all demonstrated stage pT1 (TNM 2009, AJCC 2017); grossly they were solid and tan to brown. Despite the high-grade nuclei in HOT, no aggressive clinical course was recorded in any case, although the follow-up period was relatively short.

High-grade cytology accompanied by non-aggressive clinical behavior is not a rare phenomenon in renal tumors. For example, a recently described eosinophilic solid and cystic (ESC) RCC usually shows WHO/ISUP grade 3, but in great majority of cases exhibits indolent behavior [22–24]. Similarly, high-grade morphology can also be seen in t(6;11) translocation RCC, but only few cases with aggressive behavior have been described [25].

The evidence gained from the molecular studies on cases included in this series should be considered preliminary, because only limited number of cases were analyzed; more detailed molecular analysis by next-generation sequencing was not performed. It is important however to emphasize that complete chromosomal losses or gains, as typically seen in chromophobe renal cell carcinoma, were not found in any of the cases, and 3/9 cases showed absence of any abnormalities by aCGH. Losses of the short arm or both arms of chromosome 19 were only found in 4/9 cases (1/3 cases also showed CN loss at 19p11 by molecular karyotyping), as well as loss of chromosome 1 (3/9 cases). Of note, loss of chromosome 1 or part of it is often found in RO. We also ruled out the possibility that these cases represent either an SDH-deficient RCC or t(6;11) MiTF translocation RCC.

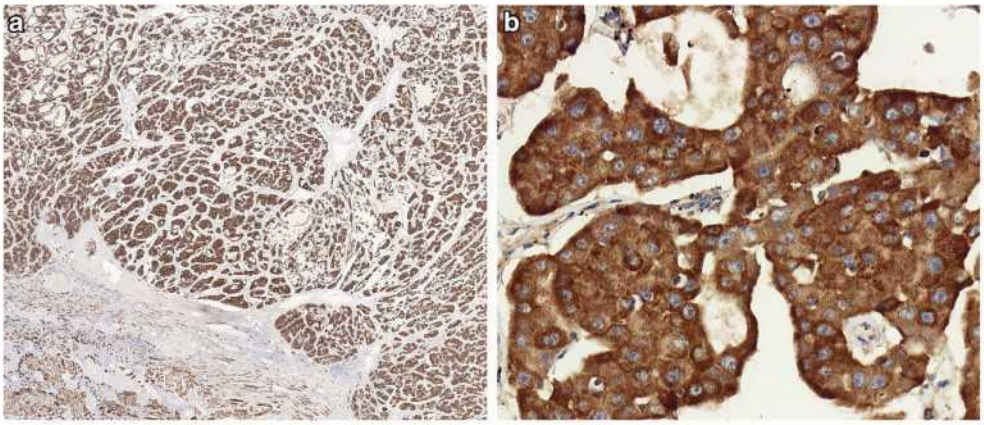

Fig. 6 **a** Staining of SDHB was retained in all cases. **b** All tumors were diffusely positive for antimitochondrial antigen

The differential diagnosis of HOT also includes several rare renal tumors. Summary of morphologic, immunohistochemical, and molecular genetic features of HOT is showed in Table 7.

Some MiTF t(6;11) translocation RCC may resemble HOT. t(6;11) translocation RCCs are arranged mostly in solid-alveolar pattern, with large pale to eosinophilic cells with prominent nuclei and nucleoli, and frequent thick-walled vessels [26, 27]. The typical morphology includes pseudorosettes, composed of basal membrane material surrounded by smaller cells with scanty cytoplasm. These tumors are immunoreactive for cathepsin K, HMB45, Melan A, and TFEB [28]. Molecular genetic analyses may help detect either breaks in *TFEB* gene or expression of TFEB protein [6, 29]. None of the HOT cases showed true pseudorosettes, but thick-walled vessels were typically found. However, islets of deep eosinophilic cells resembling architecture known for t6;11 translocation RCC were found in two cases in our series. All cases of HOT were negative for HMB45 and Melan A, but showed uniform positivity for cathepsin K, which is considered specific by some authors for t(6;11) translocation RCC [30]. We also did not find abnormalities in the *TFEB* gene in any of the analyzed cases in this study.

Oncocytic papillary renal cell carcinoma is another not fully characterized tumor subtype, which demonstrates papillary or solid-papillary architecture, voluminous, finely granular eosinophilic cytoplasm, and oncocytoma-like nuclei. Larger foci of foam cells are invariably present. Oncocytic papillary renal cell carcinoma is positive for vimentin, MIA, and AMACR in most cases. Immunoreactivity for CK7 is variable [2] [6]. Oncocytic papillary renal cell carcinoma showed frequent tri/polysomy of chromosomes 7 and 17, but this feature was not a constant finding [1] [31]. HOT in contrast lacks papillary architecture, foam cells, it is negative for vimentin, and it does not show trisomy of chromosomes 7 and 17.

Succinate dehydrogenase (SDH)-deficient RCC is a recently recognized entity in the WHO 2016 classification [6]. The most typical morphological features include the presence of smaller eosinophilic cells with cytoplasmic vacuoles and inclusions, imparting a "bubbly" appearance of the cytoplasm, which is somewhat different to the granular eosinophilic appearance found in HOT [32, 33] [7]. All SDH-deficient RCCs demonstrate negative staining for SDHB by IHC, which was in contrast positive in all cases included in this series. In the era of widespread availability of molecular testing, it is important not to interpret all genetic variants as pathogenic mutations particularly in tumors that are difficult to classify. The identification of a benign *SDHB* polymorphism [c.487 T > C (p.Ser163Pro)] in case no. 13 in which there was preserved SDHB by IHC illustrates the importance of critically examining the morphological context and functional significance of all genetic variants identified by molecular testing before attributing pathogenicity.

ESC RCC is another recently described entity, which has been found in association with the tuberous sclerosis complex [34], but it is more often sporadic [24, 35]. ESC RCC occurs predominantly in females and show solid and cystic growth, with voluminous eosinophilic cells showing cytoplasmic, coarse granularity, and rare delicate vacuoles (resembling leishmaniosis-like bodies). Great majority of ESC RCC exhibit positivity for CK20 at least focally. HOT lacked cystic areas grossly, frequently contained cells with clear cytoplasm or large cytoplasmic vacuoles, and no coarse cytoplasmic granularity or leishmaniosis-like bodies were seen. Although

Table 5 Molecular karyotypic findings

Case	LOH	CN gain	CN loss
1	2p12-11.2; 3p21.31-21.2; 7q31.31; 16p11.2-11.1	7p22.3	7q11.21; 19p11; 22q11.23; Xp11.21; Xp11.22-11.21
2	16p11.2-11.1; Xp22.13-22.12	13q34; 17q25	7q11.21; Xq11.1; Xq24-25; Xp11.21; Xp11.22-11.21
3	7q31.31; 11p11.2; 16p11.2-11.1; Xp22.13; Xp11.22; Xq11.1	13q34; 22q11.23	7q11.21; 8p11.22; Xq24-25; Xp11.21; Xp11.22-11.21

Table 6 Molecular genetic findings: analysis of *SDH*, *TFEB*, and aCGH

Case	SDH (SDHB, SDHC, SDHD)	TFEB	TFE3	aCGH
1	Negative	Negative	NA	Loss of chr 1, loss of chr 19p
2	Negative	Negative	Negative	Loss of chr 19p
3	Negative	Negative	Negative	Loss of chr 19
4	Negative	Negative	Negative	Negative
5	Negative	Negative	Negative	Negative
6	negative	Negative	Negative	Loss of chr 1
7	NA	NA	Negative	NA
8	Negative	Negative	Negative	NA
9	Negative	Negative	Negative	NA
10	Negative	Negative	Negative	Negative
11	Negative	Negative	Negative	NA
12	Negative	Negative	Negative	Loss of chr 1, gain of chr 19p
13	c.487 T > C p.(Ser163Pro)	Negative	NP	NA
14	Negative	Negative	Negative	Gain of chr 5q, loss of chr 9q

NA not analyzable, *NP* not performed

5/14 HOT cases contained rare, isolated cells positive for CK20, they did not show more extensive areas of positivity.

In summary, we report a group of distinct renal oncocytic tumors with high-grade nuclear features, which we designated HOT. Despite some morphologic similarities, primarily to renal oncocytoma, chromophobe renal cell carcinoma, HOCT, and t(6;11) translocation RCC, these tumors do not fit into any of these categories. They are also different from some less common, novel, or emerging renal entities with eosinophilic features. Most of the HOT were small and of low stage and despite the high-grade nuclear features, they did not show aggressive clinical course. However, this cohort is relatively small and with short follow-up. We hope that this report will allow surgical pathologists to re-evaluate and study tumors previously considered "unclassified," hopefully resulting in identification of additional examples, and leading to their better characterization and classification.

Contributions Huiying He and Ondrej Hes: revision of all cases, evaluation of immunohistochemistry. Kiril Trpkov and Ondrej Hes: design of study. Petr Martinek: molecular genetics. Ozlem Tanas Isikci, Kristyna Pivovarcikova: evaluation of immunohistochemistry. Anthony J Gill: evaluation of SDHB mutation and SDHB staining interpretation. Cristina Maggi-Galuzzi, Reza Alaghehbandan, Maria Tretiakova, Jose Ignacio Lopez, Sean Williamson, Delia Perez Montiel, Maris Sperga, Eva Comperat, Fadi Brimo, Michael Bonert, and Ali Yilmaz: case contribution, providing follow up data, and help with discussion. Kveta Michalova, David Slouka: follow up information, photodocumentation, Kristyna Prochazkova, Milan Hora: evaluation of clinical data. Michal Michal: discussion.

Funding The study was supported by the Charles University Research Fund (project number Q39) and by the project Institutional Research Fund of University Hospital Plzen (FN 00669806).

Compliance with ethical standards

Study design has been approved by local ethical committee (Charles University, Medical School Plzen) LEK FN Plzeň.

Table 7 Summary of the key features of high-grade oncocytic tumor (HOT)

Clinical	Female predominance, usually low stage, good prognosis
Gross	Solid, tan, mahogany-brown, single tumors
Light microscopy	Architecture: solid and nested, occasionally tubulocystic or trabecular
	Cytology: oncocytic cells with mostly round to oval nuclei, prominent nucleoli (WHO/ISUP grade 3). Focally cells with clear to pale cytoplasm
Immunohistochemistry	Positive: AE1/AE3, CK18, PAX 8, MIA, SDHB, cathepsin K, CD10
	Negative: TFE3, HMB45, Melan-A, vimentin
Molecular karyotype	LOH: 16p11.2-11.1 (3/3), 7q31.31 (2/3)
	CN loss: 7q11.21 (3/3), Xp11.21 (3/3), Xp11.22-11.21 (3/3), Xq24-25 (2/3) CN gain: 13q34 (2/3)
aCGH	Chr. 19 loss (4/9): 3 with 19p loss and 1 with loss of 19p and q)
	Chr. 1 (3/9)

LOH loss of heterozygosity, *CN* copy number

Conflict of interest The authors declare that they have no conflict of interest.

References

1. Hes O, Brunelli M, Michal M, Cossu Rocca P, Hora M, Chilosi M, Mina M, Boudova L, Menestrina F, Martignoni G (2006) Oncocytic papillary renal cell carcinoma: a clinicopathologic, immunohistochemical, ultrastructural, and interphase cytogenetic study of 12 cases. Ann Diagn Pathol 10:133–139. https://doi.org/10.1016/j.anndiagpath.2005.12.002
2. Lefevre M, Couturier J, Sibony M, Bazille C, Boyer K, Callard P, Vieillefond A, Allory Y (2005) Adult papillary renal tumor with oncocytic cells: clinicopathologic, immunohistochemical, and cytogenetic features of 10 cases. Am J Surg Pathol 29:1576–1581
3. Pavlovich CP, Walther MM, Eyler RA, Hewitt SM, Zbar B, Linehan WM, Merino MJ (2002) Renal tumors in the Birt-Hogg-Dube syndrome. Am J Surg Pathol 26:1542–1552
4. Petersson F, Gatalica Z, Grossmann P, Perez Montiel MD, Alvarado Cabrero I, Bulimbasic S, Swatek A, Straka L, Tichy T, Hora M, Kuroda N, Legendre B, Michal M, Hes O (2010) Sporadic hybrid oncocytic/chromophobe tumor of the kidney: a clinicopathologic, histomorphologic, immunohistochemical, ultrastructural, and molecular cytogenetic study of 14 cases. Virchows Archiv : Int J Pathol 456:355–365. https://doi.org/10.1007/s00428-010-0898-4
5. Srigley JR, Delahunt B, Eble JN, Egevad L, Epstein JI, Grignon D, Hes O, Moch H, Montironi R, Tickoo SK, Zhou M, Argani P, Panel IRT (2013) The International Society of Urological Pathology (ISUP) Vancouver classification of renal neoplasia. Am J Surg Pathol 37:1469–1489. https://doi.org/10.1097/PAS.0b013e318299f2d1
6. Moch H, Humphrey PA, Ulbright TM, Reuter VE (2016) WHO classification of tumours of the urinary system and male genital organs IARC, Lyon, p 356
7. Williamson SR, Gadde R, Trpkov K, Hirsch MS, Srigley JR, Reuter VE, Cheng L, Kunju LP, Barod R, Rogers CG, Delahunt B, Hes O, Eble JN, Zhou M, McKenney JK, Martignoni G, Fleming S, Grignon DJ, Moch H, Gupta NS (2017) Diagnostic criteria for oncocytic renal neoplasms: a survey of urologic pathologists. Hum Pathol 63:149–156. https://doi.org/10.1016/j.humpath.2017.03.004
8. Steiner P, Andreasen S, Grossmann P, Hauer L, Vanecek T, Miesbauerova M, Santana T, Kiss K, Slouka D, Skalova A (2018) Prognostic significance of 1p36 locus deletion in adenoid cystic carcinoma of the salivary glands. Virchows Archiv : Int J Pathol. https://doi.org/10.1007/s00428-018-2349-6
9. Sperga M, Martinek P, Vanecek T, Grossmann P, Bauleth K, Perez-Montiel D, Alvarado-Cabrero I, Nevidovska K, Lietuvietis V, Hora M, Michal M, Petersson F, Kuroda N, Suster S, Branzovsky J, Hes O (2013) Chromophobe renal cell carcinoma—chromosomal aberration variability and its relation to Paner grading system: an array CGH and FISH analysis of 37 cases. Virchows Archiv: Int J Pathol 463:563–573. https://doi.org/10.1007/s00428-013-1457-6
10. Perrino CM, Grignon DJ, Williamson SR, Idrees MT, Eble JN, Cheng L (2018) Morphological spectrum of renal cell carcinoma, unclassified: an analysis of 136 cases. Histopathology 72:305–319. https://doi.org/10.1111/his.13362
11. Amin MB, Crotty TB, Tickoo SK, Farrow GM (1997) Renal oncocytoma: a reappraisal of morphologic features with clinicopathologic findings in 80 cases. Am J Surg Pathol 21:1–12
12. Trpkov K, Yilmaz A, Uzer D, Dishongh KM, Quick CM, Bismar TA, Gokden N (2010) Renal oncocytoma revisited: a clinicopathological study of 109 cases with emphasis on problematic diagnostic features. Histopathology 57:893–906. https://doi.org/10.1111/j.1365-2559.2010.03726.x
13. Foix MP, Dunatov A, Martinek P, Mundo EC, Suster S, Sperga M, Lopez JI, Ulamec M, Bulimbasic S, Montiel DP, Alaghehbandan R, Peckova K, Pivovarcikova K, Daum O, Rotterova P, Skenderi F, Prochazkova K, Dusek M, Hora M, Michal M, Hes O (2016) Morphological, immunohistochemical, and chromosomal analysis of multicystic chromophobe renal cell carcinoma, an architecturally unusual challenging variant. Virchows Archiv : Int J Pathol 469:669–678. https://doi.org/10.1007/s00428-016-2022-x
14. Hes O, Vanecek T, Perez-Montiel DM, Alvarado Cabrero I, Hora M, Suster S, Lamovec J, Curik R, Mandys V, Michal M (2005) Chromophobe renal cell carcinoma with microcystic and adenomatous arrangement and pigmentation–a diagnostic pitfall. Morphological, immunohistochemical, ultrastructural and molecular genetic report of 20 cases. Virchows Archiv : Int J Pathol 446:383–393. https://doi.org/10.1007/s00428-004-1187-x
15. Ohe C, Kuroda N, Keiko M, Tomoki K, Masatsugu M, Shun S, Shintaro T, Naoki H, Hes O, Michal M, Tadashi M, Yoshiko U (2014) CHromophobe renal cell carcinoma with neuroendocrine differentiation/morphology: a clinicopathological and genetic study of three cases. Human Pathol: Case Rep 1:31–39
16. Peckova K, Martinek P, Ohe C, Kuroda N, Bulimbasic S, Condom Mundo E, Perez Montiel D, Lopez JI, Daum O, Rotterova P, Kokoskova B, Dubova M, Pivovarcikova K, Bauleth K, Grossmann P, Hora M, Kalusova K, Davidson W, Slouka D, Sulc M, Buzrla P, Hynek M, Michal M, Hes O (2015) Chromophobe renal cell carcinoma with neuroendocrine and neuroendocrine-like features. Morphologic, immunohistochemical, ultrastructural, and array comparative genomic hybridization analysis of 18 cases and review of the literature. Ann Diagn Pathol 19:261–268. https://doi.org/10.1016/j.anndiagpath.2015.05.001
17. Delongchamps NB, Galmiche L, Eiss D, Rouach Y, Vogt B, Timsit MO, Vieillefond A, Mejean A (2009) Hybrid tumour 'oncocytoma-chromophobe renal cell carcinoma' of the kidney: a report of seven sporadic cases. BJU Int 103:1381–1384. https://doi.org/10.1111/j.1464-410X.2008.08263.x
18. Mai KT, Dhamanaskar P, Belanger E, Stinson WA (2005) Hybrid chromophobe renal cell neoplasm. Pathol Res Pract 201:385–389. https://doi.org/10.1016/j.prp.2005.03.008
19. Petersson F, Gatalica Z, Grossmann P, Montiel MDP, Cabrero IA, Bulimbasic S, Swatek A, Straka L, Tichy T, Hora M, Kuroda N, Legendre B, Michal M, Hes O (2010) Sporadic hybrid oncocytic/chromophobe tumor of the kidney: a clinicopathologic, histomorphologic, immunohistochemical, ultrastructural, and molecular cytogenetic study of 14 cases. Virchows Arch 456:355–365. https://doi.org/10.1007/s00428-010-0898-4
20. Hes O, Petersson F, Kuroda N, Hora M, Michal M (2013) Renal hybrid oncocytic/chromophobe tumors—a review. Histol Histopathol 28:1257–1264
21. Eble JN, Delahunt B (2018) Emerging entities in renal cell neoplasia: thyroid-like follicular renal cell carcinoma and multifocal oncocytoma-like tumours associated with oncocytosis. Pathology 50:24–36. https://doi.org/10.1016/j.pathol.2017.09.005
22. Li Y, Reuter VE, Matoso A, Netto GJ, Epstein JI, Argani P (2018) Re-evaluation of 33 'unclassified' eosinophilic renal cell carcinomas in young patients. Histopathology 72:588–600. https://doi.org/10.1111/his.13395
23. McKenney JK, Przybycin CG, Trpkov K, Magi-Galluzzi C (2018) Eosinophilic solid and cystic renal cell carcinomas have metastatic potential. Histopathology 72:1066–1067. https://doi.org/10.1111/his.13457
24. Trpkov K, Hes O, Bonert M, Lopez JI, Bonsib SM, Nesi G, Comperat E, Sibony M, Berney DM, Martinek P, Bulimbasic S, Suster S, Sangoi A, Yilmaz A, Higgins JP, Zhou M, Gill AJ, Przybycin CG, Magi-Galluzzi C, McKenney JK (2016) Eosinophilic, solid, and cystic renal cell carcinoma:

clinicopathologic study of 16 unique, sporadic neoplasms occurring in women. Am J Surg Pathol 40:60–71. https://doi.org/10.1097/PAS.0000000000000508

25. Peckova K, Vanecek T, Martinek P, Spagnolo D, Kuroda N, Brunelli M, Vranic S, Djuricic S, Rotterova P, Daum O, Kokoskova B, Vesela P, Pivovarcikova K, Bauleth K, Dubova M, Kalusova K, Hora M, Michal M, Hes O (2014) Aggressive and nonaggressive translocation t(6;11) renal cell carcinoma: comparative study of 6 cases and review of the literature. Ann Diagn Pathol 18:351–357. https://doi.org/10.1016/j.anndiagpath.2014.10.002
26. Argani P, Ladanyi M (2006) The evolving story of renal translocation carcinomas. Am J Clin Pathol 126:332–334. https://doi.org/10.1309/EAEJTJGD5J4J3B4F
27. Argani P, Lae M, Hutchinson B, Reuter VE, Collins MH, Perentesis J, Tomaszewski JE, Brooks JS, Acs G, Bridge JA, Vargas SO, Davis IJ, Fisher DE, Ladanyi M (2005) Renal carcinomas with the t(6;11)(p21;q12): clinicopathologic features and demonstration of the specific alpha-TFEB gene fusion by immunohistochemistry, RT-PCR, and DNA PCR. Am J Surg Pathol 29:230–240
28. Martignoni G, Tardarico, R., Pea, M., Pecciarini, L., Gobbo, S. (2005) t6;11 renal cell tumor. A clinicopathological study of two cases in adults. Modern Pathol 18:155A
29. Argani P, Yonescu R, Morsberger L, Morris K, Netto GJ, Smith N, Gonzalez N, Illei PB, Ladanyi M, Griffin CA (2012) Molecular confirmation of t(6;11)(p21;q12) renal cell carcinoma in archival paraffin-embedded material using a break-apart TFEB FISH assay expands its clinicopathologic spectrum. Am J Surg Pathol 36:1516–1526. https://doi.org/10.1097/PAS.0b013e3182613d8f
30. Martignoni G, Bonetti F, Chilosi M, Brunelli M, Segala D, Amin MB, Argani P, Eble JN, Gobbo S, Pea M (2012) Cathepsin K expression in the spectrum of perivascular epithelioid cell (PEC) lesions of the kidney. Mod Pathol 25:100–111. https://doi.org/10.1038/modpathol.2011.136
31. Pitra T, Pivovarcikova K, Alaghehbandan R, Hes O (2017) Chromosomal numerical aberration pattern in papillary renal cell carcinoma: review article. Ann Diagn Pathol. https://doi.org/10.1016/j.anndiagpath.2017.11.004
32. Gill AJ, Pachter NS, Clarkson A, Tucker KM, Winship IM, Benn DE, Robinson BG, Clifton-Bligh RJ (2011) Renal tumors and hereditary pheochromocytoma-paraganglioma syndrome type 4. N Engl J Med 364:885–886. https://doi.org/10.1056/NEJMc1012357
33. Gill AJ, Pachter NS, Chou A, Young B, Clarkson A, Tucker KM, Winship IM, Earls P, Benn DE, Robinson BG, Fleming S, Clifton-Bligh RJ (2011) Renal tumors associated with germline SDHB mutation show distinctive morphology. Am J Surg Pathol 35:1578–1585. https://doi.org/10.1097/PAS.0b013e318227e7f4
34. Guo J, Tretiakova MS, Troxell ML, Osunkoya AO, Fadare O, Sangoi AR, Shen SS, Lopez-Beltran A, Mehra R, Heider A, Higgins JP, Harik LR, Leroy X, Gill AJ, Trpkov K, Campbell SC, Przybycin C, Magi-Galluzzi C, McKenney JK (2014) Tuberous sclerosis-associated renal cell carcinoma: a clinicopathologic study of 57 separate carcinomas in 18 patients. Am J Surg Pathol 38:1457–1467. https://doi.org/10.1097/PAS.0000000000000248
35. Trpkov K, Abou-Ouf H, Hes O, Lopez JI, Nesi G, Comperat E, Sibony M, Osunkoya AO, Zhou M, Gokden N, Leroy X, Berney DM, Werneck Cunha I, Musto ML, Athanazio DA, Yilmaz A, Donnelly B, Hyndman E, Gill AJ, McKenney JK, Bismar TA (2017) Eosinophilic solid and cystic renal cell carcinoma (ESC RCC): further morphologic and molecular characterization of ESC RCC as a distinct entity. Am J Surg Pathol 41:1299–1308. https://doi.org/10.1097/PAS.0000000000000838

1.7 Chromofóbní renální karcinom, nový pohled na tradiční jednotku a její varianty

(komentář 3 publikací)

Chromophobe renal cell carcinoma with neuroendocrine and neuroendocrine-like features. Morphologic, immunohistochemical, ultrastructural, and array comparative genomic hybridization analysis of 18 cases and review of the literature.
Peckova K, Martinek P, Ohe C, Kuroda N, Bulimbasic S, Condom Mundo E, Perez Montiel D, Lopez JI, Daum O, Rotterova P, Kokoskova B, Dubova M, Pivovarcikova K, Bauleth K, Grossmann P, Hora M, Kalusova K, Davidson W, Slouka D, Miroslav S, Buzrla P, Hynek M, Michal M, Hes O.
Ann Diagn Pathol. 2015 Aug;19(4):261-8.

Expanding the morphologic spectrum of chromophobe renal cell carcinoma: A study of 8 cases with papillary architecture.
Michalova K, Tretiakova M, Pivovarcikova K, Alaghehbandan R, Perez Montiel D, Ulamec M, Osunkoya A, Trpkov K, Yuan G, Grossmann P, Sperga M, Ferak I, Rogala J, Mareckova J, Pitra T, Kolar J, Michal M, Hes O.
Ann Diagn Pathol. 2020 Feb;44:151448. doi: 10.1016/j.anndiagpath.2019.151448.

Morphological, immunohistochemical, and chromosomal analysis of multicystic chromophobe renal cell carcinoma, an architecturally unusual challenging variant.
Foix MP, Dunatov A, Martinek P, Mundó EC, Suster S, Sperga M, Lopez JI, Ulamec M, Bulimbasic S, Montiel DP, Alaghehbandan R, Peckova K, Pivovarcikova K, Ondrej D, Rotterova P, Skenderi F, Prochazkova K, Dusek M, Hora M, Michal M, Hes O.
Virchows Arch. 2016 Dec;469(6):669-678

Skupina „eosinofilních renálních tumorů“ je velkou diferenciálně diagnostickou výzvou, kdy situaci částečně znesnadňuje i fakt, že v posledních letech tato kategorie renálních tumorů expandovala o nové významné jednotky. I tak však vzhledem k frekvenci výskytu zůstávají RO a chromofóbní renální karcinom (ChRCC) nejvýznamnější zástupci skupiny.

Chromofóbní RCC ve své typické a plně vyjádřené morfologii nepředstavuje obtížnou diagnózu a k definitivnímu zaklasifikování tumoru diagnózou ChRCC často postačuje obyčejný hematoxylin-eozin (HE). Diagnostickou výzvou jsou však tumory s překryvnou morfologií mezi RO a ChRCC, či některé z variant ChRCC. To je i oblast, na kterou cílí literatura zabývající se ChRCC v posledních letech.

Notoricky známá dogmata pojící se s ChRCC (častější přítomnost dediferenciace do sarkomatoidního RCC v porovnání s jinými typy RCC a stanoviska doporučených postupů, které nedoporučují ChRCC gradovat pomocí ISUP/WHO gradingového systému) zůstávají u této jednotky neměnná.

1.7.1 Chromophobe renal cell carcinoma with neuroendocrine and neuroendocrine-like features. Morphologic, immunohistochemical, ultrastructural, and array comparative genomic hybridization analysis of 18 cases and review of the literatur

Pro účely studie bylo z celkem 624 ChRCC archivovaných v plzeňském registru nádorů vybráno 18 případů morfologicky suspektních pro možnou neuroendokrinní diferenciaci. Jako sugestivní histologický vzhled byly považovány znaky: 1) trabekulární/palisádující/ribbon-like, gyriformní, insulární, glandulární a solidní architektonika; 2) uniformní polygonální buňky tvořící drobné ostrůvky a 3) kribriformní uspořádání v kombinaci s palisádováním. Vybrané suspektní případy byly dále analyzovány za pomoci imunohistochemie, elektronové mikroskopie, arrayCGH a FISH.

Případy byly na základě detekované imunohistochemické exprese neuroendokrinních markerů rozděleny do dvou skupin - ChRCC s neuroendokrinní diferenciací (ChRCCND) a ChRCC s „neuroendocrine-like“ vzhledem (ChRCCND-L). Klinické údaje o dalším průběhu onemocnění byly dostupné u 11/18 pacientů (v délce trvání 0,5 až 12 let). Skupina ChRCCND čítala celkem čtyři případy, věkové rozmezí pacientů bylo mezi 49 a 79 roky, velikost tumorů od 2,2 do 22 cm. ChRCCND byly fokálně pozitivní v CD56 (4/4), synaptofyzinu (4/4), chromograninu A (1/4) a neuron-specifické enoláze/NSE (3/4). Ultrastrukturální analýza pomocí elektronové mikroskopie prokázala špatně zachovaná neuroendokrinní granula u 2/4 analyzovatelných ChRCCND. U 2/4 ChRCCND bylo klinicky zdokumentováno agresivní chování s metastatickým rozsevem. Skupina CRCCND-L zahrnovala 14 případů, pacienti byly ve věkovém rozmezí od 34 do 74 let, velikost tumorů se pohybovala mezi 3,8 - 16,5 cm. Všechny studované CRCCND-L byly ve většině negativní či velmi slabě fokálně pozitivní v průkazu výše jmenovaných neuroendokrinních markerů. Všechny tumory (18/18) byly pozitivních v imunohistochemickém barvení CK7 a CD117. Ztráta chromozomů 1, 2, 6 a 10 byla zastižena ve všech analyzovatelných ChRCCND, zatímco ve skupině ChRCCND-L byly prokázány mnohotné ztráty chromozomů 1, 2, 6, 10, 13, 17 a 21 a zisk chromozomů 4, 11, 12, 14, 15, 16, 19 a 20.

ChRCCND, zejména v případech s limitovaným diagnostickým materiálem (např. renální punkce pod CT kontrolou), představuje tumor s výrazně problematickou diferenciální diagnózou. Tumory přicházející do diferenciální diagnózy s ChRCCND jsou zejména karcinoid, uroteliální karcinom s neuroendokrinní diferenciací a metastázy.

Annals of Diagnostic Pathology 19 (2015) 261–268

Contents lists available at ScienceDirect

Annals of Diagnostic Pathology

Chromophobe renal cell carcinoma with neuroendocrine and neuroendocrine-like features. Morphologic, immunohistochemical, ultrastructural, and array comparative genomic hybridization analysis of 18 cases and review of the literature ☆

Kvetoslava Peckova, MD [a], Petr Martinek, MSc [a], Chisato Ohe, MD [b], Naoto Kuroda, MD [c], Stela Bulimbasic, MD, PhD [d], Enric Condom Mundo, MD [e], Delia Perez Montiel, MD [f], Jose I. Lopez, MD [g], Ondrej Daum, MD, PhD [a], Pavla Rotterova, MD, PhD [a], Bohuslava Kokoskova, MD [a], Magdalena Dubova, MD [a], Kristyna Pivovarcikova, MD [a], Kevin Bauleth, MD [a], Petr Grossmann, PhD [a], Milan Hora, MD [h], Kristyna Kalusova, MD [h], Whitney Davidson, MD [i], David Slouka, MD, PhD [j], Sulc Miroslav, MD [k], Petr Buzrla, MD [l], Mirka Hynek, MD, PhD [m], Michal Michal, MD [a], Ondrej Hes, MD, PhD [a,n,*]

[a] Department of Pathology, Charles University, Medical Faculty and Charles University Hospital Plzen, Plzen, Czech Republic
[b] Department of Diagnostic Pathology, Kansai Medical University, Hirakata Hospital, Osaka, Japan
[c] Department of Diagnostic Pathology, Kochi Red Cross Hospital, Kochi, Japan
[d] Department of Pathology, University Hospital Dubrava, Zagreb, Croatia
[e] Department of Pathology, Bellvitge University Hospital, Barcelona, Spain
[f] Department of Pathology, Instituto Nacional de Cancerologia, Mexico City, Mexico
[g] Department of Pathology, Cruces University Hospital, Barakaldo, Spain
[h] Department of Urology, Charles University, Medical Faculty and Charles University Hospital Plzen, Plzen, Czech Republic
[i] Department of Pathology and Laboratory Medicine, University of Kansas Medical Center, Kansas City, KS
[j] Department of Otorhinolaryngology, Charles University, Medical Faculty and Charles University Hospital Plzen, Plzen, Czech Republic
[k] Bioptical Laboratory Chomutov, Chomutov, Czech Republic
[l] Department of Pathology, University Hospital Ostrava, Ostrava, Czech Republic
[m] Department of Radiology, Medical Faculty and Charles University Hospital Plzen, Plzen, Czech Republic
[n] Biomedical Centre, Charles University, Medical Faculty and Charles University Hospital Plzen, Plzen, Czech Republic

ARTICLE INFO

Keywords:
Kidney
Chromophobe renal cell carcinoma
Neuroendocrine differentiation
Immunohistochemistry
Chromosomal numerical aberrations
aCGH

ABSTRACT

Chromophobe renal cell carcinoma (CRCC) with neuroendocrine differentiation (CRCCND) has only recently been described. Eighteen cases of CRCC with morphologic features suggestive of neuroendocrine differentiation were selected from among 624 CRCCs in our registry. The tissues were fixed in neutral formalin, embedded in paraffin, cut into 4- to 5-μm-thick sections, and stained with hematoxylin and eosin. As CRCC with neuroendocrine features, tumors with following morphology were suggested: (1) trabecular/palisading/ribbon-like, gyriform, insular, glandular, and solid pattern; (2) uniform polygonal cells formed in small islets; and (3) cribriform pattern in combination with palisading. Selected cases were further analyzed using immunohistochemistry, electron microscopy, array comparative genomic hybridization, and fluorescence in situ hybridization. Cases were classified as CRCCND or CRCC with neuroendocrine-like features (CRCCND-L) based on the immunohistochemical expression of neuroendocrine markers: CRCCND, 4 cases, age range 49 to 79 years, size ranged from 2.2 to 22 cm, and CRCCND-L, 14 cases, age range 34 to 74 years, size range 3.8 to 16.5 cm. Follow-up information was available for 11 of 18 patients aged 0.5 to 12 years. Two of 4 CRCCNDs showed aggressive clinical course with metastatic spreading. Chromophobe renal cell carcinomas with neuroendocrine differentiation were focally positive for CD56 (4/4), synaptophysin (4/4), chromogranin A (1/4), and neuron-specific enolase (3/4). All 14 CRCCND-Ls were mostly negative or very weakly focally positive for some of the aforementioned markers. All 18 tumors were positive for cytokeratin 7 and CD117. Ultrastructural analysis showed poorly preserved neuroendocrine granules only in 2 of 4 analyzed CRCCNDs. Losses

☆ The study was supported by the Charles University Research Fund (project no. P36) and by the project CZ.1.05/2.1.00/03.0076 from European Regional Development Fund.
* Corresponding author at: Department of Pathology, Charles University, Medical Faculty and Charles University Hospital Plzen, Alej Svobody 80, 304 60 Plzen, Czech Republic.
E-mail address: hes@medima.cz (O. Hes).

http://dx.doi.org/10.1016/j.anndiagpath.2015.05.001

of chromosomes 1, 2, 6, and 10 were found in all analyzable CRCCNDs, whereas multiple losses (chromosomes 1, 2, 6, 10, 13, 17, and 21) and gains (chromosomes 4, 11, 12, 14, 15, 16, 19, and 20) were found in CRCCND-L.

1. Introduction

Chromophobe renal cell carcinoma (CRCC) represents approximately 5% of renal carcinomas. Microscopically, these tumors are described as mostly solid or solid alveolar; however, the morphologic spectrum has expanded to include microcystic, adenomatoid, and focal papillary arrangements [1-4].

Chromophobe renal cell carcinoma with true neuroendocrine differentiation (CRCCND) and CRCC with a neuroendocrine-like pattern (CRCCND-L) have only recently been described; a limited number of cases have been reported [5-7].

In this study, we attempt to distinguish and compare true neuroendocrine differentiation in CRCC to CRCC with a neuroendocrine-like pattern and to evaluate the biological nature of both forms.

2. Materials and methods

The tissues were fixed in neutral formalin, embedded in paraffin, cut into 4- to 5-μm-thick sections, and stained with hematoxylin and eosin.

We selected 18 cases of CRCC with morphologic features suggestive of neuroendocrine differentiation from among 624 CRCCs in our files. As CRCCs with neuroendocrine features, tumors with following morphology were suggested: (1) palisading/ribbon-like, gyriform patterns; (2) insular pattern; and (3) cribriform/pseudorosettoid pattern or small cell islets in combination with palisading.

Selected cases were further analyzed using immunohistochemistry (IHC), electron microscopy, array comparative genomic hybridization (aCGH), and fluorescence in situ hybridization (FISH).

3. Immunohistochemistry

The immunohistochemical study was performed using a Ventana Benchmark XT automated stainer (Ventana Medical System, Inc, Tucson, AZ) on formalin-fixed, paraffin-embedded (FFPE) tissue. The following primary antibodies were used: cytokeratin 7 (CK7) (OV-TL12/30, monoclonal, 1:200; DakoCytomation, Glostrup, Denmark), c-kit (CD 117, polyclonal, RTU; DakoCytomation), CD56 (1B6, monoclonal, 1:100; Leica Biosystems, Newcastle, UK), Ki-67 (MIB1, monoclonal, 1:1000; Dako, Glostrup, Denmark), synaptophysin (polyclonal, 1:350; LabVision, Fremont, CA), chromogranin A (monoclonal, DAK-A3, 1:600; DakoCytomation), CD99 (O13, monoclonal, 1:200; Ventana, Mannheim, Germany), cytokeratin 20 (CK20) (Ks20.8, monoclonal, 1:250; DakoCytomation). The primary antibodies were visualized using the supersensitive streptavidin-biotin-peroxidase complex (Biogenex, Fremont, CA). Appropriate positive and negative controls were used.

4. Ultrastructure

Electron microscopy evaluation was performed on 7 cases. Small pieces of FFPE from 3 cases of CRCCND and 4 cases of CRCCND-L were deparaffinized and further routinely processed for ultrastructural analysis. Semithin sections of epoxy-embedded tissue were stained with toluidine blue and examined by light microscopy. Ultrathin sections from representative areas were cut, stained with uranyl acetate and lead citrate, and examined with a Jeol (Tokyo, Japan) JEM 1400 Transmission Electronic Microscope.

Table 1
Clinicopathologic features

Case	Age	Sex	Site	Size (cm)	Color	Pattern	Follow up (y)
CRCCND							
1.[a]	79	M	Right	22 × 12 × 10	Brownish	SCI	3.5 AWD (CT scan, lymph nodes mediastinum)
2.	66	F	Left	12 cm	Yellow	SCI	Metastatic spreading in time of diagnosis, 0.5 AWD (local recurrence and bone meta)
3.	67	M	Right	5.6	Yellowish	PSC	LE
4.[a]	49	M	Left	Diam. 2.2	Beige	SCI	1 AW after partial nephrectomy
CRCCND-L							
1.	70	M	Right	2.6 × 3 × 2.3	Brown	P	AW 8/2014
2.	69	F	NA	12 × 5	Brown	PSC	NA
3.	74	F	Right	16.5	Yellow hemorrhagic, atrophic kidney	PSC	LE
4.	47	F	NA	3.8	NA	PSC	NA
5.	67	F	Left	7.3 × 6.8	Grayish	SC PR	LE
6.	46	M	Left	10 × 8 × 2	Grayish	SCI	3 y AW, then LE
7.	51	M	Left	8 × 7 × 6	Brownish	PSC	LE
8.	72	M	NA	NA	NA	SCPR	LE
9.	72	F	left	6.4	Pink to tan	PSC	AW 8/2014
10.	51	M	Left	Diam. 5	Yellow	PSC	AW 8/2014
11.	34	F	Left	14 × 11 × 10.5	Yellow	P	AW 8/14
12.	70	M	Right	13 × 10 × 9	Brown	P	AW 8/2014
13.	63	M	Left	Diam. 5.5	Brown	PSC	AW 2010, then LE
14.	49	F	NA	Diam. 13	NA	P	AW 9/14

Abbreviations: M, male; F, female; SCI, small cell islets; PSC, palisading and small cell areas; P, palisading; SCPR, small cells and pseudorosettes; AWD, alive with disease; CT, computed tomography; meta, metastasis; LE, loss of evidence; Diam., diameter; AW, alive and well; NA, not available.

[a] Cases have been published previously.

5. Molecular genetic methods

5.1. DNA extraction

DNA from FFPE tumor and nontumor tissues (when available) of each case was extracted using QIAsymphony DNA Mini Kit (Qiagen, Hilden, Germany) on automated extraction system (QIAsymphony SP; Qiagen) according to the manufacturer's supplementary protocol for FFPE samples (purification of genomic DNA from FFPE tissue using the QIAamp DNA FFPE Tissue Kit and Deparaffinization Solution). Concentration and purity of isolated DNA were measured using Nanodrop ND1000 (NanoDrop Technologies, Inc, Wilmington, DE). DNA integrity was examined by amplification of control genes in multiplex PCR, producing fragments from 100 to 600 base pairs (bp). Only cases with DNA integrity equal to or higher than 400 bp were used for further analysis by aCGH.

5.2. Fluorescence in situ hybridization

For each specimen, a 4-μm-thick, FFPE section was placed on a positively charged slide. The hematoxylin and eosin–stained slide was examined for determination of areas for cell counting. Another unstained slide was routinely deparaffinized and incubated in the 1× Target Retrieval Solution Citrate pH 6 (Dako) for 40 minutes at 95°C and subsequently cooled for 20 minutes at room temperature in the same solution. The slide was washed in deionized water for 5 minutes, and the tissue was digested in protease solution with pepsin (0.5 mg/mL) (Sigma Aldrich, St Louis, MO) in 0.01 M HCl at 37°C for 15 minutes. The slide was then immersed in deionized water for 5 minutes, dehydrated in a series of ethanol solutions (70%, 85%, and 96% for 2 minutes each), and air dried. Fluorescence in situ hybridization probes, shown in Table 1 (VYSIS/Abbott Molecular, Des Plaines, IL), were mixed with water and hybridization buffers according to the manufacturer's protocol. An appropriate amount of probe mix was applied to the specimen, covered with a glass cover slip, and sealed with rubber cement. The slide was then incubated in a ThermoBrite instrument (StatSpin/Iris Sample Processing, Westwood, MA) with codenaturation at 85°C for 8 minutes and hybridization at 37°C for 16 hours. The rubber-cemented cover slip was removed, and the slide was placed in posthybridization wash solution (compounded of saline-sodium citrate buffer (SSC) and detergent nonyl phenoxypolyethoxylethanol (NP-40) at a ratio of 2× SSC/0.3% NP-40) at 72°C for 2 minutes. Finally, the slide was air dried in the dark, counterstained with 4′,6-diamidino-2-phenylindole (DAPI I; VYSIS), cover slipped, and immediately examined.

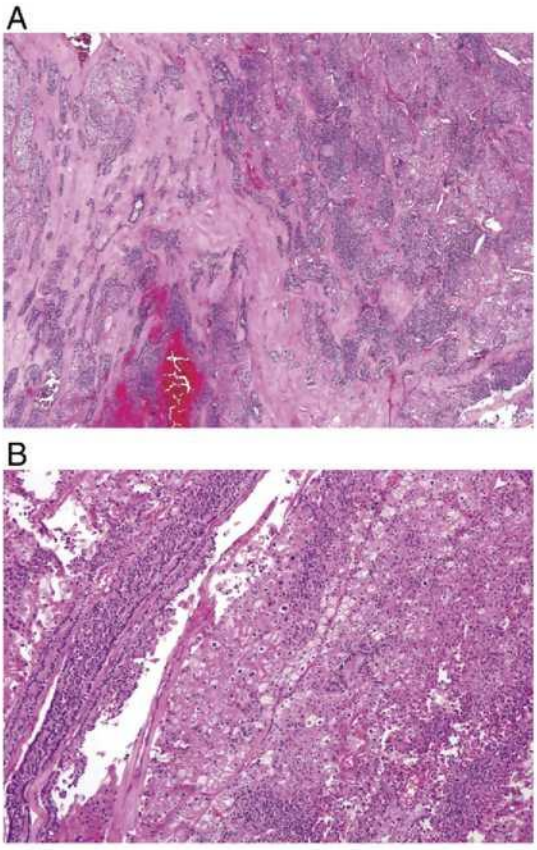

Fig. 2. Tumorous cells arranged in palisading structures in a background of dense fibrotic stroma in a case of CRCC with neuroendocrine differentiation (CRCCND case 1) (A). Cords of small neoplastic cells crossing areas composed of otherwise typical large polygonal cells with raisinoid nuclei (CRCCND case 3) (B).

5.3. Fluorescence in situ hybridization interpretation

The areas of the specimen with tumor were examined on an Olympus BX51 fluorescence microscope using an objective ×100 and filter sets triple bandpass (DAPI/Spectrum Green/Spectrum Orange) and single bandpass (Spectrum Green and Spectrum Orange). Scoring of aneuploidy was performed by counting the number of fluorescent signals in 100 randomly selected, nonoverlapping

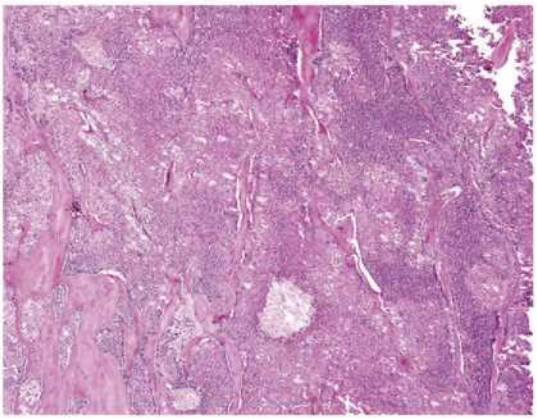

Fig. 1. Low-power view showing solid alveolar architecture of CRCC with neuroendocrine differentiation. Areas of small uniform cells are clearly visible in the right side of the picture (CRCCND case 4).

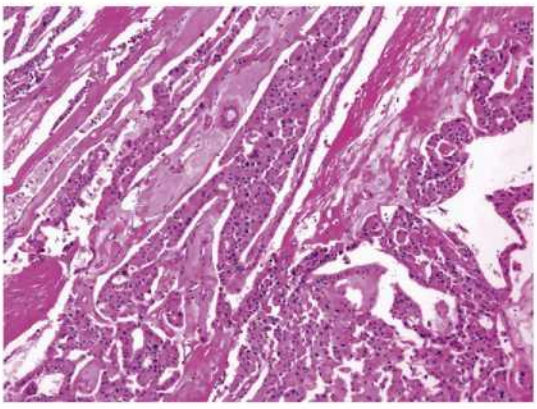

Fig. 3. Cords of neoplastic cells with inconspicuous palisading architecture in case of chromophobe RCC with neuroendocrine-like differentiation (CRCCND-L case 5).

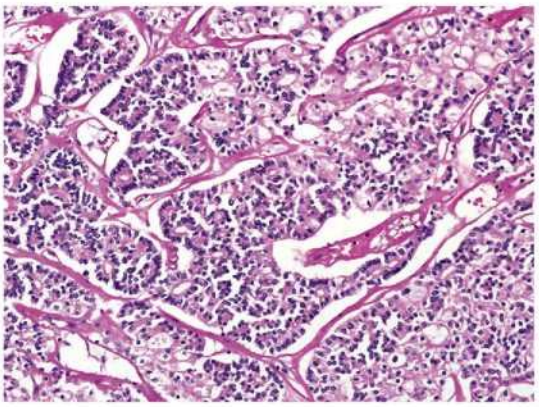

Fig. 4. Cribriform pattern in CRCC with neuroendocrine-like differentiation (CRCCND-L case 8).

tumor cell nuclei. Each slide was independently enumerated by 2 observers (PM and PG). The cut-off values used for each probe were established in a previous study [8].

5.4. Array comparative genomic hybridization

A CytoChip Focus Constitutional (BlueGnome Ltd, Cambridge, UK) microarray processor was used for analysis. CytoChip Focus Constitutional uses BAC technology and covers 143 regions of known significance with 1-Mb spacing across a genome. Probes are spotted in triplicates. First, 400 ng of gDNA was labeled using the Fluorescent Labeling System (BlueGnome Ltd). The procedure consisted of Cy3 labeling of a test sample and Cy5 labeling of a reference sample. MegaPool Reference DNA of opposite sex was used as a reference sample (Kreatech Diagnostics, Amsterdam, The Netherlands). Each labeled pair was mixed, dried, and hybridized overnight at 47°C using ArrayIt hybridization cassettes (Arrayit Corporation, Sunnyvale, CA). Posthybridization washing was done using SSC buffers with increasing stringency. Dried microarrays were scanned with InnoScan 900 (Innopsys, Carbonne, France) at a resolution of 5 μm.

5.5. Image and data analyses

Scanned images were analyzed and quantified using BlueFuse Multi software (BlueGnome Ltd). BlueFuse Multi uses Bayesian algorithms to generate intensity values for each Cy5- and Cy3-labeled spot on the array according to an appropriate .gal file. The reported changes were browsed and interpreted using BlueFuse Multi as well. Cut-off values were set to a log 2 ratio of −0.193 for loss and 0.170 for gain.

6. Results

Tumors were defined as CRCCND or CRCCND-L based on morphologic, immunohistochemical, and ultrastructural examinations.

The clinicopathologic features of the 4 patients with CRCCND are summarized in Table 1. Three of the patients were male, and 1 was female with ages ranging from 49 to 79 years (mean, 65.25 years; median, 66.5 years). Tumor size ranged from 2.2 to 22 cm in greatest dimension (mean, 10.45 cm; median, 8.8 cm); the cut surface of the tumor was yellow/yellowish in 2 cases and brownish/beige in 2 cases. Follow-up data were available for 3 of 4 patients with follow-up period ranging from 0.5 to 3.5 years. Tumors in the CRCCND group exhibited aggressive behavior in 2 of 3 patients for whom follow-up information was available.

The second group included 14 patients with CRCCND-L tumors; clinicopathologic data are available in Table 1. Within this group, there were 7 males and 7 females whose ages ranged from 34 to 74 years (mean, 59.64 years; median, 65 years). Tumor size ranged from 3.0 to 16.5 cm in greatest dimension (mean, 9.0 cm; median, 8 cm), and the cut surface of the tumor was brown/brownish in 5 cases, yellow/yellowish in 3 cases, grayish in 2 cases, and pink to tan in 1 case. Information regarding tumor color and consistency was not available in the 3 remaining cases. Follow-up information was available for 8 of 14 patients with no evidence of aggressive clinical course discovered in any of the cases of CRCCND-L.

6.1. Morphology

The morphologic patterns are summarized in Table 1. A typical dual cell population was found in every examined case. Characteristic raisinoid nuclei and perinuclear clearing were observed in all cases, albeit only focally in some cases. Regarding CRCCND, islets of small neoplastic cells were found in 3 of 4 tumors (Fig. 1), whereas palisading and small cell areas were detected in 1 of 4 tumors (Fig. 2A and B). As for CRCCND-L, we observed palisading and small cell areas in 7 of 14 cases (Fig. 3), palisading/ribbon-like pattern in 4 of 14 cases, small cell areas in 2 of 14 cases, and small cells with cribriform pattern/pseudorosettes (Fig. 4) in 1 of 14 cases.

Table 2
Results of immunohistochemical examination

Case	chrom	Syn	NSE	CD56	CK7	CD117	Ki-67	CD99	CK20
CRCCND									
1	−	Weak Foc++	Foc+++	Foc+++	+++	+++	8-10/HPF	−	−
2	−	+++	+++	Foc+	Foc++	+++	10-12/HPF	−	−
3	Foc+	Foc+++	Foc+++	Foc+	+++	+++	10-12/HPF	SC	−
4	−	+++	Foc+++	+++	+++	+++	10-12/HPF	−	−
CRCCND-L									
1	−	−	+	Foc+	Foc+++	+++	6-10/HPF	−	−
2	−	−	−	−	Foc++	++	4-5/HPF	−	−
3	−	−	−	−	+++	++	3-5/HPF	−	−
4	−	Foc+	−	−	+++	+++	6-7/HPF	−	SC
5	−	−	Foc+++	−	+++	+++	5-7/HPF	−	−
6	−	−	Foc+++	−	+++	+++	10-14/HPF	−	−
7	−	−	Foc+++	−	+++	+++	2-5/HPF	−	−
8	−	−	−	−	+++	+++	10-12/HPF	−	−
9	−		Foc++	−	+++	+++	8-10/HPF	−	−
10	−	−	−	−	Foc++	+++	3-7/HPF	−	−
11	−	−	+++	−	−	++	5-8/HPF	−	−
12	−	−	−	−	Foc++	++	4-6/HPF	−	−
13	−	−	−	−	+++	+++	2-5/HPF	NP	NP
14	−	−	Foc+++	−	+++	+++	1-2/HPF	NP	NP

Abbreviations: −, negative; +, weak positivity; ++, moderate positivity; +++, strong positivity; Foc, focal; NP, not performed; HPF, high-power field; SC, single cells; chrom, chromogranin; syn, synaptophysin.

6.2. Immunohistochemistry

The results of immunohistochemical examination are summarized in Table 2 (CRCCND and CRCCND-L). All of the tumors in the CRCCND group expressed markers considered to be typical for CRCC (CD117 and CK7) and were negative for vimentin (single positive cells). All tumors classified in this group were immunoreactive for synaptophysin, CD56, and neuron-specific enolase (NSE), although the positivity was often focal. A single case was focally and weakly positive for chromogranin A (Fig. 5A, B and C). Concerning the CRCCND-like group, all but 1 of the tumors were reactive for CD117 and CK7. Generally speaking, they were negative for neuroendocrine markers (synaptophysin, CD56, and NSE) or displayed variable positivity for NSE (7/14 cases). None of these tumors was positive for chromogranin A.

6.3. Ultrastructure

Electron-dense structures (granules) were found within the cytoplasm in 2 of 3 cases of CRCCND; however, the exact origin of such structures cannot be fully elucidated due to the presence of fixation artifacts. Such structures were not present in the 4 analyzed cases of CRCCND-L.

6.4. Array comparative genomic hybridization

Complete results of aCGH and FISH are summarized in Table 3. Losses of chromosomes 1, 2, 6, 10, and 17 were the most frequent finding in CRCCND (Fig. 6), whereas multiple losses (chromosomes 1, 2, 6, 10, 13, 17, and 21) and gains (chromosomes 4, 11, 12, 14, 15, 16, 19, and 20) were most frequently found in CRCCND-L (Fig. 7).

Table 4 summarizes comparative features of both CRCCND and CRCCND-L.

7. Discussion

Chromophobe renal cell carcinoma is a renal cell neoplasm, typically described as a solid alveolar tumor. These tumors are often composed of a dual population of cells, large leaf-like cells with abundant pale cytoplasm and well-defined borders variably intermixed with smaller eosinophilic cells embedded in a fine reticular setting. Large wrinkled nuclei, usually referred to as "raisinoid," are another characteristic feature of these tumors. One relatively common subtype of CRCC is the eosinophilic variant, which is composed mostly of smaller eosinophilic cells and is distinguished from classic CRCC according to the proportion of cell populations [9]. Additional variants of CRCC including those with microcystic, pigmented, and oncocytic morphologies have also been described [1,2,10,11].

Neuroendocrine differentiation within CRCC has been described only recently [5-7]. The histologic features of this extremely rare variant of CRCC are characterized by an admixture of classical and eosinophilic cells with regions of features consistent with neuroendocrine differentiation. These features include the formation of tubular, glandular, and insular patterns with rosettoid formations, intense granular eosinophilic cytoplasm, and dense hyaline stroma. In these areas, the neuroendocrine differentiation can be confirmed by immunohistochemical positivity for chromogranin, synaptophysin, CD56, and NSE, whereas the typical CRCC regions do not express these neuroendocrine markers.

Although sarcomatoid features can be observed in all types of renal cell carcinoma (RCC), 1 study suggests that CRCC is the most common RCC subtype with such dedifferentiation [12]. Clinically, this differentiation represents high-grade transformation of relatively indolent CRCC into a neoplasm with aggressive course and unfavorable prognosis. The neoplastic cells in sarcomatoid areas mostly express epithelial markers, and their epithelial origin can be immunohistochemically and ultrastructurally confirmed [12]. This sarcomatoid component may mimic or even differentiate into several different types of heterologous mesenchymal tumors such as osteosarcoma, rhabdomyosarcoma, chondrosarcoma, or liposarcoma [13-17].

One case report even describes the combination of CRCC, collecting duct RCC, and sarcomatoid differentiation within the same tumor [18].

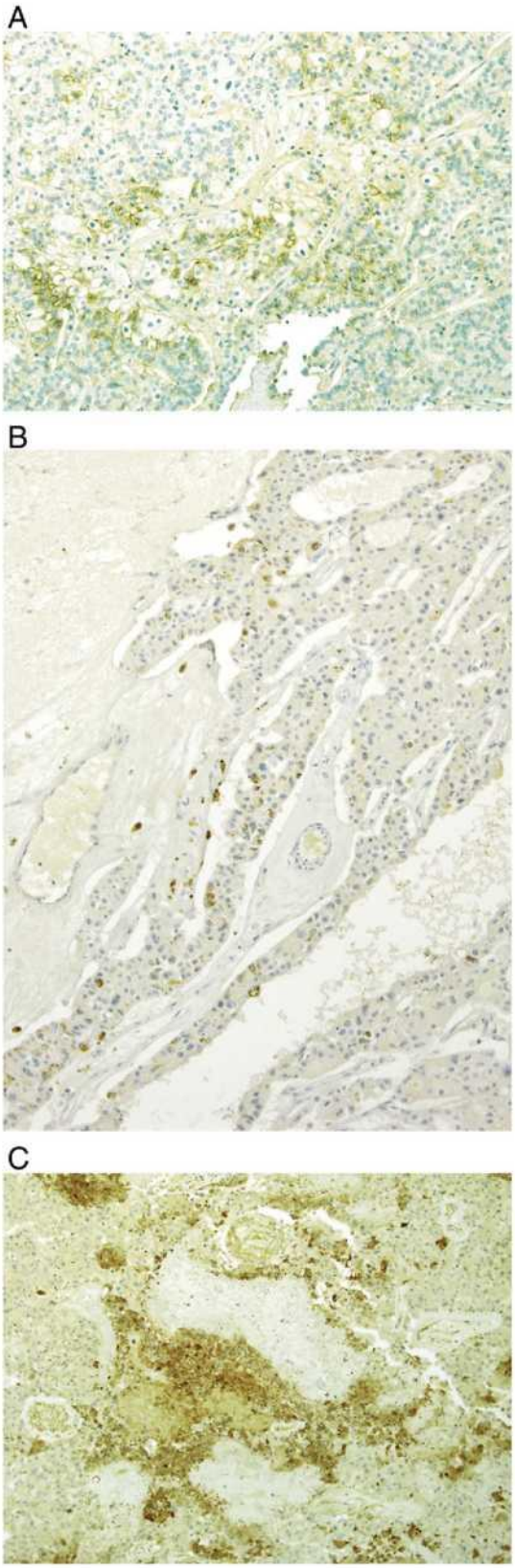

Fig. 5. Immunohistochemical examination of CRCC with neuroendocrine differentiation disclosed focal positivity for CD56 (A), synaptophysin (B), and NSE (C).

In this study, we have focused on the changes occurring in the epithelial component of certain CRCC subtypes. Only 1 of the 18 cases studied included areas of sarcomatoid differentiation. This particular case was CRCC with neuroendocrine differentiation and has also been published in previous studies [6,7]. Microscopically, the tumor was composed of 3 histologic components: an area of typical CRCC, a neuroendocrine carcinoma component, and a sarcomatoid component. The area with neuroendocrine differentiation was purely epithelial with no signs of sarcomatoid differentiation. The remaining 17 tumors analyzed were CRCC without areas of sarcomatoid transformation.

Neuroendocrine differentiation is a well-known phenomenon and occurs in tumors such as gastrointestinal adenocarcinoma, small and large cell carcinoma of the lung, urothelial carcinoma, prostatic adenocarcinoma, ovarian carcinosarcoma, and certain breast carcinomas [19-23].

The morphologic features suggesting neuroendocrine differentiation consist of organoid growth patterns characterized by trabecular, insular, palisading, ribbon, and rosette-like architecture. The tumor cells are uniform and polygonal with finely eosinophilic cytoplasm. Nuclei are round to oval with haphazardly distributed nuclear chromatin (frequently with a "salt and pepper" pattern), inconspicuous nucleoli, and scant to moderate cytoplasm. Necrosis is usually absent. Highly vascularized fibrovascular stroma, stromal hyalinization, cartilage, or bone formation as well as the presence of amyloid can be observed [24].

The morphologic features of CRCCND should be supported by IHC and/or ultrastructural examinations. Chromogranin A, synaptophysin, CD56, and NSE are often used as IHC markers of neuroendocrine differentiation with chromogranin A and synaptophysin being the most common. Both of the aforementioned markers are specific to neuroendocrine differentiation, although synaptophysin manifests much higher sensitivity than chromogranin A. CD56 is not a specific neuroendocrine marker and should not be considered as confirmation of neuroendocrine differentiation in the absence of synaptophysin/chromogranin positivity. Neuron-specific enolase, despite its name, is also not specific for neuroendocrine cells/tumors [24]. Ultrastructurally, the presence of neurosecretory or endosecretory granules is sometimes helpful. In this study, all available CRCCs with patterns suggesting possible neuroendocrine differentiation were examined by IHC with selected cases also being analyzed by ultrastructure. Of 18 cases, we confirmed real neuroendocrine differentiation in only 4 of them. The remaining 14 tumors exhibiting morphology compatible with neuroendocrine differentiation turned out to be examples of architectural/morphologic variability only.

Table 3
Results of molecular genetic analysis

Case	aCGH	FISH
CRCCND		
1	−1, −2, −6, −10, −17, −21	n7, −17
2	−1, −2, −3, −6, +7, −9, −10, −11, −13, −14, −17	+7, n17
3	NA	NT
4	−1, −2, −4, −5[a], −6, −9, −10, −13, −16p, −17, −21	NT
CRCCND-L		
1	No changes	NT
2	+11, +14	NT
3	−1, −2, +3, +4pter-4q31.21, −4q31.21-qter, −5, −6, +7, −8pter-8q13, −8q24.22, +8q13-8qter, +9pter-9q21.13, +9q21-9qter, −10, −11, +12, −13, −14, +15, +16, −17, +18, +19, +20, −21, +22	+7, −17
4	NT	NT
5	−1, −2, −6, −10, −13, −17, −21	n7, −17
6	+4, +5, +8, +11, +12, +14, +15, +16, +19, +20	+8, n10
7	NT	NT
8	−1, −3, −6, −10, −17, −21	NA
9	NA	NT
10	NT	NT
11	NT	NT
12	−1, −2, −6, −10, −13, −17, −18, −21	NA
13	NT	NT
14	NT	NT

Abbreviations: NT, not tested; NA, not analyzable; +, gain of chromosome; −, loss of chromosome; n, normal status (disomy).
[a] Only in area with neuroendocrine differentiation.

The presence of multiple losses of chromosomes 1, 2, 6, 10, 13, 17, and 21 has been considered a genetic hallmark of both classic and eosinophilic CRCCs. Although the presence of multiple chromosomal gains in CRCC has also been reported [10,25], these findings have been regarded as an uncommon phenomenon with CRCC generally believed to have a hypodiploid genome with the chromosomal losses described above. However, recent articles in which larger cohorts of cases were analyzed have described a more variable genetic pattern with multiple losses as well as with multiple gains. In these studies, chromosomal gains were most frequently detected on chromosomes 4, 7, 15, 19, and 20 [8,26,27]. These findings indicate that the molecular-genetic abnormalities in CRCC can encompass a considerably broader spectrum than was previously suggested. Our study reveals losses of chromosomes 1, 2, 6, and 10 in all analyzable neuroendocrine CRCC with multiple losses (chromosomes 1, 2, 6, 10, 13,

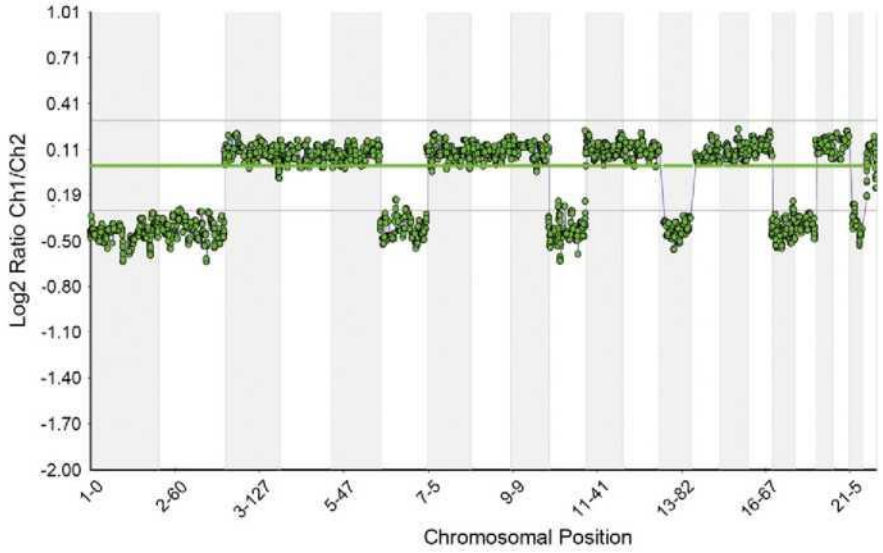

Fig. 6. Array comparative genomic hybridization fused chart of CRCC with neuroendocrine differentiation case with losses of chromosomes 1, 2, 6, 10, 13, 17, 18, and 21.

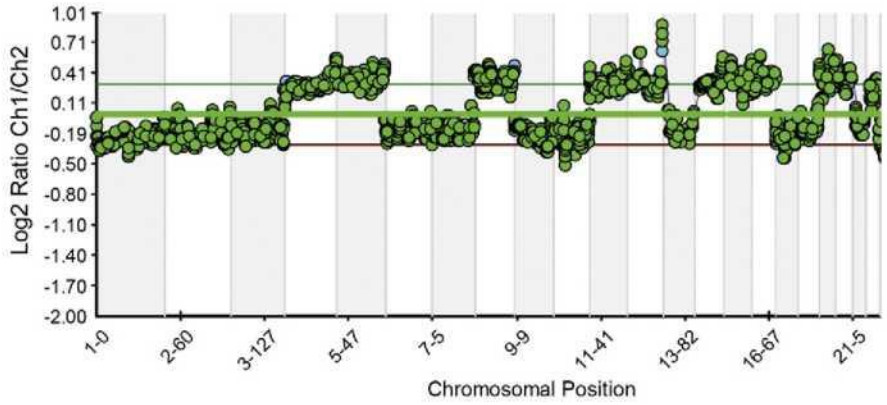

Fig. 7. Array comparative genomic hybridization fused chart of CRCCND-L with gains of chromosomes 4, 5, 8, 11, 12, 14, 15, 16, 19, and 20.

17, and 21) and gains (chromosomes 4, 11, 12, 14, 15, 16, 19, and 20) in neuroendocrine-like CRCC. These findings further enrich the spectrum of chromosomal anomalies on CRCC.

Chromophobe RCC has generally been regarded as an indolent tumor with a more favorable prognosis than other common RCCs. As for CRCCND, it remains unclear whether neuroendocrine differentiation influences clinical course and prognosis; the rarity of CRCCND makes it difficult to assess clinical outcomes, and few cases have been published to date [5-7].

Two cases (nos. 1 and 4) from our series were previously reported by Kuroda et al [6] and Ohe et al [7]. One of these new patients (case 2) presented with a 12-cm primary tumor and metastatic spreading at the time of diagnosis. She is alive with disease with 0.5 years of follow-up revealing local recurrence and bone metastasis. The second patient (case 3) presented with a 5.6-cm tumor with no available follow-up data. Chromophobe renal cell carcinoma with neuroendocrine differentiation exhibited aggressive behavior with relatively large tumor size (12 and 22 cm) in 2 of our 4 cases. Although few cases have been reported and follow-up information is not always complete, our data are in concordance with the hypothesis that neuroendocrine differentiation may represent advanced tumor stage [6]. Some authors have suggested a possible link between loss of chromosomes 4, 5, and 16p and neuroendocrine differentiation in CRCC; however, this finding was not confirmed in our series [7]. It appears that CRCCND may represent a more aggressive tumor than conventional CRCC, but further large-scale study is needed to elucidate this issue.

Most RCC patients are treated surgically following the discovery of a renal mass by modern imaging techniques, but in certain cases, a core biopsy is indicated. In such cases, making a definitive diagnosis from such limited material is often difficult. The most problematic tumors in the differential diagnosis are carcinoid, transitional cell carcinoma (TCC) with neuroendocrine features, and outside metastases.

Primary renal carcinoid tumors are rare, and their histogenesis within the kidney remains uncertain. Although malignant, the biological behavior of renal carcinoid tumors is considered to be more indolent than that of most RCC [24]. Microscopically, the tumors are composed of monomorphic round to polygonal cells with round to oval nuclei showing evenly distributed chromatin. These cells are arranged in trabecular, ribbon-like, gyriform, insular, glandular, and solid patterns. Immunohistochemically, tumor cells demonstrate variable positivity for neuroendocrine markers such as chromogranin A, synaptophysin, and NSE. In addition, renal carcinoids frequently display immunoreactivity for CD99. Ultrastructurally, the neoplastic cells contain abundant dense core neurosecretory granules [24]. Raisinoid nuclei and perinuclear clearing (halo) are not characteristics of renal carcinoid. The presence of such findings, along with immunohistochemical examination, could help to resolve diagnostic problems. However, the neuroendocrine component in CRCCND can mimic carcinoid features, especially if only limited material is available. In such cases, immunoreactivity for CD99 can be especially useful, as it has not been observed in CRCCND.

Transitional cell carcinoma can also feature neuroendocrine differentiation [20], exhibiting overlapping morphologic characteristic with CRCCND and making differential diagnosis complicated. The typical microscopic pattern of this variant of TCC is a mosaic arrangement of tumor cells resembling Merkel neuroendocrine carcinoma of skin. The dual cell population with raisinoid nuclei and perinuclear clearing found in CRCCND can be a helpful morphologic distinction. Immunohistochemically, CK20 can be used for distinction between these 2 entities, although other immunostaining qualities tend to be similar. However, in unusual TCC or in cases with high grade, CK20 is usually only weakly positive or entirely negative. CD117 is reported as negative in TCC, which may serve as another immunohistochemical marker for differentiation between TCC and CRCCND. In cases where a whole kidney specimen is available, well-performed sampling is nearly always helpful. It is usually possible to find areas where the urothelial origin of the lesion is obvious and it is not necessary to apply extensive immunohistochemical examination. Careful sampling of the renal pelvis in deeply located tumors can also help to find TCC in situ or

Table 4
Summary of morphologic, immunohistochemical, ultrastructural, and molecular genetic features of CRCCND and CRCCND-L.

	CRCCND	CRCCND-L
Morphology/pattern	SCI, PSC	SCI, PSC, P, SC PR
Immunohistochemistry	Chrom−+, Syn +, CD56+, NSE+	Chrom−, Syn−+, CD56−+, NSE+
Ultrastructure[a]	Neurosecretory granules +	Neurosecretory granules −
Chromosomal numerical aberrations	Loss of chromosomes 1, 2, 6, 10, 17	Multiple losses of chromosomes 1, 2, 6, 10, 13, 17, 21 and gains of chromosomes 4, 11, 12, 14, 15, 16, 19, 20

Abbreviations: −+, focally, weakly positive in single case; +, positive; −, negative.
[a] Ultrastructural study was performed on limited number of the cases.

to discover the transition from more typical TCC to areas with neuroendocrine differentiation.

Finally, metastases of neuroendocrine carcinomas from other organs can also cause diagnostic difficulties. The morphology, immunohistochemistry, and ultrastructure of such lesions can resemble the neuroendocrine component in CRCCND making it important to look carefully for the chromophobe component. Definitive resolution usually requires clinical and radiologic correlation in these cases.

8. Conclusions

1. Morphologic features suggestive of neuroendocrine differentiation are rarely seen in CRCC. In the majority of such cases, true neuroendocrine differentiation cannot be demonstrated; thus, these features often simply represent an architectural growth pattern variant.
2. True CRCCND is distinguished from CRCCND-L based on the expression of neuroendocrine markers and the presence of neuroendocrine granules.
3. Chromosomal losses (chromosomes 1, 2, 6, and 10) are mostly found in CRCCND, whereas some CRCCND-L cases show both losses and gains of multiple chromosomes.
4. CRCCND appears to have metastatic potential based on the fact that 2 of 4 reported cases behaved aggressively. Nevertheless, further research with additional cases is required to highlight this rare and peculiar variant of RCC.

Disclosure of conflict of interest

All authors declare no conflict of interest.

References

[1] Michal M, Hes O, Svec A, Ludvikova M. Pigmented microcystic chromophobe cell carcinoma: a unique variant of renal cell carcinoma. Ann Diagn Pathol 1998;2:149–53 [PubMed PMID: 9845733].
[2] Hes O, Vanecek T, Perez-Montiel DM, Alvarado Cabrero I, Hora M, Suster S, et al. Chromophobe renal cell carcinoma with microcystic and adenomatous arrangement and pigmentation—a diagnostic pitfall. Morphological, immunohistochemical, ultrastructural and molecular genetic report of 20 cases. Virchows Arch 2005;446:383–93 [PubMed PMID: 15756595].
[3] Dundr P, Pesl M, Povysil C, Tvrdik D, Pavlik I, Soukup V, et al. Pigmented microcystic chromophobe renal cell carcinoma. Pathol Res Pract 2007;203:593–7 [PubMed PMID: 17658700].
[4] Kuroda N, Iiyama T, Moriki T, Shuin T, Enzan H. Chromophobe renal cell carcinoma with focal papillary configuration, nuclear basaloid arrangement and stromal osseous metaplasia containing fatty bone marrow element. Histopathology 2005;46:712–3 [PubMed PMID: 15910607].
[5] Parada DD, Pena KB. Chromophobe renal cell carcinoma with neuroendocrine differentiation. APMIS 2008;116:859–65 [PubMed PMID: 19024610].
[6] Kuroda N, Tamura M, Hes O, Michal M, Gatalica Z. Chromophobe renal cell carcinoma with neuroendocrine differentiation and sarcomatoid change. Pathol Int 2011;61:552–4 [PubMed PMID: WOS:000294976700009. English].
[7] Ohe C, Kuroda N, Keiko M, Tomoki K, Masatsugu M, Shun S, et al. Chromophobe renal cell carcinoma with neuroendocrine differentiation/morphology: a clinicopathological and genetic study of three cases. Hum Pathol Case Rep 2014;1:31–9.
[8] Sperga M, Martinek P, Vanecek T, Grossmann P, Bauleth K, Perez-Montiel D, et al. Chromophobe renal cell carcinoma–chromosomal aberration variability and its relation to Paner grading system: an array CGH and FISH analysis of 37 cases. Virchows Arch 2013;463:563–73 [PubMed PMID: 23913167].
[9] Thoenes W, Storkel S, Rumpelt HJ, Moll R, Baum HP, Werener S. Chromophobe renal cell carcinoma and its variants. A report on 32 cases. J Pathol 1988;155:277–87.
[10] Brunelli M, Eble JN, Zhang S, Martignoni G, Delahunt B, Cheng L. Eosinophilic and classic chromophobe renal cell carcinomas have similar frequent losses of multiple chromosomes from among chromosomes 1, 2, 6, 10, and 17, and this pattern of genetic abnormality is not present in renal oncocytoma. Mod Pathol 2005;18:161–9 [PubMed PMID: 15467713].
[11] Kuroda N, Tanaka A, Yamaguchi T, Kasahara K, Naruse K, Yamada Y, et al. Chromophobe renal cell carcinoma, oncocytic variant: a proposal of a new variant giving a critical diagnostic pitfall in diagnosing renal oncocytic tumors. Med Mol Morphol 2013;46:49–55 [PubMed PMID: 23338778].
[12] Akhtar M, Tulbah A, Kardar AH, Ali MA. Sarcomatoid renal cell carcinoma: the chromophobe connection. Am J Surg Pathol 1997;21:1188–95 [PubMed PMID: 9331291].
[13] Magro G, Lopes M, Amico P, Puzzo L. Chromophobe renal cell carcinoma with extensive rhabdomyosarcomatous component. Virchows Arch 2005;447:894–6 [PubMed PMID: 16021511].
[14] Itoh T, Chikai K, Ota S, Nakagawa T, Takiyama A, Mouri G, et al. Chromophobe renal cell carcinoma with osteosarcoma-like differentiation. Am J Surg Pathol 2002;26:1358–62 [PubMed PMID: 12360051].
[15] Quiroga-Garza G, Khurana H, Shen S, Ayala AG, Ro JY. Sarcomatoid chromophobe renal cell carcinoma with heterologous sarcomatoid elements. A case report and review of the literature. Arch Pathol Lab Med 2009;133:1857–60 [PubMed PMID: 19886723].
[16] Anila KR, Mathew AP, Somanathan T, Mathews A, Jayasree K. Chromophobe renal cell carcinoma with heterologous (liposarcomatous) differentiation: a case report. Int J Surg Pathol 2012;20:416–9 [PubMed PMID: 22134633].
[17] Petersson F, Michal M, Franco M, Hes O. Chromophobe renal cell carcinoma with liposarcomatous dedifferentiation—report of a unique case. Int J Clin Exp Pathol 2010;3:534–40 [PubMed PMID: 20606735, Pubmed Central PMCID: 2897100].
[18] Husain A, EBJ, Trpkov K. Composite chromophobe renal cell carcinoma with sarcomatoid differentiation containing osteosarcoma, chondrosarcoma, squamous metaplasia and associated collecting duct carcinoma: a case report. Anal Quant Cytol Histol 2014;36:235–40.
[19] Dittus CFC, Saha D, Magee A. A rare case of ovarian carcinosarcoma with neuroendocrine differentiation. J Community Support Oncol 2004;12:71–4.
[20] Eble JN, Sauter G, Epstein JI, Sesterhenn I. WHO Classification of Tumours. Tumours of the urinary system and male genital organs. Pathology and GeneticsLyon: IARC Press; 2004.
[21] La Rosa SSF. High-grade poorly differentiated neuroendocrine carcinomas of the gastroenteropancreatic system: from morphology to proliferation and back. Endocr Pathol 2014;52:193–8.
[22] Caplin ME, Baudin E, Ferolla P, Filosso P, Garcia-Yuste M, Lim E, et al. Pulmonary neuroendocrine (carcinoid) tumors: European Neuroendocrine Tumor Society expert consensus and recommendations for best practice for typical and atypical pulmonary carcinoids. Ann Oncol 2015;2 [PubMed PMID: 25646366].
[23] Rekhtman N. Neuroendocrine tumors of the lung: an update. Arch Pathol Lab Med 2010;134:1628–38 [PubMed PMID: 21043816].
[24] Kuroda N, Tanaka A, Ohe C, Mikami S, Nagashima Y, Inoue K, et al. Review of renal carcinoid tumor with focus on clinical and pathobiological aspects. Histol Histopathol 2013;28:15–21 [PubMed PMID: 23233056].
[25] Gunawan B, Bergmann F, Braun S, Hemmerlein B, Ringert RH, Jakse G, et al. Polyploidization and losses of chromosomes 1, 2, 6, 10, 13, and 17 in three cases of chromophobe renal cell carcinomas. Cancer Genet Cytogenet 1999;110:57–61 [PubMed PMID: 10198624].
[26] Vieira J, Henrique R, Ribeiro FR, Barros-Silva JD, Peixoto A, Santos C, et al. Feasibility of differential diagnosis of kidney tumors by comparative genomic hybridization of fine needle aspiration biopsies. Genes Chromosomes Cancer 2010;49:935–47 [PubMed PMID: 20629095].
[27] Tan MH, Wong CF, Tan HL, Yang XJ, Ditlev J, Matsuda D, et al. Genomic expression and single-nucleotide polymorphism profiling discriminates chromophobe renal cell carcinoma and oncocytoma. BMC Cancer 2010;10:196 [PubMed PMID: 20462447, Pubmed Central PMCID: 2883967].

1.7.2 Expanding the morphologic spectrum of chromophobe renal cell carcinoma: A study of 8 cases with papillary architecture

Chromofóbní renální karcinom je typicky uspořádán solidně alveolárně, může však též vykazovat i jinou architektoniku. Do studie bylo zařazeno 8 ChRCC s prominentním papilárním růstem, architektonikou velmi raritně popisovanou u ChRCC.

Z 972 ChRCC v plzeňském registru nádorů bylo identifikováno 8 ChRCC s papilárním růstem. U případů bylo provedeno imunohistochemické vyšetření a arrayCGH za účelem vyšetření možných chromozomálních aberací. Pacienti byli 3 muži a 5 žen, ve věkovém rozmezí od 30 do 84 let (průměr 57,5 let, medián 60 let). Velikost tumorů se pohybovala od 2 do 14 cm (průměr 7,5 cm, medián 6,6 cm). Údaje o dalším průběhu onemocnění byly dostupné u 7/8 pacientů, v délce trvání 1-61 měsíců (průměr 20,1 měsíců, medián 12 měsíců), u šesti pacientů bez známek agresivního chování, jeden z pacientů zemřel. Histologicky, byly všechny tumory tvořeny duální populací buněk a sestávaly z variabilní proporce „leaf-like" struktur z buněk se světlou cytoplasmou a eosinofilních buněk. Papilární komponenta tvořila 15-100% objemu nádorové masy (průměr 51%, medián 50%). Sarkomatoidní diferenciace byla identifikována pouze u případu s letálním průběhem. Imunohistochemicky byly všechny tumory pozitivní v CK7, CD117 a v Halově koloidním železe. Dále bylo 5/8 případů pozitivních v PAX8, 3/8 v TFE3 a 2/8 v katepsinu K. Ve všech případech byly vimentin, AMACR a HMB45 průkaz negativní. Exprese fumaráthydratázy byla zachována ve všech případech. Proliferační aktivita byla nízká, s MIB1 indexem < 1% v 7/8 případů a MIB1 indexem < 5% u 1/8 tumoru. U 3 případů bylo možné provést aCGH, ve všech případech byl chromozomální aberační status variabilní s četnými ztrátami a zisky chromozomů.

Chromofóbní renální karcinom s papilárním růstem je velmi vzácnou renální neoplázií, která je však diagnostickou výzvou. Hlavní pomocné znaky pro správnou diagnózu jsou u těchto lézí především cytologické znaky konzistentní s diagnózou klasického ChRCC. V rámci diferenciální diagnózy renálních neoplázií s papilární architektonikou přichází v úvahu renální neoplázie s popsaným agresivním chováním (např. Xp11 translokační RCC, FHRCC) proto je důležité odlišit tyto neoplázie od ChRCC s papilárním růstem. Na podkladě dat získaných touto limitovanou studií není zřejmé, že by přítomnost papilární architektoniky měla mít negativní prognostický dopad, ačkoliv pro definitivní verifikaci tohoto tvrzení je potřeba dalších studií na větším množství případů.

Annals of Diagnostic Pathology 44 (2020) 151448

Contents lists available at ScienceDirect

Annals of Diagnostic Pathology

journal homepage: www.elsevier.com/locate/anndiagpath

Original Contribution

Expanding the morphologic spectrum of chromophobe renal cell carcinoma: A study of 8 cases with papillary architecture

Kvetoslava Michalova[a], Maria Tretiakova[b], Kristyna Pivovarcikova[a], Reza Alaghehbandan[c], Delia Perez Montiel[d], Monika Ulamec[e], Adeboye Osunkoya[f], Kiril Trpkov[g], Gao Yuan[g], Petr Grossmann[a], Maris Sperga[h], Ivan Ferak[i], Joanna Rogala[a], Jana Mareckova[a], Tomas Pitra[j], Jiri Kolar[j], Michal Michal[a], Ondrej Hes[a,*]

[a] Department of Pathology, Charles University, Medical Faculty and Charles University Hospital Plzen, Czech Republic
[b] Department of Pathology, University of Washington, Seattle, WA, USA
[c] Department of Pathology, Faculty of Medicine, University of British Columbia, Royal Columbian Hospital, Vancouver, BC, Canada
[d] Department of Pathology, Institute Nacional de Cancerologia, Mexico City, Mexico
[e] Ljudevit Jurak Pathology Department, University Clinical Hospital "Sestre milosrdnice", Pathology Department, School of Dental Medicine, University of Zagreb, Croatia
[f] Department of Pathology, Emory Hospital, Atlanta, USA
[g] Department of Pathology and Laboratory Medicine, Calgary Laboratory Services and University of Calgary, Calgary, AB, Canada
[h] Department of Pathology, University of Split, Croatia
[i] Department of Pathology, AGEL, Novy Jicin, Czech Republic
[j] Department of Urology, Charles University, Medical Faculty and Charles University Hospital Plzen, Czech Republic

ARTICLE INFO

Keywords:
Chromophobe renal cell carcinoma
Papillary
Immunohistochemistry
Copy number variation
CNV

ABSTRACT

Although typically arranged in solid alveolar fashion, chromophobe renal cell carcinoma (RCC) may also show several other architectural growth patterns. We include in this series 8 chromophobe RCC cases with prominent papillary growth, a pattern very rarely reported or only mentioned as a feature of chromophobe RCC, which is lacking wider recognition The differential diagnosis of such cases significantly varies from the typical chromophobe RCC with its usual morphology, particularly its distinction from papillary RCC and other relevant and clinically important entities.

Of 972 chromophobe RCCs in our files, we identified 8 chromophobe RCCs with papillary growth. We performed immunohistochemistry and array Comparative Genomic Hybridisation (aCGH) to investigate for possible chromosomal aberrations.

Patients were 3 males and 5 females with age ranging from 30 to 84 years (mean 57.5, median 60 years). Tumor size was variable and ranged from 2 to 14 cm (mean 7.5, median 6.6 cm). Follow-up was available for 7 of 8 patients, ranging from 1 to 61 months (mean 20.1, median 12 months). Six patients were alive with no signs of aggressive behavior, and one died of the disease. Histologically, all cases were composed of dual cell population consisting of variable proportions of leaf-like cells with pale cytoplasm and eosinophilic cells. The extent of papillary component ranged from 15 to 100% of the tumor volume (mean 51%, median 50%). Sarcomatoid differentiation was identified only in the case with fatal outcome. Immunohistochemically, all tumors were positive for CK7, CD117 and Hale's Colloidal Iron. PAX8 was positive in 5 of 8 cases, TFE3 was focally positive 3 of 8 tumors, and Cathepsin K was focally positive in 2 of 8 tumors. All cases were negative for vimentin, AMACR and HMB45. Fumarate hydratase staining was retained in all tested cases. The proliferative activity was low (up to 1% in 7, up to 5% in one case). Three cases were successfully analyzed by aCGH and all showed a variable copy number variation profile with multiple chromosomal gains and losses. *Conclusions:* Chromophobe RCC demonstrating papillary architecture is an exceptionally rare carcinoma. The diagnosis can be challenging, although the cytologic features are consistent with the classic chromophobe RCC. Given the prognostic and therapeutic implications of accurately diagnosis other RCCs with papillary architecture (i.e., Xp11.2 translocation RCC, *FH*-deficient RCC), it is crucial to differentiate these cases from chromophobe RCC with papillary architecture. Based on this limited series, the presence of papillary architecture does not appear to have negative prognostic impact. However, its wider recognition may allow in depth studies on additional examples of this rare morphologic variant.

* Corresponding author.
E-mail address: hes@medima.cz (O. Hes).

https://doi.org/10.1016/j.anndiagpath.2019.151448

1. Introduction

Chromophobe RCC is an indolent renal neoplasm with specific morphologic features demonstrated by dual population of pale leaf-like and eosinophilic cells encountered in various proportions. The cells have accentuated cellular borders, hyperchromatic wrinkled nuclei and perinuclear halos. In most cases, chromophobe RCC demonstrates solid-alveolar growth. Several architectural morphologic patterns (or variants) have also been described, including chromophobe RCC with pigmented microcystic adenomatoid/multicystic growth [1-4], chromophobe RCC with neuroendocrine differentiation [5-9] and renal oncocytoma-like variant [10]. In this report, we expand the morphologic spectrum of chromophobe RCC by presenting a cohort of 8 cases with distinct and prominent papillary architecture. Differential diagnosis in such cases encompasses a wide spectrum of neoplasms and is different than in cases showing typical architectural growth of chromophobe RCC or from other described patterns.

The aim of this study was to improve our understanding of this rare architectural variant and to discuss its differential diagnosis in the relevant context, incorporating the entities where incorrect diagnosis would have prognostic and therapeutic implications.

2. Materials and methods

The 8 cases of chromophobe RCC with papillary architecture were identified and selected out of 972 chromophobe RCC documented in the Plzen tumor registry. The clinical information and follow-up data were obtained when available. Generally, the cases were collected over a period of two years (2017–2019). None of the cases included in the study has been previously reported. Tissues for light microscopy were formalin fixed and embedded in paraffin using the routine procedure. In general four to five-μm-thick sections were cut from the tissue blocks and stained with hematoxylin and eosin (H&E) and Hale's colloidal iron. When possible, the same tissue block from each case was used for the immunohistochemical (IHC) study and for the genetic analysis.

2.1. Immunohistochemistry

The IHC analysis was performed using a Ventana BenchMark ULTRA (Ventana Medical System, Inc., Tucson, Arizona). The following primary antibodies were used: CK7 (monoclonal, OV-TL12/30, 1:200, Dako, Glostrup, Denmark), CD117 (polyclonal, 1:800, Dako), vimentin (monoclonal, V9, RTU, Ventana Medical System, Inc., Tucson, Arizona), PAX8 (monoclonal, MRQ-50, RTU, Ventana Medical System, Inc.), AMACR (monoclonal, 13H4, RTU, Dako), Ki-67 (monoclonal, MIB-1, 1:400, Dako), TFE3 (monoclonal, MRQ-37, RTU, Ventana Medical System, Inc.), HMB45 (monoclonal, HMB45, 1:400, Ventana Medical System, Inc.), Cathepsin K (monoclonal, 3F9, 1:100, Abcam, Cambridge, UK), Fumarate hydratase (FH) (monoclonal, J-13, 1:3000, Santa Cruz, Wien, Austria). The primary antibodies were visualized using either alkaline phosphatase or peroxidase-based detecting systems (both from Ventana Medical System, Inc.).

2.2. DNA extraction

Representative tumor areas from the formalin-fixed paraffin-embedded (FFPE) samples were marked using H&E slides and were macro dissected. DNA from FFPE tumor tissue was extracted using QIAsymphony DNA Mini Kit (Qiagen, Hilden, Germany) on an automated extraction system (QIAsymphony SP; Qiagen) according to the manufacturer's supplementary protocol for FFPE samples. The concentration and the purity of the isolated DNA were measured using NanoDrop ND-1000 and DNA integrity was examined by amplification of control genes in a multiplex polymerase chain reaction (PCR).

2.3. Low pass whole genome sequencing

SurePlex DNA amplification system (Illumina, San Diego, CA) was used to generate DNA templates of tumor samples. DNA amplification in this setting is highly representative, which allows the resulting product to be suitable for copy number variation (CNV) detection. The library of all samples was prepared using Nextera DNA Sample Prep Kit (Illumina, San Diego, CA) using MiSeq sequencer. CNV analysis was performed using BlueFuse Multi software with the Veriseq plugin (Illumina, San Diego, CA). Following quality control filters for valid samples were set at a minimum 1 million reads per sample, with average quality score and average alignment score > 30, and overall noise < 0.3. Thresholds for CNV calling were set based on the group of samples with known CNV that were validated using array comparative genomic hybridisation (aCGH) and fluorescence in-situ hybridization (FISH). The percentage of tumor in the DNA sample was considered when calling the lower frequency CNVs. Thresholds for CNVs were set individually for each case, typically with the copy number of 1.5 for loss and 2.5 for gain. CNVs spanning less than the whole length of a chromosomal arm were not called. FISH was also used for confirmation of the three analyzable cases, as previously described [11] (results not shown). Aberrations on gonosomes were excluded from the results. CNV detection using low pass whole genome sequencing was shown to produce similar and comparable results as in the fresh frozen tissue [12].

3. Results

3.1. Clinicopathologic features

The clinicopathologic characteristics are summarized in Table 1. There were 3 males and 5 females with the age range (at the time of diagnosis) from 30 to 84 years (mean 57.5, median 60 years). Follow-up

Table 1
Clinical features and morphology.

Case	Age (years)	Sex	Size (cm)[a]	TNM, AJCC 2017	Follow-up (months)	Morphology					
						Papillary (%)	Adenomatous (%)	Solid (%)	Microcalcif	Pigment	Necrosis
1	55	M	12	pT3a, pNx	AND 12	100	0	0	Yes	No	Yes
2	39	M	3	pT1a, pNx	AND 48	15	85	0	No	Yes	No
3	75	F	2	pT1a, pNx	AND 2	15	70	15	No	Yes	No
4	84	F	13	pT3a, pN1	DOD 3	20	0	30[b]	No	No	No
5	67	M	9.6	pT3a, pNx	NA	80	20	0	No	No	Yes
6	65	F	3.5	pT1a, pNx	AND 14	40	60	0	No	No	No
7	30	F	14	pT2b, pNx	AND 61	80	20	0	No	Yes	No
8	45	F	2.9	pT1a, pNx	AND 1	50	10	10	Yes	Yes	No

M: male; F: female; AND: alive no evidence of disease; NA: not available; DOD: death of disease; Microcalcif: microcalcification

[a] Greatest dimension

[b] Sarcomatoid dedifferentiation.

was available for 7 patients and ranged from 1 to 61 months (mean 20.1, median 12 months). Six patients were alive with no evidence of disease progression, while 1 died of the disease 3 months after the surgery. There was no association with Birt-Hogg-Dubé syndrome in any patient. Three patients presented with pT3a stage, 1 with pT2b and 4 with pT1a.

Tumor size showed a broad range from 2 to 14 cm (mean 7.5, median 6.6). Tumors were described as solid, solid-cystic with focal hemorrhages on gross examination (Fig. 1). Histologically, the tumors were arranged in papillary, adenomatoid and solid structures. The extent of papillary component ranged from 15% to 100% of the tumor volume (mean 51%, median 50%) (Fig. 2). The papillae contained delicate fibrovascular cores without foamy histiocytes (Fig. 3). All cases consisted of two cell populations of pale leaf-like and eosinophilic cells that were represented in variable proportions. Typical raisinoid nuclei were present in all cases (Fig. 4).

Cytologically, the cells in the papillary structures did not differ from those found in the other areas showing a typical chromophobe RCC morphology. Case 2 was predominantly composed of eosinophilic oncocytic cells with mostly centrally located, round nuclei. In this case, raisinoid nuclei (without halos) as well as rounded nuclei with perinuclear halos were identified only at the periphery of the tumor. Amorphous rough microcalcifications and/or psammoma bodies and extracellular dark brown pigment (lipofuscin and/or hemosiderin) were also occasionally found (for details see Table 1) (Fig. 5). Sarcomatoid differentiation involving about 50% of the tumor was present in Case 4.

3.2. Immunohistochemical and histochemical features

The results are summarized in Table 2. All tumors were positive for CK7 (Fig. 6), CD117 (Fig. 7), and Hale's colloidal iron. PAX8 was positive in 7 of 8 cases. TFE3 was focally positive in 3 of 8 tumors. All cases were negative for vimentin, AMACR, Cathepsin K and HMB45. FH staining was retained in all evalauted cases. The proliferative activity was low with Ki-67 proliferative index of 1% in 7 tumors and 5% in the remaining case.

3.3. Chromosomal aneuploidy study

The results are summarized in Table 2. Three cases included in the current study were analyzable. Case 3 revealed loss of chromosome 1p36.33–p36.22, −9q21.11–q34.3, Case 4 showed gains of chromosomes 4, 5, 7, 12, 14, 15q11.2 - q25.3, 18, 19, 20 and 22 and Case 7 showed losses of chromosomes 1, 2, 6, 10 and 17.

4. Discussion

Papillary architecture can occur in a broad spectrum of renal tumors and is by no means specific for papillary RCC. In fact, the papillary morphology represents one of the most common architectural configurations encountered in renal neoplasms. Prominent papillary pattern is however not widely recognized as a morphological feature of chromophobe RCC [13,14]. Papillary arrangement as a focal feature in these tumors has been only rarely mentioned in the literature [13,15-17]. To our best knowledge, only 1 chromophobe RCC with predominant papillary morphology has been documented [17]. This case was reported in one of the largest series of chromophobe RCC published to date, comprising 145 cases [17], and was therefore not discussed in detail. The 8 cases included in this study exhibited a prominent papillary architecture, representing 15% to 100% of the tumor volume. The other architectural patterns observed in these cases were tubulary to cribriform, and solid. The diagnosis of chromophobe RCC was based on the typical cytological features, i.e. on a combination of enlarged pale and leaf-like cells and smaller population of eosinophilic cells. In all cases, raisinoid nuclei and perinuclear clearing were identified. Case 2 exhibited similar features to oncocytic chromophobe RCC, another rare variant [10]. Nuclear features typical for chromophobe RCC were identified only at the periphery of this case. Immunophenotype, showing positivity with CK7, CD117, Hale, low Ki-67 index and negativity with vimentin, was also consistent with chromophobe RCC. Uniformly negative staining with AMACR also argued against the diagnosis of papillary RCC. The cytogenetic features further supported our diagnosis, as multiple chromosomal losses and gains pathognomonic for chromophobe RCC [18-23] were detected in all 3 analyzable cases.

It has been hypothesized that certain morphological features of chromophobe RCC may influence its otherwise indolent clinical course. Neuroendocrine differentiation may occur as the result of dedifferentiation with a potentially negative impact on prognosis [5-7,9]. In our series, Case 4 behaved aggressively and the patient succumbed to the disease 3 months after the surgery. In addition to papillary arrangement, this case also showed sarcomatoid differentiation. Its presence in chromophobe RCC worsens its prognosis by reducing 10-year cancer specific survival rate from 90% to 27% [24,25]. According to one of the largest series on sarcomatoid chromophobe RCC, the mean percentage of tumor showing sarcomatoid differentiation was 67% [26]. Therefore, it is most likely that the aggressive clinical behavior in Case 4 was owing to the presence of sarcomatoid transformation, which comprised about 50% of the tumor, rather than by the papillary component. The remaining 7 cases lacked sarcomatoid areas and all 6 with available clinical information had an indolent clinical course.

The differential diagnostic work-up should be primarily based on the careful cytomorphologic evaluation. Tumors composed mainly of pale cells may be misdiagnosed as papillary RCC with clear cell change, clear cell RCC, or as Xp11.2 translocation RCC. The presence of characteristic cytomorphologic features of chromophobe RCC is however sufficient to make or to strongly suggest the correct diagnosis in most cases.

Papillary RCC can occasionally demonstrate clear cell change [27-30], which is probably caused by the phagocytic activity of the carcinoma cells or by the local microenviroment [29]. This phenomenon is illustrated by the tendency of clear cells to cluster in the vicinity of areas of necrosis and hemorrhage. However, no such zonal distribution was observed in any of the cases in the current series. Psammoma bodies can be also seen in both tumor types, but other structures typical of papillary RCC, such as aggregates of foamy macrophages and cholesterol clefts were not observed in this case series. In contrary to chromophobe RCC, papillary RCC typically stains with AMACR and vimentin. As multiple chromosomal imbalances including chromosomal losses and gains may be found in both papillary [22,31-33] and

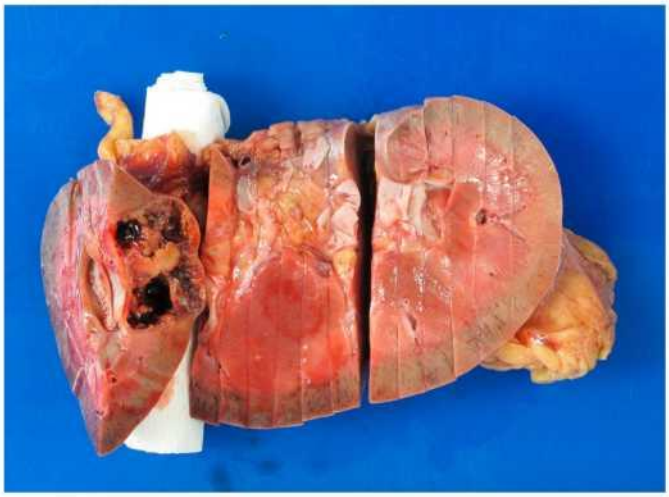

Fig. 1. The tumors were solid or solid-cystic with focal hemorrhages on gross section.

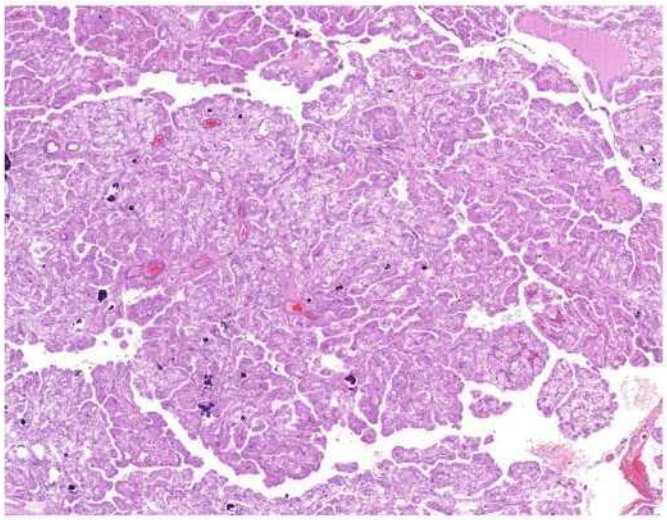

Fig. 2. The tumors were arranged in papillary, adenomatoid and solid structures.

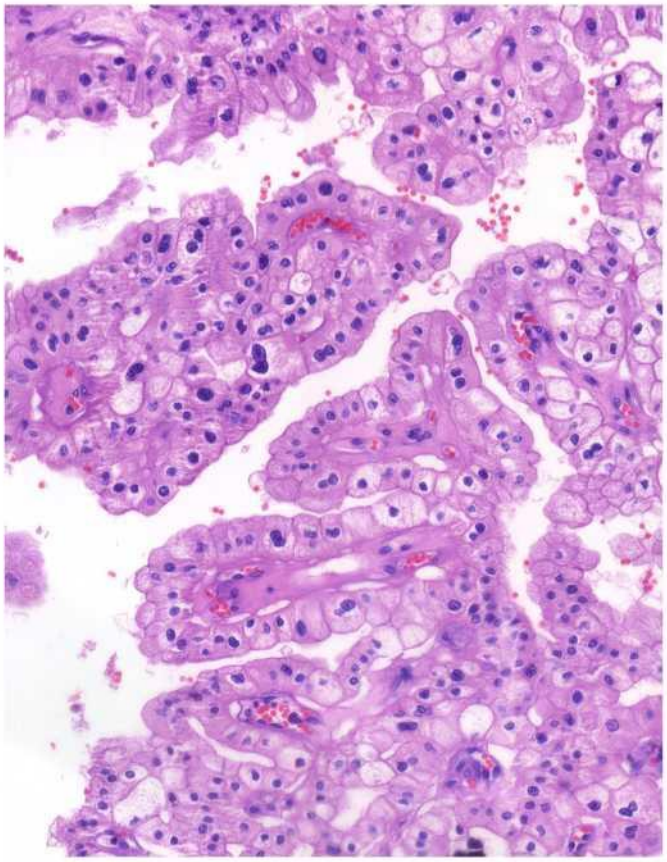

Fig. 3. The papillae contained delicate fibrovascular cores lined by large pale epithelial cells and smaller eosinophilic epithelial cells.

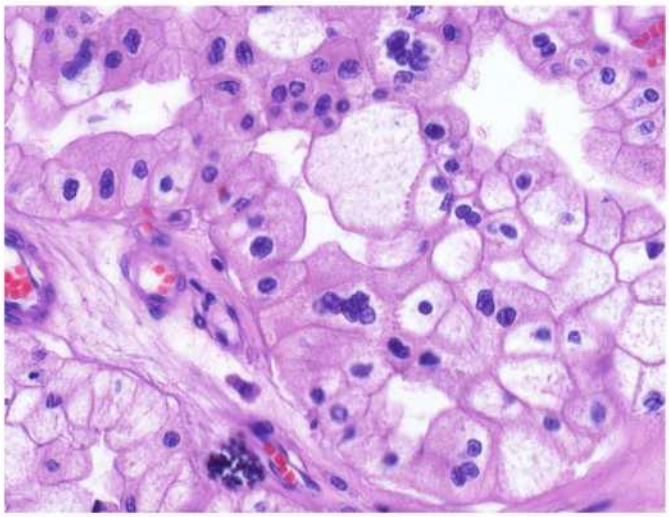

Fig. 4. Typical raisinoid nuclei were prominent and present in all cases.

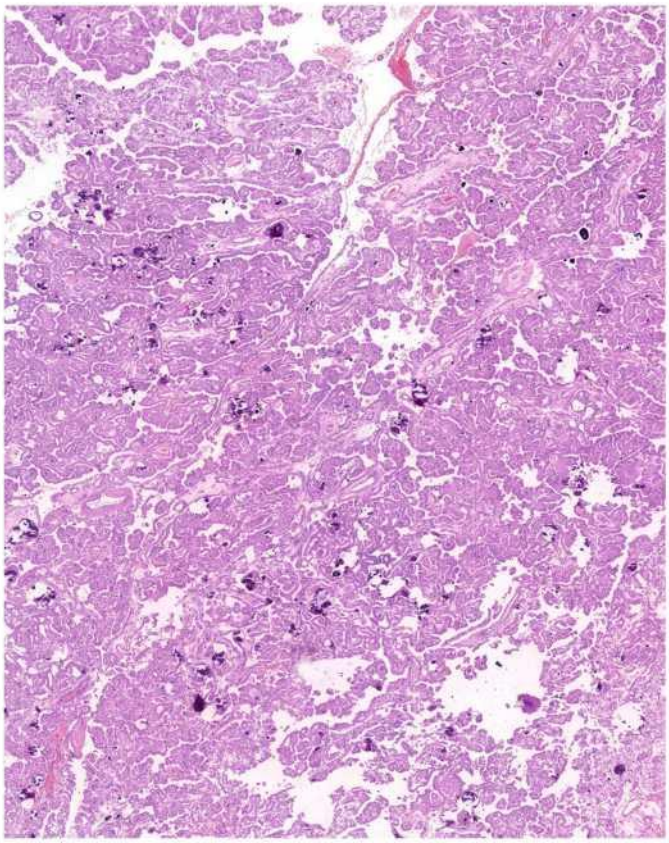

Fig. 5. Amorphous rough microcalcifications, psammoma bodies, and lipochrome were found in several cases.

chromophobe RCC, the results of the cytogenetic analyses should always be correlated with the morphologic and immunohistochemical features.

Papillary structures can also rarely occur in low-grade clear cell RCC [27-29,34-36]. Apart from the differences in the cytomorphology, the vascular pattern in clear cell RCC may offer a helpful diagnostic clue. Pseudoacinar and fascicular patterns are more common in clear cell RCC, whereas reticular pattern is more often present in chromophobe RCC [37]. Likewise, vimentin reactivity and an absence of reactivity for CD117 are uniformly present in clear cell RCC, but are typically not found in chromophobe RCC. In contrast to the traditional view that clear cell RCC are CK7 negative, CK 7 positivity can be often found in the low-grade clear cell RCC [38]. Although CK7 can be strongly positive in such cases, it is invariably focal, in contrast to the strong and diffuse positivity found in chromophobe RCC. In addition, cytogenetic methods for detection of *VHL* mutation, *VHL* hypermethylation or LOH 3p may also help to establish the diagnosis of clear cell RCC in equivocal cases.

It has become evident that Xp11.2 translocation RCC represents a morphologically heterogeneous group of tumors [39]. Histological

Table 2
Results of immunohistochemical and molecular genetic analysis.

Case	CK 7	CD117	vim	PAX8	AMACR	Ki-67	TFE3	HMB45	Hale's	cath K	FH	aCGH
1	+ + +	+ + +	−	+ + +	−	1%	−	−	+ + +	−	+ + +	NA
2	+ + +	+	−	+ + +	−	1%	foc + +	−	+ + +	−	+ + +	NA
3	+ + +	+ +	−	+ + +	−	1%	−	−	+ + +	−	+ + +	−1p36.33–p36.22, −9q21.11–q34.3.
4	+ + +	+ +	−	−	−	5%	foc + +	−	+ + +	−	+ + +	+4, +5, +7, +12, +14, +15q11.2–q25.3, +18, +19, +20, +22.
5	+ + +	+	−	foc +	−	1%	−	−	+ + +	−	NP	NP
6	+ + +	+	−	+	−	1%	−	−	+ + +	−	+ + +	NA
7	+ + +	+ +	−	+	−	1%	−	−	+ + +	−	+ + +	−1, −2, −6, −10, −17
8	+ + +	+ + +	−	+ + +	−	1%	foc +	−	+ +	−	+ + +	NA

vim: vimentin; cath K: cathepsin K; FH: fumarat hydratase; foc:focal aCGH: array Comparative Genomic Hybridization; NP: not performed; NA: not analyzable.

features similar to the cases described in this series may theoretically observed only in a subset of Xp11.2 translocation RCCs demonstrating an *ASPL-TFE3* fusion. These tumors are characterized by papillary and nested structures, lined by epithelioid clear and eosinophilic cells, often intermingled with psammoma bodies. Although the positive immune reaction for TFE3 is considered relatively specific for Xp11.2 translocation RCC, frequent false positive (or negative) results are well documented [40]. TFE3 was focally positive in 3 of the cases in this series, while the remaining 5 were negative. The fraction of positive neoplastic cells was however typically below 20% and can be considered as non-specific. FISH analysis for further confirmation was not performed. Cathepsin K is another widely used marker in the diagnosis of the translocation RCC, but its expression depends on the type of *TFE3* fusion partner. *ASPL-TFE3* RCC is typically negative for Cathepsin K, which has no discriminatory value in this situation [41,42]. In our series, Cathepsin K was negative in all cases. The key diagnostic test in this setting relies on the use of break-apart FISH or RT-PCR, which are necessary for diagnostic confirmation of Xp11.2 translocation RCC.

Case 2 was predominantly eosinophilic, resembling an oncocytic papillary RCC, which is a malignant renal tumor characterized by papillary structures lined by eosinophilic (oncocytic) cells with rounded, low-grade nuclei, lacking perinuclear clearing [43,44]. The nuclei in Case 2 closely resembled those found in oncocytic papillary RCC. However, after closer evaluation, cells with raisinoid nuclei (without halo) and rounded nuclei encircled by halos were identified at the periphery of the neoplasm. Scattered foci of foamy macrophages, typical of oncocytic papillary RCC, can serve as another useful discriminatory feature and no such features were documented in this case. Comparison of immunoprofile of papillary and chromophobe RCC was already discussed. The cytogenetic data available on the oncocytic

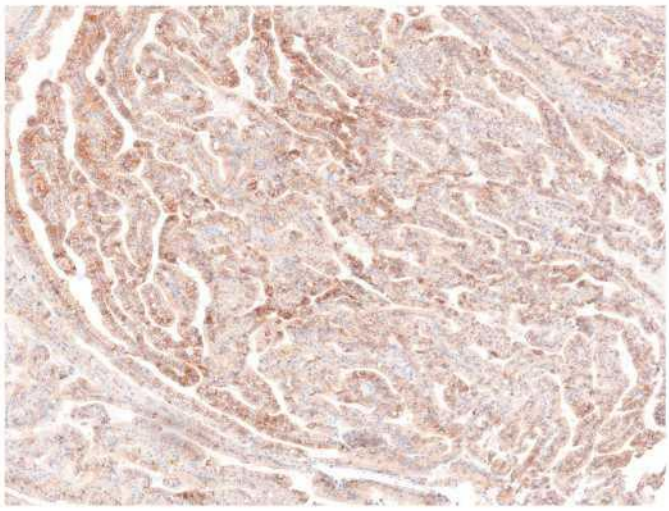

Fig. 7. All cases were positive for CD117; staining pattern was predominantly membranous.

papillary RCC are somewhat inconsistent, and some indicate cytogenetic similarities to type 1 papillary RCC (demonstrating polysomy of chromosomes 7, 17 and loss of Y), whereas other cases were documented with diploid status of 7, 17 and Y or even diploid status of all chromosomes [45]. In the current study, Case 2 was cytogenetically not analyzable.

Fumarate hydratase (*FH*)-deficient RCC often demonstrates papillary architecture with large cells containing abundant eosinophilic

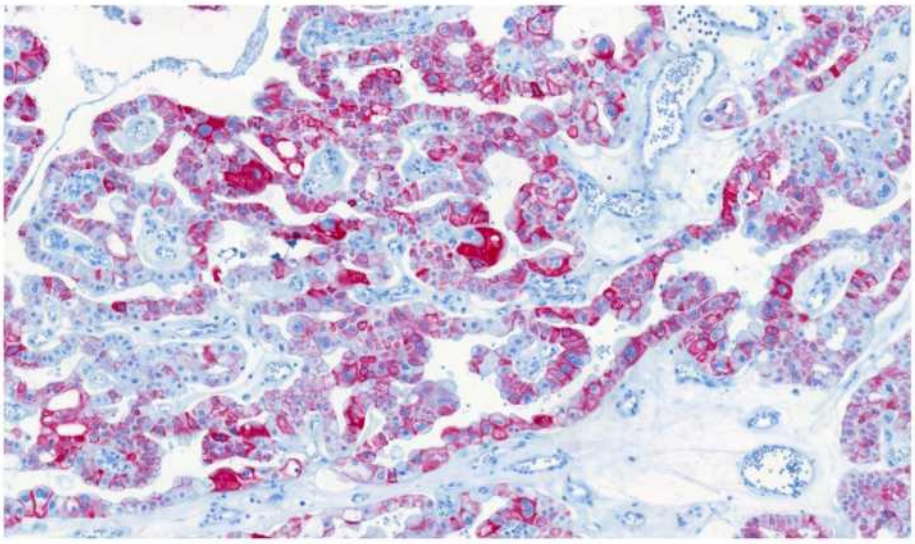

Fig. 6. Strong diffuse positivity was found for CK7 in all cases.

cytoplasm. The typical finding includes large viral-like nucleoli [46], which were not seen in our cases. Another helpful morphologic feature can be the detection of multiple architectural patterns in *FH*-deficient RCC [47]. The overall high-grade morphology and an advanced pathologic stage at the time of diagnosis underscore the aggressiveness of *FH*-deficient RCC and with the IHC loss of FH and the overexpression of S-(2-succino)-cysteine can help in this differential scenario. In all evaluated cases in this study, the FH staining was retained. The detection of the *FH* gene mutation on chromosome 1q42.3-q43 can also confirm the diagnosis.

In summary, we expand the morphologic spectrum of chromophobe RCC by presenting 8 cases demonstrating a prominent papillary architecture, which is a feature exceptionally rarely documented in these neoplasms. Although our study is limited, it seems that the presence of papillary architecture does not affect the indolent clinical course of chromophobe RCC. In contrast to chromophobe RCC demonstrating classic architecture, the presence of prominent papillary structures in this tumor alters the list of entities that should be considered in the differential diagnosis. It is therefore important to distinguish chromophobe RCC with papillary features in particular from the biologically aggressive entities, such as *FH*-deficient RCC or Xp11.2 translocation RCC. The correct diagnosis in this setting can usually be rendered or strongly suggested by identifying the typical cytomorphology of chromophobe RCC.

Compliance with ethical standards

Neither ethics approval nor informed consent was required for our study.

Funding

The study was supported by the Charles University Research Fund (project number Q39) and by the project Institutional Research Fund of University Hospital Plzen (FNPl 00669806).

Declaration of competing interest

All authors declare no conflict of interest.

References

[1] Hes O, Vanecek T, Perez-Montiel DM, Alvarado Cabrero I, Hora M, Suster S, et al. Chromophobe renal cell carcinoma with microcystic and adenomatous arrangement and pigmentation–a diagnostic pitfall. Morphological, immunohistochemical, ultrastructural and molecular genetic report of 20 cases. Virchows Archiv : An International Journal of Pathology 2005;446:383–93.
[2] Michal M, Hes O, Svec A, Ludvikova M. Pigmented microcystic chromophobe cell carcinoma: a unique variant of renal cell carcinoma. Ann Diagn Pathol 1998;2:149–53.
[3] Dundr P, Pesl M, Povysil C, Tvrdik D, Pavlik I, Soukup V, et al. Pigmented microcystic chromophobe renal cell carcinoma. Pathol Res Pract 2007;203:593–7.
[4] Foix MP, Dunatov A, Martinek P, Mundo EC, Suster S, Sperga M, et al. Morphological, immunohistochemical, and chromosomal analysis of multicystic chromophobe renal cell carcinoma, an architecturally unusual challenging variant. Virchows Archiv : An International Journal of Pathology. 2016;469:669–78.
[5] Peckova K, Martinek P, Ohe C, Kuroda N, Bulimbasic S, Condom Mundo E, et al. Chromophobe renal cell carcinoma with neuroendocrine and neuroendocrine-like features. Morphologic, immunohistochemical, ultrastructural, and array comparative genomic hybridization analysis of 18 cases and review of the literature. Ann Diagn Pathol 2015;19:261–8.
[6] Parada DD, Pena KB. Chromophobe renal cell carcinoma with neuroendocrine differentiation. APMIS : Acta Pathologica, Microbiologica, et Immunologica Scandinavica 2008;116:859–65.
[7] Kuroda N, Tamura M, Hes O, Michal M, Gatalica Z. Chromophobe renal cell carcinoma with neuroendocrine differentiation and sarcomatoid change. Pathol Int 2011;61:552–4.
[8] Mokhtar GA, Al-Zahrani R. Chromophobe renal cell carcinoma of the kidney with neuroendocrine differentiation: a case report with review of literature. Urology Annals 2015;7:383–6.
[9] Ohe C, Matsuura K, Kai T, Moriyama M, Sugiguchi S, Terahata S, et al. Chromophobe renal cell carcinoma with neuroendocrine differentiation/morphology: a clinicopathological and genetic study of three cases. Human Pathology: Case Reports 2014;1:31–9.
[10] Kuroda N, Tanaka A, Yamaguchi T, Kasahara K, Naruse K, Yamada Y, et al. Chromophobe renal cell carcinoma, oncocytic variant: a proposal of a new variant giving a critical diagnostic pitfall in diagnosing renal oncocytic tumors. Med Mol Morphol 2013;46:49–55.
[11] Sperga M, Martinek P, Vanecek T, Grossmann P, Bauleth K, Perez-Montiel D, et al. Chromophobe renal cell carcinoma–chromosomal aberration variability and its relation to Paner grading system: an array CGH and FISH analysis of 37 cases. Virchows Archiv : An International Journal of Pathology. 2013;463:563–73.
[12] Munchel S, Hoang Y, Zhao Y, Cottrell J, Klotzle B, Godwin AK, et al. Targeted or whole genome sequencing of formalin fixed tissue samples: potential applications in cancer genomics. Oncotarget. 2015;6:25943–61.
[13] Przybycin CG, Cronin AM, Darvishian F, Gopalan A, Al-Ahmadie HA, Fine SW, et al. Chromophobe renal cell carcinoma: a clinicopathologic study of 203 tumors in 200 patients with primary resection at a single institution. Am J Surg Pathol 2011;35:962–70.
[14] Din NU, Fatima S, Ahmad Z. Chromophobe renal cell carcinoma: a morphologic and immunohistochemical study of 45 cases. Ann Diagn Pathol 2013;17:508–13.
[15] Kuroda N, Iiyama T, Moriki T, Shuin T, Enzan H. Chromophobe renal cell carcinoma with focal papillary configuration, nuclear basaloid arrangement and stromal osseous metaplasia containing fatty bone marrow element. Histopathology. 2005;46:712–3.
[16] Karashima T, Kuroda N, Taguchi T, Matsumoto M, Hiroi M, Nao T, et al. Chromophobe renal cell carcinoma, eosinophilic variant with papillary growth: a case report. Int J Clin Exp Pathol 2015;8:13590–5.
[17] Amin MB, Paner GP, Alvarado-Cabrero I, Young AN, Stricker HJ, Lyles RH, et al. Chromophobe renal cell carcinoma: histomorphologic characteristics and evaluation of conventional pathologic prognostic parameters in 145 cases. Am J Surg Pathol 2008;32:1822–34.
[18] Moch H, Cubilla AL, Humphrey PA, Reuter VE, Ulbright TM. The 2016 WHO classification of tumours of the urinary system and male genital organs-part a: renal, penile, and testicular tumours. Eur Urol 2016;70:93–105.
[19] Brunelli M, Eble JN, Zhang S, Martignoni G, Delahunt B, Cheng L. Eosinophilic and classic chromophobe renal cell carcinomas have similar frequent losses of multiple chromosomes from among chromosomes 1, 2, 6, 10, and 17, and this pattern of genetic abnormality is not present in renal oncocytoma. Modern Pathology : An Official Journal of the United States and Canadian Academy of Pathology, Inc. 2005;18:161–9.
[20] Speicher MR, Schoell B, du Manoir S, Schrock E, Ried T, Cremer T, et al. Specific loss of chromosomes 1, 2, 6, 10, 13, 17, and 21 in chromophobe renal cell carcinomas revealed by comparative genomic hybridization. Am J Pathol 1994;145:356–64.
[21] Hagenkord JM, Gatalica Z, Jonasch E, Monzon FA. Clinical genomics of renal epithelial tumors. Cancer Genet 2011;204:285–97.
[22] Kim HJ, Shen SS, Ayala AG, Ro JY, Truong LD, Alvarez K, et al. Virtual-karyotyping with SNP microarrays in morphologically challenging renal cell neoplasms: a practical and useful diagnostic modality. Am J Surg Pathol 2009;33:1276–86.
[23] Yokomizo A, Yamamoto K, Furuno K, Shiota M, Tatsugami K, Kuroiwa K, et al. Histopathologic subtype-specific genomic profiles of renal cell carcinomas identified by high-resolution whole-genome single nucleotide polymorphism array analysis. Oncol Lett 2010;1:1073–8.
[24] Volpe A, Novara G, Antonelli A, Bertini R, Billia M, Carmignani G, et al. Chromophobe renal cell carcinoma (RCC): oncological outcomes and prognostic factors in a large multicentre series. BJU Int 2012;110:76–83.
[25] de Peralta-Venturina M, Moch H, Amin M, Tamboli P, Hailemariam S, Mihatsch M, et al. Sarcomatoid differentiation in renal cell carcinoma: a study of 101 cases. Am J Surg Pathol 2001;25:275–84.
[26] Lauer SR ZM, Master VA, Osunkoya AO. Chromophobe renal cell carcinoma with sarcomatoid differentiation. A clinicopathologic study of 14 cases. Anal Quant Cytol Histol35:77–84.
[27] Ross H, Martignoni G, Argani P. Renal cell carcinoma with clear cell and papillary features. Arch Pathol Lab Med 2012;136:391–9.
[28] Klatte T, Said JW, Seligson DB, Rao PN, de Martino M, Shuch B, et al. Pathological, immunohistochemical and cytogenetic features of papillary renal cell carcinoma with clear cell features. J Urol 2011;185:30–5.
[29] Gobbo S, Eble JN, Maclennan GT, Grignon DJ, Shah RB, Zhang S, et al. Renal cell carcinomas with papillary architecture and clear cell components: the utility of immunohistochemical and cytogenetical analyses in differential diagnosis. Am J Surg Pathol 2008;32:1780–6.
[30] Petersson F, Sperga M, Bulimbasic S, Martinek P, Svajdler M, Kuroda N, et al. Foamy cell (hibernoma-like) change is a rare histopathological feature in renal cell carcinoma. Virchows Archiv : An International Journal of Pathology. 2014;465:215–24.
[31] Saleeb RM, Brimo F, Farag M, Rompre-Brodeur A, Rotondo F, Beharry V, et al. Toward biological subtyping of papillary renal cell carcinoma with clinical implications through histologic, immunohistochemical and molecular analysis. Am J Surg Pathol 2017;41:1618–29.
[32] Antonelli A, Tardanico R, Balzarini P, Arrighi N, Perucchini L, Zanotelli T, et al. Cytogenetic features, clinical significance and prognostic impact of type 1 and type 2 papillary renal cell carcinoma. Cancer Genet Cytogenet 2010;199:128–33.
[33] Vieira J, Henrique R, Ribeiro FR, Barros-Silva JD, Peixoto A, Santos C, et al. Feasibility of differential diagnosis of kidney tumors by comparative genomic hybridization of fine needle aspiration biopsies. Genes Chromosomes Cancer 2010;49:935–47.
[34] Salama ME, Worsham MJ, DePeralta-Venturina M. Malignant papillary renal tumors with extensive clear cell change: a molecular analysis by microsatellite

analysis and fluorescence in situ hybridization. Arch Pathol Lab Med 2003;127:1176–81.
[35] Haudebourg J, Hoch B, Fabas T, Cardot-Leccia N, Burel-Vandenbos F, Vieillefond A, et al. Strength of molecular cytogenetic analyses for adjusting the diagnosis of renal cell carcinomas with both clear cells and papillary features: a study of three cases. Virchows Archiv : An International Journal of Pathology. 2010;457:397–404.
[36] Alaghehbandan R, Ulamec M, Martinek P, Pivovarcikova K, Michalova K, Skenderi F, et al. Papillary pattern in clear cell renal cell carcinoma: Clinicopathologic, morphologic, immunohistochemical and molecular genetic analysis of 23 cases. Ann Diagn Pathol 2019;38:80–6.
[37] Ruiz-Sauri A, Garcia-Bustos V, Granero E, Cuesta S, Sales MA, Marcos V, et al. Distribution of vascular patterns in different subtypes of renal cell carcinoma. A morphometric study in two distinct types of blood vessels. Pathology Oncology Research : POR 2018;24:515–24.
[38] Gonzalez ML, Alaghehbandan R, Pivovarcikova K, Michalova K, Rogala J, Martinek P, et al. Reactivity of CK7 across the spectrum of renal cell carcinomas with clear cells. Histopathology. 2019;74:608–17.
[39] Inamura K. Translocation renal cell carcinoma: an update on clinicopathological and molecular features. Cancers. 2017;9.
[40] Hayes M, Peckova K, Martinek P, Hora M, Kalusova K, Straka L, et al. Molecular-genetic analysis is essential for accurate classification of renal carcinoma resembling Xp112 translocation carcinoma. Virchows Archiv : an international journal of pathology 2015;466:313–322.
[41] Martignoni G, Gobbo S, Camparo P, Brunelli M, Munari E, Segala D, et al. Differential expression of cathepsin K in neoplasms harboring TFE3 gene fusions. Modern Pathology : An Official Journal of the United States and Canadian Academy of Pathology, Inc 2011;24:1313–9.
[42] Argani P, Zhong M, Reuter VE, Fallon JT, Epstein JI, Netto GJ, et al. TFE3-fusion variant analysis defines specific clinicopathologic associations among Xp11 translocation cancers. Am J Surg Pathol 2016;40:723–37.
[43] Lefevre M, Couturier J, Sibony M, Bazille C, Boyer K, Callard P, et al. Adult papillary renal tumor with oncocytic cells: clinicopathologic, immunohistochemical, and cytogenetic features of 10 cases. Am J Surg Pathol 2005;29:1576–81.
[44] Hes O, Brunelli M, Michal M, Cossu Rocca P, Hora M, Chilosi M, et al. Oncocytic papillary renal cell carcinoma: a clinicopathologic, immunohistochemical, ultrastructural, and interphase cytogenetic study of 12 cases. Ann Diagn Pathol 2006;10:133–9.
[45] Michalova K, Steiner P, Alaghehbandan R, Trpkov K, Martinek P, Grossmann P, et al. Papillary renal cell carcinoma with cytologic and molecular genetic features overlapping with renal oncocytoma: analysis of 10 cases. Ann Diagn Pathol 2018;35:1–6.
[46] Chen YB, Brannon AR, Toubaji A, Dudas ME, Won HH, Al-Ahmadie HA, et al. Hereditary leiomyomatosis and renal cell carcinoma syndrome-associated renal cancer: recognition of the syndrome by pathologic features and the utility of detecting aberrant succination by immunohistochemistry. Am J Surg Pathol 2014;38:627–37.
[47] Muller M, Guillaud-Bataille M, Salleron J, Genestie C, Deveaux S, Slama A, et al. Pattern multiplicity and fumarate hydratase (FH)/S-(2-succino)-cysteine (2SC) staining but not eosinophilic nucleoli with perinucleolar halos differentiate hereditary leiomyomatosis and renal cell carcinoma-associated renal cell carcinomas from kidney tumors without FH gene alteration. Modern Pathology : An Official Journal of the United States and Canadian Academy of Pathology, Inc. 2018;31:974–83.

1.7.3 Morphological, immunohistochemical, and chromosomal analysis of multicystic chromophobe renal cell carcinoma, an architecturally unusual challenging variant

Chromofóbní renální karcinom je typicky tvořen různou kombinací velkých slabě eosinofilních buňek a menších oxyfilních buněk s granulární cytoplasmmou uspořádaných v solidně-alveolárně. V literatuře jsou popsány různé varianty ChRCC.

V rámci prezentované studie bylo morfologicky, imunohistochemicky a molekulárně-geneticky (arrayCGH) analyzováno 10 případů ChRCC se specifickým multicystickým vzhledem. Případy pocházely od 6 mužů a 4 žen, pacienti byli ve věkovém rozmezí 50 - 89 let. Velikost tumorů se pohybovala mezi 1,2 – 20 cm (průměr 5,32 cm; medián 3 cm). U žádného z tumorů nebylo zdokumentováno agresivní chování. V tumorech byly pozorovány 2 odlišné typy růstu – jednak cysty variabilní velikosti připomínající multiloculární cystickou neoplázii nízkého maligního potenciálu a dále i komprimované cystické a tubulární struktury vytvářející štěrbinovité prostory. Konstantně byla u tumorů pozorována typická „rozinkovitá/raisenoidní“ jádra, všechny případy byly prosty nekrotických okrsků. Polovina případů měla eosinofilní/onkocytickou cytologii buněk, depozita pigmentu (lipochmrom) a mikrokalcifikace. Druhá polovina byla složená spíše z bledé či smíšené populace buněk. Všechny tumory vykazovali pozitivitu v imunohistochemickém barvení EMA, CK7, OSCAR, CD117, parvalbuminu, MIA a PAX8. Naopak negativní byly všechny tumory ve vimentinu, TFE3, CAIX, HMB45, katepsinu K a v průkazu AMACR. Proliferační aktivita značená protilátkou Ki67 byla pod 1%. Molekulárně-genetické vyšetření prokázalo mnohotné chromozomální ztráty v 2/5 analyzovatelných případů, 3/5 případů byly bez chromozomálních numerických aberací.

Chromofóbní renální karcinom může být velmi vzácně uspořádán multicysticky, patrně by se u těchto případů mohlo jednak o extrémní formu mikrocystické adenomatoidní pigmentované varianty ChRCC. Spektrum renálních neoplázií, které přicházejí do diferenciální diagnózy v rámci této vzácné varianty ChRCC, je odlišné než u klasického ChRCC, i když imunohistochemický profil klasického ChRCC a multicystické varianty ChRCC jsou překryvné. Chromozonální numerický aberační status byl v analyzovaných případech variabilní. Všechny případy se manifestovaly indolentním průběhem onemocnění.

Virchows Arch (2016) 469:669–678
DOI 10.1007/s00428-016-2022-x

ORIGINAL ARTICLE

Morphological, immunohistochemical, and chromosomal analysis of multicystic chromophobe renal cell carcinoma, an architecturally unusual challenging variant

Maria Pané Foix[1,2] · Ana Dunatov[3] · Petr Martinek[4] · Enric Condom Mundó[1,2] · Saul Suster[5] · Maris Sperga[6] · Jose I. Lopez[7] · Monika Ulamec[8] · Stela Bulimbasic[9] · Delia Perez Montiel[10] · Reza Alaghehbandan[11] · Kvetoslava Peckova[4] · Krystina Pivovarcikova[4] · Daum Ondrej[4] · Pavla Rotterova[4] · Faruk Skenderi[12] · Kristyna Prochazkova[13] · Martin Dusek[4] · Milan Hora[13] · Michal Michal[4] · Ondrej Hes[4,14]

Received: 26 May 2016 / Revised: 27 July 2016 / Accepted: 5 September 2016 / Published online: 15 September 2016

Abstract Chromophobe renal cell carcinoma (ChRCC) is typically composed of large leaf-like cells and smaller eosinophilic cells arranged in a solid-alveolar pattern. Eosinophilic, adenomatoid/pigmented, or neuroendocrine variants have also been described. We collected 10 cases of ChRCC with a distinct multicystic pattern out of 733 ChRCCs from our registry, and subsequently analyzed these by morphology, immunohistochemistry, and array comparative genomic hybridization. Of the 10 patients, 6 were males with an age range of 50–89 years (mean 68, median 69). Tumor size ranged between 1.2 and 20 cm (mean 5.32, median 3). Clinical follow-up was available for seven patients, ranging 1–19 years (mean 7.2, median 2.5). No aggressive behavior was documented. We observed two growth patterns, which were similar in all tumors: (1) variable-sized cysts, resembling multilocular cystic neoplasm of low malignant potential and (2) compressed cystic and tubular pattern with slit-like spaces. Raisinoid nuclei were consistently present while necrosis was absent in all cases. Half of the cases showed eosinophilic/oncocytic cytology, deposits of pigment (lipochrome) and microcalcifications. The other half was composed of pale or mixed cell populations. Immunostains for epithelial membrane antigen (EMA), CK7, OSCAR, CD117, parvalbumin, MIA, and Pax 8 were positive in all tumors while negative for vimentin, TFE3, CANH 9, HMB45, cathepsin K, and AMACR. Ki67 immunostain was positive in up to 1 % of neoplastic cells. Molecular genetic

✉ Ondrej Hes
hes@medima.cz

1 Department of Pathology, Bellvitge University Hospital, Bellvitge Biomedical Research Institute (IDIBELL), Barcelona, Spain

2 Department of Pathology and Experimental Therapeutics, School of Medicine, University of Barcelona, Barcelona, Spain

3 Department of Pathology, University of Split, Split, Croatia

4 Department of Pathology, , Medical Faculty and Charles University Hospital Plzen, Charles University, Alej Svobody 80, 304 60 Pilsen, Czech Republic

5 Department of Pathology, Medical College of Wisconsin, Milwaukee, WI, USA

6 Department of Pathology, East University, Riga, Latvia

7 Department of Pathology, Cruces University Hospital, Biocruces Research Institute, University of the Basque Country, Barakaldo, Spain

8 "Ljudevit Jurak" Pathology Department, Clinical Hospital Center "Sestre milosrdnice", Zagreb, Croatia

9 Department of Pathology, Clinical Hospital Center Zagreb, Zagreb, Croatia

10 Department of Pathology, Instituto Nacional de Cancerologia, Mexico City, Mexico

11 Department of Pathology, Faculty of Medicine, Royal Columbian Hospital, University of British Columbia, Vancouver, BC, Canada

12 Department of Pathology, Clinical Center of the University of Srajevo, Sarajevo, Bosnia and Herzegovina

13 Department of Urology, Medical Faculty and Charles University Hospital, Charles University, Plzen, Czech Republic

14 Biomedical Centre, Faculty of Medicine in Lzen, Charles University in Prague, Plzen, Czech Republic

examination revealed multiple chromosomal losses in two fifths analyzable tumors, while three cases showed no chromosomal numerical aberrations. ChRCC are rarely arranged in a prominent multicystic pattern, which is probably an extreme form of the microcystic adenomatoid pigmented variant of ChRCC. The spectrum of tumors entering the differential diagnosis of ChRCC is quite different from that of conventional ChRCC. The immunophenotype of ChRCC is identical with that of conventional ChRCC. Chromosomal numerical aberration pattern was variable; no chromosomal numerical aberrations were found in three cases. All the cases in this series have shown an indolent and non-aggressive behavior.

Keywords Kidney · Chromophobe renal cell carcinoma · Multicystic · Immunohistochemistry · ArrayCGH

Introduction

Chromophobe renal cell carcinoma (ChRCC) is the third most common type of adult renal epithelial tumor, accounting for approximately 5 % of renal carcinomas [1, 2]. ChRCC usually carries a more favorable prognosis than clear cell renal cell carcinoma (CCRCC). However, sarcomatoid differentiation, which is associated with worse prognosis, is found in approximately 8 % of ChRCC [2].

ChRCC usually shows solid or solid-alveolar architectural patterns, composed of a combination of cells with leaf-like morphology and pale cytoplasm, and smaller eosinophilic cells with oncocytic cytoplasm. The two main recognized ChRCC morphologic variants are classic and eosinophilic. However, the morphological spectrum has expanded to pigmented microcystic adenomatoid, oncocytoma-like, ChRCC with neuroendocrine differentiation, and ChRCC with focal papillary proliferations [3–10].

In this study, we describe a subset of ChRCC tumors with a pure multicystic architecture using morphologic, immunohistochemical, and array comparative genomic hybridization (aCGH) features.

Material and methods

From 733 ChRCCs in the Plzen Tumor Registry, 10 cases of ChRCC with a multicystic pattern were selected. The tissues had been fixed in neutral formalin, embedded in paraffin, cut into 4–5-μm-thin sections and stained with hematoxylin and eosin (H&E). One to seven paraffin blocks were available for each case. All tumors were independently reviewed by two pathologists (MPF and OH). Clinicopathologic and follow-up data were collected using medical records available from each participating institution. Selected cases were further analyzed using immunohistochemistry and aCGH.

Immunohistochemistry

The immunohistochemical study was performed using a Ventana Benchmark XT automated immunostainer (Ventana Medical System, Inc., Tucson, AZ, USA) on formalin fixed, paraffin embedded tissue. Primary antibodies against the following antigens were employed: epithelial membrane antigen (EMA) (E29, monoclonal, DakoCytomation, Carpinteria CA, 1:1000); cytokeratin 7 (OV-TL12/30, monoclonal, DakoCytomation, 1:200); OSCAR (OSCAR, 1:500, Covance, Herts, UK, 1:500), racemase/AMACR (P504S, monoclonal, Zeta, Sierra Madre, CA, 1:50); vimentin (D9, monoclonal, NeoMarkers, Westinghouse, CA, 1:1000); parvalbumin (PA-235, monoclonal, Sigma Aldrich, St. Luis, MO, 1:500): antimelanosome (HMB45, monoclonal, DakoCytomation, 1:200); Ki-67 (MIB1, monoclonal, Dako, Glostrup, Denmark, 1:1000); c-kit (CD117, polyclonal, Dako, Glostrup, Denmark, 1:300); carbonic anhydrase IX (rhCA9, monoclonal, RD systems, Abingdon, GB, 1:100); TFE3 (polyclonal, Abcam, Cambridge, UK, 1:100), cathepsin K (3F9, monoclonal, Abcam, 1:100); progesterone receptor (monoclonal, 1E2, Ventana, RTU); estrogen receptor (monoclonal, SP1, Ventana, RTU); antimitochondrial antigen (113-1, monoclonal, Biogenex, Fremont, CA, 1:500); smooth muscle actin (1A4, monoclonal, DakoCytomation, 1:1000); desmin (D33, monoclonal, Dako, 1:100); CD31 (JC70A, monoclonal, DakoCytomation, 1:50); CD34 (QBEnd-10, monoclonal, Dako, 1:100); and PAX-8 (polyclonal, Cell Marque, Rocklin, CA, 1: 25). The primary antibodies were visualized using the supersensitive streptavidin-biotin-peroxidase complex (BioGenex). Appropriate positive controls were employed.

Molecular genetic methods

DNA extraction

DNA was extracted from formalin-fixed paraffin-embedded (FFPE) tumor and non-tumor tissues (when available) of each case using QIAsymphony DNA Mini Kit (QIAGEN, Hilden, Germany) on an automated extraction system (QIAsymphony SP, QIAGEN) according to the manufacturer's supplementary protocol for FFPE samples (purification of genomic DNA from FFPE tissue using the QIAamp DNA FFPE Tissue Kit and Deparaffinization Solution). Concentration and purity of isolated DNA were measured using NanoDrop ND1000 (NanoDrop Technologies Inc., Wilmington, DE, USA). DNA integrity was examined by amplification of control genes in multiplex PCR, producing fragments from 100 to

600 base pairs. Only cases with DNA integrity equal to or higher than 400 bp were used for further analysis by aCGH.

Array comparative genomic hybridization

A CytoChip Focus Constitutional (BlueGnome Ltd., Cambridge, UK) microarray processor was used for analysis. CytoChip Focus Constitutional uses BAC technology and covers 143 regions of known significance with 1-Mb spacing across a genome. Probes were spotted in triplicate. First, 400 ng of gDNA was labeled using the Fluorescent Labeling System (BlueGnome Ltd., Cambridge, UK). The procedure consisted of Cy3 labeling of a test sample and Cy5 labeling of a reference sample. MegaPool Reference DNA of opposite sex was used as a reference sample (Kreatech Diagnostics, Amsterdam, Netherlands). Each labeled pair was mixed, dried, and hybridized overnight at 47 °C using ArrayIt hybridization cassettes (Arrayit Corporation, CA, USA). Posthybridization washing was done using SSC buffers with increasing stringency. Dried microarrays were scanned with InnoScan 900 (Innopsys, France) at a resolution of 5 μm.

Image and data analysis: scanned images were analyzed and quantified using BlueFuse Multi software (BlueGnome Ltd., Cambridge, UK). BlueFuse Multi uses Bayesian algorithms to generate intensity values for each Cy5 and Cy3 labeled spot on the array according to an appropriate .gal file. The reported changes were browsed and interpreted using BlueFuse Multi as well. Cutoff values were set to a log 2 ratio of −0.193 for loss and 0.170 for gain.

Results

The clinicopathological features of the 10 selected cases are summarized in Table 1. Six patients were male with an age range of 50–89 years (mean 68, median 69). Tumor size ranged between 1.2 and 20 cm (mean 5.32, median 3.7). Clinical follow-up was available for seven patients, ranging 1–19 years (mean 7.2, median 2.5). An aggressive clinical course was not observed in any of these patients.

At gross examination, tumors were relatively well-demarcated. No grossly visible angioinvasion or invasion into the renal sinus, pelvicalyceal system, or perirenal fat was encountered. The tumor cut surface was brown in three cases, tan/yellow in three cases, and tan to gray in one case. Gross information on color and consistency of the tumor was not available in three cases.

Morphologic features are presented in Table 2. The majority of the tumors showed predominantly eosinophilic/oncocytic morphology (6/10), a smaller proportion of cases demonstrating a pale and leaf-like neoplastic cell population (3/10) and one case a mixture of both. Raisinoid nuclei with perinuclear halo were present in all cases, with occasional binucleated cells. All cases were low grade according to the Paner grading system (grade 1 or 2). No cases with grade 3 or sarcomatoid differentiation were noted.

By histology, we separated the cases into two groups based on architectural pattern. The first group of seven cases included tumors showing a prominent multicystic pattern (Fig. 1). These were all demarcated, three with a fibrous pseudocapsule. Cysts were irregular in shape and size. Glands appeared cribriform focally in some tumors. Septa of the cysts were thin, mostly lined by a single layer of neoplastic cells. However, larger aggregates of mostly eosinophilic/oncocytic cells were present within the septa. Deposits of dark brown pigment (lipofuscin and hemosiderin) were focally present in four cases. Dystrophic calcification was noted in four cases. Necrosis was not present.

Tumors in the second group (3/10) had a more solid appearance due to arrangement of neoplastic cells in compressed elongated tubules resembling a solid architectural appearance (no true solid areas were seen) (Fig. 2). The whole tumor was

Table 1 Clinicopathologic data

Case	Age (years)	Sex	Size (cm)	Site	color	FU (years)
1	56	F	4.0	L	Brown/yellow	19 AW
2	68	F	3.0	L	Yellow	6 AW
3	70	M	5.0	R	Pink/yellow	4 AW
4	64	F	1.2	R	NA	LFU
5	72	M	2.5	R	Brown	2.5 AW
6	50	M	20.0	NA	NA	LFU
7	74	M	NA	NA	NA	LFU
8	67	M	3.7	R	Dark brown	15 NED, then DOD
9	89	F	7.0	R	Tan	1 AW
10	70	M	1.5	R	Tan/gray	3 AW

M male, *F* female, *L* left, *R* right, *FU* follow-up, *AW* alive and well, *LFU* lost for follow-up, *NED* no evidence of disease, *DOD* death of other disease, *NA* not available

Table 2 Basic morphological features

Case	Architecture	Percentage of cysctic component (%)	Cell type (predominant)	Capsule	Calcifications	Necrosis	Pigment	*P* grade
1	cystic	80	Eosinophil	P	P	A	P	1
2	cystic	100	Pale cells	A	A	A	P	1
3	Cystic/aden	60	Pale cells	A	A	A	P	2
4	Slit-like	100	Eosinophil	A	A	A	A	1
5	Cystic	100	Pale cells	A	P	A	A	2
6	Cystic/aden	80	Eosinophil	P	P	A	A	2
7	Cystic	100	Eosinophil	P	P	A	P	2
8	Slit-like	100	Eosinophil	A	A	A	A	2
9	Cystic/aden	70	Pale/Eosinophil	A	A	A	A	2
10	Slit-like/cyst	100	Eosinophil	A	A	A	P	1

P grade Paner grading, *P* present, *A* absent, *aden* adenomatous, *eosinophil* eosiniphilic cells

exclusively composed of tubules. Lumina of compressed elongated tubules displayed a slit-like pattern. In all three cases, the tumors were well-demarcated and without pseudocapsule. None of the cases showed necrosis or calcification, while focal pigment deposits were present in one case (Fig. 3).

Results of immunohistochemical examinations are summarized in Table 3. All tumors were positive for CK 7, OSCAR, CD117, EMA, parvalbumin, antimitochondrial antigen, and Pax 8. It should be noted that CK 7 positivity was moderate to strong with a rather patchy pattern in seven cases. Immunoreactivity for CD117 was diffuse but varied in intensity, ranging from weak (three cases) to strong (four cases). Proliferative activity as indicated by nuclear Ki67 staining was low (<1 %) in all cases. All tumors were negative for vimentin, AMACR, CANH IX, estrogen and progesterone receptors, TFE3, HMB45, cathepsin K, CD31, and CD34.

Table 4 presents aCGH results of the five cases suitable for aCGH analysis. Multiple losses of chromosomes 1p, 2q, 6, 13, 17, 21, and X were found in two cases. Three cases showed no numerical chromosomal aberrations.

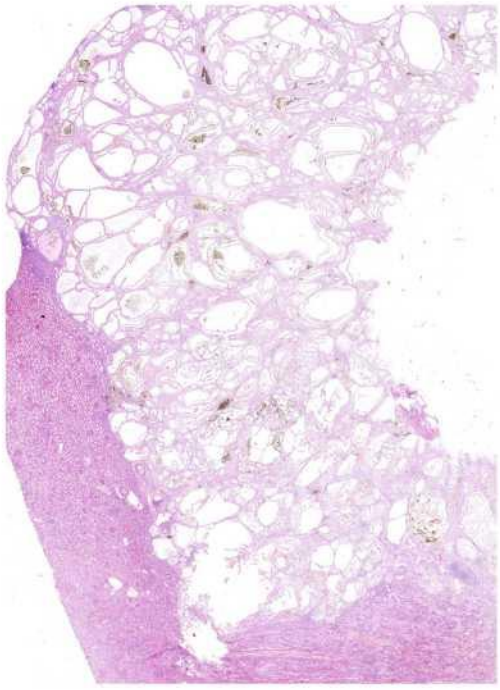

Fig. 1 Histotopogram showing multicystic nature of this rare morphologic variant of chromophobe RCC

Discussion

Chromophobe renal cell carcinomas represent approximately 5 % of all renal cell carcinomas. They are usually well-demarcated and composed of an admixture of smaller eosinophilic cells and larger clear cells with prominent cell membranes (leaf-like cells) (Fig. 4). The nuclei are usually irregular, with a raisinoid appearance and perinuclear clearing (halo) (Fig. 5). Binucleated cells are not rare. Tumors are typically arranged in a solid sheet-like pattern, separated by incomplete vascular septa [11].

Two main morphological variants are traditionally recognized: the classical variant demonstrating both cell types with

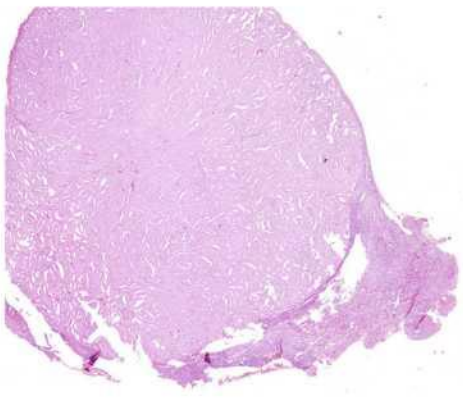

Fig. 2 Three tumors were composed of compressed cystic spaces/large tubules

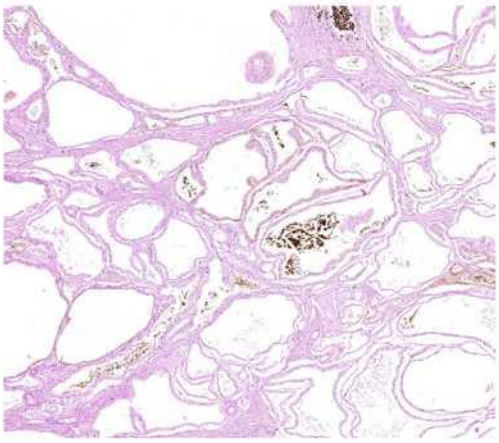

Fig. 3 Deposits of dark brown pigment (lipochrome) were seen in 5/10 tumors

a solid-alveolar growth pattern and the eosinophilic variant composed almost exclusively of smaller eosinophilic cells [2]. Several additional morphological variants have been described. The oncocytic variant is characterized by a solid mass of proliferating cells with typical oncocytic cytoplasm and minimal variation in size. Nuclei are round and centrally located and a perinucelar halo is mostly absent. Nonetheless, the immunohistochemical marker profile and pattern of numerical chromosomal aberrations are characteristic of ChRCC [4].

The adenomatoid microcystic pigmented variant of ChRCC has some features similar to those seen in our cases [3, 5, 6]. The cystic areas contain a mixture of eosinophilic and paler cells, both with the typical raisinoid nuclei and a perinuclear halo. The adenomatous structures in the adenomatoid microcystic pigmented variant are lined by smaller cylindrical cells with basal nuclei. Complex architecture and cribriform formations, similar to those seen in intraductal carcinoma of the breast, can also be observed in the adenomatoid microcystic pigmented variant of ChRCC, as well as areas with prominent fibrous stroma. Raisinoid nuclear shape has also been described in this variant. These cases characteristically contain areas with light to dark brown pigmentation corresponding to lipochrome [5]. Tumors in our series were multicystic even at low magnification. No compact solid areas were noted and lipochrome deposits were seen in four cases. We perceive multicystic ChRCC as the extreme end of the morphologic spectrum of ChRCC with adenomatoid microcystic pattern.

ChRCCs with neuroendocrine differentiation have been recently described [8, 9, 12]. Although many cases of ChRCC may show a neurondocrine-like morphological pattern, few show true neuroendocrine differentiation by immunohistochemical staining for neuroendocrine markers (chromogranin, synaptophysin, CD56 and neuron-specific enolase) or electron microscopy confirming neuroendocrine granules. Cytologic features are not remarkably different from classic ChRCC and from cases examined in this study.

Table 3 Results of immunohistochemical examination

Case	Vim	CK 7	OSC	EMA	CD117	AMACR	CAN	PAX8	Parv	PR/ER	TFE3	HMB	Cath	MIA	SMA	Des	CD31/34	Ki67 (%)
1	–	+++	+++	+++	+	–	–	+	+++	–	–	–	–	+++	Stroma+	–	–	~1
2	–	++	+++	+++	++	–	–	+	+	–	–	–	–	+++	Stroma+++	–	–	~1
3	–	Patchy++	+++	++	++	–	–	+	++	–	–	–	–	+++	–	–	–	~1
4	–	+++	+++	+++	+++	–	–	+	+++	–	–	–	–	+++	–	–	–	~1
5	–	Patchy+++	++	+++	+	–	–	+	+++	–	–	–	–	++	–	–	–	~1
6	–	Patchy+++	++	+++	+++	–	–	+	+++	–	–	–	–	+++	Capsule+	Stroma foc+	–	~1
7	–	Patchy+++	+++	+++	+	–	–	++	+++	–	–	–	–	+++	Stroma++	–	–	~1
8	–	Patchy+++	+++	+++	+++	–	–	++	+++	–	–	–	–	+++	Stroma+	–	–	~1
9	–	Patchy++	++	+++	+++	–	–	++	+++	–	–	–	–	++	Stroma+	–	–	~1
10	–	Patchy++	+++	+++	++	–	–	++	+++	–	–	–	–	+++	–	–	–	~1

VIM vimentin, *OSC* OSCAR, *CAN* carbonic anhydrase 9, *Parv* parvalbumin, *HMB* HMB45, *Cath* cathepsin K, *MIA* antimitochondrial antigen, *SMA* smooth muscle actin, *Des* desmin, – negative, + weak positivity, ++ moderate positivity, +++ strong positivity, *foc* focal

Table 4 Results of arrayCGH

Case	kgd	aCGH
1	300	NP
2	300	NP
3	200	NP
4	400	Normal
5	400	−1p, −2q, −6
6	600	Normal
7	200	NP
8	100	NP
9	600	−1p, −6, −13, −17, −21, −*X*
10	600	Normal

aCGH array comparative genomic hybridisation, *NP* not performed, *Normal* no chromosomal numerical abberations

Chromophobe carcinomas occasionally undergo sarcomatoid differentiation, with high-grade transformation associated with aggressive clinical course and unfavorable prognosis [13]. Histologically, these lesions can differentiate into heterologous elements such as osteosarcoma, rhabdomyosarcoma, chondrosarcoma, or even liposarcoma [14–19]. No sarcomatoid differentiation was identified in our series.

Architecturally, our cases were all multicystic without solid component but two different patterns emerged. A multicystic appearance, with large cystic spaces, slightly irregular in shape and size was found in seven cases while the other three appeared rather compact at low magnification but at higher magnification appeared to be composed of elongated compressed tubules and cysts, resulting in growth pattern with slit-like spaces. Raisinoid shape of nuclei, considered as landmark of all ChRCC, with perinuclear clearing (halo) was a constant finding in all our cases. Hence, cytologic features in were not different between the two patterns (large cysts and slit-like cysts) and similar to those of conventional ChRCC (Fig. 6).

Immunohistochemical stains performed in this series showed a profile similar to that of conventional ChRCC [20–22]. Our cases were positive for PAX 8, parvalbumin, antimitochondrial antigen, and CD117. The latter has been suggested as a useful stain to differentiate ChRCCs and oncocytomas from other renal neoplasms [23] and was at least weakly positive in all cases. CK 7 staining was patchy in 30 % and diffuse in 70 % but strong in all cases. Of seven multicystic CHRCC with patchy CK 7 staining 2 were weakly but diffusely positive for CD117 while the remaining cases were diffusely and strongly positive (Fig. 7). These results are in concordance with those of previous studies reporting CK 7 staining in approximately 76 % of ChRCC (range 50–100 %). Focal CK 7 staining therefore does not exclude a diagnosis of CHRCC [22, 24–26].

EMA and OSCAR were diffusely positive in all cases. Actin staining was positive in the stroma of six tumors.

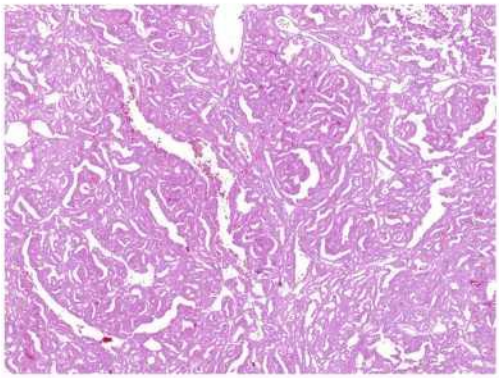

Fig. 4 Tumor composed of predominantly eosinophilic neoplastic cells

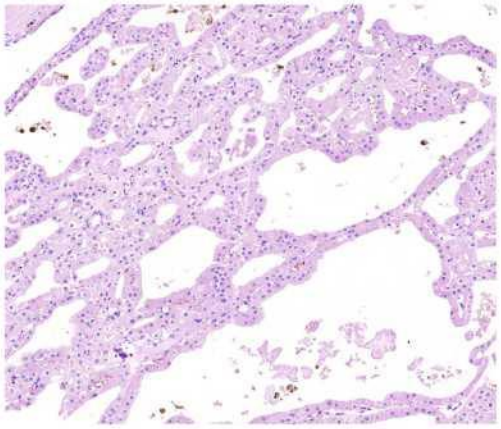

Fig. 5 Tumor composed of large pale cells with perinuclear halo and raisinoid nuclei

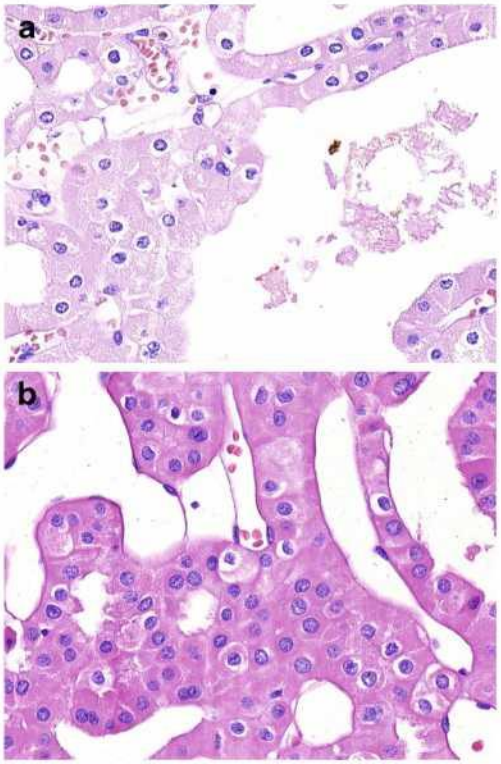

Fig. 6 **a**, **b** Large nuclei with wrinkled edge were constant finding in all 10 cases

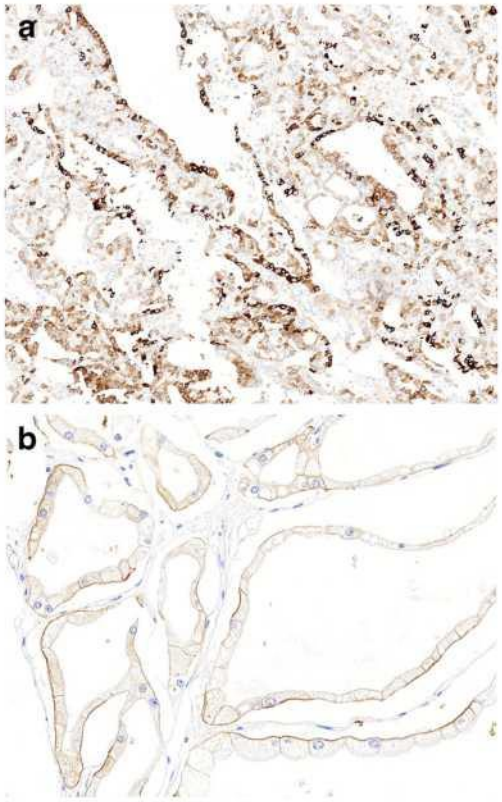

Fig. 7 **a**, **b** All tumors were positive for CK 7, as well as for CD117

Ki67-based proliferation index was low (<1 %) in all cases. Reactivity for other markers including hormone receptors (ER/PR), melanocytic markers, TFE3, cathepsin K, and endothelial markers was not observed in any case.

Previous molecular genetic studies performed on ChRCC revealed some recurrent alterations which are now considered a genetic hallmark for this entity. Multiple losses of chromosomes 1, 2, 6, 10, 13, 17, and 21 are usually detected in both classic and eosinophilic ChRCC [27]. Furthermore, some studies showed gains in chromosomes 4, 7, 15, 19, and 20 [28–31], but the significance of these numerical chromosomal aberrations is not entirely clear. These findings do suggest, however, that the spectrum of chromosomal anomalies of ChRCC may be broader than as yet reported. In two of our five cases suitable for arrayCGH analysis, we found multiple losses of chromosomes 1p, 2q, 6, 13, 17, 21, and X while the remaining three showed no numerical chromosomal aberrations. Absence of chromosomal aberrations has been reported for renal oncocytomas. Our three cases without chromosomal aberrations were predominantly composed of eosinophilic cells but raisinoid nuclei with perinuclear clearing were also present and the immunohistochemical marker pattern these cases was consistent with CHRCC. We emphasize that cases of ChRCC with a normal numerical chromosomal status have been reported previously in the literature [27, 32–36].

In the differential diagnosis of multicystic ChRCC, the following diagnoses should be considered: cystic/multicystic variant of renal oncocytoma, multilocular cystic clear cell carcinoma/neoplasm of low malignant potential (MCCCC), granular/eosinophilic high-grade variant of clear renal cell carcinoma (CCRCC), tubulocystic renal cell carcinoma (TCRCC), and mixed epithelial stromal tumor (MEST)/cystic nephroma (CN).

The cystic/multicystic variant of renal oncocytoma has been reported recently and also is included in the most recent WHO classification [11, 37, 38]. Although such cases occasionally show prominent cystic areas, foci of solid tumor with the typical islets of oncocytic cells in a background of fibrotic stroma can be easily identified, if sampling is adequate. Furthermore, cytomorphologic features, notably raisinoid nuclei, perinuclear clearing, and at least focal presence of a dual cell population strongly point towards the diagnosis of ChRCC.

Multilocular cystic clear cell carcinoma/neoplasm of low malignant potential (MCCCC) typically presents as a multicystic lesion without conspicuous solid areas [11, 39]. The cysts are lined by low-grade clear cells (maximum grade 2 according to the ISUP grading system) with a variable amount of usually pale cytoplasm or atrophic flattened epithelium. Architecture of multilocular cystic clear cell carcinoma/neoplasm is very similar to that of our tumors and yet, cytologically, our cases differ significantly from MCCCC. Pale, leaf-like cells as well as smaller oncocytic cells are completely different from clear cell elements characteristic of MCCCC. Further, raisinoid nuclei, which we easily encountered in our cases, have never been described in MCCCC. In addition, MCCCC expresses vimentin and CANH 9 but, as a rule, not CK 7, parvalbumin, antimitochondrial antigen, or CD117 [11].

The granular/eosinophilic high grade variant of clear renal cell carcinoma (CCRCC) are occasionally, at least focally, arranged in a multicystic pattern. High-grade CCRCCs usually have architectural and cytological features different from multicystic ChRCC. They mostly show alveolar or acinar growth patterns with delicate thin-walled blood vessels and abundant cytoplasmic lipid vacuoles and glycogen deposits [2, 40]. On the other hand, the typical ChRCC morphology (i.e., raisinoid nuclei with perinuclear clearing) is usually not observed in typical CCRCC. Marker profiles are also different, CCRCC expressing CANH 9, CD10, and vimentin, while CD117 and CK 7 are usually negative, although CK7 can be focally positive in up to 15 % of CCRCC.

Tubulocystic renal cell carcinoma (TCRCC) presents grossly as a solid or spongy mass. On microscopic examination, the lesion shows multiple cystic spaces lined by a single layer of flat, cuboidal, or low columnar cells. These cells have a moderate amount of eosinophilic cytoplasm and can show a hobnail appearance [41–43]. In contrast, the cystic areas in cystic ChRCC are lined by larger cells with wide, usually eosinophilic cytoplasm and typical irregular nuclei. The neoplastic cells in TCRCC are usually monotonous while tumor cells in ChRCC can show some degree of polymorphism, with

presence of both eosinophilic and leaf-like cells. TCRCC is usually positive for CK 18, CK 19, EMA, CD10, high molecular weight cytokeratin 34betaE12, and vimentin, while negative for CK7 [44]. Genome abnormalities of both entities are also different, TCRCC displaying mainly gains of chromosomes 7 and 17 [11, 45] although TCRCC with normal numerical chromosomal status have been reported recently [46].

Another renal tumor presenting with predominantly cystic morphology is mixed epithelial stromal tumor (MEST)/cystic nephroma (CN) [47, 48]. The currently accepted concept is that CN of adult onset and MEST are the same tumor at the two ends of the morphological spectrum of a single entity. This concept is supported not only by clinical data but also by morphology and molecular genetic analyses [11]. These tumors mostly occur in perimenopausal women. Histologically, MEST is defined as a dimorphic tumor with an epithelial component lining cystic structures embedded in a spindle cell Mullerian type of stroma [49]. The stromal component is usually of ovarian type and typically expresses estrogen and progesterone receptors, as well as desmin, smooth muscle actin, and vimentin. Of note, pediatric CN is a completely different tumor, unrelated to MEST. Of our 10 patients, 4 were female and none of the tumors showed morphologic features resembling Mullerian differentiation. In addition, the cytological features of cystic ChRCC in our series were different from the cell populations described in MEST. Immunoreactivity for estrogen or progesterone receptors was not noted.

We conclude that in rare cases, ChRCC displays a prominent multicystic pattern which we perceive as an extreme form of the microcystic adenomatoid pigmented variant of ChRCC. The immunophenotype of multicystic ChRCC is identical to that of conventional ChRCC but its differential diagnosis is quite different from that of conventional ChRCC. Its pattern of numerical chromosomal aberrations is variable and in three cases, none were found. All our cases have shown an indolent, non-aggressive behavior.

Compliance with ethical standards Study design has been approved by local ethical committee (Charles University, Medical School Plzen) LEK FN Plzeň.

Funding The study was supported by the Charles University Research Fund (project number P36), by the project FN 00669806, and by SVV 260283.

Conflict of interest All authors declare no conflict of interest

References

1. Amin MB, Amin MB, Tamboli P, Javidan J, Stricker H, de-Peralta Venturina M, Deshpande A, Menon M (2002) Prognostic impact of histologic subtyping of adult renal epithelial neoplasms: an experience of 405 cases. Am J Surg Pathol 26(3):281–291
2. Amin MB, Paner GP, Alvarado-Cabrero I, Young AN, Stricker HJ, Lyles RH, Moch H (2008) Chromophobe renal cell carcinoma: histomorphologic characteristics and evaluation of conventional pathologic prognostic parameters in 145 cases. Am J Surg Pathol 32(12):1822–1834. doi:10.1097/PAS.0b013e3181831e68
3. Michal M, Hes O, Svec A, Ludvikova M (1998) Pigmented microcystic chromophobe cell carcinoma: a unique variant of renal cell carcinoma. Ann Diagn Pathol 2(3):149–153
4. Kuroda N, Tanaka A, Yamaguchi T, Kasahara K, Naruse K, Yamada Y, Hatanaka K, Shinohara N, Nagashima Y, Mikami S, Oya M, Hamashima T, Michal M, Hes O (2013) Chromophobe renal cell carcinoma, oncocytic variant: a proposal of a new variant giving a critical diagnostic pitfall in diagnosing renal oncocytic tumors. Medical molecular morphology 46(1):49–55. doi:10.1007/s00795-012-0007-7
5. Hes O, Vanecek T, Perez-Montiel DM, Alvarado Cabrero I, Hora M, Suster S, Lamovec J, Curik R, Mandys V, Michal M (2005) Chromophobe renal cell carcinoma with microcystic and adenomatous arrangement and pigmentation—a diagnostic pitfall. Morphological, immunohistochemical, ultrastructural and molecular genetic report of 20 cases. Virchows Archiv: an international journal of pathology 446(4):383–393. doi:10.1007/s00428-004-1187-x
6. Dundr P, Pesl M, Povysil C, Tvrdik D, Pavlik I, Soukup V, Dvoracek J (2007) Pigmented microcystic chromophobe renal cell carcinoma. Pathol Res Pract 203(8):593–597. doi:10.1016/j.prp.2007.05.005
7. Kuroda N, Iiyama T, Moriki T, Shuin T, Enzan H (2005) Chromophobe renal cell carcinoma with focal papillary configuration, nuclear basaloid arrangement and stromal osseous metaplasia containing fatty bone marrow element. Histopathology 46(6):712–713. doi:10.1111/j.1365-2559.2005.02032.x
8. Parada DD, Pena KB (2008) Chromophobe renal cell carcinoma with neuroendocrine differentiation. APMIS 116(9):859–865
9. Kuroda N, Tamura M, Hes O, Michal M, Gatalica Z (2011) Chromophobe renal cell carcinoma with neuroendocrine differentiation and sarcomatoid change. Pathol Int 61(9):552–554. doi:10.1111/j.1440-1827.2011.02689.x
10. Thoenes W, Storkel S, Rumpelt HJ, Moll R, Baum HP, Werner S (1988) Chromophobe cell renal carcinoma and its variants—a report on 32 cases. J Pathol 155(4):277–287. doi:10.1002/path.1711550402
11. Moch H, Humphrey PA, Ulbright TM, Reuter VE (2016) WHO classification of tumours of the urinary system and male genital organs (World Health Organization classification of tumours). IARC Press, Lyon, 356 pp
12. Peckova K, Martinek P, Ohe C, Kuroda N, Bulimbasic S, Condom Mundo E, Perez Montiel D, Lopez JI, Daum O, Rotterova P, Kokoskova B, Dubova M, Pivovarcikova K, Bauleth K, Grossmann P, Hora M, Kalusova K, Davidson W, Slouka D, Miroslav S, Buzrla P, Hynek M, Michal M, Hes O (2015) Chromophobe renal cell carcinoma with neuroendocrine and neuroendocrine-like features. Morphologic, immunohistochemical, ultrastructural, and array comparative genomic hybridization analysis of 18 cases and review of the literature. Ann Diagn Pathol 19(4):261–268. doi:10.1016/j.anndiagpath.2015.05.001
13. Akhtar M, Tulbah A, Kardar AH, Ali MA (1997) Sarcomatoid renal cell carcinoma: the chromophobe connection. Am J Surg Pathol 21(10):1188–1195
14. Itoh T, Chikai K, Ota S, Nakagawa T, Takiyama A, Mouri G, Shinohara N, Yamashita T, Suzuki S, Koyanagi T, Nagashima K (2002) Chromophobe renal cell carcinoma with osteosarcoma-like differentiation. Am J Surg Pathol 26(10):1358–1362
15. Magro G, Lopes M, Amico P, Puzzo L (2005) Chromophobe renal cell carcinoma with extensive rhabdomyosarcomatous component.

Virchows Archiv: an international journal of pathology 447(5): 894–896. doi:10.1007/s00428-005-0026-z

16. Quiroga-Garza G, Khurana H, Shen S, Ayala AG, Ro JY (2009) Sarcomatoid chromophobe renal cell carcinoma with heterologous sarcomatoid elements. A case report and review of the literature. Archives of pathology & laboratory medicine 133(11):1857–1860. doi:10.1043/1543-2165-133.11.1857
17. Anila KR, Mathew AP, Somanathan T, Mathews A, Jayasree K (2012) Chromophobe renal cell carcinoma with heterologous (liposarcomatous) differentiation: a case report. Int J Surg Pathol 20(4):416–419. doi:10.1177/1066896911429298
18. Petersson F, Michal M, Franco M, Hes O (2010) Chromophobe renal cell carcinoma with liposarcomatous dedifferentiation—report of a unique case. International journal of clinical and experimental pathology 3(5):534–540
19. Husain A, Eigl BJ, Trpkov K (2014) Composite chromophobe renal cell carcinoma with sarcomatoid differentiation containing osteosarcoma, chondrosarcoma, squamous metaplasia and associated collecting duct carcinoma: a case report. Analytical and quantitative cytopathology and histopathology 36(4):235–240
20. Cochand-Priollet B, Molinie V, Bougaran J, Bouvier R, Dauge-Geffroy MC, Deslignieres S, Fournet JC, Gros P, Lesourd A, Saint-Andre JP, Toublanc M, Vieillefond A, Wassef M, Fontaine A, Groleau L (1997) Renal chromophobe cell carcinoma and oncocytoma. A comparative morphologic, histochemical, and immunohistochemical study of 124 cases. Archives of pathology & laboratory medicine 121(10):1081–1086
21. DeLong W, Sakr W (1996) Chromophobe renal cell carcinoma: a comparative histochemical and immunohistochemical study. J Urol Pathol 4:1–8
22. Taki A, Nakatani Y, Misugi K, Yao M, Nagashima Y (1999) Chromophobe renal cell carcinoma: an immunohistochemical study of 21 Japanese cases. Modern pathology: an official journal of the United States and Canadian Academy of Pathology, Inc 12(3):310–317
23. Petit A, Castillo M, Santos M, Mellado B, Alcover JB, Mallofre C (2004) KIT expression in chromophobe renal cell carcinoma: comparative immunohistochemical analysis of KIT expression in different renal cell neoplasms. Am J Surg Pathol 28(5):676–678
24. Wu SL, Kothari P, Wheeler TM, Reese T, Connelly JH (2002) Cytokeratins 7 and 20 Immunoreactivity in chromophobe renal cell carcinomas and renal oncocytomas. Modern pathology: an official journal of the United States and Canadian Academy of Pathology, Inc 15(7):712–717
25. Mathers ME, Pollock AM, Marsh C, O'Donnell M (2002) Cytokeratin 7: a useful adjunct in the diagnosis of chromophobe renal cell carcinoma. Histopathology 40(6):563–567. doi:10.1046/j.1365-2559.2002.01397.x
26. Liu L, Qian J, Singh H, Meiers I, Zhou X, Bostwick DG (2007) Immunohistochemical analysis of chromophobe renal cell carcinoma, renal oncocytoma, and clear cell carcinoma: an optimal and practical panel for differential diagnosis. Archives of pathology & laboratory medicine 131(8):1290–1297. doi:10.1043/1543-2165(2007)131[1290:IAOCRC]2.0.CO;2
27. Brunelli M, Eble JN, Zhang S, Martignoni G, Delahunt B, Cheng L (2005) Eosinophilic and classic chromophobe renal cell carcinomas have similar frequent losses of multiple chromosomes from among chromosomes 1, 2, 6, 10, and 17, and this pattern of genetic abnormality is not present in renal oncocytoma. Modern pathology: an official journal of the United States and Canadian Academy of Pathology, Inc 18(2):161–169. doi:10.1038/modpathol.3800286
28. Gunawan B, Bergmann F, Braun S, Hemmerlein B, Ringert RH, Jakse G, Fuzesi L (1999) Polyploidization and losses of chromosomes 1, 2, 6, 10, 13, and 17 in three cases of chromophobe renal cell carcinomas. Cancer Genet Cytogenet 110(1):57–61
29. Brunelli M, Gobbo S, Cossu-Rocca P, Cheng L, Hes O, Delahunt B, Pea M, Bonetti F, Mina MM, Ficarra V, Chilosi M, Eble JN, Menestrina F, Martignoni G (2007) Chromosomal gains in the sarcomatoid transformation of chromophobe renal cell carcinoma. Modern pathology: an official journal of the United States and Canadian Academy of Pathology, Inc 20(3):303–309. doi:10.1038/modpathol.3800739
30. Tan MH, Wong CF, Tan HL, Yang XJ, Ditlev J, Matsuda D, Khoo SK, Sugimura J, Fujioka T, Furge KA, Kort E, Giraud S, Ferlicot S, Vielh P, Amsellem-Ouazana D, Debre B, Flam T, Thiounn N, Zerbib M, Benoit G, Droupy S, Molinie V, Vieillefond A, Tan PH, Richard S, Teh BT (2010) Genomic expression and single-nucleotide polymorphism profiling discriminates chromophobe renal cell carcinoma and oncocytoma. BMC Cancer 10:196. doi:10.1186/1471-2407-10-196
31. Vieira J, Henrique R, Ribeiro FR, Barros-Silva JD, Peixoto A, Santos C, Pinheiro M, Costa VL, Soares MJ, Oliveira J, Jeronimo C, Teixeira MR (2010) Feasibility of differential diagnosis of kidney tumors by comparative genomic hybridization of fine needle aspiration biopsies. Genes, chromosomes & cancer 49(10):935–947. doi:10.1002/gcc.20805
32. Speicher MR, Schoell B, du Manoir S, Schrock E, Ried T, Cremer T, Storkel S, Kovacs A, Kovacs G (1994) Specific loss of chromosomes 1, 2, 6, 10, 13, 17, and 21 in chromophobe renal cell carcinomas revealed by comparative genomic hybridization. Am J Pathol 145(2):356–364
33. Verdorfer I, Hobisch A, Hittmair A, Duba HC, Bartsch G, Utermann G, Erdel M (1999) Cytogenetic characterization of 22 human renal cell tumors in relation to a histopathological classification. Cancer Genet Cytogenet 111:61–70
34. Bugert P, Gaul C, Weber K, Herbers J, Akhtar M, Ljungberg B, Kovacs G (1997) Specific genetic changes of diagnostic importance in chromophobe renal cell carcinomas. Laboratory investigation; a journal of technical methods and pathology 76(2):203–208
35. Iqbal MA, Akhtar M, Ali MA (1996) Cytogenetic findings in renal cell carcinoma. Hum Pathol 27(9):949–954
36. Sperga M, Martinek P, Vanecek T, Grossmann P, Bauleth K, Perez-Montiel D, Alvarado-Cabrero I, Nevidovska K, Lietuvietis V, Hora M, Michal M, Petersson F, Kuroda N, Suster S, Branzovsky J, Hes O (2013) Chromophobe renal cell carcinoma—chromosomal aberration variability and its relation to Paner grading system: an array CGH and FISH analysis of 37 cases. Virchows Archiv: an international journal of pathology 463(4):563–573. doi:10.1007/s00428-013-1457-6
37. Zhang Q, Ma J, Wu CY, Zhang DH, Zhao M (2015) Tubulocystic oncocytoma of the kidney: a case study and review of literature with focus on implications for differential diagnosis. International journal of clinical and experimental pathology 8(11):14786–14792
38. Skenderi F, Ulamec M, Vranic S, Bilalovic N, Peckova K, Rotterova P, Kokoskova B, Trpkov K, Vesela P, Hora M, Kalusova K, Sperga M, Perez Montiel D, Alvarado Cabrero I, Bulimbasic S, Branzovsky J, Michal M, Hes O (2016) Cystic renal oncocytoma and tubulocystic renal cell carcinoma: morphologic and immunohistochemical comparative study. Applied immunohistochemistry & molecular morphology: AIMM / official publication of the Society for Applied Immunohistochemistry 24(2):112–119. doi:10.1097/pai.0000000000000156
39. Eble JN, Bonsib SM (1998) Extensively cystic renal neoplasms: cystic nephroma, cystic partially differentiated nephroblastoma, multilocular cystic renal cell carcinoma, and cystic hamartoma of renal pelvis. Semin Diagn Pathol 15(1):2–20
40. Tickoo SK, Lee MW, Eble JN, Amin M, Christopherson T, Zarbo RJ, Amin MB (2000) Ultrastructural observations on mitochondria and microvesicles in renal oncocytoma, chromophobe renal cell carcinoma, and eosinophilic variant of conventional (clear cell) renal cell carcinoma. Am J Surg Pathol 24(9):1247–1256

41. MacLennan GT, Farrow GM, Bostwick DG (1997) Low-grade collecting duct carcinoma of the kidney: report of 13 cases of low-grade mucinous tubulocystic renal carcinoma of possible collecting duct origin. Urology 50(5):679–684. doi:10.1016/s0090-4295(97)00335-x
42. MacLennan GT, Bostwick DG (2005) Tubulocystic carcinoma, mucinous tubular and spindle cell carcinoma, and other recently described rare renal tumors. Clin Lab Med 25(2):393–416. doi:10.1016/j.cll.2005.01.005
43. Hora M, Urge T, Eret V, Stransky P, Klecka J, Kreuzberg B, Ferda J, Hyrsl L, Breza J, Holeckova P, Mego M, Michal M, Petersson F, Hes O (2011) Tubulocystic renal carcinoma: a clinical perspective. World J Urol 29(3):349–354. doi:10.1007/s00345-010-0614-7
44. Khalaf I, El-Badawy N, Shawarby MA (2013) Tubulocystic renal cell carcinoma, a rare tumor entity: review of literature and report of a case. Afr J Urol 19(1):1–6. doi:10.1016/j.afju.2012.12.001
45. Tran T, Jones CL, Williamson SR, Eble JN, Grignon DJ, Zhang S, Wang M, Baldridge LA, Wang L, Montironi R, Scarpelli M, Tan PH, Simper NB, Comperat E, Cheng L (2015) Tubulocystic renal cell carcinoma is an entity that is immunohistochemically and genetically distinct from papillary renal cell carcinoma. Histopathology. doi:10.1111/his.12840
46. Michal M, Syrucek M (1998) Benign mixed epithelial and stromal tumor of the kidney. Pathol Res Pract 194(6):445–448. doi:10.1016/s0344-0338(98)80038-1
47. Adsay NV, Eble JN, Srigley JR, Jones EC, Grignon DJ (2000) Mixed epithelial and stromal tumor of the kidney. Am J Surg Pathol 24(7):958–970
48. Kum JB, Grignon DJ, Wang M, Zhou M, Montironi R, Shen SS, Zhang S, Lopez-Beltran A, Eble JN, Cheng L (2011) Mixed epithelial and stromal tumors of the kidney: evidence for a single cell of origin with capacity for epithelial and stromal differentiation. Am J Surg Pathol 35(8):1114–1122. doi:10.1097/PAS.0b013e3182233fb6
49. Zhou M, Yang XJ, Lopez JI, Shah RB, Hes O, Shen SS, Li R, Yang Y, Lin F, Elson P, Sercia L, Magi-Galluzzi C, Tubbs R (2009) Renal tubulocystic carcinoma is closely related to papillary renal cell carcinoma: implications for pathologic classification. Am J Surg Pathol 33(12):1840–1849. doi:10.1097/PAS.0b013e3181be22d1

1.8 Vzácné renální neoplázie

(komentář 3 publikací)

Mixed Epithelial and Stromal Tumor of the Kidney: Mutation Analysis of the DICER 1 Gene in 29 Cases.
Vanecek T, Pivovarcikova K, Pitra T, Peckova K, Rotterova P, Daum O, Davidson W, Montiel DP, Kalusova K, Hora M, Ondic O, Dubova M, Michal M, Hes O.
Appl Immunohistochem Mol Morphol. 2015 Oct 27. 2017 Feb;25(2):117-121.

Primary Renal Well-differentiated Neuroendocrine Tumor (Carcinoid): Next-Generation Sequencing Study of 11 Cases.
Pivovarcikova K, Agaimy A, Martinek P, Alaghehbandan R, Perez Montiel D, Alvarado Cabrero I, Rogala J, Kuroda N, Rychly B, Gasparov S, Michalova K, Michal M, Hora M, Pitra T, Tuckova I, Laciok S, Mareckova J, Hes O.
Histopathology. 2019 Mar 9. doi: 10.1111/his.13856

Distinctive renal cell tumor simulating atrophic kidney with 2 types of microcalcifications. Report of 3 cases.
Hes O, de Souza TG, Pivovarcikova K, Grossmann P, Martinek P, Kuroda N, Kacerovska D, Svajdler M, Straka L, Petersson F, Hora M, Michal M.
Ann Diagn Pathol. 2014 Apr;18(2):82-8.

Smíšený epiteliální a stromální tumor (MEST) a adultní cystický nefrom (ACN) jsou benigní bifazické tumory sestávající z epiteliální a stromální komponenty. Ačkoli MEST a ACN mají jisté morfologické rozdíly (makroskopické i mikroskopické), oba tumory jsou považovány za jedinou neoplastickou entitu variabilního morfologického vzhledu – dva konce morfologického spektra [53]. Současná WHO klasifikace (2016), řadí MEST a ACN společně do kategorie "Mixed epithelial and stromal tumor family" (MESTF) [24]. Pediatrický cystický nefrom (PCN) je zcela odlišnou neoplastickou jednotkou, která kromě zavádějícího názvu nemá s tumory MESTF co dočinění, což dokazují i výsledky molekulárně genetických studií [10, 48].

Primární dobře diferencovaný neuroendokrinní tumor (NET) ledviny je velmi vzácnou renální neoplázií, doposud bylo ve světové literatuře reportováno lehce přes 100 případů těchto tumorů. Vzhledem k raritě výskytu primárních renálních NET nedošlo v posledních letech na poli těchto neoplázií k převratným objevům a všechny nově vycházející práce spíše jen potvrzují už známé a dříve publikované poznatky. Dle provedených studií nejsou tyto tumory nikterak molekulárně-geneticky ani imunohistochemicky specifické, morfologický vzhled je totožný jako u neuroendokrinních neoplázií v jiných lokalizacích. Současná WHO (2016) klasifikuje neuroendokrinní tumory ledvin do tří kategorií (dobře diferencovaný neuroendokrinní tumor, velkobuněčný neuroendokrinní karcinom a malobuněčný neuroendokrinní karcinom) [24]. Vzhledem ke změnám v klasifikaci gastrointestinálních neuroendokrinních tumorů by se dalo předpokládat, že nová a právě připravovaná WHO klasifikace renálních neoplázií pozmění nomenklaturu primární renálních neuroendokrinních tumorů právě po vzoru gastrointestinální klasifikace.

Atrofii ledviny napodobující léze (Atrophic kidney-like lesion/AKLL) je raritní renální léze popsaná v literatuře na velmi limitovaném počtu případů. Jedná se o

lokalizovanou, kompaktní, ohraničenou nodulární lézi typicky s relativně tlustostěnným pouzdrem [45]. Vzhledem k popsanému solitárnímu výskytu a prezentaci pod obrazem lokalizované masy se celkem logicky nabízí neoplastická etiologie léze. Na stranu druhou, některé popsané znaky zase hovoří proti neoplastickému původu léze (mohlo by se jednat i o lokalizované regresivní změny renálního parenchymu). Mikroskopicky léze sestává z folikulárně uspořádaných struktur, tvořených plochými až atrofickými buňkami (imunofenotypem odpovídají podocytům – tyto struktury by tak mohli reprezentovat cysticky dilatované glomeruly), mezi folikly bývají přítomny atrofické tubuly s denzním kolagenním stromatem a malé kolabované glomeruly. V tumoru bývají přítomny mikrokalcifikace (psammomakalcifikace či amorfní depozita) [17].

1.8.1 Mixed Epithelial and Stromal Tumor of the Kidney: Mutation Analysis of the DICER 1 Gene in 29 Cases

Termíny „cystický nefrom“ a „MEST“ jsou považovány za synonyma označující jedinou nozologickou jednotku, tumor vznikající u dospělých pacientů. Cystický nefrom u pediatrických pacientů (PCN) je patrně kompletně odlišná jednotka, u níž byla prokázána přítomnost mutace genu *DICER1*. Dosavadní literatura však neposkytovala relevantní údaj o stavu *DICER1* genu u CN/MEST dospělých pacientů. Proto bylo v rámci této studie v plzeňském registru nádorů vyhledáno celkem 29 případů adultních CN/MEST s dostatečnou kvalitou DNA, u nichž byl analyzován právě gen *DICER1* (za pomoci PCR a přímého sekvenování).

Převážná většina analyzovaných CN/MEST (28/29 případů) vykazovala benigní morfologii, u jediného případu byl diagnostikován maligní MEST/CN se sarkomatoidní diferenciací stromální komponenty. Všech 29 případů bylo negativních v průkazu mutace genu *DICER1* v tzv. hot-spot kodonech 1705, 1709, 1809, 1810, 1813 a 1814.

Výsledky této studie tak jasně ukazují, že na molekulárně-genetické úrovni nemají MEST/CN a PCN společné znaky. Na podkladě výsledků a dříve stanovených morfologických rozdílů mezi PCN a MEST/CN považujeme za důležité striktně rozlišovat mezi těmito dvěma jednotkami a doporučujeme používat termín „cystický nefrom“ pouze pro pediatrické pacienty a vyvarovat se užívání tohoto názvu u adultních MEST.

Mixed Epithelial and Stromal Tumor of the Kidney: Mutation Analysis of the *DICER 1* Gene in 29 Cases

Tomas Vanecek, PhD, Kristyna Pivovarcikova, MD,* Tomas Pitra, MD,† Kvetoslava Peckova, MD,* Pavla Rotterova, MD, PhD,* Ondrej Daum, MD, PhD,* Whitney Davidson, MD,‡ Delia Perez Montiel, MD,§ Kristyna Kalusova, MD,† Milan Hora, MD, PhD,† Ondrej Ondic, MD,* Magdalena Dubova, MD,* Michal Michal, MD,* and Ondrej Hes, MD, PhD*‖*

Abstract: Cystic nephroma (CN) and mixed epithelial stromal tumor (MEST) of the kidney have been considered as synonymous terms describing a single nosologic entity in adult patients. Cystic nephroma in pediatric patients (PCN) is, apparently, a completely different nosologic entity. Although the presence of *DICER 1* mutations is well established in PCN, nothing is currently known about the *DICER 1* gene status in adult MEST/CN. About 33 cases of MEST/CN were selected from the Plzen Tumor Registry; 4 cases were later excluded from the study due to low DNA quality. About 28 of the studied tumors displayed a benign morphology, whereas 1 was diagnosed as a malignant MEST/CN with sarcomatoid differentiation of the stromal component. All 29 samples analyzed using polymerase chain reaction and direct sequencing, including the case with the malignant morphology, were negative for mutation in *DICER 1* hot-spot codons 1705, 1709, 1809, 1810, 1813, and 1814. Our results show that MEST/CN has no relation to PCN on a molecular genetic level. On the basis of our findings and the established morphologic differences between PCN and MEST/CN, we conclude that the term CN should be used for pediatric cases only and should be avoided in adult cases of MEST.

Key Words: kidney, mixed epithelial and stromal tumor, cystic nephroma, pediatric cystic nephroma, *DICER 1* gene mutation

(*Appl Immunohistochem Mol Morphol* 2017;25:117–121)

Received for publication May 18, 2015; accepted July 22, 2015.

From the Departments of *Pathology; †Urology, Charles University, Medical Faculty and Charles University Hospital Plzen; Biomedical Centre, Faculty of Medicine in Plzen, Charles University in Prague, Plzen, Czech Republic; §Department of Pathology, Instituto Nacional de Cancerologia, Mexico City, Mexico; and ‡Department of Pathology and Laboratory Medicine, University of Kansas Medical Center, Kansas City, KS.

Supported by the Charles University Research Fund (project number P36) and by the project CZ.1.05/2.1.00/03.0076 from the European Regional Development Fund.

The authors declare no conflict of interest.

Reprints: Ondrej Hes, MD, PhD, Department of Pathology, Charles University, Medical Faculty and Charles University Hospital Plzen, Alej Svobody 80, Pilsen 304 60, Czech Republic (e-mail: hes@medima.cz).

The term mixed epithelial stromal tumor (MEST) of the kidney was established in 1998 by Michal and Syrucek,[1] whereas the whole concept of MEST was proposed by Michal[2] in 2000 and confirmed later the same year by Adsay et al.[3] Several studies have been published since 2000 that discuss at length the relationship between cystic nephroma (CN) and MEST. The current theory is that CN of adult onset and MEST are the same tumor: 2 ends of the morphologic spectrum of 1 entity. This concept is supported not only by clinical data but also by morphology and molecular genetic analyses.[4–10] The molecular genetic study of MEST and CN has been performed by Zhou et al.[7] Unsupervised clustering of mRNA expression profiles in their report demonstrated that MEST and CN had very similar expression profiles that were distinct from other renal tumors.

The currently preferred term for this entity is MEST.[11] Cystic nephroma in pediatric patients (PCN) is a completely different tumor[7] (for further reference, see below). Unfortunately, the name CN is currently used to describe these distinct entities; however, this will no longer be the case in the new upcoming WHO classification 2016, and the term CN will be preserved for pediatric tumors only (O.H., unpublished data). PCN is a tumor characterized by a multicystic architecture with septa lined by flat to cuboidal epithelial cells. The majority of the tumors occur before the fifth year of life.[12,13] The relation of PCN to Wilms tumor and cystic partially differentiated nephroblastoma is mentioned in the literature.[14,15]

DICER 1 is located on chromosome 14q32.13 and encodes proteins belonging to the RNase III family. It acts as an endoribonuclease, cleaving double-stranded RNA, and is required mainly by the RNA interference pathway to produce active miRNA and siRNA molecules that play a role in a gene repression.[16]

PCN bears biallelic alteration of the *DICER 1* gene. Although the role of *DICER 1* mutations is well recognized in PCN, no data are available regarding the presence/absence of *DICER 1* mutations in adult MEST/CN. In this study, we analyzed mutation hot spots of the *DICER 1* gene in a series of MEST/CN cases.

MATERIALS AND METHODS

A total of 33 cases of MEST/CN were retrieved from among more than 19,500 renal tumors in the files of

the Pilsen Tumor Registry. One to 33 blocks were available for each case. The tumors were reevaluated by at least 2 pathologists (Kristyna Pivovarcikova, O.H.). Tissue for light microscopy was fixed in 10% buffered formalin, embedded in paraffin, cut into 5-μm sections, and stained with hematoxylin and eosin.

The quality of DNA was evaluated, and 4 cases were excluded from further molecular genetic study on the basis of low DNA quality.

MOLECULAR GENETICS

DNA was extracted using the QIAsymphony DNA Mini Kit (Qiagen, Hilden, Germany) on an automated extraction system (QIAsymphony SP, Qiagen) according to the manufacturer's supplementary protocol for paraffin embedded, formalin fixed (FFPE) samples (purification of genomic DNA from FFPE tissue using the QIAamp DNA FFPE Tissue Kit and deparaffinization solution). The concentration and the purity of the extracted DNA were measured using the NanoDrop ND-1000 (NanoDrop Technologies Inc., Wilmington, DE).

For hot-spot mutation analysis [codons 1705, 1709, 1809, 1810, 1813, and 1814, all localized in the RNaseIIb domain of *DICER1*,[23] 50 ng of DNA was added to a reaction that consisted of 12.5 μL of HotStar Taq polymerase chain reaction Master Mix (Qiagen), 10 pmol of each primer (Table 1), and distilled water up to 25 μL. The amplification program was as follows: denaturation at 95°C for 14 minutes, 40 cycles of denaturation at 95°C for 1 minute, annealing at 60°C for 1 minute, extension at 72°C for 1 minute, and finally, incubation at 72°C for 7 minutes.

Successfully amplified polymerase chain reaction products were purified with magnetic particles Agencourt AMPure (Agencourt Bioscience Corporation, A Beckman Coulter Company, Beverly, MA). Products were then sequenced bidirectionally using a Big Dye Terminator Sequencing kit (PE/Applied Biosystems, Foster City, CA) and purified with magnetic particles Agencourt CleanSEQ (Agencourt Bioscience Corporation) according to the manufacturers' protocols before being run on an automated sequencer ABI Prism 3130xl (Applied Biosystems) at a constant voltage of 13.2 kV for 20 minutes.

All sequences were compared with reference sequence NG_016311.1 by BLAST (http://blast.ncbi.nlm.nih.gov/Blast.cgi).

RESULTS

The basic clinicopathologic data are summarized in Table 2. The patients studied included 5 men and 28 women whose ages ranged from 33 to 92 years (mean, 58.79; median, 59 y). The tumor size was measured in the greatest dimension and ranged from 0.9 to 25 cm (mean, 7.34; median, 6.5 cm). Of the 33 MEST in our study, 31 showed no morphologic signs of aggressive behavior, whereas the other 2 displayed characteristics most consistent with the diagnosis of malignant MEST. A review of corresponding pathology reports revealed that all of the neoplasms were described as well-circumscribed but not encapsulated. Benign tumors were characterized primarily by a multicystic and solid architecture with ovarian (Müllerian)-type stroma and cysts lined by hobnail-shaped epithelial cells (Figs. 1A–C). In cases of malignant neoplasms, tumors were multicystic, with a stromal component containing polymorphic, spindled cells and occasional mitotic figures; the epithelial component in both of these tumors lacked malignant morphologic features. The first malignant case was diagnosed as low-grade sarcoma not otherwise specified arising in MEST (case 25), whereas the second case was diagnosed

TABLE 1. Primer Pairs for Hot-Spot Mutation Analysis of the *DICER 1* Gene[17]

Primer Name	Sequence 5′-3′	Analyzed Codons
DICER1-hs1F	TGGGGATCAGTTGCTATGTG	1705, 1709
DICER1-hs1R	CGGGTCTTCATAAAGGTGCT	
DICER1-hs2F	TGGACTGCCTGTAAAAGTGG	1809, 1810, 1813, 1814
DICER1-hs2R	ATGTAAATGGCACCAGCAAG	

TABLE 2. Basic Clinicopathologic Features and Results of *DICER 1* Gene Molecular Genetic Analysis

Case	Sex	Age (y)	Side	Size (cm)	DICER1—Hot-Spots
1	F	47	U	U	–
2	F	72	U	U	–
3	F	39	U	1.0	–
4	F	52	U	3.5	–
5	M	48	U	U	–
6	F	89	L	2.0	–
7	F	74	U	U	–
8	F	63	U	8.0	–
9	F	49	U	9.0	–
10	F	62	U	6.0	–
11	F	71	U	25.0	–
12	F	58	U	8.5	–
13	F	53	R	5.0	–
14	F	44	R	U	–
15	F	36	R	13.0	–
16	F	33	L	U	–
17	F	59	U	13.0	–
18	M	92	L	0.9	–
19	F	64	U	9.0	–
20	F	47	R	6.5	–
21	F	59	R	5.5	–
22	F	65	R	6.0	Not analyzable
23	F	37	R	U	–
24	F	49	U	10.0	–
25*	F	75	U	2.5	–
26	F	74	U	U	–
27	F	78	R	U	Not analyzable
28	M	64	U	8.0	–
29	F	48	L	8.0	–
30	F	53	R	6.0	–
31	M	50	U	3.0	–
32*	M	69	U	9.5	Not analyzable
33	F	67	U	U	Not analyzable

Size denotes the tumor size in the greatest dimension.
*Malignant.
F indicates female; L, left kidney; M, male; R, right kidney; U, unknown; –, negative.

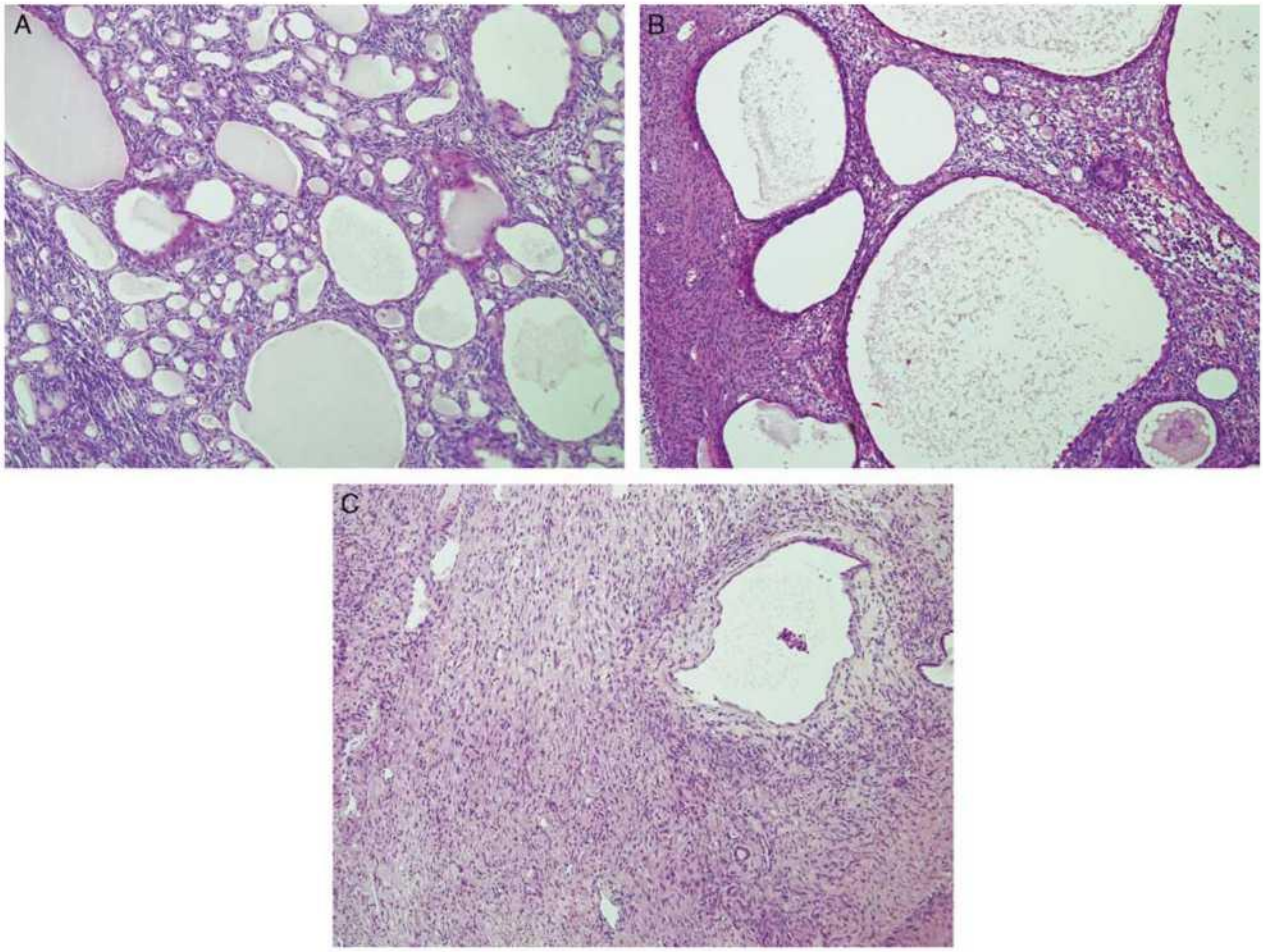

FIGURE 1. MEST/CN is a tumor characterized by both multicystic and solid architecture (A) with the overall appearance depending on the proportion of cystic and solid components (B). The lesional stroma is described as ovarian (Müllerian) type and cysts are lined by epithelium with variable morphology (C).

as spindle cell sarcoma not otherwise specified arising in MEST (case 32) (Figs. 2A, B).

DICER 1 gene mutation hot-spot analysis was performed successfully on 29 of the 33 cases of MEST/CN. All 28 benign samples and the single analyzable malignant sample were negative for mutation in codons 1705, 1709, 1809, 1810, 1813, and 1814 (Table 2).

DISCUSSION

CN was first described by Edmunds in a case report in 1892. His report included a single, hand-drawn plate of an encapsulated cystic tumor in an 18-year-old girl; no microscopic picture of the lesion or histologic description was part of the report. It is very unlikely that the tumor presented by Edmunds was either PCN or MEST/CN; it would be extremely unusual for these tumors to occur in an 18-year-old patient and they do not normally have a well-formed capsule such as that described in Edmunds' paper. It remains a mystery as to which tumor was being described in the above-mentioned case report, but the name CN has since been used many times and has been associated with at least 2 different entities.[18]

MEST/CN has a strong female predilection (up to 8:1) and occurs mostly in perimenopausal women. A few reports have proposed an association with estrogen therapy (the majority of the male cases). Radiologically, MEST/CN are a complex of solid tumor and multicystic lesions, mostly classified as Bosniak 3 or 4.[19] The vast majority of the reported cases follow a benign clinical course, although a few cases have been described as aggressive malignant tumors with sarcomatoid differentiation or carcinomatous change within the epithelial component.[17,20]

MEST/CN is a tumor characterized by both a multicystic and a solid architecture with the overall appearance depending on the proportion of cystic and solid components. The lesional stroma is described as ovarian (Müllerian) type, and cysts are lined by an epithelium with a variable morphology. Most commonly, the epithelial cells have a hobnail appearance, but tumors with a columnar to cylindrical morphology resembling the cervical, the colonic,

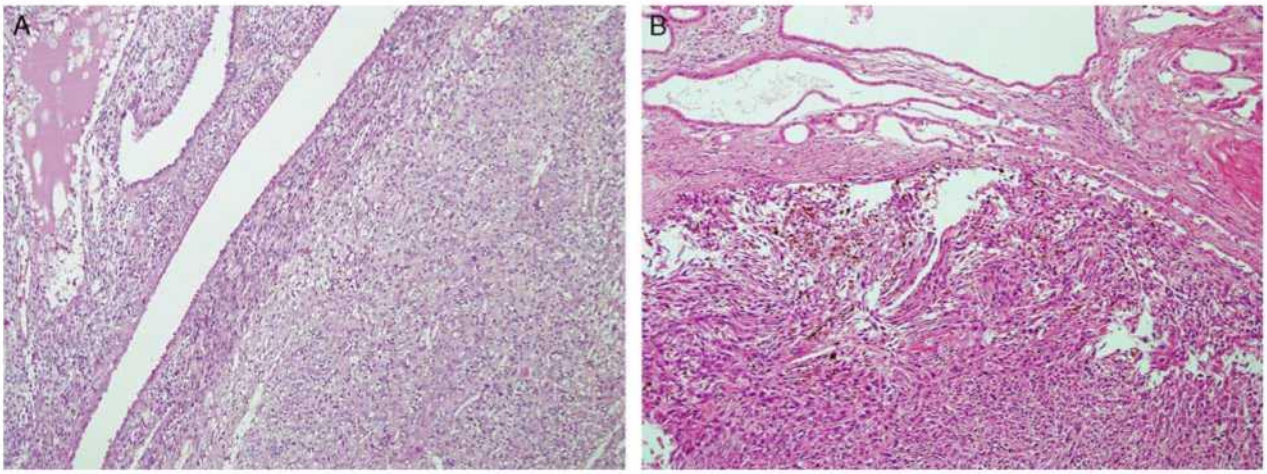

FIGURE 2. A, The first malignant case was diagnosed as low-grade sarcoma NOS arising in MEST. B, The second case was diagnosed as spindle cell sarcoma NOS arising in MEST.

or even the tubular type of epithelium have been documented. Structures resembling corpus albicans in the ovary, lipomatous differentiation, and structures identical to ovarian adenofibromas have also been reported.[21]

PCN is a tumor characterized by its occurrence in pediatric patients, with the majority arising before the fifth year of life and a strong male predominance (up to 4:1).[18,22] PCN are typically expansile, noncapsulated masses that are well demarcated from the normal kidney parenchyma. Most of these tumors are solitary; however, cases of bilateral lesions have been described. Tumors are typically multicystic with septa lined by flattened, cuboidal epithelial cells; the septal stroma is composed mostly of spindle cell elements. PCN, cystic partially differentiated nephroblastoma, and cystic Wilms' tumor are thought to represent a spectrum of a single etiological entity, with PCN at the benign end, cystic Wilms tumor at the malignant end, and cystic partially differentiated nephroblastoma occupying the intermediate position. PCN and stage 1 cystic partially differentiated nephroblastoma are often treated with surgery alone. The International Society of Pediatric Oncology (SIOP) protocols for Wilms' tumor advocate preoperative chemotherapy, which may be unnecessary and potentially harmful in PCN and in pT 1 cystic partially differentiated nephroblastoma.[15]

Doros and colleagues studied PCN and cystic partially differentiated nephroblastomas, including cases of sarcoma with morphologic features of pleuropulmonary blastoma arising in PCN. They found that *DICER1* mutations are a major genetic event in the development of PCN, and also that PCN and pleuropulmonary blastoma have similar *DICER1* loss of function and "hotspot" missence mutation rates. The relationship between PCN, medulloepithelioma, Sertoli-Leydig cell tumors, and pleuropulmonary blastoma, on a molecular genetic level, has also been proposed by others.[23,24] Cases of familial PCN have also been documented.[25–27]

We are not aware of any previous study describing the role of *DICER 1* gene mutations in MEST/CN. In our study, we analyzed 28 cases of benign MEST/CN with DNA suitable for *DICER 1* gene mutation analysis. None of the cases were positive for mutations within hot-spot regions of the *DICER 1* gene. Only 1 malignant MEST/CN from our cohort was suitable for genetic analysis. Even in this case, we were not able to find mutations within hot-spot regions of the *DICER 1* gene. Our findings can thus be considered as another argument for a strict differentiation between PCN and tumors from the MEST/CN group occurring in adult patients.

On the basis of the results of our study and others performed previously, it is possible to conclude that MEST/CN is a tumor that has no relation to PCN on the morphologic or the molecular genetic level. The term CN should be used for pediatric cases only and should be avoided as a synonym for adult cases of MEST.

REFERENCES

1. Michal M, Syrucek M. Benign mixed epithelial and stromal tumor of the kidney. *Pathol Res Pract*. 1998;194:445–448.
2. Michal M. Benign mixed epithelial and stromal tumor of the kidney. *Pathol Res Pract*. 2000;196:275–276.
3. Adsay NV, Eble JN, Srigley JR, et al. Mixed epithelial and stromal tumor of the kidney. *Am J Surg Pathol*. 2000;24:958–970.
4. Jevremovic D, Lager DJ, Lewin M. Cystic nephroma (multilocular cyst) and mixed epithelial and stromal tumor of the kidney: a spectrum of the same entity? *Ann Diagn Pathol*. 2006;10:77–82.
5. Bisceglia M, Galliani CA, Senger C, et al. Renal cystic diseases: a review. *Adv Anat Pathol*. 2006;13:26–56.
6. Turbiner J, Amin MB, Humphrey PA, et al. Cystic nephroma and mixed epithelial and stromal tumor of kidney: a detailed clinicopathologic analysis of 34 cases and proposal for renal epithelial and stromal tumor (REST) as a unifying term. *Am J Surg Pathol*. 2007;31:489–500.
7. Zhou M, Kort E, Hoekstra P, et al. Adult cystic nephroma and mixed epithelial and stromal tumor of the kidney are the same disease entity: molecular and histologic evidence. *Am J Surg Pathol*. 2009;33:72–80.
8. Mohanty SK, Parwani AV. Mixed epithelial and stromal tumors of the kidney: an overview. *Arch Pathol Lab Med*. 2009;133:1483–1486.

9. Lane BR, Campbell SC, Remer EM, et al. Adult cystic nephroma and mixed epithelial and stromal tumor of the kidney: clinical, radiographic, and pathologic characteristics. *Urology*. 2008;71:1142–1148.
10. Montironi R, Mazzucchelli R, Lopez-Beltran A, et al. Cystic nephroma and mixed epithelial and stromal tumour of the kidney: opposite ends of the spectrum of the same entity? *Eur Urol*. 2008;54:1237–1246.
11. Srigley JR, Delahunt B, Eble JN, et al. The International Society of Urological Pathology (ISUP) Vancouver Classification of Renal Neoplasia. *Am J Surg Pathol*. 2013;37:1469–1489.
12. Boybeyi O, Karnak I, Orhan D, et al. Cystic nephroma and localized renal cystic disease in children: diagnostic clues and management. *J Pediatr Surg*. 2008;43:1985–1989.
13. Luithle T, Szavay P, Furtwangler R, et al. Group SGS. Treatment of cystic nephroma and cystic partially differentiated nephroblastoma–a report from the SIOP-GPOH study group. *J Urol*. 2007;177:294–296.
14. Joshi VV, Banerjee AK, Yadav K, et al. Cystic partially differentiated nephroblastoma: a clinicopathologic entity in the spectrum of infantile renal neoplasia. *Cancer*. 1977;40:789–795.
15. van den Hoek J, de Krijger R, van de Ven K, et al. Cystic nephroma, cystic partially differentiated nephroblastoma and cystic Wilms' tumor in children: a spectrum with therapeutic dilemmas. *Urol Int*. 2009;82:65–70.
16. Hannon GJ, Rossi JJ. Unlocking the potential of the human genome with RNA interference. *Nature*. 2004;431:371–378.
17. Sukov WR, Cheville JC, Lager DJ, et al. Malignant mixed epithelial and stromal tumor of the kidney with rhabdoid features: report of a case including immunohistochemical, molecular genetic studies and comparison to morphologically similar renal tumors. *Hum Pathol*. 2007;38:1432–1437.
18. Michal M, Hes O, Kuroda N, et al. What is a cystic nephroma? *Am J Surg Pathol*. 2010;34:126–127. Author reply 7.
19. Hora M, Hes O, Michal M, et al. Extensively cystic renal neoplasms in adults (Bosniak classification II or III) possible "common" histological diagnoses: multilocular cystic renal cell carcinoma, cystic nephroma, and mixed epithelial and stromal tumor of the kidney. *Int Urol Nephrol*. 2005;37:743–750.
20. Svec A, Hes O, Michal M, et al. Malignant mixed epithelial and stromal tumor of the kidney. *Virchows Arch*. 2001;439:700–702.
21. Michal M, Hes O, Bisceglia M, et al. Mixed epithelial and stromal tumors of the kidney. A report of 22 cases. *Virchows Arch*. 2004;445:359–367.
22. Madewell JE, Goldman SM, Davis CJ Jr, et al. Multilocular cystic nephroma: a radiographic-pathologic correlation of 58 patients. *Radiology*. 1983;146:309–321.
23. Doros LA, Rossi CT, Yang J, et al. DICER1 mutations in childhood cystic nephroma and its relationship to DICER1-renal sarcoma. *Mod Pathol*. 2014;27:1267–1280.
24. Schultze-Florey RE, Graf N, Vorwerk P, et al. DICER1 syndrome: a new cancer syndrome. *Klin Padiatr*. 2013;225:177–178.
25. Bahubeshi A, Bal N, Rio Frio T, et al. Germline DICER1 mutations and familial cystic nephroma. *J Med Genet*. 2010;47:863–866.
26. Bal N, Kayaselcuk F, Polat A, et al. Familial cystic nephroma in two siblings with pleuropulmonary blastoma. *Pathol Oncol Res*. 2005;11:53–56.
27. Ashley RA, Reinberg YE. Familial multilocular cystic nephroma: a variant of a unique renal neoplasm. *Urology*. 2007;70:179.e9–179.e10.

1.8.2 Distinctive renal cell tumor simulating atrophic kidney with 2 types of microcalcifications. Report of 3 cases¨

Studie prezentuje tři případy primárních renálních „tumorů“ připomínajících atrofickou ledvinu se specifickým makroskopickým, mikroskopickým, imunohistochemickým a molekulárně-genetickým pozadím.

Nádory se vyskytly u 2 žen a 1 muže, pacienti ve věkovém rozmezí 29-35 let. Tumory byly makroskopicky kulaté, enkapsulované. Dostupné údaje o dalším průběhu onemocnění (v délce trvání 2 - 14 let, průměr 8 roků) neprokázaly agresivní potenciál. Nádory měly podobnou morfologii jako atrofický renální parenchym - sestávaly z foliklů různé velikosti, které byly vyplněny eosinofilním sekretem, vzácně přítomny i okrsky s „kolabovanými“ folikly. Okolní stroma bylo řídké a fokálně fibrotické. Pozorovány byly dva typy kalcifikací (psammomakalcifikace a amorfní tmavě modře se barvící depozita). Nádory byly silně imunoreaktivní v barvení OSCAR, CD10 a vimentinu a slabě pozitivní v CAM5.2, AE1/3, WT1 a katepsinu K. Naopak negativní byly tumory v CK20, CA IX, parvalbuminu, HMB45, TTF1, TFE3, chromograninu A, thyroglobulinu, PAX8 a ALK. Pro molekulárně genetické testování byl vhodný pouze jeden tumor, u něhož nebyla prokázána ani mutace *VHL* genu, ani metylace *VHL*, bez numerických aberací (v aCGH), bez LOH 3p. Analýza klonality odhalila monoklonální povahu tumoru.

V rámci této práce jsme tak popsali doposud neznámý „tumor“ ledviny, který: 1) připomínal atrofický renální parenchym či nodulární strumu štítné žlázy, 2) obsahoval leiomyomatózní pouzdro a dva typy kalcifikací, 3) tumory byly bez mitóz, atypií, nekróz a hemorrhagií a téměř bez Ki-67 pozitivity, 4) doposud vykazovaly benigní biologické chování.

Annals of Diagnostic Pathology 18 (2014) 82–88

Contents lists available at ScienceDirect

Annals of Diagnostic Pathology

Distinctive renal cell tumor simulating atrophic kidney with 2 types of microcalcifications. Report of 3 cases ☆,☆☆

Ondrej Hes, MD, PhD [a,b], Tulio Geraldo de Souza, MD [c], Kristyna Pivovarcikova, MUC [a], Petr Grossmann, PhD [a], Petr Martinek, MSc [a], Naoto Kuroda, MD [d], Denisa Kacerovska, MD, PhD [a], Marian Svajdler, MD [e], Lubomir Straka, MD [f], Fredrik Petersson, MD, PhD [g], Milan Hora, MD, PhD [b,h], Michal Michal, MD [a,*]

[a] Department of Pathology, Faculty of Medicine in Plzeň, Charles University in Prague, Pilsen, Czech Republic
[b] Biomedical Centre, Faculty of Medicine in Plzeň, Charles University in Prague, Pilsen, Czech Republic
[c] Department of Pathology, Hospital Aliança, Salvador, Bahia, Brazil
[d] Department of Pathology, Red Cross Hospital Kochi, Kochi, Japan
[e] Department of Pathology, Pasteur University Hospital Kosice, Kosice, Slovak Republic
[f] Klinicka Patologia Presov, Presov, Slovak Republic
[g] Department of Pathology, National University Health System, Singapore, Singapore
[h] Department of Urology, Faculty of Medicine in Plzeň, Charles University in Prague, Pilsen, Czech Republic

ARTICLE INFO

Keywords:
Kidney
Atrophic renal parenchyma-like tumor
Thyroid-like renal tumor
Comparative genomic hybridization
HUMARA

ABSTRACT

We report 3 cases of primary renal cell tumor simulating atrophic kidney with distinct gross, morphologic, immunohistochemical, and molecular genetic features. The tumors were retrieved out of more than 17 000 renal tumors from the Plzen Tumor Registry. Tissues for light microscopy had been fixed, embedded, and stained with hematoxylin and eosin using routine procedures. The tumors were further analyzed using immunohistochemistry, array comparative genomic hybridization, and human androgen receptor. Analyses of *VHL* gene and loss of heterozygosity (LOH) 3p were also performed. The patients were 2 women and 1 man, with ages ranging from 29 to 35 years (mean, 31.3 years). Grossly, the neoplasms were encapsulated and round with largest diameter of 3.5 cm (mean, 3.2 cm). Follow-up available for all patients ranged from 2 to 14 years (mean, 8 years). No aggressive behavior was noted. Histologically, akin to atrophic (postpyelonephritic) kidney parenchyma, the tumors were composed of follicles of varying sizes that were filled by eosinophilic secretion. Rare areas contained collapsed follicles. Each follicle was endowed with a small capillary. The stroma was loose, inconspicuous, and focally fibrotic. Two types of calcifications were noted: typical psammoma bodies and amorphous dark-blue stained calcified deposits. Immunohistochemically, tumors were strongly positive for cytokeratins (OSCAR), CD10, and vimentin, with weak immunopositivity for CAM5.2 and AE1-AE3. WT1 and cathepsin K were weakly to moderately focally to diffusely positive. Tumors were negative for cytokeratin 20, carbonic anhydrase IX, parvalbumin, HMB45, TTF1, TFE3, chromogranin A, thyroglobulin, PAX8, and ALK. Only 1 case was suitable for molecular genetic analyses. No mutations were found in the *VHL* gene; no methylation of *VHL* promoter was noted. No numerical aberrations were found by array comparative genomic hybridization analysis. LOH for chromosome 3p was not detected. Analysis of clonality (human androgen receptor) revealed the monoclonal nature of the tumor. We describe an unknown tumor of the kidney that (1) resembles renal atrophic kidney or nodular goiter of thyroidal gland; (2) contains a leiomyomatous capsule and 2 types of calcifications; (3) lacks mitoses, atypias, necroses, and hemorrhages and nearly lack Ki-67 positivity; and (4) so far showed benign biological behavior.

1. Introduction

We report 3 cases of a primary renal cell tumor microscopically simulating atrophic kidney with distinct gross, morphologic, and immunohistochemical features, which has not so far been reported, to the best of our knowledge. Comparative genomic hybridization (CGH) analysis and analysis of clonality using X-chromosomal inactivation pattern and human androgen receptor (HUMARA) locus were used to better understand the nature of this tumor and to distinguish it from the kidney with atrophic changes.

☆ The study was supported by the Charles University Research Fund (project number P36), by the project CZ.1.05/2.1.00/03.0076 from European Regional Development Fund, and by Charles University Fund SVV 06805.

☆☆ Conflict of interest statement: The authors declare that they have no conflict of interest.

* Corresponding author at: Department of Pathology, Medical Faculty and Charles University Hospital Plzen, Charles University, Alej Svobody 80, 304 60 Pilsen, Czech Republic.
E-mail address: michal@medima.cz (M. Michal).

1092-9134/$ – see front matter © 2014 Elsevier Inc. All rights reserved.
http://dx.doi.org/10.1016/j.anndiagpath.2013.12.003

2. Materials and methods

The tumors were retrieved out of more than 17 000 renal cases from the Plzen Tumor Registry. Two of 3 cases were sent to the authors (O.H., M.M.) for the second opinion, and case 3 was contributed by Dr Souza from Hospital Aliança, Salvador, Brazil. Tissues for light microscopy have been fixed in 4% formaldehyde and embedded in paraffin using routine procedures. Five-micrometer-thick sections were cut and stained with hematoxylin and eosin.

3. Immunohistochemistry

The immunohistochemical study was performed using a Ventana Benchmark XT automated stainer (Ventana Medical System, Inc, Tucson, Arizona). The following primary antibodies were used: epithelial membrane antigen (E29, monoclonal; 1:1000; DAKO, Carpinteria, California), cytokeratins (CKs; CAM5.2, monoclonal, 1:200; Becton-Dickinson, San Jose, California), Pan Ab-1 (AE1-AE3, monoclonal, 1:1000; BioGenex, San Ramon, California), CK7 (OV-TL12/30, monoclonal, 1:200; DAKO), CK18 (DC 10, monoclonal, 1:100; DAKO), CK19 (M 0888, monoclonal, 1:100; DAKO), CK20 (M7019, monoclonal, 1:100; DAKO), CK OSCAR (OSCAR, monoclonal, 1:2000; Covance, Princetown, New Jersey), CK NMF 116 (MNF 116, monoclonal, 1:100; DAKO), racemase/AMACR (P504S, monoclonal, 1:50; Zeta, Sierra Madre, California), vimentin (D9, monoclonal, 1:1000; NeoMarkers, Westinghouse, California), Ki-67 (MIB1, monoclonal, 1:1000; DAKO, Glostrup, Denmark), melanoma marker (HMB45, monoclonal, 1:200; DAKO), CD10 (56C6, monoclonal, 1:100; Abcam, Cambridge, UK), carbonic anhydrase IX (rhCA9, monoclonal, 1:100; RD Systems, Abingdon, GB, UK), TFE3 (polyclonal, 1:100; Abcam), TFE 3 (monoclonal, MRQ 37, RTU; Cell Marque, Rocklin, California), ALK (monoclonal, 5A4, 1:400; Novocastra, Newcastle, UK), cathepsin K (3F9, monoclonal, 1:100; Abcam), WT1 (GF-H2, monoclonal, 1:150; DAKO), synaptophysin (polyclonal, 1:400; Thermo Scientific, Cheshire, UK), chromogranin A (DAK A3, monoclonal, 1:300; DAKO), S 100 protein (polyclonal, 1:400; DAKO), TTF-1 (SPT24, monoclonal, 1:400; Novocastra), thyroglobulin (polyclonal, RTU; DAKO), parvalbumin (PARV-19, monoclonal, 1:500; Sigma, St Luis, Missouri), CD34 (monoclonal, QBEnd10, 1:100; DAKO), desmin (monoclonal, D33, 1:2000; DAKO), smooth muscle actin (monoclonal, 1A4, RTU; Ventana-Roche), PAX2 (polyclonal, 1:100; Invitrogen, Camarillo, California), and PAX8 (polyclonal, 1:100; Abcam). Appropriate positive controls were used.

4. Molecular genetic study

4.1. DNA extraction

DNA from formalin-fixed paraffin-embedded (FFPE) tumor and nontumor tissues was extracted using a QIAsymphony DNA Mini Kit (Qiagen, Hilden, Germany) on automated extraction system (QIAsymphony SP; Qiagen), according to the manufacturer's supplementary protocol for FFPE samples (purification of genomic DNA from FFPE tissue using the QIAamp DNA FFPE Tissue Kit and Deparaffinization Solution). Concentration and purity of isolated DNA was measured using NanoDrop ND-1000 (NanoDrop Technologies Inc, Wilmington, Delaware). DNA integrity was examined by amplification of control genes in a multiplex polymerase chain reaction (PCR).[1]

4.2. Array CGH

4.2.1. A microarray processing

A CytoChip Focus Constitutional (BlueGnome Ltd, Cambridge, UK) was used for analysis. CytoChip Focus Constitutional uses BAC technology and covers 143 regions of known significance with 1-Mb spacing across a genome. Probes are spotted in triplicates. First, 400 ng of DNA was labeled using the Fluorescent Labeling System (BlueGnome Ltd). The procedure included Cy3 labeling of a test sample and Cy5 labeling of a reference sample. The labeled reference and the test sample were mixed, dried, and hybridized overnight at 47°C using Arrayit hybridization cassette (Arrayit Corporation, Sunnyvale, California). Posthybridization washing was done using SSC buffers with increasing stringency. Dried microarray was scanned with InnoScan 900 (Innopsys, Carbonne, France) at a resolution of 5 μm.

4.2.2. Image and data analysis

Scanned image was analyzed and quantified by BlueFuse Multi software (BlueGnome Ltd). BlueFuse Multi uses Bayesian algorithms to generate intensity values for each Cy5- and Cy3-labeled spot on the array according to an appropriate.gal file. The results were annotated using BlueFuse Multi, as well. Cutoff values for log 2 ratio were set to −0,193 for loss and to 0.170 for gain.[2]

4.3. VHL gene mutation analysis and promoter methylation

Mutation analysis of coding sequence and exon-intron junctions of the *VHL* gene was performed using PCR and direct sequencing. Detection of promoter methylation was performed via methylation-specific PCR, as described by Herman et al.[3] Bisulfite conversion, PCR primers, and setup are shown in a previous study.[4]

4.4. 3p loss of heterozygosity analysis

For LOH analysis of neoplastic tissue DNA, 10 short tandem repeat markers (D3S666, D3S1270, D3S1300, D3S1581, D3S1597, D3S1600, D3S1603, D3S1768, D3S2338, and D3S3630) located on the short arm of chromosome 3 (3p) were chosen from the database (GenBank UniSTS). The method is described in details in a previous study.[4]

4.5. Analysis of clonality using HUMARA locus

Clonality analysis was performed according to the previously described method based on the digestion of differentially methylated X-chromosomal DNA with methylation-sensitive restriction enzyme followed by PCR amplification of a CAG repeat located in HUMARA. DNA from tumor and nontumor tissues was digested by restriction enzyme *Hha*I and amplified as described previously.[5]

DNA from tumor and nontumor tissues was digested by restriction enzyme *Hha*I and amplified as described previously.[6]

Polymerase chain reaction products were examined by a fragment analysis on Abi3130*xl*. Peak heights of the 2 alleles were measured for each specimen. A corrected ratio (CR) was assessed by dividing the ratio (allele 1/allele2) of the digested sample by the ratio (allele1/allele 2) of the undigested sample. A final clonality ratio was determined by dividing the CR of the tumor DNA by the CR of the nontumor DNA. Sample was considered monoclonal if the final ratio was higher than 1.5 or lower than 0.66.

5. Results

5.1. Case 1

A 30-year-old woman has been followed up for 11 years for hyperurikemia and nephrolithiasis. Radical right nephrectomy was performed. The tumor was located in the renal cortex between the upper pole and part of the kidney. No infiltration into the adjacent perirenal structures or into the renal sinus was noted. There was no relationship of the lesion to the renal pelvis. The tumor was excised fragmented in 8 pieces, and estimated overall size of the tumor was 3 cm in largest diameter.

Grossly, it was difficult to appreciate whether tumor was encapsulated because of the surgical fragmentation of the excised tissue. At follow-up, 14 years after nephrectomy, the patient is

Fig. 1. The tumor is tan to brown in color grossly. Small microcysts imparting a focal honeycomb appearance are discernible on the cut surface. No hemorrhage or necroses are noted. Case 2.

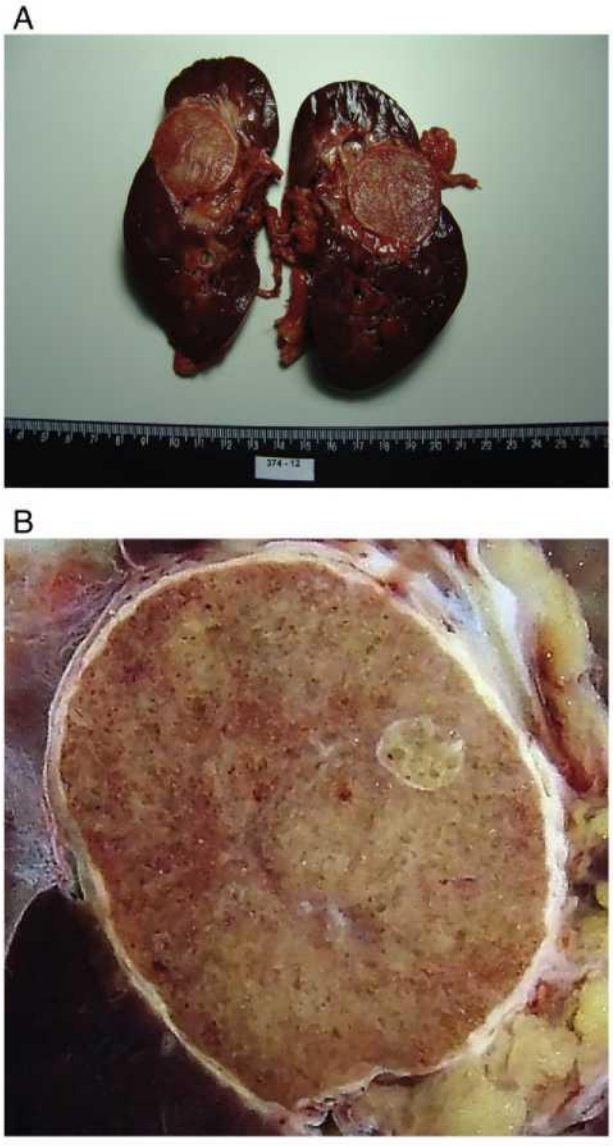

Fig. 2. The tumor is located in the central part of the kidney with extension to the sinus and cortex, is round in shape, and measures 3.5 cm in the largest diameter. The gross appearance strongly suggests that the lesion is a neoplasm and not postpyelonephritic atrophic scar. Case 3.

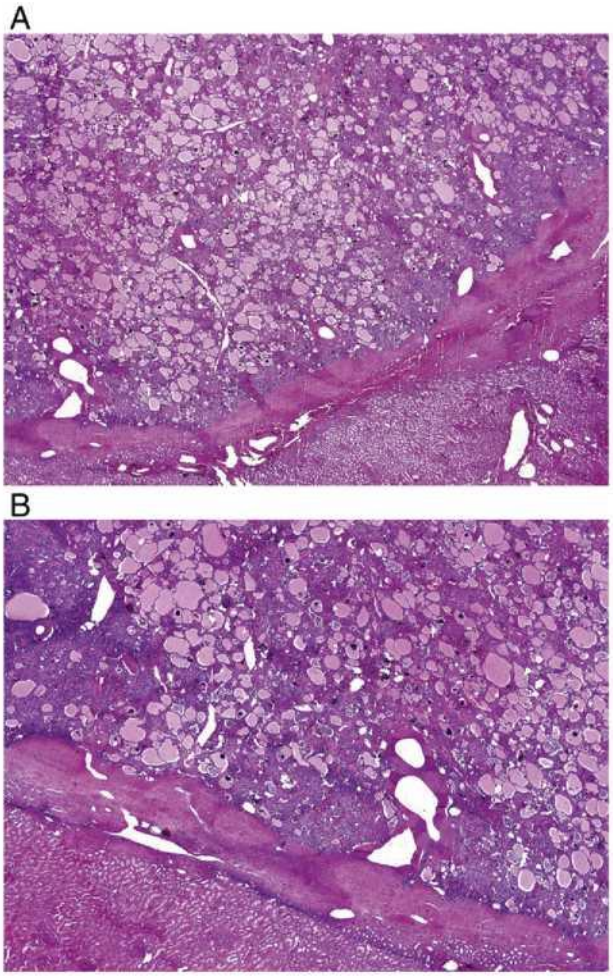

Fig. 3. The leiomyomatous capsule surrounding the neoplasms contains well-formed and abortively thick vessels. Numerous calcifications throughout the tumors can be appreciated even on the small-power magnification. A, Case 2. B, Case 3. Hematoxylin and eosin stain.

currently alive, without signs of recurrence or metastatic behavior; laboratory tests revealed hyperthyroidism, hyperurikemia, and gout.

5.2. Case 2

In a 35-year-old man, a renal tumor was incidentally disclosed during a workup for mediastinal Hodgkin lymphoma by ultrasonography. The renal neoplasm was located in the cortex with extension toward the renal sinus. No connection of the lesion to the pelveocalyceal system was found. The tumor was well demarcated and oval shaped with 3 cm in largest diameter, and it had a distinct white capsule. The neoplasm was tan to brown and solid on the cut surface; however, on closer inspection, small microcysts were observed, imparting a focal honeycomb or sponge-like appearance (Fig. 1). No hemorrhages or necroses were noted. The patient has been followed up for 8 years, revealing no signs of recurrence or metastases. No progression of Hodgkin lymphoma was observed.

5.3. Case 3

The patient was a 29-year-old woman. A tumor, causing no clinical symptoms, was incidentally found in the left kidney on a regular checkup. The neoplasm was located in the central part of the kidney with extension both into the sinus and cortex. It was round shaped and measured 3.5 cm in the largest diameter (Fig. 2A). The tumor was encapsulated, with finely microcystic surface on the cut surface

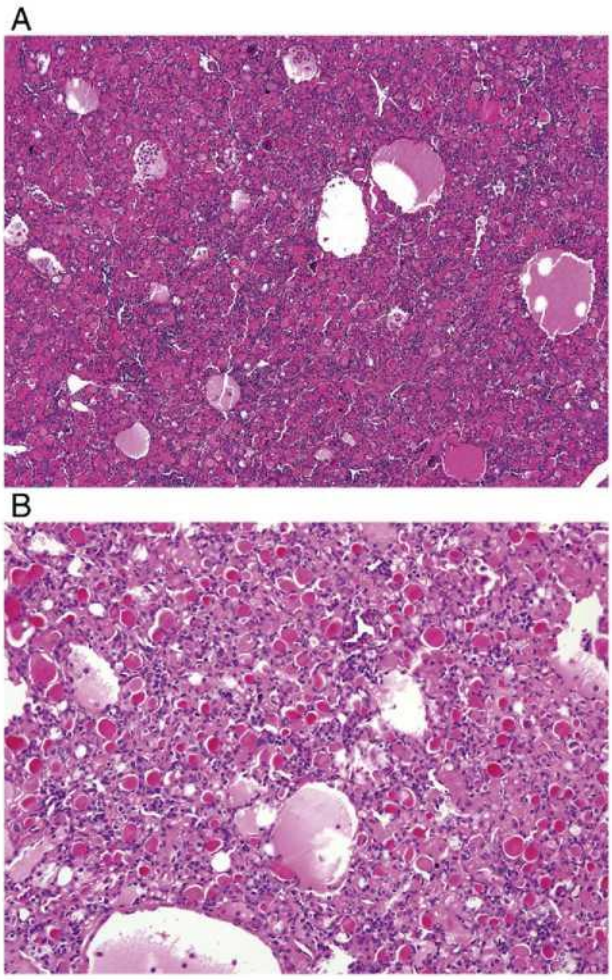

Fig. 4. Note a similarity to the thyroid gland. A, Case 1. B, Case 2.

resembling a bath sponge or honeycomb with 1 yellow nodule within a tumorous mass. The main tumorous mass was pink to brownish. The capsule was well formed and white. No grossly visible hemorrhages or necroses were present (Fig. 2B). The patient has been followed up for 2 years every 3 months since the nephrectomy with no signs of recurrent disease or metastatic behavior.

The histological picture was remarkably identical in all 3 tumors. The neoplasms had a capsule formed by excessive smooth muscle of

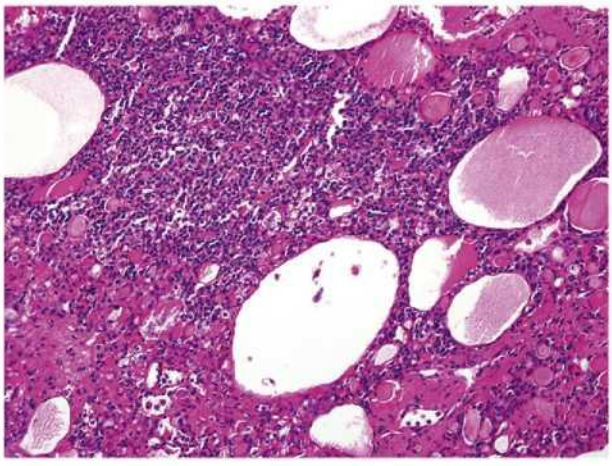

Fig. 5. Rare areas of tumors are composed of collapsed follicles arranged in small alveoli. Case 1. Hematoxylin and eosin stain.

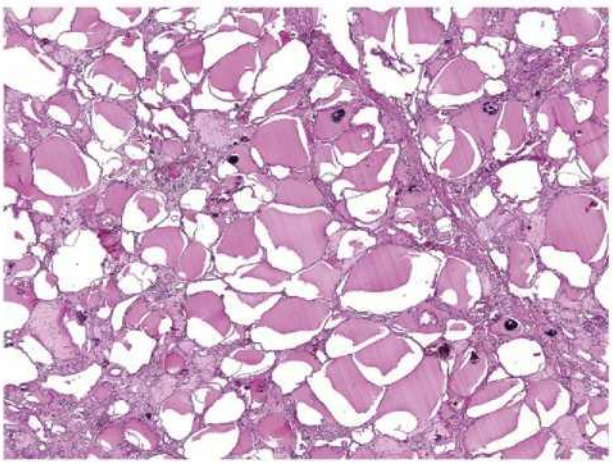

Fig. 6. Areas composed of large follicles only. Case 3. Hematoxylin and eosin stain.

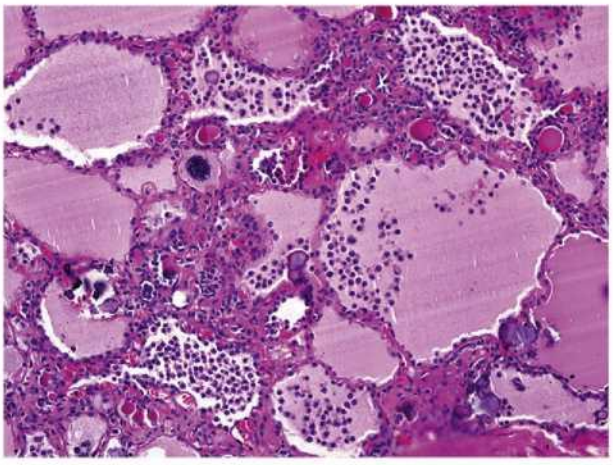

Fig. 7. The tumor cells lining larger follicles in a hobnail pattern. Note tumor cells detached from the follicle into the colloid. Case 3. Hematoxylin and eosin stain.

vessel walls, which were well and less well formed and thick (Fig. 3A, B). The overall microscopic appearance was that of an atrophic kidney, with the tumor bulk being composed of follicles of varying sizes. The smallest follicles were as small as 30 μm, whereas the largest ones were on close inspection discernible by naked eye resulting in a

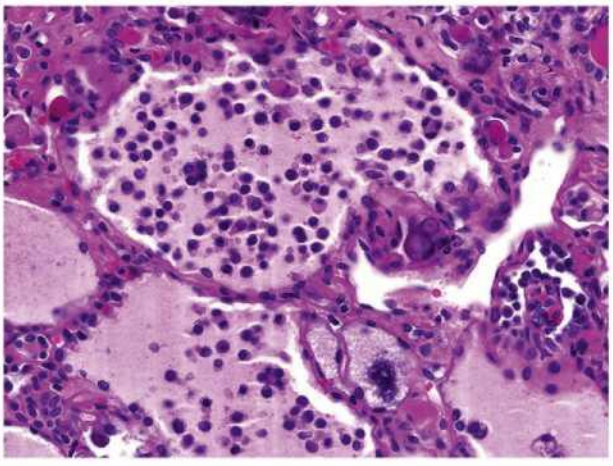

Fig. 8. The tumor cell floating in the colloid resembling plasma cells. Case 3. Hematoxylin and eosin stain.

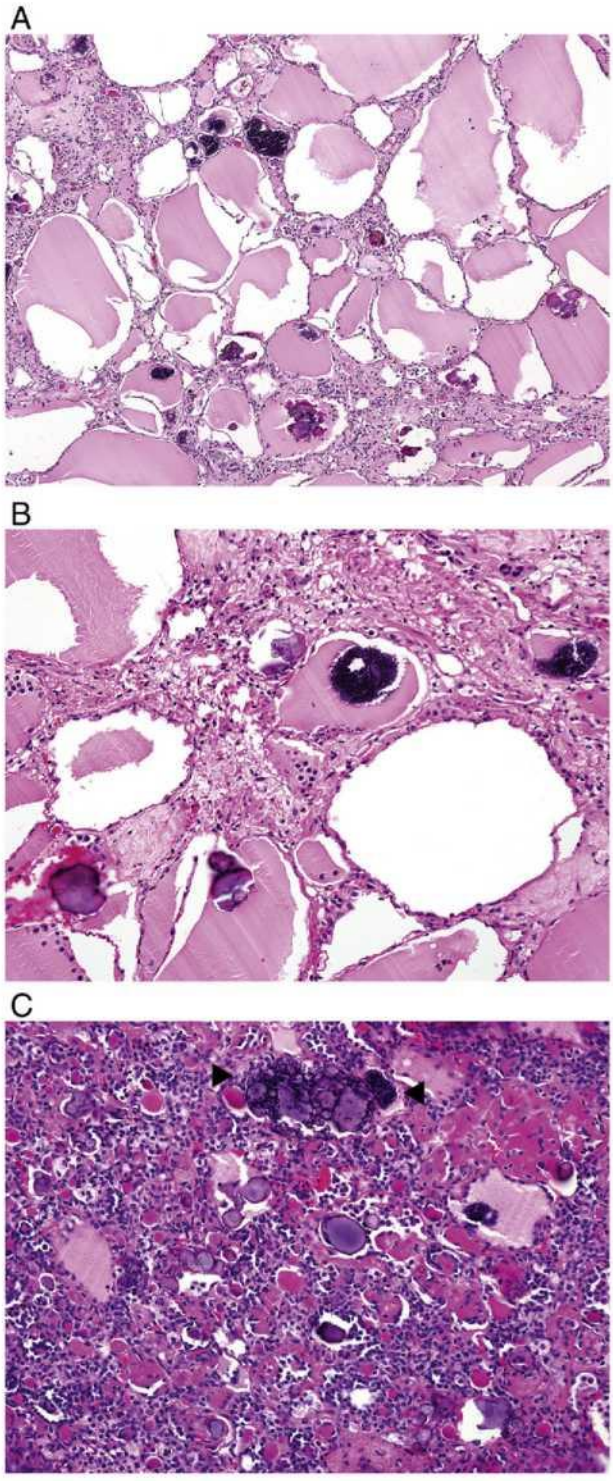

Fig. 9. Two types of calcifications located either inside the follicles or within the follicle walls can be recognized. One type is reminiscent of a typical psammoma body, and the second type is composed of amorphous dark-blue stained calcified deposits. A, Case 1. B, Case 2. Rare calcifications display features of both types. C, Case 3 (arrow). Hematoxylin and eosin stain.

sponge-like appearance. The follicles were filled with eosinophilic secretions. Usually, the smaller the follicles, the deeper pink was the color of the secretion. The secretion of the largest follicles had often "moth-eaten" clear peripheries, similar to those seen in the follicles of the thyroid gland (Fig. 4A, B). Collapsed follicles were focally present (Fig. 5), and some areas consisted of large follicles only (Fig. 6). On higher magnification, it was apparent that each follicle was endowed with a small capillary, which ran in the stroma between the adjacent follicles. The follicles were formed by cells with small round to slightly cleaved nuclei with indistinct nucleoli, which lined larger follicles in a hobnail pattern with shedding of the neoplastic cells into a colloid-filled lumen (Fig. 7). The tumor cells floating in the colloid had morphology remarkably similar to plasma cells (Fig. 8). The tumorous stroma was loose, inconspicuous, and focally fibrotic.

Other distinctive features of all tumors were calcifications, of which 2 types were recognized, both located either inside the follicles or within the follicle walls. One type of calcification resembled a typical psammoma body, whereas the other one was composed of amorphous dark-blue stained calcified deposits (Fig. 9A, B). Rarely, there were calcifications that had features of both of these types in all tumors (Fig. 9C).

6. Immunohistochemistry

The tumors were strongly positive for CKs (OSCAR), vimentin, and CD10 and weakly positive for CAM5.2 and AE1-AE3. OSCAR stained detached cells inside the follicles in a dot-like paranuclear pattern (Fig. 10), whereas AE1-AE3 stained mostly the epithelium of small follicles. Cytokeratin 7, CK18, MNF116, and epithelial membrane antigen immunoreactivity was similar to that of AE1-AE3. Focal strong positivity was noted for CK19. PAX2 was weakly positive in all 3 cases. Positivity for WT1 ranged from weak and focal to moderate and diffuse. The same pattern of positivity was noted for cathepsin K. Staining for CK20, carbonic anhydrase IX, parvalbumin, HMB45, TTF1, TFE3, chromogranin A, thyroglobulin, ALK, S100 protein, racemase/AMACR, and PAX8 was negative. The capsule was positive for smooth muscle actin (3/3) and focally for desmin (1/3) and for CD34 (2/3). Ki-67 positivity was very rare, and several high-power fields had to be reviewed to find a single Ki-67–positive cell.

7. Molecular genetic findings

Only case 3 had sufficient DNA quality to perform molecular genetic analyses. No mutations were found in the *VHL* gene. Methylation of *VHL* promoter was not detected. No significant numerical aberrations were found in array CGH analysis (Fig. 11) on chromosomes 1 to 22. Loss of heterozygosity for chromosome 3p was not detected. Analysis of clonality (Fig. 12) revealed a final clonality ratio of 0.072, indicating monoclonality of the sample.

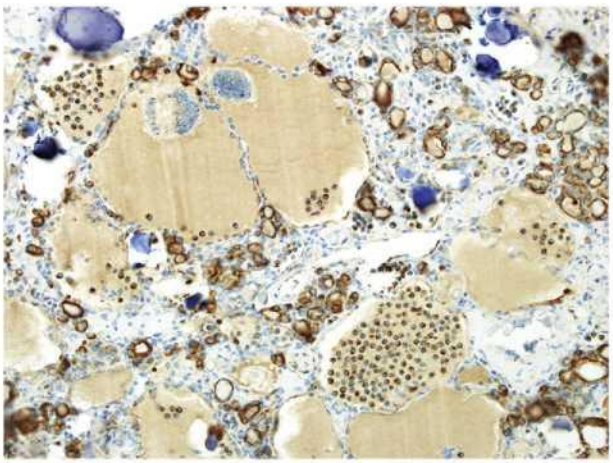

Fig. 10. Detached cells inside the follicles are stained by OSCAR in a dot-like paranuclear pattern. Case 3.

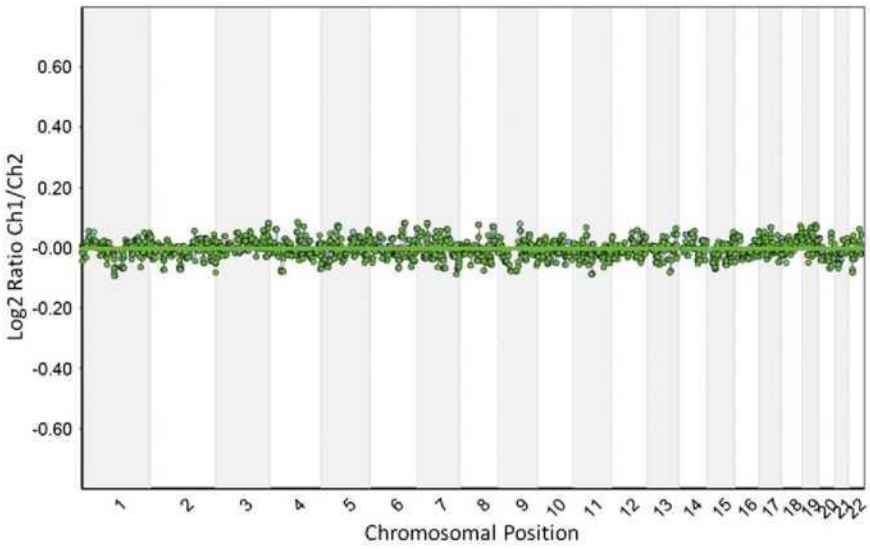

Fig. 11. No significant numerical aberrations were found in array CGH analysis on chromosomes 1 to 22.

8. Discussion

Since the beginning of late 1990s, we were aware of a distinctive lesion of the kidney that morphologically resembled an atrophic kidney, but it was considered as a neoplasm by clinicians. One of us (M.M.) saw 2 additional examples of this neoplasm in the files of a different institution in the 1990 (these 2 cases are not included in this series). The lesions, similar to atrophic kidneys, were composed of densely packed follicles filled with eosinophilic colloid secretions resulting in a thyroid-like appearance. Such a thyroid-like appearance in renal pathology was repeatedly described in patients with postpyelonephritic disease or postischemic renal scarring.[7–9] Because the first case we received was surgically excised by a surgeon fragmented in many pieces, it was not readily apparent to us whether the lesion was encapsulated, precluding further speculations whether the lesion represented a true neoplasm or merely a segmental renal atrophy. After receiving the other 2 lesions with distinct encapsulation and identical histopathologic features, it became apparent that the 3 lesions are identical and represent a neoplasm (Figs. 1 and 2). The neoplastic nature of the lesions was further proved by the analysis of clonality using HUMARA locus, which revealed a clonality ratio of 0.072, indicating monoclonality of the sample in case 3. Array CGH revealed no alteration, but this can be seen in many tumors in which neoplastic process is triggered by a mechanism different from unbalanced chromosomal abnormalities. In addition, there were no entrapped cortical or medullar tubuli and no obsolete glomeruli within tumorous mass, which is regularly the case with atrophic areas in postpyelonephritic kidneys.

Two distinctive types of calcifications reminiscent of those seen in thyroid neoplasms are further unique feature of the lesions. We are

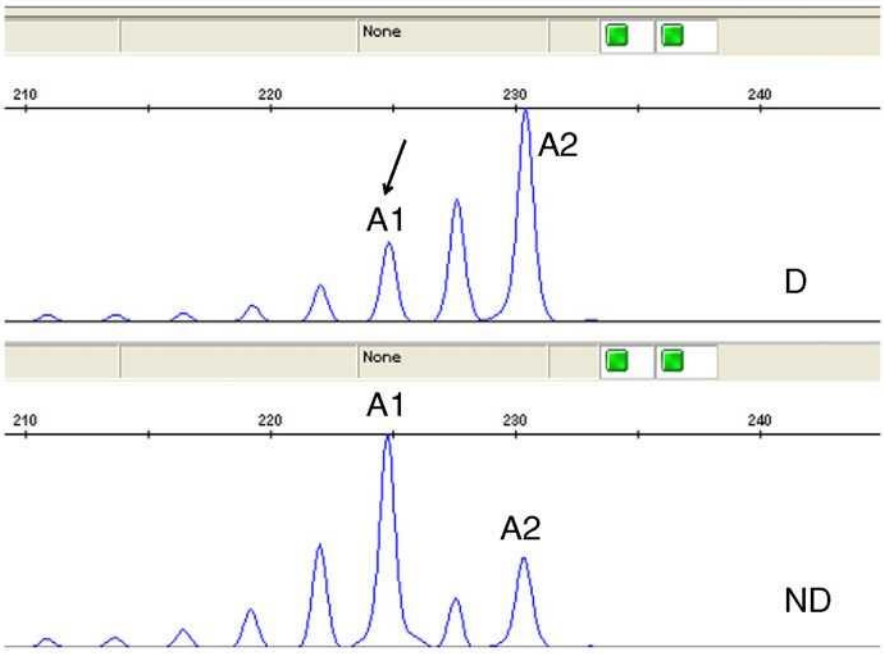

Fig. 12. Analysis of clonality of sample in case 3. Apparent reduction of peak height of the longer allele is visible (A1) in *Hha*I-digested (D) sample compared with nondigested sample (ND). Only minor change in peak height was detected in nontumor tissue (not shown).

not aware of any renal neoplasm containing similar calcifications. Given the above-described constellation of clinicopathologic features, we think that the 3 cases represent a distinct entity.

Even if the lesions we describe do not come close to any renal neoplasms in appearance, 2 renal lesions should be discussed in the differential diagnosis, that is, multilocular multicystic renal cell carcinoma and thyroid-like follicular renal cell carcinoma (TFRCC).

Multilocular multicystic renal cell carcinoma is an unusual but well-defined multicystic variant of clear renal cell carcinoma histologically characterized by thin fibrous septa lined by clear cells. Our cases can be easily distinguished by the lack of a clear cell component and much less conspicuous vascularity. In addition, genetically, and in contrast to most cases of multilocular multicystic renal cell carcinoma,[10,11] we were not able to detect the *VHL* gene mutations or LOH3p in the case available for molecular genetic analysis.

Because of similarity of our lesions to a thyroid gland tissue, there should be discussed differential diagnosis of TFRCC, which is an extremely rare and unusual renal tumor. This entity has not been included in the World Health Organization 2004 classification, but many renal pathologists recognize it as a distinct renal tumor.[12–16] Our cases are easily distinguished from TFRCC by the fact that they resembled much more an entirely atrophic kidney or at most a benign thyroid goiter rather than any known type of a thyroidal malignant neoplasm. In fact, a lesion that is morphologically difficult to differentiate from renal atrophy cannot be mistaken with any type of malignant tumor. In addition, our cases were entirely devoid of mitoses, atypias, necroses, and hemorrhage, and it was even very difficult to find a single Ki-67–positive cell in many microscopical fields in all 3 tumors in our series. We usually found 1 Ki-67–positive cell after reviewing multiple microscopical high-power fields of the tumors.

A very interesting and constant feature in our cases was the capsule composed of a leiomyomatous tissue. Because the capsule contained many incased abortive as well as well-formed thick-walled vessel reacting immunohistochemically with smooth muscle actin and desmin antibodies, and because the kidney is otherwise devoid of any structure containing smooth muscles under normal conditions, we infer that this capsule is derived from smooth muscle of the vessel walls. This feature, capsule composed of leiomyomatous smooth muscles, is not unique to the tumor we describe here. It is a constant feature of tumor recently described as renal angiomyoadenomatous tumor (RAT).[17,18] We have currently nearly 40 cases of RAT in our files, and all contain identical leiomyomatous capsules. In contrast to RAT, where the smooth muscle proliferations not only are always seen in the capsule and but also permeate the whole tumor, accounting for up to 90% of the tumor volume in some cases of RAT, in the lesion cases we describe herein the smooth muscle component was strictly confined to the capsule.

In summary, we describe a new tumor of the kidney that resembles a postpyelonephritic atrophic kidney or nodular goiter of the thyroidal gland. It contains a leiomyomatous capsule and 2 distinct types of calcifications, located either inside the follicles or within the follicle walls. One type of calcification resembles a typical psammoma body, and the other one is composed of amorphous dark-blue stained calcified deposits. Owing to the lack of mitoses, atypias, necroses, hemorrhage, near absence of Ki-67 positivity, and uneventful follow-up, we consider the tumor to be a benign neoplasm.

References

[1] van Dongen JJ, Langerak AW, Bruggemann M, et al. Design and standardization of PCR primers and protocols for detection of clonal immunoglobulin and T-cell receptor gene recombinations in suspect lymphoproliferations: report of the BIOMED-2 Concerted Action BMH4-CT98-3936. Leukemia 2003;17:2257–317.

[2] Petersson F, Vanecek T, Michal M, et al. A distinctive translocation carcinoma of the kidney; "rosette forming," t(6;11), HMB45-positive renal tumor: a histomorphologic, immunohistochemical, ultrastructural, and molecular genetic study of 4 cases. Hum Pathol 2012;43:726–36.

[3] Herman JG, Graff JR, Myohanen S, Nelkin BD, Baylin SB. Methylation-specific PCR: a novel PCR assay for methylation status of CpG islands. Proc Natl Acad Sci U S A 1996;93:9821–6.

[4] Petersson F, Grossmann P, Hora M, et al. Renal cell carcinoma with areas mimicking renal angiomyoadenomatous tumor/clear cell papillary renal cell carcinoma. Hum Pathol 2013;44:1412–20.

[5] Allen RC, Zoghbi HY, Moseley AB, Rosenblatt HM, Belmont JW. Methylation of Hpall and Hhal sites near the polymorphic CAG repeat in the human androgen-receptor gene correlates with X chromosome inactivation. Am J Hum Genet 1992;51:1229–39.

[6] Kazakov DV, Curik R, Vanecek T, Mukensnabl P, Michal M. Nodular hyperplasia of the bartholin gland: a clinicopathological study of two cases, including detection of clonality by HUMARA. Am J Dermatopathol 2007;29:385–7.

[7] Kimmelstiel P, Kim OJ, Beres JA, Wellman K. Chronic pyelonephritis. Am J Med 1961;30:589–607.

[8] Kincaid-Smith P. Vascular obstruction in chronic pyelonephritic kidneys and its relation to hypertension. Lancet 1955;269:1263–9.

[9] Laberke HG, Klingebiel T, Quack G. A contribution to the morphology and pathogenesis of thyroid-like lesions in the kidney. Pathol Res Pract 1983;176:284–96.

[10] von Teichman A, Comperat E, Behnke S, Storz M, Moch H, Schraml P. VHL mutations and dysregulation of pVHL- and PTEN-controlled pathways in multilocular cystic renal cell carcinoma. Mod Pathol 2011;24:571–8.

[11] Williamson SR, Halat S, Eble JN, et al. Multilocular cystic renal cell carcinoma: similarities and differences in immunoprofile compared with clear cell renal cell carcinoma. Am J Surg Pathol 2012;36:1425–33.

[12] Amin MB, Gupta R, Ondrej H, et al. Primary thyroid-like follicular carcinoma of the kidney: report of 6 cases of a histologically distinctive adult renal epithelial neoplasm. Am J Surg Pathol 2009;33:393–400.

[13] Angell SK, Pruthi R, Freiha FS. Primary thyroidlike carcinoma of the kidney. Urology 1996;48:632–5.

[14] Dhillon J, Tannir NM, Matin SF, Tamboli P, Czerniak BA, Guo CC. Thyroid-like follicular carcinoma of the kidney with metastases to the lungs and retroperitoneal lymph nodes. Hum Pathol 2011;42:146–50.

[15] Jung SJ, Chung JI, Park SH, Ayala AG, Ro JY. Thyroid follicular carcinoma-like tumor of kidney: a case report with morphologic, immunohistochemical, and genetic analysis. Am J Surg Pathol 2006;30:411–5.

[16] Khoja HA, Almutawa A, Binmahfooz A, Aslam M, Ghazi AA, Almaiman S. Papillary thyroid carcinoma-like tumor of the kidney: a case report. Int J Surg Pathol 2012;20:411–5.

[17] Michal M, Hes O, Havlicek F. Benign renal angiomyoadenomatous tumor: a previously unreported renal tumor. Ann Diagn Pathol 2000;4:311–5.

[18] Michal M, Hes O, Nemcova J, et al. Renal angiomyoadenomatous tumor: morphologic, immunohistochemical, and molecular genetic study of a distinct entity. Virchows Arch 2009;454:89–99.

1.8.3 Primary renal well-differentiated neuroendocrine tumour (carcinoid): next-generation sequencing study of 11 cases

Dobře diferencovaný neuroendokrinní tumor (NET) ledviny je velmi vzácnou renální neoplázií - doposud bylo v literatuře publikováno méně než 100 případů. Dostupná data o molekulárně-genetickém pozadí těchto lézí jsou tak logicky velmi limitovaná.

V rámci této studie jsme analyzovali 11 dobře diferencovaných neuroendokrinních tumorů za pomoci sekvenování nové generace (NGS), ve snaze identifikovat genetické alterace charakteristické pro tuto entitu. Analyzované tumory byly pozitivní v synaptofyzinu (11/11), exprimovaly INSM1 (10/11 tumorů), chromogranin A (8/11) a CD56 (3/11). Cytoplazmatická pozitivita CD99 zastižena v 8/11 případů a silná jaderná exprese ATRX byla zaznamenána ve všech případech. Molekulárně-genetická analýza aberace *VHL* genu prokázala negativitu ve všech případech. Ztráta heterozygozity 3p21 byla detekována ve 3/9 analyzovatelných případech. NGS bylo úspěšně provedeno v 9/11 případů. Pomocí NGS bylo identifikováno celkem 56 různých genetických alterací, což představuje v průměru 5 variant na tumor. U všech analyzovaných případů bez prokázané mutace v *ATRX* a *DAXX*. Nejčastěji odhalené mutované geny byly *CDH1* a *TET2* s třemi mutacemi ve 2 případech. Mutace v genech *AKT3, ROS1, PIK3R2, BCR* a *MYC* byly zastiženy ve 2 případech. Zbylých 41 studií detekovaných genových mutacích bylo zastiženo pouze individuálně v různých případech. Ve 4 případech zastižené mutace postihovaly geny asociované s angiogenezí.

Mutační profil primárních NET ledviny je vysoce variabilní, žádná z detekovaných mutací nemůže být považována za specifickou pro renální NET.

Histopathology

Histopathology 2019, **75**, 104–117. DOI: 10.1111/his.13856

Primary renal well-differentiated neuroendocrine tumour (carcinoid): next-generation sequencing study of 11 cases

Kristyna Pivovarcikova,[1] Abbas Agaimy,[2] Petr Martinek,[1] Reza Alaghehbandan,[3] Delia Perez-Montiel,[4] Isabel Alvarado-Cabrero,[5] Joanna Rogala,[6] Naoto Kuroda,[7] Boris Rychly,[8] Slavko Gasparov,[9] Kvetoslava Michalova,[1] Michal Michal,[1] Milan Hora,[10] Tomas Pitra,[10] Inna Tuckova,[11] Simon Laciok,[12] Jana Mareckova[1] & Ondrej Hes[1]

[1]*Department of Pathology, Faculty of Medicine in Plzen, Charles University in Prague, Pilsen, Czech Republic,* [2]*Department of Pathology, University of Erlangen, Erlangen, Germany,* [3]*Department of Pathology, Faculty of Medicine, University of British Columbia, Royal Columbian Hospital, Vancouver, British Columbia, Canada,* [4]*Department of Pathology, INCAN,* [5]*Department of Pathology, Centro Medico, Mexico City, Mexico,* [6]*Department of Pathology, Wojewódzki Szpital Specjalistyczny, Wroclaw, Poland,* [7]*Department of Diagnostic Pathology, Kochi Red Cross Hospital, Kochi, Japan,* [8]*Department of Pathology, Cytopathos, Bratislava, Slovakia,* [9]*Department of Pathology, School of Medicine, Zagreb, Croatia,* [10]*Department of Urology, Faculty of Medicine in Plzeň Charles University in Prague, Pilsen,* [11]*Department of Pathology, Central Military Hospital Prague, Prague, and* [12]*Department of Pathology, Regional Hospital Havirov, Havirov, Czech Republic*

Date of submission 20 December 2018
Accepted for publication 6 March 2019
Published online *Article Accepted* 9 March 2019

Pivovarcikova K, Agaimy A, Martinek P, Alaghehbandan R, Perez-Montiel D, Alvarado-Cabrero I, Rogala J, Kuroda N, Rychly B, Gasparov S, Michalova K, Michal M, Hora M, Pitra T, Tuckova I, Laciok S, Mareckova J & Hes O (2019) *Histopathology* **75**, 104–118. https://doi.org/10.1111/his.13856

Primary renal well-differentiated neuroendocrine tumour (carcinoid): next-generation sequencing study of 11 cases

Aims: Primary renal well-differentiated neuroendocrine tumour (NET) (hereafter referred to as renal NET) is rare, with ~100 cases having been reported in the literature. There are also limited data on the molecular–genetic background of primary renal NETs.

Methods and results: We analysed 11 renal NETs by using next-generation sequencing (NGS) to identify characteristic genetic aberrations. All tumours were positive for synaptophysin, and also expressed insulinoma-associated protein 1 (10/11), chromogranin-A (8/11), and CD56 (3/11). Cytoplasmic positivity of CD99 was present in eight of 11 cases, and strong nuclear expression of α-thalassaemia/mental retardation syndrome X-linked (ATRX) was retained in all 11 cases. Molecular–genetic analysis of aberration of *VHL* gave negative results in all cases. Loss of heterozygosity on chromosome 3p21 was found in three of nine analysable cases. NGS was successful in nine cases, showing a total of 56 variants being left after the updated filtering process, representing an average of five variants per sample. All analysable cases were negative for *ATRX* and *DAXX* (death-domain associated protein X) mutations. The most frequently mutated genes were *CDH1* and *TET2*, with three mutations in two cases. Mutations in *AKT3*, *ROS1*, *PIK3R2*, *BCR* and *MYC* were found in two cases. The remaining 41 genes were found to be mutated only in individual cases. In four cases, the mutations affected a subset of genes related to angiogenesis.

Conclusions: Overall, the mutation profile of primary renal NETs is variable, and none of the studied genes or affected pathways seems to be specific for renal NET.

Keywords: carcinoid, kidney, next-generation sequencing, primary, well-differentiated neuroendocrine tumour

Address for correspondence: O Hes, Department of Pathology, Charles University, Medical Faculty and Charles University Hospital Plzen, Alej Svobody 80, 304 60 Pilsen, Czech Republic. e-mail: hes@medima.cz

Introduction

Primary neuroendocrine neoplasms (NENs) of the kidney are tumours arising within the renal parenchyma that show neuroendocrine differentiation on the basis of morphology and immunohistochemistry. According to the current World Health Organization (WHO) classification of renal tumours, two major subtypes of primary renal NENs are well-differentiated neuroendocrine tumour (NET) (carcinoid and atypical carcinoid tumours) and poorly differentiated neuroendocrine carcinoma, which may be further subdivided into large-cell and small-cell variants.[1] These tumours recapitulate the characteristic appearance of NETs in other anatomical sites, in particular gastrointestinal (GI), pancreatic and pulmonary NENs.

Primary well-differentiated renal NET (hereafter referred to as renal NET) is rare, with ~100 cases reported in the literature, mainly as case reports or small series (the largest original study described 21 tumours).[2–45]

Only limited data are available on the molecular–genetic background of primary renal NETs, with loss of heterozygosity (LOH) on chromosome 3p21 (LOH 3p) the most frequently reported finding.[1,11,35] In this study, we analysed 11 primary renal NETs by next-generation sequencing (NGS) in a trial to identify their characteristic genetic aberrations.

Materials and methods

An institutional Ethics Review was obtained for the study. Nineteen cases of primary renal NET were retrieved from 26 000 renal neoplasms in the Plzen tumour registry (<0.1% of all registered renal tumours). All cases were reviewed by three pathologists (K.P., A.A., and O.H.). Clinical and follow-up data were collected by reviewing institutional medical records, and by contacting consulting pathologists and attending clinicians. Five cases were excluded because the quality of the material was too low for molecular–genetic analysis, and two other cases were excluded because of limited clinical information, specifically because we were not able to confirm that the tumour arose in the kidney. One more case was also excluded because it was not possible to determine whether the tumour was a primary renal tumour or a metastasis from the stomach.

Finally, 11 cases with available detailed clinical history and radiographic evaluation were selected and further analysed by the use of morphology, immunohistochemistry, *VHL* analysis, and NGS.

Tissues for light microscopy were fixed in 4% formaldehyde and embedded in paraffin by a routine procedure. Four-micrometre-thick sections were cut from the tissue blocks and stained with haematoxylin and eosin (H&E). There were 1–19 tissue blocks (median, 2) for each case, and all original H&E-stained slides were reviewed and evaluated. One representative block was selected for immunohistochemical and molecular–genetic studies. Tumour grading was performed by one of the authors (A.A.) after reviewing H&E-stained slides to identify the neuroendocrine pattern in each case and assessing the Ki67 labelling index. The latter was performed with an image-guided approach, in which the most proliferating hotspot area was identified and a high-power image subsequently printed in colour. Positively stained tumour nuclei were manually counted, in a total of 500 cells. The proliferation index was then calculated as a percentage, and a grade was assigned in accordance with the most recent WHO recommendation for well-differentiated NENs (NET grade 1, <3%; NET grade 2, 3–20%; and NET grade 3, >20%).[46]

IMMUNOHISTOCHEMISTRY

The immunohistochemical analysis was performed with a Ventana BenchMark ULTRA (Ventana Medical Systems, Tucson, AZ, USA). The following primary antibodies were used: anti-chromogranin (DAK-A3, monoclonal; Dako, Glostrup, Denmark; dilution 1:600), anti-synaptophysin (polyclonal; Thermo Fisher Scientific, Waltham, MA, USA; dilution 1:350), anti-CD56 (1B6, monoclonal; Novocastra, Newcastle upon Tyne, UK; dilution 1:400), anti-CD99 (H036-1.1, monoclonal; Thermo Fisher Scientific; dilution 1:50), anti-α-thalassaemia/mental retardation syndrome X-linked (ATRX) (polyclonal; Sigma-Aldrich, Darmstat, Germany; dilution 1:400), anti-insulinoma-associated protein 1 (INSM1) (monoclonal, sc-271408; Santa Cruz Biotechnology, Dallas, TX, USA; dilution 1:1000), anti-succinate dehydrogenase B subunit (SDHB) (polyclonal; Sigma Aldrich, St Louis, MO, USA; dilution 1:50), anti-S100 (polyclonal; Ventana; RTU), anti-PAX8 (polyclonal; Cell Marque, Rocklin, CA, USA; dilution 1:25), anti-melanosome (HMB45, monoclonal; DakoCytomation, Glostrup, Denmark, dilution 1:200), and anti-Ki67 (MIB1, monoclonal; Dako; dilution 1:1000). Appropriate positive and negative controls were used.

MOLECULAR–GENETIC STUDY

VHL analysis

Mutation analysis of *VHL* was performed with Sanger sequencing and hypermethylation of the *VHL* promoter was detected with bisulfite conversion.

Methylation statusand LOH 3p was detected by short tandem repeats fragmentation analysis as described previously.[47]

Targeted NGS

An NGS panel of 271 cancer-related genes (Comprehensive Cancer Panel; Qiagen, Hilden, Germany) was used to analyse 11 tumour and normal tissue sample pairs (including a group of angiogenesis-related genes): *CTNNB1*, *ERBB2*, *FGFR2*, *FLT4*, *GATA2*, *GREM1*, *HOXB13*, *KDR*, *NF1*, *NOTCH1*, *PIK3CA*, *PLCG1*, *PTEN*, *RUNX1*, *TNFAIP3*, and *VHL*. The samples were isolated by macrodissection from formalin-fixed paraffin-embedded blocks. DNA was isolated with the Qiagen DNA mini-kit, and 250 ng of DNA was used to construct the library. QIAseq technology with molecular barcodes allowed for more specific allele frequency determination as well as PCR error reduction. Technical duplicates and positive controls were used to ensure quality control of the analysis parameters. The library was sequenced on Illumina's Nextseq 500, aiming at an average coverage of $\times 600$ to detect an allele frequency of 10% with 95% sensitivity (Illumina, San Diego, CA, USA). Variants were called with Qiagen's proprietary pipeline, and subsequently filtered for a 10% allele frequency and a minimal coverage of $\times 100$ after deduplication of molecular barcodes. Variants with a frequency of >1% in the GnomAD database were excluded, as were known benign variants according to the ClinVar database.[48] Variants found in both tumour and non-tumour tissues were excluded. The remaining subset was visualised and checked for the possibility of being artefacts (homopolymer or otherwise difficult PCR regions). The COSMIC annotations were checked for its cancer relevance.[49] Detailed base-to-base coverage analysis and manual visualisation with Integrative Genomics Viewer[50] were performed to ensure that the entire coding regions of *ATRX* and *DAXX* (death-domain associated protein X) were thoroughly analysed.

Results

Basic clinicopathological data are summarised in Table 1. The patients were four males and seven females, ranging in age from 38 to 87 years (mean, 58 years; median, 56 years). Information on tumour size was available for all 11 cases, and showed a mean size of 81 mm in greatest diameter (range, 30–195 mm; median, 79 mm).

The majority of patients showed no additional masses clinically or radiographically. Four patients had distant metastases at the time of diagnosis or shortly after surgery, but these metastases were much smaller than the primary renal tumour and were multiple in nature. In this context, the clinical status and medical history were consistent with the diagnosis of a primary renal NET.

Follow-up data were available for nine of 11 patients, ranging from 1 to 108 months (mean follow-up, 36 months; median, 12 months). Three patients died of disease 1 month to 1 year after resection. Two patients were alive but with progression of the disease (lymph node metastasis). Metastatic spread was documented in lymph nodes (2/10), liver (3/10), and bones (3/10). Only four patients were alive and disease-free at last follow-up.

The gross findings are summarised in Table 1. The tumours were predominantly located in the interpolar area of the kidney (6/11) and were mostly well demarcated, with no definitive capsule; however, in one case a thick whitish pseudocapsule had partially developed (Figure 1A). Invasion of the renal pelvis was noted in two cases. No grossly identifiable necrosis or haemorrhage was reported. No case was associated with a horseshoe kidney or with other tumours. No association with syndromic disease was documented.

Microscopically, the tumours showed a prominent organoid neuroendocrine growth pattern (Figure 1B), with ribbons, trabecular or solid–insular cell arrangements, and occasional palisading. More than one growth pattern, at least focally, was also noted. Spindling was seen in two cases (one focally and one diffusely, closely reminiscent of pulmonary spindle cell carcinoids) (Figure 1C). The tumours were composed of uniform cells with round to oval nuclei, with finely granular and dispersed chromatin and inconspicuous nucleoli. The cytoplasm was pale eosinophilic to amphophilic (Figure 1D). Neither calcification nor necrosis was detected in any case. In the two cases with infiltration of the renal pelvis, no urothelial dysplasia, urothelial carcinoma *in situ* or invasive urothelial carcinoma was documented. No structures resembling paraganglioma, particularly 'Zellballen', were identified. Mitotic figures were rare, ranging from 1 to 2 per 10 high-power fields. No atypical mitoses were noted. On the basis of the Ki67 grading of NETs in the GI and pancreatic systems, nine tumours were graded as grade 1, one case grade 2 and one case grade 3.

Immunohistochemical evaluation confirmed a neuroendocrine nature in all 11 cases (Table 2). Synaptophysin staining was diffusely positive in all 11 cases (seven of 11, strong and diffuse; four of 11, moderate) (Figure 2A). INSM-1 staining was strong

Table 1. Clinicopathological features

Case	Sex	Age (years)	Side	Size (greatest dimension) (mm)	Gross findings	Stage (UICC 2017)	Follow-up (months)	Current status	NET grade
Case 1	F	55	L	70	Central part of kidney, renal pelvis involvement	pT1b	55	ANED	G1
Case 2	F	66	R	30	Well-demarcated white tumour, limited to the kidney, subcapsular location	pT1a	108	ANED	G1
Case 3	M	55	NA	90+ smaller satellite nodules up to 14	Central part of the kidney with several smaller satellite nodules	pT2a	96	AWD (metastases in the retroperitoneal lymph node)	G1
Case 4	M	38	R	80	NA	NA	LFU	NA	G1
Case 5	F	63	R	60	Infiltration of renal sinus	pT3a	LFU	NA	G1
Case 6	F	87	L	80	Thin pseudocapsule, limited to the kidney	pT2a	24	ANED	G3
Case 7	F	44	L	79	Well-demarcated, soft brown tumour	pT2a	12	ANED	G1
Case 8	F	68	R	65	Nodular, haemorrhagic mass with soft consistency, infiltration of renal sinus and pelvis	pT3a	4	AWD (metastases in the para-aortal lymph nodes)	G1
Case 9	M	44	L	195	Infiltration of renal sinus	pT3a	1	DOD (metastases to bones and liver)	G2
Case 10	F	56	R	100	Without sinus or renal pelvis involvement	pT2a	12	DOD (metastases to bones and liver)	G1
Case 11	M	62	R	40	Infiltration of renal sinus	pT3a	12	DOD (metastases to bones and liver)	G1

ANED, Alive with no evidence of disease; AWD, Alive with disease; DOD, Dead of disease; L, Left; F, Female; LFU, Lost to follow-up; M, Male; NA, Not available; NET, Neuroendocrine tumour; R, Right; UICC, International Union Against Cancer.

and diffuse in nine of 11 cases (Figure 2B), moderate and focal in one case, and one case was completely negative for INSM-1. Chromogranin-A positivity was confirmed in eight of 11 cases (Figure 2C), however positivity was focalin six of 11 cases. CD56 showed weak to moderate positivity in three cases. Cytoplasmic positivity of CD99 was detected in eight of 11 cases; it was diffuse and weak to moderate in four cases, focal and weak in two cases, and focal and strong in two cases. Strong nuclear expression of ATRX was detected in all 11 cases (Figure 2D).

The results of molecular–genetic analysis are summarised in Tables 3 and 4. Analysis of aberration of *VHL* gave negative results in all cases. LOH 3p was found in three of nine analysable cases.

Next-generation sequencing was successfully performed in nine of 11 cases. A total of 56 variants were left after the updated filtering process, representing an average of five variants per sample. All analysable cases were negative for mutation of *ATRX* (6/11) and *DAXX* (9/11). The filtering process eliminated some of the most frequent variants in our set, which have been determined to be non-pathogenic (some of *NF1*, *FLT4*, and several other variants). Overall, the clinical significance varied from pathogenic (*RIT1*), across probably pathogenic (*MED12*), to conflicting interpretations of pathogenicity (*RET*, *MET*, *BCOR*, *CTNNB1*, *HNF1A*, *PALB2*, and others). The clinical significance of the most commonly detected variants was not clear. The most frequently

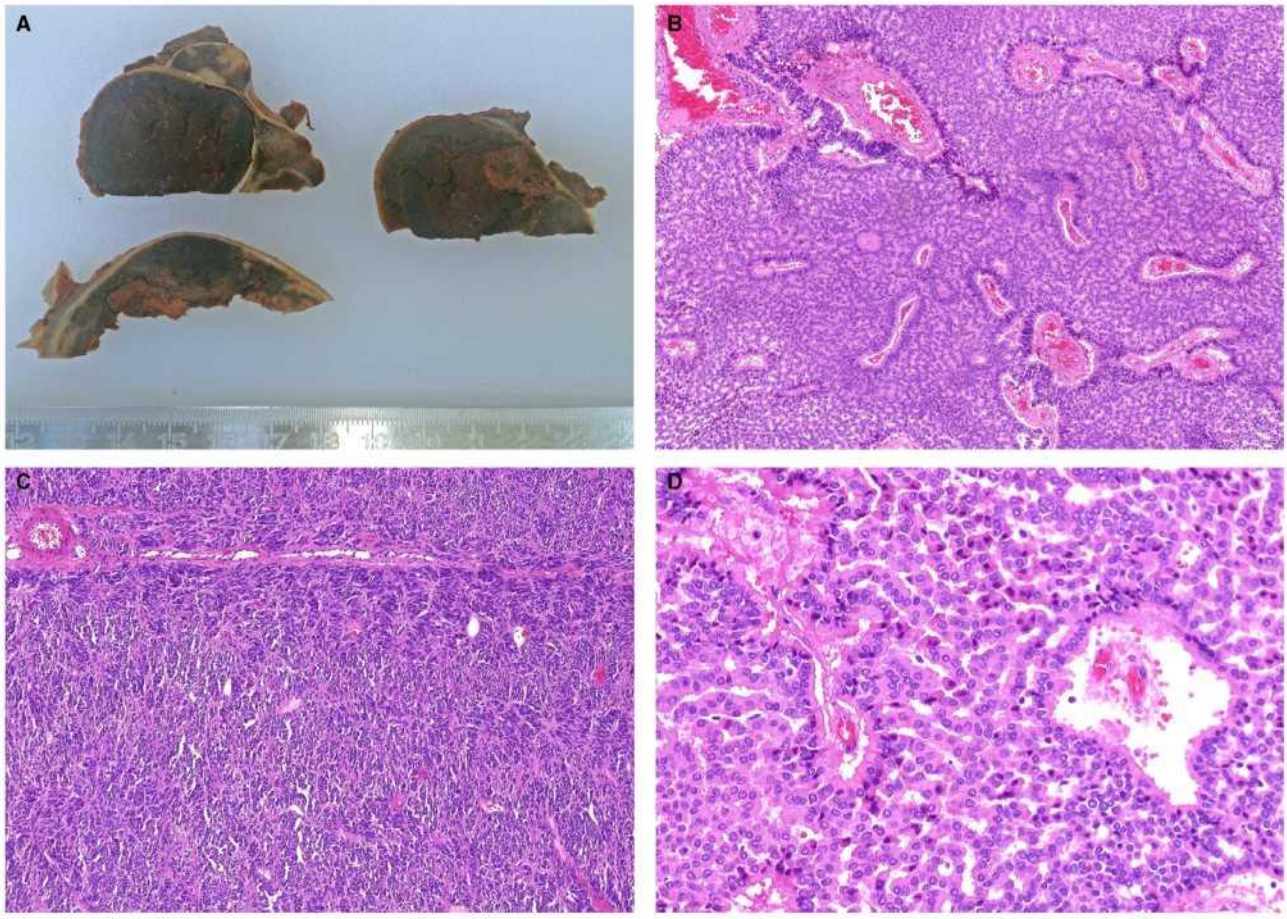

Figure 1. A, The tumours were mostly well demarcated, with no definitive capsule; however, in one case, a thick whitish pseudocapsule had partially developed. B, Renal neuroendocrine tumour with typical morphology, a palisading pattern, and low-grade cytological features. C, Only rarely was tumour composed of spindle cell elements organised mainly in ribbons. D, The tumours were mostly composed of uniform cells with round to oval nuclei. The cytoplasm was pale eosinophilic to amphophilic.

mutated genes were *CDH1* and *TET2*, with three mutations in two cases. Mutations in *AKT3*, *ROS1*, *PIK3R2*, *BCR* and *MYC* were found in two cases.

The remaining 41 genes were found to be mutated only in individual cases. There were four positive cases associated with genes related to angiogenesis. The mutated genes were *NF1*, *CTNNB1*, *GATA2*, and *NOTCH1*; each variant was in a different case. Two of the angiogenesis-related variants in *GATA2* and *CTNNB1* belonged to cases with documented aggressive behaviour (cases 3 and 11, respectively).

Discussion

Primary renal carcinoid tumour was first reported by Resnick *et al.* in 1966.[2] Since then, <100 cases have been published either as case reports or as small case series.[2–45]

Interesting coincidences were reported in renal NETs. According to a review study by Romero *et al.*, up to 26.8% of published cases were associated with another renal pathology.[26] In particular, renal NETs were often associated with developmental disorders, especially horseshoe kidney.[29] In fact, the rate of renal NETs arising in horseshoe kidney is proposed to be as high as 15–17.8%.[14,26] The isthmic part of horseshoe kidney is usually involved.[26] One case was described in a patient with autosomal dominant polycystic kidney disease.[20] Associations between renal NETs and other renal malignancies have rarely been described as case reports (i.e. clear cell papillary renal cell carcinoma[40] and chromophobe renal cell carcinoma[34]). However, renal NETs are frequently reported to develop in association with renal teratomas.[27] The concurrent finding of renal NET and a mature cystic teratoma has been reported in 10 previously published cases in the literature,[41] and the rate of coincidence of these two tumours is proposed to be as high as 14.3% of all cases.[26] Interestingly,

Table 2. Results of immunohistochemical examination

Case	Synaptophysin	Chromogramin	CD56	CD99	INSM1	ATRX	SDHB	PAX8	S100	HMB45
Case 1	+++	Foc. +++	–	Foc. +	+++	+++	+++	–	–	–
Case 2	+++	Foc. +	++	+	+++	+++	++	–	–	–
Case 3	+++	+	–	–	+++	+++	+++	–	Foc. +	–
Case 4	+++	+++	+	–	+++	+++	++	–	–	–
Case 5	++	Foc. +++ (SCs)	–	Foc. +	+++	+++	++	–	–	–
Case 6	++	–	–	Foc. +++	+++	+++	+++	–	Foc +	–
Case 7	+++	Foc. ++	–	+	+++	+++	++	–	–	–
Case 8	+++	Foc. +++	–	–	–	+++	++	–	–	–
Case 9	Dif. ++Foc. +++	–	Dif. +Foc. ++	++	Foc. ++	+++	+++	–	–	–
Case 10	+++	–	–	Dif. +Foc. +++	+++	+++	++	–	–	–
Case 11	++	Foc. +++ (SC)	–	++	+++	+++	+++	–	–	–

ATRX, α-thalassaemia/mental retardation syndrome X-linked; Dif. Diffusely; Foc., Focally (up to 50%); INSM1, Insulinoma-associated protein 1; SC, Single cell; –, Negative; +, Weakly positive; ++, Moderately positive; +++, Strongly positive.

the occurrence of concurrent horseshoe kidney, renal NET and teratoma in the same patient was documented in six of these 10 published cases[5,15,19,37]; two mature teratomas even underwent malignant transformation into adenocarcinoma.[27,41] We were not able to corroborate any similar associations with the above conditions in our cases. All cases described in this study arose from normal kidney; no other neoplasms were documented.

The histogenesis of NETs in the kidney is uncertain, as neuroendocrine cells are not found in normal renal parenchyma.[51] Several histogenetic theories have been proposed to explain the origin of primary renal NETs. The absence of PAX2 and PAX8 staining in well-differentiated NETs of the kidney[33] supports the theory that these tumours are derived from non-renal elements.[3]

Renal NET is a neoplasm with no gender predilection, and occurs over a wide age range, with the majority presenting in the fourth to seventh decades. The basic clinical symptoms are related to the mass effect, including abdominal or flank pain, but other symptoms are also known (i.e. haematuria, constipation, fever, and weight loss).[26] Renal NET presents as an incidental finding in more than one-quarter of the patients[26] and it was present in 80% of cases in the study of Aung *et al.*[35] Carcinoid syndrome is a rare clinical presentation described in <5% of patients.[38] None of our cases was associated with carcinoid syndrome. Tumours often present in a higher stage at diagnosis, frequently with metastatic involvement at the time of diagnosis or with metastatic spread early after surgery (in more than half of cases).[28,33] It is extremely important to exclude the metastatic origin of the renal lesion before considering the tumour as a primary renal NEN.

Renal NETs have the histological appearance of NETs in other anatomical sites, in particular pancreatic and, to some degree, pulmonary NETs. They show a predominantly trabecular or ribbon-like arrangement admixed with solid nests with peripheral palisading. The neoplastic cells have round or oval nuclei with granular and finely dispersed chromatin ('salt and pepper-like' pattern) and inconspicuous nucleoli.[26] Calcification may be present (from small psammomatous calcification to large calcified regions); haemorrhage and necrosis are infrequent.[28] These tumours are positive for synaptophysin (the most commonly positive marker), chromogranin-A,[28,33] CD99,[33] and CD56,[44] but negative for thyroid transcription factor 1, Wilms tumour 1,[28,33] PAX2 and PAX8, CDX2,[33] antiRCC, and CD10.[44] Ultrastructurally, renal NET contains numerous membrane-bound cytoplasmic neuroendocrine granules,[44] and many tumour cells have rounded perinuclear conglomerates of condensed intermediate filaments.[9] In this study, we used classic neuroendocrine immunohistochemical markers such as chromogranin A, synaptophysin, and CD56, as well as a novel marker, INSM1, to support the morphological

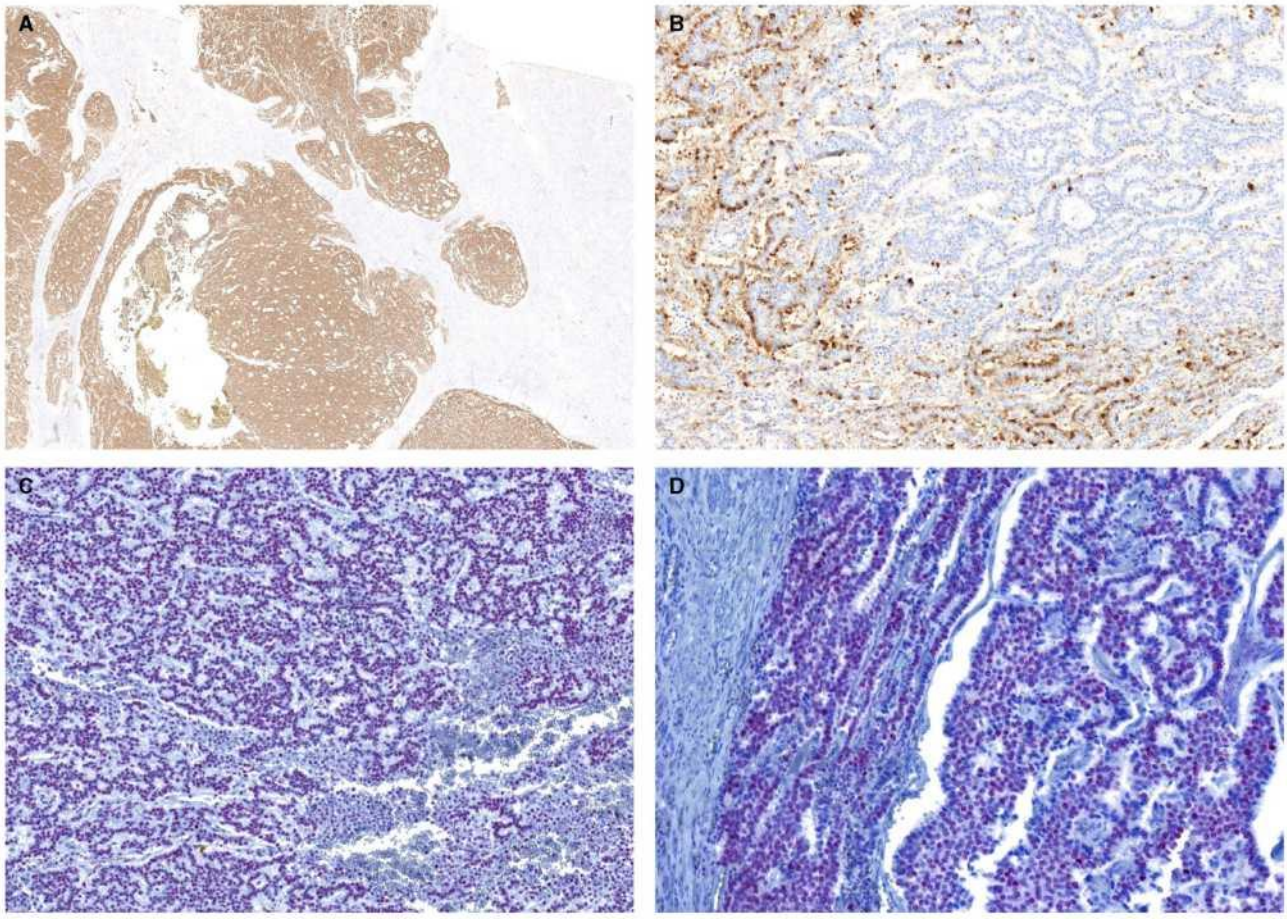

Figure 2. **A**, Synaptophysin was diffusely positive in all cases; however, the intensity of staining was variable. **B**, Insulinoma-associated 1 (INSM1) positivity was strong and diffuse in all but one case. **C**, Chromogranin A was positive in eight cases to a variable extent (ranging from focal to diffuse positivity). **D**, Strong nuclear expression of α-thalassaemia/mental retardation syndrome X-linked (ATRX) was detected in all cases.

diagnosis of NET and to confirm the neuroendocrine nature of the lesions in our registry. INSM1 is a transcription factor that plays a pivotal role in neuroendocrine differentiation, and it has been proposed as a promising immunohistochemical marker of NENs.[52]

Renal NETs may follow an aggressive clinical course.[9] However, it seems that the disease usually has a prolonged clinical course despite widespread metastatic dissemination.[28] Furthermore, published data suggest a better prognosis for primary renal NETs arising in horseshoe kidney than for those arising in normal kidneys.[21] In this series, the majority of renal NETs were grade 1. It is striking that most of the cases had a very low proliferation index rate (<1% in five cases). On the basis of the Ki67 grading of NETs in the GI and pancreatic systems, nine tumours were grade 1, one case grade 2 and one case grade 3. It should be noted that the prognostic relevance of grading and the best Ki67 rate cut-off to use for renal NET remains to be defined in future larger series.

There are data suggesting that the loss of ATRX/DAXX expression is associated with an aggressive phenotype in pancreatic NETs.[53] However, no definitive data on ATRX as a prognostic marker for NET have been provided to date. All cases in our series had retained ATRX expression, including cases with apparently aggressive behaviour and cases with a non-aggressive clinical course.

The majority of cases in our study were located in the central part of the kidney, which localisation raised the question of whether NETs originated within the urothelium or within the renal parenchyma. We were not able to identify any dysplasia, carcinoma *in situ* or urothelial carcinoma in the renal pelvis or calyces. Furthermore, no record of urothelial

Table 3. Overview of molecular and genetic findings

Case	*VHLM*	LOH 3p	*VHL* sequencing	NGS number of variants	*ATRX*	*ATRX* LOD (%)	*DAXX*	*DAXX* LOD (%)
Case 1	Negative	Negative	Negative	1	Negative	17	Negative	7
Case 2	Negative	Negative	Negative	5	Negative	7	Negative	7
Case 3	Negative	NA	Negative	8	NA	NA	NA	NA
Case 4	Negative	Positive	Negative	3	Negative	11	Negative	3
Case 5	Negative	Negative	Negative	8	Negative	14	Negative	8
Case 6	Negative	NA	Negative	6	NA	NA	Negative	4
Case 7	Negative	NA	Negative	4	NA	NA	NA	NA
Case 8	Negative	Positive	Negative	6	Negative	3	Negative	1
Case 9	Negative	Negative	Negative	NA	NA	NA	Negative	5
Case 10	Negative	Positive	Negative	NA	NA	NA	Negative	8
Case 11	Negative	Negative	Negative	15	Negative	5	Negative	3

ATRX, α-thalassaemia/mental retardation syndrome X-linked; DAXX, Death-domain associated protein X; LOD, Limit of detection; LOH 3p, Loss of heterozygosity on chromosome 3p21; NA, Not analysable; NGS, Next-generation sequencing; *VHLM*, Hypermethylation status of *VHL*.

carcinoma associated with our cases was found in the medical records.

The differential diagnosis of renal NETs includes large-cell neuroendocrine carcinoma, Ewing sarcoma/primitive neuroectodermal tumour, t6;11 transcription factor EB translocation renal cell carcinoma, and metastasis from extrarenal origins. The key differential diagnostic features are summarised in Table 5. In our series, the majority of patients had only renal tumour at the time of diagnosis; however, in two cases, metastatic spread was found 1 and 2 months after surgery, respectively.

There is limited information on the molecular–genetic background of renal NETs. The genetic features of renal NETs have rarely been studied, perhaps because of the rarity of such tumours and the limited availability of suitable material.[11,12,28,32,35] Aung *et al.* described one of the largest studies to date dealing with the genetic profile of renal NETs.[35] They studied 11 cases of well-differentiated NET of the kidney, three of which were analysed for molecular alterations: LOH 3p was confirmed in two of three cases.[35] el-Naggar *et al.* made similar findings in their analysed case.[11] Kuroda *et al.* reported monosomy of chromosome 3 in three of four cases, monosomy of chromosome 13 in one of four cases, and LOH 3p in one of two cases, and detected *VHL* mutation in two cases.[32] van den Berg *et al.* analysed one case of well-differentiated NET in a horseshoe kidney, and showed karyotype 47,XX,+13[8]/46,XX,t(13;14)(q31;q11.2)[5]/46,XX[2].[12] In our study, we found LOH 3p in three of nine analysable cases. Mutation analyses of *VHL* and the hypermethylation status of the *VHL* promoter gave negative results in all cases.

We used an NGS panel of 271 cancer-related genes, including a group of angiogenesis-related genes, in our study. The most frequently mutated genes were *CDH1* and *TET2*, with three mutations in two cases. *CDH1* encodes cadherin cell-adhesion protein, which is correlated with gastric, breast, colorectal, thyroid and ovarian cancers. Loss of function resulting from mutation of this gene is thought to contribute to cancer progression by increasing proliferation, invasion, and/or metastasis. Loss-of-function mutation of *TET2* is found in a variety of haematooncological diseases as a risk factor that is activated by a second hit. Mutations in *AKT3*, *ROS1*, *PIK3R2*, *BCR* and *MYC* were found in two cases. The products of *AKT3*, *CDH1* and *PIK3R2* form part of the phosphoinositide 3-kinase (PI3K)–AKT–mammalian target of rapamycin (mTOR) signalling pathway, which controls many cell processes including proliferation, growth, and survival, and is one of the most frequently dysregulated pathways in human cancers. It is associated with tumour progression and resistance to cancer therapies.[54,55] *AKT3* is a member of the AKT family, and encodes a serine threonine kinase, which regulates many processes, including

Table 4. List of variants detected with next-generation sequencing

Case	Variant frequency	Gene symbol	HGVSp variant description	dbSNP ID	Clinical significance
Case 1	0.11	*AKT3*	NP_005456.1:p.Ser210Ala	–	–
Case 2	0.46	*PDGFRB*	NP_002600.1:p.Gln222His	COSM5695183	–
	0.45	*HGF*	NP_000592.3:p.Ser228Ala	rs139457161	Uncertain significance
	0.49	*ABL1*	NP_009297.2:p.Ser991Leu	rs2229067	Not provided
	0.12	*CREBBP*	NP_004371.2:p.Pro1947Leu	–	–
	0.54	*ZNF217*	NP_006517.1:p.Glu349Lys	rs141467941	–
Case 3	0.27	*ALK*	NP_004295.2:p.Trp614Ter	–	–
	0.14	*GATA2*	NP_001139133.1:p.Met221Ile	–	–
	0.50	*PDGFRA*	NP_001334757.1:p.Leu834Ser	–	–
	0.11	*CTNNA1*	NP_001310911.1:p.Ala850Thr	–	–
	0.13	*EGFR*	NP_005219.2:p.Gln163Ter	–	–
	0.27	*PAX5*	NP_057953.1:p.Gly273Glu	–	–
	0.14	*RAD51*	NP_597994.3:p.Ser99Pro	–	–
	0.11	*DOT1L*	NP_115871.1:p.Pro472Ser	–	–
Case 4	0.52	*IDH1*	NP_001269316.1:p.Val303Ala	–	–
	0.49	*PIK3R2*	NP_005018.1:p.Ala727Thr	rs149081991	–
	0.40	*EP300*	NP_001420.2:p.Asn2209_Gln2213delinsLys	rs587778256	Conflicting interpretations
	0.51	*TET2*	NP_001120680.1:p.Leu34Phe	rs111948941	Not provided
	0.60	*TET2*	NP_001120680.1:p.His1778Arg	rs62621450	Not provided
Case 5	0.43	*MTOR*	NP_004949.1:p.Met1083Val	rs56164650	–
	0.46	*MCL1*	NP_068779.1:p.Ala227Val	rs11580946	–
	0.54	*ROS1*	NP_002935.2:p.Ile537Met	rs28639589	–
	0.47	*RET*	NP_066124.1:p.Tyr791Phe	rs141467941	Conflicting interpretations
	0.42	*BIRC3*	NP_001156.1:p.Arg401Lys	rs17881197	–
	0.66	*PALB2*	NP_078951.2:p.Leu337Ser	rs45494092	Conflicting interpretations
	0.12	*NF1*	NP_001035957.1:p.Thr467Ile	COSM1666611	–
	0.46	*PIK3R2*	NP_005018.1:p.Ala727Thr	rs149081991	–
Case 6	0.13	*AKT3*	NP_005456.1:p.His139Tyr	COSM6062426	–
	0.43	*LRP1B*	NP_061027.2:p.Thr4298Ser	rs139037100	–
	0.13	*SF3B1*	NP_036565.2:p.Gly179Glu	–	–
	0.43	*ERBB4*	NP_005226.1:p.Gly879Arg	COSM2716044	–
	0.11	*CDH1*	NP_004351.1:p.Gly134Glu	–	–
	0.46	*CDH1*	NP_004351.1:p.Ala592Thr	rs35187787	Conflicting interpretations

Table 4. *(Continued)*

Case	Variant frequency	Gene symbol	HGVSp variant description	dbSNP ID	Clinical significance
Case 7	0.67	*CDK6*	NP_001138778.1:p.Asp110Asn	rs35654944	Uncertain significance
	0.30	*NOTCH1*	NP_060087.3:p.Asp452Glu	–	–
	0.38	*BCR*	NP_004318.3:p.Asp752Glu	rs12484731	–
	0.40	*BCR*	NP_004318.3:p.Tyr910Cys	rs35537221	–
Case 8	0.53	*GEN1*	NP_001123481.2:p.Lys882Glu	rs77424145	–
	0.48	*MYC*	NP_002458.2:p.Asn26Ser	rs4645959	–
	0.48	*KMT2A*	NP_001184033.1:p.Glu502Lys	rs9332772	Uncertain significance
	0.30	*IKZF3*	NP_036613.2:p.Gly234Ala	rs112301322	–
	0.51	*TCF3*	NP_003191.1:p.Lys101Arg	rs41275842	–
	0.49	*CRLF2*	NP_071431.2:p.Val244Met	COSM5019349	Not provided
Case 9	Not analysable				
Case 10	Not analysable				
Case 11	0.31	*RIT1*	NP_001243750.1:p.Phe99Cys	rs868208063	Pathogenic
	0.43	*DDR2*	NP_001014796.1:p.Met441Ile	rs34722354	–
	0.14	*CTNNB1*	NP_001091679.1:p.Thr41Ala	rs121913412	Conflicting interpretations, other
	0.58	*EPHA3*	NP_005224.2:p.Ala550Ser	–	–
	0.45	*TET2*	NP_001120680.1:p.Gly355Asp	rs61744960	Not provided
	0.52	*PRDM1*	NP_001189.2:p.Ser354Asn	rs143040512	Not provided
	0.53	*ROS1*	NP_002935.2:p.Ile537Met	rs28639589	–
	0.40	*MYC*	NP_002458.2:p.Asn26Ser	rs4645959	–
	0.20	*CDKN2B*	NP_004927.2:p.Ala129Pro	–	–
	0.14	*ARID2*	NP_689854.2:p.Lys1813Glu	–	–
	0.56	*FLT3*	NP_004110.2:p.Asp324Asn	rs35602083	Not provided
	0.21	*CDH1*	NP_004351.1:p.Leu564Ter	–	–
	0.14	*AXIN2*	NP_004646.3:p.Thr673Pro	–	–
	0.11	*SOX9*	NP_000337.1:p.Thr239Pro	–	–
	0.33	*MED12*	NP_005111.2:p.Gly44Ser	rs199469669	Other

proliferation and cell survival through serine and/or threonine phosphorylation of a range of downstream substrates.[56,57] *ROS1* encodes a proto-oncogene tyrosine kinase receptor that activates downstream signalling pathways related to cell differentiation and proliferation, including the PI3K–AKT–mTOR pathway. *PIK3R2* (phosphatidylinositol 3-kinase regulatory subunit) encodes a part of the PI3K heterodimer (the other part being encoded by *PIK3CA*). Membrane phospholipid phosphatidylinositol (3,4,5)-trisphosphate, which is a product of phosphorylation by PI3K, activates AKT, which triggers downstream activation of the mTOR complex. The most direct known and predicted interactions of all genes mutated more than once in our group and their closest neighbours are visualised in Figure 3 (according to the String

Table 5. Differential diagnostic features of renal neuroendocrine tumour

	Histology	IHC	Genetics	Note
NET	Trabecular, sheet-like or nested pattern, uniform cells with inconspicuous nucleoli	Synaptophysin, chromogranin, CD56, INSM1, CD99, keratins, S100-negative (sustentacular cells rarely present)	No definitive genetic landmark	Mutation of *ATRX/DAXX* in pancreatic NETs
HGNC	Trabecular, sheet-like or nested pattern. Large cells with prominent nuclei, brisk mitotic activity, and necrosis	Synaptophysin, chromogranin, CD56, INSM1, CD99, keratins	No definitive genetic landmark	
PNET	Solid sheets of primitive small uniform cells, and irregular nests with fibrovascular septa	CD99, FLI1, ERG, NKX2.2, PAX7, synaptophysin	*EWSR1–FLI1EWSR1–ERGEWSR1–FEVEWSR1–ETV1EWSR1–E1AFEWSR1–ZSGFUS–ERGEWSR1–ERGEWSR1–ETV4EWSR1–POU5F1EWSR1–PATZ1EWSR1–SP3EWSR1–NFATC2FUS–FEV*	
TFEB RCC	Usually solid nested pattern with pseudorosettes, and dual cell populations	Melan A, HMB45, TFEB	Translocation of *TFEB*	
Paraganglioma	Nests of polygonal cells ('Zellballen'), and a delicate capillary network	Chromogranin, synaptophysin, S100 (weak in chromaffin cells; strong in sustentacular cells), GATA3, catecholamine-synthesising enzymes (also positive in a proportion of NETs), SDHB†	*SDH* mutations†	Keratins negative (rarely positive, mostly in spinal paragangliomas and duodenal gangliocytic paraganglioma)
MS	Similar to renal tumours; usually a diagnosis of exclusion			

ATRX, α-thalassaemia/mental retardation syndrome X-linked; DAXX, Death-domain associated protein X; HGNC, High-grade neuroendocrine carcinoma; IHC, Immunohistochemistry; INSM1, Insulinoma-associated protein 1; MS, Metastasis; PNET, Primitive neuroectodermal tumour; SHDB, Succinate dehydrogenase B subunit; TFEB RCC, Transcription factor EB translocation renal cell carcinoma.
*In SDH-deficient cases.

database).[58] Some cases had single mutations in genes whose products are also involved in the PI3K–AKT–mTOR pathway (*MTOR*), are directly regulated by it (*MYC*),[59] or indirectly interact with it (*CTNNB1* and *ABL1*). Regarding the subset of genes related to angiogenesis, there were four positive cases that showed the following mutated genes: *NF1*, *CTNNB1*, *GATA2*, and *NOTCH1* (each variant was in a different case). Identification of a germline or somatic *NF1* aberration can be challenging, as *NF1* is one of the largest human genes,[60] and a wide spectrum of mutation types was observed in *NF1*. Furthermore, many highly homologous *NF1* pseudogene sequences are scattered throughout the human genome, and can often interfere with PCR-based diagnostic tests (despite the absence of any obvious mutational hotspots or recurrent mutations).[61] With this knowledge, most of the alterations of *NF1* were eliminated as non-pathogenic after an updated manual filtering process by the use of available databases and the literature.[48,49,62]

Unfortunately, on the basis of our results and the findings of other investigators, there is not a distinct molecular genetic marker that can be used as a prognosticator for predicting the behaviour of such tumours.

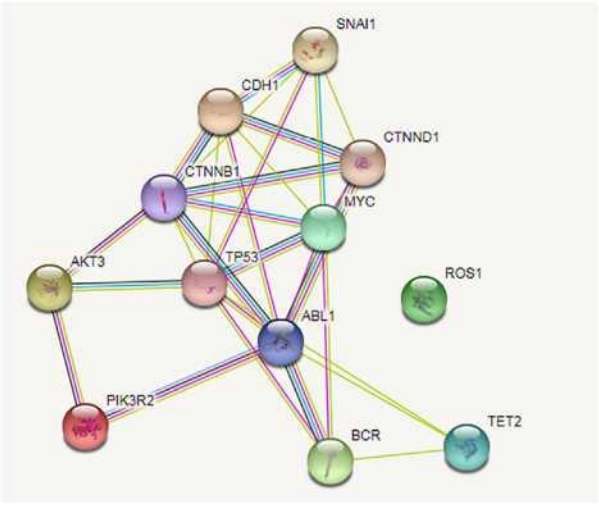

Figure 3. Schematic representation of interactions between genes found to be mutated more than once in our group. The line colours represent known interactions (magenta—experimentally determined; cyan—from curated databases) and predicted interactions (green—gene neighbourhood; light green—from text mining; grey—coexpression; violet—protein homology).

Neuroendocrine tumours constitute a heterogeneous group of neoplasms with several anatomical sites of origin (central nervous system, respiratory tract, larynx, GI tract, thyroid, skin, breast, and urogenital system).[63] The nomenclature varies significantly according to the organ of origin.[64] NETs are sporadic in the majority of cases, but may be associated with hereditary syndromes (i.e. multiple endocrine neoplasia types 1 and type 2, von Hippel–Lindau syndrome, neurofibromatosis type 1, tuberous sclerosis, Carney complex, hyperparathyroidism–jaw tumour syndrome, and hereditary small-intestine NET).[65,66]

Whole genome sequencing approaches have underlined the very low mutation rate of well-differentiated NET of all organs as compared with other malignancies.[66] Molecular alterations have been among the most studied in pancreatic NETs (PanNETs). Several novel germline mutations were described recently. Furthermore, recurring features have been reported, such as inactivation of *MEN1*, *VHL*, and *TSC1/2*, hyperactivation of the PI3K–mTOR pathway and inactivation of *ATRX/DAXX* in a proportion of PanNET cases.[67,68] Another group of NETs studied with molecular–genetic techniques were lung carcinoids (typical carcinoid and atypical carcinoid), which often have alterations in the chromatin-remodelling genes *MEN1*, *PSIP1*, and *ARID1A*.[69] On the other hand, lung neuroendocrine carcinomas frequently have inactivating mutations in *TP53* and *RB1*, amplification of *MYC* family members, and genetic alterations in the PI3K–AKT–mTOR signalling pathway.[70]

This study had a number of limitations, including a relatively low number of cases examined with molecular–genetic testing, despite the fact that this was one of the largest series of renal NETs in the literature. Additionally, it was both crucial and challenging to precisely determine the origin of renal NETs by using available clinical data. The other challenge that we faced in this study was to ensure that no urothelial dysplasia or malignancy was associated with the tumours, given that most of them were located in the central portion of the kidney.

Conclusions

Overall, the mutation profile in renal NETs is variable, and none of the studied genes or affected pathways seems to be specific for renal NETs.

The most frequently observed genetic changes in renal NETs were mutations in *CDH1* and *TET2*, followed by LOH 3p and mutations in *AKT3*, *ROS1*, *PIK3R2*, *BCR*, and *MYC*. Some of the more frequently mutated genes point to the PI3K–AKT signalling pathway.

Acknowledgements

This study was supported by the Charles University Research Fund (project number Q39) and project FN 00669806. Informed, written consent was not required according to the Local Ethics Committee. Studies were performed according to the Declaration of Helsinki. The procedures were approved by the Local Ethics Committee (EK LF and FN Plzen, Charles University, 02.03.2015).

Conflicts of interest

All authors declare no conflicts of interest.

Author contributions

K. Pivovarcikova: case selection, immunohistochemistry control, results evaluation, and writing of manuscript. A. Agaimy: case evaluation, grading, and discussion. P. Martinek: genetic analyses. R. Alaghehbandan: study design and discussion. D. Perez-Montiel: contribution with a case (including clinicopathologic data). J. Rogala: contribution with a

case (including clinicopathologic data). N. Kuroda: contribution with a case (including clinicopathologic data). B. Rychly: contribution with a case (including clinicopathologic data). S. Gasparov: contribution with a case (including clinicopathologic data). K. Michalova: case selection, and immunohistochemistry control. M. Michal: study design. M. Hora: clinical information. T. Pitra: clinical information. I. Tuckova: contribution with a case (including clinicopathologic data). S. Laciok: contribution with a case (including clinicopathologic data). J. Mareckova: evaluation of immunohistochemical staining. O. Hes: study design, results evaluation, discussion, and figures.

References

1. Moch H, Humphrey PA, Ulbright TM, Reuter VE eds. *World Health Organization classification of tumours of the urinary system and male genital organs*. 4th ed. Lyon: IARC Press, 2016.
2. Resnick ME, Unterberger H, McLoughlin PT. Renal carcinoid producing the carcinoid syndrome. *Med. Times* 1966; **94**: 895–896.
3. Zak FG, Jindrak K, Capozzi F. Carcinoidal tumor of the kidney. *Ultrastruct. Pathol.* 1983; **4**: 51–59.
4. Fetissof F, Benatre A, Dubois MP, Lanson Y, Arbeille-Brassart B, Jobard P. Carcinoid tumor occurring in a teratoid malformation of the kidney. An immunohistochemical study. *Cancer* 1984; **54**: 2305–2308.
5. Fetissof F, Lanson Y, Dubois MP, Jobard P. Renal carcinoma with argyrophil cells. *Ann. Pathol.* 1984; **4**: 361–364.
6. Juma S, Nickel JC, Young I. Carcinoids of the kidney: case report and literature review. *Can. J. Surg.* 1989; **32**: 384–386.
7. Unger PD, Russell A, Thung SN, Gordon RE. Primary renal carcinoid. *Arch. Pathol. Lab. Med.* 1990; **114**: 68–71.
8. Huettner PC, Bird DJ, Chang YC, Seiler MW. Carcinoid tumor of the kidney with morphologic and immunohistochemical profile of a hindgut endocrine tumor: report of a case. *Ultrastruct. Pathol.* 1991; **15**: 655–661.
9. Raslan WF, Ro JY, Ordonez NG *et al.* Primary carcinoid of the kidney. Immunohistochemical and ultrastructural studies of five patients. *Cancer* 1993; **72**: 2660–2666.
10. Schlussel RN, Kirschenbaum AM, Levine A, Unger P. Primary renal carcinoid tumor. *Urology* 1993; **41**: 295–297.
11. el-Naggar AK, Troncoso P, Ordonez NG. Primary renal carcinoid tumor with molecular abnormality characteristic of conventional renal cell neoplasms. *Diagn. Mol. Pathol.* 1995; **4**: 48–53.
12. van den Berg E, Gouw AS, Oosterhuis JW *et al.* Carcinoid in a horseshoe kidney. Morphology, immunohistochemistry, and cytogenetics. *Cancer Genet. Cytogenet.* 1995; **84**: 95–98.
13. Takeshima Y, Inai K, Yoneda K. Primary carcinoid tumor of the kidney with special reference to its histogenesis. *Pathol. Int.* 1996; **46**: 894–900.
14. Krishnan B, Truong LD, Saleh G, Sirbasku DM, Slawin KM. Horseshoe kidney is associated with an increased relative risk of primary renal carcinoid tumor. *J. Urol.* 1997; **157**: 2059–2066.
15. Lodding P, Hugosson J, Hansson G. Primary carcinoid tumour with ossification masquerading as calyx stone in a horseshoe kidney. *Scand. J. Urol. Nephrol.* 1997; **31**: 575–578.
16. Begin LR, Guy L, Jacobson SA, Aprikian AG. Renal carcinoid and horseshoe kidney: a frequent association of two rare entities – a case report and review of the literature. *J. Surg. Oncol.* 1998; **68**: 113–119.
17. McCaffrey JA, Reuter VV, Herr HW, Macapinlac HA, Russo P, Motzer RJ. Carcinoid tumor of the kidney. The use of somatostatin receptor scintigraphy in diagnosis and management. *Urol. Oncol.* 2000; **5**: 108–111.
18. Yoo J, Park S, Jung Lee H, Jin Kang S, Kee Kim B. Primary carcinoid tumor arising in a mature teratoma of the kidney: a case report and review of the literature. *Arch. Pathol. Lab. Med.* 2002; **126**: 979–981.
19. McVey RJ, Banerjee SS, Eyden BP, Reeve RS, Harris M. Carcinoid tumor originating in a horseshoe kidney. *In Vivo* 2002; **16**: 197–199.
20. Shibata R, Okita H, Shimoda M *et al.* Primary carcinoid tumor in a polycystic kidney. *Pathol. Int.* 2003; **53**: 317–322.
21. Tal R, Lask DM, Livne PM. Metastatic renal carcinoid: case report and review of the literature. *Urology* 2003; **61**: 838xv–838xvii.
22. Daneshmand S, Chandrasoma S, Wilson S. Primary renal carcinoid tumor. *Sci. World J.* 2004; **4**: 378–380.
23. Kawajiri H, Onoda N, Ohira M *et al.* Carcinoid tumor of the kidney presenting as a large abdominal mass: report of a case. *Surg. Today* 2004; **34**: 86–89.
24. Mufarrij P, Varkarakis IM, Studeman KD, Jarrett TW. Primary renal carcinoid tumor with liver metastases detected with somatostatin receptor imaging. *Urology* 2005; **65**: 1002.e19–1002.e21.
25. Shurtleff BT, Shvarts O, Rajfer J. Carcinoid tumor of the kidney: case report and review of the literature. *Rev. Urol.* 2005; **7**: 229–233.
26. Romero FR, Rais-Bahrami S, Permpongkosol S, Fine SW, Kohanim S, Jarrett TW. Primary carcinoid tumors of the kidney. *J. Urol.* 2006; **176**: 2359–2366.
27. Armah HB, Parwani AV. Primary carcinoid tumor arising within mature teratoma of the kidney: report of a rare entity and review of the literature. *Diagn. Pathol.* 2007; **2**: 15.
28. Hansel DE, Epstein JI, Berbescu E, Fine SW, Young RH, Cheville JC. Renal carcinoid tumor: a clinicopathologic study of 21 cases. *Am. J. Surg. Pathol.* 2007; **31**: 1539–1544.
29. Rodriguez-Covarrubias F, Gomez X, Valerio JC, Lome-Maldonado C, Gabilondo F. Carcinoid tumor arising in a horseshoe kidney. *Int. Urol. Nephrol.* 2007; **39**: 373–376.
30. Lane BR, Chery F, Jour G *et al.* Renal neuroendocrine tumours: a clinicopathological study. *BJU Int.* 2007; **100**: 1030–1035.
31. Lane BR, Jour G, Zhou M. Renal neuroendocrine tumors. *Indian J. Urol.* 2009; **25**: 155–160.
32. Kuroda N, Alvarado-Cabrero I, Sima R *et al.* Renal carcinoid tumor: an immunohistochemical and molecular genetic study of four cases. *Oncol. Lett.* 2010; **1**: 87–90.
33. Jeung JA, Cao D, Selli BW *et al.* Primary renal carcinoid tumors: clinicopathologic features of 9 cases with emphasis on novel immunohistochemical findings. *Hum. Pathol.* 2011; **42**: 1554–1561.
34. Roy S, Hooda S, Huang GJ, Pantanowitz L, Parwani AV. A novel case of concurrent renal tumors: chromophobe renal cell carcinoma and carcinoid tumor of the kidney with brief review of renal neuroendocrine tumors. *Int. J. Surg. Pathol.* 2012; **20**: 531–535.
35. Aung PP, Killian K, Poropatich CO, Linehan WM, Merino MJ. Primary neuroendocrine tumors of the kidney: morphological and molecular alterations of an uncommon malignancy. *Hum. Pathol.* 2013; **44**: 873–880.

36. Korkmaz T, Seber S, Yavuzer D, Gumus M, Turhal NS. Primary renal carcinoid: treatment and prognosis. *Crit. Rev. Oncol. Hematol.* 2013; **87**: 256–264.
37. Sun K, You Q, Zhao M, Yao H, Xiang H, Wang L. Concurrent primary carcinoid tumor arising within mature teratoma and clear cell renal cell carcinoma in the horseshoe kidney: report of a rare case and review of the literature. *Int. J. Clin. Exp. Pathol.* 2013; **6**: 2578–2584.
38. Lamb L, Shaban W. Primary renal carcinoid tumor: a radiologic review. *Radiol. Case Rep.* 2014; **9**: 923.
39. Ouyang B, Ma X, Yan H, He J, Xia C, Yu H. Renal carcinoid tumor with liver metastasis followed up postoperatively for 9 years. *Diagn. Pathol.* 2015; **10**: 182.
40. Anderson DA, Tretiakova MS. Primary renal carcinoid with bilateral multiple clear cell papillary renal cell carcinomas. *Case Rep. Pathol.* 2017; **2017**: 9672368.
41. Higgins A, Eisa W, Walton J, Baber J, Zhu S, Williams H. Metastatic mucinous adenocarcinoma and carcinoid tumor arising from a mature cystic teratoma of a horseshoe kidney. *Urol. Case Rep.* 2017; **11**: 39–41.
42. Mardi K, Negi L, Srivastava S. Well differentiated neuroendocrine tumor of the kidney: report of a rare case with review of literature. *Indian J. Pathol. Microbiol.* 2017; **60**: 105–107.
43. Seker KG, Sam E, Sahin S *et al.* Partial nephrectomy in horseshoe kidney: primary carcinoid tumor. *Arch. Ital. Urol. Androl.* 2017; **89**: 316–318.
44. Gu X, Cheng M, Herrera GA. Kidney carcinoid tumor: histological, immunohistochemical and ultrastructural features. *Ultrastruct. Pathol.* 2018; **42**: 18–22.
45. Rosenberg JE, Albersheim JA, Sathianathen NJ, Murugan P, Weight CJ. Five new cases of primary renal carcinoid tumor: case reports and literature review. *Pathol. Oncol. Res.* 2018. E-pub ahead of print. https://doi.org/10.1007/s12253-018-0481-x
46. Lloyd RV, Osamura RY, Kloppel G, Rosai J eds. *World Health Organization classification of tumours of endocrine organs*. 4th ed. Lyon: IARC Press, 2017.
47. Petersson F, Grossmann P, Hora M *et al.* Renal cell carcinoma with areas mimicking renal angiomyoadenomatous tumor/-clear cell papillary renal cell carcinoma. *Hum. Pathol.* 2013; **44**: 1412–1420.
48. Landrum MJ, Lee JM, Benson M *et al.* Clinvar: improving access to variant interpretations and supporting evidence. *Nucleic Acids Res.* 2018; **46**: D1062–D1067.
49. Bamford S, Dawson E, Forbes S *et al.* The COSMIC (Catalogue of Somatic Mutations in Cancer) database and website. *Br. J. Cancer* 2004; **91**: 355–358.
50. Robinson JT, Thorvaldsdottir H, Winckler W *et al.* Integrative genomics viewer. *Nat. Biotechnol.* 2011; **29**: 24–26.
51. Guy L, Begin LR, Oligny LL, Brock GB, Chevalier S, Aprikian AG. Searching for an intrinsic neuroendocrine cell in the kidney. An immunohistochemical study of the fetal, infantile and adult kidney. *Pathol. Res. Pract.* 1999; **195**: 25–30.
52. Yoshida A, Makise N, Wakai S, Kawai A, Hiraoka N. INSM1 expression and its diagnostic significance in extraskeletal myxoid chondrosarcoma. *Mod. Pathol.* 2018; **31**: 744–752.
53. Yadav R, Kakkar A, Sharma A, Malik PS, Sharma MC. Study of clinicopathological features, hormone immunoexpression, and loss of ATRX and DAXX expression in pancreatic neuroendocrine tumors. *Scand. J. Gastroenterol.* 2016; **51**: 994–999.
54. Sarris EG, Saif MW, Syrigos KN. The biological role of PI3K pathway in lung cancer. *Pharmaceuticals* 2012; **5**: 1236–1264.
55. Morgan TM, Koreckij TD, Corey E. Targeted therapy for advanced prostate cancer: inhibition of the PI3K/AKT/mTOR pathway. *Curr. Cancer Drug Targets* 2009; **9**: 237–249.
56. Wright GL, Maroulakou IG, Eldridge J *et al.* VEGF stimulation of mitochondrial biogenesis: requirement of AKT3 kinase. *FASEB J.* 2008; **22**: 3264–3275.
57. Moriya C, Jinnin M, Yamane K *et al.* Expression of matrix metalloproteinase-13 is controlled by IL-13 via PI3K/AKT3 and PKC-delta in normal human dermal fibroblasts. *J. Invest. Dermatol.* 2011; **131**: 655–661.
58. Szklarczyk D, Morris JH, Cook H *et al.* The STRING database in 2017: quality-controlled protein–protein association networks, made broadly accessible. *Nucleic Acids Res.* 2017; **45**: D362–D368.
59. Cunningham JT, Ruggero D. New connections between old pathways: PDK1 signaling promotes cellular transformation through PLK1-dependent MYC stabilization. *Cancer Discov.* 2013; **3**: 1099–1102.
60. Yap YS, McPherson JR, Ong CK *et al.* The NF1 gene revisited – from bench to bedside. *Oncotarget* 2014; **5**: 5873–5892.
61. Philpott C, Tovell H, Frayling IM, Cooper DN, Upadhyaya M. The NF1 somatic mutational landscape in sporadic human cancers. *Hum. Genomics* 2017; **11**: 13.
62. O'Leary NA, Wright MW, Brister JR *et al.* Reference sequence (RefSeq) database at NCBI: current status, taxonomic expansion, and functional annotation. *Nucleic Acids Res.* 2016; **44**: D733–D745.
63. Oronsky B, Ma PC, Morgensztern D, Carter CA. Nothing but NET: a review of neuroendocrine tumors and carcinomas. *Neoplasia* 2017; **19**: 991–1002.
64. Kim JY, Hong SM, Ro JY. Recent updates on grading and classification of neuroendocrine tumors. *Ann. Diagn. Pathol.* 2017; **29**: 11–16.
65. Gut P, Komarowska H, Czarnywojtek A *et al.* Familial syndromes associated with neuroendocrine tumours. *Contemp. Oncol.* 2015; **19**: 176–183.
66. Di Domenico A, Wiedmer T, Marinoni I, Perren A. Genetic and epigenetic drivers of neuroendocrine tumours (NET). *Endocr. Relat. Cancer* 2017; **24**: R315–R334.
67. Mafficini A, Scarpa A. Genomic landscape of pancreatic neuroendocrine tumours: the International Cancer Genome Consortium. *J. Endocrinol.* 2018; **236**: R161–R167.
68. Scarpa A, Chang DK, Nones K *et al.* Whole-genome landscape of pancreatic neuroendocrine tumours. *Nature* 2017; **543**: 65–71.
69. Fernandez-Cuesta L, Peifer M, Lu X *et al.* Frequent mutations in chromatin-remodelling genes in pulmonary carcinoids. *Nat. Commun.* 2014; **5**: 3518.
70. Simbolo M, Mafficini A, Sikora KO *et al.* Lung neuroendocrine tumours: deep sequencing of the four World Health Organization histotypes reveals chromatin-remodelling genes as major players and a prognostic role for TERT, RB1, MEN1 and KMT2D. *J. Pathol.* 2017; **241**: 488–500.

2 ZÁVĚR

Zde prezentované práce jsou součástí literatury poskytující nový pohled na renální nádorovou patologii a jsou tak jedny z tisíců činitelů vývoje a progrese morfologického a diagnostického poznání v tomto odvětví patologie. Dostupná literatura nabízí množství dat a záplavu rozličných studií, orientace v dostupných pramenech může být nezřídka komplikovaná, i to však patří nejen do vědeckého života, ale i do každodenní praxe rutinního klinického lékaře. Věříme, že ač naše práce se většinou zabývají velmi úzkou problematikou a soustředí se často na velmi drobné detaily, jsou v kontextu většího množství a rozsáhlejších studií literaturou přispívající k utváření komplexního celku.

3 SEZNAM POUŽITÉ LITERATURY

1. Al-Obaidy KI, Eble JN, Cheng L, Williamson SR, Sakr WA, Gupta N, Idrees MT, Grignon DJ (2019) Papillary Renal Neoplasm With Reverse Polarity: A Morphologic, Immunohistochemical, and Molecular Study. The American journal of surgical pathology 43:1099-1111.
2. Al-Obaidy KI, Eble JN, Nassiri M, Cheng L, Eldomery MK, Williamson SR, Sakr WA, Gupta N, Hassan O, Idrees MT, Grignon DJ (2020) Recurrent KRAS mutations in papillary renal neoplasm with reverse polarity. Modern pathology 33:1157-1164.
3. Argani P, Antonescu CR, Couturier J, Fournet JC, Sciot R, Debiec-Rychter M, Hutchinson B, Reuter VE, Boccon-Gibod L, Timmons C, Hafez N, Ladanyi M (2002) PRCC-TFE3 renal carcinomas: morphologic, immunohistochemical, ultrastructural, and molecular analysis of an entity associated with the t(X;1)(p11.2;q21). The American journal of surgical pathology 26:1553-1566
4. Argani P, Antonescu CR, Illei PB, Lui MY, Timmons CF, Newbury R, Reuter VE, Garvin AJ, Perez-Atayde AR, Fletcher JA, Beckwith JB, Bridge JA, Ladanyi M (2001) Primary renal neoplasms with the ASPL-TFE3 gene fusion of alveolar soft part sarcoma: a distinctive tumor entity previously included among renal cell carcinomas of children and adolescents. The American journal of pathology 159:179-192.
5. Argani P, Reuter VE, Zhang L, Sung YS, Ning Y, Epstein JI, Netto GJ, Antonescu CR (2016) TFEB-amplified Renal Cell Carcinomas: An Aggressive Molecular Subset Demonstrating Variable Melanocytic Marker Expression and Morphologic Heterogeneity. The American journal of surgical pathology 40:1484-1495.
6. Argani P, Zhang L, Reuter VE, Tickoo SK, Antonescu CR (2017) RBM10-TFE3 Renal Cell Carcinoma: A Potential Diagnostic Pitfall Due to Cryptic Intrachromosomal Xp11.2 Inversion Resulting in False-negative TFE3 FISH. The American journal of surgical pathology 41:655-662.
7. Argani P, Zhong M, Reuter VE, Fallon JT, Epstein JI, Netto GJ, Antonescu CR (2016) TFE3-Fusion Variant Analysis Defines Specific Clinicopathologic Associations Among Xp11 Translocation Cancers. The American journal of surgical pathology 40:723-737.
8. Delahunt B, Eble JN (1997) Papillary renal cell carcinoma: a clinicopathologic and immunohistochemical study of 105 tumors. Modern pathology 10:537-544.
9. Denize T, Just PA, Sibony M, Blons H, Timsit MO, Drossart T, Jakubowicz D, Broudin C, Morini A, Molina T, Vano Y, Auvray-Kuentz M, Richard S, Mejean A, Gimenez Roqueplo AP, Burnichon N, Verkarre V (2021) MET alterations in biphasic squamoid alveolar papillary renal cell carcinomas and clinicopathological features. Modern pathology 34:647-659. doi: 10.1038/s41379-020-0645-6.
10. Fernandez-Martinez L, Villegas JA, Santamaria I, Pitiot AS, Alvarado MG, Fernandez S, Torres H, Paredes A, Blay P, Balbin M (2017) Identification of somatic and germ-line DICER1 mutations in pleuropulmonary blastoma, cystic nephroma and rhabdomyosarcoma tumors within a DICER1 syndrome pedigree. BMC cancer 17:146.
11. Foster EA, Levine, A.J. (1963) Mucin production in metastatic carcinomas. Cancer 16:506-509.
12. Grignon DJ, Ro JY, Ayala AG (1988) Primary mucin-secreting adenocarcinoma of the kidney. Archives of pathology & laboratory medicine 112:847-849.

13. Han G, Yu W, Chu J, Liu Y, Jiang Y, Li Y, Zhang W (2017) Oncocytic papillary renal cell carcinoma: A clinicopathological and genetic analysis and indolent clinical course in 14 cases. Pathology, research and practice 213:1-6.
14. He H, Trpkov K, Martinek P, Isikci OT, Maggi-Galuzzi C, Alaghehbandan R, Gill AJ, Tretiakova M, Lopez JI, Williamson SR, Montiel DP, Sperga M, Comperat E, Brimo F, Yilmaz A, Pivovarcikova K, Michalova K, Slouka D, Prochazkova K, Hora M, Bonert M, Michal M, Hes O (2018) "High-grade oncocytic renal tumor": morphologic, immunohistochemical, and molecular genetic study of 14 cases. Virchows Archiv 473:725-738.
15. Hes O, Brunelli M, Michal M, Cossu Rocca P, Hora M, Chilosi M, Mina M, Boudova L, Menestrina F, Martignoni G (2006) Oncocytic papillary renal cell carcinoma: a clinicopathologic, immunohistochemical, ultrastructural, and interphase cytogenetic study of 12 cases. Annals of diagnostic pathology 10:133-139.
16. Hes O, Condom Mundo E, Peckova K, Lopez JI, Martinek P, Vanecek T, Falconieri G, Agaimy A, Davidson W, Petersson F, Bulimbasic S, Damjanov I, Jimeno M, Ulamec M, Podhola M, Sperga M, Pane Foix M, Shelekhova K, Kalusova K, Hora M, Rotterova P, Daum O, Pivovarcikova K, Michal M (2016) Biphasic Squamoid Alveolar Renal Cell Carcinoma: A Distinctive Subtype of Papillary Renal Cell Carcinoma? The American journal of surgical pathology 40:664-675.
17. Hes O, de Souza TG, Pivovarcikova K, Grossmann P, Martinek P, Kuroda N, Kacerovska D, Svajdler M, Straka L, Petersson F, Hora M, Michal M (2014) Distinctive renal cell tumor simulating atrophic kidney with 2 types of microcalcifications. Report of 3 cases. Annals of diagnostic pathology 18:82-88.
18. Chen YB, Mirsadraei L, Jayakumaran G, Al-Ahmadie HA, Fine SW, Gopalan A, Sirintrapun SJ, Tickoo SK, Reuter VE (2019) Somatic Mutations of TSC2 or MTOR Characterize a Morphologically Distinct Subset of Sporadic Renal Cell Carcinoma With Eosinophilic and Vacuolated Cytoplasm. The American journal of surgical pathology 43:121-131.
19. Kim SS, Cho YM, Kim GH, Kee KH, Kim HS, Kim KM, Kim JH, Choi C (2020) Recurrent KRAS mutations identified in papillary renal neoplasm with reverse polarity-a comparative study with papillary renal cell carcinoma. Modern pathology 33:690-699.
20. Kojima F, Bulimbasic S, Alaghehbandan R, Martinek P, Vanecek T, Michalova K, Pivovarcikova K, Michal M, Hora M, Murata SI, Sugawara E, Rogala J, Limani R, Hes O (2019) Clear cell renal cell carcinoma with Paneth-like cells: Clinicopathologic, morphologic, immunohistochemical, ultrastructural, and molecular analysis of 13 cases. Annals of diagnostic pathology 41:96-101.
21. Kunju LP, Wojno K, Wolf JS, Jr., Cheng L, Shah RB (2008) Papillary renal cell carcinoma with oncocytic cells and nonoverlapping low grade nuclei: expanding the morphologic spectrum with emphasis on clinicopathologic, immunohistochemical and molecular features. Human pathology 39:96-101.
22. Lefevre M, Couturier J, Sibony M, Bazille C, Boyer K, Callard P, Vieillefond A, Allory Y (2005) Adult papillary renal tumor with oncocytic cells: clinicopathologic, immunohistochemical, and cytogenetic features of 10 cases. The American journal of surgical pathology 29:1576-1581.
23. Merino MJ, Torres-Cabala C, Pinto P, Linehan WM (2007) The morphologic spectrum of kidney tumors in hereditary leiomyomatosis and renal cell carcinoma (HLRCC) syndrome. The American journal of surgical pathology 31:1578-1585.

24. Moch H, Humphrey PA, Ulbright TM, Reuter VE (2016) WHO classification of tumours of the urinary system and male genital organs. IARC, Lyon
25. Muller M, Guillaud-Bataille M, Salleron J, Genestie C, Deveaux S, Slama A, de Paillerets BB, Richard S, Benusiglio PR, Ferlicot S (2018) Pattern multiplicity and fumarate hydratase (FH)/S-(2-succino)-cysteine (2SC) staining but not eosinophilic nucleoli with perinucleolar halos differentiate hereditary leiomyomatosis and renal cell carcinoma-associated renal cell carcinomas from kidney tumors without FH gene alteration. Modern pathology 31:974-983.
26. Nilsson H, Lindgren D, Axelson H, Brueffer C, Saal LH, Lundgren J, Johansson ME (2020) Features of increased malignancy in eosinophilic clear cell renal cell carcinoma. The Journal of pathology 252:384-397.
27. Peckova K, Vanecek T, Martinek P, Spagnolo D, Kuroda N, Brunelli M, Vranic S, Djuricic S, Rotterova P, Daum O, Kokoskova B, Vesela P, Pivovarcikova K, Bauleth K, Dubova M, Kalusova K, Hora M, Michal M, Hes O (2014) Aggressive and nonaggressive translocation t(6;11) renal cell carcinoma: comparative study of 6 cases and review of the literature. Annals of diagnostic pathology 18:351-357.
28. Petersson F, Bulimbasic S, Hes O, Slavik P, Martinek P, Michal M, Gomolcakova B, Hora M, Damjanov I (2012) Biphasic alveolosquamoid renal carcinoma: a histomorphological, immunohistochemical, molecular genetic, and ultrastructural study of a distinctive morphologic variant of renal cell carcinoma. Annals of diagnostic pathology 16:459-469.
29. Pitra T, Pivovarcikova K, Alaghehbandan R, Hes O (2017) Chromosomal numerical aberration pattern in papillary renal cell carcinoma: Review article. Annals of diagnostic pathology.
30. Pivovarcikova K, Grossmann P, Hajkova V, Alaghehbandan R, Pitra T, Perez Montiel D, Sperga M, Rogala J, Slisarenko M, Bartos Vesela A, Svajdler P, Michalova K, Rotterova P, Hora M, Michal M, Hes O (2021) Renal cell carcinomas with tubulopapillary architecture and oncocytic cells: Molecular analysis of 39 difficult tumors to classify. Annals of diagnostic pathology 52:151734.
31. Pivovarčíková K, Martínek P, Trpkov K, Alaghehbandan R, Magi-Galluzzi C, Condom ME, Berney D, Suster S, Gill A, Rychlý B, Michalová K, Pitra T, Hora M, Michal M, Hes O (2019) Fumarate hydratase deficient renal cell carcinoma and fumarate hydratase deficient-like renal cell carcinoma: Morphologic comparative study of 23 genetically tested cases. Ceskoslovenska patologie 55(4):244-249
32. Rao Q, Williamson SR, Zhang S, Eble JN, Grignon DJ, Wang M, Zhou XJ, Huang W, Tan PH, Maclennan GT, Cheng L (2013) TFE3 break-apart FISH has a higher sensitivity for Xp11.2 translocation-associated renal cell carcinoma compared with TFE3 or cathepsin K immunohistochemical staining alone: expanding the morphologic spectrum. The American journal of surgical pathology 37:804-815.
33. Rogala J, Kojima F, Alaghehbandan R, Agaimy A, Martinek P, Ondic O, Ulamec M, Sperga M, Michalova K, Pivovarcikova K, Pitra T, Hora M, Ferak I, Mareckova J, Michal M, Hes O (2020) Papillary renal cell carcinoma with prominent spindle cell stroma - tumor mimicking mixed epithelial and stromal tumor of the kidney: Clinicopathologic, morphologic, immunohistochemical and molecular genetic analysis of 6 cases. Annals of diagnostic pathology 44:151441. doi: 10.1016/j.anndiagpath.2019.151441
34. Ross H, Argani P (2010) Xp11 translocation renal cell carcinoma. Pathology 42:369-373.

35. Rotterova P, Martinek P, Alaghehbandan R, Prochazkova K, Damjanov I, Rogala J, Suster S, Perez-Montiel D, Alvarado-Cabrero I, Sperga M, Svajdler M, Michalova K, Pivovarcikova K, Daum O, Hora M, Dusek M, Ondic O, Stehlikova A, Michal M, Hes O (2018) High-grade renal cell carcinoma with emperipolesis: Clinicopathological, immunohistochemical and molecular-genetic analysis of 14 cases. Histology and histopathology 33(3):277-287.
36. Saleeb RM, Brimo F, Farag M, Rompre-Brodeur A, Rotondo F, Beharry V, Wala S, Plant P, Downes MR, Pace K, Evans A, Bjarnason G, Bartlett JMS, Yousef GM (2017) Toward Biological Subtyping of Papillary Renal Cell Carcinoma With Clinical Implications Through Histologic, Immunohistochemical, and Molecular Analysis. The American journal of surgical pathology 41(12):1618-1629.
37. Siadat F, Trpkov K (2020) ESC, ALK, HOT and LOT: Three Letter Acronyms of Emerging Renal Entities Knocking on the Door of the WHO Classification. Cancers (Basel) 12(1):168.
38. Skenderi F, Ulamec M, Vanecek T, Martinek P, Alaghehbandan R, Foix MP, Babankova I, Montiel DP, Alvarado-Cabrero I, Svajdler M, Dubinsky P, Cempirkova D, Pavlovsky M, Vranic S, Daum O, Ondic O, Pivovarcikova K, Michalova K, Hora M, Rotterova P, Stehlikova A, Dusek M, Michal M, Hes O (2017) Warthin-like papillary renal cell carcinoma: Clinicopathologic, morphologic, immunohistochemical and molecular genetic analysis of 11 cases. Annals of diagnostic pathology 27:48-56.
39. Smith NE, Illei PB, Allaf M, Gonzalez N, Morris K, Hicks J, Demarzo A, Reuter VE, Amin MB, Epstein JI, Netto GJ, Argani P (2014) t(6;11) renal cell carcinoma (RCC): expanded immunohistochemical profile emphasizing novel RCC markers and report of 10 new genetically confirmed cases. The American journal of surgical pathology 38:604-614.
40. Smith SC, Sirohi D, Ohe C, McHugh JB, Hornick JL, Kalariya J, Karia S, Snape K, Hodgson SV, Cani AK, Hovelson D, Luthringer DJ, Martignoni G, Chen YB, Tomlins SA, Mehra R, Amin MB (2017) A distinctive, low-grade oncocytic fumarate hydratase-deficient renal cell carcinoma, morphologically reminiscent of succinate dehydrogenase-deficient renal cell carcinoma. Histopathology 71:42-52.
41. Tanas Isikci O, He H, Grossmann P, Alaghehbandan R, Ulamec M, Michalova K, Pivovarcikova K, Montiel DP, Ondic O, Daum O, Prochazkova K, Hora M, Michal M, Hes O (2018) Low-grade spindle cell proliferation in clear cell renal cell carcinoma is unlikely to be an initial step in sarcomatoid differentiation. Histopathology 72:804-813.
42. Toro JR, Nickerson ML, Wei MH, Warren MB, Glenn GM, Turner ML, Stewart L, Duray P, Tourre O, Sharma N, Choyke P, Stratton P, Merino M, Walther MM, Linehan WM, Schmidt LS, Zbar B (2003) Mutations in the fumarate hydratase gene cause hereditary leiomyomatosis and renal cell cancer in families in North America. American journal of human genetics 73:95-106.
43. Trpkov K, Hes O, Agaimy A, Bonert M, Martinek P, Magi-Galluzzi C, Kristiansen G, Luders C, Nesi G, Comperat E, Sibony M, Berney DM, Mehra R, Brimo F, Hartmann A, Husain A, Frizzell N, Hills K, Maclean F, Srinivasan B, Gill AJ (2016) Fumarate Hydratase-deficient Renal Cell Carcinoma Is Strongly Correlated With Fumarate Hydratase Mutation and Hereditary Leiomyomatosis and Renal Cell Carcinoma Syndrome. The American journal of surgical pathology 40:865-875.
44. Trpkov K, Hes O, Williamson SR, Adeniran AJ, Agaimy A, Alaghehbandan R, Amin MB, Argani P, Chen YB, Cheng L, Epstein JI, Cheville JC, Comperat E, da Cunha

IW, Gordetsky JB, Gupta S, He H, Hirsch MS, Humphrey PA, Kapur P, Kojima F, Lopez JI, Maclean F, Magi-Galluzzi C, McKenney JK, Mehra R, Menon S, Netto GJ, Przybycin CG, Rao P, Rao Q, Reuter VE, Saleeb RM, Shah RB, Smith SC, Tickoo S, Tretiakova MS, True L, Verkarre V, Wobker SE, Zhou M, Gill AJ (2021) New developments in existing WHO entities and evolving molecular concepts: The Genitourinary Pathology Society (GUPS) update on renal neoplasia. Modern pathology doi: 10.1038/s41379-021-00779-w

45. Trpkov K, Williamson SR, Gill AJ, Adeniran AJ, Agaimy A, Alaghehbandan R, Amin MB, Argani P, Chen YB, Cheng L, Epstein JI, Cheville JC, Comperat E, da Cunha IW, Gordetsky JB, Gupta S, He H, Hirsch MS, Humphrey PA, Kapur P, Kojima F, Lopez JI, Maclean F, Magi-Galluzzi C, McKenney JK, Mehra R, Menon S, Netto GJ, Przybycin CG, Rao P, Rao Q, Reuter VE, Saleeb RM, Shah RB, Smith SC, Tickoo S, Tretiakova MS, True L, Verkarre V, Wobker SE, Zhou M, Hes O (2021) Novel, emerging and provisional renal entities: The Genitourinary Pathology Society (GUPS) update on renal neoplasia. Modern pathology doi: 10.1038/s41379-021-00737-6
46. Val-Bernal JF, Mayorga M, Garcia-Arranz P, Gomez-Roman JJ (1998) Mucin secretion in papillary (chromophil) renal cell carcinoma. The American journal of surgical pathology 22:1037-1040.
47. Val-Bernal JF, Salcedo W, Val D, Parra A, Garijo MF (2013) Mucin-secreting clear cell renal cell carcinoma. A rare variant of conventional renal cell carcinoma. Annals of diagnostic pathology 17:226-229.
48. Vanecek T, Pivovarcikova K, Pitra T, Peckova K, Rotterova P, Daum O, Davidson W, Montiel DP, Kalusova K, Hora M, Ondic O, Dubova M, Michal M, Hes O (2017) Mixed Epithelial and Stromal Tumor of the Kidney: Mutation Analysis of the DICER 1 Gene in 29 Cases. Applied immunohistochemistry & molecular morphology 25:117-121.
49. Wei MH, Toure O, Glenn GM, Pithukpakorn M, Neckers L, Stolle C, Choyke P, Grubb R, Middelton L, Turner ML, Walther MM, Merino MJ, Zbar B, Linehan WM, Toro JR (2006) Novel mutations in FH and expansion of the spectrum of phenotypes expressed in families with hereditary leiomyomatosis and renal cell cancer. Journal of medical genetics 43:18-27.
50. Williamson SR, Kum JB, Goheen MP, Cheng L, Grignon DJ, Idrees MT (2014) Clear cell renal cell carcinoma with a syncytial-type multinucleated giant tumor cell component: implications for differential diagnosis. Human pathology 45:735-744.
51. Xia QY, Rao Q, Shen Q, Shi SS, Li L, Liu B, Zhang J, Wang YF, Shi QL, Wang JD, Ma HH, Lu ZF, Yu B, Zhang RS, Zhou XJ (2013) Oncocytic papillary renal cell carcinoma: a clinicopathological study emphasizing distinct morphology, extended immunohistochemical profile and cytogenetic features. International journal of clinical and experimental pathology 6:1392-1399.
52. Xia QY, Wang XT, Fang R, Wang Z, Zhao M, Chen H, Chen N, Teng XD, Wang X, Wei X, Ye SB, Li R, Ma HH, Lu ZF, Zhou XJ, Rao Q (2020) Clinicopathologic and Molecular Analysis of the TFEB Fusion Variant Reveals New Members of TFEB Translocation Renal Cell Carcinomas (RCCs): Expanding the Genomic Spectrum. The American journal of surgical pathology 44:477-489.
53. Zhou M, Kort E, Hoekstra P, Westphal M, Magi-Galluzzi C, Sercia L, Lane B, Rini B, Bukowski R, Teh BT (2009) Adult cystic nephroma and mixed epithelial and stromal tumor of the kidney are the same disease entity: molecular and histologic evidence. The American journal of surgical pathology 33:72-80.

PODĚKOVÁNÍ

Prof. MUDr. Ondřeji Hesovi, Ph.D. - za odborné vedení, předané znalosti, nápady, nabídnutou příležitost a kamarádský přístup.

Prof. MUDr. Michalu Michalovi – za poskytnuté zázemí a podporu.

MUDr. Mariánu Švajdlerovi, Ph.D. – za ochotu a pomoc ve specializačním výcviku.

Prof. MUDr. Milanu Horovi, Ph.D. a MUDr. Tomáši Pitrovi, Ph.D. - za inspirativní mezioborovou spolupráci, bez níž by většina dokončených projektů nikdy nevznikla.

Nefrologickému oddělení I. IK FN Plzeň – za vlídné přijetí, vloženou důvěru a jejich dobrou práci.

Kolektivu Šiklova Ústavu Patologie a Bioptické laboratoře s.r.o. za poskytnuté zázemí.